TR-1224-01

ANALYSIS AND RECOMMENDATION OF SEPARATION REQUIREMENTS FOR ROTORCRAFT OPERATION AT AIRPORTS AND HELIPORTS

SAMUEL W. FERGUSON
Systems Technology, Inc.
2672 Bayshore-Frontage Road, Suite 505
Mountain View, California 94043

J. DAVID KOCUREK
Computational Methodology Associates
2900 Steve Drive
Hurst, Texas 76054

September 1986

FINAL REPORT

Document is available to the U.S. public through the National Technical Information Service, Springfield, Virginia 22161.

Prepared for

U.S. DEPARTMENT OF TRANSPORTATION

TRANSPORTATION SYSTEMS CENTER

KENDAL SQUARE

CAMBRIDGE, MASSACHUSETTS 02142

NOTICE

PREFACE

The analysis work presented in this report is part of an ongoing effort by the Federal Aviation Administration (FAA) to develop improved rotorcraft separation standards. The subject of this report, **Analysis and Recommendation of Separation Requirements for Rotorcraft Operation at Airports and Heliports**, is specifically oriented toward hazards created by rotorwash in scenarios involving hover and low-speed ground and/or air taxi of rotorcraft. Other ongoing efforts by the FAA are directed toward the investigation of separation requirements involving hazard generating rotorcraft and other rotorcraft/fixed-wing aircraft in flight up and away from the ground.

The authors would like to acknowledge the contributions of three people who provided guidance and direction in this analysis effort: the contracting officer's technical representative, Dr. David Burnham; the FAA sponsor for this project, Mr. Peter Massoglia; and Mr. Don Harris of the Naval Air Test Center. In addition, the authors would like to thank Mrs. Sharon Duerksen and Mr. William Dawson for their help in preparing the interim and final reports.

METRIC CONVERSION FACTORS

Approximate Conversions to Metric Measures

Symbol	When You Know	Multiply by	To Find	Symbol
		LENGTH		
in	inches	*2.5	centimeters	cm
ft	feet	30	centimeters	cm
yd	yards	0.9	meters	m
mi	miles	1.6	kilometers	km
		AREA		
in^2	square inches	6.5	square centimeters	cm^2
ft^2	square feet	0.09	square meters	m^2
yd^2	square yards	0.8	square meters	m^2
mi^2	square miles	2.6	square kilometers	km^2
	acres	0.4	hectares	ha
		MASS (weight)		
oz	ounces	28	grams	g
lb	pounds	0.45	kilograms	kg
	short tons (2000 lb)	0.9	tonnes	t
		VOLUME		
tsp	teaspoons	5	milliliters	ml
Tbsp	tablespoons	15	milliliters	ml
fl oz	fluid ounces	30	milliliters	ml
c	cups	0.24	liters	l
pt	pints	0.47	liters	l
qt	quarts	0.95	liters	l
gal	gallons	3.8	liters	l
ft^3	cubic feet	0.03	cubic meters	m^3
yd^3	cubic yards	0.76	cubic meters	m^3
		TEMPERATURE (exact)		
°F	Fahrenheit temperature	5/9 (after subtracting 32)	Celsius temperature	°C

*1 in = 2.54 (exactly). For other exact conversions and more detailed tables, see NBS Misc. Publ. 286, Units of Weights and Measures, Price $2.25, SD Catalog No. C13.10:286.

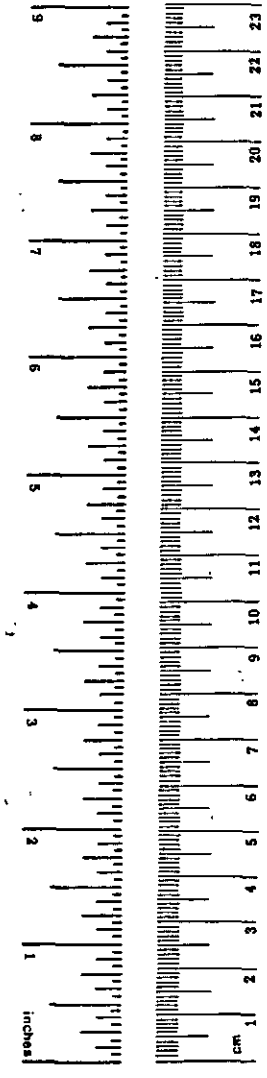

Approximate Conversions from Metric Measures

Symbol	When You Know	Multiply by	To Find	Symbol
		LENGTH		
mm	millimeters	0.04	inches	in
cm	centimeters	0.4	inches	in
m	*meters*	3.3	*feet*	ft
m	meters	1.1	yards	yd
km	kilometers	0.6	miles	mi
		AREA		
cm^2	square centimeters	0.16	square inches	in^2
m^2	square meters	1.2	square yards	yd^2
km^2	square kilometers	0.4	square miles	mi^2
ha	hectares (10,000 m^2)	2.5	acres	
		MASS (weight)		
g	grams	0.035	ounces	oz
kg	kilograms	2.2	pounds	lb
t	tonnes (1000 kg)	1.1	short tons	
		VOLUME		
ml	milliliters	0.03	fluid ounces	fl oz
l	liters	2.1	pints	pt
l	liters	1.06	quarts	qt
l	liters	0.26	gallons	gal
m^3	cubic meters	35	cubic feet	ft^3
m^3	cubic *meters*	1.3	cubic yards	yd^3
		TEMPERATURE (exact)		
°C	Celsius temperature	9/5 (then add 32)	Fahrenheit temperature	°F

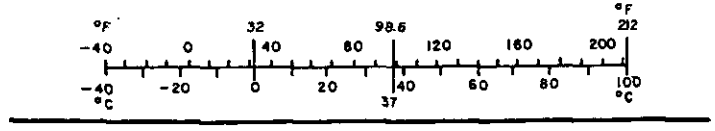

TABLE OF CONTENTS

TABLE OF CONTENTS (Continued)

TABLE OF CONTENTS (Concluded)

LIST OF TABLES

LIST OF TABLES (Concluded)

LIST OF FIGURES

LIST OF FIGURES (Continued)

LIST OF FIGURES (Continued)

LIST OF FIGURES (Continued)

LIST OF FIGURES (Continued)

LIST OF FIGURES (Continued)

LIST OF FIGURES (Continued)

LIST OF FIGURES (Continued)

LIST OF FIGURES (Concluded)

LIST OF ABBREVIATIONS

AFCS	Automatic flight control system
AGL	Above ground level
c.g.	Center of gravity
CMA	Computational Methodology Associates
DAIP	Distance along the interaction plane
deg	Degree
DFRC	Distance from rotor center
dia	Diameter
DL	Disc loading
FAA	Federal Aviation Administration
FOD	Foreign object damage
ft	Foot, feet
HROTOR	Rotor height above the ground
IGE	In ground effect
kt,kts	Knot(s)
lb,lbs	Pound(s)
MAX	Maximum
msec	Millisecond(s)
mm	Millimeter(s)
NASA	National Aeronautics and Space Administration
NTIS	National Technical Information Service
OGE	Out-of-ground effect
PSF	Pounds per square foot
ROTHAZ	Rotorcraft Hazard Analysis Program

LIST OF ABBREVIATIONS (Concluded)

rpm	Revolutions per minute
STI	Systems Technology, Inc.
V/STOL	Vertical/short takeoff and landing

LIST OF SYMBOLS

A	Particulate cloud vortex rollup constant
A_F	Maximum drag area (ft^2)
A_I	Object impact area (ft^2)
a_{3d}	Wing lift curve slope (1/deg)
B	Number of rotor blades
C_D	Coefficient of drag (ND)
C_T	Rotor thrust coefficient (ND)
C_u, C_z	Wall jet growth function constants (ND)
C_1, C_2	Ground vortex positional constants (ND)
C_3	Particulate cloud radial boundary calculation constant (ND)
D	Rotor diameter (ft)
D'	Fuselage generated side force (lb)
D_e	Jet exhaust diameter (ft)
DL	Disc loading (lb/ft^2)
D_P	Terrain particle size (in)
D_W	Diameter of reference water particles (in)
E_P	Kinetic energy of object (ft-lb)
E_P/A_I	Kinetic energy to impact area ratio (lb/ft)
e	Exponential mathematical function
F_{peak}	Peak overturning force (lb)
F_x	Incremental calculated peak forces on personnel (lb)
GW	Gross weight (lb)
GW_{max}	Maximum rotorcraft gross weight (lb)
GW'	(0.95)(empty weight of the aircraft + 100 lb)

H	Rotor height above ground (ft)
H_c	Maximum particulate cloud height (ft)
HI	Hazard index (lb/ft)
ΔH	Incremental vertical height (ft)
K	Span correction factor for vortex strength calculations (ND)
K_T	Terrain erosion factor (ND)
k_g	Ground effect induced velocity correction factor (ND)
k_{wind}	Wind effect correction factor (ND)
L'	Wing generated lift (lb)
ln	Natural logarithmic mathematical function
ℓ_V	Particulate cloud vortex radial arm position length (ft)
M_{peak}	Peak overturning moment (ft-lbs)
m_p	Mass of the particle (slugs)
n_s	Shear layer exponent (ND)
P_o	Total downwash pressure (lb/ft^2)
Q_{peak}	Peak velocity dynamic pressure (lb/ft^2)
Q_x	Incremental peak dynamic pressure values for personnel force calculations (lb/ft^2)
q_F	Peak dynamic pressure (lb/ft^2)
q_N	Dynamic pressure at the jet nozzle or at the effective rotor slipstream diameter (lb/ft^2)
q_s	Dynamic pressure along the ground (lb/ft^2)
$q_{s_{eff}}$	Effective surface dynamic pressure (lb/ft^2)
$q_{s_{max}}$	Maximum surface dynamic pressure (lb/ft^2)

LIST OF SYMBOLS (Continued)

$\lvert\bar{q}\rvert$	Magnitude of induced velocity due to the ground vortex (ft/sec)
R	Rotor radius (ft)
R_c	Particulate cloud radial boundary (ft)
R_V	Radial distance to the center of the particulate cloud vortex core (ft)
r	Rotor radial station (ft)
r_{ip}	Rotor radial station (total length) along the interaction plane (ft)
r_j	Rotor radial station (ft)
$(r/R)_j$	Initial wall jet radius (ND)
S	Wing area (ft^2)
T_f	Twin rotor wall jet interference correction factor (ND)
t	Axial distance from jet nozzle exit (ft)
U_N	Induced velocity of a fully developed rotor slipstream (ft/sec)
$\bar{U}$	Average induced velocity at the rotor disk in ground effect (ft/sec)
$\bar{U}_M$	Mean momentum velocity at the jet nozzle exit or, analogously, the mean velocity of the fully accelerated rotor slipstream (ft/sec)
$\bar{U}_{OGE}$	Average induced velocity at the rotor disk influenced by the out-of-ground effect (ft/sec)
u	Local velocity within the wall jet (ft/sec)
u_h	Horizontal velocity component (ft/sec)
u_m	Maximum radial wall jet velocity (ft/sec)
u_v	Vertical velocity component (ft/sec)
V	Forward flight velocity (ft/sec)

V_f	Rotorcraft translational speed (kt)
VK	Minimum rotorwash velocity required to overturn a fixed-wing aircraft (kt)
V_{min}	Minimum air velocity required to maintain partical or object flight (ft/sec)
V_p	Partical or object velocity (ft/sec)
V_{peak}	Peak velocity of air mass in personnel peak force and moment calculations (ft/sec)
V_{space}	Distance experimentally measured between trailing vortices (ft)
v_i	Induced velocity (ft/sec)
W_p	Particle weight (lb)
W_h	Width of a person (ft)
X_F	Vertical moment arm from the wheel to the point of application of D' (ft)
X_{LG}	Moment arm of the landing gear (one-half the wheel stance) (ft)
X_W	Moment arm from the c.g. of the light aircraft to the point of application of L' (ft)
x/R	Radial distance to the evaluation point in the wall jet (ND)
x_g	Longitudinal location of the ground vortex core from the center of the rotor (ft)
x_{ip}	x component of interaction plane coordinate system along the ground (ft)
y_{ip}	y component of interaction plane coordinate system along the ground 9ft)
Z_V	Vertical distance to the center of the dust cloud vortex core (ft)
Z_x	Vertical height in the wall jet profile for the evaluation station for peak force and moment calculations (ft)

z	Height in the wall jet profile (ft)
z_b	Maximum height of the wall jet profile (ft)
z_g	Vertical height location of the ground vortex core (ft)
z_h	Vertical coordinate at which the profile velocity is one-half its maximum velocity (ft)
z_{ip}	z component of interaction plane coordinate system along the ground (ft)
z_m	Maximum velocity height in the wall jet profile (ft)
α	Wing angle of attack (deg)
β	Particle size parameter (ND)
Γ_g	Ground vortex strength (ft^2/sec)
Γ_{tip}	Tip vortex strength (ft^2/sec)
Γ_w	Trailer vortex strength (ft^2/sec)
ΔH	Incremental vertical height (ft)
Γ	Vortex strength (ft^2/sec)
λ	Inflow ratio (ND)
μ	Advance or tip speed ratio (ND)
μ^*	Ratio of the free or translational airspeed to the average induced flow speed through the rotor tip path plane (ND)
π	Constant (3.1416)
ρ_A	Ambient air density ($slug/ft^3$)
ρ_p	Terrain particle density (lb/ft^3)
ρ_W	Density of water (lb/ft^3)
σ'	Air density ratio (ND)

LIST OF SYMBOLS (Concluded)

ϕ_o	Particulate cloud vortex rollup constant (ND)
Ω	Rotor rotational speed (rad/sec)
χ	Trailer angle (deg)

SECTION I

INTRODUCTION

The safe operation of rotorcraft, for the purpose of avoiding rotorwash-related accidents in close proximity to the ground, has historically been primarily the responsibility of the rotorcraft pilot. In the execution of this task, however, the rotorcraft pilot has usually been provided with only minimal help and guidance. The Federal Aviation Administration (FAA), in an effort to provide more guidance, has initiated a program to develop the capability to better understand, model, and predict with analysis many of the more important types of rotorwash-related hazards. This report presents one approach to the development of a rotorwash hazard analysis methodology as well as **recommended separation requirements for rotorcraft operation at airports and heliports.** This study also provides a computer program (to be run on IBM PC or PC-compatible computers) that can be used as an analysis tool in studying potential rotorwash hazard scenarios.

The presentation of the information in this report is broken down into three major groupings. The end products of this effort, an executive summary and recommended separation requirements for rotorcraft operation at airports and heliports, are presented in Section II for easy reference rather than at the end of the report in accordance with the developmental chronology of the project. The associated background information for the recommended separation requirements are presented in Sections VII and VIII, respectively. The second major grouping in this report comprises Sections III and IV, which present the mathematical models that were developed to analytically investigate the rotorcraft downwash flowfields of interest as well as their correlation/validation. The third major grouping is made up of Sections V and VI, which are respectively devoted to the development of a hazard analysis methodology and to mathematical modeling/analysis of the rotorwash hazards for which separation requirements are subsequently proposed. Appendices contain, among other things,

the user's guide for and a listing of the ROTHAZ computer program that was developed as an aid to the analysis effort.

SECTION II

EXECUTIVE SUMMARY AND RECOMMENDED ROTORCRAFT SEPARATION REQUIREMENTS AND PROCEDURES

A. EXECUTIVE SUMMARY

Historically, rotorcraft pilots have been held primarily responsible for the avoidance (or prevention) of rotorwash-related accidents, and only minimal guidance has been made available to pilots to aid them in this task. The Federal Aviation Administration (FAA), in response to a need for more information and guidance, has initiated a program whose goal is to develop the capability to better understand, model, and predict with analysis various types of rotorwash-related hazards. Recommended separation guidelines for use by pilots as well as air traffic controllers and heliport designers are also a program goal. This report presents one approach toward the development of a hazard analysis methodology as well as recommended separation requirements for rotorcraft operation at airports and heliports (as applicable primarily to the hover and low-speed air- and ground-taxi modes of flight).

As an aid to better understanding the results presented in this report, it is important to begin with a brief discussion of the tasks required by the contract statement of work (Contract DTRS-57-85-C-00039, Study of the Upset Potential of the Rotorcraft Downwash Flow Field in Order to Define Separation Standards for Rotorcraft Operations at Airports and Heliports). These tasks (with their titles expanded) include:

Task 1: Development of a Downwash Flow Field Model

Task 2: Development of a Hazard Analysis Model

Task 3: Quantification of Safety Factors and Recommendation of Research to Reduce or Eliminate Safety Factors

Task 4: Recommendation of Separation Requirements.

The initial step in the research effort was the development of a task specific work plan for the project. For Tasks I and II, the developed work plan was essentially identical. The subtasks that were defined included:

1. A literature review of the subject
2. A development of the analytical model(s)
3. A computer implementation of the model(s)
4. Validation of the model(s) with experimental data
5. Detailed documentation of the developed model(s).

The literature search was initially considered to be one of the most important phases of the entire project, and, in retrospect, this assumption was quite correct. One of the reasons this task was so critically important was due to the fact that the subject areas applicable to this type of research are not popular and are therefore infrequently investigated. Another important reason involved the need to progress quickly in the research to support the development of an FAA planning document to aid in heliport design. The last reason the literature search was so important was that, as with most research projects, resources (time and funds) were limited; therefore, minimizing duplication of work already available in the literature helped to stretch available resources.

The literature searches for Tasks I and II were conducted simultaneously. This was done to minimize the required calendar time as well as to obtain a better perspective on how the two tasks interfaced with one another and to identify where voids existed in the data base that would have to be filled in order to complete the required tasks. One of the most difficult parts of this effort involved the identification of the important hazards that needed to be analyzed. It was discovered quite early in the research effort that there were no identifiable U.S. Government or other civilian-related accident data bases from which to obtain examples nor were there comprehensive statistics on common types of rotorwash-related accidents. Subsequent to discussion with FAA personnel on

this problem, the decision was made to contact the U.S. military safety centers to see if further guidance could be provided from their accident data bases. The U.S. Army Safety Center at Ft. Rucker, Alabama, was particularly helpful in this regard; they were able to supply a significant number of "sanitized" accident reports for numerous types of rotorwash-related accidents. Following review of these data, it seemed that an analysis of the most frequently occurring military rotorwash-related accidents would be quite appropriate for developing the hazard model and subsequently making recommendations for separation criteria. This decision was based on the discovery that most of the accidents reported by the military did not seem to be related particularly to military operations or to specific types of military rotorcraft. In many of the cases reported, the accidents could easily have been civilian accidents. In some of these cases, the accidents being reported actually occurred at civilian-operated airports and heliports (e.g., civilian hospital heliports were involved in several rotorwash-related accidents). More detailed information on the hazard analysis methodolgy used in this research is provided in Section V.

In concluding the discussion on the literature search, it should be noted that an appendix (Appendix E) listing the documents identified as important reading on the subject of rotorwash-related accidents has been provided in this final report.

Upon completion of the literature search effort, collected information was used to aid development of both the downwash and the hazard analysis models. These mathematical models were then implemented on a computer to maximize their usefulness during the detailed analysis phases of the project. Before the models were utilized extensively, however, an effort was made to correlate the model results with flight test or other experimental data wherever possible.

The assumption was made early in the project that all analytical results from the research effort would be challenged. This assumption is still believed to be completely valid, because any recommended separation criteria resulting from the research are bound to have at least some eventual impact on the operational use and economics of civilian rotorcraft. Without validation of mathematical models wherever possible and a clear

statement of all assumptions and safety factors involved, it would clearly be hard to accept any recommended separation criteria different from those presently practiced by the rotorcraft industry on a daily basis. (The recommended separation criteria presented herein are stated conservatively for safety purposes at the present time and can probably be modified somewhat if recommended research is conducted.) In some cases, the quantitative flight test and/or experimental data that was needed for mathematical model correlation was found to be available. In some cases, only qualitative data was identified from which only subjective measures of correlation could be obtained. Correlation is presented in detail for the downwash flowfield models in Section IV and for various components of the hazard models in Section VI.

Upon completion of the Task I and II models and correlation of the models, documentation of the tasks was completed so that interim working papers could be provided to the Government for review of the project.

The next major task in the project was to utilize the mathematical models in helping to develop various forms of recommended separation criteria and to identify and develop any safety factors that might be required (i.e., as a result of a lack of flight test or experimental data for correlation with a particular mathematical model or analysis methodology). This phase of the research initiated the Task III and IV efforts. The Task III goal was to identify and, if possible, eliminate as much nontechnical "guesstimation" in the analysis process as possible prior to the formulation of recommended separation criteria. As these efforts progressed, the recommendations for further research became more clearly identifiable, particularly with respect to their priorities. The details of the recommendations for further research as identified by this task are provided in Section VIII. The highest priority items are those involving the experimental measurement of the effects of wind on rotorwash, the quantification of rotorwash flowfields for small rotorcraft (less than 3000 lbs), and an investigation of what intensities of rotorwash are hazard thresholds to untrained and unprotected civilian personnel from the standpoints of being bothersome, discomforting, and physically hazardous (i.e., as a function of body build and body weight).

As Task III was concluded, the work on Task IV was advanced considerably due to the fact that these two tasks were much more closely coupled than was originally perceived. The task specific work plan for Task IV included:

1. Contact and review with appropriate organizations to discuss the topic of safe rotorcraft separation criteria in general
2. Development of recommended separation criteria (based on all previous work in this research effort)
3. Documentation and justification of recommended separation standards.

The task of discussing and reviewing separation criteria with appropriate organizations and personnel was not as effective as originally planned. One hindrance to successful completion of this task resulted from a lack of organized infrastructure within the Government and military that could provide guidance on the subjects of interest through written policies, detailed and concise accident records, and/or active committee groups working on rotorwash-related problems. Discussions were held with some members of the FAA air traffic control section; however, no extensive field analysis work or interviewing was conducted with air traffic controllers or pilots who regularly work or fly in heavily congested heliport or airport situations. It is suggested in Section VIII that further research also be conducted in this area to provide for increased insight into the recommendation of improved separation criteria.

Discussion on the methodology utilized in developing the recommended separation criteria are presented in Section VII. Let it suffice to say here that the guiding words or phrases utilized in this process centered upon the concepts of

1. Simplicity
2. Ease of implementation in the appropriate operational scenario
3. Fairness of application to various types of rotorcraft and operators.

It was clearly understood from the beginning of the project that no criteria could be developed that would please all parties and interests involved. The factor that was given highest priority in criteria development was that **personnel**, particularly those untrained for exposure in the rotorcraft hazard environment, **should be protected with conservatively recommended separation criteria.** The intent of the authors in these situations is to force complaints that are registered against the recommended criteria to have to be justified either by existing data (not identified by this study) or through future research (such as that recommended by Section VIII) before the recommended separation criteria may be altered. The loss of human life or the careless injury of innocent bystanders cannot be allowed to occur through the application of liberally devised separation criteria when those criteria are not based on sound technical decision making processes using sound technical information.

The presentation of the recommended separation requirements for rotorcraft operation at airports and heliports, the final outcome of this study, are presented in the next subsection. These recommendations are stated in an advisory format rather than a regulatory format. It is left to the users of these recommendations to reformat them as specifically required.

B. RECOMMENDED ROTORCRAFT SEPARATION REQUIREMENTS AND PROCEDURES

The recommended separation requirements and procedures presented in this section are the outcome of the analysis effort presented in subsequent sections of this report. These recommendations are intended to insure that safe and practical separation distances are maintained in all weather conditions between hazard generating rotorcraft (those rotorcraft that generate a significant rotorwash flowfield, e.g. in a low IGE hover) and personnel, animals, structures, and various types of vehicles on the ground (e.g., parked rotorcraft, fixed-wing aircraft, and ground vehicles). For ideal weather conditions, therefore, it is acknowledged that some may consider these recommendations to be too restrictive.

The recommended requirements and procedures proposed are also believed to be presented in a practical format that is consistent with the way in which civilian rotorcraft are operated. For several of the proposed recommendations, a choice of more than one approach is provided, each of which attempts to accomplish the same end result. A review and discussion of background information directly associated with these recommended rotorcraft separation requirements and procedures is provided in Section VII. The rest of the report provides the rationale, justification, and methodology that was used to develop and quantify the proposed criteria and procedures in their present format.

1. Recommendation 1

Many rotorwash-related accidents could be avoided if each airport and heliport was designed for the rotorcraft traffic that it handles. This statement is particularly true with respect to the physical size of the rotorcraft involved. It is recommended, therefore, that all airports and heliports be authorized on a nonemergency basis to operate only rotorcraft of specifically named types or of specifically defined size classifications. This authorization should be stated officially in the appropriate documentation involved with the certification of the airport or heliport as well as in pilot mission planning literature (e.g., maps and airport and heliport directories). If the choice is made not to specify by name the type(s) of rotorcraft authorized to use a particular facility, then it is suggested that the rotorcraft size classifications utilized for hazard classification purposes be the Classes A, B, and C of Table 1, where the hazard index (HI) is equal to the product of the disc loading (lb/ft^2) multiplied by the rotor radius (ft). (See Section VII for a detailed discussion on the hazard index parameter concept and on the size classification breakpoints recommended in Table 1.)

TABLE 1

ROTORCRAFT HAZARD CLASSES

Class	Size Classification
A	HI $\leq$ 110
B	110 $<$ HI $\leq$ 260
C	HI $>$ 260

2. Recommendation 2

After the decision has been made to authorize a particular airport or heliport to operate a specific rotorcraft type or size class (or combination of types and size classes), it then becomes important to maintain safe separation distances between the hazard-generating rotorcraft and personnel, structures, and other types of aircraft, rotorcraft, or ground vehicles. Since rotorcraft are operated in many different ways, it is recommended that two different types of operational airport/heliport scenarios be used in the specification of safe separation criteria. It is hoped that specification of separation criteria in this way will also simplify practical implementation.

a. Operational Scenario No. 1. The first operational scenario for which recommendations are made includes all heliports that normally accommodate only one rotorcraft at a time. (Examples of these heliports are discussed in Ref. 1.) Recommended separation requirements for this scenario are simple in comparison with other scenarios, since there is no need to regulate rotorcraft operations in close proximity to other rotorcraft or fixed-wing aircraft. To provide flexibility for future use, two different formats are suggested for definition of safe separation distances. The first format, presented in Fig. 1, recommends separation distance as a function of the rotorcraft hazard classification (review Table 1). Recommended separation distances are specified in feet between the center of the rotor of the hazard-generating rotorcraft and the various types of personnel, structures, and other vehicles that might be involved. The SEPARATION DISTANCE CATEGORY definitions are:

Separation Distance Category	Rotorcraft Hazard Class		
	A	B	C
X	40 ft*	60 ft	160 ft
Y	80 ft	190 ft	360 ft
Z	160 ft	330 ft	500 ft

* or rotor radius + 10 ft

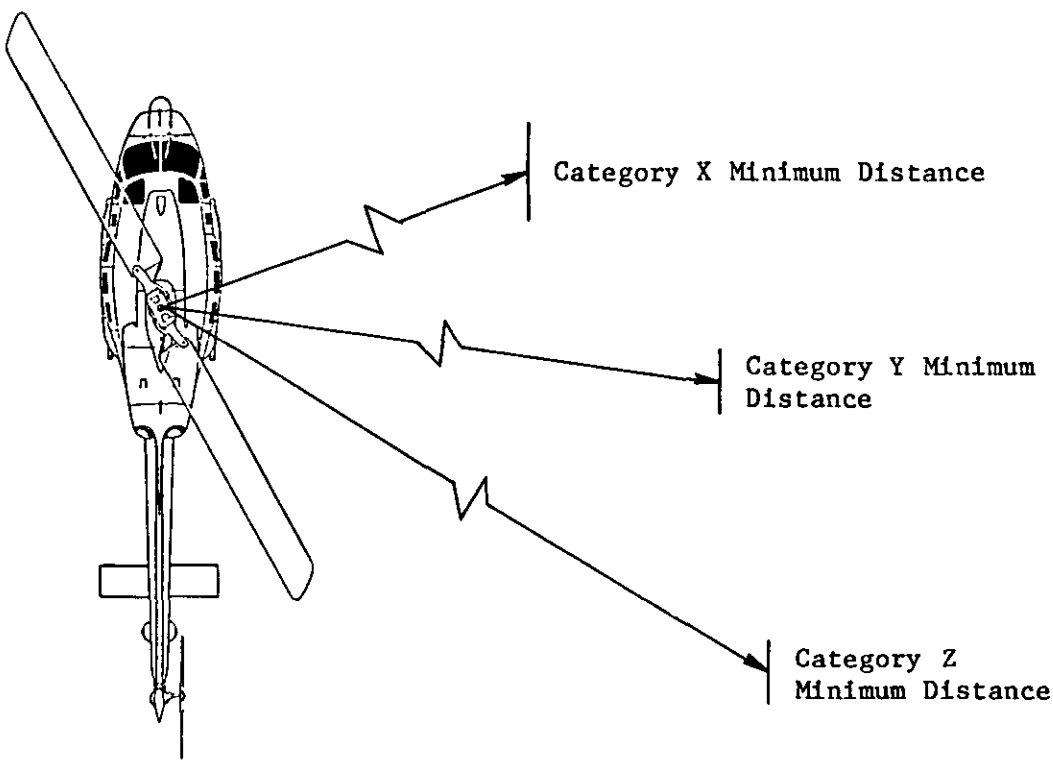

Figure 1. Recommended Rotorcraft Separation Requirements for Scenarios Where Only One Rotorcraft Can be Landed and Shut Down or Parked at a Time

Class.	Definition
X	Minimum separation distance to all secured objects, equipment, vehicles, and structures. (The region located within this radial distance should be kept clear of all types of objects at all times.)
Y	Minimum separation distance to untrained and unprotected personnel who are anticipating an encounter with rotorwash (i.e., people casually watching a helicopter land). These personnel must be prohibited from gaining unauthorized access to the hazard generating rotorcraft by either a restraining fence or wall.
Z	Minimum separation distance to all unsecured equipment, vehicles, structures, or unsuspecting personnel.

An example suggesting the use of this criteria is presented in Fig. 2.

The second recommended format utilizes equations to calculate minimum required separation distances as a direct function of the hazard index and hazard type. This format is much more useful in allowing the heliport designer to specify ahead of time:

1. The exact type(s) of rotorcraft that can be operated from the heliport (e.g., maximum disc loading, rotor radius).

and,

2. The types of potential hazards that will be involved with the unique layout of the heliport to be designed.

These equations, presented in Fig. 3, provide the opportunity to customize a heliport design as a function of available resources and the type of traffic expected.

b. Operational Scenario No. 2. The second operational scenario for which recommendations are made includes all the various types of rotorcraft operations conducted in close proximity to other rotorcraft and/or to fixed-wing aircraft. Recommended minimum separation distances (between the center of the rotor of the hazard-generating rotorcraft and personnel, structures, vehicles, fixed-wing aircraft, and other rotorcraft) are provided in Fig. 4, where definitions for the HAZARD AVOIDANCE DISTANCE CATEGORIES are:

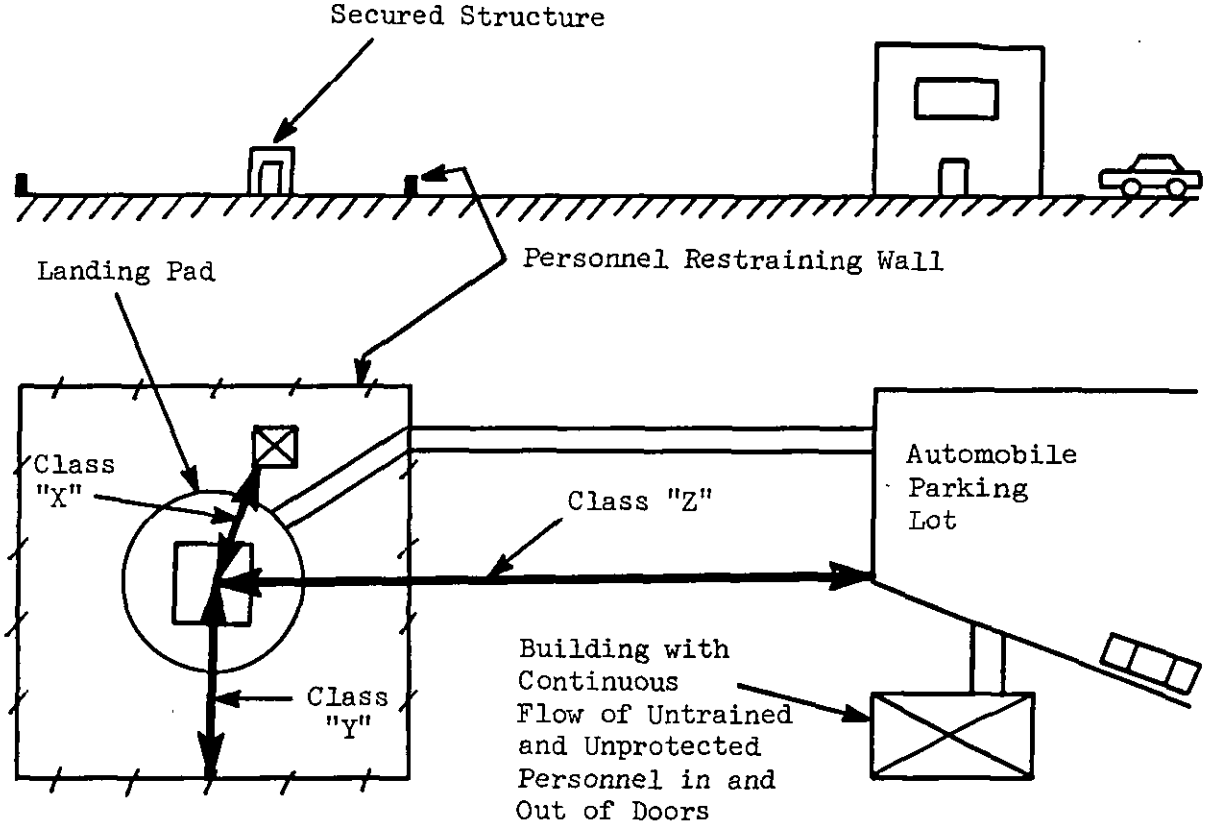

Figure 2. Example Illustration of the Use of the Single Rotorcraft Heliport Category Distances

Class	Equation
X	$RSD = 32.51 + (1.3258)(HI) + (-0.0008)(HI)^2$
Y	$RSD = 0.7635 + (0.9571)(HI) + (-0.0006)(HI)^2$
Z	$RSD = -6.1505 + (0.2868)(HI) + (-0.00002)(HI)^2$

NOTE: Equations may not be applicable for rotorcraft hazard index values of less than 30.

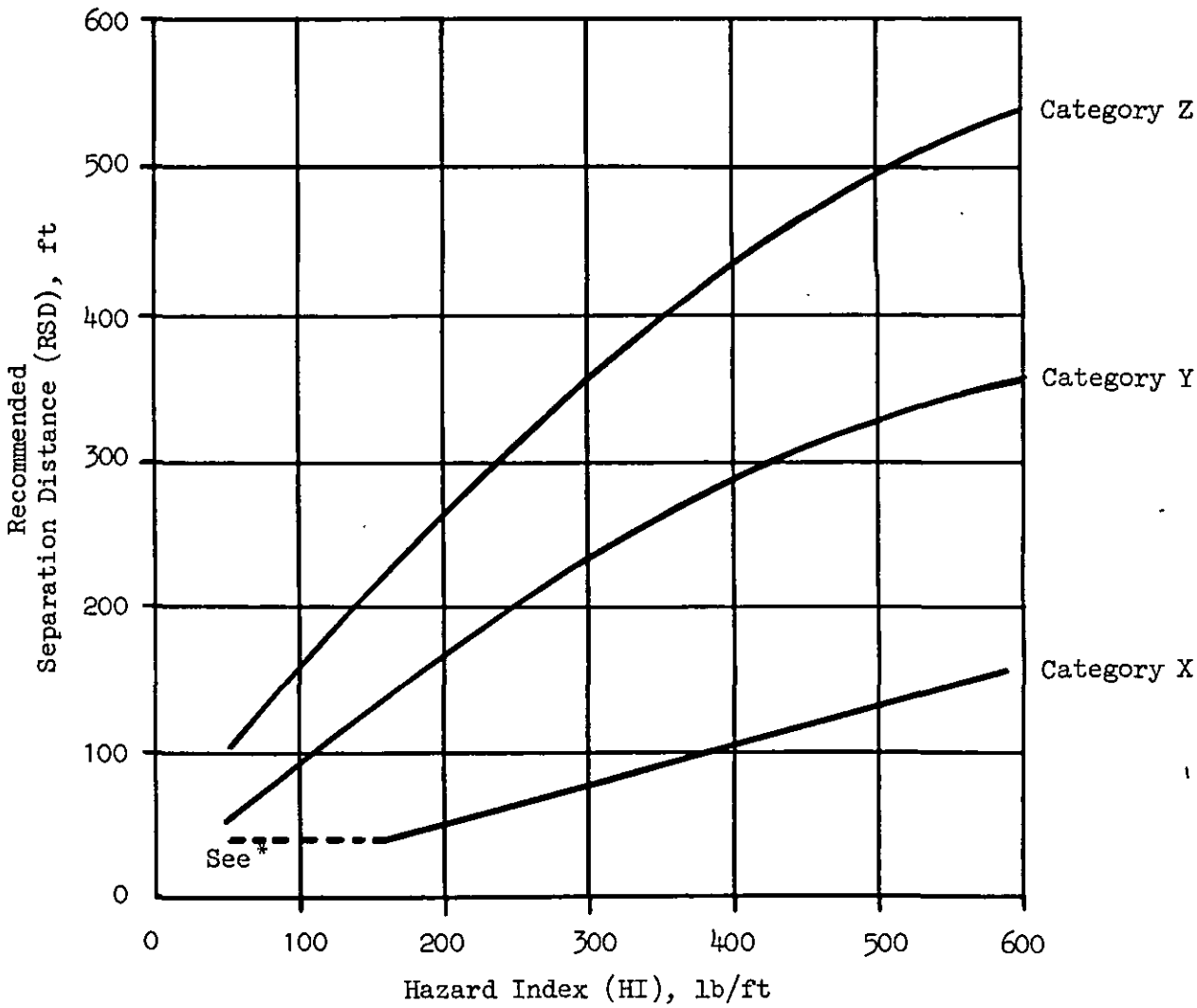

*Requirement exists to insure that adequate rotor tip clearance is maintained.

Figure 3. An Alternative Format for Recommended Rotorcraft Separation Requirements for Scenarios Where Only One Rotorcraft Can be Landed and Shut Down or Parked at a Time

Hazard Avoidance Distance Category	Rotorcraft Hazard Class		
	A	B	C
I	160 ft	330 ft	500 ft
II	70 ft	120 ft	180 ft
III	70 ft	120 ft	180 ft

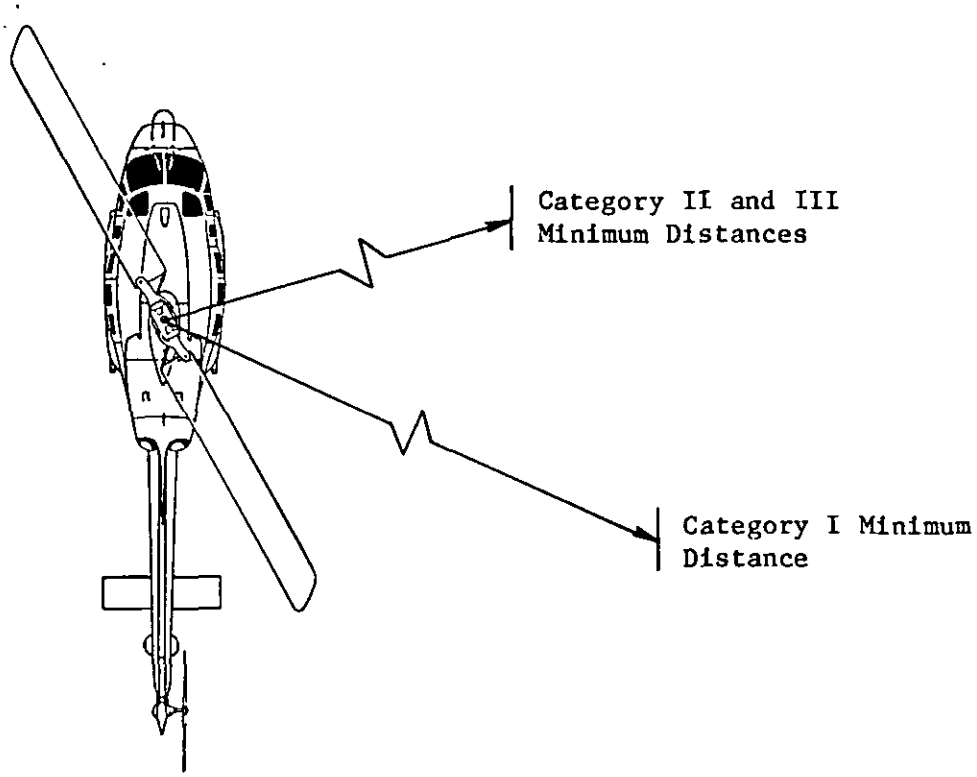

Figure 4. Recommended Rotorcraft Separation Requirements for all Scenarios Except Those Involving Heliports Where Only One Rotorcraft Can be Landed at a Time

Class.	Definition
I	Minimum separation distance required between the hazard generating rotorcraft and the general public (unauthorized personnel), loading or unloading operations, maintenance operations, unsecured light fixed-wing aircraft or rotorcraft, public parking lots, and structures with open doors/windows as well as all potentially hazardous situations not clearly covered by Categories II or III.
II	Minimum separation distance required between the hazard generating rotorcraft and secured ready-for-flight rotorcraft, parked and secured (tied down) fixed-wing aircraft and rotorcraft, secure rotorcraft support equipment, and structures meeting uniform building codes.
III	Minimum separation distance required between the hazard-generating rotorcraft and unsecured (always assumed) equipment, objects, and vehicles not required in routine rotorcraft operations (e.g., trash barrels, tarps, construction materials, maintenance equipment) since these items can contribute to the creation of other types of hazards (i.e., to the rotorwash generating rotorcraft itself). Humans and animals are not permitted nearby, and their presence immediately results in a Classification I requirement.

The format recommended in Fig. 4 is designed to be similar to the first of the two formats discussed previously (Fig. 1). The two formats are different in that the "Separation Distance" categories have been replaced with the more general "Hazard Avoidance Distance" categories, which are tied more directly to the rotorcraft's operational environment. The alternative equation format for this second scenario is provided in Fig. 5.

3. Recommendation 3

As an aid to further avoiding potentially hazardous situations at airports and heliports, the following procedural guidelines are recommended for future implementation:

a. The rotorcraft manufacturer should provide a statement in the pilot manuals of certificated rotorcraft providing quantitative/qualitative guidance concerning the rotorwash hazard potential and how it is influenced by ambient winds.

Class	Equation
I	$RSD = 32.51 + (1.3258)(HI) + (-0.0008)(HI)^2$
II,III	$RSD = 34.61 + (0.3376)(HI) + (-0.0002)(HI)^2$

NOTE: Equations may not be applicable for rotorcraft hazard index values of less than 30.

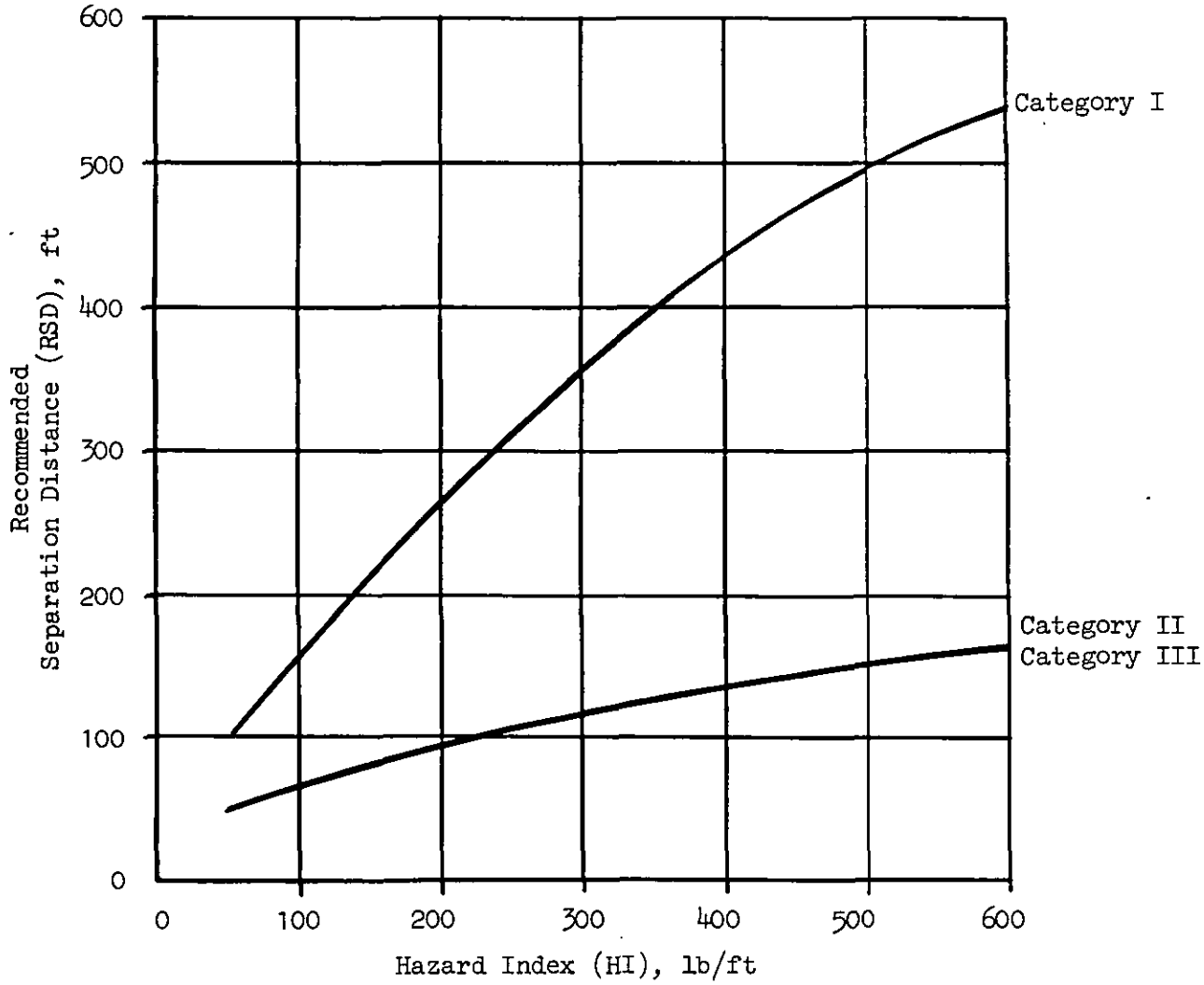

Figure 5. An Alternative Format for Recommended Rotorcraft Separation Requirements for All Scenarios Except Those Involving Heliports Where Only One Rotorcraft Can be Landed at a Time

b. All runways, taxiways, and authorized rotorcraft parking positions should be clearly marked in order to help insure that rotorcraft pilots do not stray inadvertently off approved routes for rotorcraft movement.

c. Rotorcraft should not be allowed under any conditions to ground or air taxi between loading or unloading personnel (except for authorized and trained ramp personnel) and the exit routes from their location to terminal buildings, other structures, or parking lots. (This requirement exists for avoidance of rotorwash as well as other crash related hazards.)

d. All rotorcraft operations that are not of the usual operational type (e.g., maintenance run-up, blade track and balance) should be isolated from all other normal rotorcraft operations to as great an extent as possible. The effect of wind should be accounted for in the locations chosen for these types of rotorcraft operations in order to insure that hazardous levels of rotorwash are not blown into areas of the heliport or airport used for normal operations.

e. Operational rotorcraft traffic patterns should be designed so that the prevailing ambient wind blows rotorwash away from all personnel, structures, vehicles, fixed-wing aircraft, and other rotorcraft. Heliport and airport design and general operating procedures should also be developed using historically developed ambient wind speed and direction data in such a way as to minimize rotorwash hazard potential.

f. All unauthorized and unessential personnel should be prevented from obtaining access to runway, taxiway, or ramp areas.

g. All personnel required to be in close proximity to potentially hazardous levels of rotorwash should be provided equipment for eye protection and written documentation that explains the rotorwash hazard problem and techniques for their personal protection.

SECTION III

DEVELOPMENT OF A ROTORCRAFT DOWNWASH FLOWFIELD MODEL

This section describes the approach, methods, and working equations required to implement three rotor-induced downwash/outwash flow field models which were developed as Task I of this contract (Ref. 2). These three aerodynamic models are designed to be used as predictive tools in determining, classifying, and estimating downwash and wake hazard potential as influenced by the flight regime and configuration of the rotorcraft of interest. The presented models are developed with emphasis toward rotorcraft operations in close proximity to the ground. This mode of operation results in the prominent wake flow characteristics which are known to present the greatest hazard potential.

The most important flow field model, the radial wall jet, occurs while the rotorcraft is hovering near the ground where the downwash wake impinges and flows outward along the ground. This outward flow can produce serious erosion of the ground, recirculation and foreign object damage (FOD), as well as debris and wind hazards to personnel, equipment, structures, adjacent rotorcraft or aircraft, and to the generating rotorcraft itself. This radial wall jet model is also extended to include modeling of the upwash deflection zone which occurs along the plane of symmetry between the rotors of side-by-side or tandem rotorcraft.

The second model that was developed treats the ground vortex which occurs at hover with low wind conditions or at low rotorcraft flight speeds. The ground vortex phenomenon has received little attention as a potential downwash hazard source, and very little information is available to correlate this type of model. Recent studies are used, however, to guide in the estimation of the ground vortex strength, position, and probability of occurrence. With this information, a horseshoe vortex model is implemented which can be used to determine the approximate local velocity field and the hazard potential.

The third model which is developed applies primarily to higher forward airspeeds (and possibly to sideward flight) where disk edge vortices form in analogy to the familiar fixed-wing trailing vortices. This is the simplest model posed and is described using traditional fixed-wing methods through analogy.

Correlation is provided wherever possible for each of the presented mathematical models using available flight test data. The most extensive correlation analysis which is provided is for the wall jet model in both the single- and twin-rotor configurations. Data used in this correlation analysis comes from flight test evaluations of the Sikorsky CH-53E and the Bell XV-15.

A. THE WALL JET

The wall jet is the most prominent of the three major rotorwash potential hazards produced by a rotorcraft in close proximity to the ground. The high velocity slipstream of the rotor impinges on the ground and accelerates radially outward, reaching a maximum value at a distance of approximately one diameter from the rotor's axis of rotation. At this point, the static pressure in the flow has recovered to the atmospheric value; the point is defined as the beginning of the radial wall jet. Beyond this initial point, the velocity in the wall jet decreases exponentially with distance. For a twin-rotor configuration (tandem or tilt rotor), the flow fields produced by each rotor interact with each other to result in the formation of an interaction plane jet, which produces a stronger and even more pronounced outwash effect. The development of these rotorwash environments is illustrated in Fig. 6 for both the single- and twin-rotor cases.

The rotor flow field that gives rise to the wall jet is similar to the less complex free jet that impinges on a ground plane. This flow is generally subdivided into three regions, as shown in the cross section of Fig. 7. Region I is the free jet that extends from the exit nozzle of the propulsive device to a point above the ground plane at which the flow becomes influenced by the presence of the ground. The turning region,

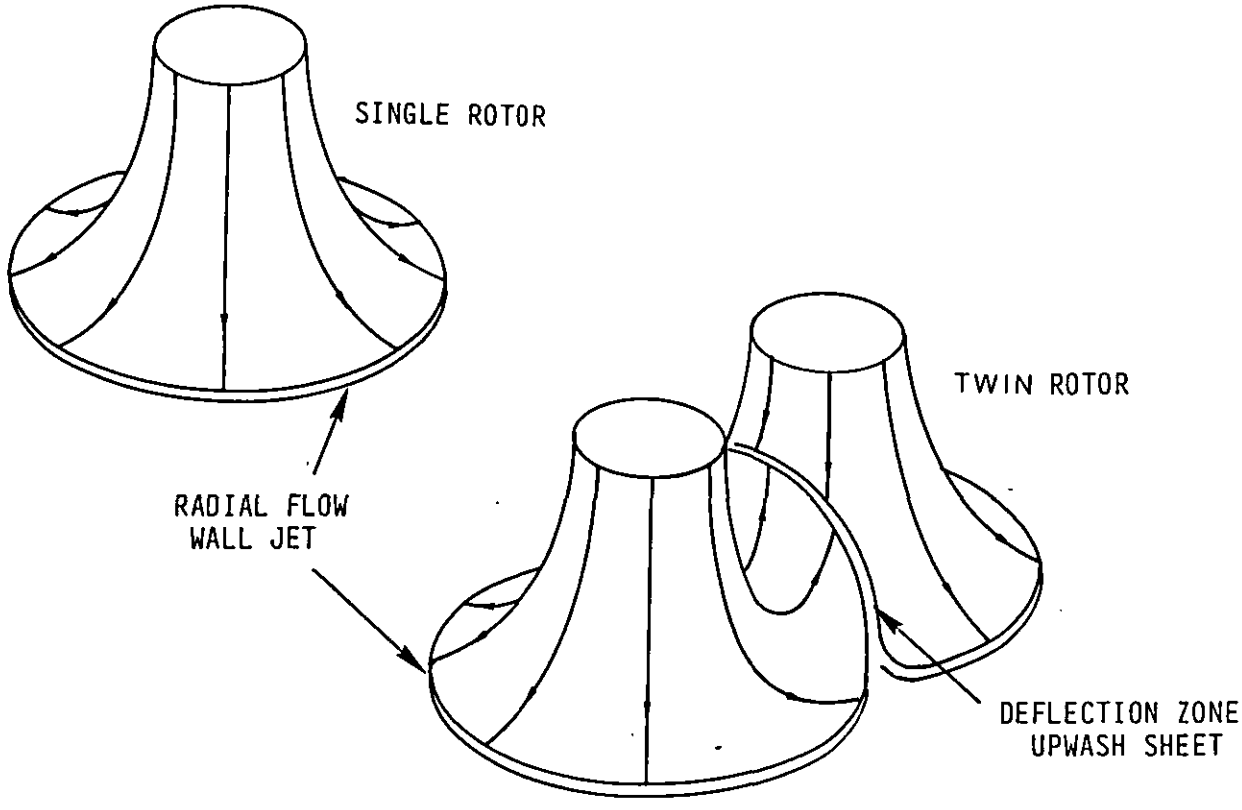

Figure 6. Radial Flow Fields of Single- and Twin-Rotor Configurations Operating in Ground Proximity

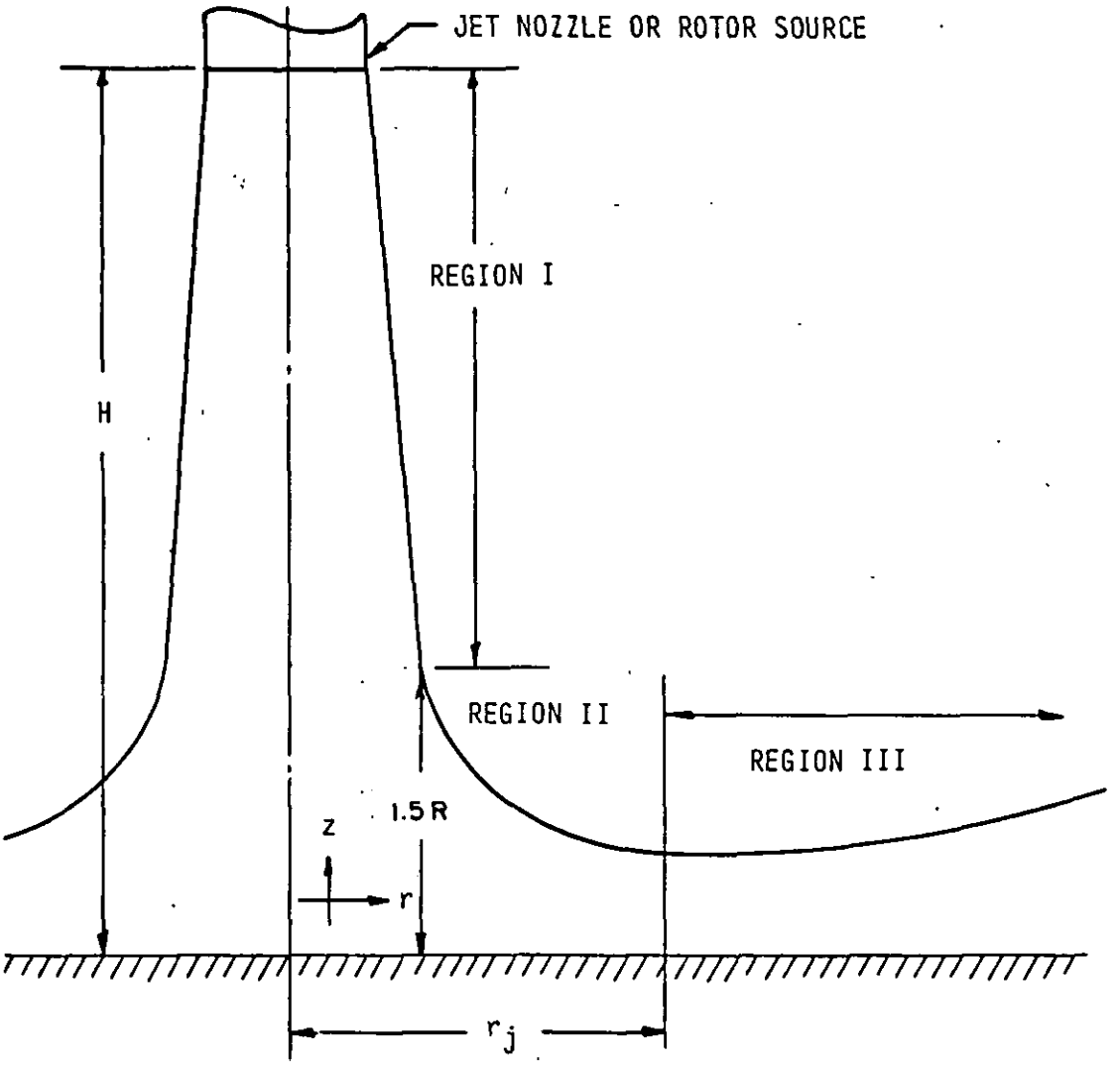

Figure 7. Cross Section of Rotor Downwash Impingement Flow

Region II, begins as the flow changes principal direction from vertical to horizontal. The static pressure is relieved from maximum at a stagnation point on the ground at the impinging jet centerline to ambient as the radial outwash develops. Region III, the wall jet region, begins at the point where the static pressure has returned to ambient pressure and the flow streamlines are parallel to the ground plane. The static pressure remains essentially constant in this region as the flow moves radially outward until the velocity of the flow is dissipated.

A significant number of the analysis approaches reviewed during this effort to model the previously described aerodynamic flow field followed the notable treatment of a uniform impinging jet that was developed by Glauert (Ref. 3). Glauert established that the velocity profiles at any radial station in the developed wall jet region are affinely related, a fact which has been verified experimentally. More recently, interest in vertical/short takeoff and landing (V/STOL) aircraft operations has focused on the quantification of the important parameters that cause ground erosion, recirculation, and equipment and personnel hazards. Hohler (Ref. 4) presents a wealth of experimental data and analytical approaches which, in combination, can provide a nominal solution to the general downwash flow field parameters when assuming a jet nozzle source. Hohler also points out unique considerations for helping to take into account the effects of a rotor or propeller downwash source, and he gives several examples of a chart method for rapidly estimating the general magnitude of certain outwash parameters.

Migdal, et al., (Ref. 5) provide further analytical detail and experimental verification for the downwash flow field in a study which focuses on the two-jet impingement configuration and the associated upwash deflection along the interaction plane. Based on conservation of mass principles and the use of the single-jet model as a building block, semi-empirical models for each of the main flow regions of the single jet are coupled to simulate the combined flow field for two jets and to provide representative estimates for experimentally measured ground-pressure distributions. The treatment of the transitional region in this analysis is very complete; however, it is dependent upon certain assumptions for the uniform jet source model.

In the process of solving the rotorwash flow field problem, the previously identified references provide valuable guidance through their respective analytical and physical descriptions of the behavior of the flow field components. However, their focus on jet sources, and the simplifying assumptions made in many instances, remove the detail required to quantify hazard avoidance criteria for rotorcraft. In particular, they are strongly tied to decay models for a uniform free-jet source and are generally concerned with impingement cases where the jet height above ground (H/D) is large (or out of ground effect).

Although derived through an experimental and analytical consideration of jets, a series of investigations, performed by Cornell Aeronautical Laboratories, Canadair Ltd., and Dynasciences Corporation (Refs. 6 through 9), were identified which better address the application of the jet flow field analogy to the quantification of the rotorcraft downwash/outwash environment. These investigations also applied the results to the quantification of associated surface erosion and dust cloud formation (or brown out) problems. Therefore, the wall jet model developed in the following sections generally parallels the Dynasciences model development (Refs. 8 and 9) with certain clarifications. References 4 and 5 are also used to provide guidance in the extrapolation of the mathematical model from the initial wall jet boundary back into the transition region.

1. Wall Jet Profile Similarity

Figure 8 presents the profile of the fully developed wall jet as provided by Glauert in Ref. 3 and reproduced in Ref. 9. The velocity profile at any radial position is similar when scaled to its maximum velocity (u_m) and the vertical coordinate (z_h) at which the profile velocity is one-half its maximum. The profile is actually composed of two matched solutions to the governing viscous flows of an inner and outer layer; however, no simple, explicit, analytical representations are directly available. To circumvent this problem and to facilitate the simulation of the wall jet, distribution functions have been assumed, as used by Midgal, et al., in Ref. 5.

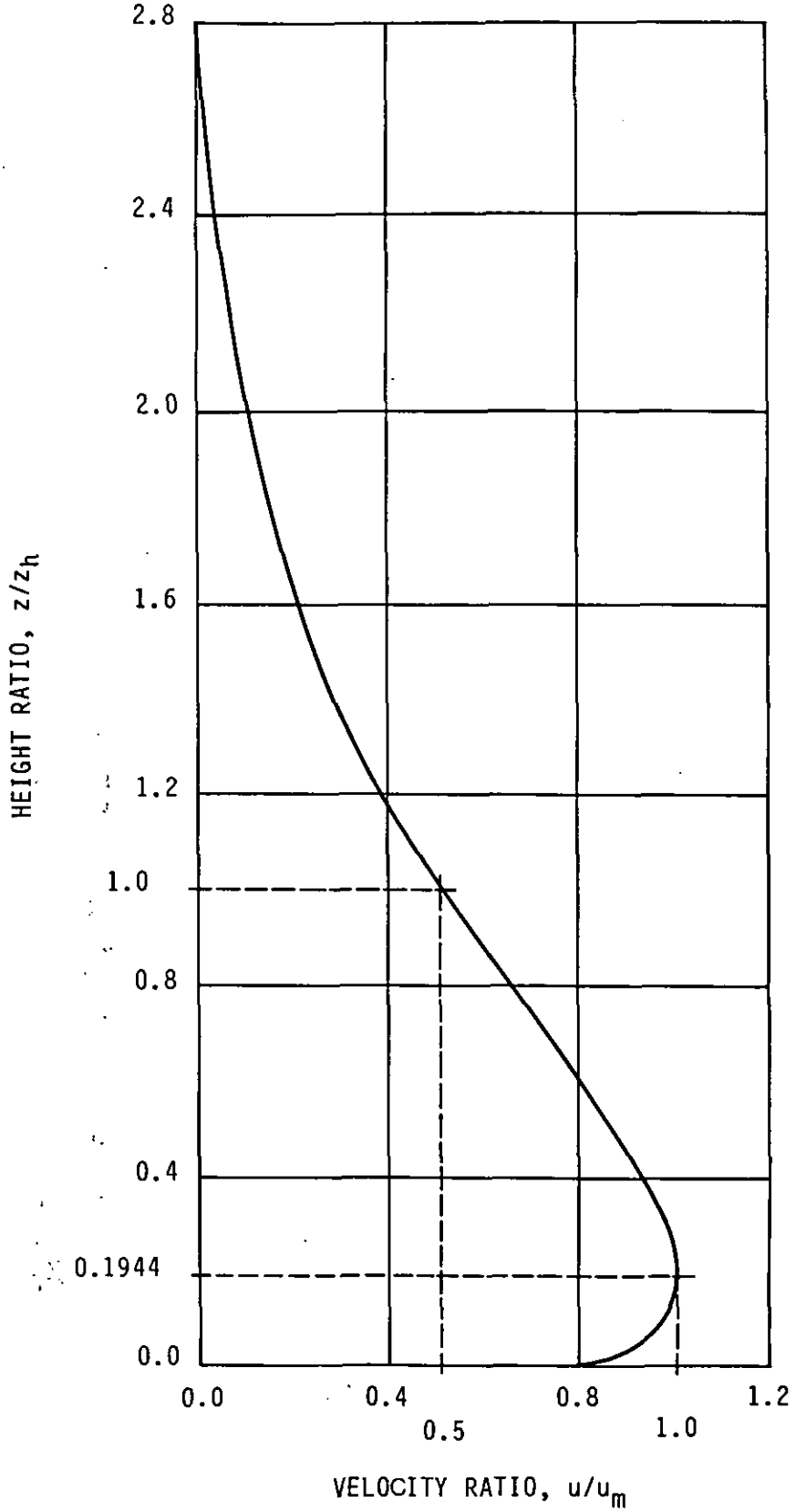

Figure 8. Nondimensional Wall Jet Vertical Velocity Profile

The inner layer is represented by the familiar turbulent boundary layer shape function

$$u/u_m = (z/z_m)^{1/7} \tag{1}$$

The outer shear layer transitions the wall jet flow to the surrounding quiescent flow field. This shear layer distribution is

$$u/u_m = \{1 - [(z-z_m)/(z_b-z_m)]^{n_s}\}^2 \tag{2}$$

The outer boundary point (z_b) and the maximum velocity point are determined from the ratios

$$z_b/z_h = 2.8 \tag{3}$$

and

$$z_m/z_h = 0.1944 \tag{4}$$

The latter constant is the limit value for the fully developed wall jet, as taken from Ref. 5, and is in agreement with Glauert's result (Ref. 3). Thus the detailed velocity profile can be constructed, given only the values for the scaling parameters u_m and z_h, since the shear layer exponent (n_s) is calculated to satisfy the ratios of the profile boundary and the maximum velocity point to the half-velocity point. The determination of the scaling parameters is then the major effort in calculating the wall jet characteristics.

The analytical procedure for calculating the wall jet region is developed in Ref. 6, which also establishes the numerical values for a number of required constants from experimental data for both uniform and nonuniform jets. References 8 and 9 extend the method to lower disk loading rotors by substituting modeling that provides for the dynamic pressure decay of the induced velocity air jet in place of modeling for free jet decay. Reference 9 further summarizes the calculation procedure; however,

several significant typographical errors were made in the typing and presentation of the working equations in the final report; these will be noted later.

2. Determination of the Scaling Parameters

The maximum radial velocity in the wall jet is of the form

$$u_m/\bar{U}_M = C_u(r/R)^{-1.143} \tag{5}$$

where $\bar{U}_M$ is the mean momentum velocity at the jet nozzle exit or, analogously, the mean velocity of the fully accelerated rotor slipstream. Similarly, the height of the half velocity point in the outer shear layer is

$$z_h/R = C_z(r/R)^{1.028} \tag{6}$$

The constants in these two equations are determined by the characteristics of the wall jet at its initial radius as non-dimensionalized by the rotor radius R. From considerations of the radial mass flow and momentum flux, as calibrated by experimental data, Ref. 6 derives the wall jet starting half velocity point as

$$(z_h/R)_j = 0.654/\{[(u_m/\bar{U}_M)_j]^2(r/R)_j\} \tag{7}$$

This equation is also presented as Eq. 15 in Ref. 9; however, in the writing or typing of this report, the exponent on the very significant velocity-squared term in the denominator of the right-hand side was omitted. (The omission was verified by checking the cited references in Ref. 9.)

It can be further assumed that the maximum radial velocity at the start of the wall jet is equal to the maximum axial velocity in an equivalent free jet at a distance from the free jet nozzle exit given by

$$\frac{t}{R} = \frac{H}{R} + \left[(r/R)_j - 1\right] \qquad (8)$$

This assumption is fully described and justified with experimental findings in Ref. 8. For a rotor, however, slipstream acceleration and the resulting wake contraction must also be accounted for; that is, t/R should be adjusted to reflect the annular area of the rotor slipstream at which the fully developed slipstream velocity occurs. The rotor slipstream contraction ratio from momentum theory is used to account for this effect; therefore, in terms of an effective slipstream diameter,

$$t/D_e = 0.707(t/R) \qquad (9)$$

The starting value for u_m can now be determined interatively as follows. First, a value of 2.0 is assumed for $(r/R)_j$, the initial wall jet radius. The equivalent free jet length and then t/D_e are calculated for the assumed value. As a function of t/D_e, the test data in Fig. 8 of Ref. 9 is used to obtain the decay of the dynamic pressure in the analogous free jet and thus the velocity at the start of the wall jet. For this investigation, the dynamic pressure is represented by

$$\frac{(q_s)_{max}}{q_N} = 1 - 0.025\left(\frac{t}{D_e}\right)^2 \qquad \text{where } \frac{t}{D_e} < 4 \qquad (10)$$

$$\frac{(q_s)_{max}}{q_N} = 2.4/\left(\frac{t}{D_e}\right) \qquad \text{where } \frac{t}{D_e} > 4 \qquad (11)$$

This formulation is compared to the test data of Ref. 9 in Fig. 9. Thus, with a value for t/D_e, the decayed dynamic pressure is determined from which an estimated starting maximum velocity is then calculated as follows

$$\frac{u_m}{U_N} = \left[\frac{(q_s)_{max}}{q_N}\right]^{1/2} \qquad (12)$$

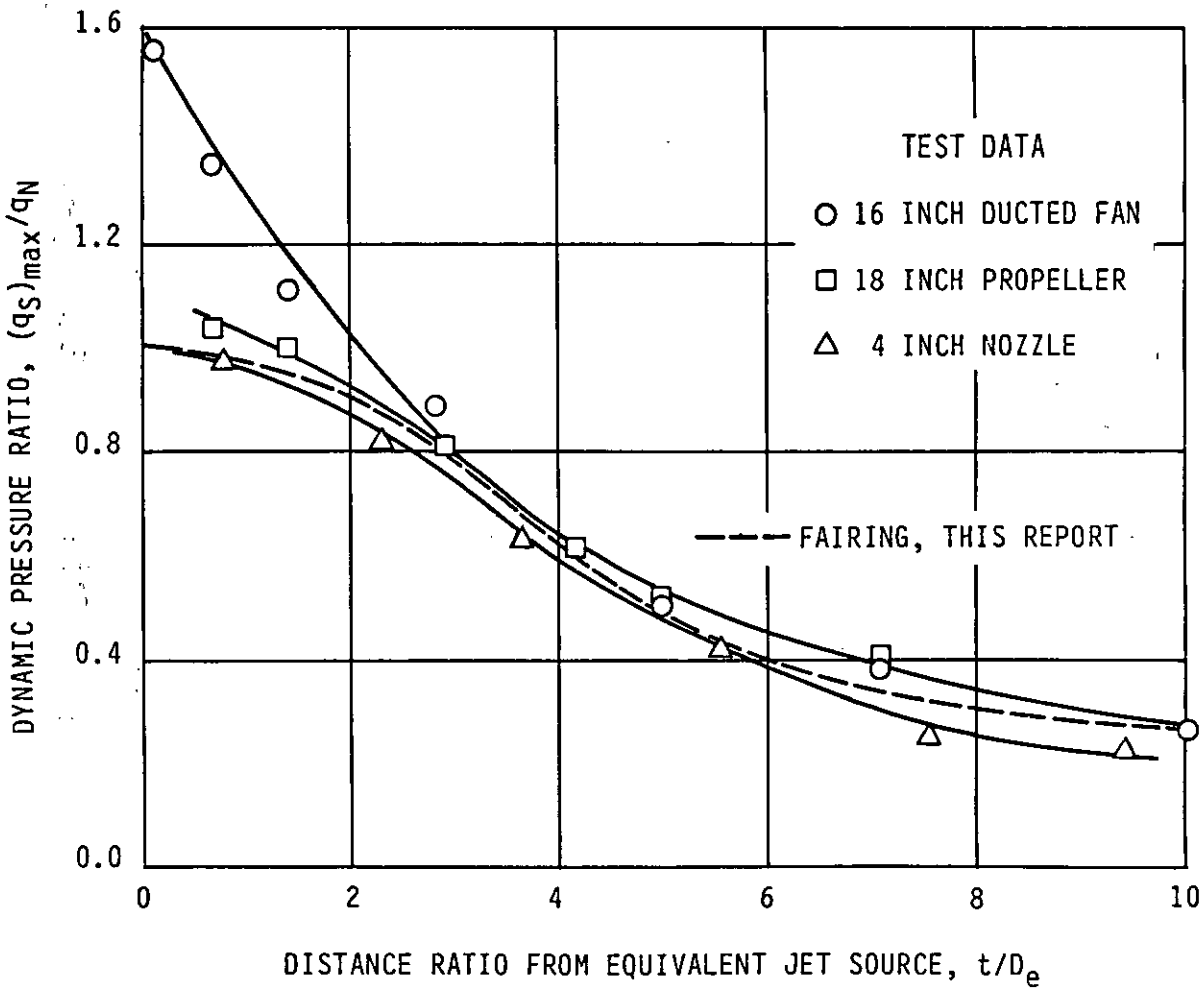

Figure 9. Measurements of Dynamic Pressure Decay with Equivalent Distance from the Jet Source

where U_N is the induced velocity of a fully developed rotor slipstream. This value is taken as the disk average from momentum theory, which is expressed as a function of the disk loading and ambient atmospheric density as

$$U_N = \left(\frac{2\ DL}{\rho_A}\right)^{1/2} \tag{13}$$

Next, the average induced velocity at the rotor disk ($\bar{U}$) is calculated with the influence of ground effect as

$$\begin{aligned} \bar{U} &= k_g\ \bar{U}_{OGE} \\ &= k_g\left(\frac{U_N}{2}\right) \end{aligned} \tag{14}$$

where k_g is the ground effect induced velocity correction factor

$$k_g = 1.0 - 0.9e^{-2(H/R)} \tag{15}$$

An improved estimate of the starting radial position of the wall jet is now calculated from

$$(r/R)_j = 2.5081\left(\bar{U}\ /u_m\right)^{0.486} \tag{16}$$

This equation, which is derived from the procedure in Ref. 6, is Eq. 21 in Ref. 9. This new value of $(r/R)_j$ is again used to calculate the equivalent length t/D_e, and the above process is repeated until $(r/R)_j$ is satisfactorily converged.

Using the final calculated values of $(r/R)_j$, $\bar{U}$, and u_m, the mean momentum velocity $\bar{U}_M$ is calculated as shown in Refs. 6 and 9 as

$$\bar{U}_M = \left\{0.3586\left[(r/R)_j\right]^{0.885}\ u_m\bar{U}^{\ 0.14}\right\}^{0.88} \tag{17}$$

This equation is presented in Ref. 9 as Eq. 22 with a typographical error in the leading constant (shown as 0.385). From Ref. 6, it is clearly seen that this constant should be 0.52/1.45 = 0.3586 as shown above.

With all of the required input parameters now calculated, the half velocity point can be calculated at the start of the wall jet using Eq. 7. The values for $(z_h)_j$ and $(u_m)_j$ can then be used to obtain values for the wall jet growth function constants which are:

$$C_u = \left(u_m/\overline{U}_M\right)_j \left[(r/R)_j\right]^{1.143} \qquad (18)$$

$$C_z = \left(z_h/R\right)_j \left[(r/R)_j\right]^{-1.028} \qquad (19)$$

The wall jet region is now fully defined for $(r/R) < (r/R)_j$ and requires only that the rotor disk loading and height above ground be specified.

3. Extrapolation in the Transition Region

The transition region is defined in this study to extend from the rotor axis to the starting point of the wall jet. The flow in this region is highly dependent upon the details associated with the rotor's radial induced velocity distribution as well as the presence of the rotorcraft's airframe, propulsive system exhaust plumes, and the induced velocity of any anti-torque devices. Figure 10 from Ref. 10 illustrates the complex streamline patterns beneath the rotor in ground effect. Of particular interest is the clearly defined region of recirculation near unit radius and a probable upwash zone near the center of rotation allowed by the rotor blade root cut-out. The apparent splitting of the streamlines also suggests an annular stagnation line on the ground plane at approximately mid-radius. In spite of this complexity, the developing outward flow of the region must be addressed, as it is of primary interest in any hazard

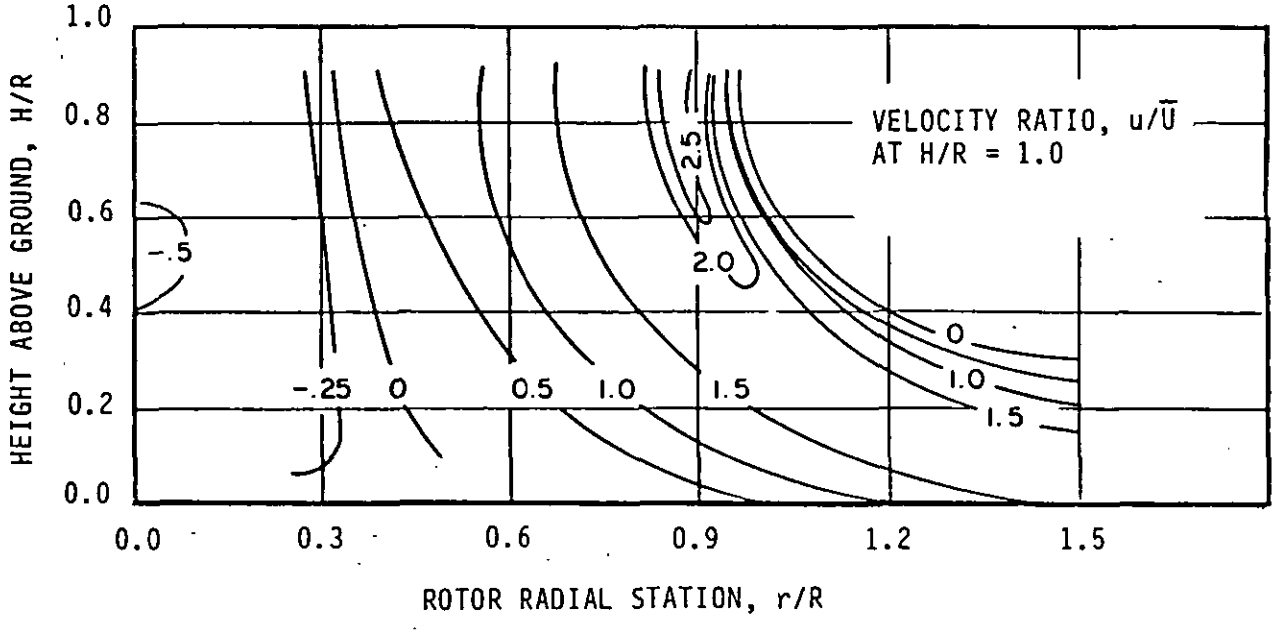

Figure 10. Measured Velocity Below Hovering Rotor in Ground Effect Shows Complexity of Real Flows

analysis. This is especially true in regards to personnel movement close to a rotorcraft.

The mathematical modeling approach has been to extrapolate the starting wall jet profile characteristics back into the transition region as guided by experimental data. The major assumption made is that the impinging rotor flow stagnates on the ground at the ground intersection with the rotor rotational axis. The maximum radial velocity (u_m) is then allowed to grow linearly to $(u_m)_j$ at unit radius, after which it is held constant until the developed wall jet begins

$$u_m = (u_m)_j r \qquad 0 \leq r \leq R \qquad (20)$$

$$u_m = (u_m)_j \qquad R \leq r \leq r_j \qquad (21)$$

The point on the developing profile where the maximum velocity occurs is treated similarly and represents the development of the radial flow's boundary layer such that

$$z_m = (z_m)_j r \qquad 0 \leq r \leq R \qquad (22)$$

$$z_m = (z_m)_j \qquad R \leq r \leq r_j \qquad (23)$$

Any further refinement to this modeling approach would require some detailed knowledge of the ground pressure distribution. In practice, however, this modified approach could be highly configuration dependent.

The profile outer boundary in the transition region is defined at the rotor axis based on the observation that the impinging flow begins to sense the presence of the ground at a rotor height of about H/R = 1.5 (Ref. 4). At this ground effect height, the impinging flow begins to slow and thus spread, initiating the outward transition. This value is therefore taken as the maximum that the outer boundary can assume. If the rotor is at or below the ground effect height, the rotor height itself is used as the limit.

$$z_b(0) = 1.5 \qquad H/R \geq 1.5 \tag{24}$$

$$z_b(0) = H/R \qquad H/R < 1.5 \tag{25}$$

To retain similarity with the fully developed wall jet, the half velocity point of the transition shear layer is taken initially as

$$z_h(0) = z_b(0)/2.8 \tag{26}$$

Then, to transition smoothly to the developed wall jet, a quadratic variation of z_h,

$$z_h(r) = [(z_h(0) - z_j)/r_j^2\ ](r - r_j)^2 + z_j \tag{27}$$

was developed, as based on correlation. The boundary variation can then be calculated as for the developed wall jet from the ratio

$$z_b(r) = 2.8 z_h(r) \tag{28}$$

This completes the analytical description of the transition region. Although necessarily simplified, this representation does simulate adequately the transition region as will be shown in the correlation section of this report. This approach also provides for rapid calculation of the profile characteristics once the starting wall jet is determined.

4. Extension of Theory to the Twin Rotor Interaction Plane

The single rotor induced velocity impingement model described in the previous section has also been used as a building block for the simulation of the twin-rotor configuration. For tandem and side-by-side rotorcraft configurations, the individual slipstreams of the rotors will exhibit both isolated (single rotor) characteristics and effects of interaction along the vertical plane of symmetry between the two rotors. In this interaction plane, the radial flows of each rotor's transition and wall jet

regions collide and form a stagnation line on the ground plane and an upwash deflection zone in which the radial flow turns upward, leaving the ground.

The presence of the rotorcraft airframe will influence the upwash depending upon the height above ground and the airframe orientation. For side-by-side rotorcraft, such as the tilt rotor, the airframe will constrain the formation of the upwash. For the tandem rotorcraft, the airframe is oriented laterally to the interaction plane and offers little resistance to the upwash. The analysis approach used in this effort is developed from Ref. 9 and neglects basically all airframe influences. The approach is therefore conservative in that the predicted deflection zone is not constrained.

The twin rotor analysis is developed by considering the interaction plane to be a thin vertical wall through which no mass flow can pass. As the radial flow from each rotor meets the wall, it is deflected up the wall at the same angle as if the flow continued along the ground. The velocity at any point on the interaction plane is then the same as the isolated radial flow at a total distance equal to the radius along the ground from the rotor axis to the interaction plane, plus the length of the run up to the plane. The geometry of the problem is illustrated in Fig. 11. The resulting vertical profile at a station along the interaction plane will also reflect only the maximum radial velocities of the colliding flows. Near the rotor, this provides a rather flat profile.

Test data cited in Ref. 9 indicates that the velocity along the interaction plane is considerably greater than that of just each rotor by itself; therefore, the individual rotor contributions are somehow additive, providing a higher dynamic pressure than suggested by the concept above. Ref. 9 graphically presents a correction factor which is analytically represented here by

$$T_f = 1.55 - 0.55e^{-1.35(x_{ip}/R)} \qquad (29)$$

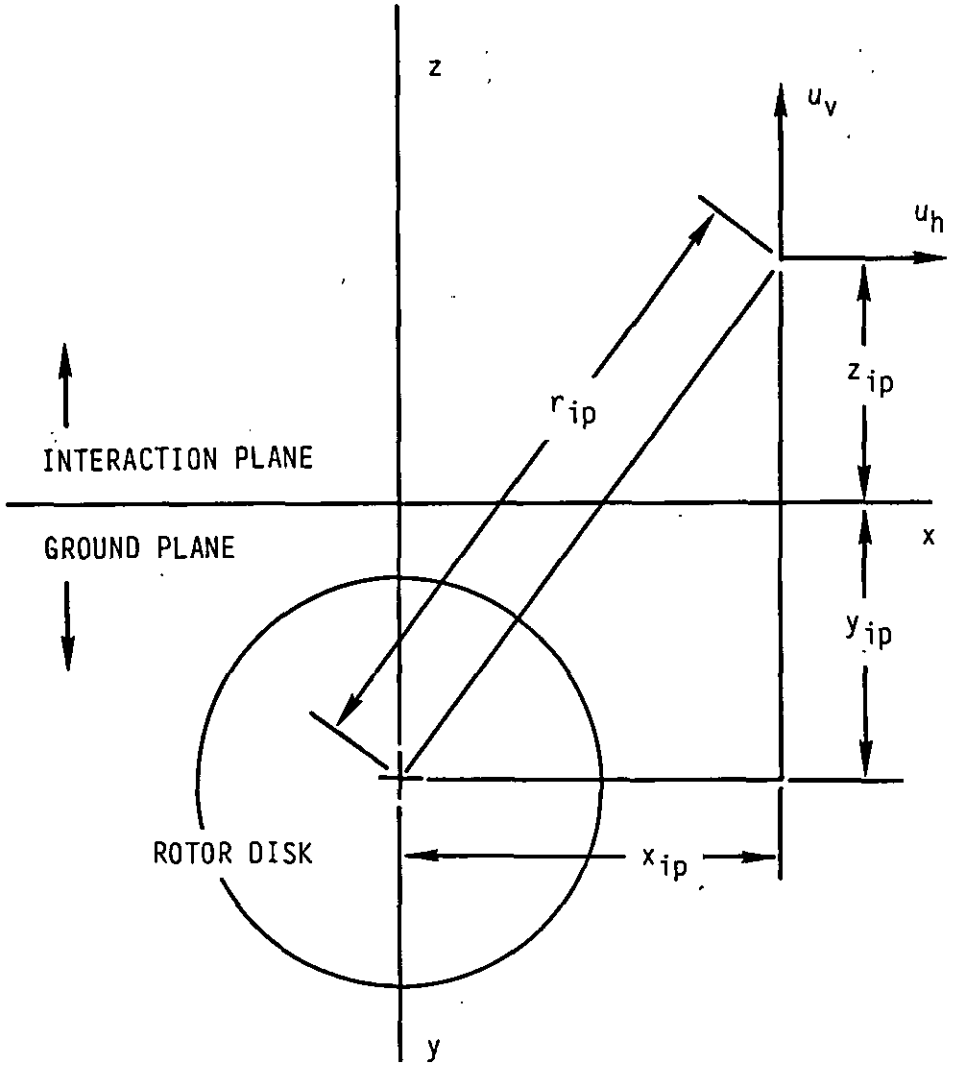

Figure 11. Geometry Description for Simulation of Interaction Plane Upwash Flow

With the correction factor and the geometry as described, the horizontal and vertical velocity components along the interaction plane are

$$u_h = T_f\, u_m(x_{ip}/r_{ip}) \tag{30}$$

$$u_v = T_f\, u_m[(y_{ip} + z_{ip})/r_{ip}] \tag{31}$$

where u_m is the maximum radial velocity calculated for a single rotor at the total distance from the rotor axis r_{ip}.

5. Addition of a Boundary Layer "Foot"

The above procedure results in a full velocity profile all the way to the ground, since the interaction plane velocity profile is built from the maximum wall jet velocity for each equivalent radius. To more realistically model the interaction plane flow, a modification was developed to provide a boundary layer footing to the interaction plane profile. The assumption is made that the foot of the interaction plane profile should be similar in structure to the radial profile boundary layer at the interaction plane's base radius as given by

$$r_{ip} = (x_{ip}^2 + y_{ip}^2)^{1/2} \tag{32}$$

This radius is then used to calculate the parameters of the initial radial profile that becomes the base ($z_{ip} = 0$) of the interaction plane profile. This calculation identifies the base profile's maximum velocity vertical position (z_m). In constructing the interaction plane profile, if $z_{ip} > z_m$, then the procedure described above is used without modification. However, for $z_{ip} < z_m$, a 1/7th power law turbulent boundary layer distribution

$$u_{ip}/u_m = (z_{ip}/z_m)^{1/7} \tag{33}$$

is substituted as for the wall jet source. For this purpose, u_m is understood to be the interaction plane velocity at z_m. This modified velocity

distribution is then resolved as before into horizontal and vertical components.

6. Nonsteady Flow and Peak Velocity Effects

The mathematical models developed in the previous subsections (both single and twin rotor) are, of course, steady and therefore simulate the nominal flow state. Experimental measurements of rotorcraft wall jet flows, and indeed all rotorcraft induced velocity fields, show the real flows to be quite unsteady in nature. The scale of these unsteady flows ranges from the periodicity associated with blade passage to the less predictable formation and dissipation of large-scale secondary flows as evidenced in wall jet data which typically shows substantial peak-to-mean velocity ratios (see flight test data as presented in Section IV). Rigorous methods for direct calculation of these types of unsteady flows as a function of time are next to impossible to derive due to the broad range of parameters which influence the problem (i.e., wind, tail rotor, and engine exhaust secondary flowfields). Therefore, practical solutions to these types of problems must usually be empirically derived.

The mathematical modeling approach that has been developed to account for the peak velocity profile effects, as specifically related to their importance in the hazard analysis, is based totally on an empirical curve fit of flight test data. The data base that has been used includes data for the CH-53E and XV-15 as presented in Refs. 11 and 12. Some data of very limited usefulness was also found in Ref. 13 for the XCH-42 (or HLH) rotor on a test stand. In reducing this flight test data, several data reduction approaches and equation formats were investigated to obtain the most useful curve fit for the ratio of the peak velocity profile to mean velocity profile. The procedure and curve fit format that was ultimately chosen for use with the presented mathematical model was chosen primarily because it best fit the available flight test data (in the time available for data reduction) after the correlation graphs presented in Section IV were evaluated. If more flight test data and data reduction time becomes available in the future, it quite possibly might be demonstratable that

another form of curve fit for calculation of the peak velocity profile is more technically appropriate.

The first step in the data reduction approach (or procedure) involved the tabulation of the velocity at a 3-ft height above the ground along both the mean and peak velocity profiles of the flight test data. A ratio was then calculated by dividing the peak velocity by the mean velocity. The purpose for using the 3-ft height was to help insure that effects due to the varying height of the boundary layer would be minimized in the process of calculating the ratio. Other procedures such as simply ratioing the peak velocities along each of the two profiles clearly yielded data that was much harder to curve fit. After tabulation of the ratio information, the data were plotted as a function of the distance at which they were measured as divided by the rotor radius (X/R). Upon completion of the scatter plot of the data, a simple linear curve fit (with a limit value) was made of the data for both the single main rotor and interaction plane data. The data that was curve fit for the single main rotor cases were taken along the azimuth that included the secondary flows of the tail rotor and engine exhausts so that the data would be for the worst case azimuth. No attempt was made to also make these derived functions a function of rotor height above the ground due to the scatter of the data. The curve fits that were chosen were not chosen on the basis of least squares regression or other techniques but, instead, were chosen to insure that the majority of the experimental data points were below the line formed by plotting the functions. This conservative assumption was thought to be a requirement due to the desire to minimize uncertainty in the hazard analysis, particularly when using the quite unsteady experimentally derived aerodynamic data as part of the analysis.

The functions that were derived using engineering judgment from the process described above are provided in Eqs. 34 and 35 where, for the single main rotor (SR) and twin rotor interaction plane (IP) at the 3-ft height the ratioed peak to mean velocity is:

$$\frac{V_{peak_{SR}}}{V_{mean_{SR}}} = 0.2444\ (X/R) + 1.4 \qquad (34)$$

$$\frac{V_{peak_{IP}}}{V_{mean_{IP}}} = 0.2444\ (X/R) + 0.8 \qquad (35)$$

Both of these ratios are reset to 2.5 if the calculated values from the equations exceed the value 2.5. These functions are also plotted in Fig. 12. The limits to these functions, at X/R break points of 4.5 and 7.0, were also estimated using the available flight data and are required in the analysis to insure that the calculated peak velocity profile does not become unreasonably large in magnitude as the mean velocity profile is reduced with increasing values of X/R. The outputs of Eqs. 34 and 35 at the 3-ft height above the ground are used in the analysis to subsequently calculate a velocity offset constant,

$$\Delta V_{SR} = V_{peak_{SR}} - V_{mean_{SR}} \qquad (36)$$

$$\Delta V_{IP} = V_{peak_{IP}} - V_{mean_{IP}} \qquad (37)$$

This calculated value is then added to each mean velocity which is calculated at each point along the respective mean velocity profile. This last step results in calculation of the desired peak velocity profile for the hazard analysis which has exactly the same shape as the mean velocity profile except for the constant offset in magnitude of the velocity at all points along the profile. Further discussion on this aspect of the mathematical model will be provided in Section IV, along with the discussion on the correlation/validation effort for the mathematical model.

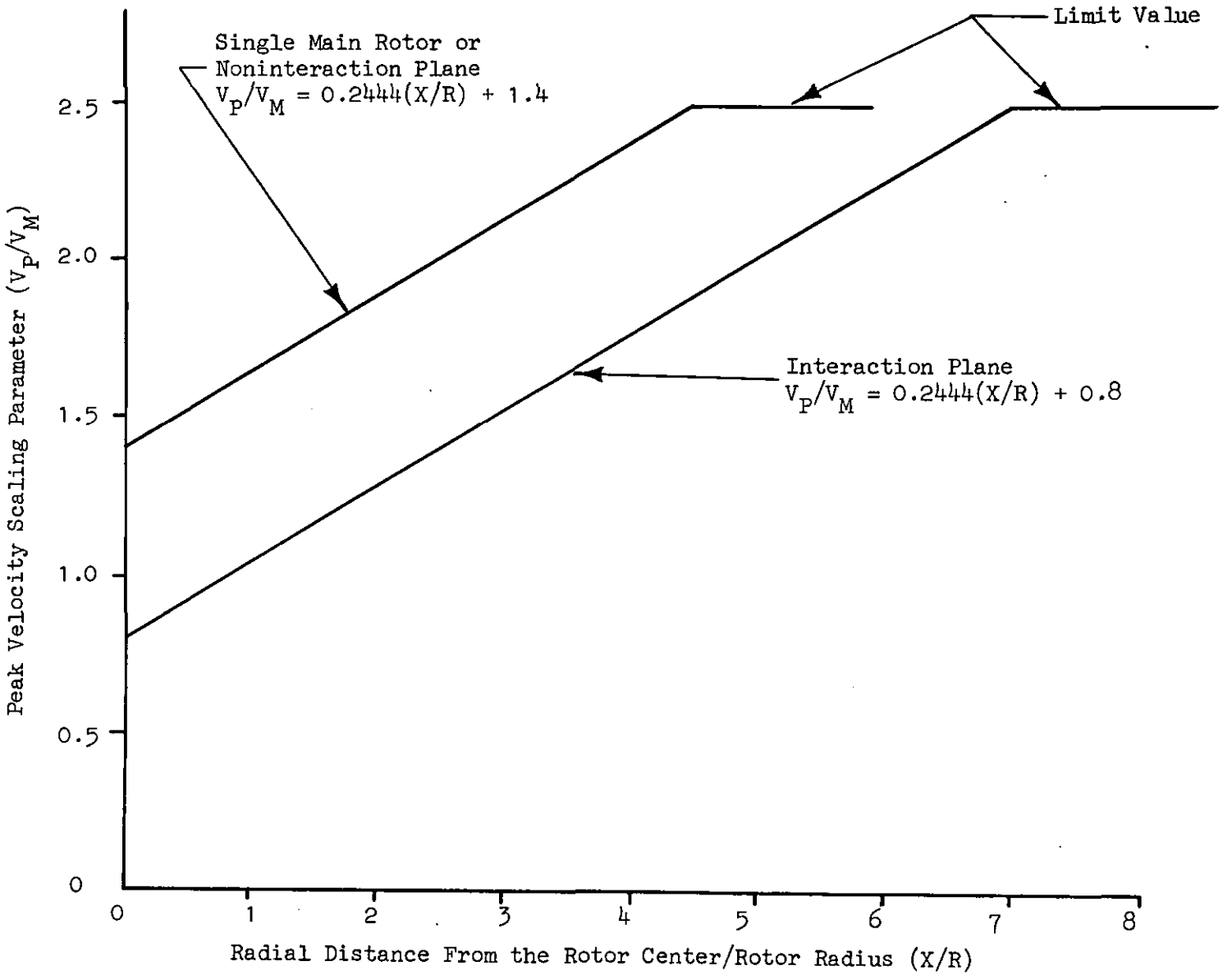

Figure 12. A Graphical Representation of the Empirically Derived Functions Used in Calculation of the Single Rotor and Interaction Plane Peak Velocity Profiles

7. The Effect of Wind on the Wall Jet Velocity Profile

An important step to be taken in bridging the gap between the mathematical models developed in this subsection for the wall jet (for a no-wind hover condition) and the ground vortex (see the next subsection) is the development of a mathematical model for the prediction of the effect of wind on outwash profile velocities. The upper operating limit for use of this mathematical model is approximately 10 kts of wind. Above this value, the model for the ground vortex becomes the more appropriate analysis tool. In developing the model, a review of the data base revealed that only a very limited amount of experimentally derived information was available to assist in development and correlation of the model. Therefore, the mathematical modeling approach chosen is conservative and simple in formulation. The references that provide at least some limited information on the effects of wind include one scale model test (Ref. 14) and three flight test experiments (Refs. 11 through 13, 15, and 16).

When first considering the possible effect of the wind on the outwash profile, one would expect the ambient wind to distort the outwash flow pattern by reducing the magnitude of the velocity profile on the upwind side by the velocity of the wind and increasing the magnitude of the velocity profile on the downwind side by the velocity of the wind. This effect is generally observed to be true as a first approximation. Upon further thought, however, this quick rationalization can be observed to be flawed in that the wind will also require a forward tilting of the rotorcraft tip path plane. This effect should tend to further decrease the profile velocities as measured in the upwind side and increase the profile velocities as measured in the downwind side. As to the actual measurement of the effect, data for an SH-3 in Refs. 15 and 16 indicates that, for prevailing winds in the 2- to 4-kt range, the effect of the wind on a helicopter is additive; in other words, the upwind side profile velocities are reduced by the ambient wind velocity, and the downwind side profile velocities are in turn increased by the same value. While mean velocity profile data on the XV-15 is not presented in Ref. 12, peak velocity profile data is presented which indicates that, along the lateral axis

(non-interaction plane), the effect of wind results in a significant increase in the spread or the pulsating nature of the measured peak velocity profiles on the upwind and downwind sides. It is hard to tell, however, whether the variation in the upwind and downwind velocity profiles may or may not be equivalent to the simple vectorial addition and subtraction of the ambient wind velocity to the profile. It is also noted in the text of Ref. 12 that a limited investigation and measurement of the effect of a 6- to 8-kt wind along the longitudinal axis or interaction plane of the XV-15 seemed to have little effect on the velocity profiles.

The most interesting data related to the effect of wind is provided in Ref. 11. Unfortunately, in this evaluation of the CH-53E, data was measured only on the less hazardous upwind side. The wind velocity during the evaluation varied between 5 and 9 kt, and the data was measured at three rotor heights above the ground (37, 77, and 117 ft). As can be seen in Fig. 13 for the two gross weights of 45000 and 56000 lbs, the reduction in mean and peak wind velocities also seems to be a function of rotor height above the ground. At the very low rotor height of 37 ft, the measured mean velocity is reduced by almost a factor of two times the ambient wind velocity. At the higher rotor height (117 ft), the reduction in mean velocity seems to be approximately equal to the measured ambient wind velocity. Comments reported in Ref. 11 from personnel who were walking through this outwash field strongly support this measured finding, and the recommendation was made that all U.S. Navy and Marine personnel be notified that approaches should always be made to a CH-53E from an upwind position.

Based on the data from these five references, a simple model has been developed in order to include the effects of ambient wind in the mathematical analysis. This model is based on the **conservative assumption** that, for rotor height to radius ratios (H/R) equal to 1.0, the upwind velocity profile is reduced by two times the ambient wind velocity and the downwind side profile is increased by two times the ambient wind velocity. This multiplier is reduced as rotor height is increased so that, at a rotor H/R of 3, the multiplier is reduced to a value of 1. Mathematically, this effect is represented as

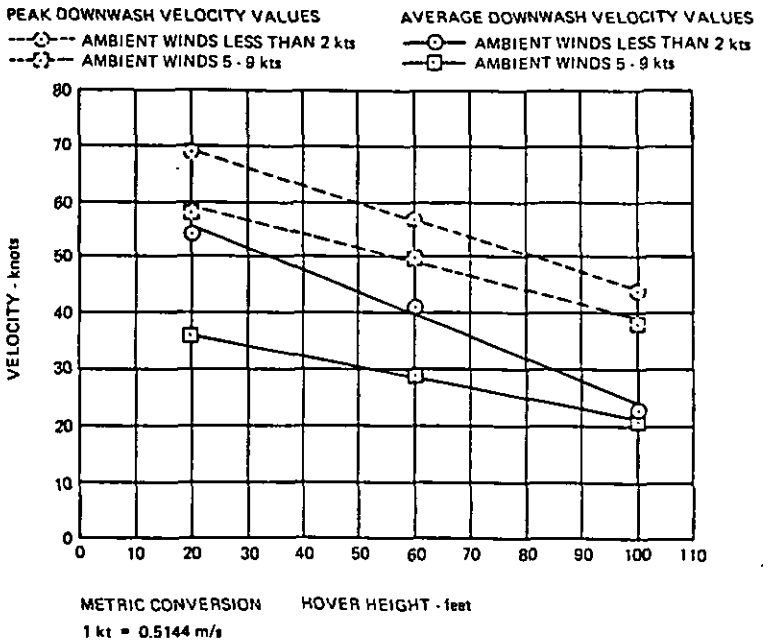

Maximum Downwash Velocities Plotted as a Function of Hover Height during a 45,000 lb (20 412 kg) Gross Weight Hover as Measured at an Ambient Upwind Position during Two Ambient Wind Conditions

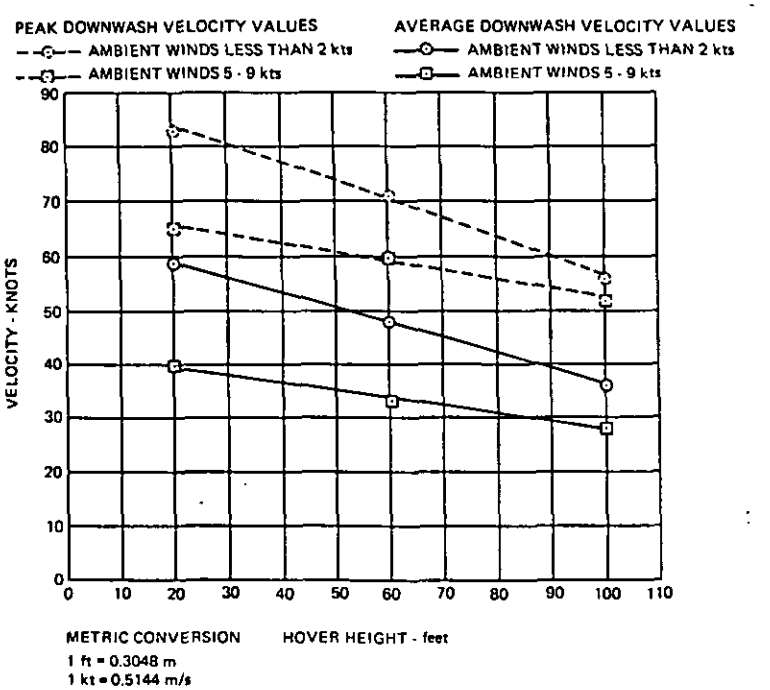

Maximum Downwash Velocities Plotted as a Function of Hover Height during a 56,000 lb (25 402 kg) Gross Weight Hover as Measured at an Ambient Upwind Position during Two Ambient Wind Conditions

(Reproduced From Ref. 11)

Figure 13. CH-53E Downwash Velocities as a Function of Rotor Height Above Ground at Gross Weights of 45000 and 56000 lbs for Winds of up to 9 kt

$$k_{wind} = -0.5(H/R) + 2.5 \qquad (38)$$

where k is limited to never being less than a value of unity.

In summary, while this approach is not extremely well founded in experimental validation, it is nevertheless a reasonably conservative approach to take based on the data for wind velocities of less than 10 kt. For wind velocities of greater than 10 kts, this mathematical correction should, however, not be considered valid. At wind velocities greater than 10 kt, the induced velocity of the rotor starts to become dramatically reduced in magnitude, and the formation of a ground vortex and trailing vortices results in the above described wind correction factor approach becoming technically unrealistic.

B. THE GROUND VORTEX

The second major flowfield element with potential for producing a rotorwash hazard is the ground vortex. This aerodynamic phenomena forms beneath the upwind edge of the rotor disk when operating in ground effect at very low advance ratios. Such a condition can occur, for instance, in very low ambient wind conditions with a rotorcraft that is in hover (i.e., position hold) or to a rotorcraft in low-speed airtaxi.

The vortex formation mechanism is simply conceived by superimposing the wind velocity with the wall jet flow, as schematically shown in Fig. 14. The ground vortex wraps from the upwind position laterally in a smooth arc, finally trailing downwind at either edge of the rotor disk and forming the characteristic horseshoe pattern.

Although the occurrence of the ground vortex is well known, as a subject for study, interest has primarily been focused on its adverse effects on rotorcraft handling characteristics. Experimental data on the vortex itself are **very limited** (almost exclusively flow visualization) and analytical approaches to quantification of the flow field details (most of which are very sophisticated) are only now emerging. Some guiding experimental research in this area has been ongoing at Princeton University. Curtiss (Refs. 17 and 18) has used the Princeton Long Track

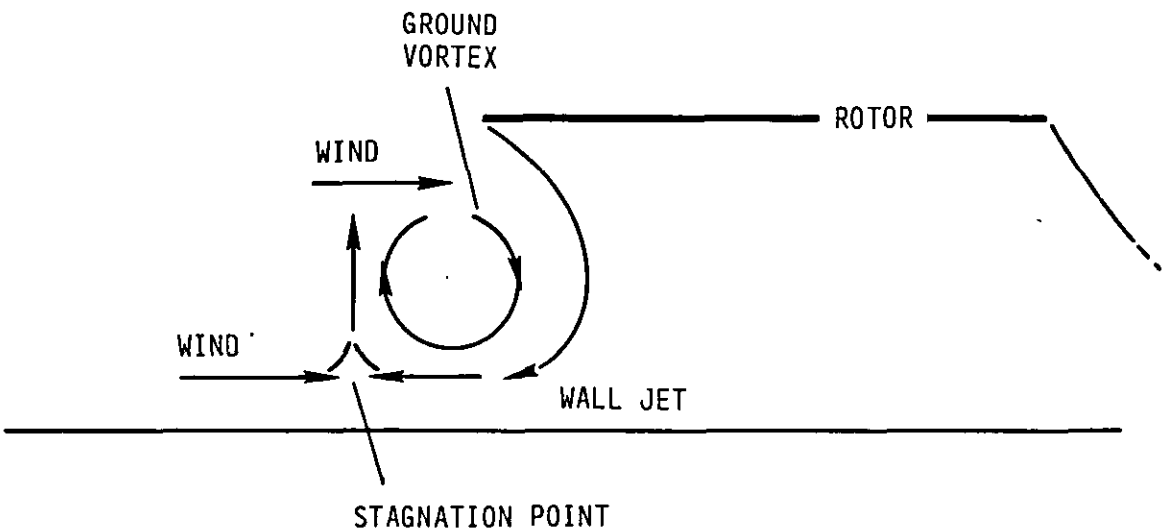

Figure 14. The Ground Vortex Forms When Wind or Translational Speed overcomes the Wall Jet

Facility to experimentally generate the ground vortex with scale model rotors and to measure the vortex's effect on rotor moment characteristics. Sun (Ref. 19), in conjunction with Curtiss, has also recently used the facility to quantify the occurrence and position of the vortex as a function of rotor height above the ground, translational speed, and collective pitch. Although the range of configurations and parameters measured in this experiment are limited, the data do identify several key trends which can be used to aid in the development of a simplified ground vortex hazard model.

Any analytical model developed for simulation of the ground vortex must address as a minimum the prediction of the occurrence of the vortex, its general shape and structure, and the behavior of its position as a function of the rotor operating conditions. Using smoke flow visualization, Sun has been able to map the position of the ground vortex, and he has identified some basic behaviors which are applied here in this study to a simple horse shoe vortex system for hazard prediction purposes.

Experimental data and data trends for aiding in the prediction of the location of the ground vortex position were measured by Sun in terms of the center of recirculation as identified forward of the rotor (upwind) in the longitudinal plane of symmetry. The identified trends show systematic behavior with advance ratio (μ) and rotor thrust coefficient (C_T). When plotting the horizontal position of the vortex $(x_g/R)^{1/2}$ as a function of μ/C_T or constant rotor height above the ground (H/D), straight line characteristics such as

$$(x_g/R)^{1/2} = C_1 + C_2(\mu/C_T) \tag{39}$$

will approximate the data. The constants C_1 and C_2 are functions of H/D. Trends for the constants are developed from the unfaired data of Figs. 4.20(a), (b), and (c) in Ref. 19. With some liberty in setting the lower limits, these trends are

$$C_1 = 1.0 + 1.2086(H/D)^{0.4374} \tag{40}$$

$$C_2 = -0.2786(H/D)^{0.6757} \quad (41)$$

Figure 15 presents these fairings as compared to the actual values chosen from the fairings of Sun's data.

The height above ground of the vortex position was seen to vary approximately linearly with advance ratio. The data available does not show any significant trends for (z_g/R) with H/D [Figs. 4.20(d), (e), and (f) of Ref. 19). The fairing developed for this parameter is

$$(z_g/R) = -10\mu + 0.6 \quad (42)$$

The remaining information now left to be specified in the development of the mathematical model is the H/D and μ ranges in which the ground vortex will occur, as well as the strength of the vortex. Consistent with other investigators, Sun's data shows that the advance ratio at which the recirculating flow leading to the ground vortex begins, and the higher advance ratio where the ground vortex is blown back and disappears beneath the rotor, can be specified as a function of the ratio of the free airspeed to the average flow speed through the rotor. This parameter (μ^*) is defined as

$$\mu^* = V_f/v_i \quad (43)$$

where V_f is the translational speed and, for the low advance ratios of interest, v_i is approximated as the value for hover induced velocity, which is

$$v_i = \Omega R(C_T/2)^{1/2} \quad (44)$$

Figure 16, reproduced from Ref. 19, shows the formation boundaries as a function of H/D and μ^*. This information may be used to estimate the probability of occurrence of the ground vortex state for hazard prediction purposes.

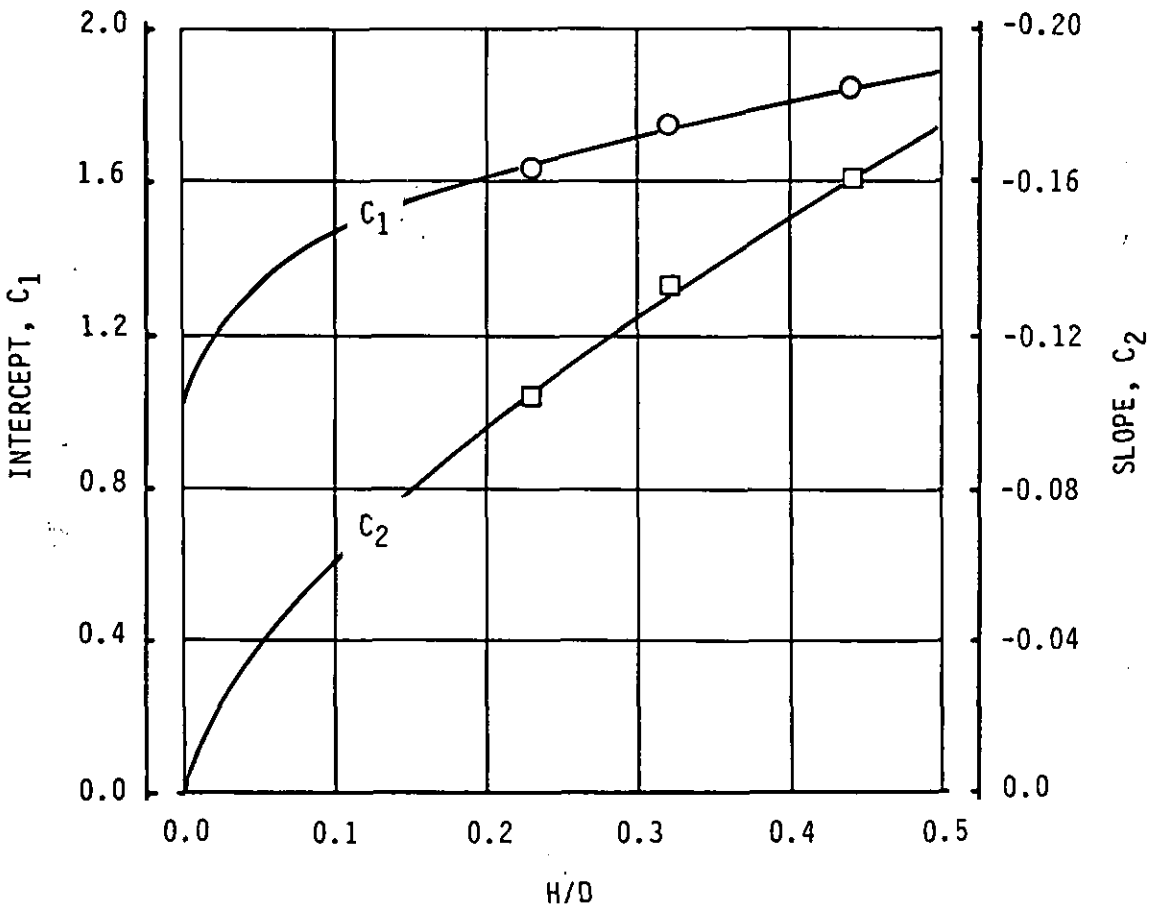

Figure 15. Fairings of Ground Vortex Positional Constants as Derived from Ref. 10

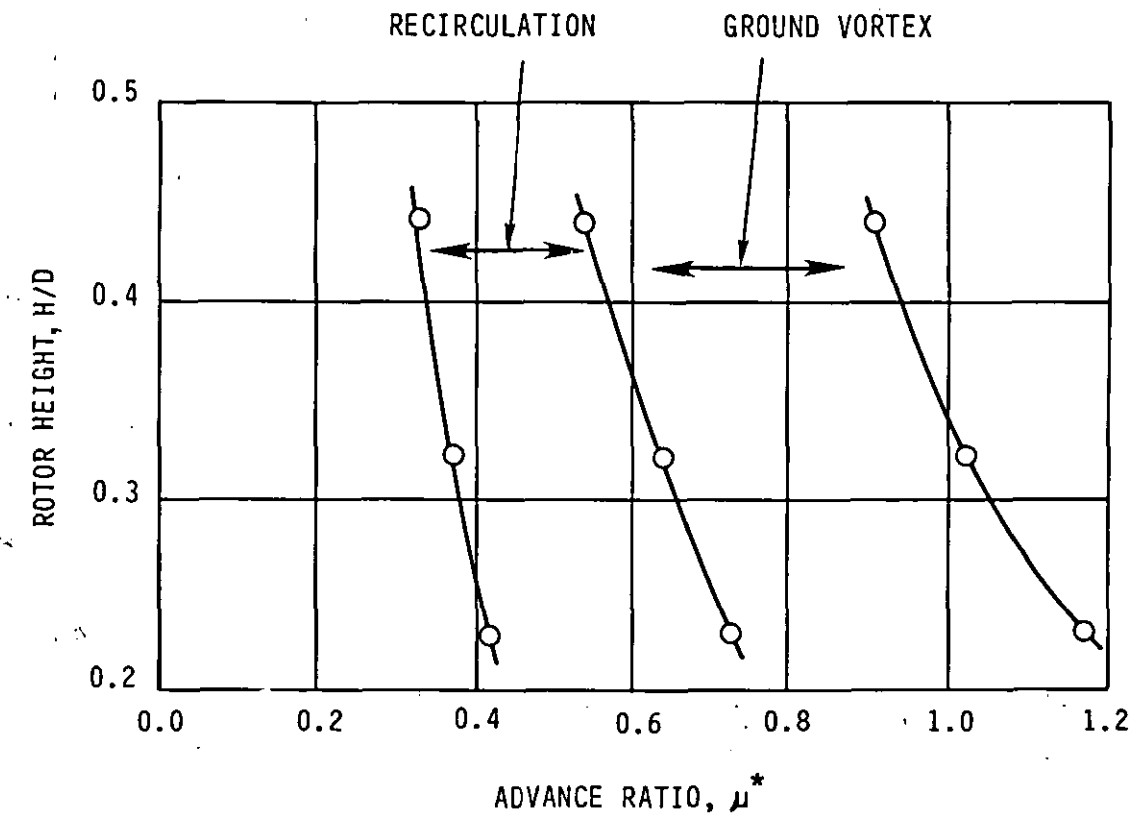

Figure 16. Boundaries for Recirculation and Ground Vortex Flow Regimes (From Ref. 19)

Guidelines to set the strength of the ground vortex are very difficult to establish because systematic experimental measurements of the ground vortex velocity field have not been made from which the strength can be calculated. Sun performed simplified free wake calculations, assuming the ground vortex position from his measurements, and iterating the vortex strength to achieve positional equilibrium. His results, shown in Fig. 17, indicate well behaved trends; however, the calculations are only for one thrust coefficient, and therefore caution must be exercised in extrapolations. To obtain a value for the ground vortex strength (Γ_g), Sun's data must be multiplied by the factor which non-dimensionalizes the data in Fig. 17, which is

$$\Gamma_{tip} = 2\pi\Omega R^2 C_T/B \qquad (45)$$

the tip vortex strength, where B is the number of rotor blades.

Using the above information, though limited in scope, it should be possible to realistically estimate the limiting, or worst case, hazard potential. With the establishment of a reasonably accurate prediction for the occurrence of the ground vortex, the positioning information described above is used to set up the horseshoe vortex geometry as shown in Fig. 18. The right-handed coordinate system is oriented such that the z-axis is positive from the system origin at the ground through the rotor disc at the center of rotation, the x-axis is positive aft (downwind), and the y-axis is positive right. Following an estimate of the vortex strength (Γ_g), the induced velocity field due to the vortex and its image system (needed to enforce the condition of no flow through the ground plane) can be calculated using the Biot-Savart law.

The following implementation of the Biot-Savart law in Cartesian coordinates is used to calculate the contributions of each straight line element of the ground vortex model. An element is considered to run from point "a" to point "b" such that the direction from "a" to "b" is consistent with the right-hand rule in view of the circulation sense. Point "c" is where the velocity is calculated. With the definitions

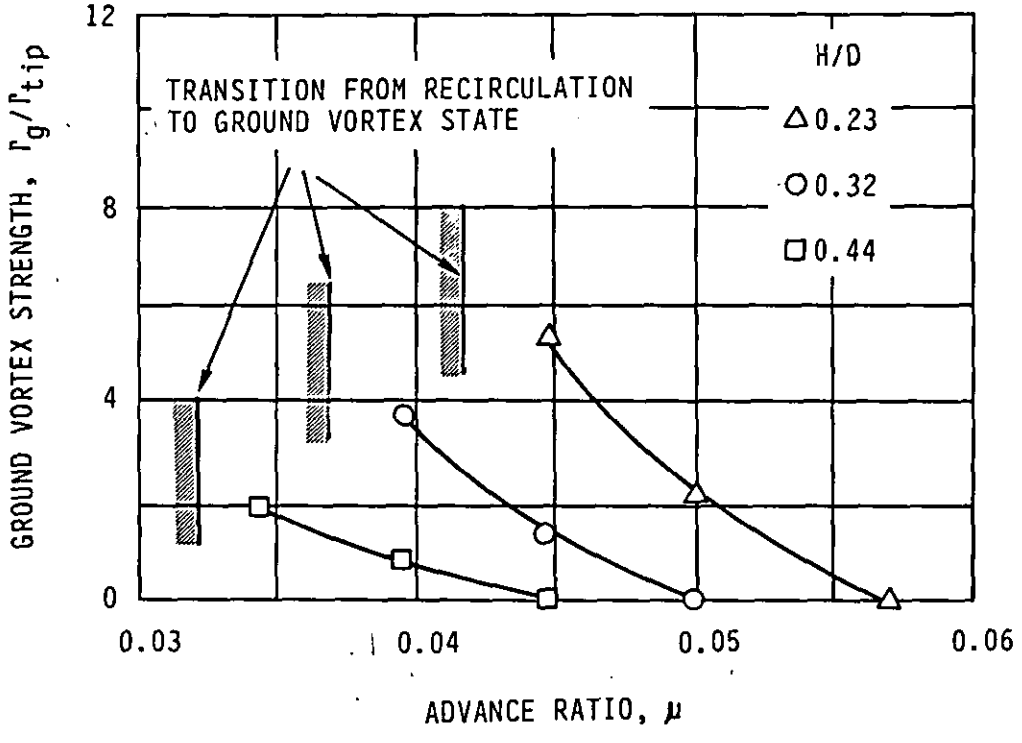

Figure 17. Calculated Ground Vortex Circulation
(From Ref. 19)

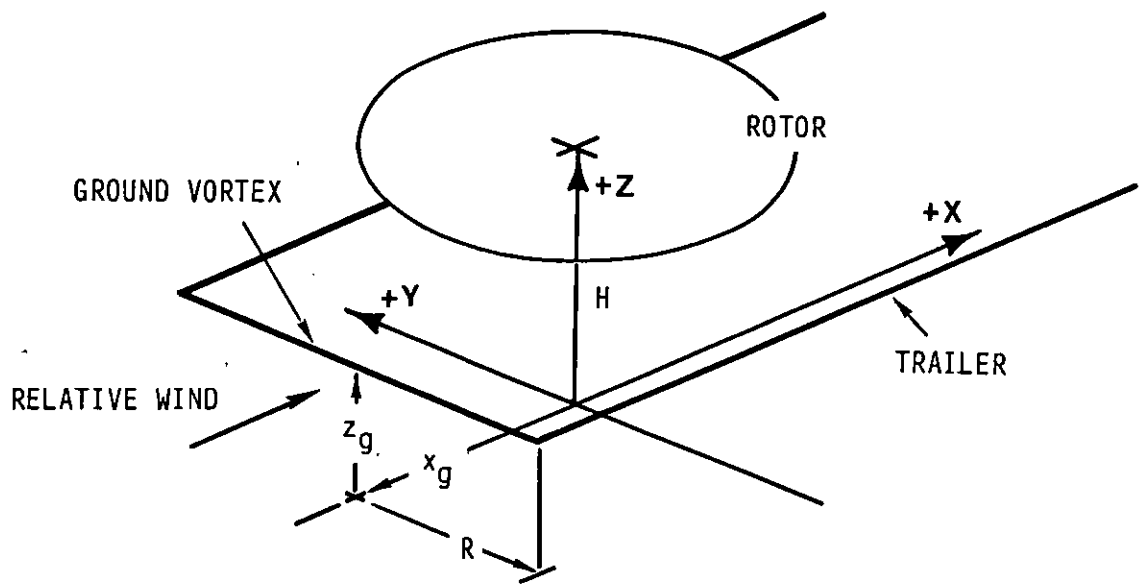

Figure 18. Horse Shoe Vortex Geometry for Calculation of Ground Vortex Hazard Potential

$$A = (x_a - x_c)^2 + (y_a - y_c)^2 + (z_a - z_c)^2 \tag{46}$$

$$B = 2[(x_a - x_b)(x_c - x_a) + (y_a - y_b)(y_c - y_a) + (z_a - z_b)(z_c - z_a)] \tag{47}$$

$$C = (x_a - x_b)^2 + (y_a - y_b)^2 + (z_a - z_b)^2 \tag{48}$$

$$Q = 4AC - B^2 \tag{49}$$

then the magnitude of the velocity induced at point "c" per unit vortex strength is

$$|\bar{q}| = [1/(2\pi Q)][(2C + B)/(A+B+C)^{1/2} - B/A^{1/2}] \tag{50}$$

for $Q \neq 0$. If $Q = 0$, then point "c" is colinear with "a" and "b," and the velocity induced is zero. If the vortex element is semi-infinite in length, as for the trailing element of the horseshoe vortex, from point "a" and passing through point "b", then the velocity magnitude becomes

$$|\bar{q}| = [1/(2\pi Q)](2C^{1/2} - B/A^{1/2}) \tag{51}$$

with the same consideration on the value Q. The total velocity is the product of $|\bar{q}|$ and the vortex strength. The Cartesian vector components of the induced velocity are obtained by multiplying the velocity magnitude by the appropriate direction cosine which, from the defined element geometry, are

$$c_x = (y_c - y_b)z_a + (y_a - y_c)z_b + (y_b - y_a)z_c \tag{52}$$

$$c_y = (z_c - z_b)x_a + (z_a - z_c)x_b + (z_b - z_a)x_c \tag{53}$$

$$c_z = (x_c - x_b)y_a + (x_a - x_c)y_b + (x_b - x_a)y_c \tag{54}$$

This formulation is easily applied to the geometry of the ground vortex system for each straight line element in turn, while summing each element's contribution, to obtain the total vector velocity at the field point of interest. Since the formulation is for a potential vortex, the velocity must be limited for distances approaching the line of action of any of the vortex elements. This can be done by assuming a solid body rotational core for the ground vortex. Without data to estimate the core radius, a value equal to the vortex height above ground is suggested.

In summary, it is recommended that the heretofore described ground vortex model be used only for **estimation** of worst case hazard potential scenarios. Until further experimental data is obtained and a more detailed correlation of results is carried out, detailed results from the presented model must be presumed suspect. Therefore, the model is considered "in development" by the authors.

C. THE FORWARD FLIGHT WAKE

As higher wind or rotor translational speeds become of interest, rotorcraft can be expected to develop the familiar fixed-wing type vortex trailers as a potential hazard. This velocity field can be estimated using a horseshoe vortex system and the Biot-Savart formulation as described in the previous section, but with a simpler geometry system positioned by the location of the rotor disk itself as shown in Fig. 19. The span of the horseshoe is the rotor diameter (2R), and the settling angle of the trailers is based on the approximation that they will initially descend at roughly one-half the mean induced velocity, v_i, through the rotor disk. The descent angle thus accounts for the fact that the velocity field (and thus the wake transport) is less at the edges of the trailed wake than at the wake's mid-span.

If the presented **idealized** geometry is accepted as adequate for estimating the order of magnitude of the velocity field's potential for producing hazards, then the problem reduces to one of relating the strength of the horseshoe vortex system to simple rotorcraft parameters. (For the following approach, the first-level rotor aerodynamic analysis and associated terms can be found in any introductory helicopter

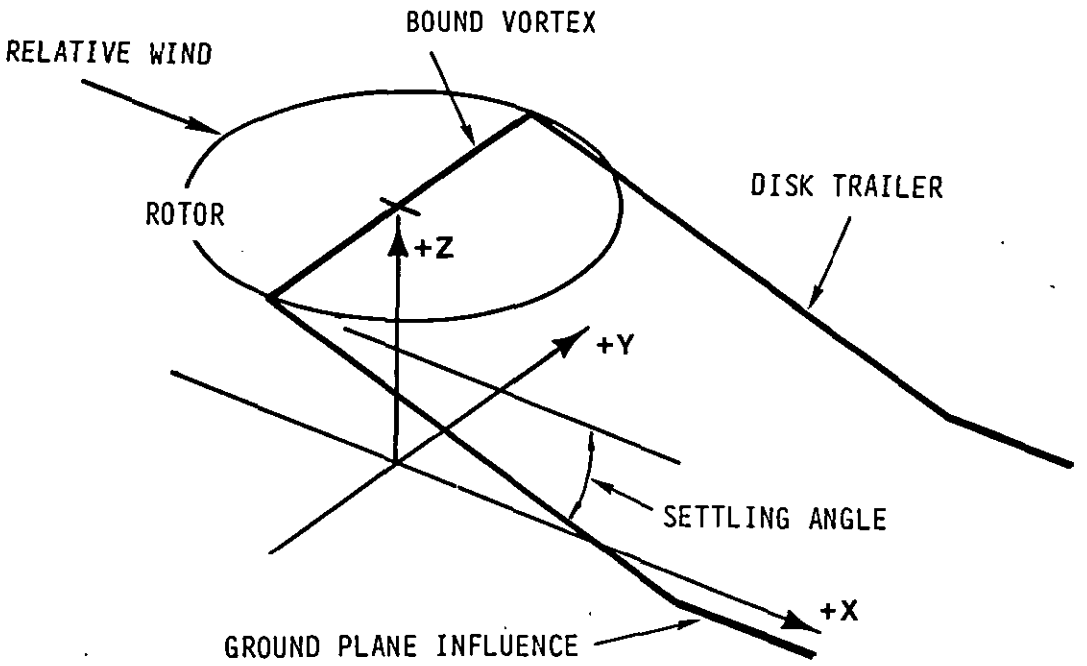

Figure 19. Horse Shoe Vortex Geometry for Calculation of Forward Flight Wake Hazard Potential

aerodynamics text.) Neglecting any rotor tip path plane inclination, the induced velocity is expressed in terms of the dimensionless inflow parameter λ, where

$$\lambda = v_i/\Omega R \tag{55}$$

and the advance ratio μ, which is

$$\mu = V_f/\Omega R \tag{56}$$

where V_f is the translational speed of the rotor (or rotorcraft). The mean value of induced velocity (inflow) through the rotor can be derived from momentum theory to be

$$\lambda = \frac{C_T/2}{(\lambda^2 + \mu^2)^{1/2}} \tag{57}$$

Thus, knowing the thrust coefficient (C_T), the advance ratio (μ), and the inflow ratio (λ); v_i can be calculated from Eq. 57 (where $v_i = \Omega R\lambda$) using successive approximation iteration.

The settling angle of the trailers is then defined from the horizontal and vertical velocities in terms of μ and λ. The trailer angle (χ) measured from the horizontal is then

$$\chi = \frac{[\tan^{-1}(\lambda/\mu)]}{2} \tag{58}$$

Consistent with the horseshoe vortex model, the rotor is now viewed as a simple wing. Considering the strength of the horseshoe vortex to be uniform everywhere along its length, or equivalently assuming the span loading of the wing to be uniform, then the strength (Γ_w) based on gross weight (GW) is

$$\Gamma_w = \frac{GW}{\rho V_f (2R)} \tag{59}$$

Substituting the definition of thrust coefficient, $C_T = T/\rho\pi R^2(\Omega R)^2$, and assuming that rotor thrust is approximately equal to rotorcraft gross weight, the vortex strength is

$$\Gamma_w = \frac{[\pi R(\Omega R)^2 C_T]}{2V_f} \qquad (60)$$

This result is equivalent to requiring the horseshoe vortex system to produce a value of downwash at the center of the rotor disk equal to the mean value over the disk as required by momentum theory.

The induced velocity in the field can now be estimated with the defined geometry and strength using the Biot-Savart law as presented in the previous subsection. As for the ground vortex case, an image system must be included. Other considerations are to provide for turning of the trailers if their descent angle is large enough to cause them to impinge the ground in the near field. Also, for descent angles calculated to be greater than 45 deg, this wake structure will not yet be developed, and care should be exercised in applying the model at very low rotor translational speeds.

Flight test results (see Section IV) demonstrate that the detailed rotor wake structure does organize itself rapidly into two distinct trailers containing the bulk of the system vorticity. A more complete model of this process would need to account for the development history of the trailers, their non-potential radial strength distributions, the development of a viscous core region, and, finally, the rate of decay of the trailers for increasing distances aft of the generating rotorcraft. These refinements are not included in the present exploratory model.

In conclusion, it should be noted that the simplified models for the ground vortex and the disc edge trailing vortices are specifically developed and implemented for use with a single main rotor configuration. Application to dual rotors (either side-by-side or tandem) is possible but highly dependent on the characteristics of the particular configuration. For instance, the degree of rotor overlap and the angle of the translational velocity relative to the plane connecting the dual rotor shafts will influence whether or not the rotors can be treated indepedently, as a single rotor, or whether their trailing wake systems are more complex than the present model is designed to estimate.

SECTION IV

VALIDATION OF THE ROTORCRAFT DOWNWASH FLOWFIELD MODEL

The mathematical models described in the previous section have been validated in this section wherever possible using flight test data for several types of rotorcraft from several sources. In this final report, however, the correlation of flight test data with mathematical models will be presented primarily for only two specific rotorcraft: the Sikorsky CH-53E and the Bell XV-15 Tilt Rotor. These rotorcraft have been chosen for presentation for two reasons: (1) the flight test data for these two rotorcraft are of higher quality than data from all other known sources and (2) there are more data available on these two rotorcraft than are available on any other known specific rotorcraft. Table 2 provides a list of the known-to-be-available sources of flight test data, the type of rotorcraft for which data are available, and a subjective/relative ranking of the quality of the data sources in comparison with each other. This subjective comparison of the data sources is based upon such factors as the type of sensors used to measure the outwash flow field, the methods of data reduction employed, the quantity of data, and the comments from the experimenters as to the quality of the data.

When correlating the mathematical models with flight test data for specific types of rotorcraft, it was discovered that two general guidelines should be followed when evaluating the quality of the correlation. (Mr. D. J. Harris, author of five of the flight test data reports listed in Table 2, was most influential in helping to establish these guidelines.) The most important of these guidelines was that any mathematical modeling changes which were made in the steady flow field modeling approach being used should be made only upon completion of correlation with as broad a data base as possible. This guideline resulted from an acknowledgement by several sources that the obtainment of downwash/outwash flight test data is not, in general, a highly repeatable process due to the unsteady nature of the whole rotorwash flowfield environment. The dynamics of this flow field are extremely susceptible to the effects of

TABLE 2. KNOWN SOURCES OF OUTWASH PROFILE FLIGHT TEST DATA FOR ROTORCRAFT

Rank*	Reference Number	Type of Rotorcraft	General Comment
1	11	Sikorsky CH-53E/ RH-53D	Mean and peak velocity profile data was reduced and presented using statistical methods. Both main rotor thrust and the helicopter position was maintained constant during testing through the use of a load cell and a tether line from the ground to the cargo hook. A large number of test configurations were also evaluated.
2	12	Bell XV-15 (Tilt Rotor)	Mean and peak velocity profile data was reduced and presented using statistical methods. Gross weight was allowed to vary some during testing.
3	15,16,20	Canadair CL-84 (Tilt Wing)	Only mean velocity profile data was reduced and presented using statistical methods.
4	13	HLH Rotor (XCH-62A)	Mean and limited peak velocity profile data was reduced and presented using statistical methods. Rotor was only evaluated at one height above the ground, because evaluation was conducted on a rotor test stand.
5	15,16,21	SH-3	Only mean velocity profile data obtained. Statistical methods not used in data reduction. Velocity sensors incapable of measurement to the same level of accuracy as in Refs. 1-4. Data from Ref. 21, while being of possibly higher quality, was very limited in quantity.
6	22	OH-58A, OH-6A AH-1G, UH-1H UH-1M, CH-47 CH-54	Only mean velocity profile data obtained. Profiles measured don't have expected profile shape and they decay inconsistently with distance. Statistical methods not used in data reduction. Velocity sensors incapable of measurement to same level of accuracy as in Refs. 1-4. Atmospheric conditions unreported. Data taken at different locations.
7	23,24,25	H-13, H-21, H-34, H-37 UH-1A, CH-47 CH-54	Data of very limited usefulness due to the data reduction process used and its age and format of presentation.

*Order of rank is based on a subjective quality comparison.

small changes in the ambient wind, the rotorcraft attitude, and the rotorcraft height above the ground (AGL). The addition of unsteady secondary flows into the rotor outwash flow field due to interaction with the turboshaft engine exhaust and the tail rotor downwash (or sidewash) has also been known to affect the profiles significantly. An example of the difference in magnitude between the statistical mean velocity profiles and the recorded peak velocity profiles (a measure of the unsteady nature of the flow field) for the CH-53E and the XV-15 (interaction plane comparison) at one arbitrarily chosen distance from the center of each rotorcraft's rotor is presented in Fig. 20. These data indicate that a significant difference does exist between the two types of measurement of velocity along the profile. This unsteady effect is also seen in the time histories of outwash velocity at a specific height above the ground as presented in Figs. 21 and 22. In the time histories for the CH-53E, data are shown for heights of 3 and 5 ft AGL. The minimum-to-maximum variation is, for means of 64 and 53 kt, respectively, on the order of 35 to 45 kt. For the XV-15, a 4 sec time history of velocity at 2 ft AGL shows a minimum-to-maximum variation in velocity from 8 to 58 kt with a mean of approximately 26 kt.

A second guideline which was suggested and followed was that no attempt should even be made to directly model and then correlate in detail the formation of the peak velocity profile. This statement does not mean that the modeling of the peak velocity profile is not important to a hazard analysis and the subsequent definition of separation standards; however, it does acknowledge the reality of the extremely complex process by which the peak velocity profile is generated. Therefore, in the hazard analysis, as suggested, this effect was taken into account using empirically derived equations or corrections to the mean velocity profile as was discussed in Section III.

A. CH-53E CORRELATION

Correlation with the CH-53E was conducted using the flight test data presented in Ref. 11. CH-53E specific input data parameters required to

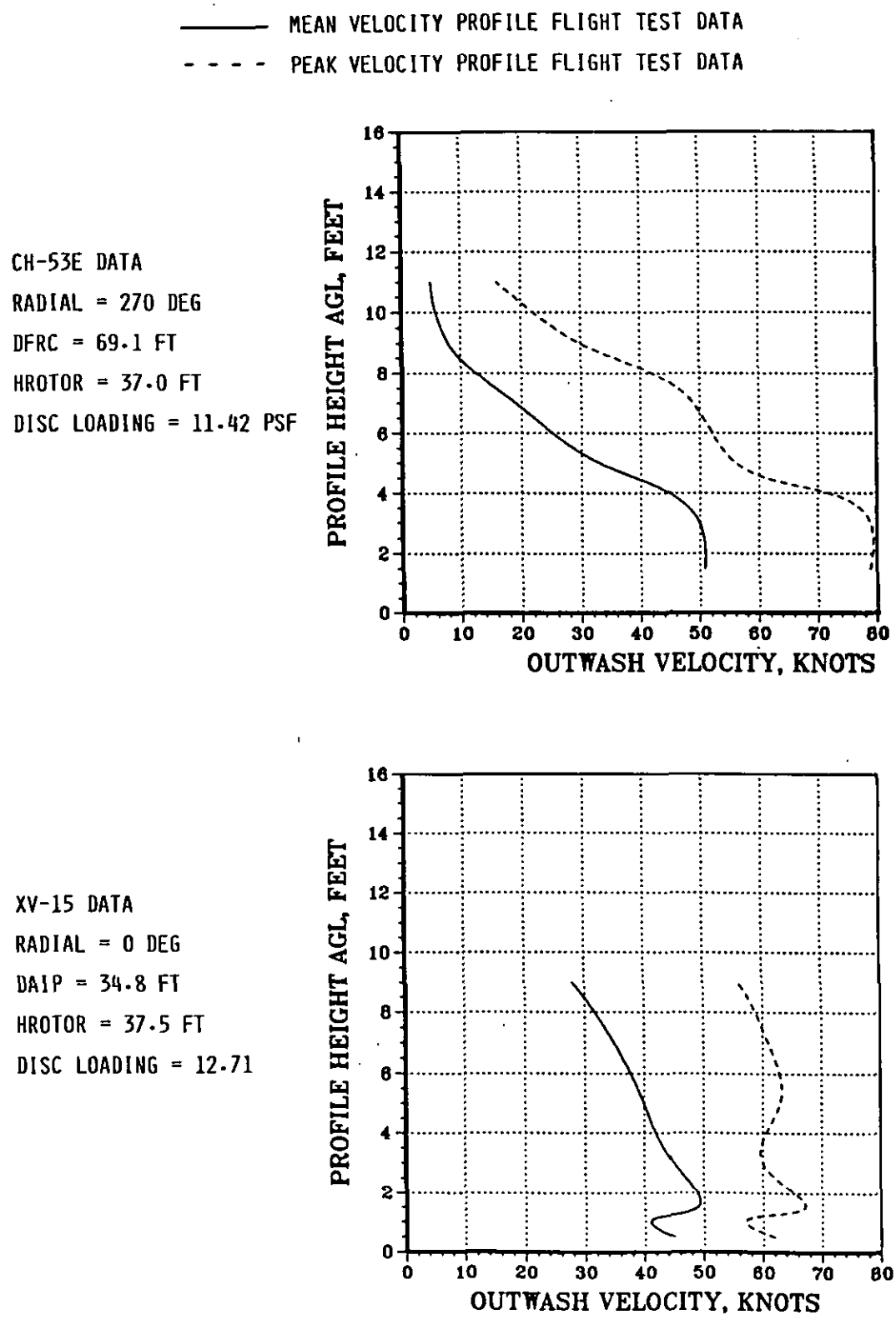

Figure 20. A Comparison of Mean and Peak Velocity Profiles for the CH-53E (Radial Comparison) and the XV-15 (Interaction Plane Comparison)

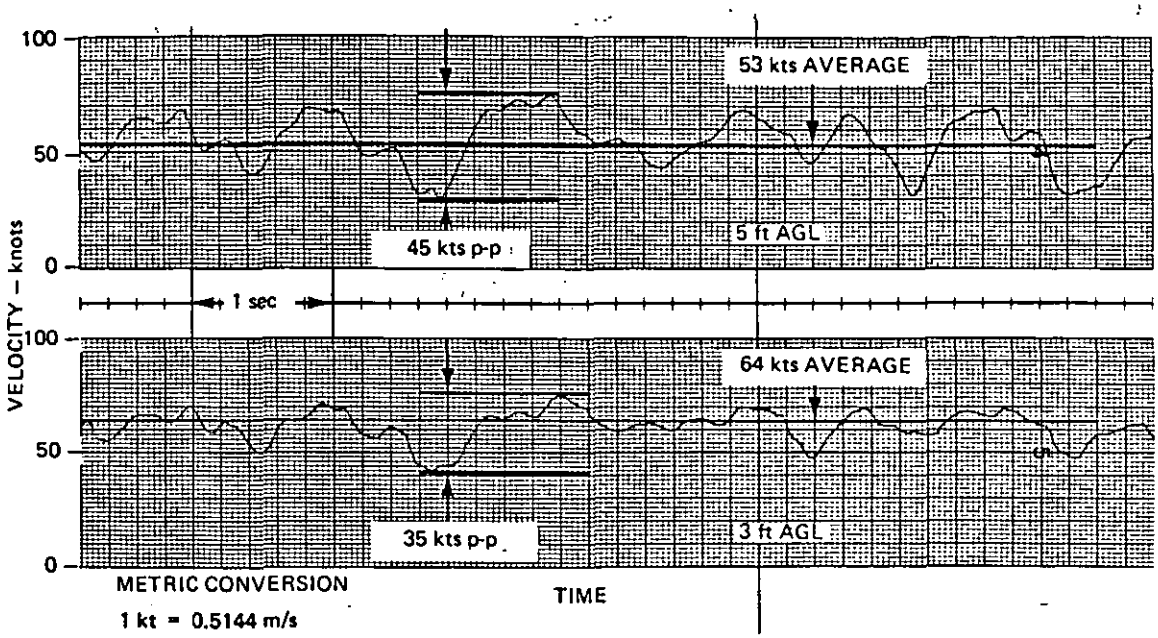

Figure 21. Time Series Strip Charts of the CH-53E Downwash Wind Velocity Magnitude at 59 ft from the Rotor Center While Hovering at a Rotor Height of 37 ft for a Gross Weight of 70000 lbs

(Reproduced From Ref. 11)

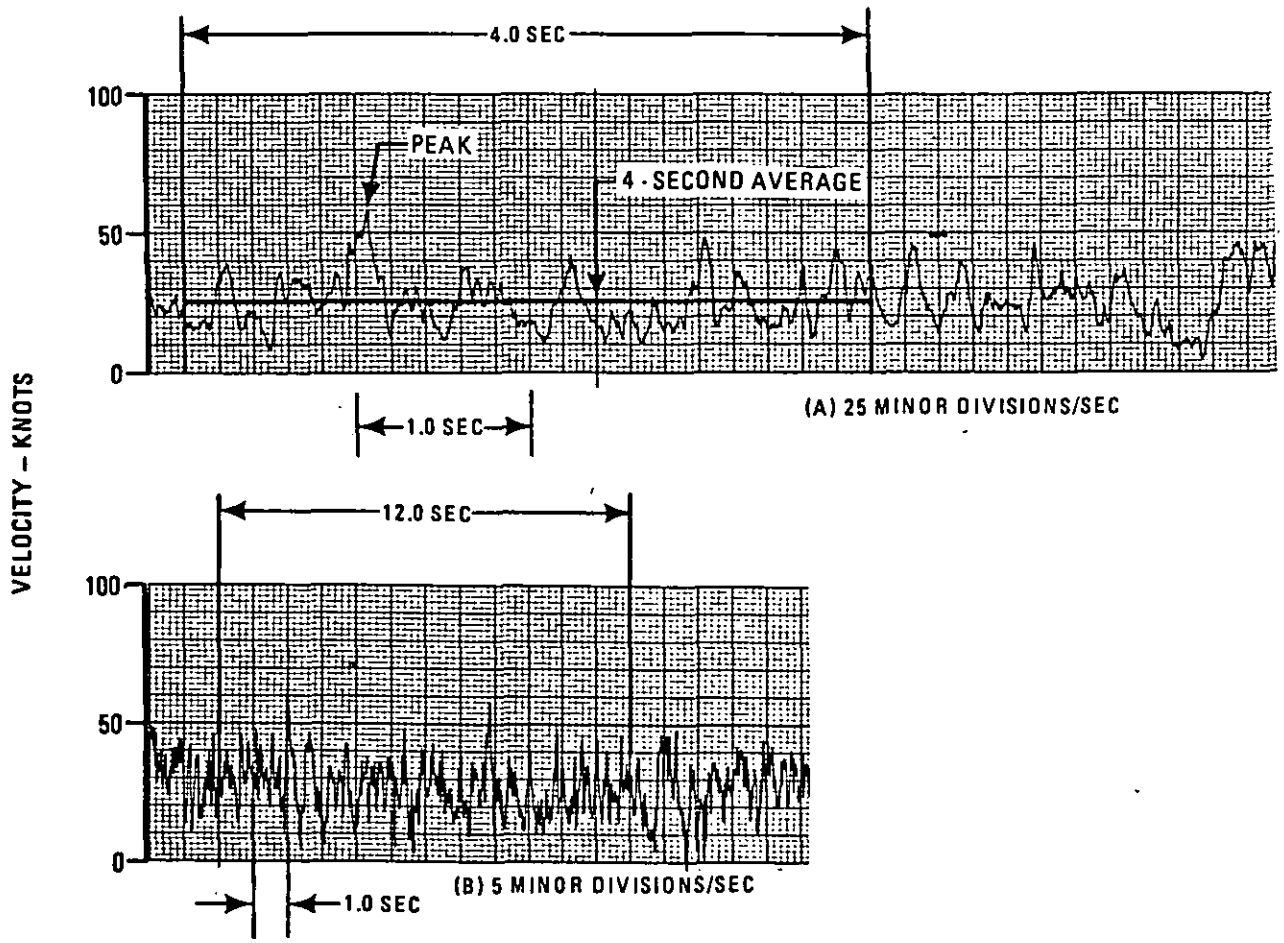

Figure 22. Time Series Strip Charts of the XV-15 Downwash Wind Velocity Magnitudes. Charts A and B Represent Horizontal Velocity Measured at 2 ft AGL and a Relative Bearing of 270 deg While the Aircraft was Hovering at 12 ft AGL (Wheel Height)

(Reproduced From Ref. 12)

execute the **ROTHAZ** analysis program (Appendices B and C) are defined in Table 3. A three-view profile of the CH-53E is presented in Fig. 23. The flight test data presented in Ref. 11 were obtained for what was considered to be the worst case azimuth of the CH-53E. This azimuth was the 270 deg radial (to the pilot's left). The eight stations at which data were measured along this radial are shown in Fig. 24. Winds during the testing were below 3 kt. It is important to note from the three-view profile that the downwash from the canted tail rotor and two of the three engine exhausts must be considered as highly influential secondary flows when profile measurements are made along the 270-deg radial position. The variations in CH-53E gross weight and rotor height above the ground which were evaluated were 45000, 56000, and 70000 lbs and 37, 77, and 117 ft, respectively. This test matrix is presented in a more comprehensive format in Table 4, along with the corresponding figure number for the flight test data comparison with the calculated **ROTHAZ** analysis output.

Correlation of flight test and calculated data for the 70000 lb maximum gross weight configuration is presented in Figs. 25 through 27 at rotor heights above the ground of 37, 77, and 117 ft, respectively. Data presented in these figures generally indicate that the calculated mean velocity profile is slightly less in magnitude than the measured flight test velocity profile at all three rotor heights. However, the empirical equation that was developed to estimate the peak velocity profile generally results in the calculated velocity profile being very close or slightly greater in magnitude than the flight test data. It should be noted that the radial stations of poorest correlation, i.e., the overprediction of velocity at a rotor height of 37 ft, are generally inside, or almost inside, the radius of the rotor. Particularly accurate prediction of the velocity profile in this transition region is probably not possible with this mathematical modeling approach which assumes a fixed profile shape due to the aforementioned impracticality of modeling the influences of engine exhaust, tail rotor downwash, nonlinear induced velocity distribution across the rotor disk, as well as some loss of mass flow due to recirculation of some percentage of the downwash velocity back up through the center of the main rotor (see transition region discussed in

TABLE 3. PROGRAM **ROTHAZ** INPUT DATA REQUIREMENTS

Rotorcraft Descriptive Parameters	CH-53E	XV-15
Number of Rotors	1	2
Distance Between the Twin Rotors (ft)	--	32.2
Rotor Radius (ft)	39.5	12.5
Gross Weight (lb)	70000.0 (MAX)	13100.0 (MAX)
Download Factor (Percent of Gross Weight)	5.0	13.0

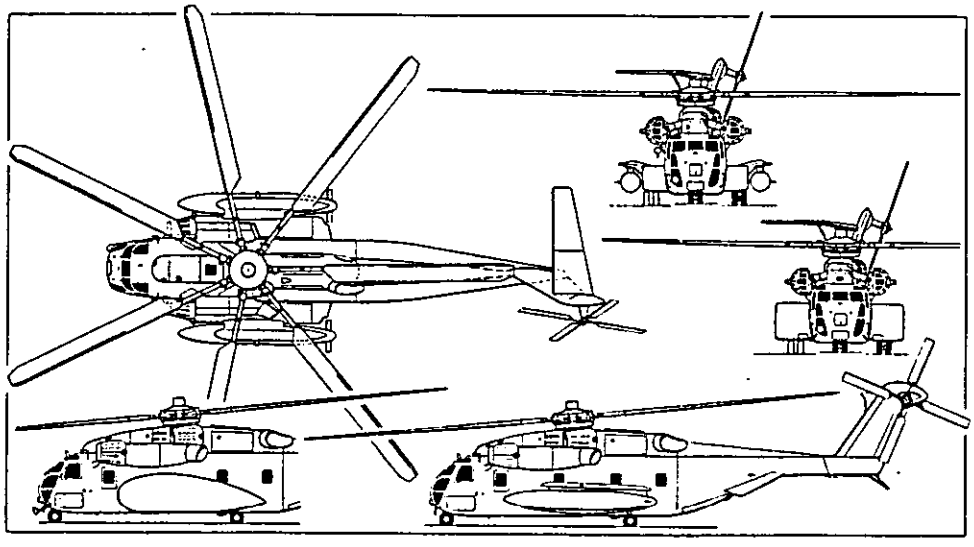

Figure 23. Sikorsky CH-53E Super Stallion, with Scrap View of Forward Fuselage and Lower Front View of MH-53E

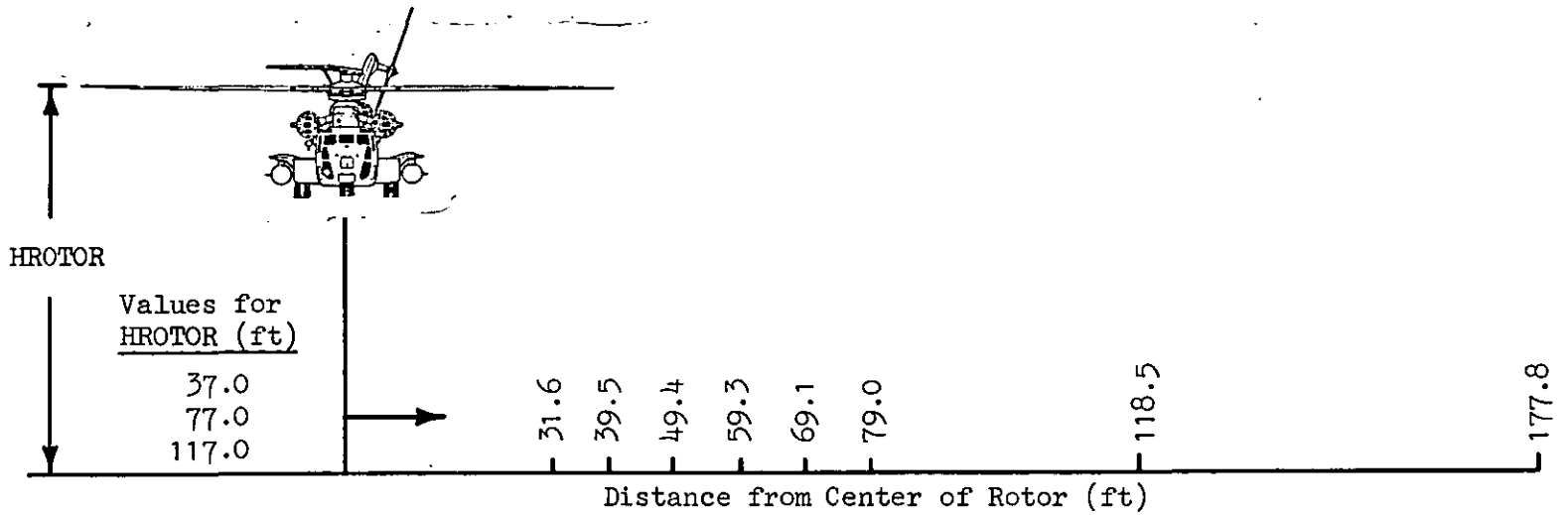

Figure 24. CH-53E Flight Test Velocity Profile Measurement Stations

TABLE 4. EVALUATION MATRIX FOR CH-53E FLIGHT TEST/MATHEMATICAL MODEL DATA CORRELATION

Figure Number	Gross Weight, lb	Disc Loading, PSF	Rotor Height, ft	Distance From Rotor Center (DFRC), ft
25,B1	70000.0	14.28	37.0	31.6,39.5,49.4,59.3,69.1,79.0,118.5,177.8
26,B2	70000.0	14.28	77.0	31.6,39.5,49.4,59.3,69.1,79.0,118.5,177.8
27,B3	70000.0	14.28	117.0	31.6,39.5,49.4,59.3,69.1,79.0,118.5,177.8
28	56000.0	11.42	37.0	59.3 118.5
B4	56000.0	11.42	37.0	31.6,39.5,49.4,59.3,69.1,79.0,118.5,177.8
29	56000.0	11.42	77.0	59.3 118.5
B5	56000.0	11.42	77.0	31.6,39.5,49.4,59.3,69.1,79.0,118.5,177.8
30	56000.0	11.42	117.0	59.3 118.5
B6	56000.0	11.42	117.0	31.6,39.5,49.4,59.3,69.1,79.0,118.5,177.8
31	45000.0	9.18	37.0	59.3 118.5
B7	45000.0	9.18	37.0	31.6,39.5,49.4,59.3,69.1,79.0,118.5,177.8
32	45000.0	9.18	77.0	59.3 118.5
B8	45000.0	9.18	77.0	31.6,39.5,49.4,59.3,69.1,79.0,118.5,177.8
33	45000.0	9.18	117.0	59.3 118.5
B9	45000.0	9.18	117.0	31.6,39.5,49.4,59.3,69.1,79.0,118.5,177.8

NOTE: All data comparisons are for mean velocity profile data measured/computed along the 270-deg azimuth radial (left side of helicopter from pilot's seat)

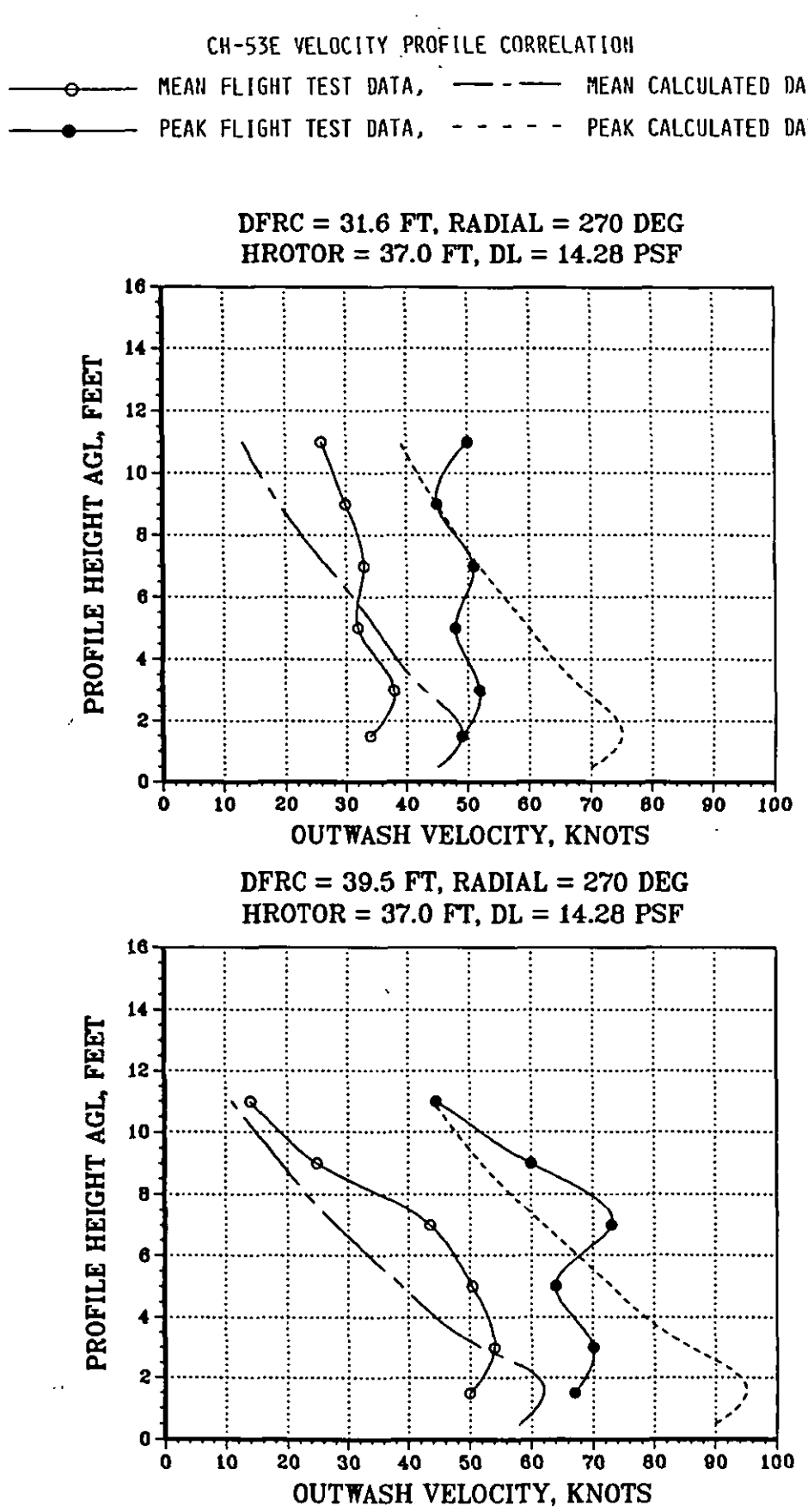

Figure 25. CH-53E Mean and Peak Velocity Profile Correlation for Eight 270-deg Azimuth Radial Stations at a Rotor Height of 37 ft and a Gross Weight of 70000 lbs

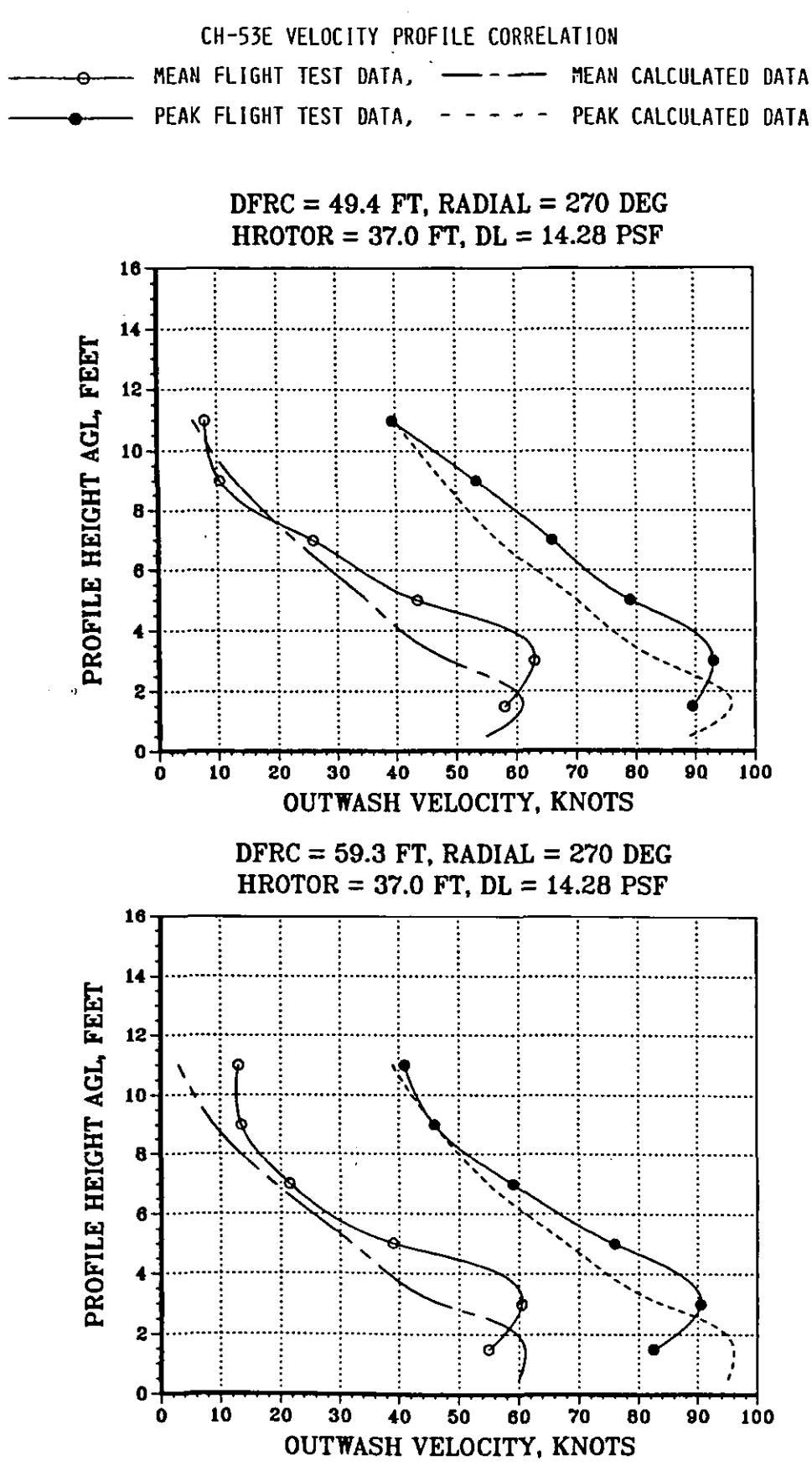

Figure 25 (Continued)

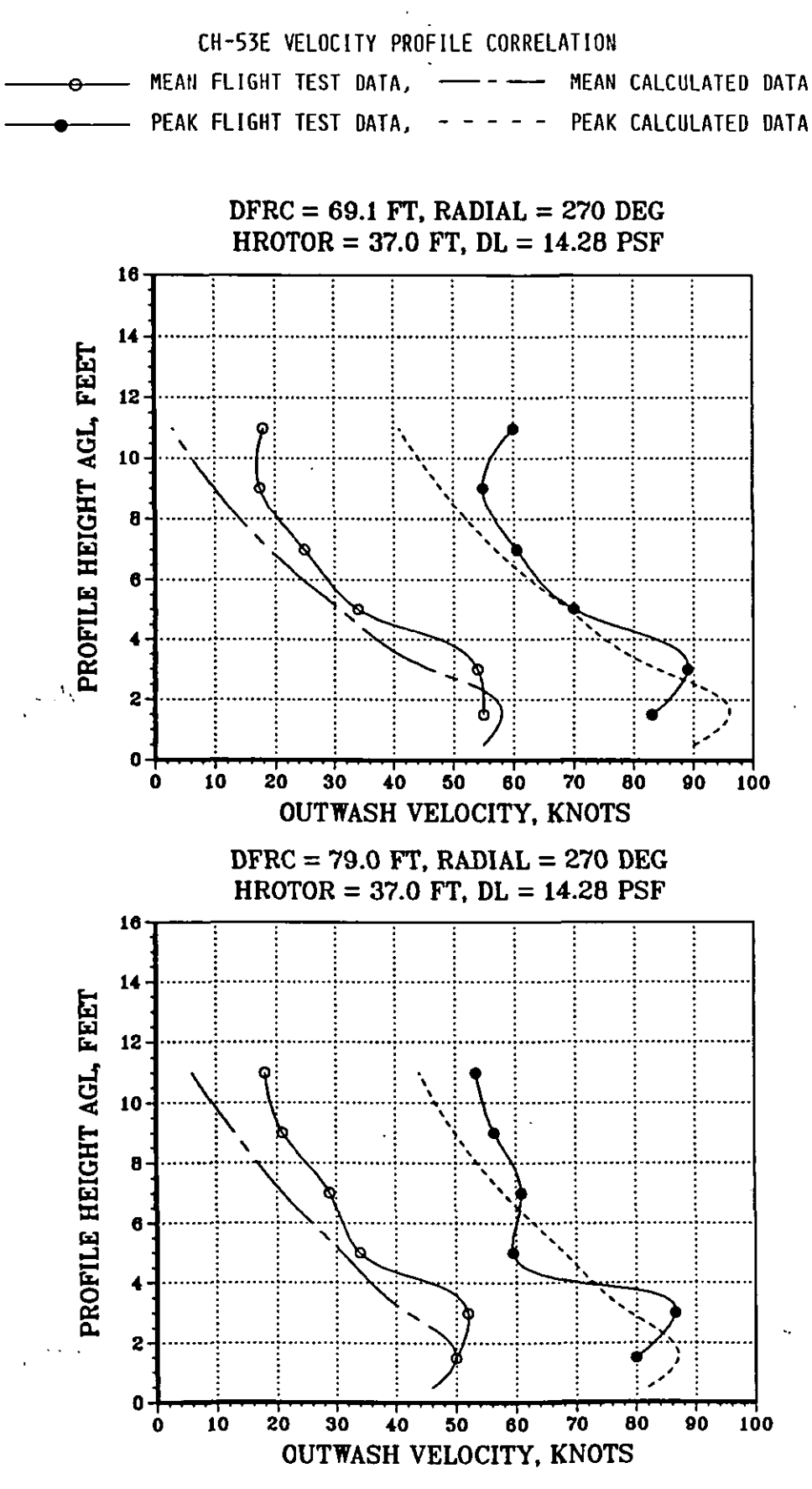

Figure 25 (Continued)

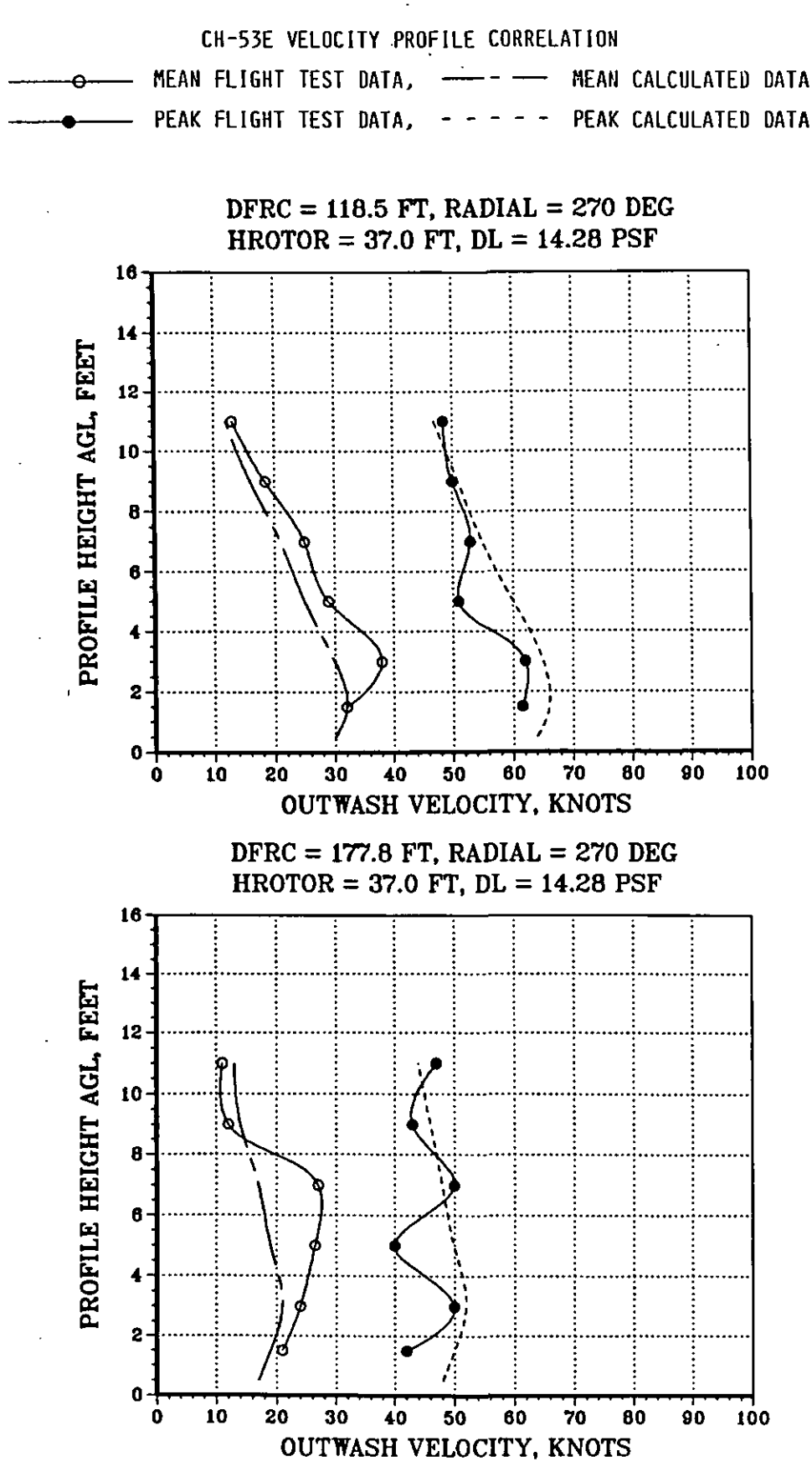

Figure 25 (Concluded)

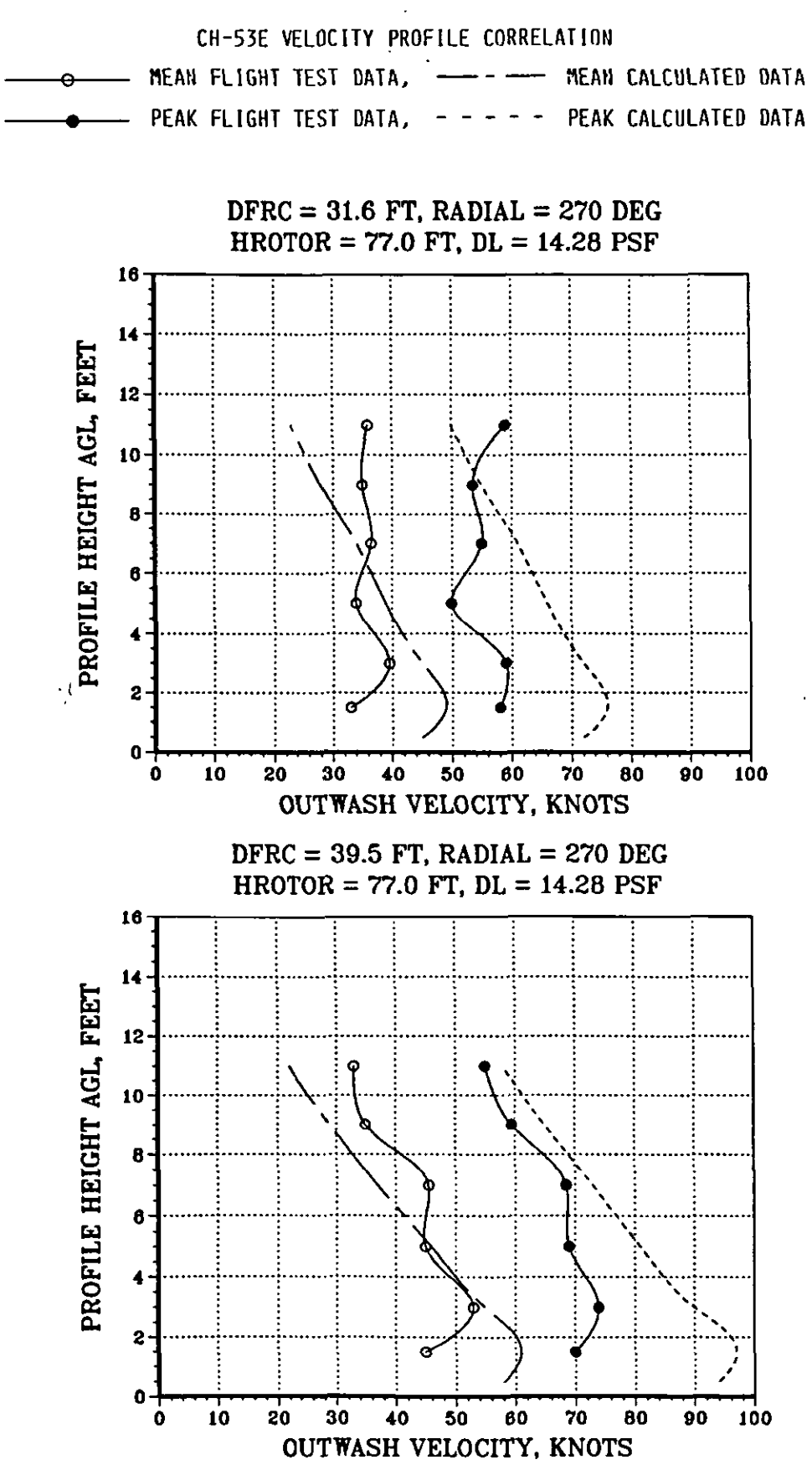

Figure 26. CH-53E Mean and Peak Velocity Profile Correlation for Eight 270-deg Azimuth Radial Stations at a Rotor Height of 77 ft and a Gross Weight of 70000 lbs

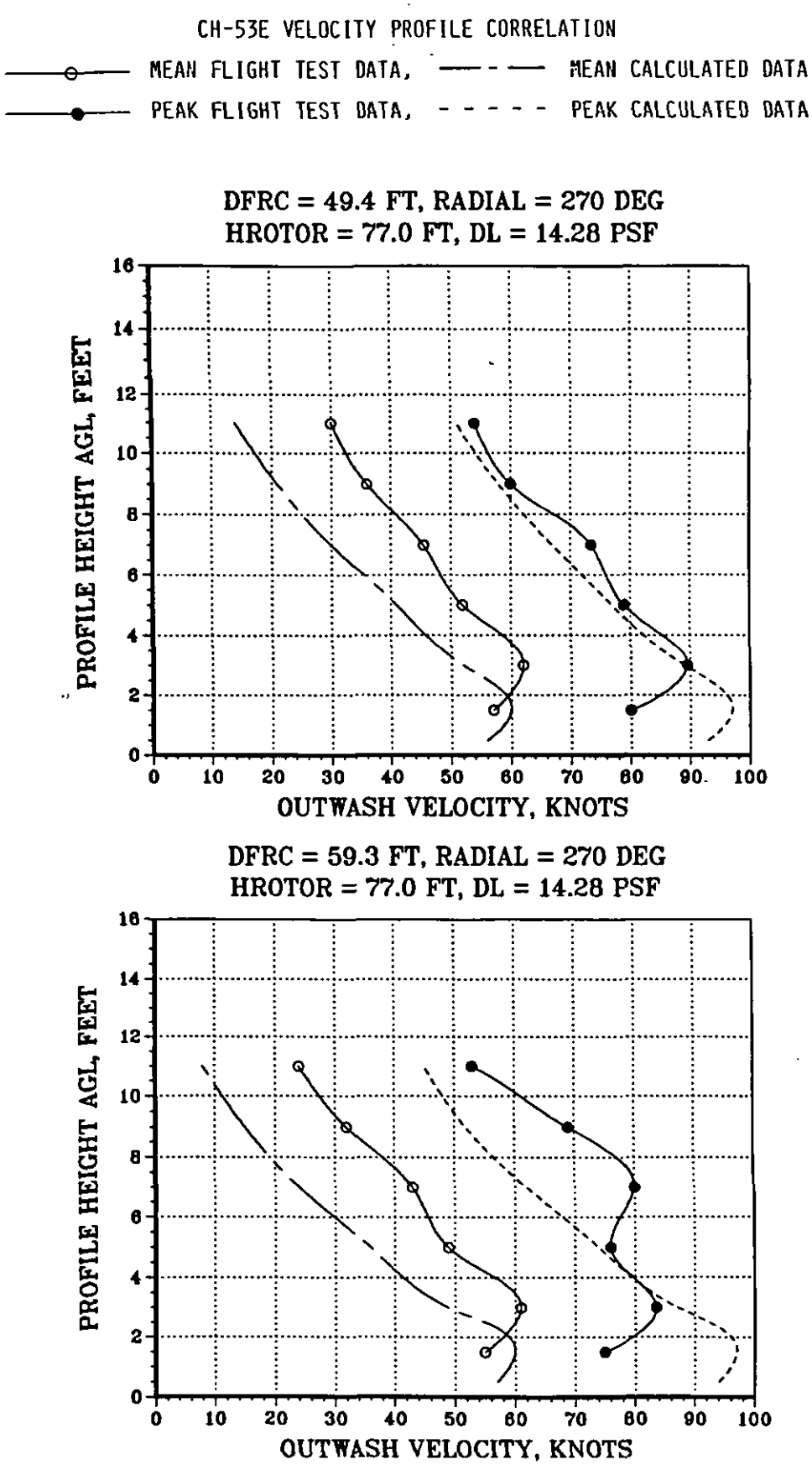

Figure 26 (Continued)

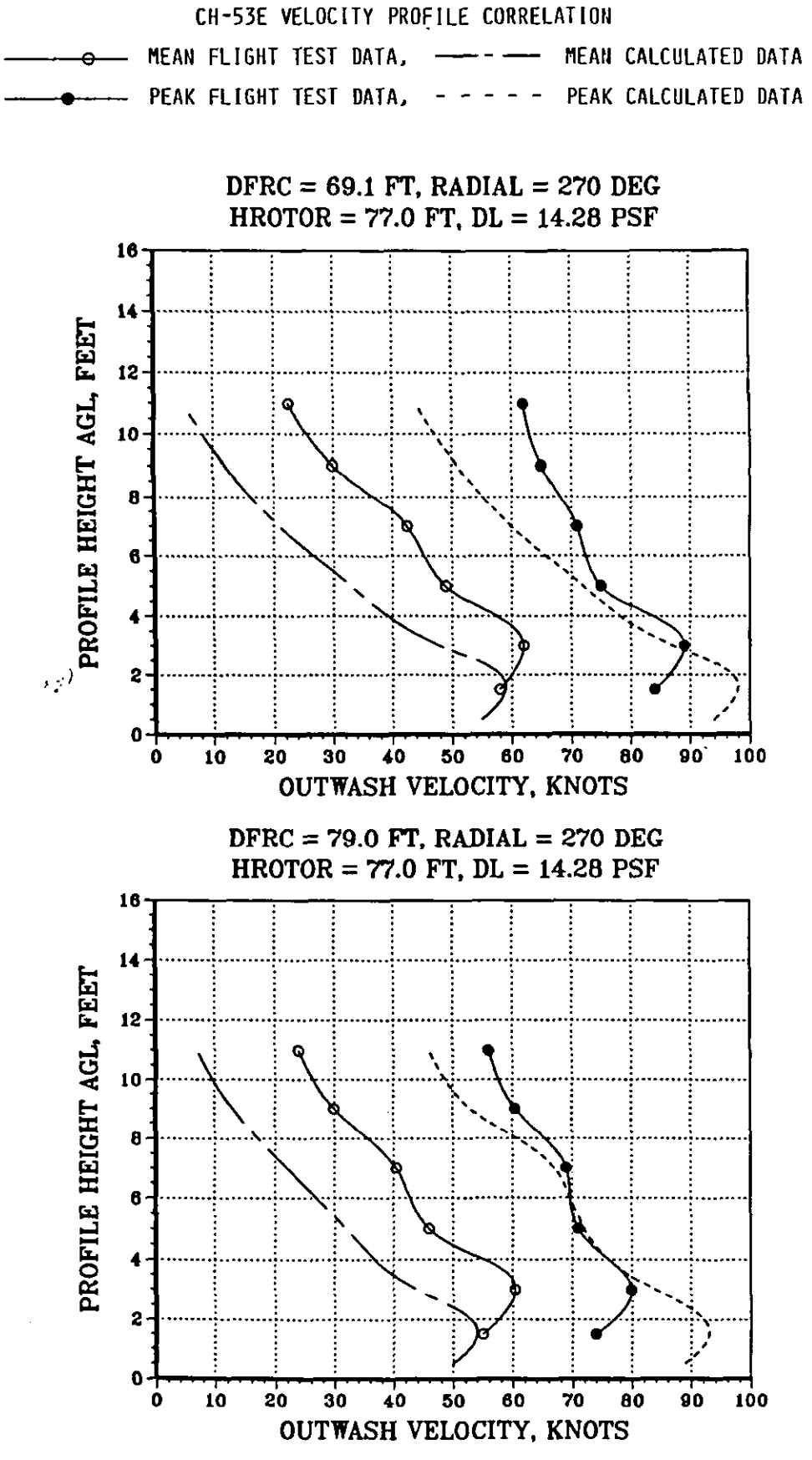

Figure 26 (Continued)

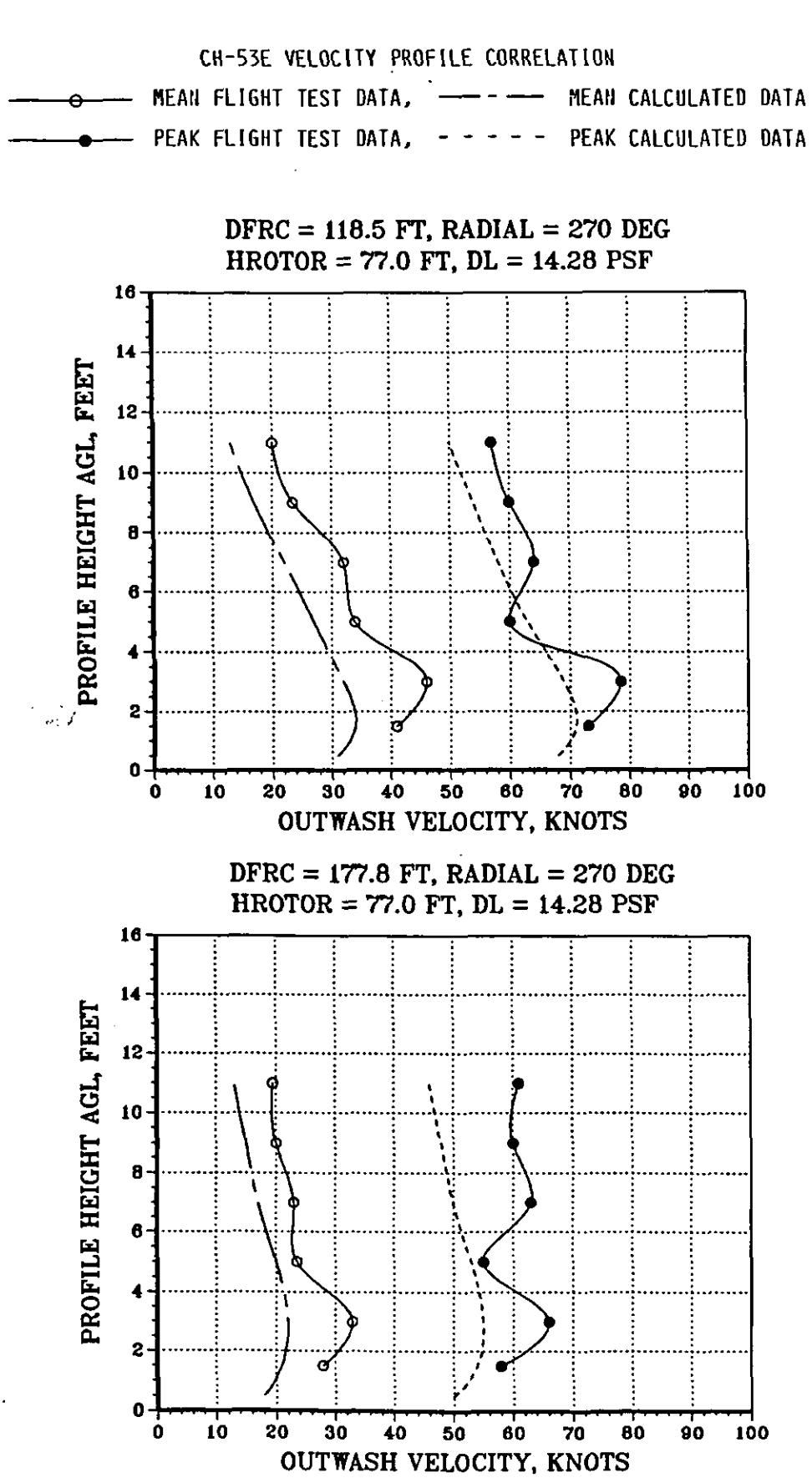

Figure 26 (Concluded)

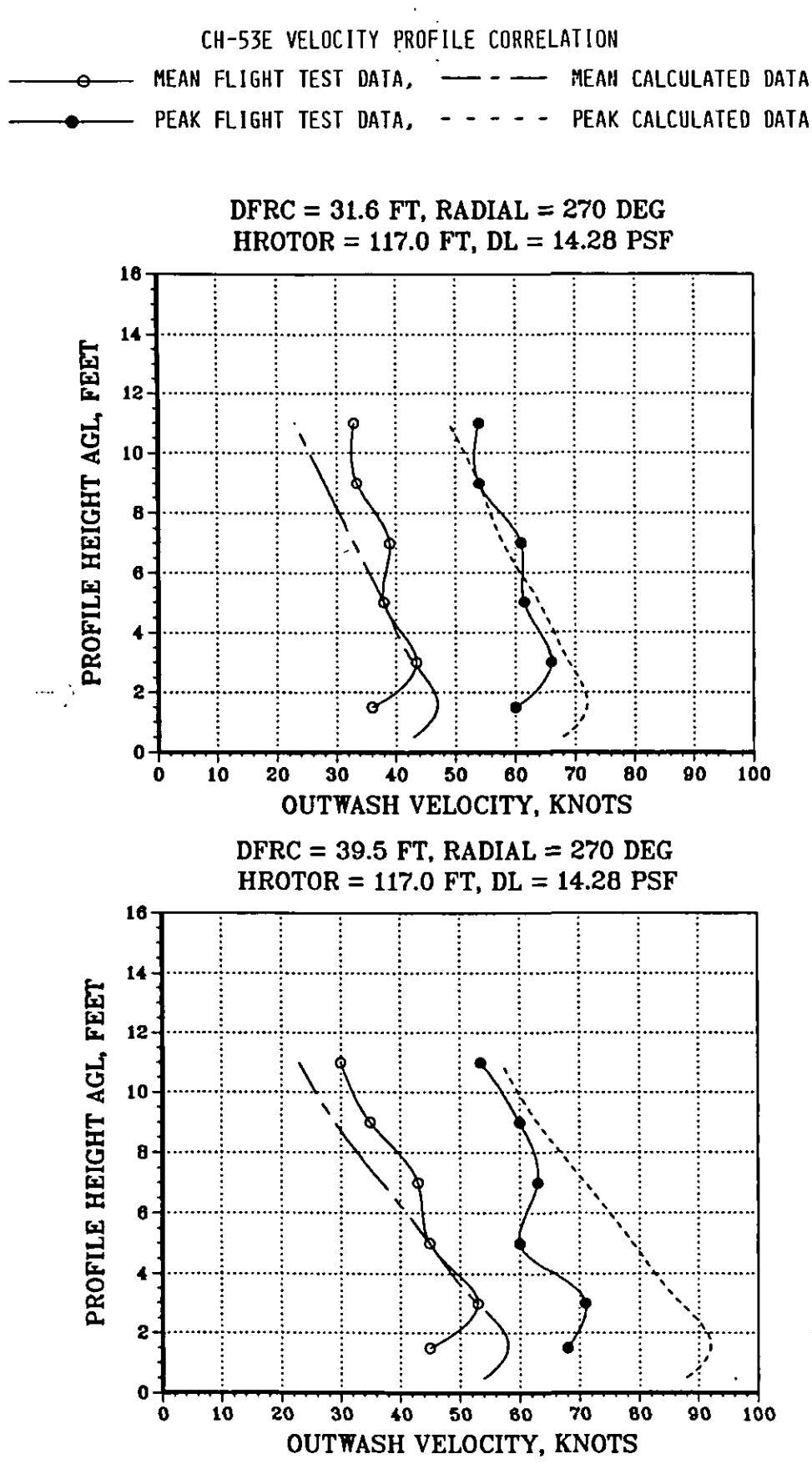

Figure 27. CH-53E Mean and Peak Velocity Profile Correlation for Eight 270-deg Azimuth Radial Stations at a Rotor Height of 117 ft and a Gross Weight of 70000 lbs

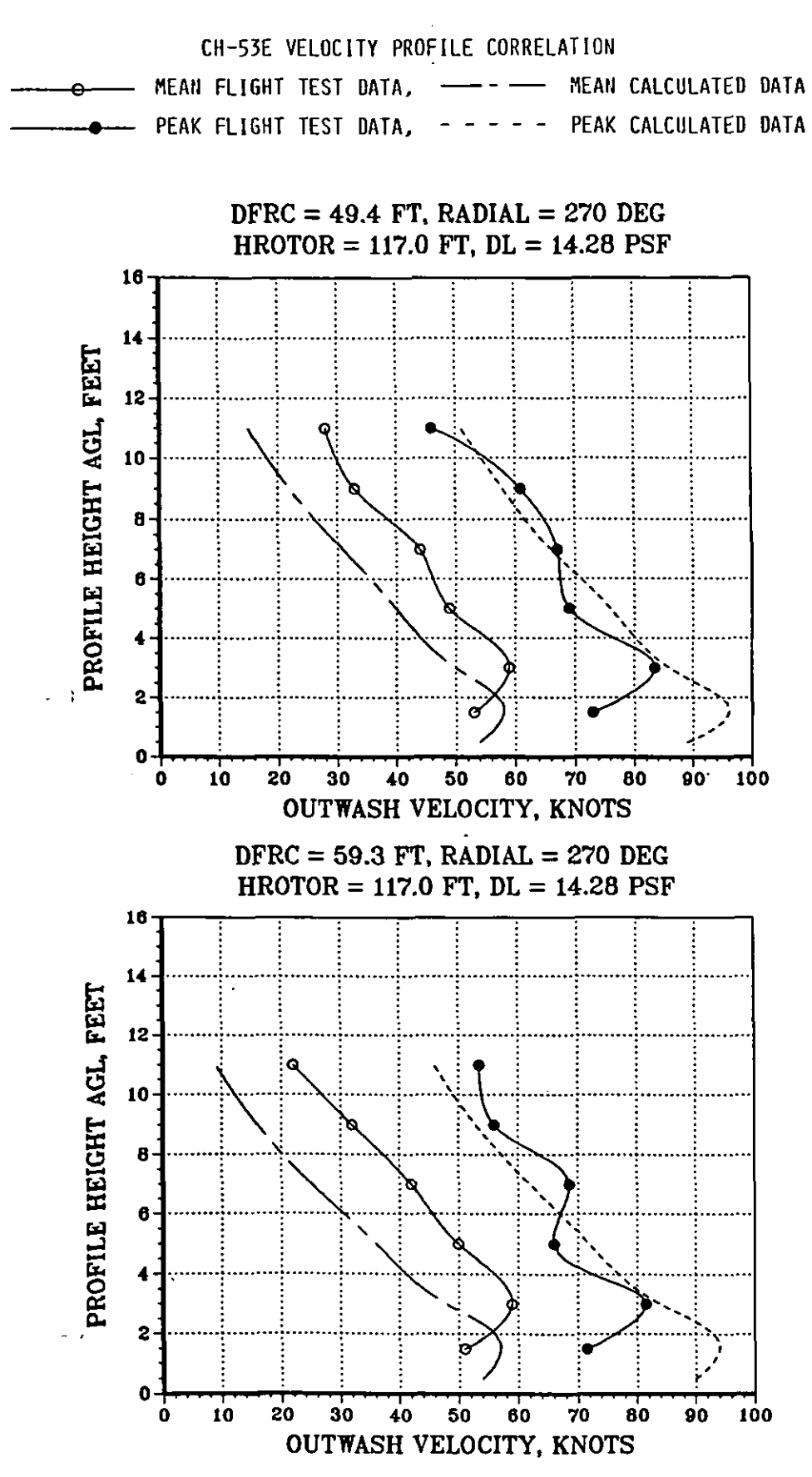

Figure 27 (Continued)

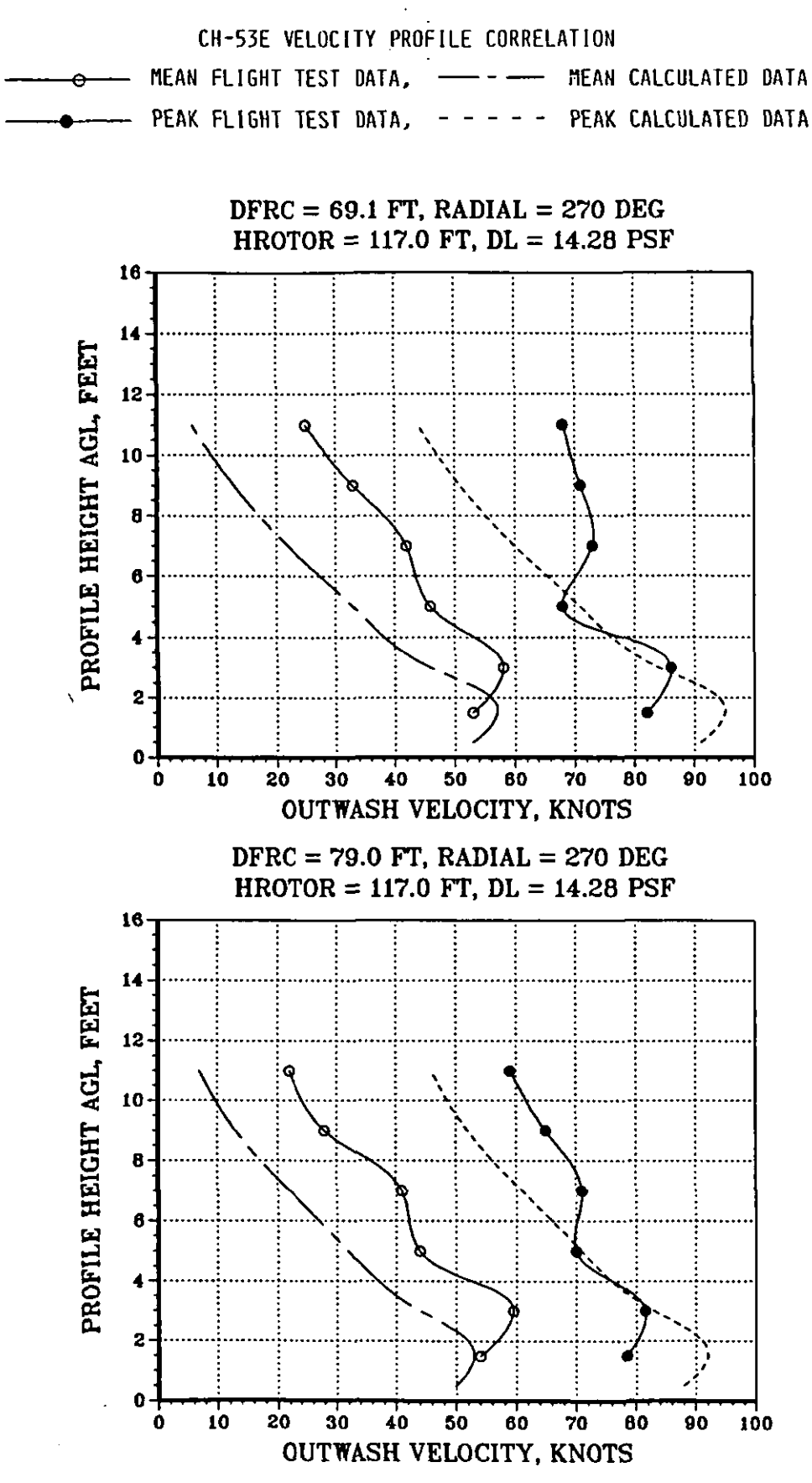

Figure 27 (Continued)

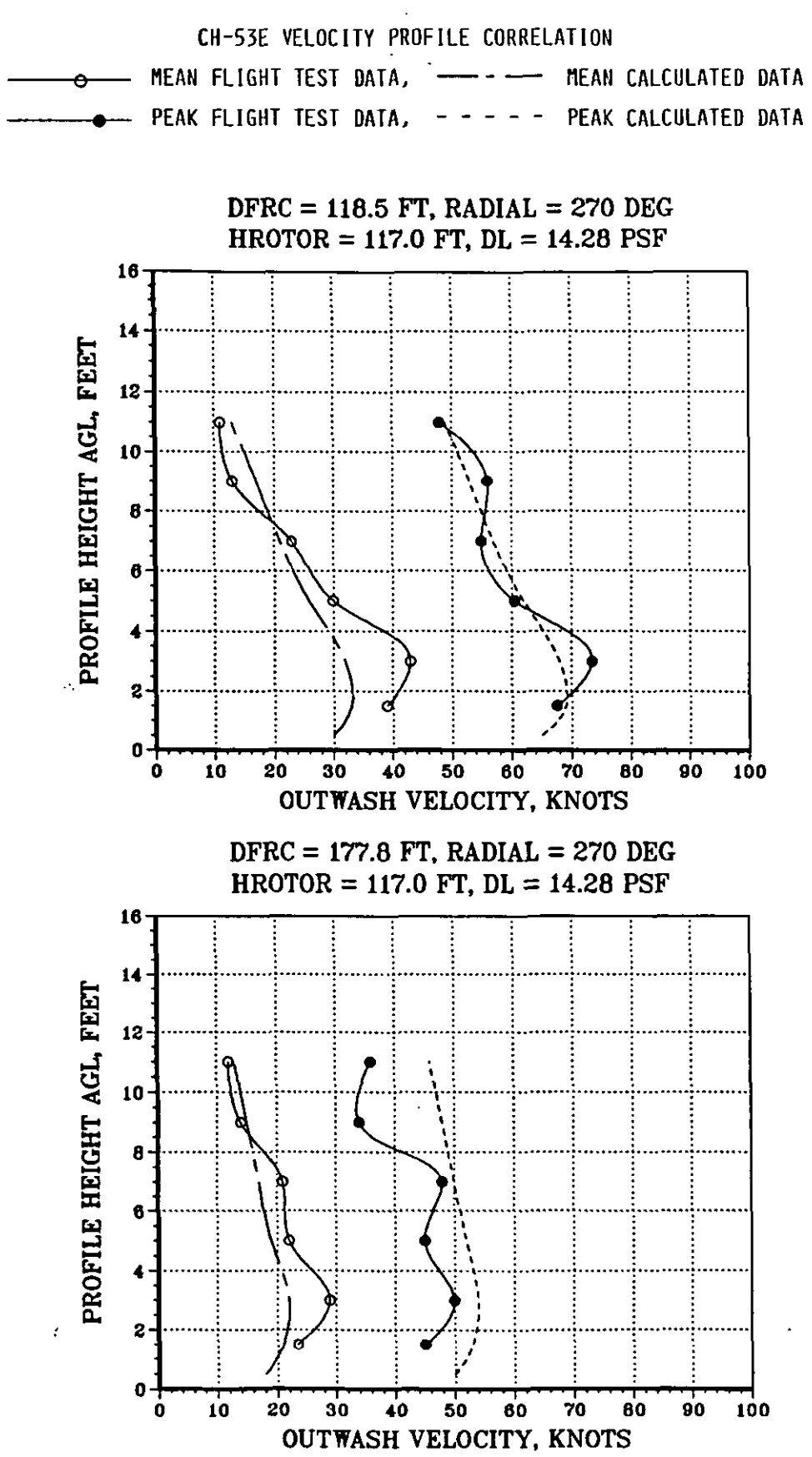

Figure 27 (Concluded)

Section III). Also, at almost all radial station positions (except for the 177.8 ft station), independent of rotor height, the calculated profile maximum velocity height is less than the almost constant value of 3 ft indicated in the flight test data. Since the flight test data was measured at only two heights in the boundary layer region (approximately 1.5 and 3.0 ft), it is believed that the faired profile of the flight test data may not be particularly accurate due to lack of sufficient data to accurately interpolate the true shape of the boundary layer. Theory and experimental results both clearly indicate that, as the outwash flow gets further from the rotor center and slows down, the boundary layer becomes thicker and the maximum velocity height increases. Overall, even with the noted discrepancies, the quality of the correlation for this particular gross weight is thought to be quite good.

A comparison and correlation of the effect of gross weight on CH-53E mean and peak velocity profiles at the radial stations at 59.3 and 118.5 ft, is presented in Figs. 28 through 33. In Figs. 28 through 30, the data for 56000 lbs are provided to compare with the previously presented data at 70000 lbs for all three of the rotor heights, and in Figs. 31 through 33, the data at 45000 lbs are likewise provided for comparison with the data at 56000 and 70000 lbs.

The comparison of these selected radial stations for variation in CH-53E gross weight reveals similar results to those presented for the 70000-lb gross weight case. A major exception to this statement appears in the correlation of the 117 ft case at both gross weights where there tends to be an overprediction of the flight test peak velocity profile data. An expanded correlation of flight test data and calculated data for all of the radial stations, rotor heights above ground, and gross weights listed in Table 4 is presented in Appendix B for the reader who is interested in further evaluation of the results.

Overall, the correlation of results between the calculated data and the CH-53E flight test data indicates at worst a very good duplication of trends. Numerous mean and peak velocity profiles of those compared are predicted quite accurately by the developed mathematical model. In contrast, while some of the other mean and peak velocity profiles are not

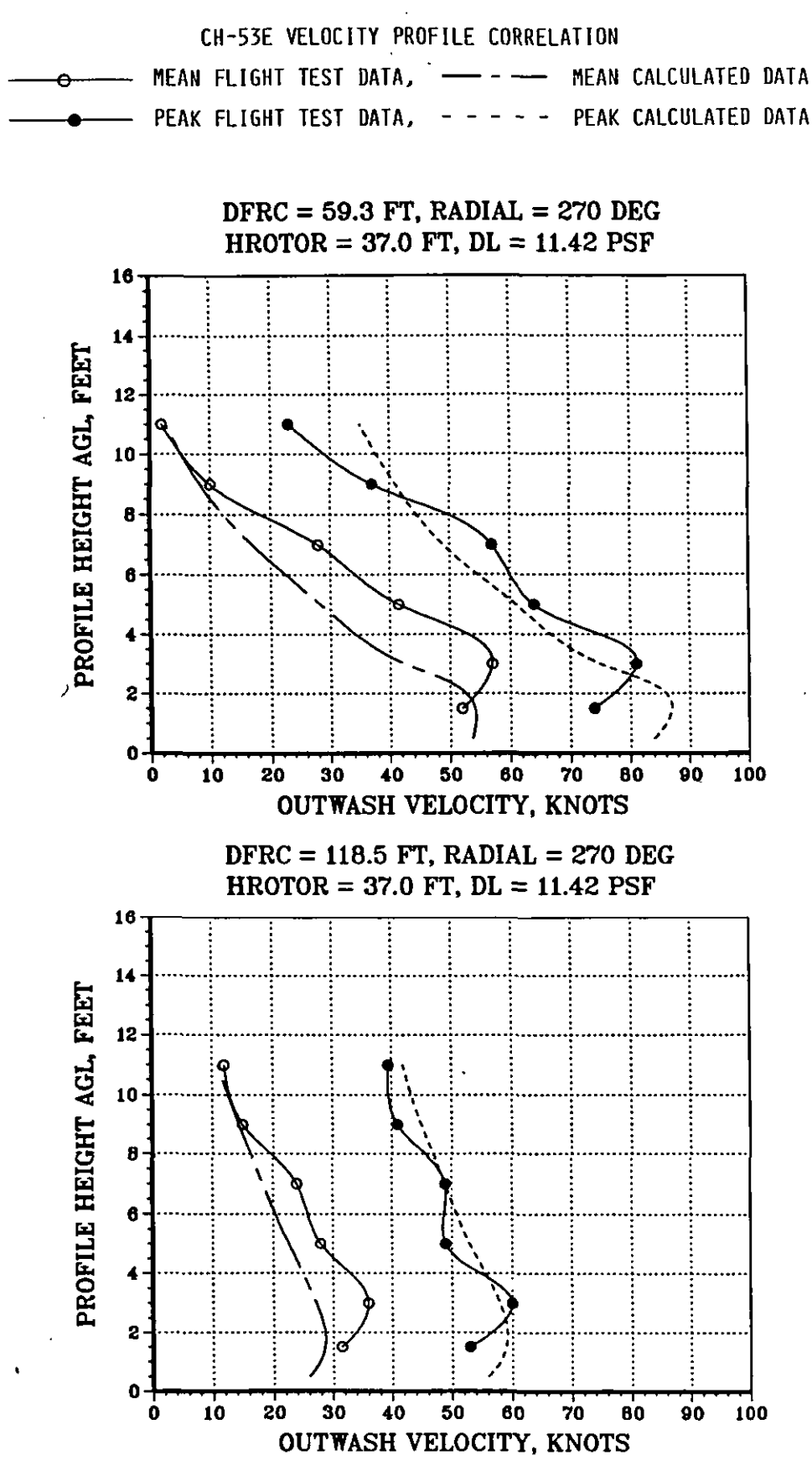

Figure 28. CH-53E Mean and Peak Velocity Profile Correlation at 56000 lbs Gross Weight for Two Stations Along the 270-deg Azimuth Radial at a Rotor Height of 37 ft

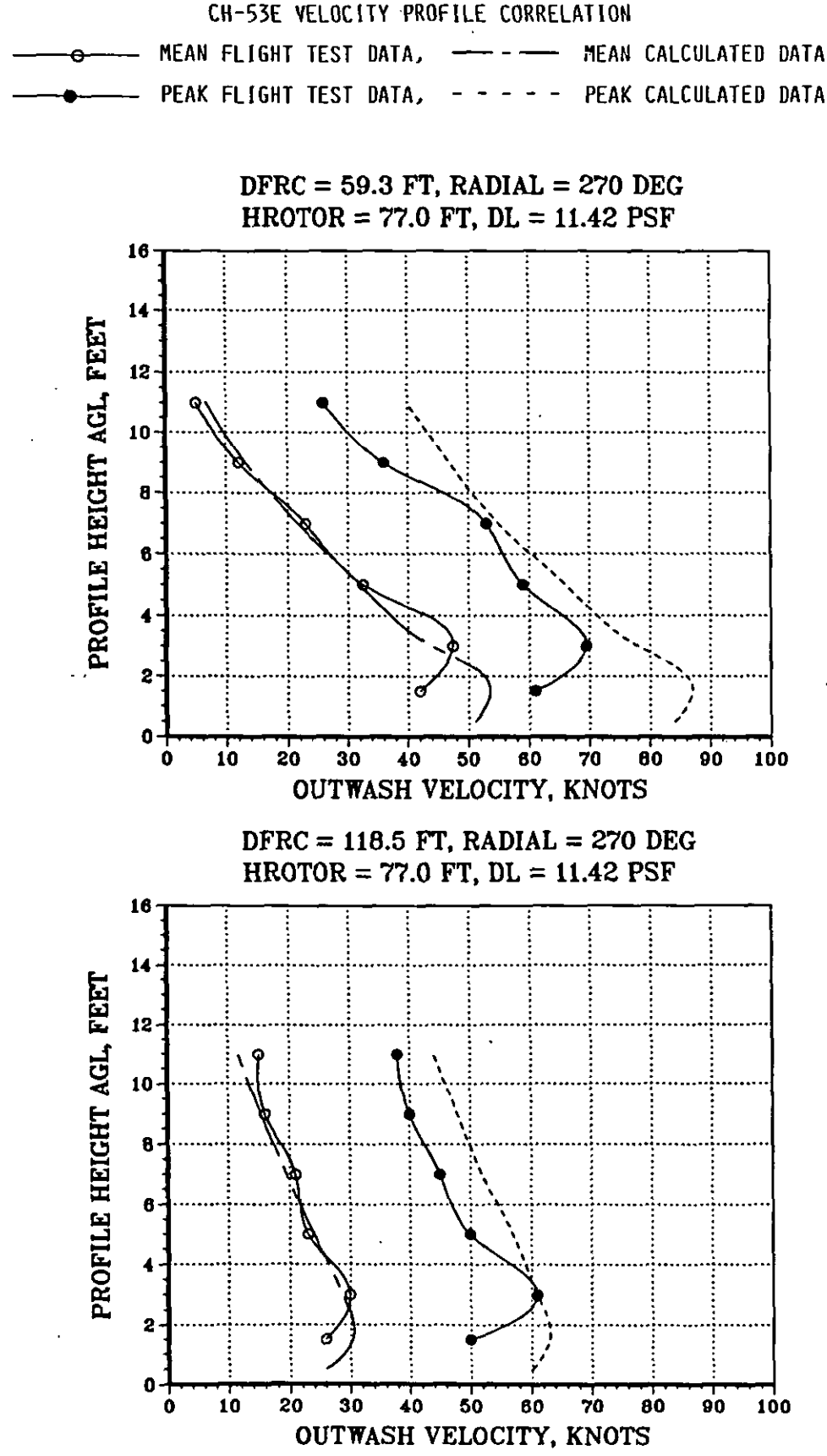

Figure 29. CH-53E Mean and Peak Velocity Profile Correlation at 56000 lbs Gross Weight for Two Stations Along the 270-deg Azimuth Radial at a Rotor Height of 77 ft

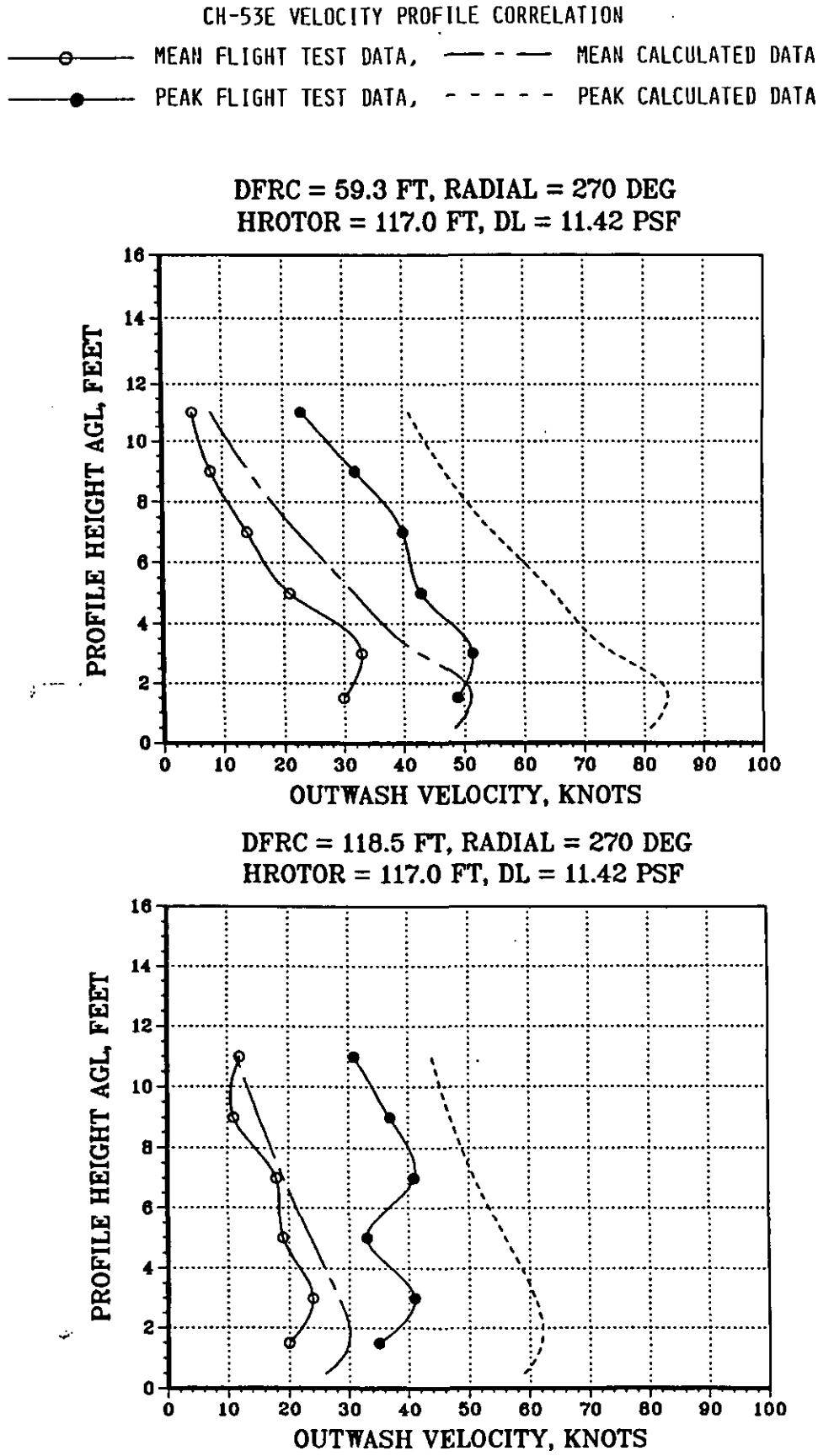

Figure 30. CH-53E Mean and Peak Velocity Profile Correlation at 56000 lbs Gross Weight for Two Stations Along the 270-deg Azimuth Radial at a Rotor Height of 117 ft

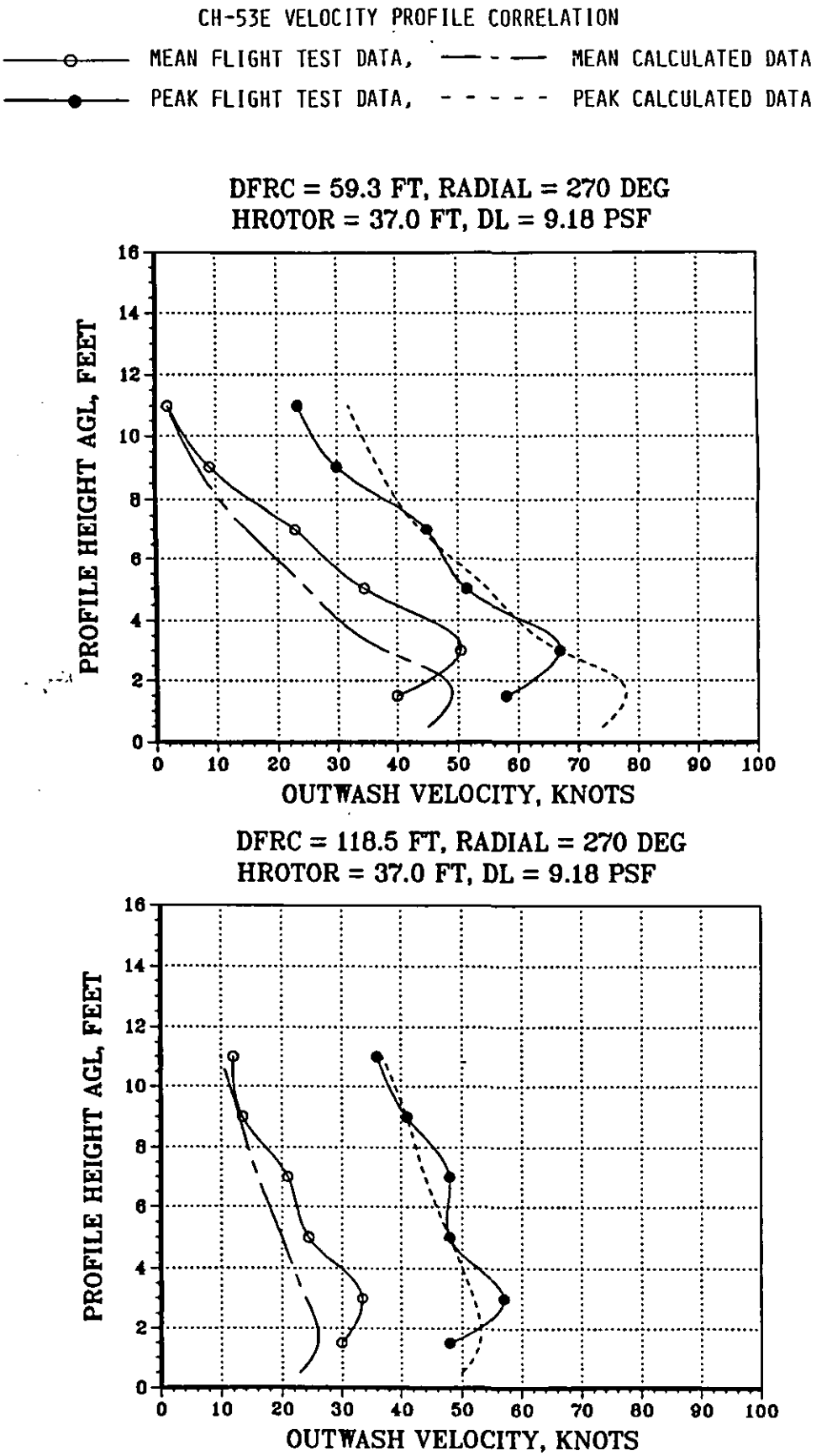

Figure 31. CH-53E Mean and Peak Velocity Profile Correlation at 45000 lbs Gross Weight for Two Stations Along the 270-deg Azimuth Radial at a Rotor Height of 37 ft

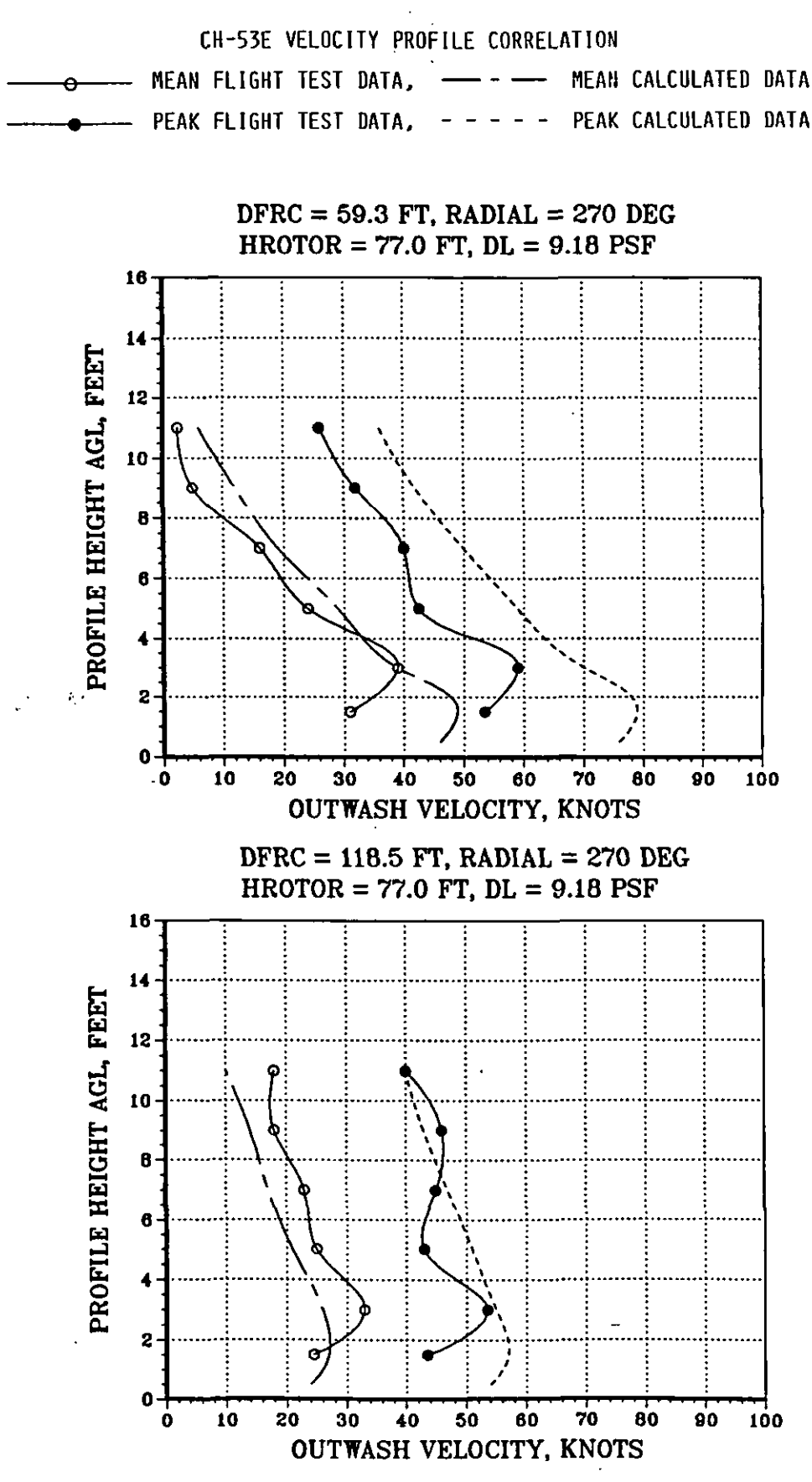

Figure 32. CH-53E Mean and Peak Velocity Profile Correlation at 45000 lbs Gross Weight for Two Stations Along the 270-deg Azimuth Radial at a Rotor Height of 77 ft

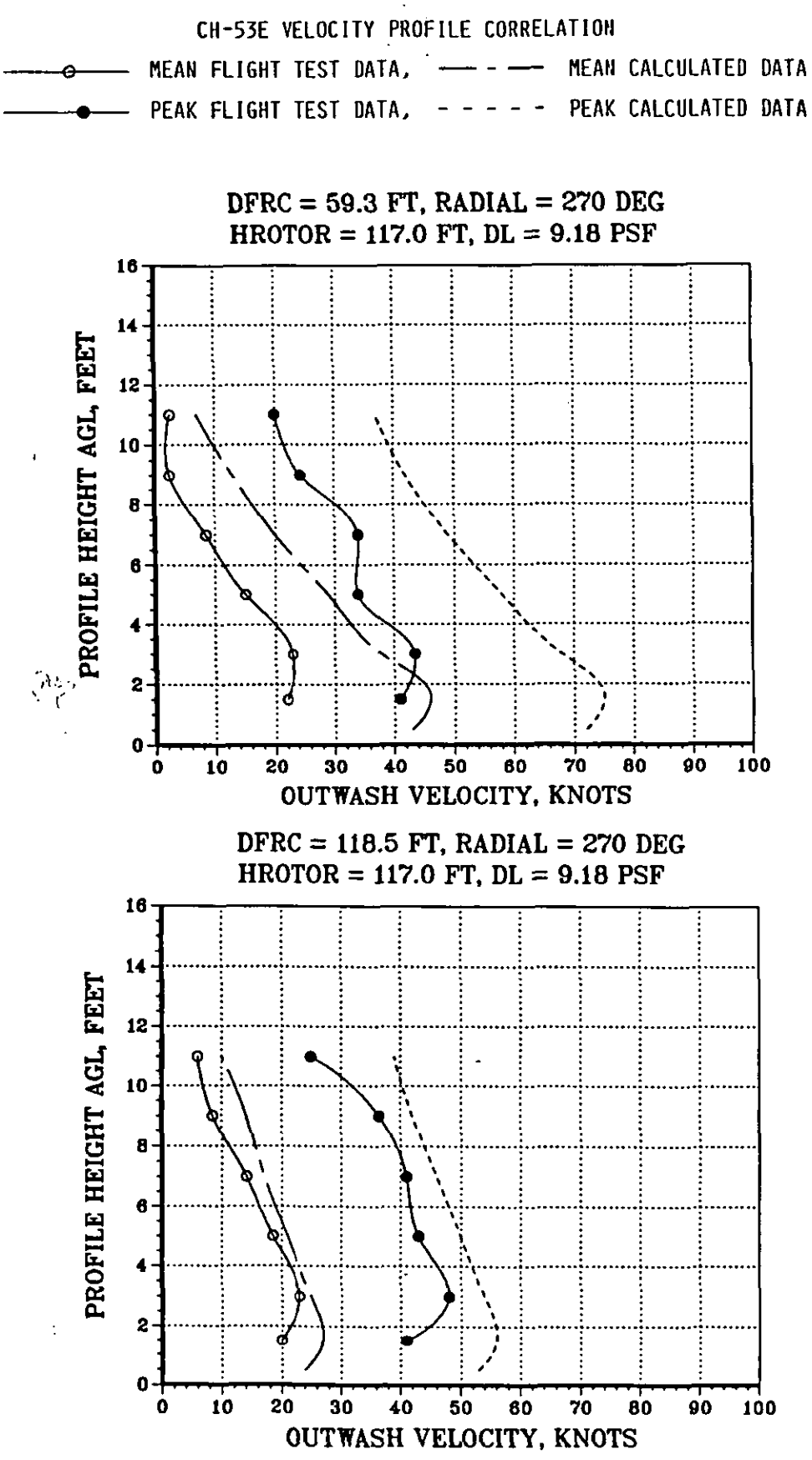

Figure 33. CH-53E Mean and Peak Velocity Profile Correlation at 45000 lbs Gross Weight for Two Stations Along the 270-deg Azimuth Radial at a Rotor Height of 117 ft

predicted as accurately as would be desired, the involved trends affecting the quality of the correlation are usually not consistent among the various cases so as to indicate any particular weakness being incorporated into the mathematical model formulation. The major weakness that seems to contribute to the failure to correlate exactly is simply the lack of complete understanding of the very complicated unsteady flow field processes that are going on inside the outwash boundaries that are being modeled by a theoretically and experimentally derived **steady flow field model.** As was discussed earlier, since the mean velocity profile calculation is primarily used in the scaling of the more important hazard-related peak velocity profile, extremely accurate prediction of the mean velocity profile, while certainly desirable, should not be looked upon as being critical to the hazard analysis.

B. XV-15 CORRELATION

Correlation with the XV-15 was conducted using flight test data presented in Ref. 12. XV-15 specific input data parameters that are required to execute the **ROTHAZ** analysis program are defined in Table 3. A three-view profile of the XV-15 is presented in Fig. 34. The flight test data presented in Ref. 12 were obtained at azimuths of 0, 180, and 270 deg (or forward, rearward, and to the left side, respectively). Six stations were evaluated along each of these radials. These station positions are described in detail in Fig. 35. Winds during the testing were below 2 kt. Data at rotor heights of 14.5, 37.5, and 62.5 ft AGL were also obtained and presented in Ref. 12 at a radial station of 15.6 ft from the center of the rotor; however, significant variations in gross weight were not evaluated. A test/correlation matrix for the XV-15, similar to that presented for the CH-53E in Table 4, is presented in Table 5.

Correlation of flight test data and calculated data as a function of the distance from the center of the rotor at a gross weight of approximately 12475 lbs and at a rotor height above the ground of 37.5 ft is presented for the 270-deg radial position (noninteraction plane) in Fig. 36. The results for this comparison indicate that the mathematical

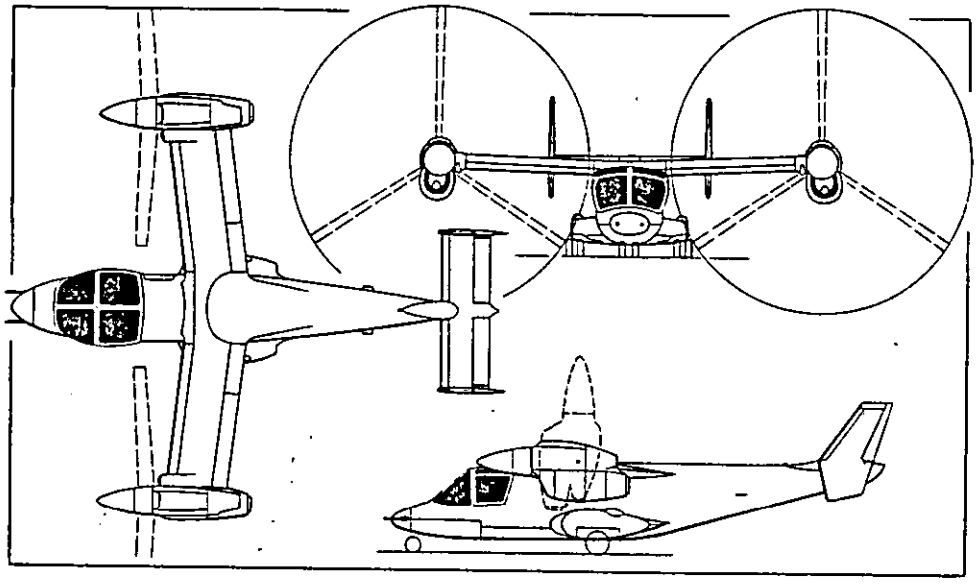

Figure 34. Bell XV-15 Tilt-Rotor Research Aircraft

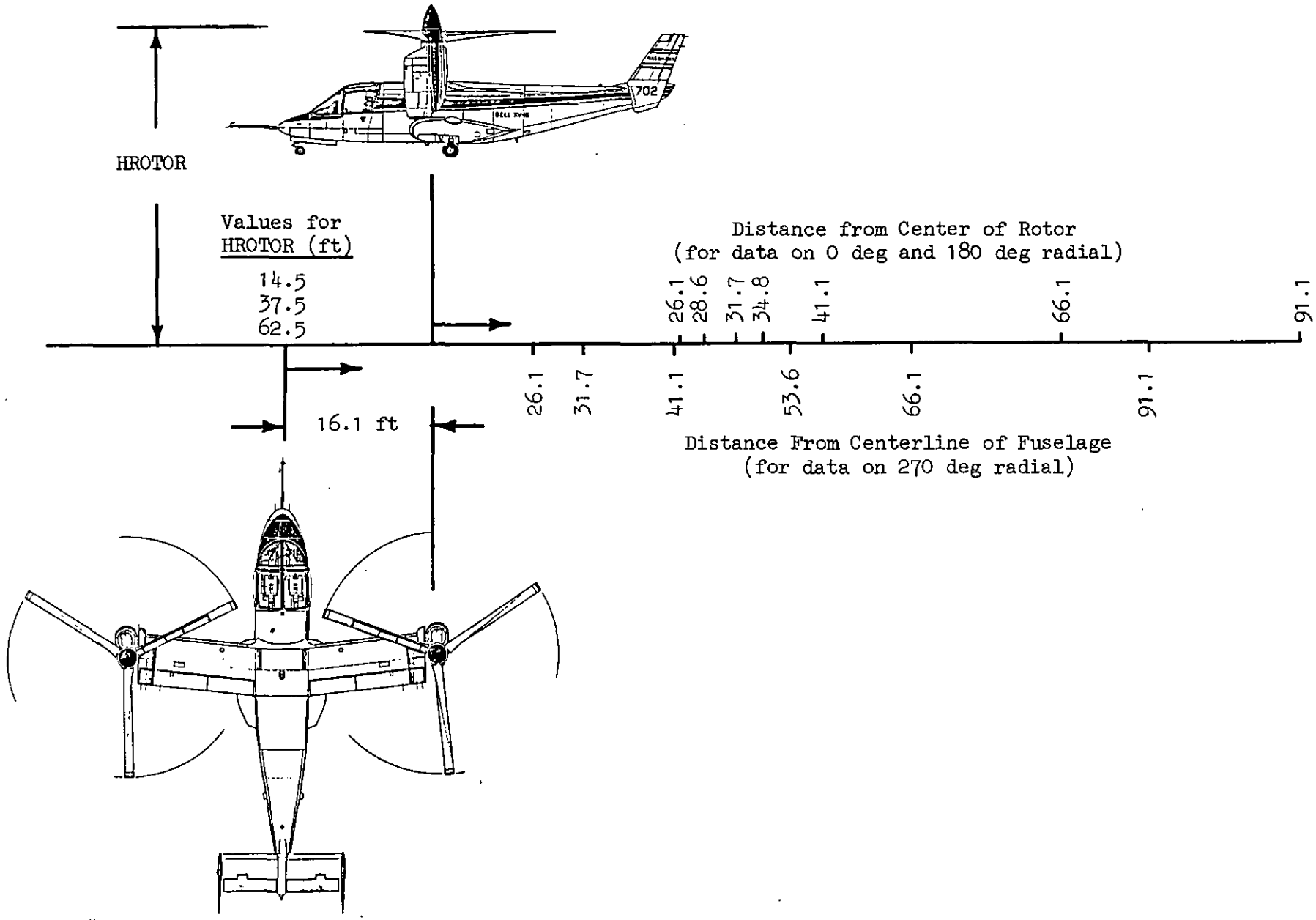

Figure 35. XV-15 Flight Test Velocity Profile Measurement Stations

TABLE 5. EVALUATION MATRIX FOR XV-15 FLIGHT TEST/MATHEMATICAL MODEL DATA CORRELATION

Figure Number	Gross Weight,[1] lb	Disc Loading,[1] PSF	Rotor Height ft	Azimuth Angle, deg	Distance From Rotor Center (DFRC) or Distance Along the Interaction Plane (DAIP)[2]
36	12475	12.71	37.5	270	10.0,15.6,25.0,37.5,50.0,75.0
37	12555	12.79	14.5,37.5,62.5	270	15.6
38	12475	12.71	37.5	0	26.1,31.7,34.8,41.1,66.1,99.1
39	12475	12.71	37.5	180	26.1,28.6,31.7,41.1,66.1,99.1
40	12555	12.79	14.5,37.5,62.5	0	31.7
41	12555	12.79	14.5,37.5,62.5	180	31.7

NOTES:

(1) Even though care has been taken to calculate realistic average gross weights, the values are average values that could vary between 12030 and 13000 lbs at the extremes.

(2) The values for DFRC are applicable along only the 270-deg azimuth radial; whereas, the values for DAIP are valid along the 0- and 180-deg azimuth radial.

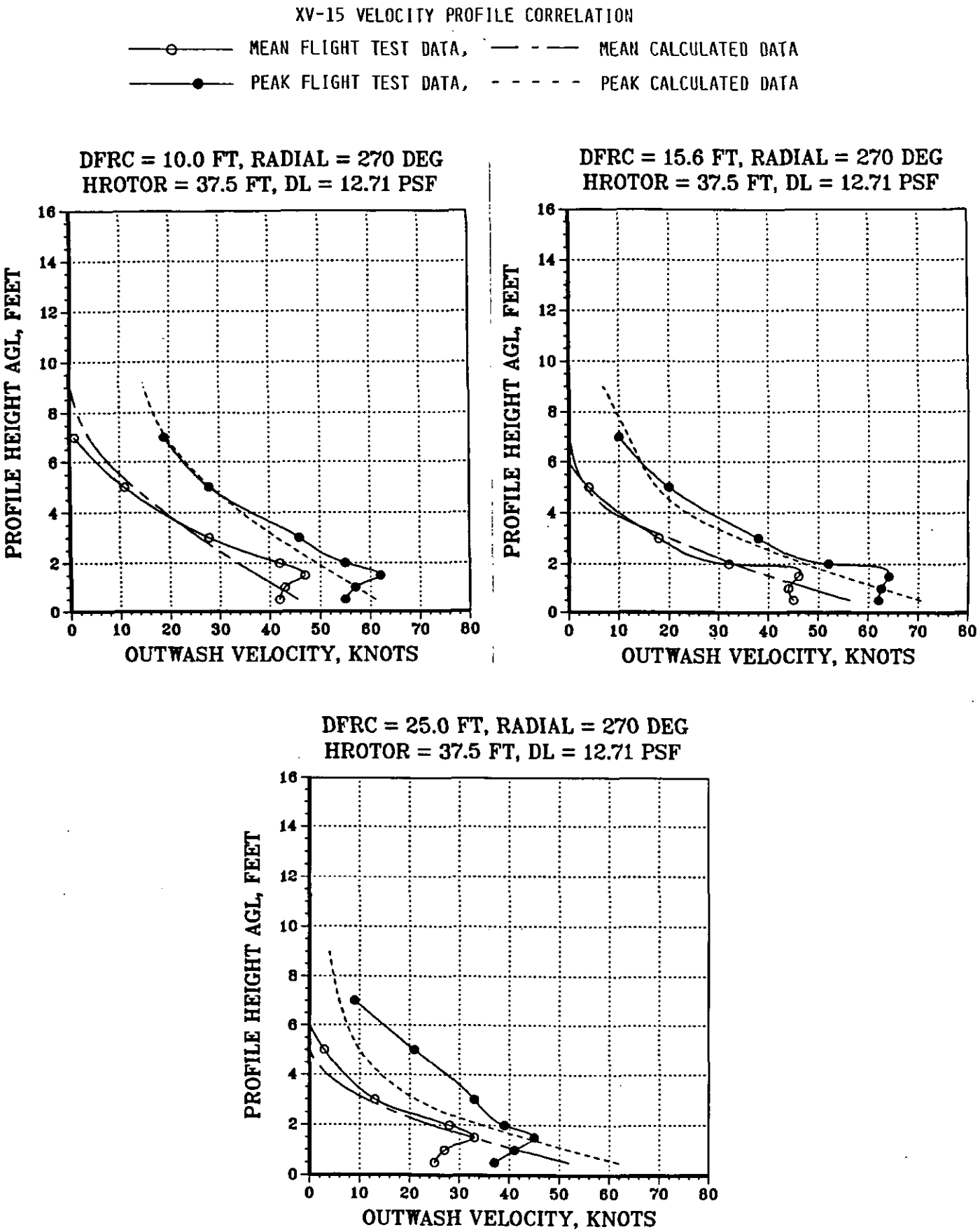

Figure 36. XV-15 Mean and Peak Velocity Profile Correlation Along the 270-deg Azimuth Radial at a Rotor Height of 37.5 ft and a Gross Weight of 12475 lbs (Average)

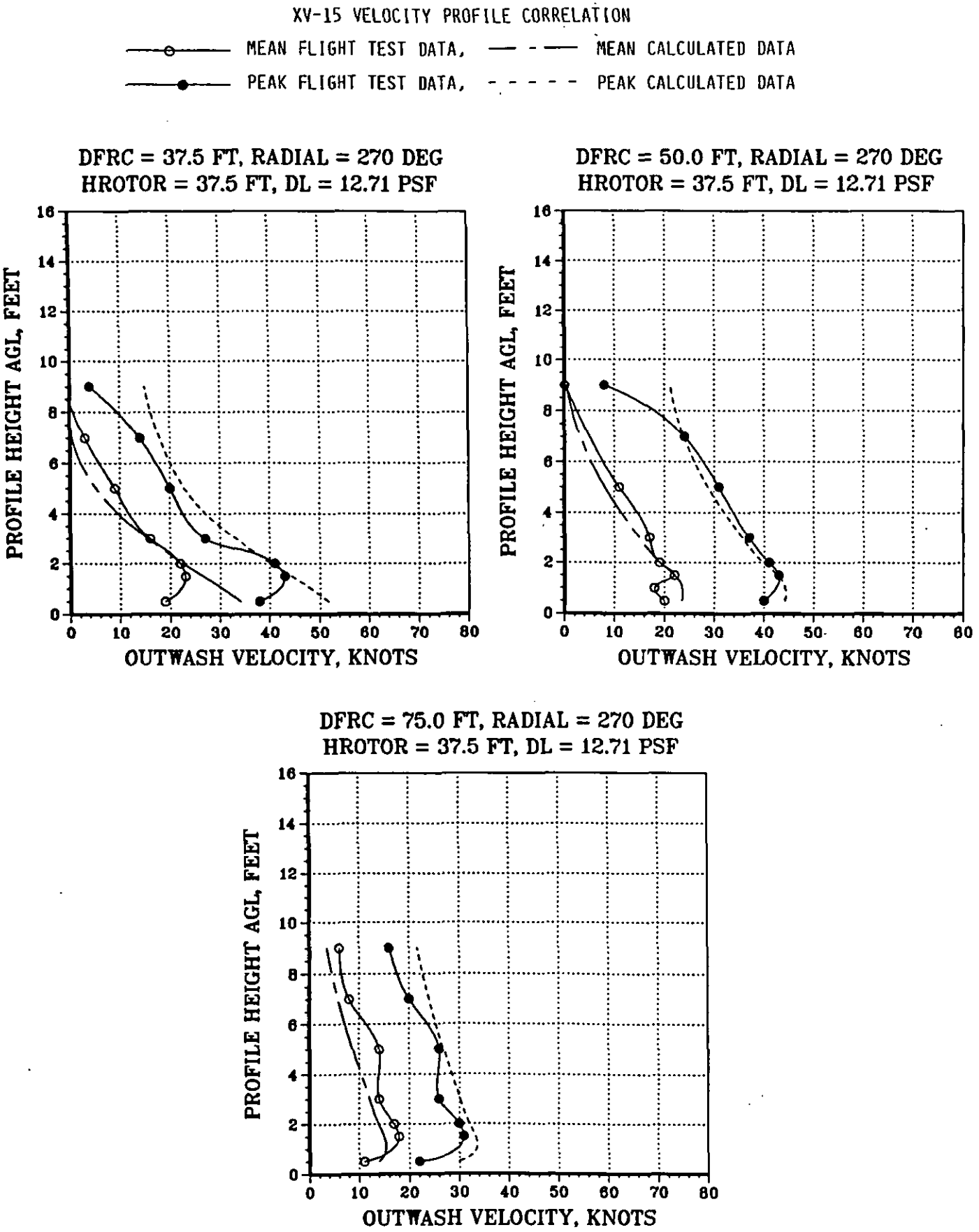

Figure 36 (Concluded)

model predicts quite accurately the XV-15 mean and peak velocity profiles for the specified flight condition. However, as was noted with the CH-53E results, the height of the maximum velocity in the profile is underpredicted, except in the far field. Data for a comparison of mean velocity profiles as a function of the variation in rotor height (at 14.5, 37.5, and 62.5 ft) at the 15.6 ft radial station are presented in Fig. 37. This limited comparison shows that the calculated velocity profiles at the three rotor heights correlate reasonably well with measured flight test profiles. The distance from the rotor which was presented in Ref. 12 for correlation is not a particularly good distance because of its extreme closeness to the tip of the rotor (within approximately 3 ft). Nevertheless, since Ref. 12 provided data for correlating only this one radial station as a function of rotor height, it is assumed that the quality of correlation at the other radial stations is similar to that presented in Fig. 36 at the rotor height of 37.5 ft.

Correlation of flight test data and calculated data along the two interaction planes between the twin rotors (radial azimuths of 0 and 180 deg) is presented as a function of the distance from the center of a line connecting the two rotors in Figs. 38 and 39. For the analysis of the interaction plane in the **ROTHAZ** analysis program, it is important to note that the mathematical model does not discriminate between the forward and aft interaction planes for a tilt rotor; instead, the analysis assumes symmetry. However, this assumption of symmetry does not seem to be fully validated by the flight test data. A comparison of the flight test velocity profiles at each of the radial stations, especially at the 41.1, 66.1, and 91.1 ft stations, indicates that a distinct difference exists in the shape of the profiles due to the influence of unknown factors. Correlation of data along the 0-deg radial indicates that the mathematical model closely predicts or overpredicts the velocity profiles of the XV-15. Along the 180-deg radial, a comparison of the data indicates a similar overprediction of the velocity profile, particularly at low profile heights, out to a radial station of greater than 41.1 ft. At the 66.1 ft and 91.1 ft radial positions, the correlation of the peak velocity profile on average is quite good.

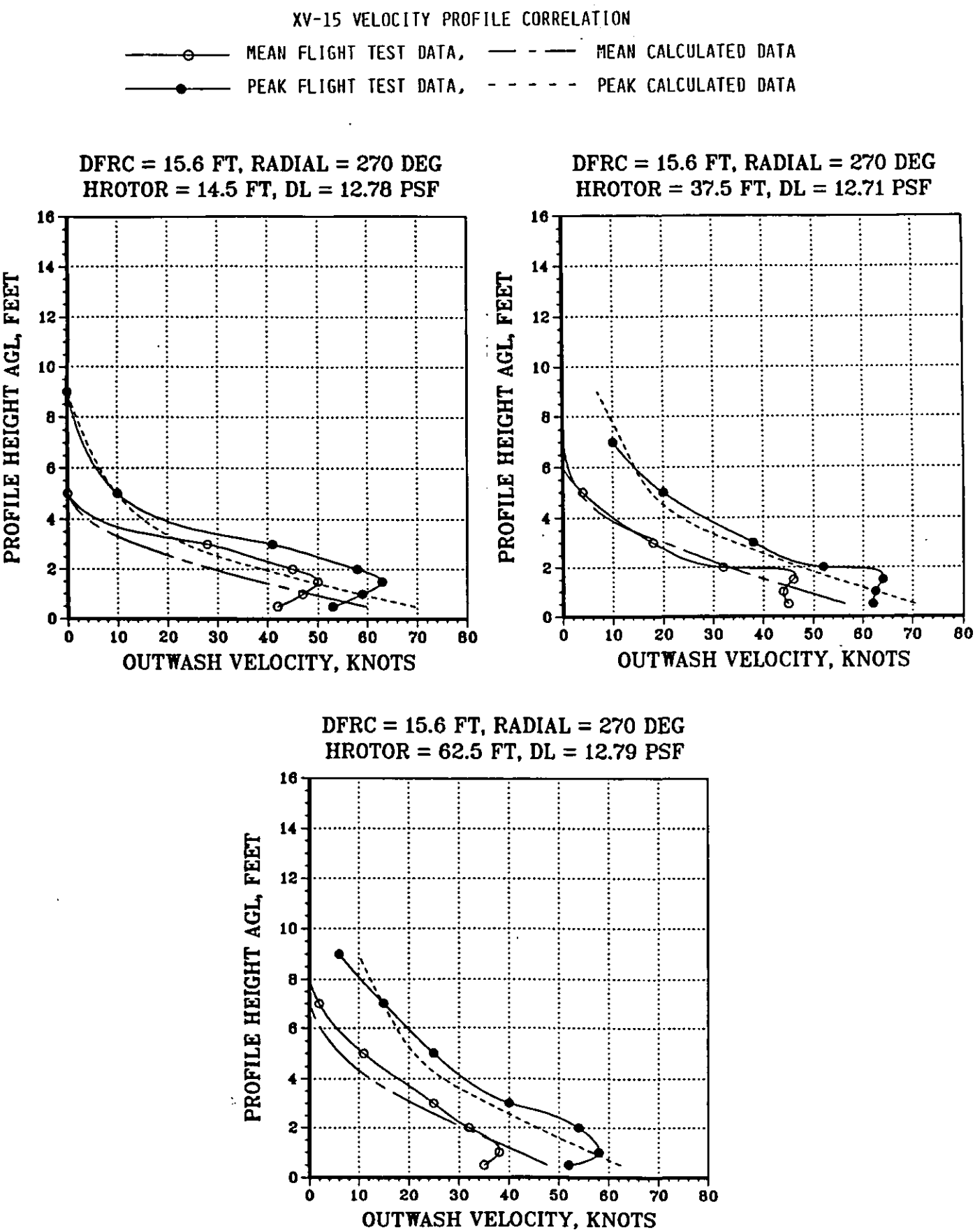

Figure 37. XV-15 Mean and Peak Velocity Profile Correlation for Three Rotor Heights and a Gross Weight of 12555 lbs (Average) at the 270-deg Azimuth Radial Station of 15.6 ft

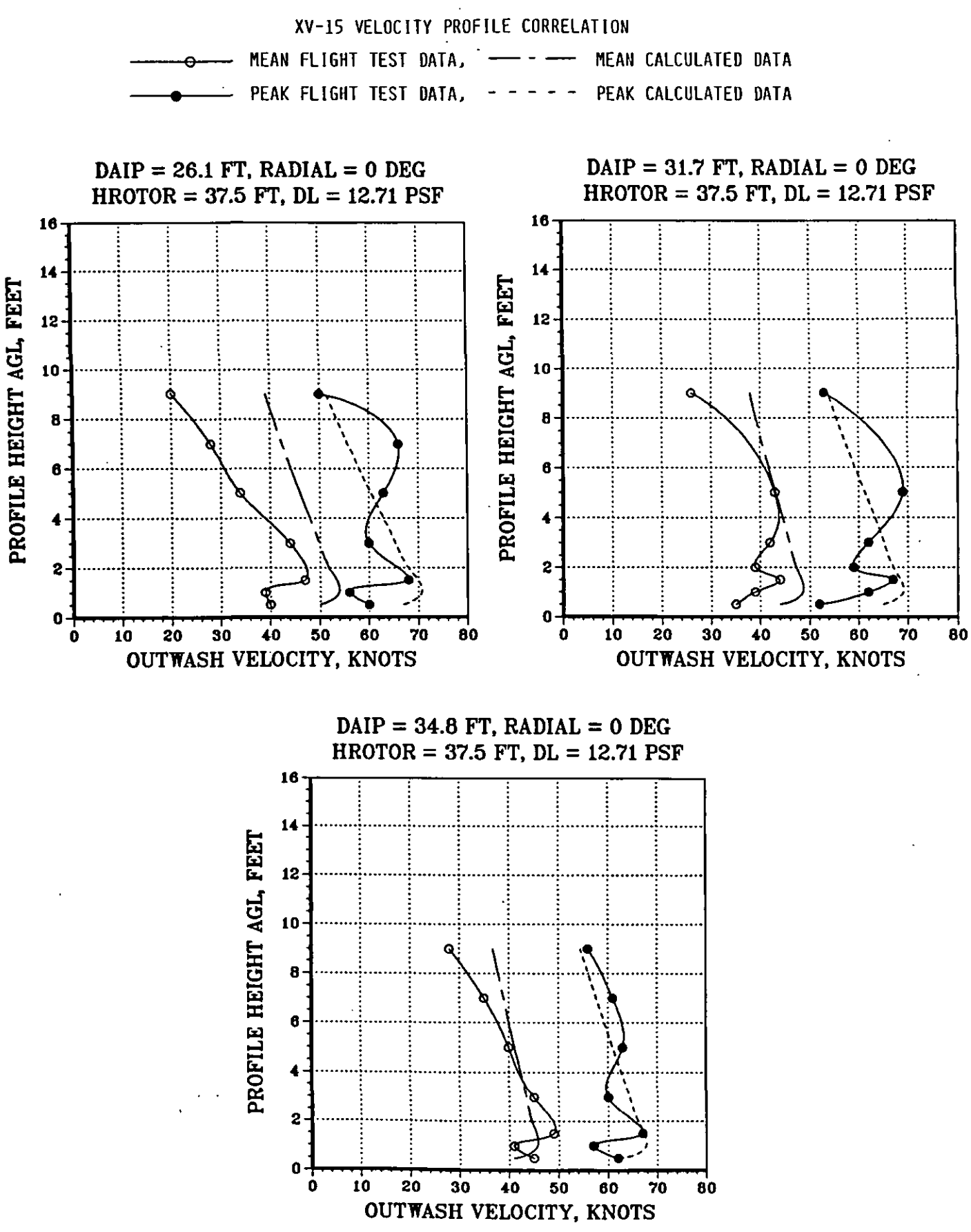

Figure 38. XV-15 Mean and Peak Velocity Profile Correlation Along the 0-deg Azimuth Radial at a Rotor Height of 37.5 ft and a Gross Weight of 12475 lbs (Average)

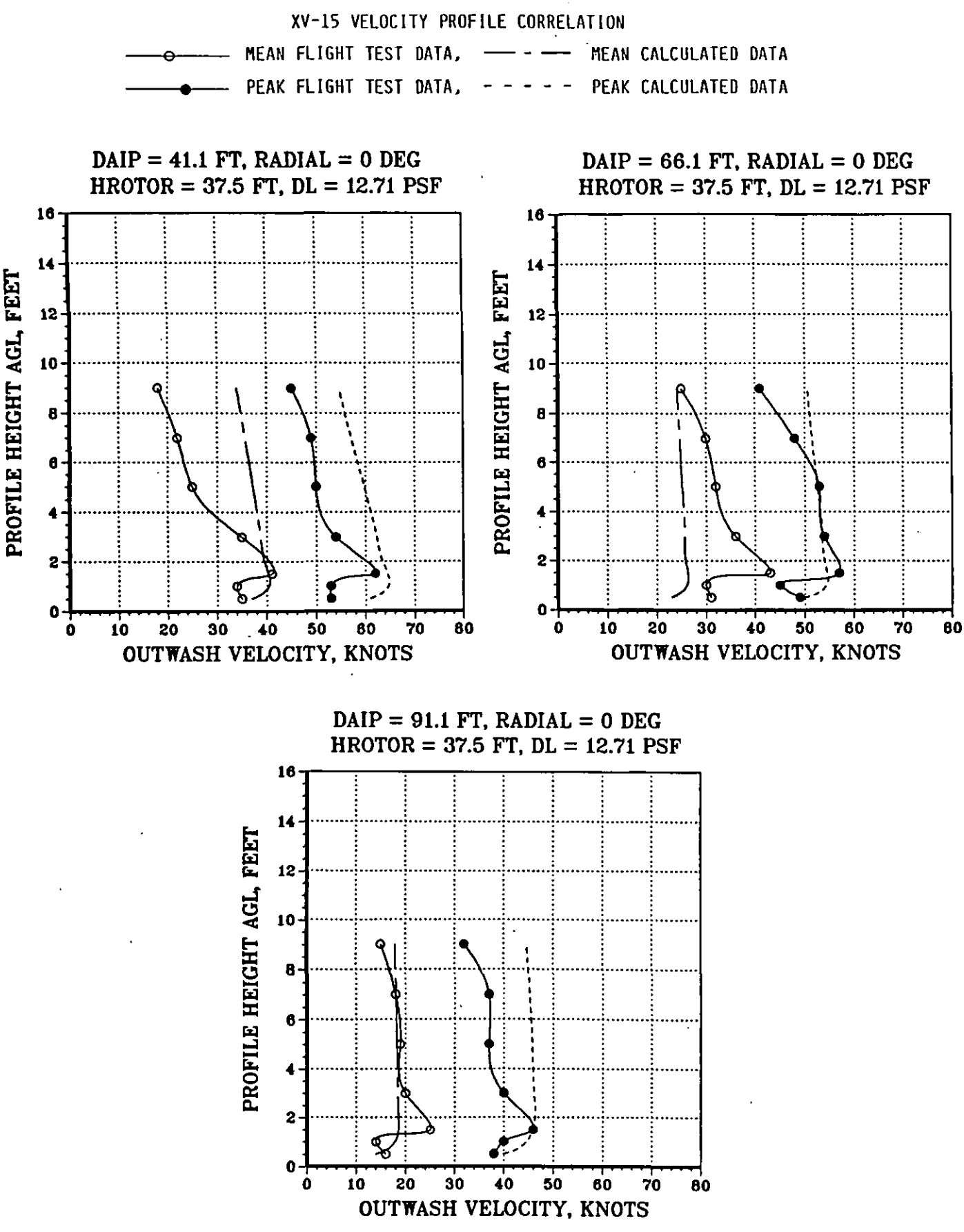

Figure 38 (Concluded)

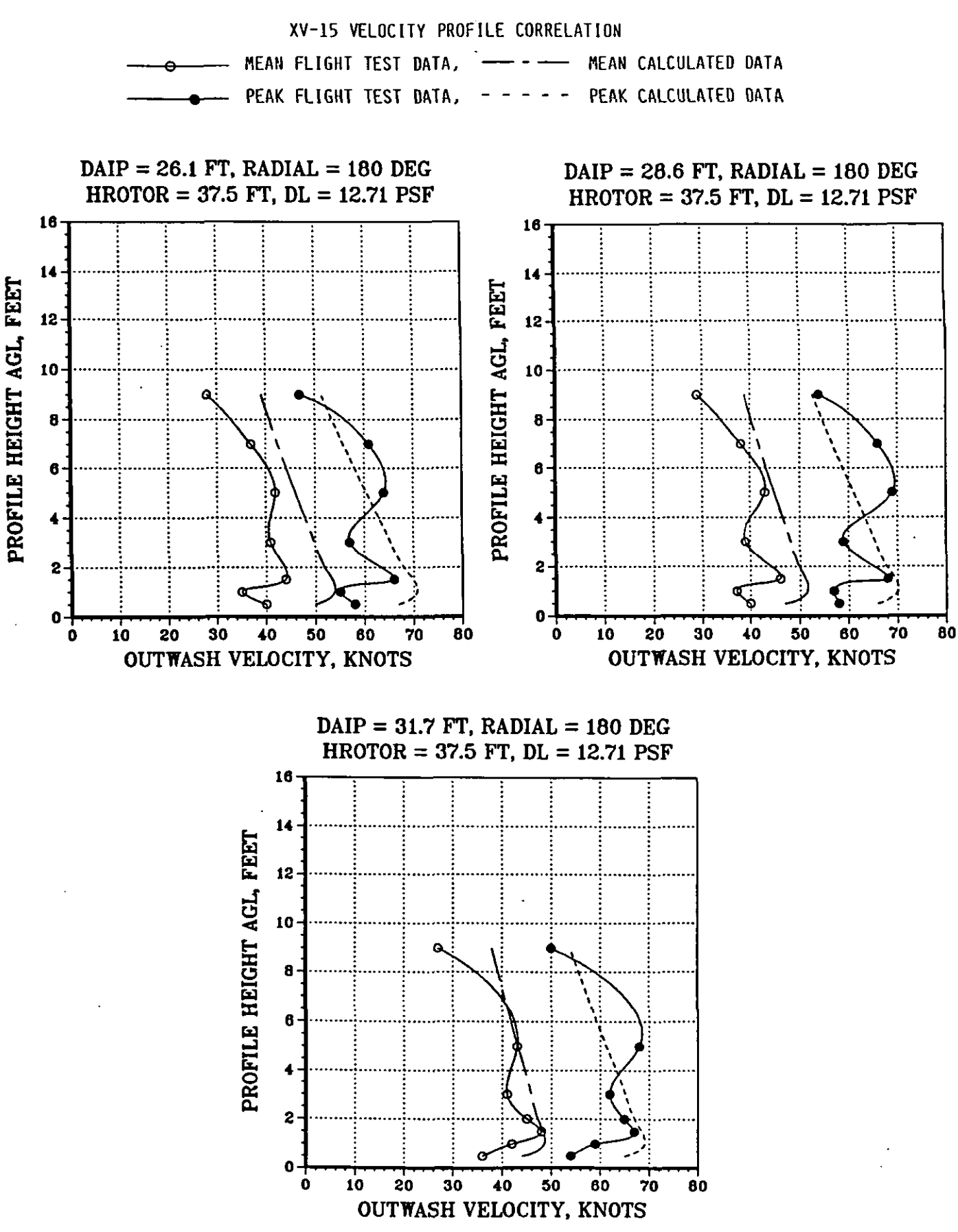

Figure 39. XV-15 Mean and Peak Velocity Profile Correlation Along the 180-deg Azimuth Radial at a Rotor Height of 37.5 ft and a Gross Weight of 12475 lbs (Average)

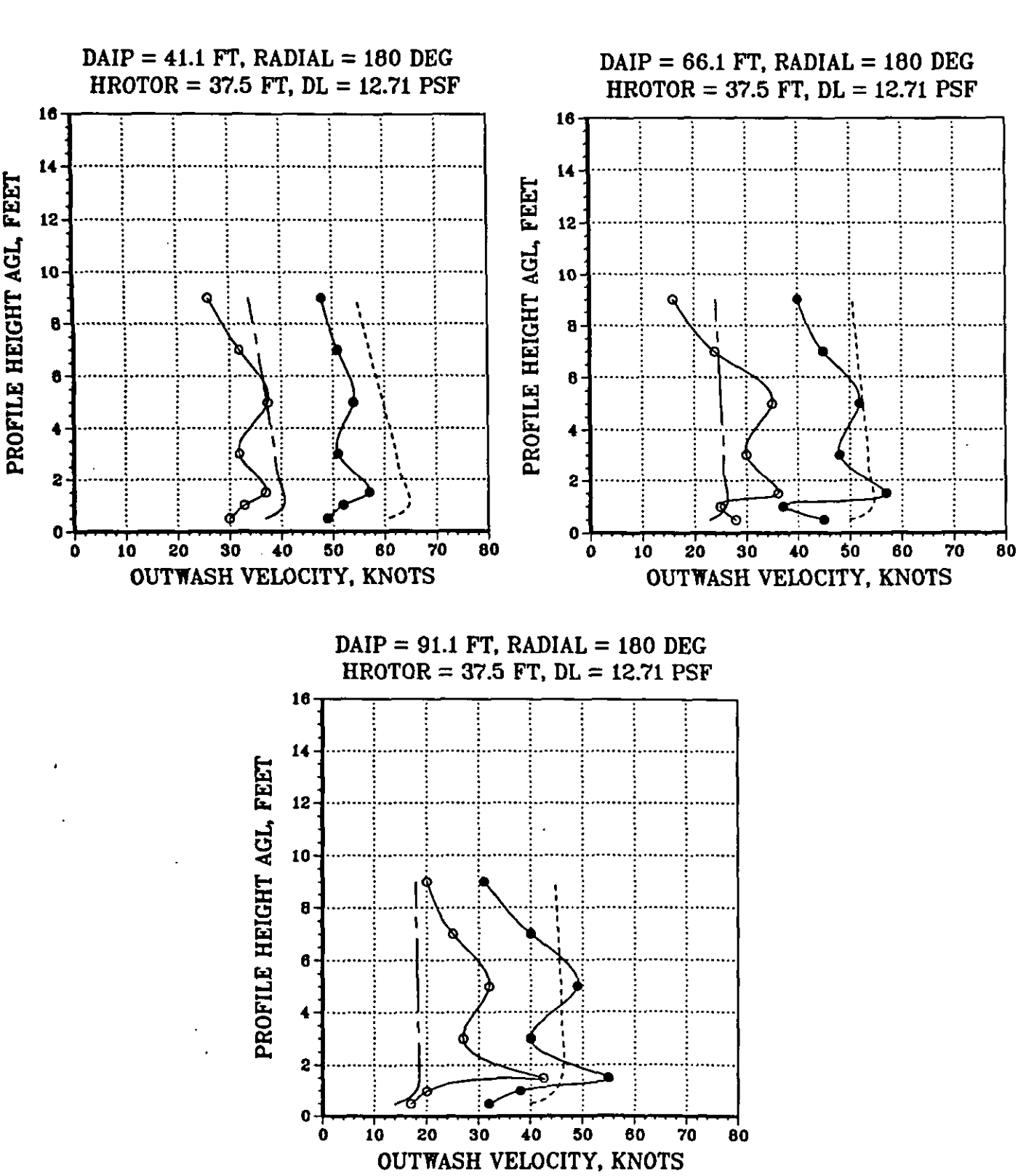

Figure 39 (Concluded)

Data for the comparison of the effect of a variation in rotor height along the interaction plane at the 15.6 ft station are presented in Figs. 40 and 41. In all cases in these two figures, the calculated velocity profiles closely predict the measured velocity profiles, except at the higher profile heights above the ground (in excess of approximately 5 ft).

Overall, the correlation of data for the XV-15 indicates a correlation quality as good as or possibly even better than that shown for the CH-53E. Limitations associated with the theories which were discussed for the CH-53E can certainly be assumed to also apply to the XV-15. However, the good correlation shown with the tilt-rotor configuration does provide confidence for making predictions associated with tandem rotor helicopters, especially along the interaction plane. This is because the tandem helicopter configuration is clearly more geometrically symmetric than the side-by-side tilt rotor along the interaction plane.

C. CORRELATION OF THE GROUND VORTEX, FORWARD FLIGHT, AND AMBIENT WIND MODELS

The mathematical models, as developed for the ambient wind, ground vortex, and forward flight effects, have each been developed using simple but sound theory. It is **still important to note,** however, that little flight test data was available for correlation with the analytical results from these models. The data that were available for correlation of the ambient wind effect are presented in Section VI. In the discussion in that section, the correlation is shown in conjunction with the correlation for overturning forces and moments as measured on personnel.

In the effort to locate flight test data for correlation with both the ground vortex and the forward flight trailing vortex models, only limited flight test data was found relating to trailing vortices. Therefore, no effort was made to validate the ground vortex model other than what was described in Section III using the model data as presented by Curtis and Sun. The trailing vortex flight test data that were located for correlation purposes were taken from unpublished memo notes (Ref. 26).

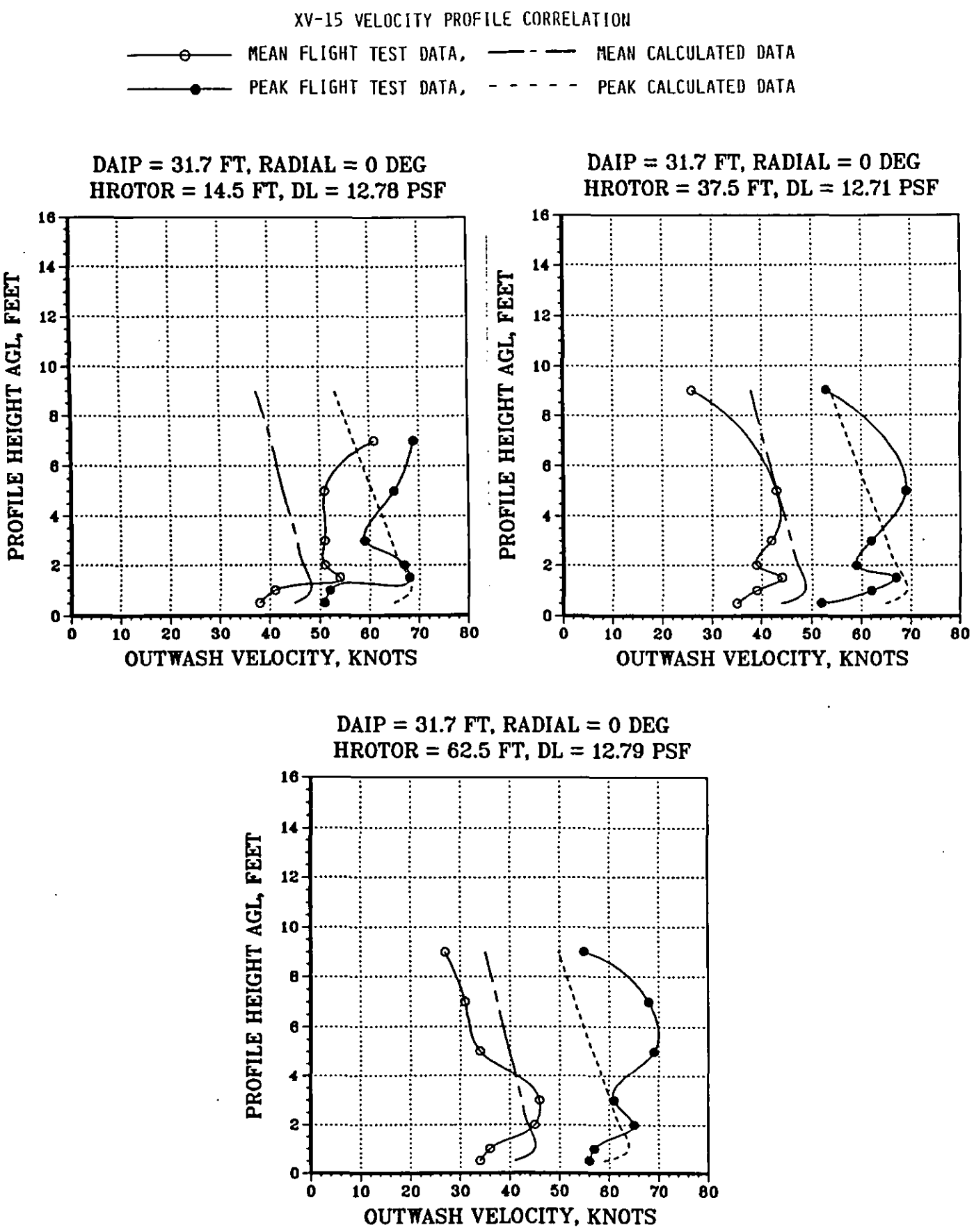

Figure 40. XV-15 Mean and Peak Velocity Profile Correlation for Three Rotor Heights and a Gross Weight of 12555 lbs (Average) at the 0-deg Azimuth Radial Station of 31.7 ft

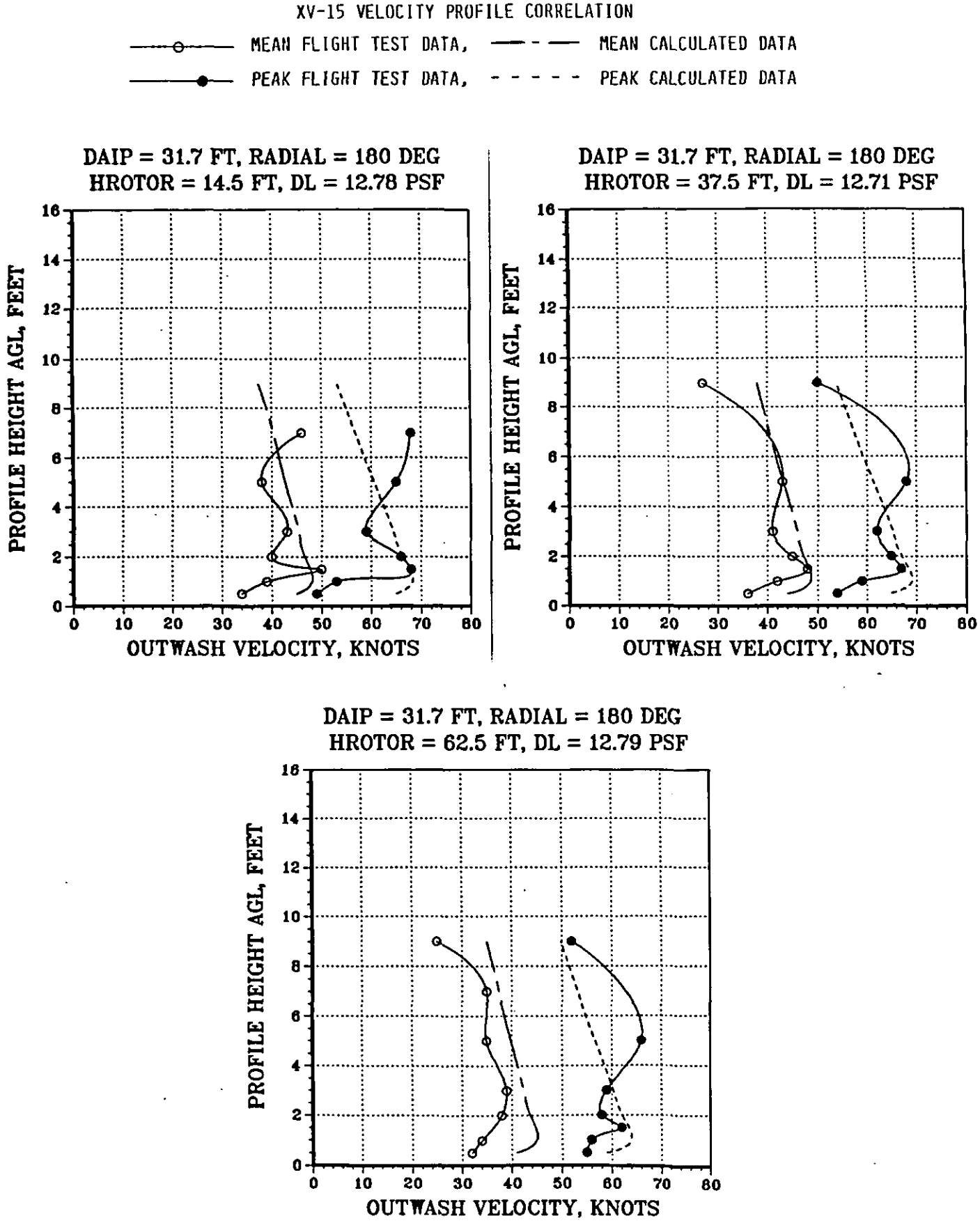

Figure 41. XV-15 Mean and Peak Velocity Profile Correlation for Three Rotor Heights and a Gross Weight of 12555 lbs (Average) at the 180-deg Azimuth Radial Station of 31.7 ft

Data on trailing vortex strength are presented in Figs. 42 and 43 as a function of airspeed for two helicopters. The helicopters are the UH-1H and the CH-54, respectively. The age of the measured vortex circulation data is approximately 20 sec, and the circulation is averaged up to a radius of five meters. (This parameter estimates the vortex hazard to a fixed-wing airplane with a five-meter semispan.) The averaged circulation, $\Gamma'(r)$, as presented in the figures, is less than the total circulation (Γ_w),

$$\Gamma_w = \frac{[\pi R(\Omega R)^2 C_T]}{2V_f} \tag{60}$$

by a factor that is a function of the core radius (r_c). Equation 61 provides this correction factor as developed for one particular model of the vortex velocity profile:

$$\Gamma'(r)/\Gamma_w = [1 - (r_c/r) \tan^{-1} (r/r_c)] \tag{61}$$

If the assumption is made that the core radii are approximately 1.3 and 2.5 meters for the UH-1H and the CH-54, respectively, then the calculated correction factors are computed to be 0.66 and 0.45.

Results, as estimated using the simplified ROTHAZ model, are presented in Figs. 42 and 43 for both corrected (dashed line) and uncorrected data (solid line). As can be seen, the uncorrected data tends to overpredict the vortex strength as measured in flight (as would be expected); whereas, the corrected data tends to underpredict the measured vortex strength, except for the low airspeed values. As airspeed is reduced below 30 kts, values of vortex strength will become estimated even more conservatively by the ROTHAZ model than would be measured in flight. (Strength would be infinite at 0 kts.) At these low values of airspeed (less than 30 kts), any predictions, as provided by a simple mathematical model, are suspect. This is due to the fact that the more fixed-wing-like horseshoe

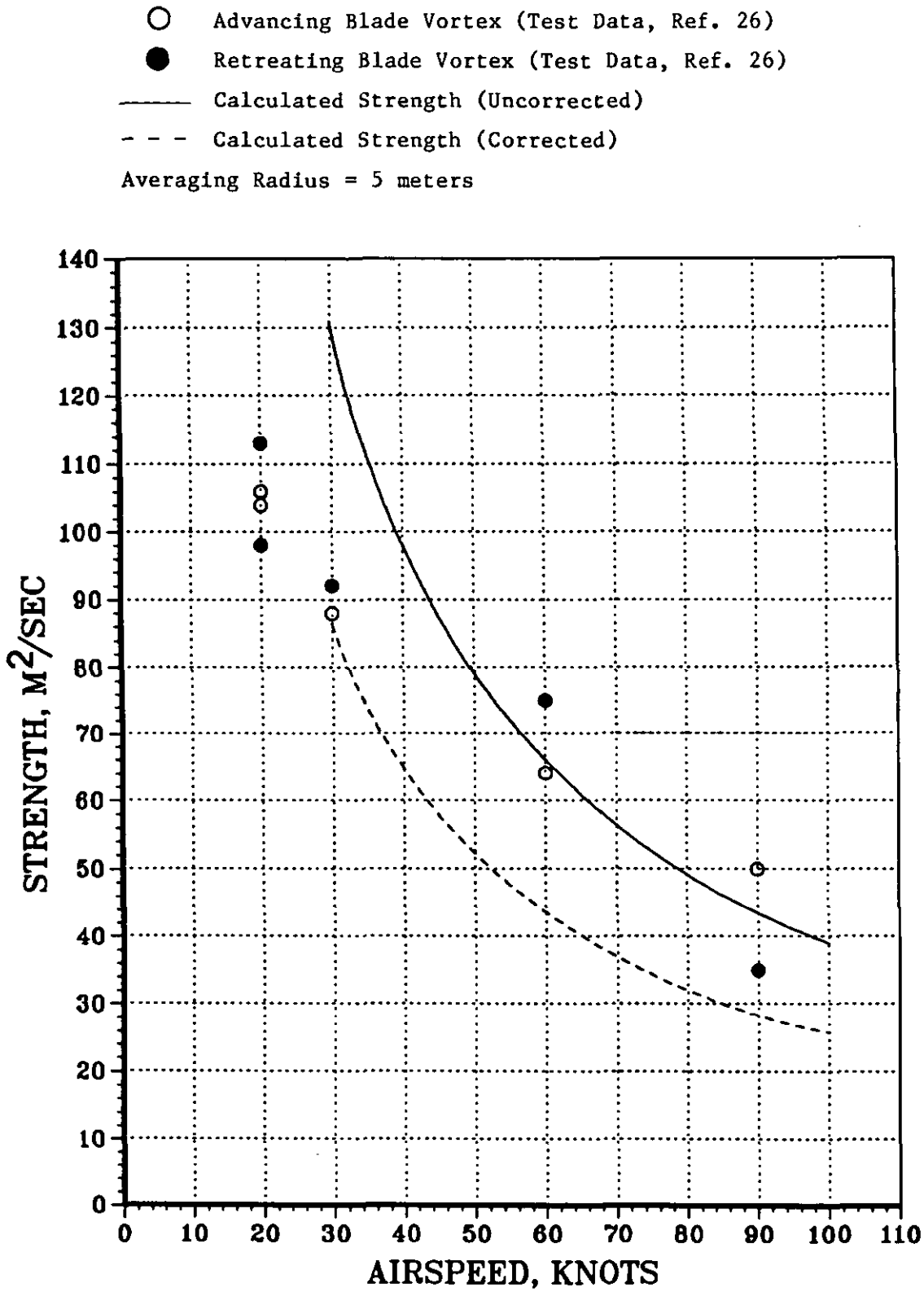

Figure 42. Correlation of Calculated and Measured UH-1H Five-Meter Wake-Vortex Strength at Age 20 sec Versus Nominal Airspeed

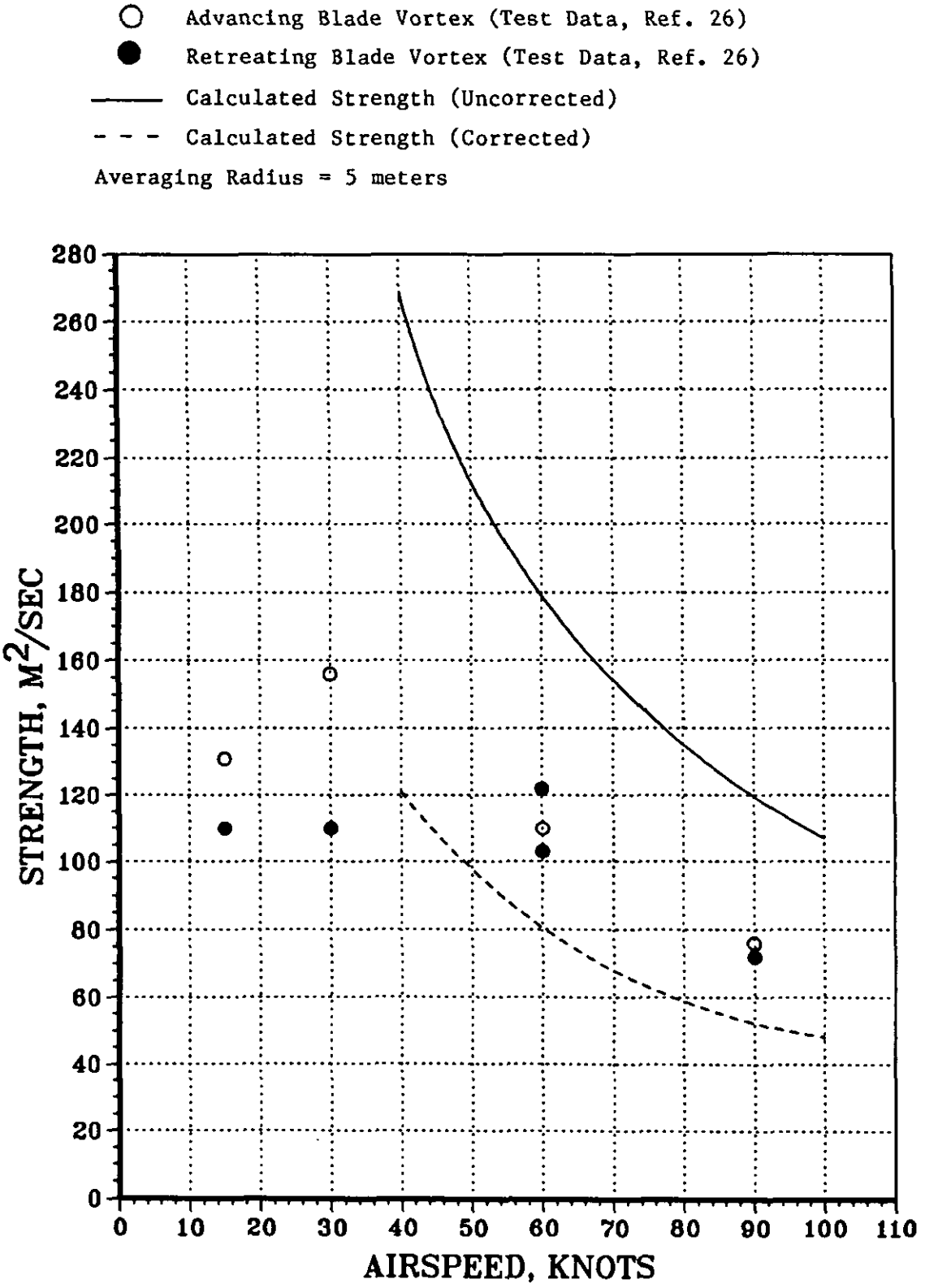

Figure 43. Correlation of Calculated and Measured CH-54 Five-Meter Wake-Vortex Strength at Age 20 sec Versus Nominal Airspeed

vortex wake structure is in transition at this airspeed range into the tubular hover wake structure.

Figures 44 and 45a have been provided as examples of velocity profiles that have been measured for trailing vortices from the UH-1H and the CH-54. The observed separations between the two vortices (one from each rotor tip), as measured in flight, are approximately 1.06 and 0.88 times the rotor diameter for the two helicopters, respectively. Given the accuracy of the experimental measurements, these values are consistent with the uniform wing loading assumption made in Eq. 60, which would predict vortex separation equal to the rotor diameter. The values of core radii used to correct the total circulation (Eq. 61) to averaged circulation were estimated from Figs. 44 and 45a.

Comparisons between the ROTHAZ-predicted data and the flight test data presented in Figs. 42 and 43 do not account for the vortex decay process. Figure 45b provides insight as to how the CH-54 five-meter averaged circulation decays as a function of time from one run to another. The initial transient measured at the beginning of each run is believed to be related to the roll up process that becomes complete in about 6 to 10 sec. Afterwards, vortex strength decays slowly. The approximately 20 sec values chosen for correlation purposes in Figs. 42 and 43 should be reasonably representative of the initial vortex strengths at the various airspeeds. It should be noted that Fig. 45b strength data do not include instrument corrections that were applied to the data presented in earlier figures.

In conclusion, it should again be emphasized that the wake vortex data presented in this section are preliminary data from an ongoing test program (Ref. 26) and are provided only for the purpose of gaining insight into the validity of using a ROTHAZ-type model for the purpose of hazard analysis. Until a more complete set of data runs for several helicopter types are measured, it is considered that the data be used with caution. The ROTHAZ model has been left configured in the more conservative form as presented in Eq. 60 for hazard analysis purposes. As more data become available for correlation, it may be desirable to alter the mathematical model formulation as presently implemented. Therefore, as suggested for

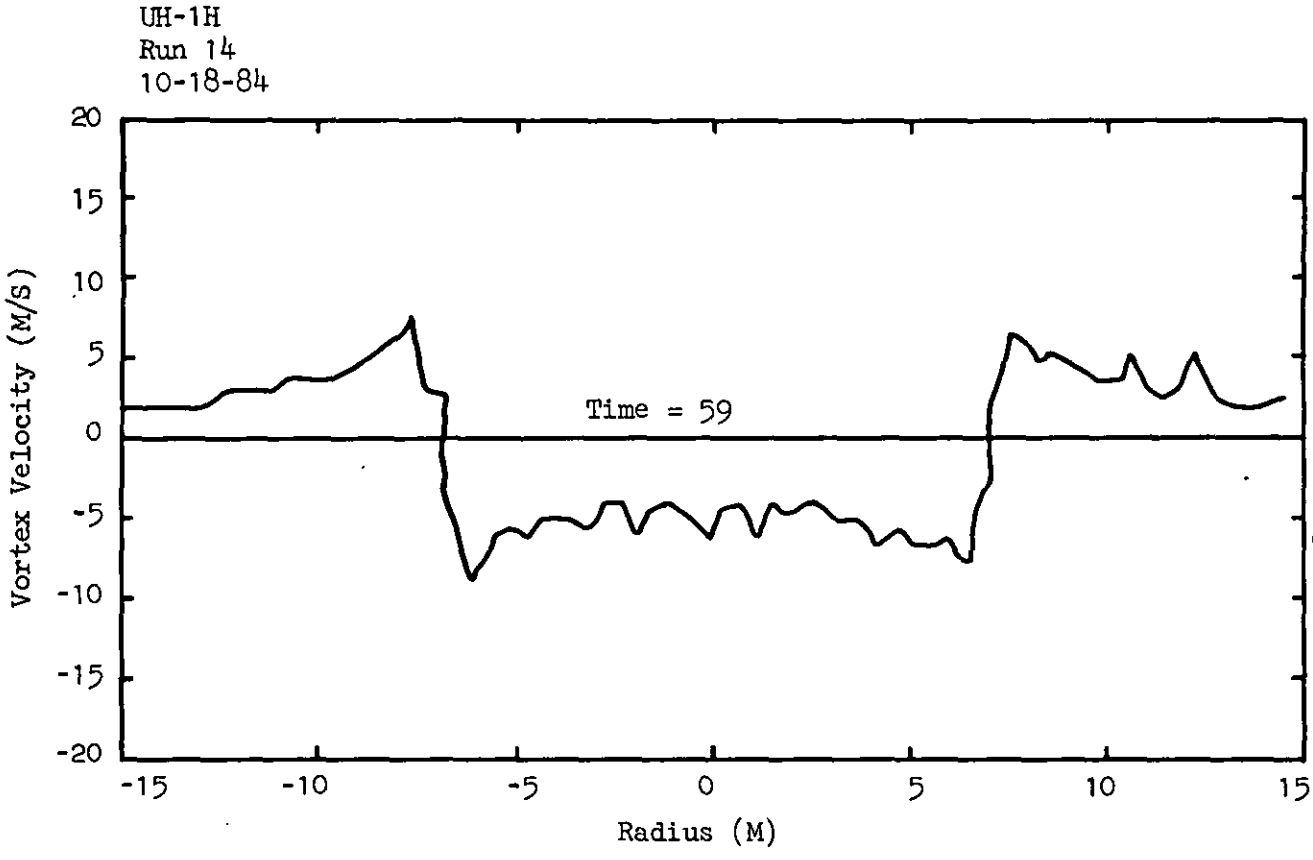

Figure 44. UH-1H Wake-Profile at Age 59 sec

(From Ref. 26)

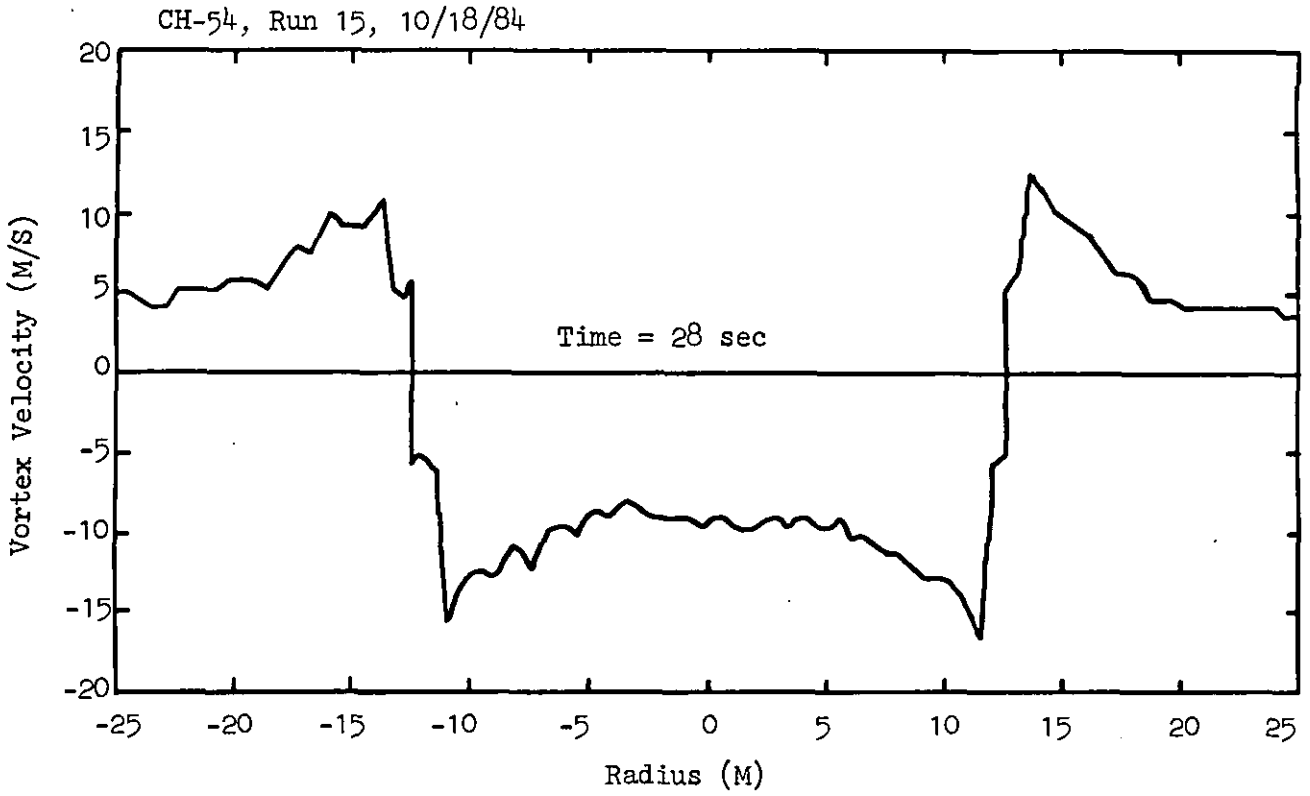

a. CH-54 Wake Profile at Age 28 sec

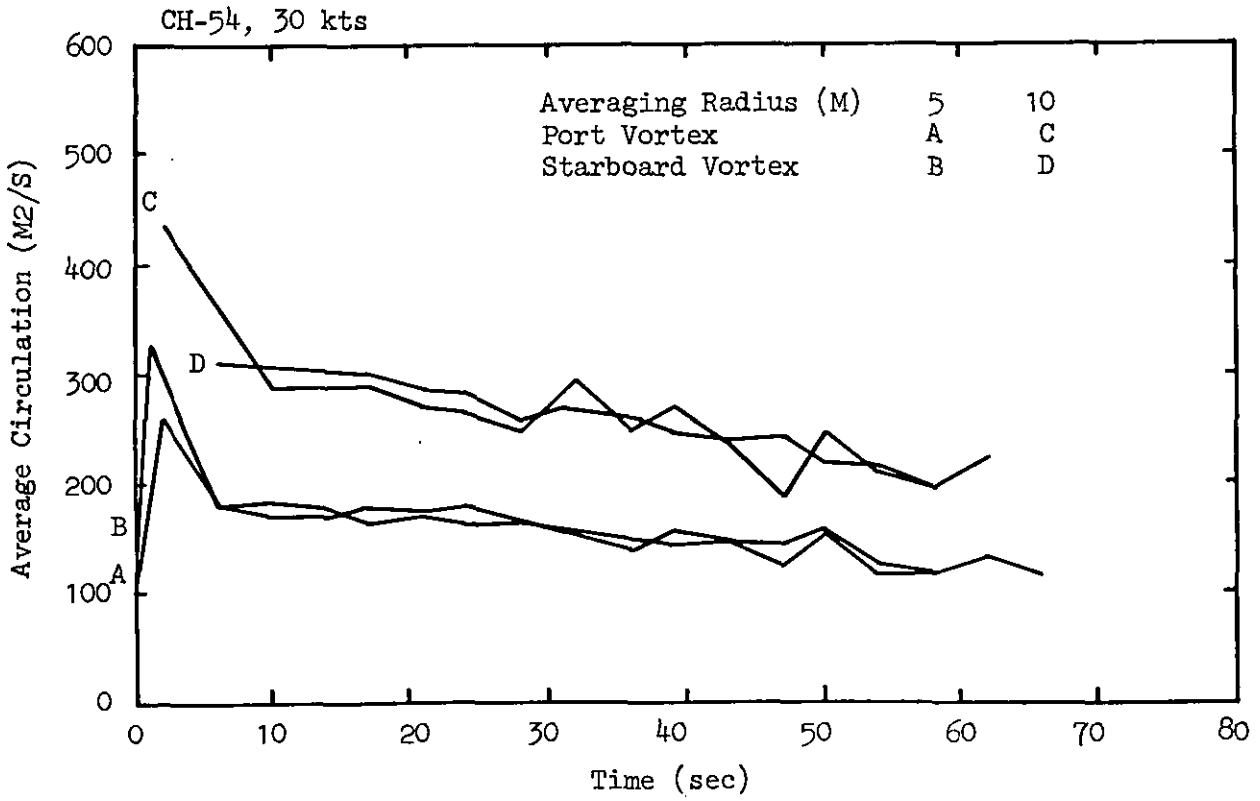

b. An Example of Vortex Strength as a Function of Time

Figure 45. CH-54 Wake Profile at Age 28 sec and an Example of Vortex Strength as a Function of Time (From Ref. 26)

the ground vortex model, the presented trailing vortex model should be used very carefully until further research and correlation work is completed.

SECTION V

DEVELOPMENT OF A HAZARD ANALYSIS METHODOLOGY

The development of a rotorwash hazard analysis methodology for the classification of hazards in relationship to their potential for damage to personnel, other rotorcraft or aircraft, vehicles, and structures is primarily a three-part process that involves:

1. Identification of potential hazards
2. Mathematical modeling of the significant hazards
3. Evaluation of the developed hazard models in the appropriate rotorcraft/hazard scenarios.

Completion of this analysis process, as described in more detail in Fig. 46, provides the information necessary to determine minimum safe distances separating the hazard generating rotorcraft of interest from personnel, various other types of vehicles, and structures that are at risk.

A. MANAGING THE ANALYSIS TASK

In conducting any study of this type, the most important task initially is to somehow bound the hazard analysis effort in order to make it more manageable. In order to accomplish this, several assumptions were made early in this analysis effort. The first assumption was that the analytical effort should concentrate on "worst offender" rotorcraft configurations only. This assumption was the result of an initial observation that analysis of "famous" or certain "popular" rotorcraft types would produce non-generalized results that would define separation standards for only a limited number of rotorcraft-scenario combinations. Separation standard requirements for new, less numerous, or less popular rotorcraft types would therefore possibly require significant additional future analysis efforts.

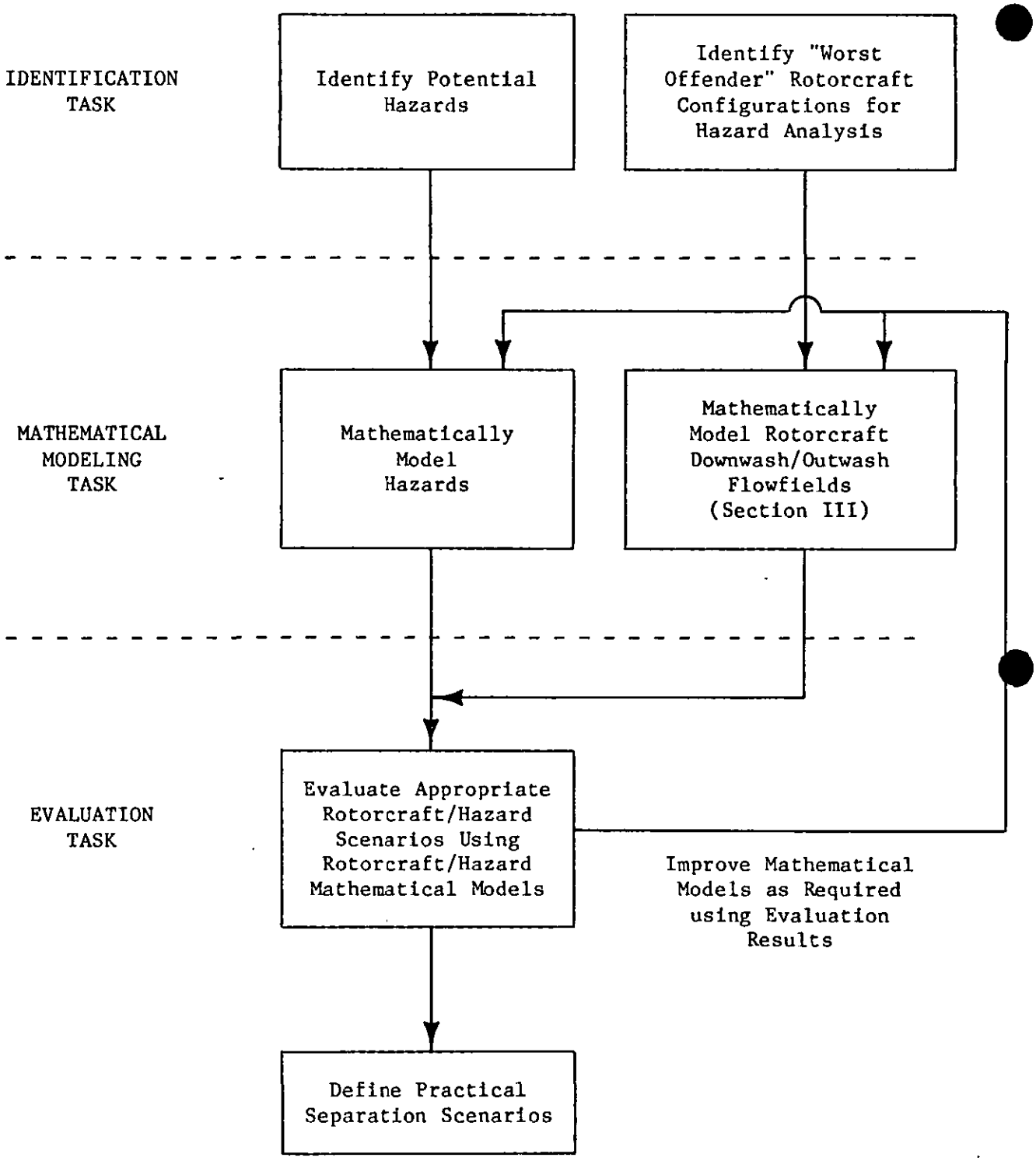

Figure 46. Hazard Analysis Methodology

A second assumption that helped in bounding the hazard analysis effort was that accidents that occurred in the past would probably be the accidents that would occur most often in the future. A list of hazards and accidents from the literature and accident data bases was therefore compiled. This list became a foundation for the majority of the hazard analysis effort.

A third assumption that was made was that proposed separation standards would be challenged, justifiably, by the FAA and particularly by the rotorcraft user community; therefore, a significant effort was made to validate wherever possible the predicted hazard analysis results with experimental data or previous accident results. This validation effort was also used to minimize requirements for safety factors on analysis results. In those areas of analysis where safety factors are required, the safety factors are clearly identified and reasoning is provided for their assigned values.

B. IDENTIFICATION OF POTENTIAL HAZARDS

The identification of the important, significant, and relevant conditions is certainly one of the most important tasks in any hazard analysis. In this rotorcraft downwash/outwash hazard analysis, primarily three sources of information were utilized in the identification process.

The first source of information that was used to identify hazards was a literature search, which was conducted simultaneously with the literature search used in the rotorcraft mathematical model development effort (Section III). Several previous hazard analysis efforts, not all applicable to civilian rotorcraft operations, were discovered and reviewed during this process. In addition, several applicable hazard analysis mathematical models were identified.

The second source of information was personal interviews. Numerous people in the civilian and military rotorcraft community (i.e., U.S. Army/Navy, rotorcraft manufacturers, rotorcraft operators, NASA, and the FAA)

were interviewed informally and asked specific questions regarding rotorwash-related hazards with which they were familiar or with which they had practical experience.

Accident data bases were the third source of information, specifically the accident data base available through the U.S. Army Safety Center at Ft. Rucker, Alabama. This accident data base provided approximately 500 descriptions of accidents occurring from January 1976 through April 1985 in which the key words "rotorwash," "downwash," and/or "outwash" were used. In general, these accident descriptions provided excellent guidance in identifying important as well as operationally and numerically significant real-world hazards that have been experienced by the largest helicopter fleet in the world, while operating in all types of environmental conditions. In summarizing the information taken from this data base, it can be stated briefly that:

1. Numerous cases of personnel injury due to flying debris were reported (i.e., eye and internal injuries requiring evacuation).

2. Rotor blade strikes on tailbooms or tunnel covers (CH-47 tandems) were numerous (independent of the number of rotor blades). In a couple of cases, these blade strikes occurred even when the blades were tied down. Drive shaft fairing, drive shaft, and main rotor blade damage was often reported. Rotorcraft during runup or shutdown were especially susceptible to these strikes.

3. Doors being blown off rotorcraft occurred very frequently (50+ cases); several cases also occurred with fixed-wing aircraft. The small helicopters (i.e., OH-58, UH-1H) were especially susceptible to this hazard. Windows and chin bubbles were often broken, and occasionally personnel were injured as a result of these accidents.

4. Damage to other fixed-wing aircraft occurred occasionally. Several cases were reported: three where a wing tip was lifted up, thereby smashing the opposite wing tip into the ground; one where a tricycle gear configuration resulted in the "aircraft" being rotated onto its tail, thereby causing tail damage; and one where there was elevator/control damage. Numerous fixed-wing aircraft and rotorcraft were reported to have been "moved" or "spun around" causing limited damage.

5. Flight (hover, air taxi, takeoff, and landing) too near other rotorcraft was the cause for numerous hard landings, some accidents, and especially overtorques by the affected rotorcraft. Formation flying was often cited as a cause, and several cases of loss of directional control (OH-58, UH-1H) were reported.

6. Accidents involving rotor blade or airframe damage (to the hazard generating rotorcraft itself) due to foreign objects (both known and unknown as to type) were, in general, too numerous to tabulate (in the hundreds). In most cases, the foreign object that struck the rotorcraft was never seen. Impact noise, poorer handling qualities, or post-flight inspection usually provided the indication that foreign object damage had occurred.

7. Examples of the types of objects being blown around and causing damage were (almost always more than one case reported):

   a. Sheet metal, corrugated metal, wood, or plastic panels (i.e., 3-ft square)

   b. Landing zone nylon/metal markers

   c. Flare/personnel parachutes

   d. Dead tree branches/brush

   e. Nylon, cloth, and plastic equipment bags as well as empty sandbags

   f. Metal landing pad planking

   g. Numerous rocks, round objects (hitting equipment, breaking glass and windshields)

   h. Maintenance stands (blown on their sides and along the ground prior to impacting other rotorcraft)

   i. Rotor blade box covers, ammunition boxes, empty 55-gallon drums.

8. Between forty and fifty cases of serious problems due to self-generated clouds of dust or dirt (brownout) or snow (whiteout) were reported where the generating rotorcraft was damaged or a hard-landing occurred. (Foreign objects, like leaves, dirt, grass, corn husks, etc., getting into rotorcraft intakes, etc., were not noted but were probably numerous under these conditions. Many hardware problems were listed with this as the assumed cause.)

9. Numerous cases were reported of tents and tarps collapsing, being picked up and blown away, or being sucked into a rotor system due to the various rotorwash effects.

10. Several camper shells were blown off pick-up trucks parked in marked parking areas next to ramps.

11. Numerous cases were reported of all types of access panel doors and driveshaft fairings being blown off, many supposedly having been secured.

The collective review of the data obtained from these three hazard identification sources resulted in the creation of a list of hazards which seemed to warrant further analytical review and study. This list of hazards is presented in Table 6.

TABLE 6

HAZARDS IDENTIFIED DURING THE INITIAL STAGES OF THE ROTORCRAFT HAZARD ANALYSIS EFFORT AS PROBABLY WARRANTING FURTHER ANALYTICAL REVIEW

1. Hazards involving personnel (i.e., overturning moments to the body as well as injury due to flying objects, such as rocks).

2. Hazards involving light airplane damage (i.e., damage due to rotation of the aircraft so as to cause wing/ground contact, control/empennage damage, and damage to doors).

3. Hazards involving other rotorcraft (i.e., rotor blade tailboom strike, door/access panel blowoff, and damage due to flying debris such as rocks).

4. Hazards related to operation in close proximity to other vehicles (i.e., automobiles) or structures.

5. Hazards related to rotorwash generated dust/garbage/debris clouds.

6. Hazards related to the nearby passage of other rotorcraft while the subject rotorcraft is on the ground or in hover with the rotor turning.

Following the construction of this list of hazards, an attempt at prioritization was made in order to better manage the modeling and analysis phase. It was hypothesized during this prioritization effort that only a few key hazards would truly define and quantify any subsequently proposed practical separation standards. The goal of the prioritization effort, while not explicitly obtainable, was therefore to define, prioritize, and analyze first those hazards that were believed to be the most important in defining and quantifying the final recommended (practical) separation standards. It was clearly recognized during this process that time and budget resources did not provide the opportunity to analyze in detail all potentially important rotorcraft/hazard topics or scenario combinations. The specific hazard topics and scenarios that were analyzed as a result of this somewhat iterative prioritization effort are presented in the next section of this report.

C. IDENTIFICATION OF "WORST OFFENDER" ROTORCRAFT CONFIGURATIONS

Early in the hazard identification/management phase of the analysis effort, it became apparent that only "worst offender" rotorcraft configurations could be analyzed. This limitation resulted from time/money resource constraints and a requirement that generic separation standards be produced instead of separation standards associated too closely with specific rotorcraft presently in commercial/military use. The identification of "worst offender" rotorcraft configurations was obtained after several iterations by developing the graph presented in Fig. 47. This figure compares the parameters of disc loading (DL) and rotor radius (R) for all of the specific rotorcraft types tabulated in Appendix A. Disc loading,

$$DL = \frac{\text{Maximum Gross Weight}}{\pi R^2} = \frac{GW}{\pi R^2} \qquad (62)$$

was chosen as a parameter for evaluation, because the induced velocity (v_i) or downwash of a rotorcraft, the hazard in this study, is a direct

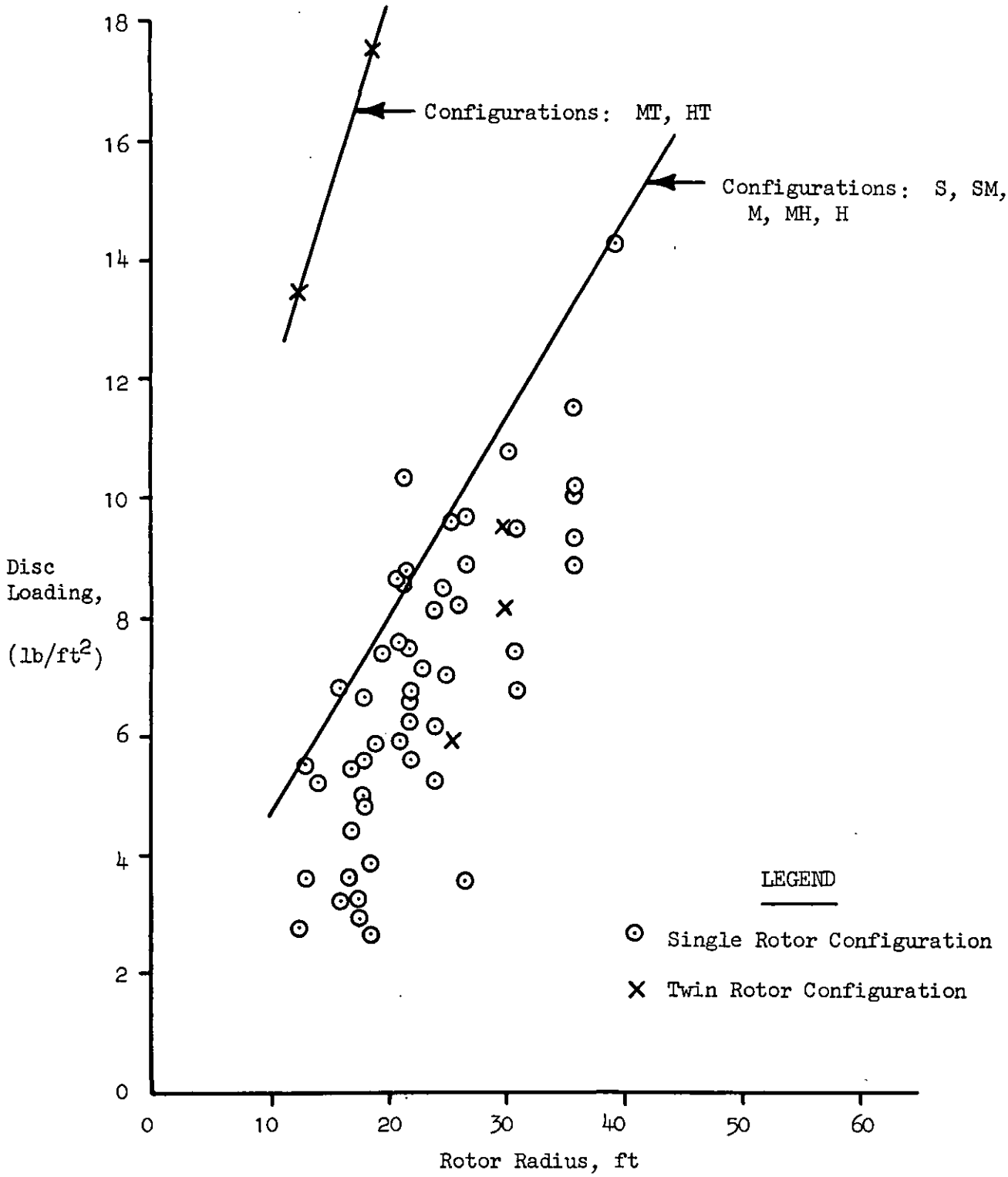

Figure 47. The Relationship of Rotorcraft Disc Loading to Rotor Radius From an Historical Perspective as Defined by Present and Announced Future Rotorcraft Designs

function of the thrust (or gross weight plus download in hover) as distributed over the surface area swept out by the rotor.

$$v_i = \sqrt{\frac{2DL}{\rho_A}} \text{ (ft/sec)} \qquad (63)$$

Rotor radius was chosen as the other plotting parameter, because this parameter is the predominant physical scaling characteristic which impacts the definition of **rotorcraft separation standards.**

As can be seen in Fig. 47, a line exists for the relationship of interest below which most (if not all) old, modern, and known future rotorcraft types can be plotted. The imaginary rotorcraft that can be plotted along this upper limit line are assumed in this analysis to be the family of "worst offenders." This line, by taking into account announced future rotorcraft types and several research rotorcraft under development, should more than adequately account for the effects of advanced technology in the development of higher disc loading rotorcraft through at least the year 2000. In reducing the "worst offender" line to specific "worst offender" rotorcraft configurations for analysis purposes, it was decided to define seven specific configurations. These "worst offender" rotorcraft configurations, as defined in detail for use with the Section III rotorwash flowfield models, are described in Table 7. Throughout the analysis, unless otherwise noted, ambient wind conditions are assumed to be 0 kt, and the atmospheric density (ρ_A) is assumed to be 0.0023769 slugs/ft^3 (this value of ρ_A is chosen because most rotorcraft generally perform best at or near sea level conditions).

As an aid to simplifying the analysis effort, the two twin-rotor configurations, "MT" and "HT," were evaluated, and they were "equivalenced" with respect to hazards with their corresponding single-main-rotor configurations. This equivalencing task was accomplished by calculating the mean and the peak velocity profiles of all seven "worst offender" configurations and then determining which single-main-rotor profiles were approximately equal in strength with the two twin-rotor interaction plane

TABLE 7

"WORST OFFENDER" ROTORCRAFT CONFIGURATIONS

Configuration Parameters	Configuration Identifier						
	S	SM	M	MH	H	MT	HT
Number of Rotors	1	1	1	1	1	2	2
Rotor Radius (ft)	15.0	20.0	25.0	30.0	40.0	12.5	19.0
Maximum Gross Weight (lb)	4453	10053	18849	31950	73388	14000	40000
Approximate Fuselage Download (percent)	1.5	1.5	2.5	3.5	5.0	13.0	10.0
Rotor Height Above Ground (ft)	10.0	12.5	15.0	17.5	20.0	12.5	20.1
Disk Loading (PSF)	6.3	8.0	9.6	11.3	14.6	14.3	17.6
Rotor Separation (ft)	--	--	--	--	--	32.2	46.5

profiles. (This profile is always the strongest profile for the twin-rotor configuration.) In the case of the "MT" configuration, the approximately equivalent single-main-rotor configuration was the "M" configuration. For the "HT" configuration, the approximately equivalent configuration was the "H" configuration. (This was a conservative equivalence, since a 35-ft radius configuration would have been a closer match if this configuration had been analyzed.) An equivalency for the CH-47D interaction plane profile (the new U.S. Army heavy lifter) was also calculated to conservatively compare with the "H" class single-main-rotor configuration. The results that are presented in the remainder of this report will therefore be assumed to apply for twin-rotor configurations according to these equivalences whenever notations to the "M" and "H" single-main-rotor configurations are specifically mentioned.

D. MATHEMATICAL MODELING AND EVALUATION OF IMPORTANT ROTORCRAFT/HAZARD SCENARIOS

With the completion of the analysis management tasks, the identification of important hazards, and the identification of "worst offender" rotorcraft configurations, it was possible to initiate the mathematical modeling and subsequent hazard evaluation tasks (Fig. 46). The mathematical modeling task provides the tools to evaluate minimum separation standards, and the evaluation task quantifies these standards into practical, useable criteria (e.g., feet, percent, rotor radii). As is shown by the feedback loop in Fig. 46, these modeling and evaluation tasks are iterative and by nature inexact due to the endless number of possible scenarios. Therefore, the development of practical, useable separation standards is not an exact science. More discussion will be presented on this subject both in the development of safety factors and in the development of the recommended separation requirements.

Throughout the remainder of this section and Section VI, the main emphasis of the work presented will be on the hazard modeling and evaluation process. In each section, the particular hazard of interest will be:

1. Introduced

2. Described and modeled

3. Validated wherever possible with experimental or accident data

4. Evaluated in appropriate scenarios (safety factors summarized)

5. Summarized.

Detailed discussion on recommended separation requirements that result from an integration of these various hazard analysis efforts will be deferred until Section VII. No attempt has been made in the next section to present the analyzed hazards in any particular order of importance. Therefore, the reader should not assume that the analyses of the individual hazards are organized in any particular order so as to present, for example, the greatest to the least potential hazard.

SECTION VI

ANALYSIS OF ROTORWASH RELATED HAZARDS

A. INTRODUCTION

This section describes the approach, methods, and working equations required to implement the rotorwash-related hazard models developed for this study. These models are designed to be used as predictive tools in estimating and classifying potential downwash and wake hazard conditions as influenced by the flight regime and the configuration of the rotorcraft of interest. The outputs from these hazard models are used to define minimum safe distances among various rotorcraft of interest, various classifications of personnel, and other aircraft, structures, or vehicles. The models presented are developed with emphasis on rotorcraft operations in close proximity to the ground. The mathematical models that have been developed for estimating the velocity fields associated with each type of rotorwash flowfield are presented in detail in Section III.

This section also describes the safety factors that have been developed with the hazard analysis models in order to insure that reasonable uncertainties are accounted for in the hazard prediction analysis process. These analytical modeling uncertainties exist due primarily to two factors:

1. The predictive accuracy of the downwash/outwash flow models (Section III) used in conjunction with the hazard models (i.e., due to wind and piloting technique).

2. The hazard models themselves due to a lack of pertinent experimental data or actual documented accident data associated with the hazard of interest which can be used in correlating the hazard model.

In situations where use of a safety factor is deemed to be unreliable or where a refined estimate could reduce the safety factor significantly, a recommendation for further research is specified along with a description

of the type of experiment that is needed (see Section VIII for this summary).

Validation of the hazard models presented in this report is provided wherever possible through correlation with available flight test, model, or previous accident data. The most extensive hazard correlation analysis that is provided is associated with the wall jet model in both the single- and twin-rotor configurations. Data used in this correlation analysis comes primarily from flight test evaluations of the Sikorsky CH-53E, the Bell XV-15, and the Sikorsky S-61 (SH-3).

B. ROTORWASH OVERTURNING FORCE AND MOMENT EFFECTS ON PERSONNEL

In the development of rotorcraft separation standards, the most important hazards to consider are those which directly involve the safety and general welfare of people (secondarily would be the safety and welfare of certain animals). Unlike buildings and equipment that can be repaired or replaced if damaged, a person (or animal) who sustains serious injury or who dies as a result of a downwash-related hazard precipitates a situation that may never be fully rectified, even in a court of law. Military research into personnel-related hazards has focused primarily on quantifying the requirements and developing regulations for the use of protective gear. This proceeds from the assumption made by the military that personnel working in the rotorcraft downwash environment will receive at least some special hazard environment training. This research has, in addition, helped to quantify the parameters that are associated with the prediction of overturning forces and moments on personnel. This subject will be the major topic of discussion in this subsection.

Only limited military research has been conducted in order to define what can be considered comfortable and uncomfortable to a person who is working while fully immersed in a rotorwash flowfield. Unfortunately, but understandably, this research has not seriously examined the civilian side of the hazard problem; therefore, minimal work has been conducted to quantify what is unpleasant, uncomfortable, or dangerous to the untrained and

therefore unsuspecting person or child who is suddenly fully or partially immersed in a rotorwash flowfield. Even less quantitative information exists to answer questions about what would happen to a person who is standing in or passing through such a hazard environment while wearing a hat, or carrying a purse or briefcase, or "towing" a **startled and scared child.**

While understandably not complete, the analysis presented in this section is nevertheless provided in order to attempt to answer some of the questions posed above; recommendations for further research work are provided in Section VIII. The proposed additional work should provide information that will greatly enhance the data base and improve quantification of the safety factors that are associated with the presented analyses. This should, in turn, lead to a better understanding of the rotorwash hazard potential and to the eventual minimization of that hazard potential.

1. Background and Literature References

Personnel immersed in the hover downwash/outwash flowfield are affected by a combination of factors such as the pressure forces generated by the horizontal velocity profile, the height of the forces above ground, the pulsating nature of the forces, and the overturning moments that are subsequently exerted. It is difficult to analyze or to assess the direct effects of velocity data on personnel for two reasons: (1) the velocity varies drastically with height and (2) the dynamic pressure created by the downwash or outwash is a function of the velocity squared. In comparing data among flight conditions or comparing data with other rotorcraft, the variation of forces is far more significant (and meaningful from a hazard standpoint) than the variation of velocity. Additionally, the force data for various altitudes and gross weights generally correlate better than velocity data. This results from the fact that the calculated force data somewhat filters variations in the measured velocity-height profile; whereas, the velocity data can only be compared directly for each corresponding height position.

Hazardous levels for forces or moments on personnel are easily calculated mathematically. Significant procedural problems do arise, however, when conducting the analysis itself. The first problem that must be resolved is associated with choosing the "appropriate" velocity profile to convert to dynamic pressure. As has been mentioned earlier, the downwash/outwash flowfield of a rotorcraft is not steady flow by any stretch of the imagination. However, the choice for conversion of the experimentally measured peak velocity profiles, instead of statistically measured mean velocity profiles, might be considered by some experimenters to be overly conservative.

A study of the literature (i.e., Refs. 11, 12, and 24) indicates that the use of the peak velocity profile in the calculation of overturning forces and moments and in the quantification of a safety standard is the correct choice. Hazardous overturning forces and moments that are associated with rotorcraft might be more appropriately entitled "destabilizing" forces and moments due to their highly oscillatory nature. In most of the literature, commentary by the authors refers to the personnel hazard as one where the forces on the human body eventually become large and oscillatory. At that point, personnel can no longer anticipate the body positioning required to move about and work safely without occasionally and unexpectedly being knocked down or overturned. This type of standard for quantification of limiting forces and moments becomes one that is quite different from that which might be set for simply overcoming forces and moments while in a fixed body position or for avoiding being knocked down while moving directly outward to escape a potentially hazardous outwash flowfield.

Two laboratory experiments have been conducted in order to attempt the quantification of limiting values for overturning forces and moments. The results of these experiments are presented in Refs. 11 and 24. In Ref. 24, test results are reported which quantify the level of unexpected uniform pressure distribution that would be required to knock a person over. These results indicate that a sudden change in force over 400 msec will cause at least limited disorientation and unbalance in a person when the peak uniform velocity profile creating the force is greater than

87 ft/sec (51 kt). A uniform peak velocity profile of greater than 126 ft/sec (75 kt) was evaluated and determined to be sufficient to instantaneously unbalance and knock over a standing or walking man. Since the work reported in Ref. 24 was an evaluation of a hazard that might occur following the loss of airliner cabin pressurization, it cannot be considered totally applicable to rotorcraft. As pointed out in that reference, "considerable judgment is necessary to successfully extend the experimental data beyond the limits for which it was intended." The data, however lacking, are nevertheless fully documented and referenceable.

Reference 11 provides a second source of experimental data to aid in the effort to quantify practical limiting overturning forces and moments; however, before discussing this experiment, it is important to depart briefly from the subject to discuss another important factor. As mentioned previously, the first problem in the analysis process involved the justification for using mean or peak velocity profile data to calculate forces. A second problem, and perhaps an even more imposing one in the evaluation process, is the establishment of personnel criteria, i.e., what size, weight, and strength percentile is to be used to model a human being for evaluating the limiting overturning forces and moments. Clearly, the physiques of an average 7-year-old child, a 25-year-old 5 ft 6 inch woman, and a professional football player are vastly different, yet they are intimately connected with the ability of each individual to overcome rotorwash-generated forces and moments. The experimental data presented in Ref. 11 attempt to address this second problem to a limited extent for the military population expected to be actively involved in operational situations involving potentially hazardous rotorwash flowfields.

Laboratory tests, as discussed in Ref. 11, were conducted for the purpose of indirectly estimating the test subjects' abilities to work against rotorwash generated wind forces. Each participant was tested in order to determine how much horizontal force could be pulled using a test fixture that consisted of a torso harness that distributed a test load across the hips and chest to a line tied 3 ft above ground level (AGL) and a weight that was lifted by the forward movement of the subject. Table 8 contains a list of subjects weights and heights. Figure 48 presents a bar chart

TABLE 8

HEIGHT AND WEIGHT OF SUBJECTS USED
DURING THE QUALITATIVE DOWNWASH SURVEYS

Subject No.	Height		Weight	
	Inches	Percentile	Pounds	Percentile
1	67	10th	133	2nd
2	73	90th	150	15th
3	74	95th	171	50th
4	74	95th	220	99th

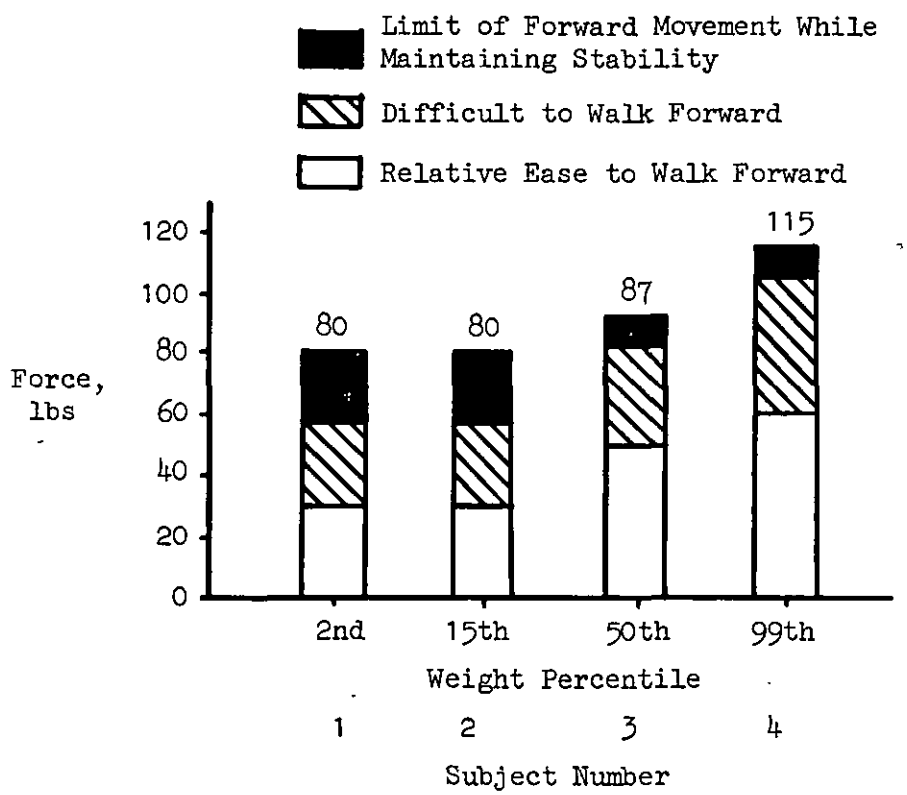

Figure 48. Capabilities of Test Subjects to Walk or Move Forward Under Various Amounts of Horizontal Restraint Loads Applied at a Position 3 ft AGL

that indicates the amount of pull force that each individual could exert. The pull test data does not, of course, duplicate the dynamically applied downwash forces. However, dynamic forces were applied during the tests, since the slightest forward or reverse movement of the body or trunk caused the weight to move up or down, thereby requiring the subject to respond dynamically to the load acceleration. The limit of postural stability was taken to be the point at which stability could no longer be maintained with some forward progress. These postural stability limits are represented by the top of the black bar in Fig. 48.

Results from this laboratory experiment were used in the rotorwash evaluations of both the Sikorsky CH-53E and the Bell XV-15 (Refs. 11 and 12). Considerable qualitative comment was also obtained from the test subjects which aids in quantifying acceptable levels of rotorwash for civilian operations. More will be said with respect to this subject in a later subsection.

2. Mathematical Modeling of Personnel

While direct measurement of overturning forces and moments from the experiments in Refs. 11 and 24 would have been ideal, it was, nevertheless, totally impractical. Therefore, "experimental" force and moment calculations must be derived indirectly using human physical dimensions, human aerodynamic coefficients, and experimentally measured mean or peak velocity profile information. In returning to the results of the first experiment (Ref. 24), it is possible to convert the 87- and 126-ft/sec overturning related velocity values into forces and moments. The "standardized" man that was assumed in this experiment had a drag coefficient (C_D) of 1.0 and was 6 ft tall and 1.1 ft wide. Using this model, the velocities convert to 60 lbs of force for purposes of unbalance and 125 lbs of force for purposes of disorientation. This converts further to moments of approximately 180 and 375 ft-lb, respectively. In comparing the forces with those presented in Fig. 48, the calculated values seem to be quite reasonable and certainly help to provide a more documentable basis for the purpose of further evaluation.

The human mathematical model that has been developed for this study (and incorporated in the ROTHAZ program of Appendix C) relies heavily upon the previously described work. Compared to the mathematical model used in Refs. 11, 12, and 24 that assumed a "standardized" person to be 6 ft tall, 1.1 ft wide, with a C_D of 1.0, other sources (i.e., Ref. 16) have assumed a "standardized" person to be only 1.0 ft wide. Hoerner, Ref. 27, points out that values for C_D can vary significantly among people, from slightly less than 1.0 to up to 1.3, especially for those wearing certain types of (bulkier) clothing. Therefore, two different "standardized" persons are used in conducting the civilian related hazard analysis reported here. These "persons" can be summarized below:

Parameter	Person Type L	Person Type S
Height, ft	6.0	4.0
Width, ft	1.1	0.8
C_D, ND	1.1	1.1

where the large or "L"-sized person is similar to those previously discussed, and the small or "S"-sized person is representative of a 7-year-old child of approximately 60 lb. A C_D value of 1.1 (not 1.0) is utilized as a limited safety factor for both sizes in the hazard evaluation process (but not in the correlation process with Refs. 11 and 12) in order to help to account for the previously discussed uncertainties inherent with the evaluation of unsuspecting civilian personnel.

Evaluations using the personnel models described above are made by first calculating the peak dynamic pressure at 0.5-ft increments up to the maximum height of the subject (Fig. 49). This can be expressed mathematically by evaluating the equation

$$Q_{peak} = \frac{1}{2} \rho_A V_{peak}^2 \qquad (64)$$

where

Q_{peak} = peak velocity dynamic pressure, lb/ft^2

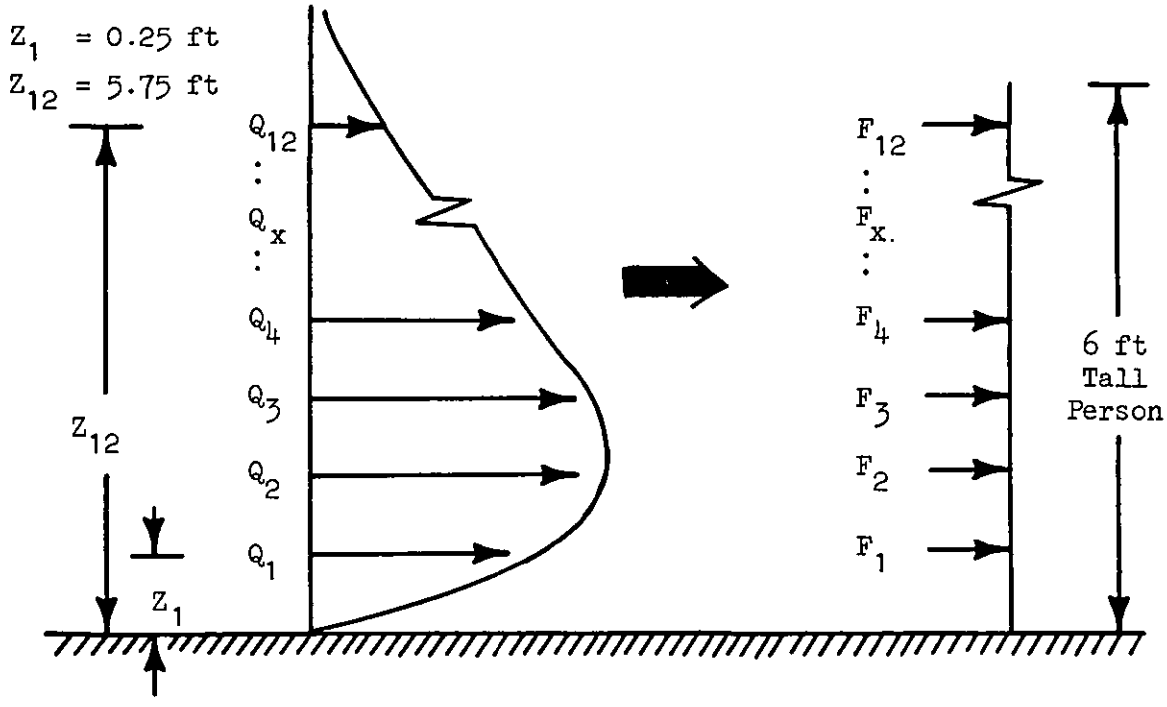

STEPS:

(1) Calculate the dynamic pressure at twelve vertical stations.

(2) Use the dynamic pressure to calculate twelve force values (multiply each Q_x value by the projected body surface area at that Z_x value, in this case 0.5 ft by 1.1 ft).

(3) Sum the twelve individual F_x values in order to obtain the total force (F_{peak}).

(4) Multiply each F_x value by its corresponding Z_x value, and sum the incremental overturning moments to obtain the total peak moment (M_{peak}).

Figure 49. Graphical Presentation of Overturning Force and Moment Calculation Procedures

and

ρ_A = atmospheric density, slugs/ft^3

V_{peak} = peak profile velocity at the point of interest, ft/sec

For an "L"-sized person, these calculations are made at twelve vertical stations (Z_x) beginning at 0.25 ft and continuing in 0.5-ft increments up to 5.75 ft. The calculations of total force and moment are then made by summing calculations made at the individual stations (Z_x).

$$F_{peak} = \sum_{x=1}^{12} (Q_{peak_x}) (C_D)(W_h)(\Delta H) \quad (65)$$

$$M_{peak} = \sum_{x=1}^{12} (Q_{peak_x})(Z_x)(C_D)(W_h)(\Delta H) \quad (66)$$

where

C_D = drag coefficient, ND

W_h = width of the person, ft

ΔH = incremental vertical height for evaluation (which in this case is 0.5 ft)

In the case of the "S"-sized person, the same approach is used; however, the value of x is evaluated at only eight vertical stations (ending at Z_x = 3.75 ft).

With a definition of the human mathematical model now completed and with use of the Section III mathematical models, it is now possible to evaluate the hazard prediction method. Before this is done, however, it is important to first correlate the output from the mathematical model with flight test data for the purpose of validating the analytical approach.

3. Quantitative Mathematical Model Validation with Experimental Data

Experimental flight test data was identified from several sources for validation of the overturning force and moment mathematical model. This data base includes data for the CH-53E (Ref. 11), RH-53D (Ref. 11), XV-15 (Ref. 12), CL-84 (Refs. 15, 16, and 20), SH-3 (Ref. 15, 16, and 21), and the HLH rotor (Ref. 13). In an effort to provide continuity with other correlation data used in this report and with the validation of the mathematical modeling (as reported in Section IV), the data from the CH-53E, XV-15, and SH-3 have been used for the correlation and presentation of results.

Correlation data for CH-53E overturning forces are presented in Figs. 50 through 52 for the gross weights of 45,000, 56,000, and 70,000 lbs, respectively. Prediction of the force distribution as a function of radial position from the peak force outward is quite good at all three gross weights at the rotor height of 37 ft. Force prediction from approximately 1.4 times the rotor radius back to the center of the rotor is overpredicted. This particular inaccuracy is not considered significantly important in the analysis, however, since this region is so close to the rotor (or under the rotor). As was noted in Section III, the mathematical model for this transition region (prior to formation of the wall jet) was considerably and conservatively simplified. At the rotor heights of 77 and 117 ft, the mathematical model clearly overpredicts the experimentally measured force. This results both from the overprediction of the maximum peak velocity value on the profile and from the prediction of the profile itself being fuller at heights between the maximum velocity point and the 6-ft height of the modeled human being. It is interesting to note that the predicted discrepancy is considerably less at the 70,000 lb (Fig. 52), or maximum gross weight condition, than it is at the much lower gross weights for the CH-53E (Figs. 50 and 51). This observation clearly indicates that the strength and shape of the experimentally measured flight test peak velocity profile varies differently with altitude for the CH-53E at various disc loadings. The cause for this phenomenon is not clearly understood at this time. Fortunately, the

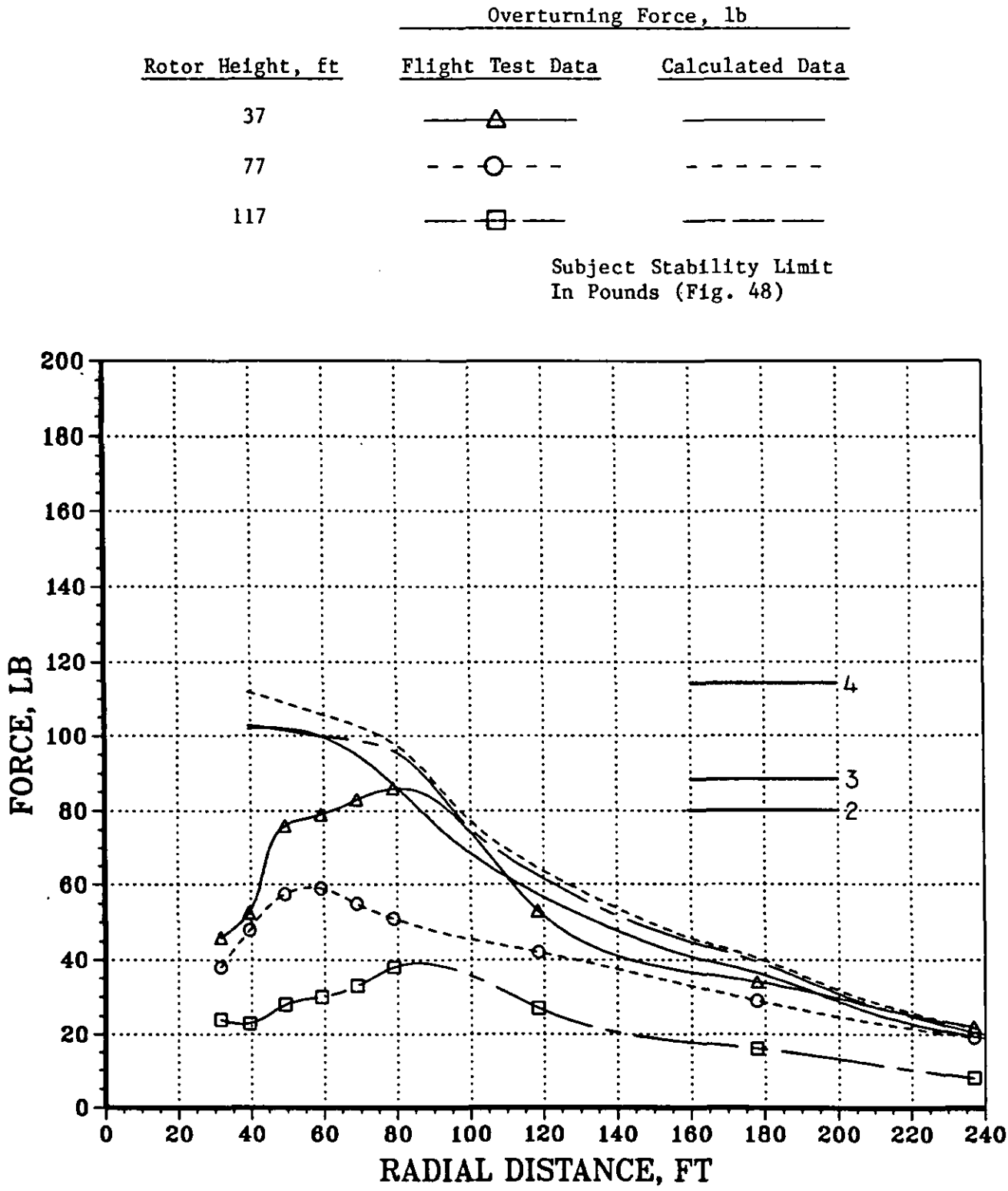

Figure 50. Correlation of Horizontal Downwash Forces on Test Subjects Plotted as a Function of Distance from the Rotor Center During Hover at 45000 lb Gross Weight

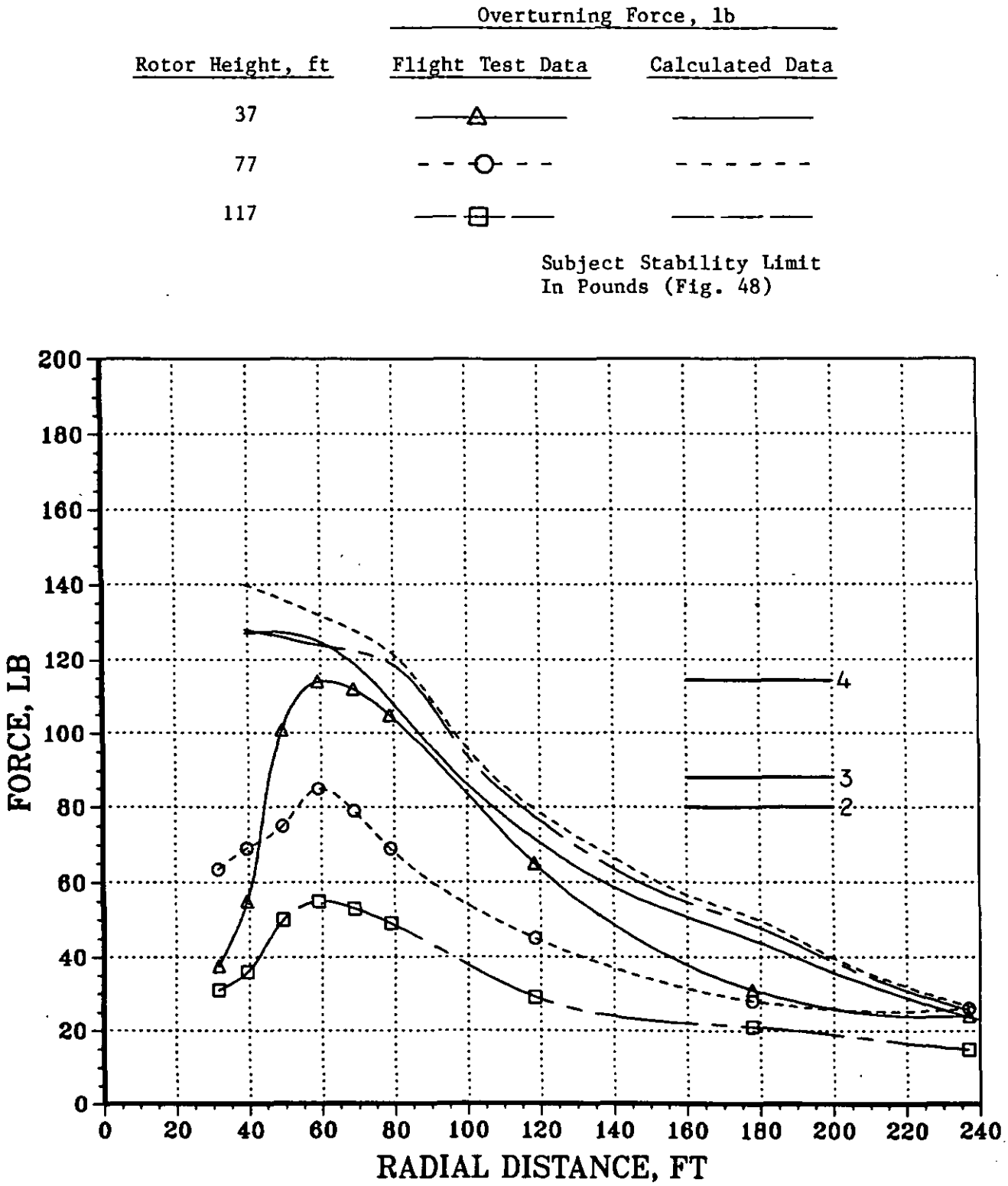

Figure 51. Correlation of Horizontal Downwash Forces on Test Subjects Plotted as a Function of Distance from the Rotor Center During Hover at 56000 lb Gross Weight

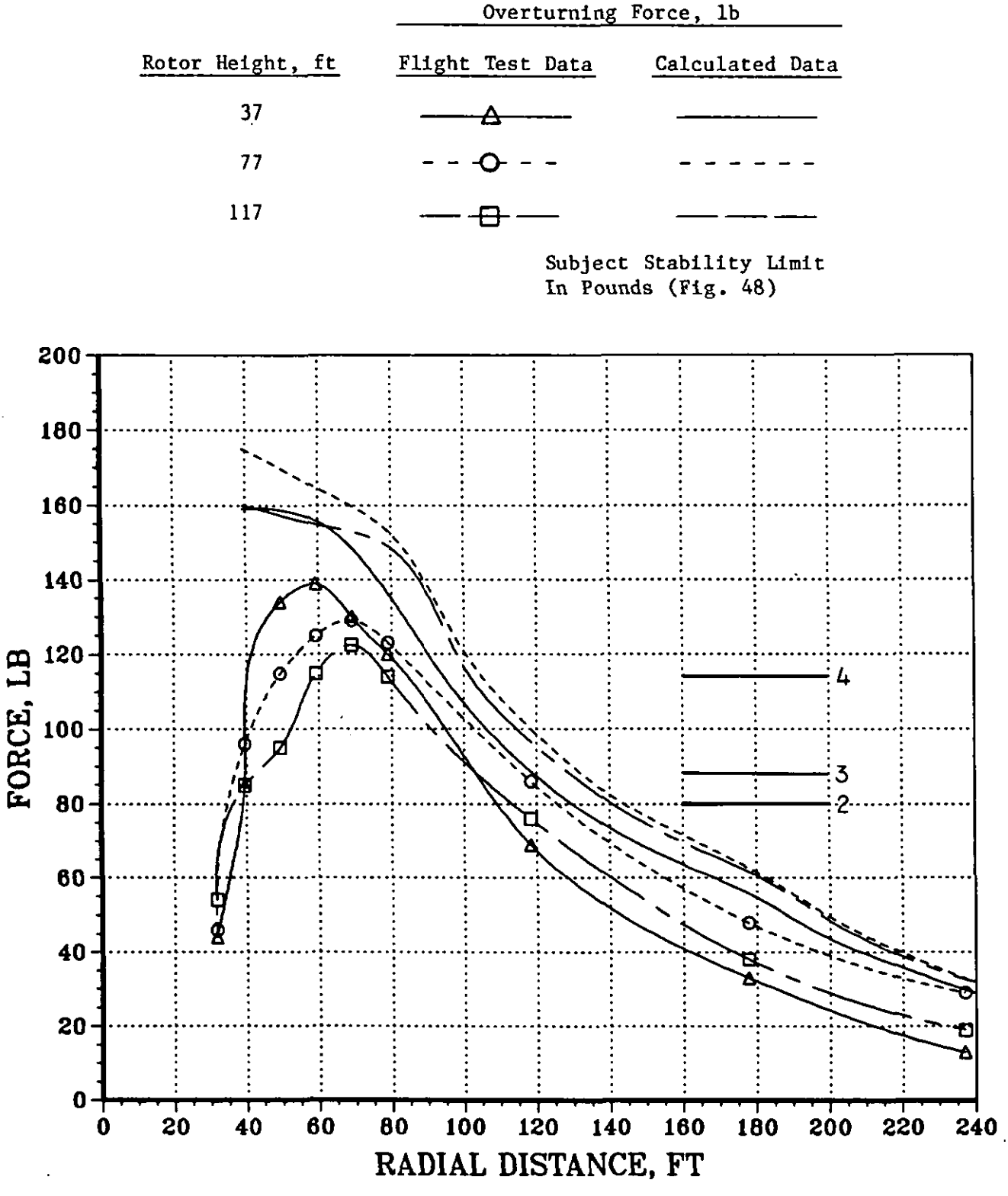

Figure 52. Correlation of Horizontal Downwash Forces on Test Subjects Plotted as a Function of Distance from the Rotor Center During Hover at 70000 lb Gross Weight

mathematical model, as empirically derived for prediction of the peak velocity profile, accounts for this worst case condition when correlated with the more important 70,000 lb maximum gross weight.

The effect of wind on the peak force generated by the CH-53E was, unfortunately, measured and presented in Ref. 11 only on the less hazardous upwind side of the CH-53E for one radial position at gross weights of 45,000 and 56,000 lbs. Correlation with this less critical azimuth is presented for the mathematical model in Figs. 53 and 54. Since the exact wind velocity was not known (Ref. 11 gives 5 to 9 kt), an assumption of 7 kt was made for correlation purposes. Results for both gross weights show fairly good correlation at the 37-ft rotor height. Correlation is poor at the 77- and 117-ft rotor heights as would be expected (see Figs. 50 through 52). Had a low wind speed value of 5 kt been used for correlation at the 37-ft height, correlation would have been improved slightly.

Experimentally measured forces for the XV-15 (Ref. 12) are presented at a rotor height of 37.5 ft at radial azimuths of 270 deg (single-rotor radial) and 0 and 180 deg (interaction plane) in Figs. 55 through 57, respectively. In general, correlation of this data indicates a tendency for the mathematical model to slightly overpredict the experimentally measured force data.

The effect of ambient winds on the peak force generated by the XV-15 along the 270-deg radial was measured in hover at 24.5 ft and presented in Ref. 12 for both the upwind and downwind sides of the XV-15 at the radial station of 15.6 ft. While these data essentially represent only a single data point, it is nevertheless another limited calibration of the hazard analysis mathematical model. Results from the flight test indicate that the variation of the peak force at 15.6 ft was 11 lbs (or 49 lbs total) above the no-wind value of approximately 38 lbs on the downwind side of the XV-15 at windspeeds of 6 to 8 kt. On the upwind side, the measured peak force was approximately 2 lb lower (or 36 lb). The almost insignificant reduction on the upwind side due to wind, when compared with the CH-53E data as measured on the upwind side, does not make good sense. Calculated data indicate that the variation should be an increase to

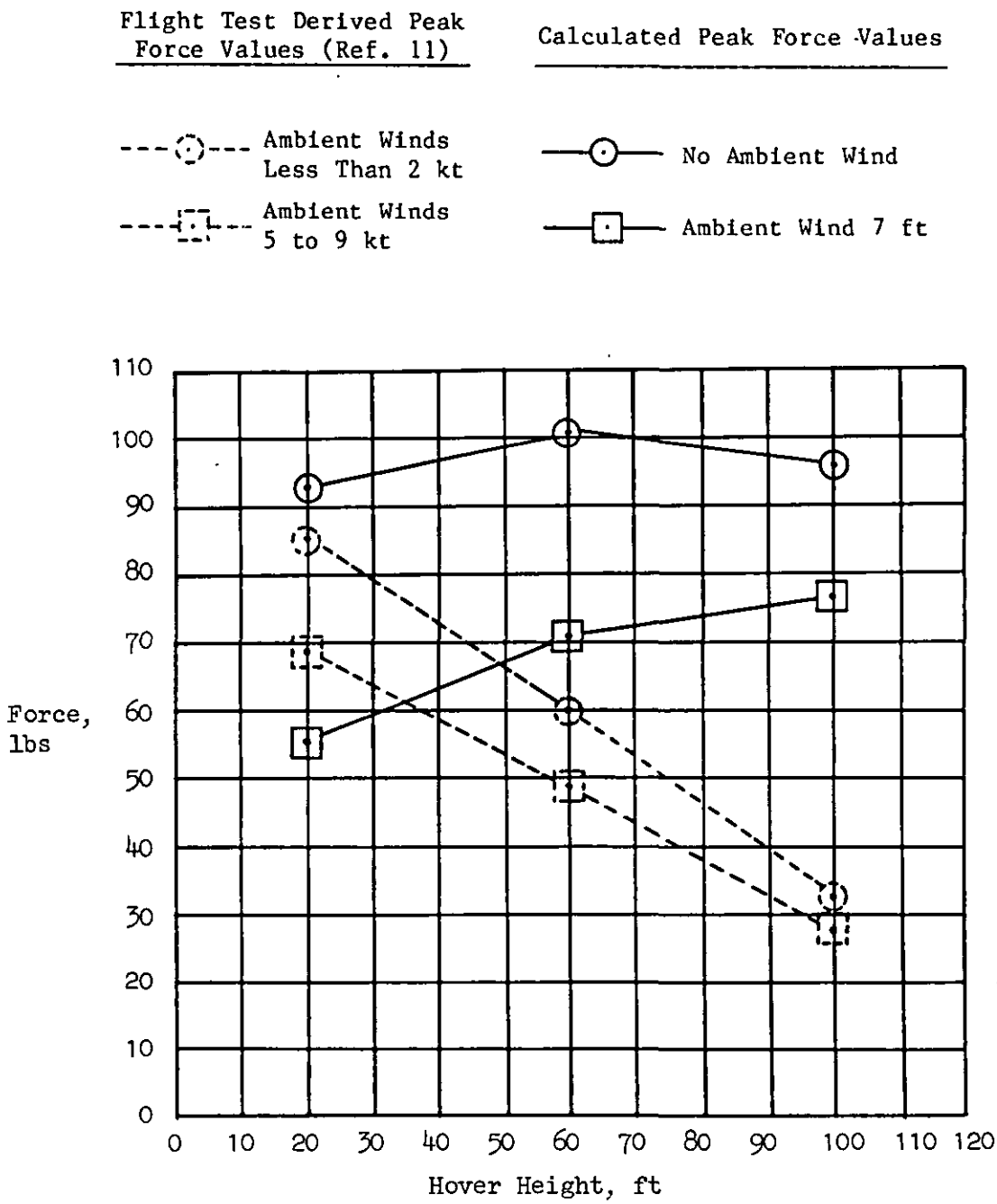

Figure 53. Correlation of Maximum Downwash Forces Plotted as a Function of Hover Height During a 45000 lb Gross Weight Hover as Measured at an Upwind Position During Two Ambient Wind Conditions

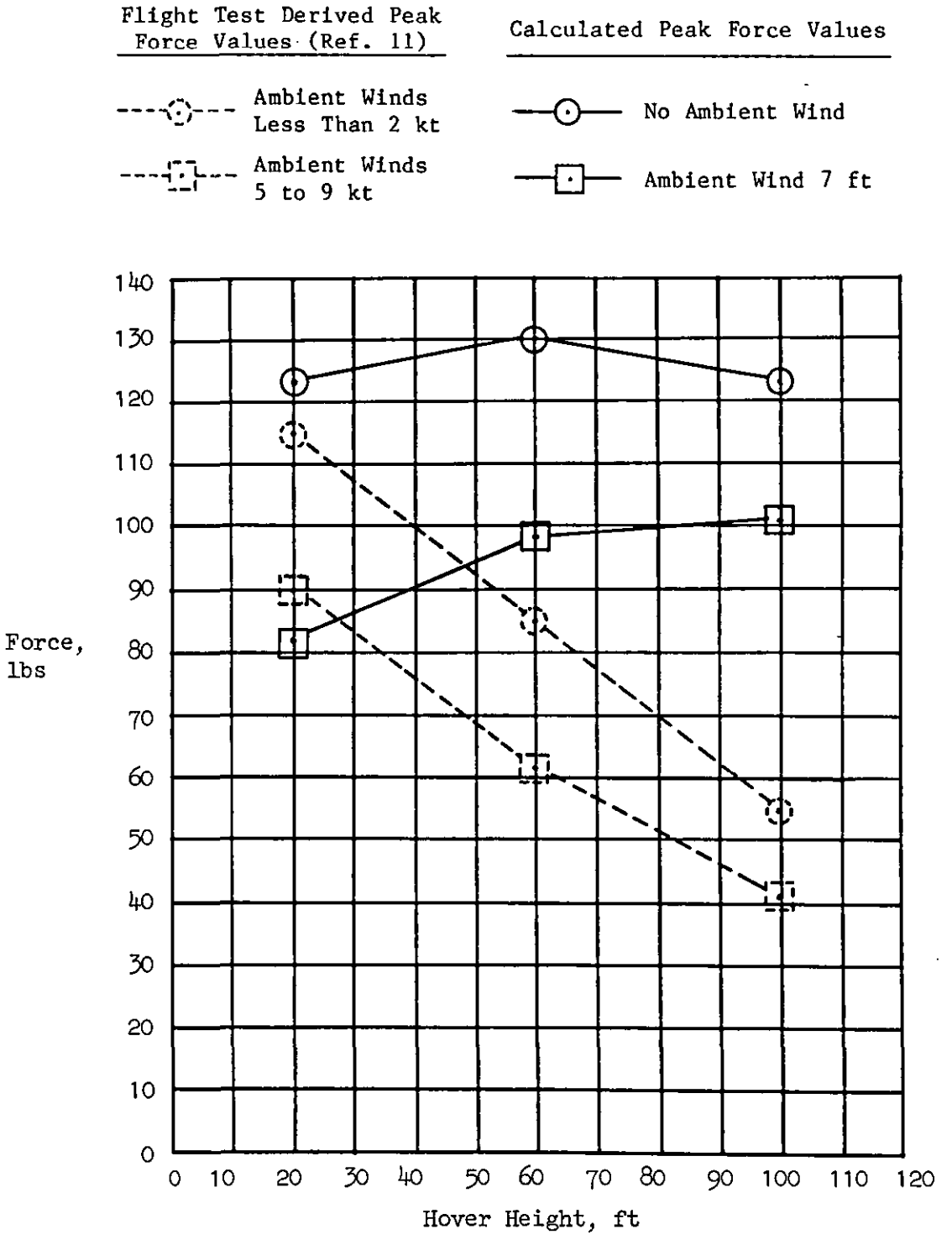

Figure 54. Correlation of Maximum Downwash Forces Plotted as a Function of Hover Height During a 56000 lb Gross Weight Hover as Measured at an Upwind Position During Two Ambient Wind Conditions

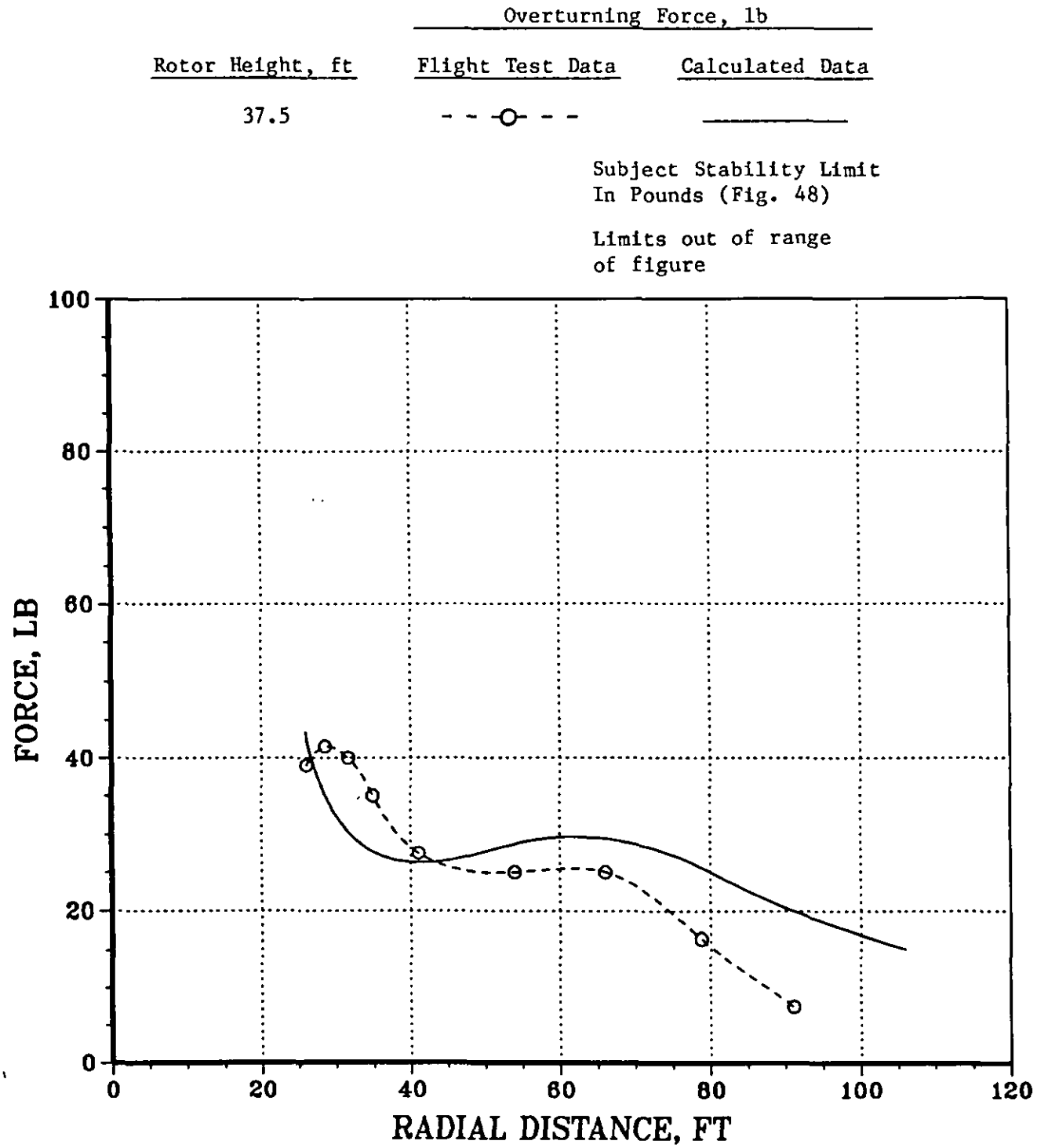

Figure 55. Correlation of Horizontal Downwash Wind Forces on Personnel at a Relative Bearing of 270-deg During Hover at a Rotor Height of 37.5 ft AGL for an Average Gross Weight of 12475 lb

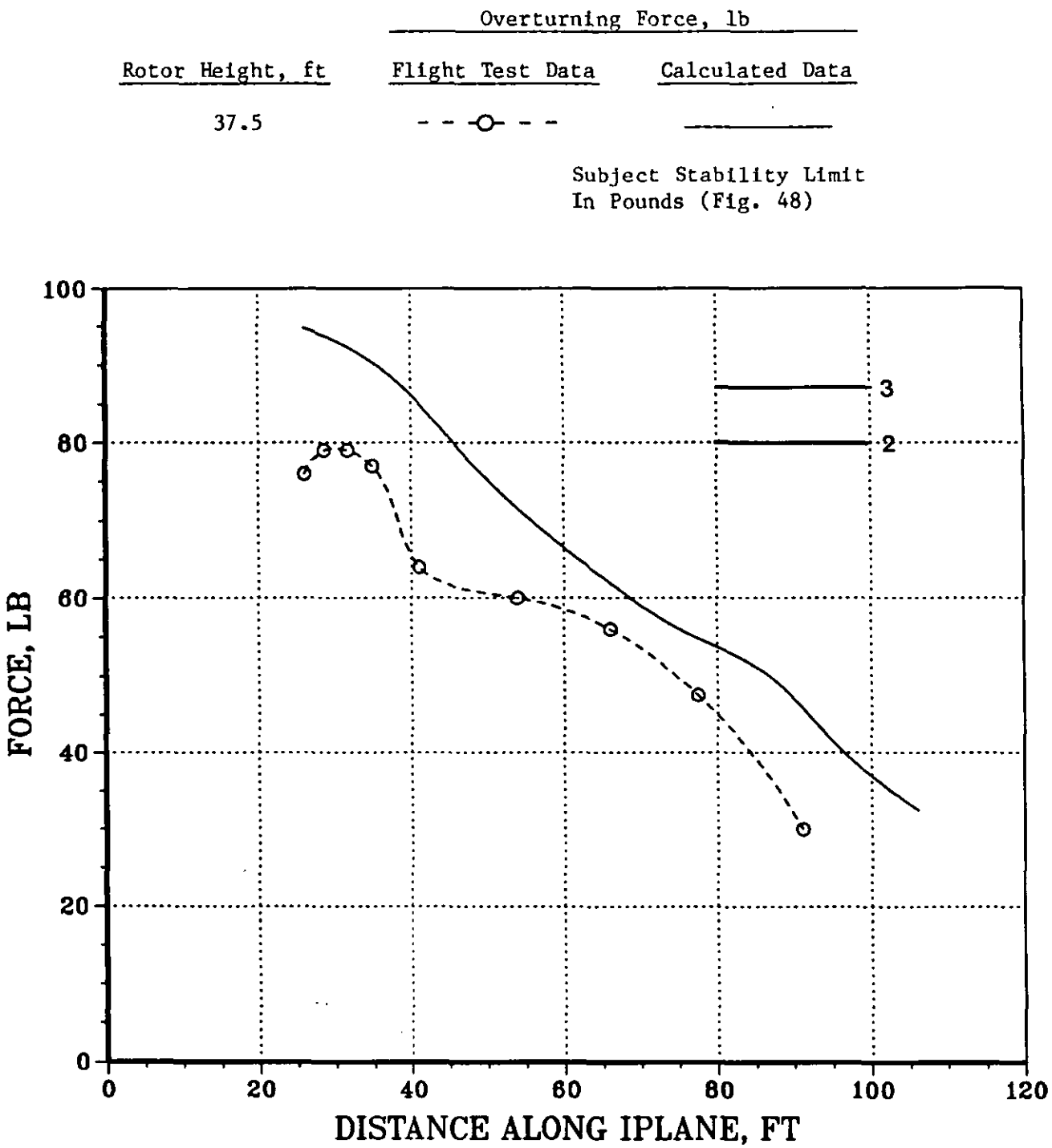

Figure 56. Correlation of Horizontal Downwash Wind Forces on Personnel at a Relative Bearing of 0-deg During Hover at a Rotor Height of 37.5 ft AGL for an Average Gross Weight of 12475 lb

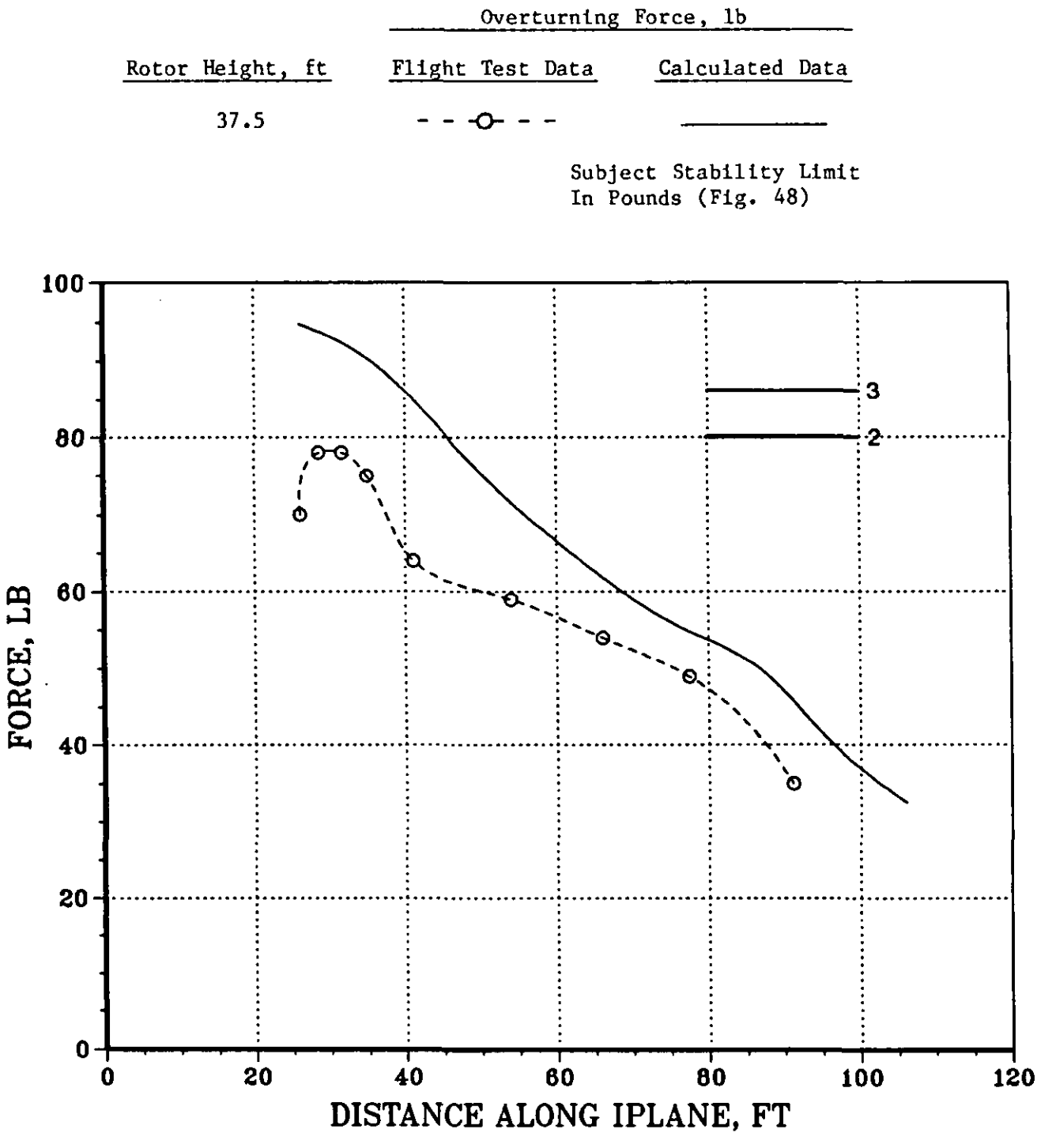

Figure 57. Correlation of Horizontal Downwash Wind Forces on Personnel at a Relative Bearing of 180-deg During Hover at a Rotor Height of 37.5 ft AGL for an Average Gross Weight of 12475 lb

60 lbs on the downwind side from a mean of 38 lbs to a reduction to 22 lbs on the upwind side.

Correlation of peak force and moment data, as measured experimentally at several distances from the rotor at rotor heights of 57 and 77 ft are presented in Figs. 58 through 61 for the Sikorsky S-61 (SH-3) (Ref. 16). This data is based on a 6-ft by 1-ft man with a C_D of 1.0 on a cold day ($\sigma' = 1.1$, $\rho_A = 0.0026146$ slugs/ft^3) which is slightly different from the previously described "Navy" man.

Results from this data comparison for both the maximum forces and moments indicate that the data correlate well for the assumption that the wind is approximately 3 kts. If the wind is assumed to be zero, the mathematical model data overpredicts the flight test data. Commentary in Ref. 16 does not provide detailed information on the ambient wind velocity, gust levels, or direction other than the statement that the wind varied from approximately 0 to 4 kts.

4. Qualitative Data That is Useful in Establishment of Separation Standards

While quantitative data, as presented in the previous section, provide guidance for calculation and correlation of overturning forces and moments, they do not provide guidance for what may or may not be acceptable levels of rotorwash that would be associated with civilian rotorcraft operations. Furthermore, definition of acceptable rotorwash levels for civilian operations is itself somewhat ill-defined. What may be acceptable and safe to an unprotected ramp employee at a heliport would be considerably different from that considered acceptable by an embarking business executive, a senior citizen, a pregnant woman, or a 7-year-old child. Therefore, before making the assumption that a certain level of overturning force or moment is acceptable for civilian operations, such as the 80-lb level of Fig. 48, it is particularly important to review some of the available qualitative data that has been reported.

Qualitative comments provided by Subjects 3 and 4 (Fig. 48) following the test with the CH-53E at the 45,000 and 56,000 lb gross weights agreed

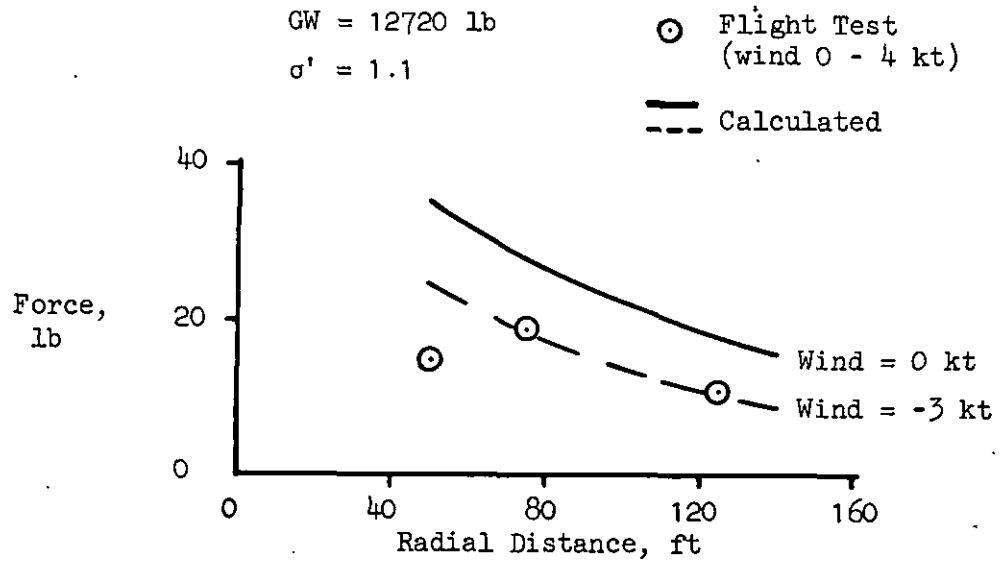

Figure 58. Correlation of Maximum Peak Forces Generated at a 57 ft Rotor Height with a Sikorsky S-61 (SH-3)

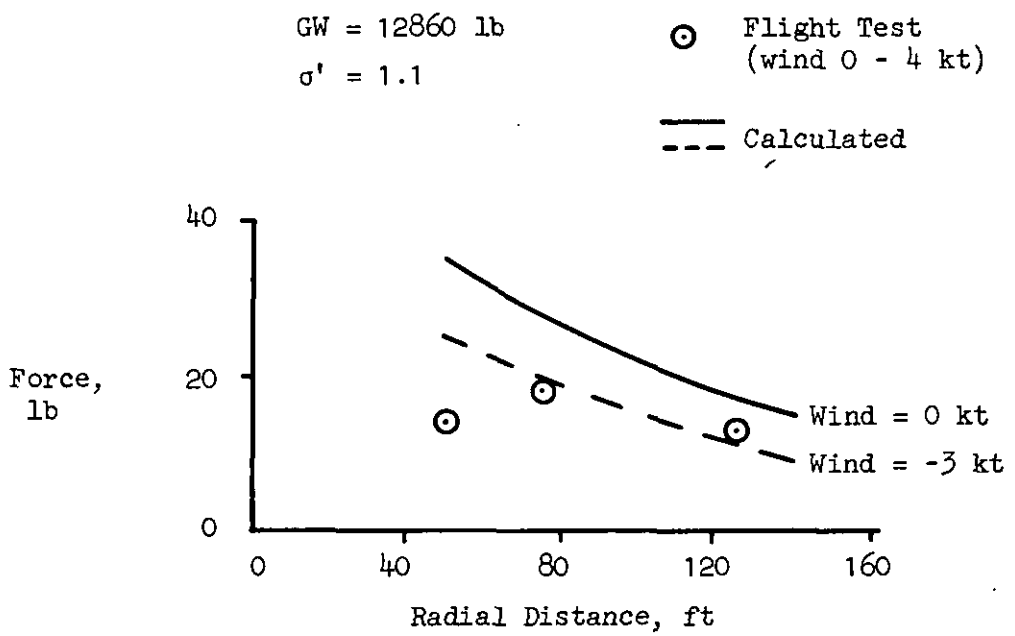

Figure 59. Correlation of Maximum Peak Forces Generated at a 77 ft Rotor Height with a Sikorsky S-61 (SH-3)

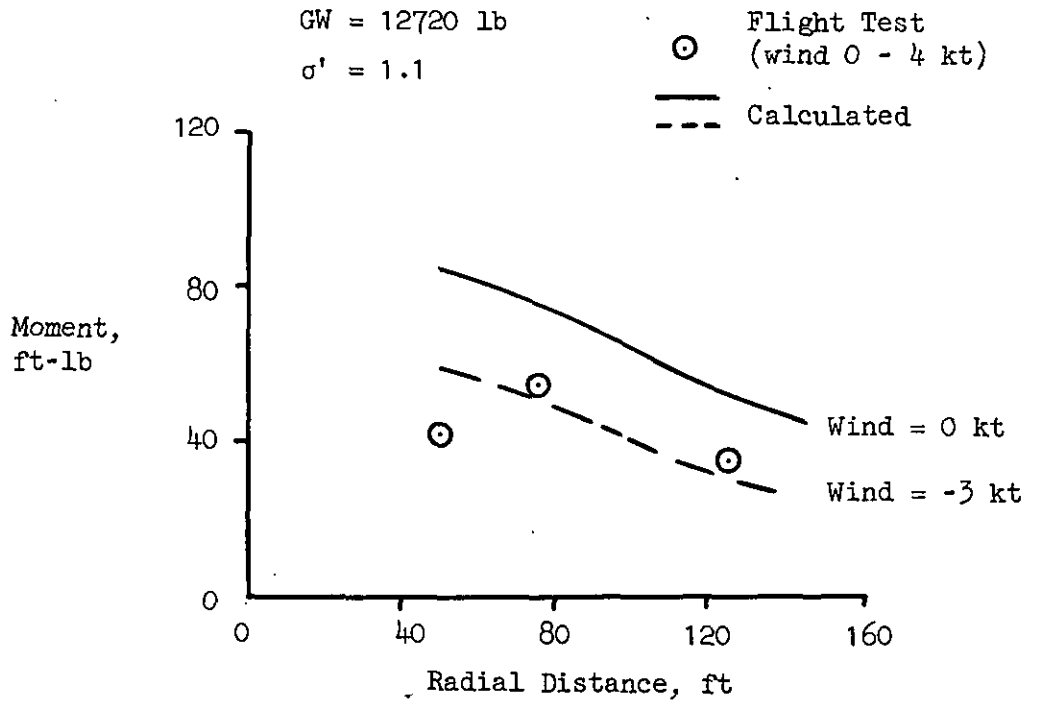

Figure 60. Correlation of Maximum Peak Moments Generated at a 57 ft Rotor Height with a Sikorsky S-61 (SH-3)

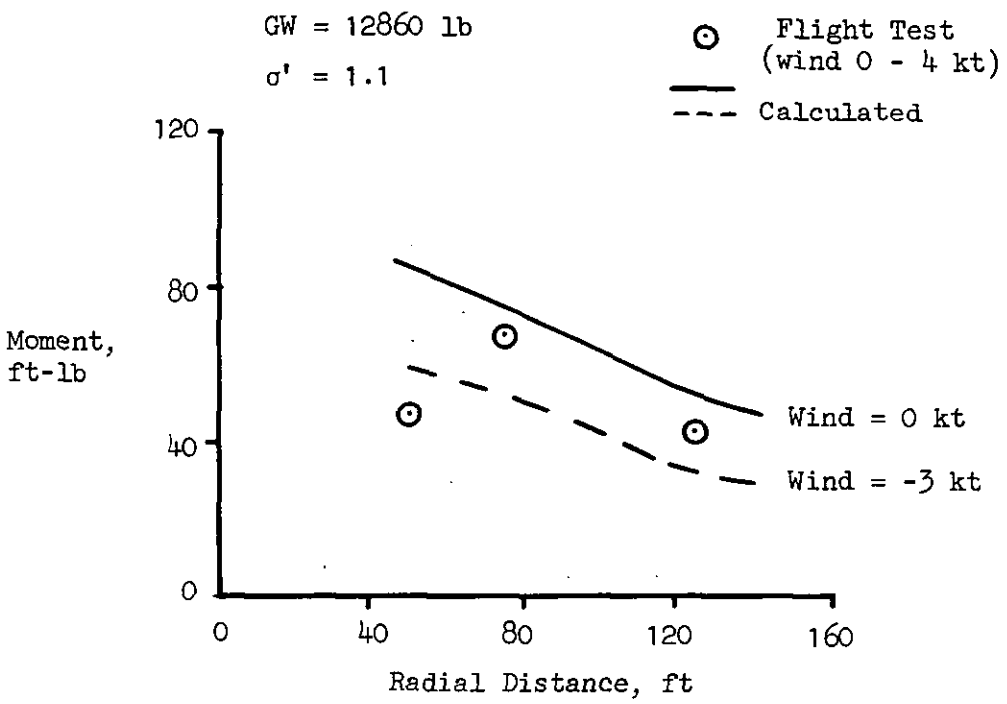

Figure 61. Correlation of Maximum Peak Moments Generated at a 77 ft Rotor Height with a Sikorsky S-61 (SH-3)

well with quantitative predictions and results from the laboratory testing used to construct Fig. 48. During the qualitative tests at the 45,000 lb gross weight, Subjects 3 and 4 experienced only minor difficulty while working in the rotorwash at the 37-ft hover and no difficulty at the two greater hover heights. The forward movement of Subject 3 was, however, completely restrained near the position marked 80 ft from the center of the test site during the 37-ft hover at 56,000 lb gross weight. During the 77-ft hover, Subject 3 could maneuver in the peak force region with some difficulty. Subject 4 could maneuver in any region of the flowfield during the 56,000 lb gross weight sequence; however, he did experience difficulty while working in the peak force region during the 37-ft hover. Subject 4 also participated in a qualitative survey during the 70,000 lb gross weight test. While he was able to completely penetrate the flowfield at all three hover heights, he did experience great difficulty while moving in the peak force region, and postural stability could not be controlled.

Further work with the CH-53E at 42,625 and 50,664 lb and with an RH-53D at 40,950 lb was conducted simultaneously with the work described above (Fig. 62). All four of the subjects listed in Table 8 participated in qualitative analysis of these flight conditions. Subjects 1, 2, and 3 indicated that the rotorwash flowfields for both aircraft caused difficulty in maintaining balance and were disorienting at even the lower disc loading (42,625 lb) of the CH-53E; however, no major differences in the degree of difficulty to maneuver in all three flowfields were reported. In general, all four subjects considered the RH-53D to have a more periodic and predictable pulsing, thus causing a constant requirement for compensation to maintain postural stability. The CH-53E steady-state flowfield pulses were not as noticeable. However, there were large time spacings between which there were large gusts that were possibly caused by the automatic flight control system (AFCS). These sudden unexpected gusts required more caution and alertness.

During the RH-53D and CH-53E tests at equivalent disc loadings (40,950 and 50,665 lb, respectively), Subjects 1 and 2 had to exert extreme effort, while maintaining only limited balance, in order to penetrate the

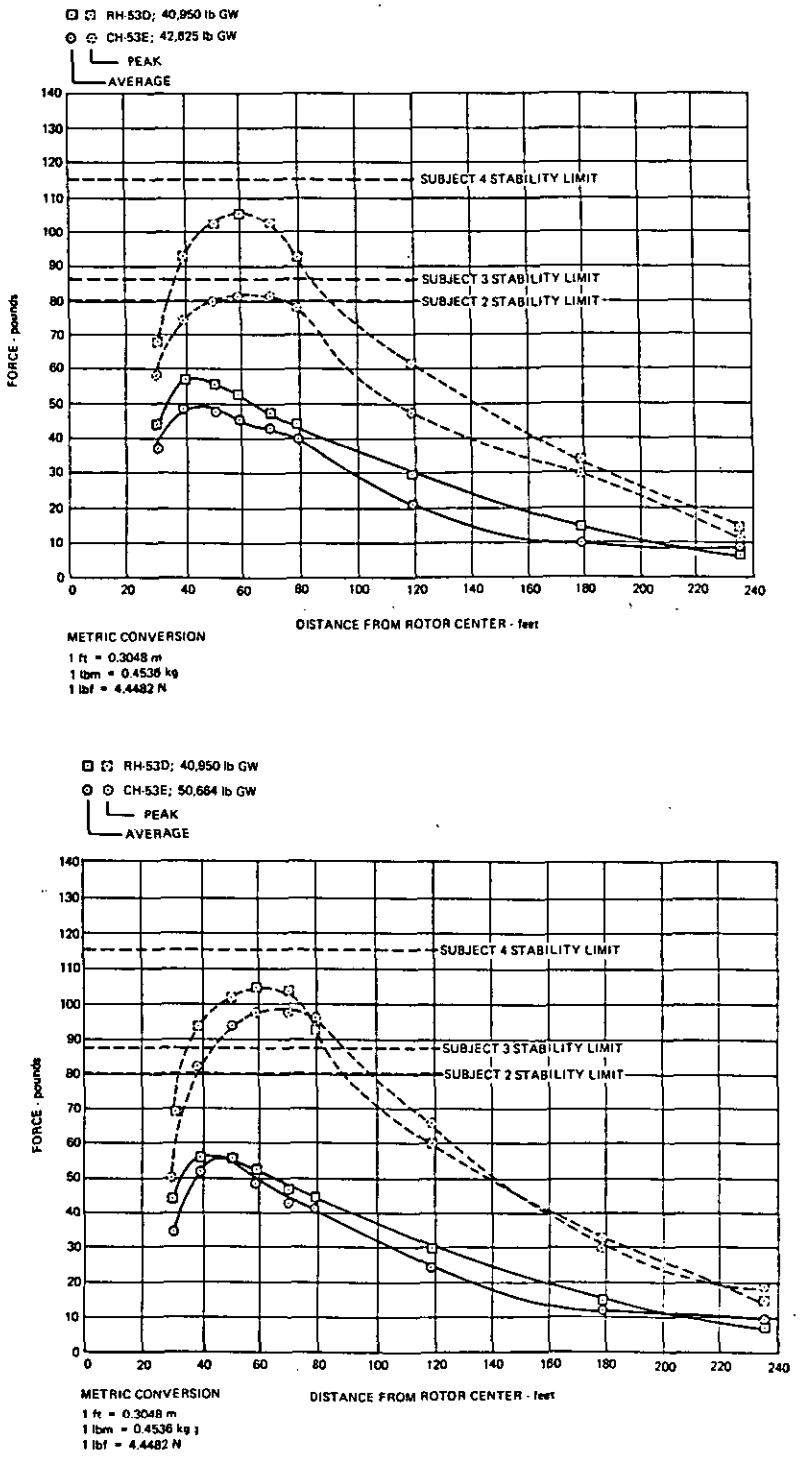

Figure 62. Comparison of CH-53E and RH-53D Horizontal Downwash Forces on Test Subjects Plotted as a Function of Distance from the Rotor Center During Hover at 37 ft with the CH-53E at 42625 lb and 50644 lb and the RH-53D at 40950 lb Gross Weight

(Reproduced From Ref. 11)

maximum force region. Subject 3 could penetrate and maintain balance at the RH-53D and CH-53E equivalent disc loading test points; however, Subject 3 was unable to penetrate the maximum velocity region (80 ft from rotor center) during the qualitative testing of the CH-53E at 56,000 lb gross weight.

Based on both of these sets of qualitative and quantative data, it was concluded that the CH-53E was no more hazardous than the RH-53D at a similar disc loading. It was also indicated from the qualitative results that up to the 50,000-lb gross weight condition, the flowfields were tolerable for trained military personnel. The CH-53E test gross weight of 56,000 lb (Fig. 51) presented difficulties to personnel over a wide range of weights and strengths that ranged from complete instability (very high hazard potential) to marginal instability (high hazard potential). It was therefore concluded that the forces and moments associated with a 50,000-lb gross weight produced the maximum wind forces to which personnel should be exposed under the CH-53E aircraft without restricting their distance from the center of the rotorcraft. It is also important to note that qualitative observations of the subjects during these tests were made under optimum conditions; the only task required during these tests was to walk through the complete flowfield from Point A to Point B. The ground surface was of rough concrete for best traction, and the rotorcraft was not moving so that the subjects could approach the flowfield at their own pace. Therefore, for civilian purposes, one might conclude that the peak force levels (approximately 80 lbs) experienced at the lower disc loading (42,625 lb) of the CH-53E were the maximum allowable (Fig. 62). This is because other variables would have to be taken into account when analyzing the downwash hazard potential as extrapolated to other classes of personnel. These classes would include factors such as age, size, weight, strength, endurance, and reflex response when subjected to the downwash, as well as environmental considerations such as the traction offered by the ground surface, loose foreign objects and grit, the difficulty of the task to be performed in the flowfield, and whether the rotorcraft is passing the person or the person is moving under the rotorcraft.

Qualitative tests were also conducted with the XV-15 (Ref. 12) during 37.5- and 62.5-ft hover tests (rotor height) using Subject 4 described in Table 8 and Fig. 48. The path of locations to which test Subject 4 walked and the locations at which he stood, both into and away from the flow direction, are shown in Fig. 63. Test Subject 4 had no problems walking or standing under the XV-15, although his forward movement was slightly impeded by the flowfield. The test subject had the most difficulty along the 0- and 180-deg relative bearing, and he noted that the flow magnitude was composed of frequent large wind gusts. Neither the test subject nor the observing test personnel noticed any differences in relative difficulty due to the variation in hover height during the test. In summary, the limited qualitative observations were in good agreement with the comparable quantitative force analysis, as presented in the previous sections and as correlated in Figs. 55 through 57. No quantitative data were obtained under the rotorcraft within a 26-ft circle centered at the XV-15 center. However, the test subjects indicated that forces in this area were extremely low. Observations by test observers and movies of the test also indicated that the velocities in this central area were relatively low in magnitude during the 37.5- and 62.5-ft hover tests. Test personnel walked erect and relaxed in this region.

Downwash wind forces on personnel were also summarized in Ref. 12 for the XV-15 by presenting the force data in Figs. 55 through 57 as four regions which have distinctive differences in degree of difficulty for personnel to maintain stability in the flowfield. These regions are shown in Fig. 64. The degree of difficulty relative to the region based on the criteria in Fig. 64 is presented in Table 9. Based on these results (although they are limited), it can be surmised that the majority of the flowfield represented by Regions III and IV present no significant problems for personnel walking, standing, or performing limited work over the range of XV-15 test conditions. Potentially, however, Regions I and II could be hazardous for people weighing less than 150 lb (25th weight percentile). In looking further at this qualitative data, it can be hypothesized that, for civilian operations, a level of outwash in Region III would be a minimum limit. When quantifying this region, the

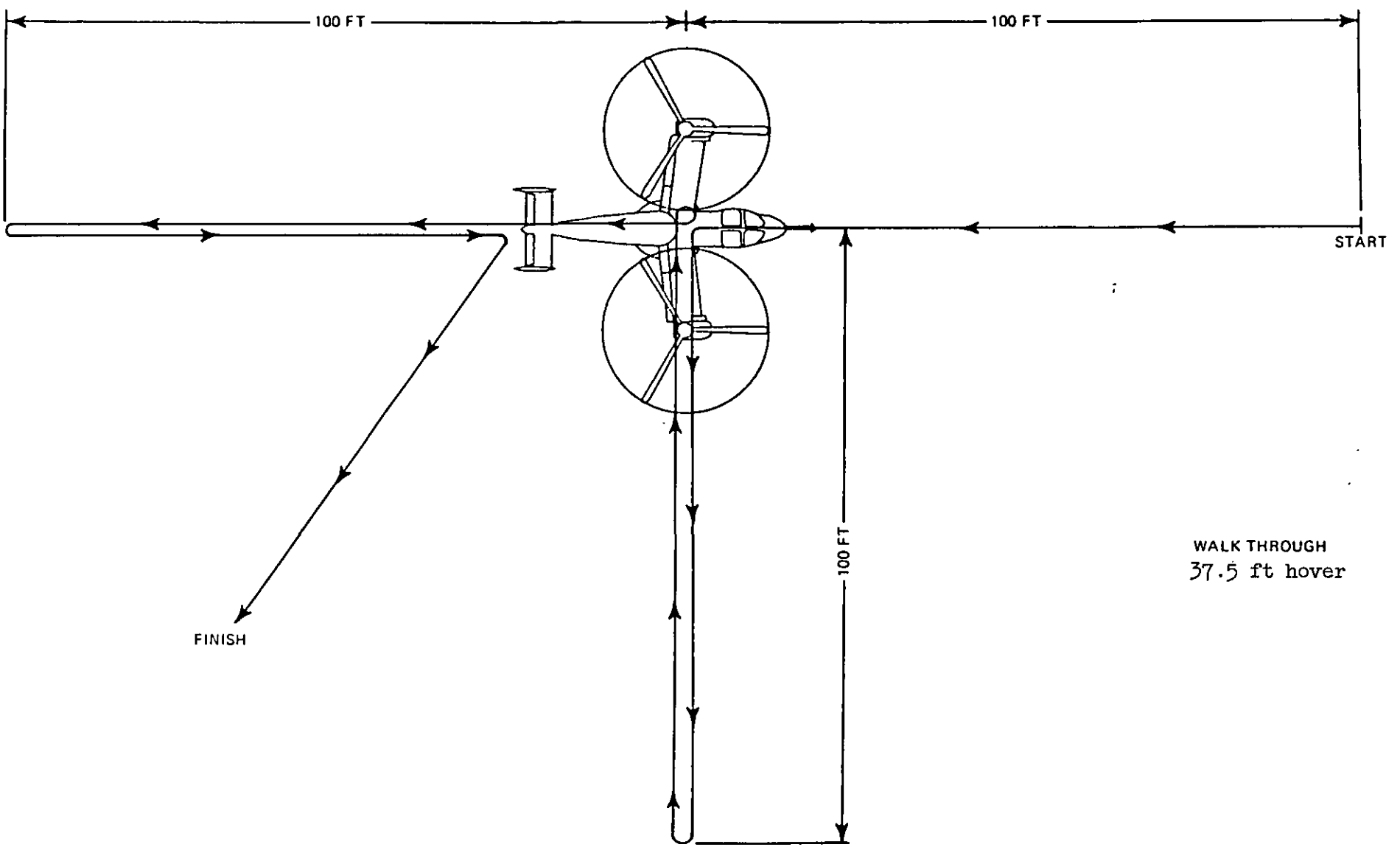

Figure 63. Path of Locations of Test Subject 4 While Conducting Qualitative Walk Around Tests Under the XV-15 Tilt-Rotor Aircraft Hovering at 37.5 and 62.5 ft

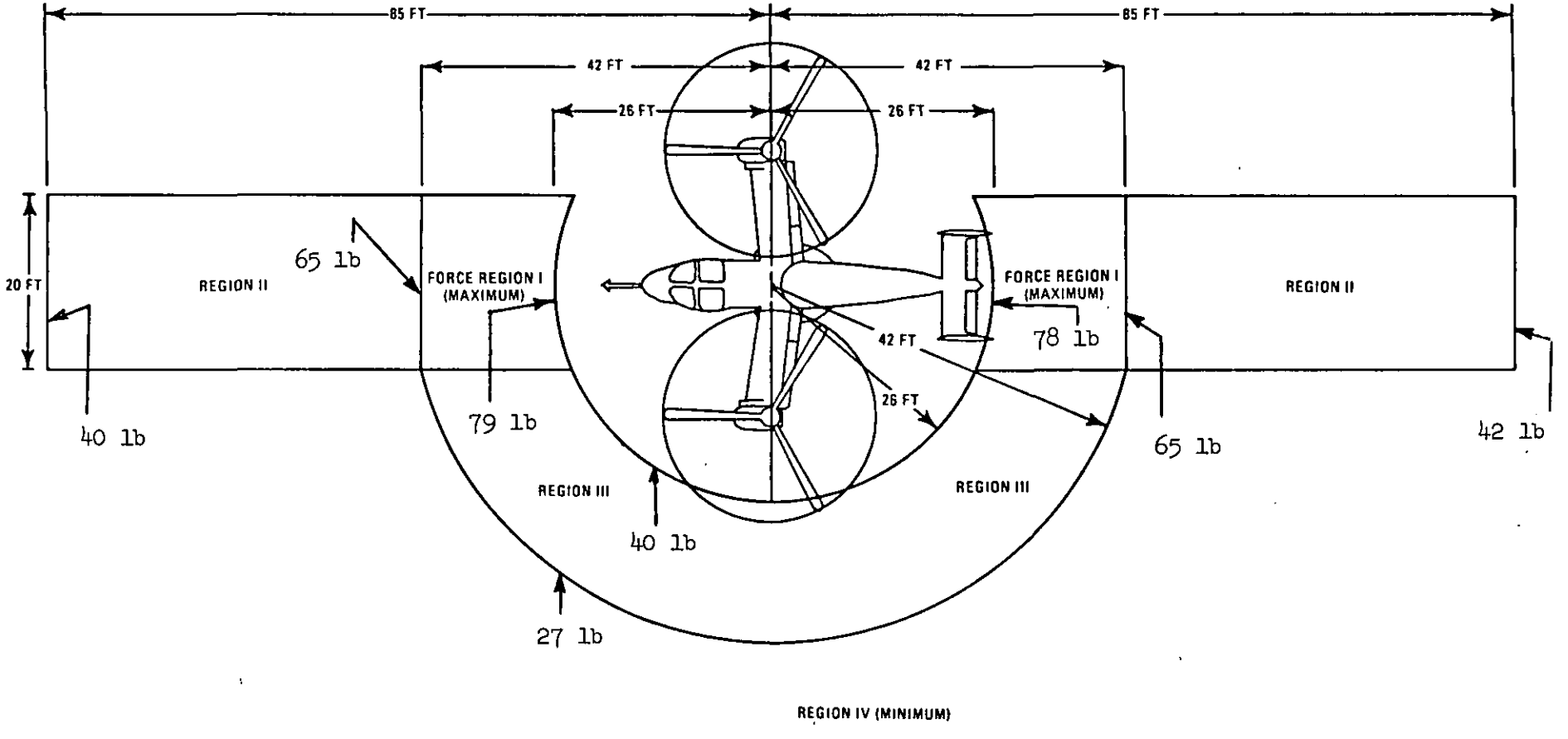

Figure 64. Regions of Different Levels of Wind Force on Personnel (Description of Level of Force in Each Region is Contained in Table 9)

TABLE 9

PERSONNEL LIMITATION IN XV-15 FLOWFIELD REGIONS

Regions[1]	Weight (Percentile[2]) - lb		
	150 (25th)	171 (75th)	220 (99th)
I	Exceeds stability limit. Hazardous.	Difficult to walk through.	Slightly difficult to walk through.
II	Very difficult to walk through.	Slightly difficult to walk through.	No difficulty to walk through.
III	Moderately difficult to walk through.	No difficulty to walk through.	No difficulty to walk through.
IV	No difficulty to walk through.	No difficulty to walk through.	No difficulty to walk through.

NOTES: (1) Regions are defined in Fig. 64.
(2) Reference 28, U.S. Marine Corps.

values of force, as presented in Figs. 55 through 57, can be extracted. Forces in Region III vary from a maximum of approximately 40 lbs at one rotor radius (12.5 ft) to a minimum of 27 lbs at 42 ft from the center of the XV-15. Likewise, forces in Region IV vary from a maximum of 27 lbs to 0 lbs at large distances away from the XV-15.

Qualitative personnel commentary from Ref. 16 for the test involving the Sikorsky S-61 (SH-3) indicated that the rotorwash at the measured disc loadings and rotor heights did not significantly impede the movement or working capabilities of any test subject. The buffetting of the outwash was random and of a low frequency. The helicopter was also not objectionably noisy such that important conversations could be conducted without undue effort.

While it might be useful to continue for documentation purposes the discussion of other qualitative results presented in the literature, it can be said that the decision as to what is or is not an acceptable level of rotorwash would not be affected signifcantly, since all of the other studies were also related in approach and methodology to those already discussed and were also not primarily interested in quantification of the civilian problem. In the next subsection, therefore, the results presented to this point, both qualitative and quanitative, are brought together to form a separation guideline by which to evaluate the previously discussed "worst offender" rotorcraft configurations.

5. Overturning Force and Moment Limits for Civilian Operations

The quantification of safe separation distances for personnel from "worst offender" rotorcraft configurations requires the specification of certain levels of forces and moments as hazardous. This task is initiated for this study by combining the results from the previous subsections into a useable format for purposes of comparison. This comparison is presented in Fig. 65 as an expansion of the data which was presented in Fig. 48. If the data in Fig. 48 is combined further with the comments of Table 9, one might propose the following limits as safe for civilian operations.

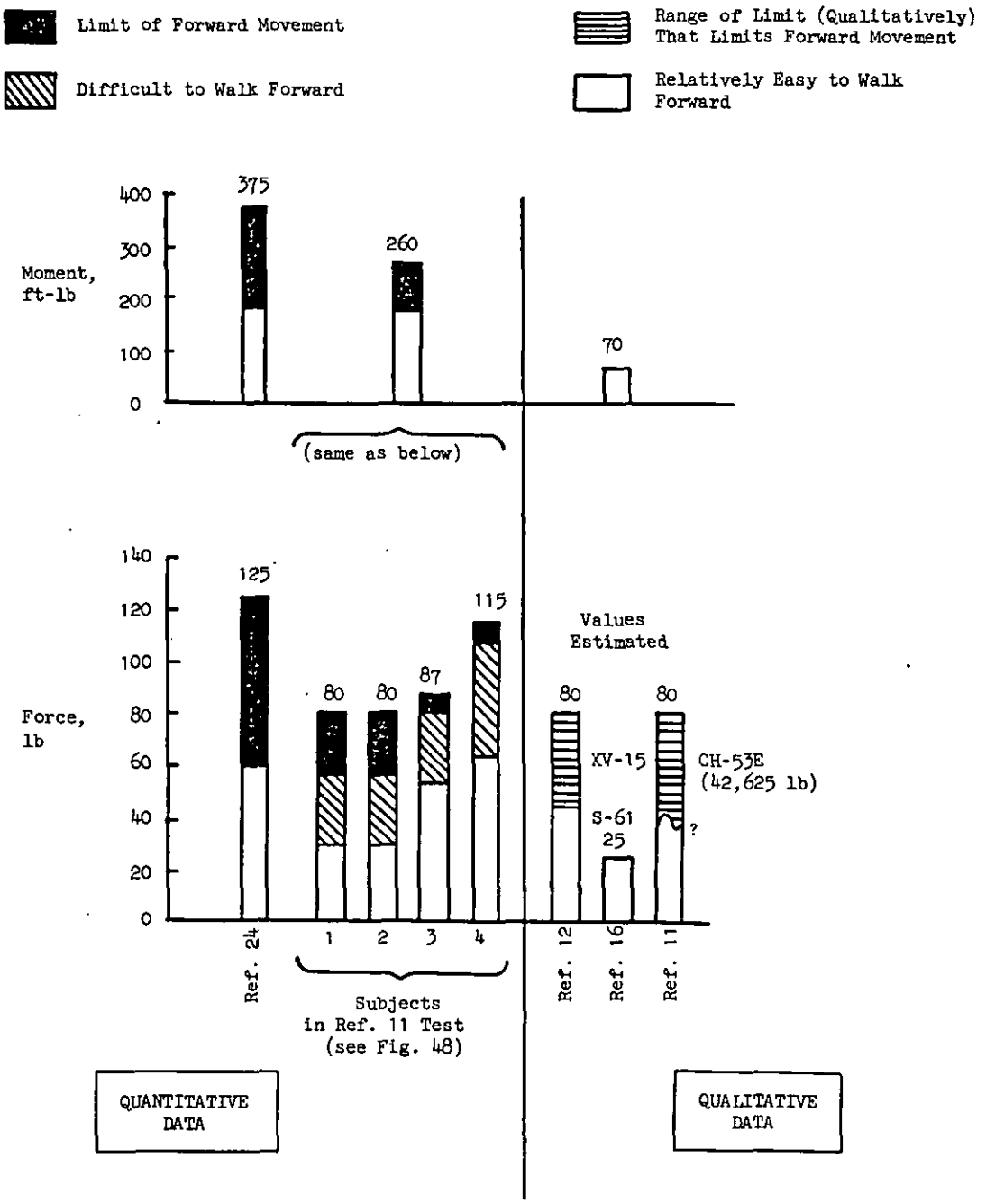

Figure 65. Summary of Quantitative and Qualitative Data Giving Important Definition of Limiting Overturning Forces and Moments

Personnel Classification	Force Limit, lb	Moment Limit, ft-lb
I: Trained and protected ramp personnel used to working in rotorcraft downwash	80	260
II: Untrained and unprotected personnel not used to rotorcraft downwash environments	40	120
III: Untrained and unprotected children likely to be walking without assistance from adults in rotorcraft downwash environment	30	60

While these limits are proposed as practical and reasonable, based on the data, there are by no means enough data to conclude conclusively that these are the best limits that could be derived if the data base were more extensive. Therefore, the reader is referred to Section VIII and the proposed experiment which, if conducted, would aid in substantiating or modifying the limits proposed above.

The limits specified for unaided children are derived from the extrapolation of Table 8 and Fig. 65 data and are shown in Fig. 66. Several children were measured and weighed for this study in order to provide a rough estimate for developing the model described for the "S" type person (or 7-year-old child) in a previous subsection as well as for aiding in the rough calculation of a force and moment limit. Based on the results that are presented in Refs. 11 and 12, body weight was judged to be the most important scaling parameter for defining a force and moment limit. The moment calculation for the "S" type person is based on an application point of 2 ft versus 3 ft for an adult.

6. Evaluation of "Worst Offender" Rotorcraft Configurations

The worst case rotorcraft configurations that were described in detail in Table 7 were evaluated at 0 and 9 kts of ambient wind velocity in order to determine their overturning force and moment hazard potential. Results

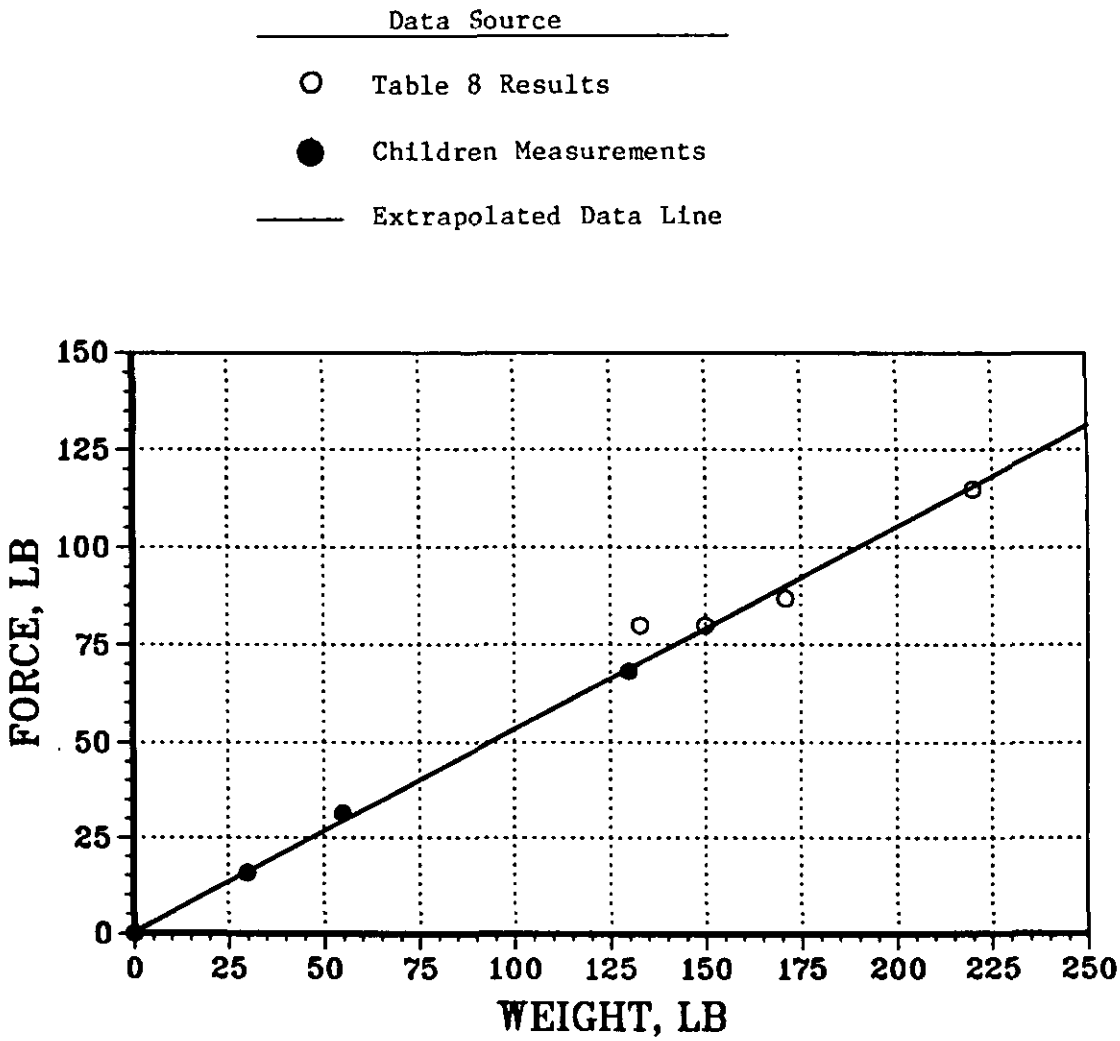

Figure 66. Extrapolation of Experimentally Measured Overturning Force Data to Smaller Personnel Weight Categories

are presented for the "L" size person in Figs. 67 through 71 for the S, SM, M, MH, and H configurations, respectively, at the most critical rotor height above the ground. For the "S"-sized rotorcraft configuration, almost no separation restriction requirements exist. When considering the safety factors that are built into the analysis process, probably the restrictions for untrained and unprotected civilian personnel would not even be required for the less hazardous civilian helicopters now in service. However, as the respective rotorcraft configurations increase in size, increasing values for separation distance do become required. This information is summarized in Fig. 72. In this figure, only separation distances that were a function of the force limit are plotted, because the separation requirements due to the forces and moments are almost exactly equal in magnitude (see tabulations in the top part of Fig. 72).

Separation requirements for the "S"-sized person are presented in Fig. 73. These results are derived by the same process as the previously presented results for the "L"-sized person; the graphs are simply not shown. As can be seen by a comparison of Figs. 72 and 73, the overturning force and moment separation requirements for the "S"-sized person are less than those proposed for the untrained and unprotected "L"-sized civilian. This is due to the fact that the smaller body size of the "S"-type person simply does not present enough surface area to the outwash flow in proportion to the body weight related criteria. These results do not imply that children are in general "safer" than the untrained and unprotected adults of Fig. 72. Instead, since unprotected children's eyes are closer to the height of the peak velocity, they may be at greater risk as a result of flying debris. (This topic will be covered in more detail in in a subsequent subsection.) What the results do indicate is that children are more probably equally as "safe" at the same separation restricted distances as the untrained and unprotected "L"-sized persons and therefore do not require special restrictions themselves. This result should make it easier to eventually determine final separation standards.

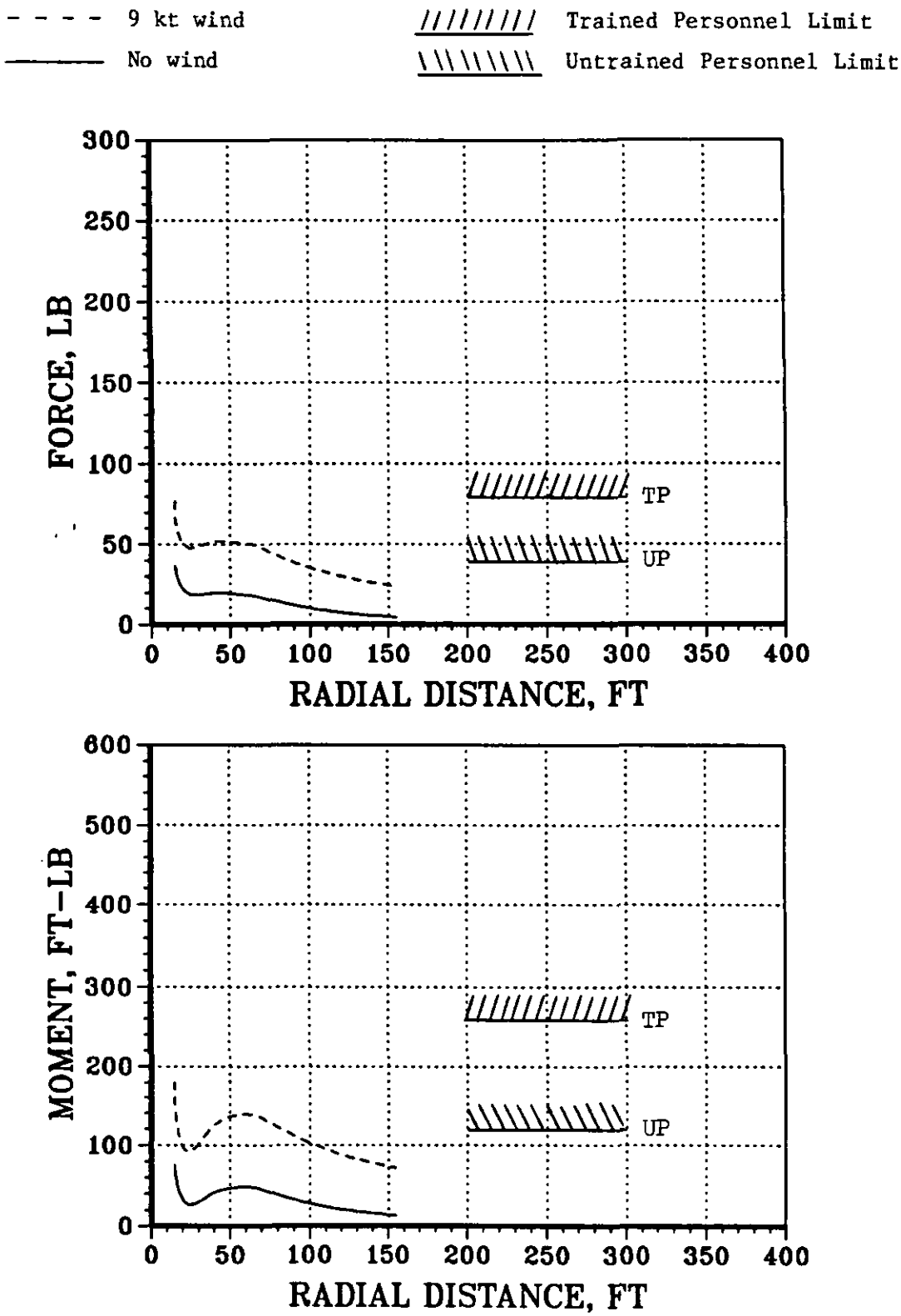

Figure 67. Peak Overturning Force and Moment Profiles for the "S"-Sized Rotorcraft as a Function of Radial Distance from the Center of the Rotorcraft

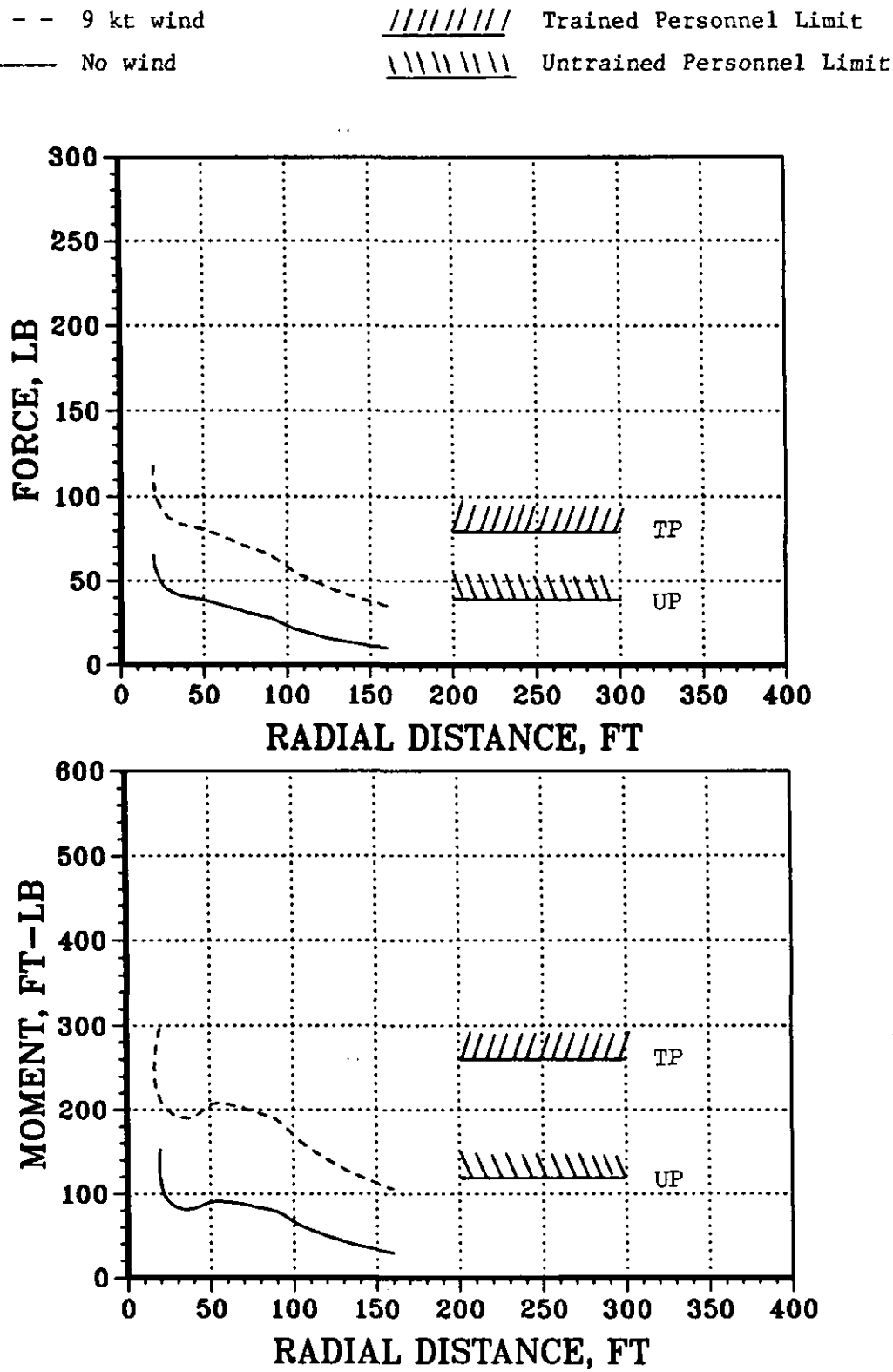

Figure 68. Peak Overturning Force and Moment Profiles for the "SM"-Sized Rotorcraft as a Function of Radial Distance from the Center of the Rotorcraft

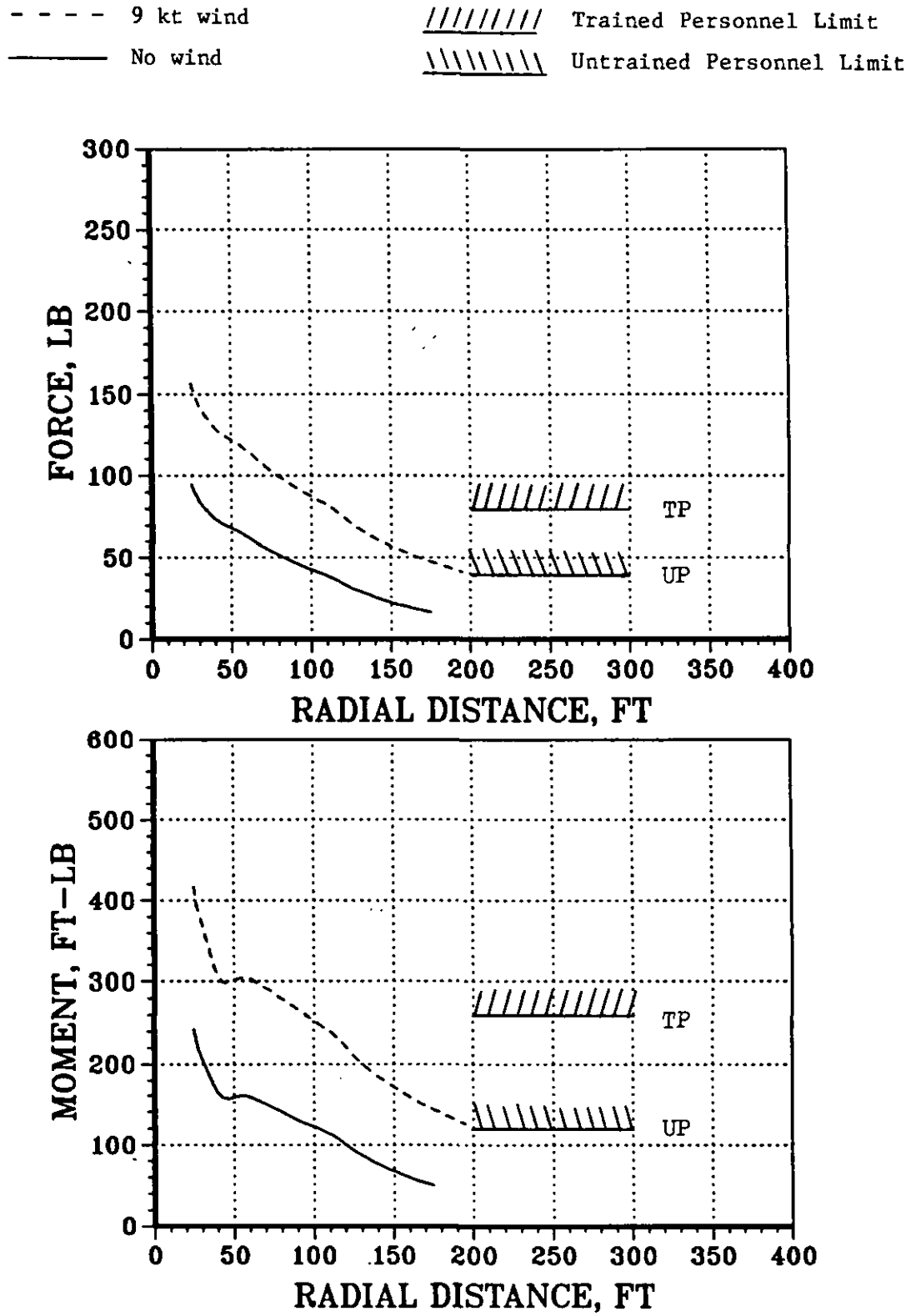

Figure 69. Peak Overturning Force and Moment Profiles for the "M"-Sized Rotorcraft as a Function of Radial Distance from the Center of the Rotorcraft

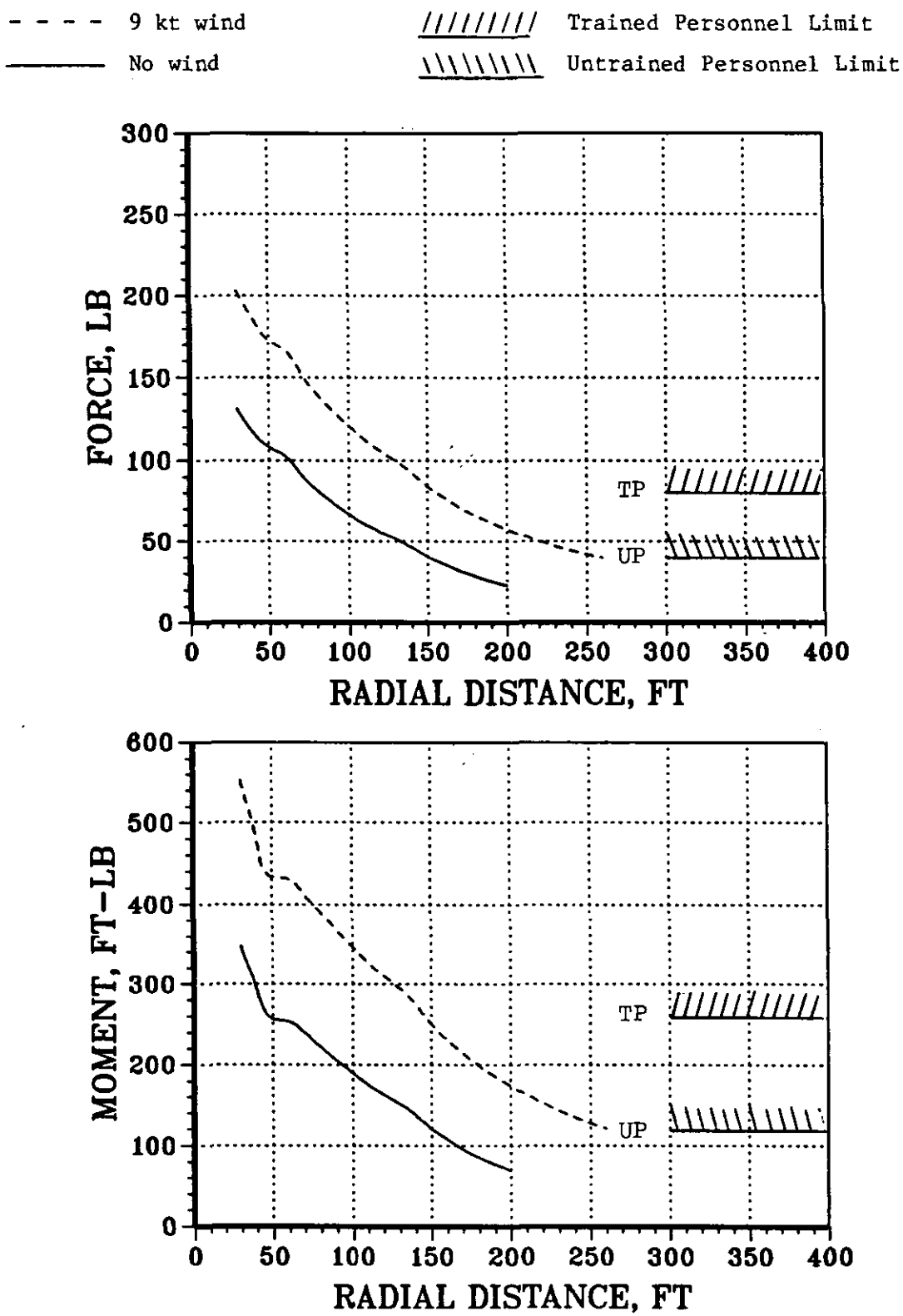

Figure 70. Peak Overturning Force and Moment Profiles for the "MH"-Sized Rotorcraft as a Function of Radial Distance from the Center of the Rotorcraft

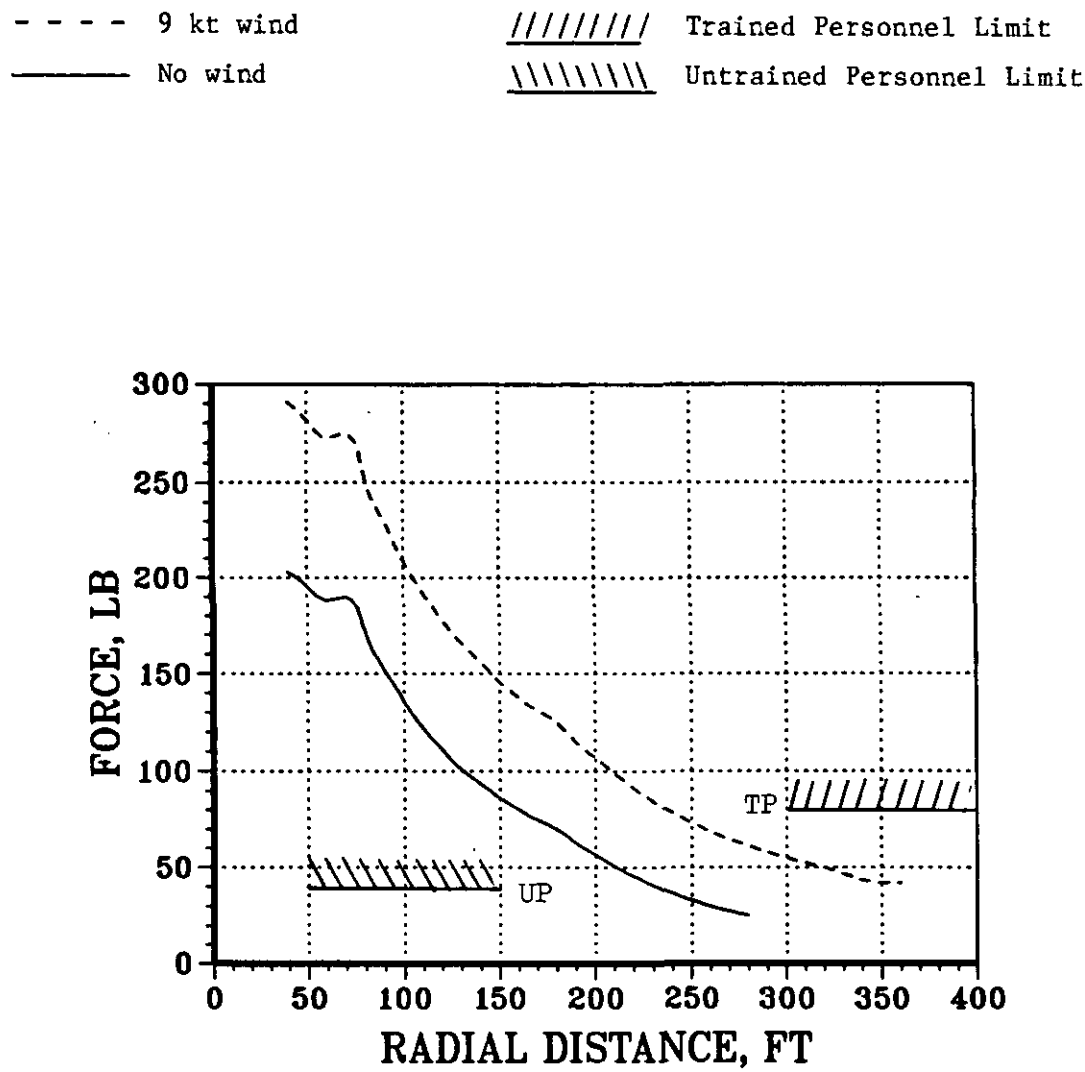

Figure 71. Peak Overturning Force and Moment Profiles for the "H"-Sized Rotorcraft as a Function of Radial Distance from the Center of the Rotorcraft

(a) Force

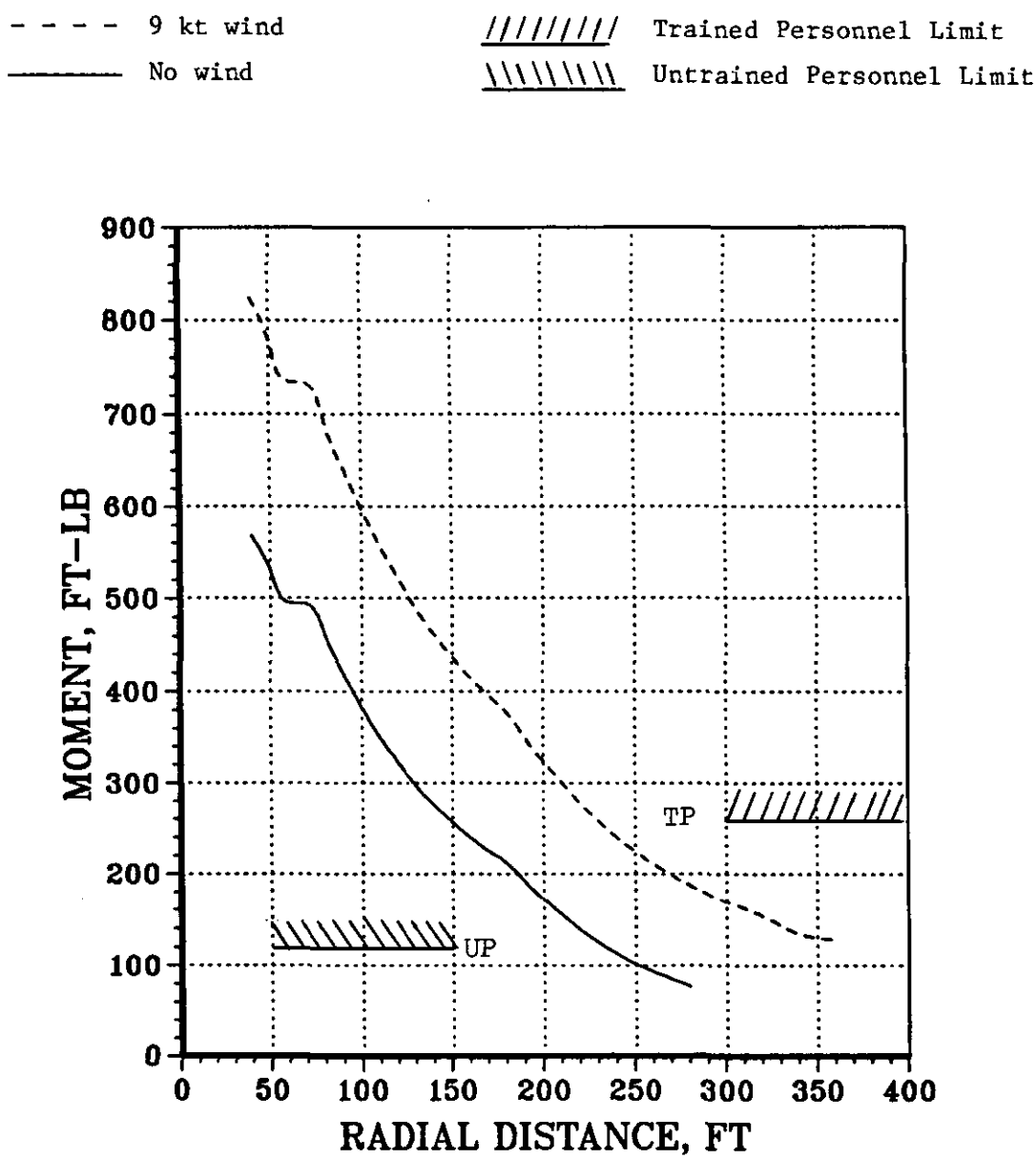

Figure 71 (Concluded)

(b) Moment

Approximate Force and Moment Limiting Radial Distances, ft or ft-lb

Limit	Personnel Type	Rotorcraft Class Size S	SM	M	MH	H
Force	TP, 0 kt	-	-	34	83	164
	TP, 9 kt	-	54	115	158	239
	UP, 0 kt	-	40	108	152	234
↓	UP, 9 kt	85	142	195	260	364
Moment	TP, 0 kt	-	-	-	48	150
	TP, 9 kt	-	24	98	148	230
	UP, 0 kt	-	24	98	150	234
↓	UP, 9 kt	85	142	198	260	370

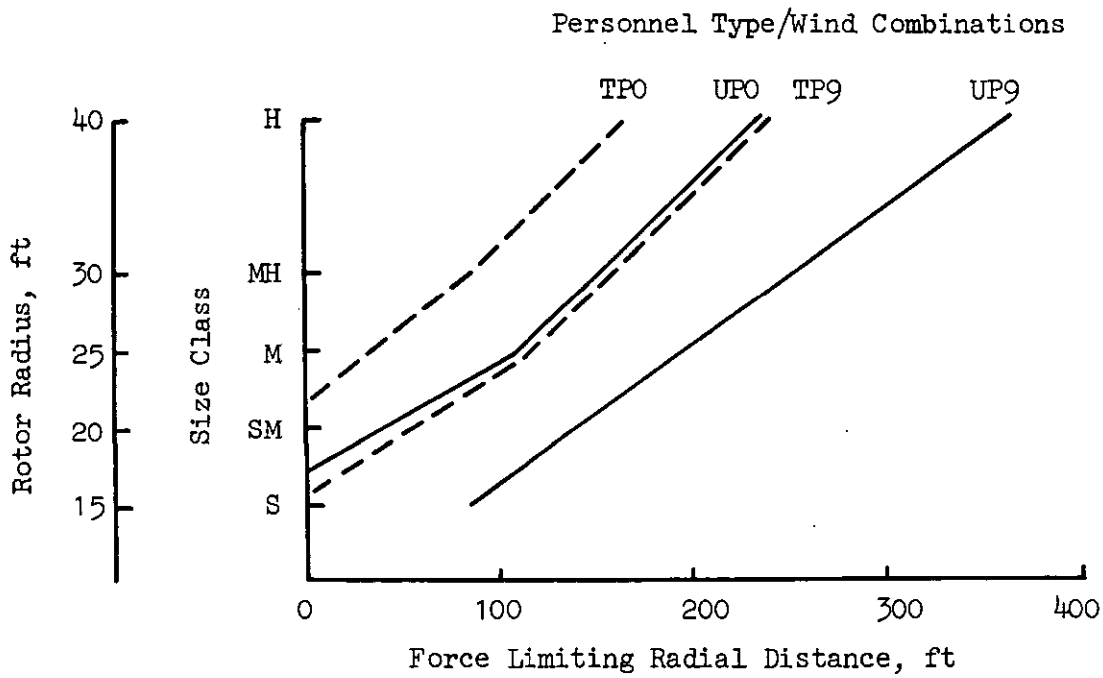

Figure 72. Overturning Force and Moment Separation Distance Requirements for "L"-Sized Personnel

Approximate Force and Moment Limiting Radial Distances, ft or ft-lb

Limit	Personnel Type	Rotorcraft Class Size S	SM	M	MH	H
Force	S, 0 kt	-	24	63	100	181
↓	S, 9 kt	22	85	128	172	254
Moment	S, 0 kt	-	-	55	100	193
↓	S, 9 kt	18	82	129	175	258

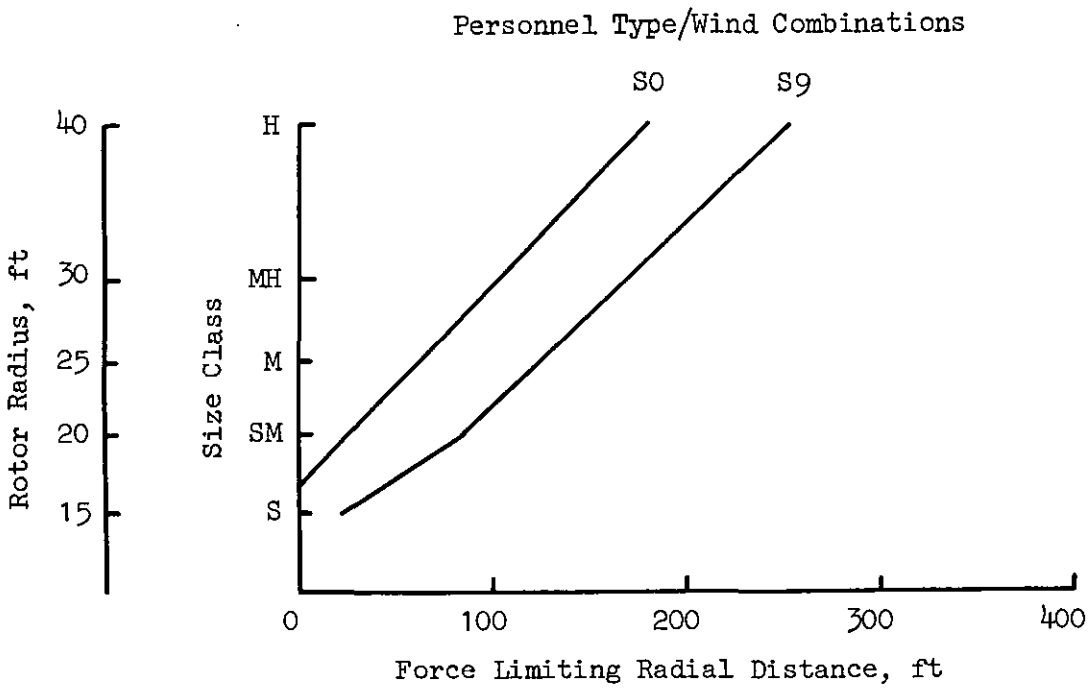

Figure 73. Overturning Force and Moment Separation Distance Requirements for "S"-Sized Personnel

7. Overturning Force and Moment Hazard Potential Resulting from Rotor Generated Vortices

An analysis was conducted simultaneously with the outwash flowfield hazard analysis in order to determine whether or not rotor generated vortices (forward flight trailing vortices and the ground vortex) present a hazard to personnel on the ground. The results from this analysis are presented in this subsection using the mathematical models which were developed in Section III.

The first task that was accomplished was simply a management one: a rough examination was made in order to decide whether or not to even conduct a detailed analysis. This task was accomplished by first correlating the developed mathematical models with the UH-1H and CH-54 flight test data as presented in Ref. 26. These results are presented in the last subsection of Section IV. Subsequent to this brief analysis, it was decided that at least some further analysis of the hazard was warranted.

Based upon the correlation results as obtained for both the vortex strength and the vortex velocity profiles (i.e., Figs. 42 through 45), three further assumptions were made in order to better manage the analysis effort. The first of these assumptions was that airspeeds of less than 30 kts should not be seriously evaluated, since the mathematical model's validity was questionable at airspeeds below this value. The second conservative assumption was that the vortices would not decay or lose strength with time. This assumption eliminated the need to predict decay rates in the vortex strength and in their position behind the rotorcraft and simply assumed that strong vortices would be laid down along the ground by a low flying rotorcraft. The third assumption made was that the maximum vortex core rotational velocity would be "approximately" 1.6 times the centerline downwash velocity (as "approximately" measured behind and along the centerline of the rotorcraft). This assumption, based on data like that presented in Figs. 44 and 45, eliminated the need to evaluate the predicted velocity field with the mathematical model at numerous positions all around the rotorcraft. This assumption also eliminated the need to model the vortex core so that calculation of peak velocity values in

each vortex could be made (for which more data would definitely be needed).

Using the methodology specified above, the "worst offender" configurations were evaluated. The "M"- and "H"-sized classes were evaluated first for the trailing vortex case at airspeeds of 30 and 50 kts. Results are presented in Table 10 for the estimated peak velocities that were calculated along the centerline of the pair of trailing vortices as well as in the core of each vortex. As can be seen from the results, if the worst case hazard is that which is predicted at 30 kt, then the peak downwash velocities for the "M" and "H" vehicles are 24 and 33 kt, respectively (without assuming any correction due to the results of Fig. 43). Assuming that a "wall" of air of this velocity exists which blows horizontal to the ground (which is a conservative assumption in itself), then, in comparison to the previously presented peak outwash profile velocities and dynamic pressures, the vortices cannot be considered a significant hazard. This is especially true if the "H"-sized class results are further corrected to account for the previously discussed "disc loading effect." Unless the vortices are laid down directly on top of unprotected personnel, then the peak values, which are very localized, cannot be expected to be large enough to be a hazard of importance when compared with the outwash flows.

These same rough cut "M" and "H" class cases were also evaluated for the ground vortex. Separation standards derived for this hazard were not significant enough to warrant further examination when the assumption was made that the rotorcraft could rapidly come to a hover and the peak outwash profile would then become the predominant and characteristic flow from which separation standard criteria would be developed.

In conclusion, when considering <u>all</u> of the conservative assumptions applied to the analysis of the trailing vortices and ground vortex, i.e.,

1. That substantial "profiles" of peak vortex velocities could strike personnel from an overturning or horizontal direction

2. That the rotorcraft would fly a profile close to the ground and lay vortices directly on personnel

TABLE 10

ESTIMATED TRAILING VORTEX GENERATED PEAK VELOCITIES

Size Class	Disc Loading, PSF	Airspeed, kts	Calculated Peak Centerline Downwash, ft/sec (kts)	Corrected* Peak Centerline Downwash, ft/sec (kts)	Calculated Peak Vortex Core Velocity ft/sec (kts)	Corrected* Peak Vortex Core Velocity ft/sec (kts)
M	9.6	30	40.4 (23.9)	30.3 (17.9)	65.9 (38.9)	49.4 (29.2)
		50	24.4 (14.5)	18.3 (10.9)	39.8 (23.6)	29.9 (17.7)
H	14.6	30	54.3 (32.2)	40.7 (24.1)	88.5 (52.5)	66.4 (39.4)
		50	35.9 (21.3)	26.9 (16.0)	58.5 (34.7)	43.9 (26.0)

*Based on results and discussion associated with Fig. 43, a conservative reduction in strength (especially for the "H" size) of 25 percent was applied to the calculated velocities.

3. That no vortex decay occurs with time or distance behind the rotorcraft

and

4. That the influence of the ground (less than 6-ft AGL where the person is) does not alter the nature of the hazardous velocities of the vortices

the velocities that were generated by the larger rotorcraft classes were not considered significant for separation standards purposes when compared to the hazardous peak outwash velocity profiles that were generated by the wall jet in hover. Therefore, for personnel safety, the recommendation from this analysis would be to keep personnel away from the taxi or takeoff/landing paths of rotorcraft with minimum separation distances to the side equal to those that would result from the case where the rotorcraft would have to come to a hover during taxi, takeoff, or landing thereby making the wall jet the critical hazard.

8. Summary of the Overturning Force and Moment Hazard Analysis

The previous subsections have supplied a technical analysis procedure for evaluating the hazard potential of overturning forces and moments on personnel caught in rotorcraft downwash/outwash flowfields. The analysis methodology that has been presented is based strongly on correlation with both laboratory experiments and test flight results (both qualitative and quantitative) for several rotorcraft. Safety factors are outlined in the analysis where they are important to a better understanding of the methodology. An experiment is also proposed (see Section VIII for details) that would aid significantly in a better quantification of safety factors as well as values for limiting forces and moments as applied to unprotected and untrained civilians. Criteria are developed based on the information available, and these criteria are utilized in the presentation of separation data for several classes of personnel in Figs. 72 and 73. Again it should be noted that the values for separation distances are based only on the overturning force and moment hazard type and no other. Results from the other types of hazards must be developed and integrated

with these results before any practical proposed separation standards can be generated.

C. ROTORWASH EFFECTS ON STRUCTURES AND GROUND VEHICLES

The potentially hazardous effects of rotorwash on structures and ground vehicles can be classified as one of two types:

1. Those that are produced by the outwash velocities themselves (converted to pressure profiles)

2. Those that are created more indirectly by the entrainment and subsequent impact of various types of debris (e.g., rocks, sand, garbage).

This section deals with the first of these two hazard types; discussion of impact damage from flying debris is reserved for Subsection E.

1. Literature Review of Peak Velocity Profile Effects on Structures

The effect of the oscillatory peak velocity profile (and therefore the pressure or wind loads) was considered to be important in heliport design, because, particularly in urban areas where real estate is limited and expensive, buildings or other structures may need to be located close to a takeoff/landing pad. A study of this hazard was identified in Ref. 29 as contracted recently by the FAA. While the results of the study presented herein are in general agreement with the results of that study, there are areas where significant differences do exist which will impact any recommended separation requirements.

In conducting the Ref. 29 study, both model and limited full-scale outwash profile data were utilized for the purpose of developing a simple mathematical model to predict the peak pressure loading on structures. Since the literature search for the study was conducted solely through NTIS, the investigators were able to identify only the full-scale and model data presented in Refs. 10, 22, and 30 through 32. Unfortunately,

none of the high quality work that was conducted by the U.S. Navy (Refs. 11, 12, 13, and 20) was discovered. An initial STI/CMA attempt to correlate the data from Ref. 22 with the mathematical models described in Section III was thought to be successful after a brief comparison of CH-54A data with Navy CH-53E (Ref. 11) data. Ultimately, however, when a more extensive correlation effort was attempted with the rest of the data in Ref. 22, the results were found to be very inconsistent and discouraging. A warning had been issued by U.S. Navy personnel at Patuxent River, Maryland, early in the study that this would probably occur; therefore, the very inconsistent results were not totally unexpected. The extremely inconsistent quality of this data was mentioned as one of the primary reasons why the U.S. Navy tests were funded as well as why very accurate velocity measurement sensors and statistical data reduction techniques were used. In conclusion, while the analytical approach that was used in Ref. 29 was generally quite good, the results were nevertheless at least partially contaminated by the poor experimental data that was used to help correlate the analytical procedure.

Results from the Ref. 29 study can be summarized generally by the data presented in Fig. 74. The curve of the ratio P_o/DL (total downwash pressure to rotorcraft disc loading) versus radial distance (x/R) was provided to enable calculations to be made quickly for the maximum expected pressure loading. The resulting calculations were then compared to the Uniform Building Code Design Requirements for wind loading as presented in Fig. 75. The only helicopter size category that was noted in the study as a possible hazard was the size category including large military helicopters such as the CH-54A. Rotorcraft such as the Bell 206L (DL = 3.86 PSF) and the Sikorsky S-76 (DL = 6.77 PSF) were shown to produce maximum pressures of less than 8.5 PSF and 14.9 PSF, respectively, at radial distances of just a few feet beyond the tip of the rotor. These pressure values are clearly less than the 15 to 20 PSF uniform loading design requirements as indicated in Fig. 75.

Conclusions drawn by the authors in the Ref. 29 study therefore indicated that both full-scale and model data revealed that maximum horizontal pressures might approach 2.0 to 2.2 times the rotorcraft disc loading.

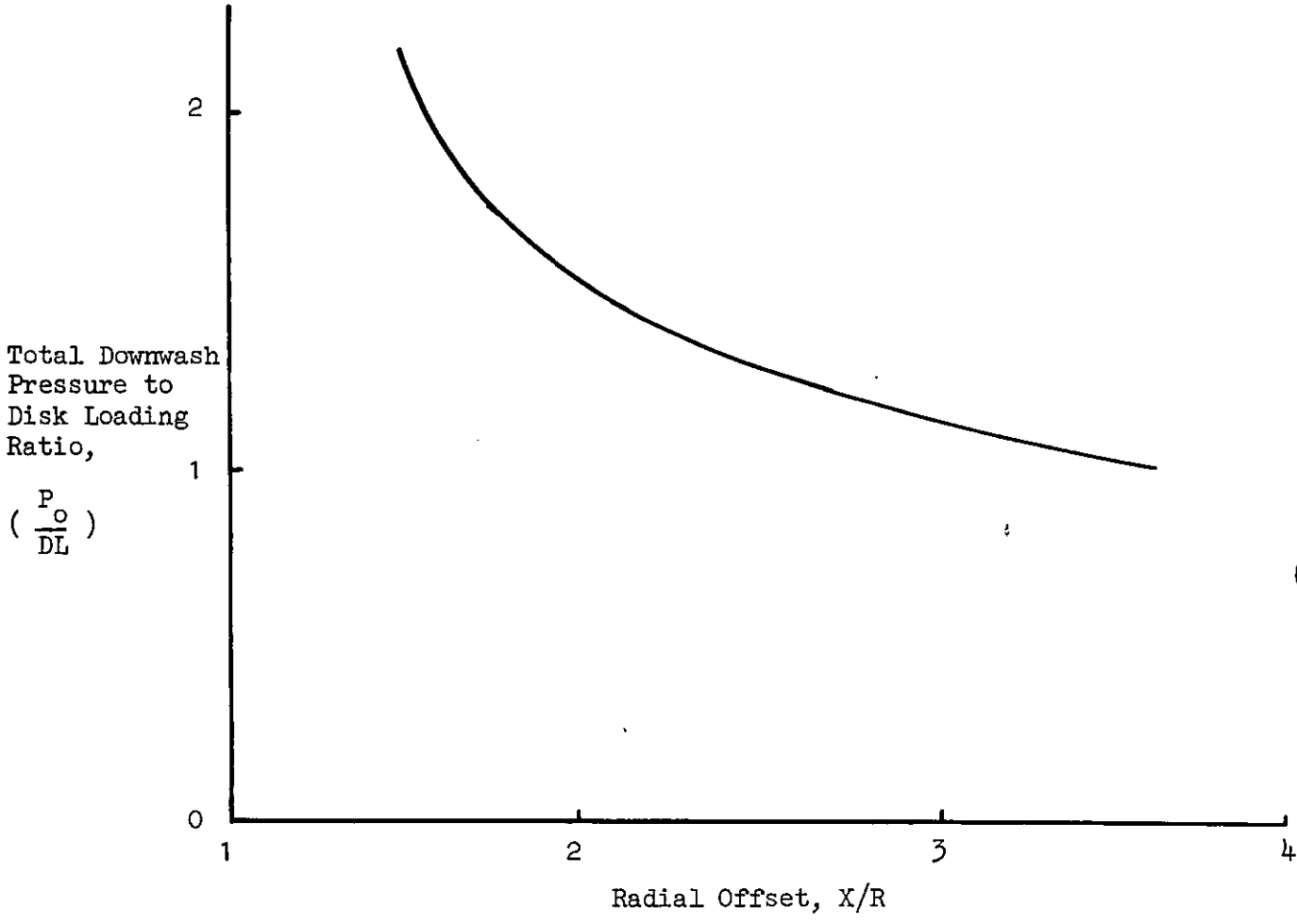

Figure 74. Pressure Distribution Envelope as a Function of Radial Offset

These peak pressure levels would then decrease quickly with increasing distance from the rotor hub. For the more commonly flown helicopters in the civilian fleet (e.g., Bell 206L and Sikorsky S-76), peak wind loads would therefore be expected to be no more than 7 to 14 lb/ft^2. Accordingly, since these pressure levels are well within the uniform building code specifications (Fig. 75), rotor outwash was deemed not to be a critical loading condition in the structural design of heliports. An extensive and impressive list of questionnaire responses were also evaluated and presented in the Ref. 29 study from more than ninety operators to substantiate this conclusion. The questionnaires indicated that operational problems associated with rotorwash were limited almost exclusively to the scattering of roof gravel and occasionally the entering of helicopter exhaust fumes into rooftop circulation vents.

2. Estimation of Peak Velocity Profile and Ambient Wind Loading Effects on Buildings

Since the basis for the whole Ref. 29 analysis hinged on the contaminated results presented in Fig. 74, the five rotorcraft configurations discussed in Section V were instead evaluated using the Section III mathematical models. Graphs of maximum expected pressure loading as a function of distance from the rotor center were then created. This data is presented in Fig. 76 for the zero velocity ambient wind case. If peak dynamic pressure loads of 15 lb/ft^2 are assumed hazardous, there is conclusively a zone for each of the three largest rotorcraft configurations where a minimum separation distance must be maintained. However, since the calculated peak pressure load is applied only over a very localized or small surface area at any specific height on any representative velocity profile (Fig. 77), it is probably quite safe to assume for structural purposes that at least a peak load of 20 lb/ft^2 must be calculated by analysis before a significant portion of structural surface area can be expected to sustain a distributed load significantly in excess of 15 lb/ft^2. It is again important to note in substantiating this assumption that the uniform building code assumes that wind loads are distributed evenly over large areas of a building (this leads to the

TABLE NO. 23-F—WIND PRESSURES FOR VARIOUS HEIGHT ZONES ABOVE GROUND[1]

HEIGHT ZONES (in feet)	WIND-PRESSURE-MAP AREAS (pounds per square foot)						
	20	25	30	35	40	45	50
Less than 30	15	20	25	25	30	35	40
30 to 49	20	25	30	35	40	45	50
50 to 99	25	30	40	45	50	55	60
100 to 499	30	40	45	55	60	70	75
500 to 1199	35	45	55	60	70	80	90
1200 and over	40	50	60	70	80	90	100

[1]See Figure No. 4. Wind pressure column in the table should be selected which is headed by a value corresponding to the minimum permissible, resultant wind pressure indicated for the particular locality.

The figures given are recommended as minimum. These requirements do not provide for tornadoes.

TABLE NO. 23-G—MULTIPLYING FACTORS FOR WIND PRESSURES—CHIMNEYS, TANKS, AND SOLID TOWERS

HORIZONTAL CROSS SECTION	FACTOR
Square or rectangular	1.00
Hexagonal or octagonal	0.80
Round or elliptical	0.60

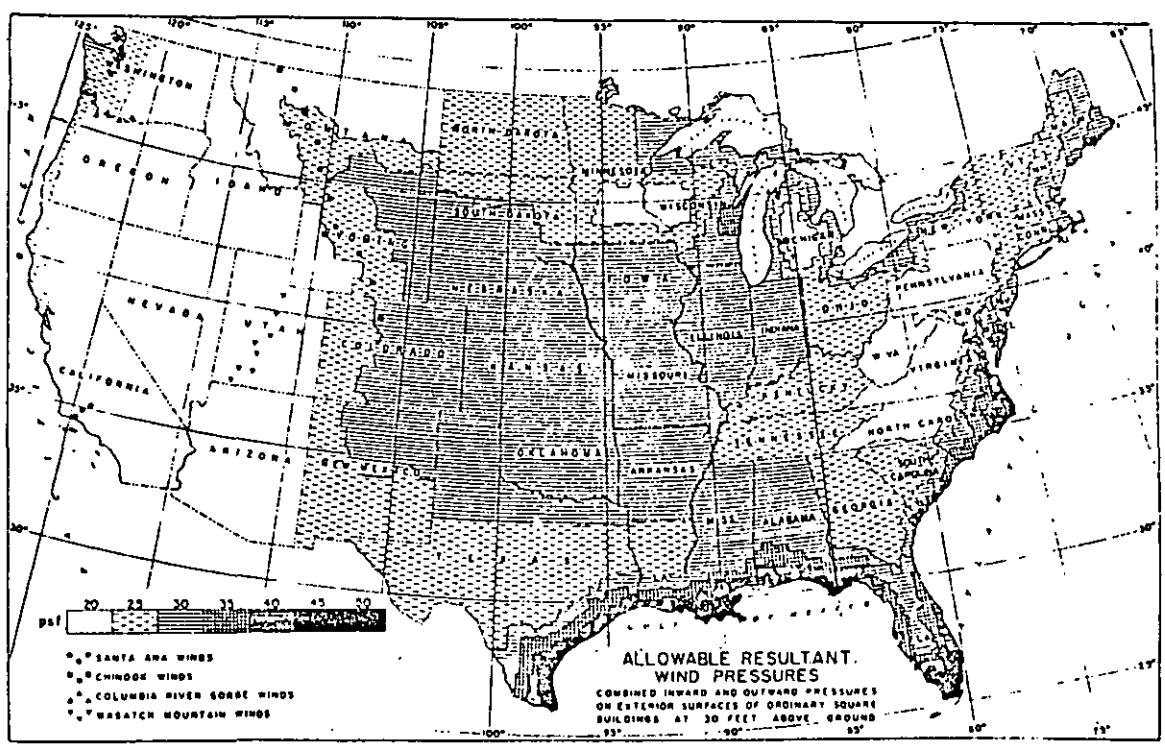

FIGURE NO. 4

Figure 75. Uniform Building Code Wind Loads

Wind = 0 kt
Rotorcraft Configurations: S, SM, M, MH, H

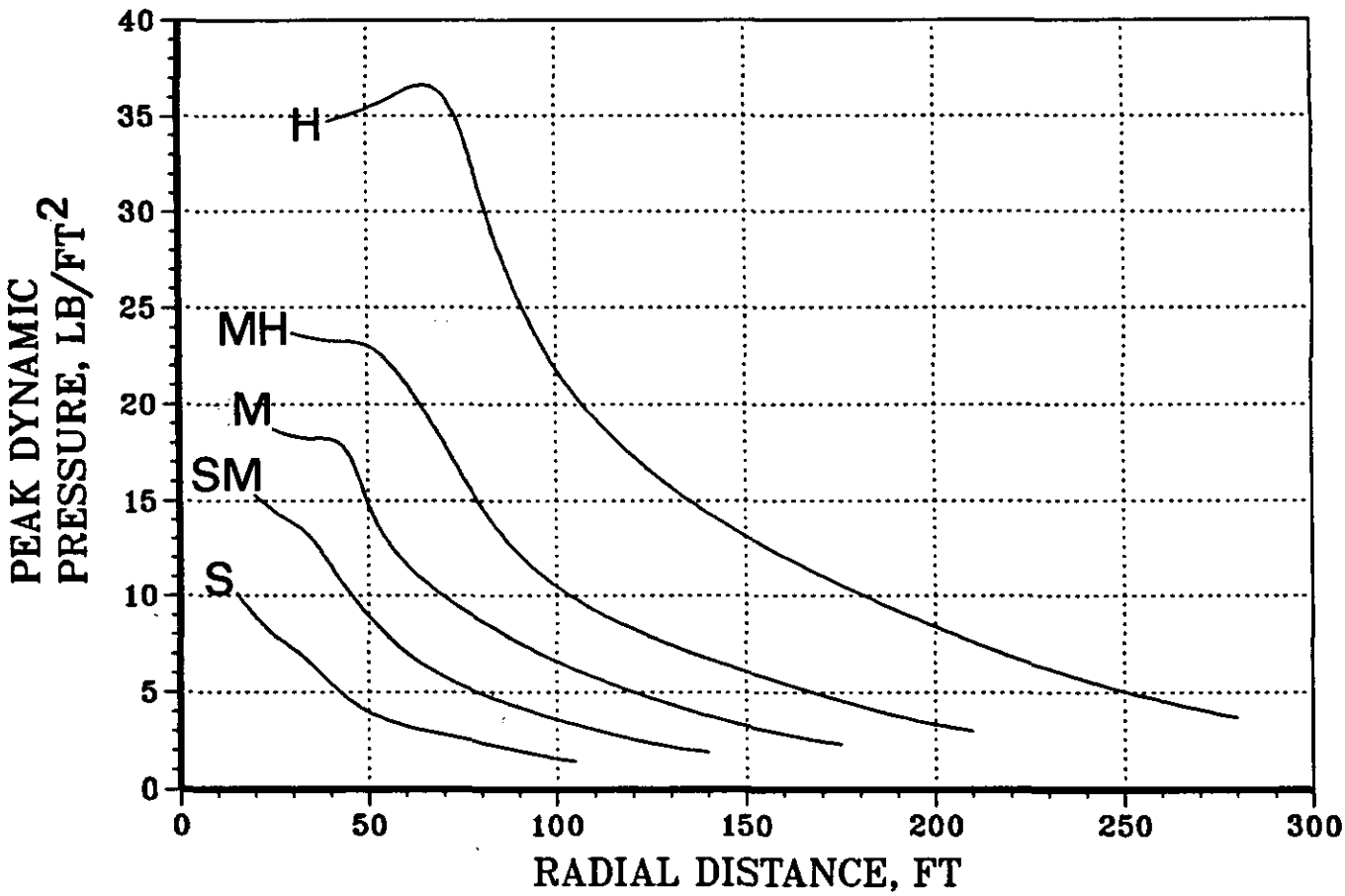

Figure 76. Peak Dynamic Pressure Loads as Calculated as a Function of Radial Distance for the "Worst Offender" Rotorcraft Configurations (Wind = 0 kts)

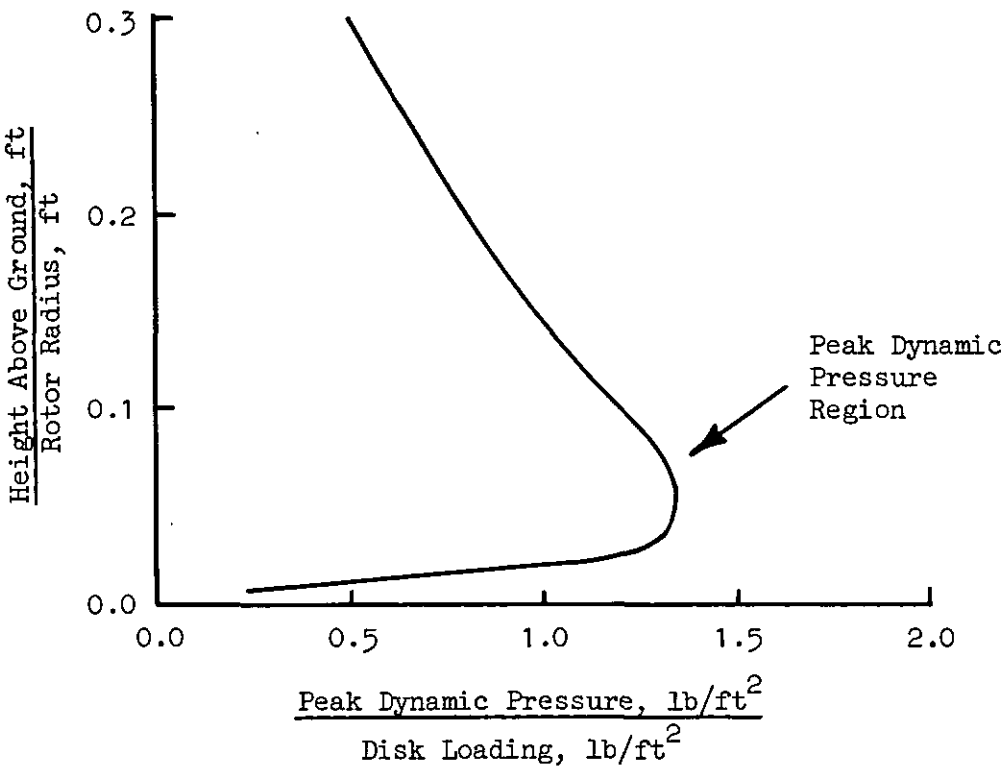

Figure 77. Outwash Profile Dynamic pressure Distribution Near the Ground Surface

calculation of much larger overall structural loads than would be expected from a rotorcraft). Based on this more realistic wind loading assumption, it can be seen in Fig. 76 that only the very large rotorcraft at very close distances to the center of the rotor can be expected to present a hazard.

With the simultaneous addition of wind, the results described above are changed considerably. Scenarios involving the addition of a wind load were not evaluated in Ref. 29. If a worst case assumption of a 9-kt crosswind is made (the limit of the mathematical model as described for the wall jet in Section III), then the peak dynamic pressure values, as plotted in Fig. 76, increase significantly to the values shown in Fig. 78. In this scenario, peak pressure loads in excess of 20 lb/ft^2 are generated by four of the five rotorcraft configurations. In all four cases, except for the 40-ft radius rotorcraft, a minimum separation distance of three rotor radii (or, more practically, 100 ft) is therefore indicated as being required.

One scenario which has not been analyzed that may have an impact on increasing separation distances is the occurrence of a sudden blast of rotorwash on a door or window that is being opened. No simple procedure is known to exist for analyzing this problem, especially when one considers the numerous types of doors and windows that can be installed in a structure. This hazard is therefore pointed out here for the record so that procedures or individual building designs can be addressed in order to eliminate the potential problem.

An evaluation of the mathematical models for the ground and the disc edge vortices indicated that separation requirements would be less stringent than those required from an analysis using the wall jet. Therefore, no results are presented for an evaluation of these forward-flight-related hazards. Good procedural common sense would suggest that rotorcraft operating in the flight regimes generating these hazardous flows should be kept clear of structures for other safety reasons.

Wind = 9 kts
Rotorcraft Configurations: S, SM, M, MH, H

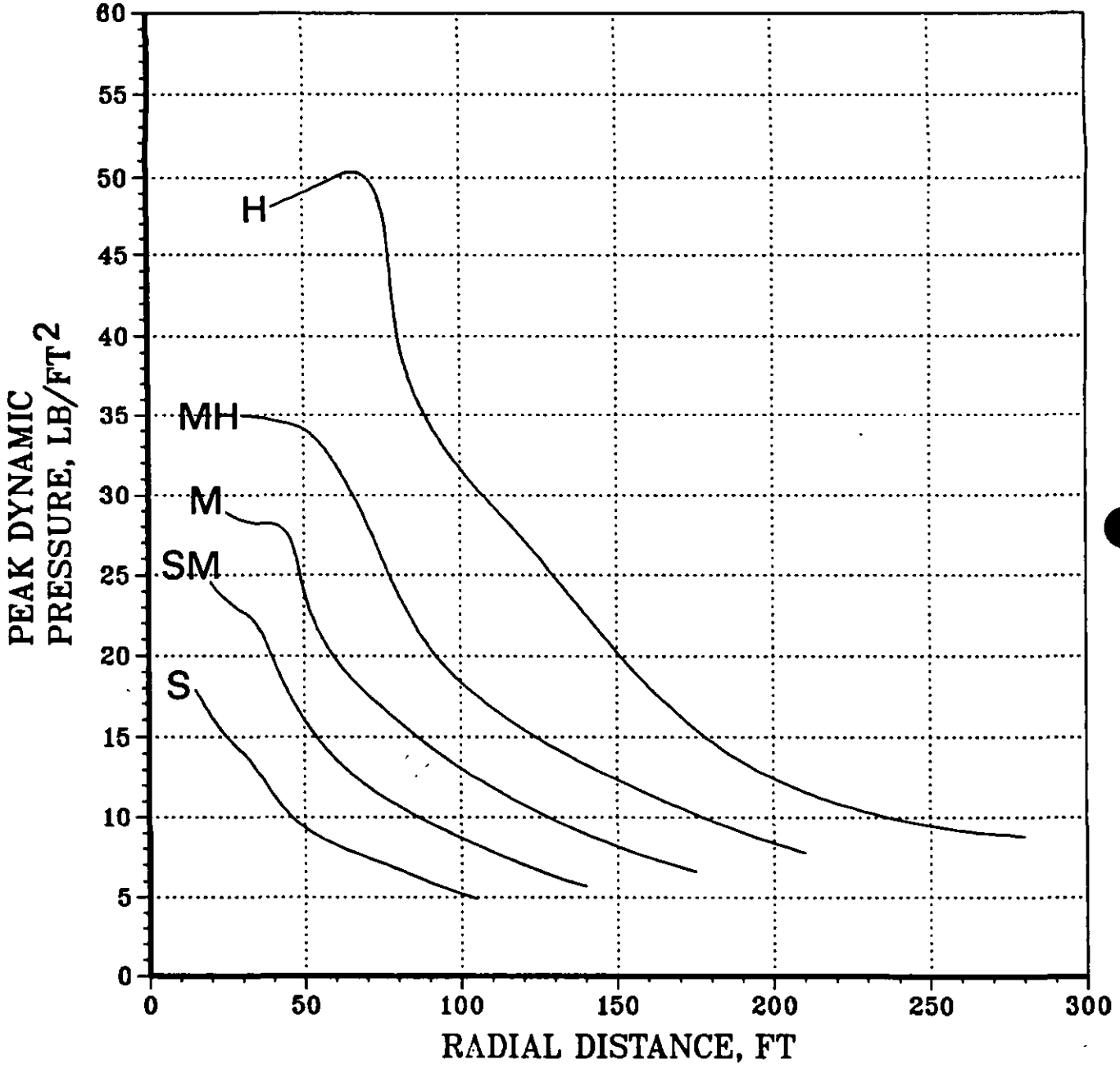

Figure 78. Peak Dynamic Pressure Loads as Calculated as a Function of Radial Distance for the "Worst Offender" Rotorcraft Configurations (Wind = 9 kts)

3. Peak Velocity Profile Effects on Vehicles

Except for a couple of reported accidents involving damage to pickup camper shells, an extensive review of the available literature did not reveal any studies or recorded accidents involving an analysis of rotorwash effects on ground vehicles. This lack of reported accidents is not too surprising when one considers the fact that most ground vehicles, because of the generally high speeds (and often gusting winds) in which they operate, are designed for this type of aerodynamic loading. For this reason, no significant amount of effort was devoted to a general analysis of this hazard.

A brief, indirect analysis was attempted in order to provide some information on the camper shell phenomenon that was reported in the two accidents. Results from this effort were inconclusive, however, due to the lack of sufficient accident information for correlation.

4. Summary of Analysis Results

An analysis of the hazard potential of rotorwash-induced loads that would be applied to buildings or structures has been made and compared to previously identified work. Results indicate that these rotorwash-induced peak pressure loads do impact the recommendation of minimum rotorcraft separation requirements. Safety factors were included in the analysis for known and projected operational rotorcraft in two ways. The first way was indigenous to the analysis methodology in that only worst case rotorcraft configurations (as discussed in Section V) were analyzed. The second way in which safety factors were included came from making the assumption that peak pressures of 20 lb/ft^2, though highly localized on a building surface, were great enough in magnitude to be potentially hazardous. The safety factor in this assumption derives from the fact that the highly localized peak pressures (often applied very low on the building surface) do not produce large cumulative loads across the exposed surface of a building. In contrast, the Uniform Building Code assumes that the wind pressure profile is relatively constant in magnitude all across the

exposed structural surface (Fig. 75). This assumption results in much larger cumulative structural pressure loads being applied to a building during its design.

Even with the conservative analysis assumptions described above being applied, the projected separation requirements resulting from this analysis are not severe. The majority of rotorcraft in civilian use (with a rotor radius of less than 27 ft) are not restricted to any separation distance for low winds. Crosswinds of up to 9 kt necessitate the application of restrictions to rotorcraft having rotor radii greater than 17 ft. Only large military rotorcraft, such as the Sikorsky CH-53E, require separation distances greater than 100 ft. It is expected, however, that most pilots of large rotorcraft will be inclined for other safety reasons to take off and land farther away from buildings than even the conservative distance recommended herein.

D. DOWNWASH/OUTWASH HAZARDS TO OTHER ROTORCRAFT

The hazard potential of rotorwash to other rotorcraft can be subclassified into three general categories, which are defined to include:

1. Hovering or taxiing rotorcraft and their effect on other parked and shutdown rotorcraft.
2. Hovering or taxiing rotorcraft and their effect on other rotorcraft with rotors turning on the ground.
3. Hovering or taxiing rotorcraft and their effect on other rotorcraft hovering or taxiing nearby.

After careful consideration of these three categories, it is easy to conclude that a detailed analysis of all of the possible hazard types and scenarios could take years. Therefore, in order to better manage the task, the available accident information was evaluated to determine which types of accidents had occurred in significant numbers. The assumed hypothesis was that accidents occurring in the past in significant numbers should be the accidents that could be reduced in number in the future. If

the most common types of hazards can be avoided through practical separation requirements, it is hoped that many of the less common hazard types will also be avoided.

The hazard types occurring most in the reviewed accident data bases included those where:

1. Doors or access panels were broken off one rotorcraft by dynamic pressure loads incurred from a passing rotorcraft's downwash (often a plexiglass window or chin bubble was also shattered by the door after it was broken off at the hinges).

2. The rotor blade of a stopped or low rpm rotor was induced by the passing rotorcraft's downwash to strike the tailboom or tail rotor driveshaft, thereby causing rotor blade, tailboom, and/or tail rotor driveshaft damage.

3. Rotorcraft flying too close to other rotorcraft were struck by downwash or trailing vortices from another nearby rotorcraft. This form of "encountered turbulence" resulted in usually either a loss of tail rotor effectiveness or a loss of rotor lift, due to the induced negative angle of attack such that the required collective and engine torque used during recovery (if made at all) resulted in an overtoruqe of the rotor and drive train.

Each of these types of hazards will be examined briefly in this section. Hazards related to one rotorcraft generating flying debris that subsequently struck another rotorcraft were also reported on numerous occasions in the accident data bases. Discussion of hazards associated with flying debris is reserved for Subsections F and G.

I. Historical Accident Data

A summary of historical accident data indicates that many operational rotorcraft accidents have occurred as the result of rotorwash from one rotorcraft impinging upon another. As stated in the previous discussion, three types of accidents were found to be of particular interest to this study. Approximate statistics for these types of accidents are summarized in Table 11; however, a significant problem exists with these statistics. In order to accommodate the format in which the information is

TABLE 11

HISTORICALLY AND STATISTICALLY IMPORTANT ACCIDENT TYPES
DIRECTLY RELATED TO ONLY ROTORWASH BLAST
OR DYNAMIC PRESSURE RELATED EFFECTS

Accident Type	**Approximate** Number of **Reported** Citations Between January 1976 and April 1985	
	Number Obtainable Only with a Brief Verbal Summary	Number Obtainable with Limited Detailed Information to Enable Some Limited Analysis
Doors, Access Panel Damage	40	12
Rotor Blade/ Tailboom Strike Damage	20	1
Wake Induced Overtorque/Loss of Control	30	4

presented, the U.S. Army Safety Center accident summaries are usually highly sanitized. As a result, many of the accidents are described in a verbal format such as, "a pilot's door was blown off a UH-1H as another UH-1H landed on the adjacent pad to the right." This does not, of course, provide sufficient information for further analysis of the accident, unless an assumption is made regarding the distance to the next landing pad. In Table 11, therefore, a comparison is made between the number of accidents that were described only in general terms and the number where information was given (i.e., "a pilot's door was blown off a UH-1H as another UH-1H landed 60 ft to the right") in some quantitative detail that would aid further analysis. (It was not practical in the time available to try to research very many of the accidents by requesting information or specific details from the original accident reports. In some of the few cases where this was done, it was found that the original accident reports were no longer available.)

2. Analysis Methodology

The analysis methodology that was chosen and developed to define separation distances for the types of hazards described previously relies more on indirect than direct analysis. The effort required in a direct analysis approach, i.e., to calculate pressure and hinge loads as well as door accelerations in order to determine when door hinges would fail, was simply beyond the scope and the available resources of this project. Even if this method had been utilized, a large body of experimental data would have been required in order to verify the analysis, especially when one considers that each rotorcraft door or hinged access panel design is different.

With the indirect analysis approach, however, the design details of doors and access panels are not important; instead, the accidents themselves were analyzed to determine the approximate rotorwash velocity values that were present at the accident location (knowing that these values of rotorwash velocites would cause a hazard). Following the analysis of a group of similar accident types, a velocity below which no

accidents occurred was estimated and assumed to be the limiting velocity beyond which a hazard was possible. It must be pointed out, however, that this analysis method also has its weaknesses. For example, the velocity of the ambient wind and the flow effects of the outwash profile around obstacles such as the rotorcraft fuselage are unknown in many instances and have to be guestimated. (These same factors, however, would also have been influential in the direct analysis approach.)

In conclusion, while accident data do exist for the analysis of the rotorcraft hazards as previously discussed, the data are not extensive enough to validate conclusively any hazard analysis in detail. The results presented here, pending further detailed validation, must therefore be used only for "rule of thumb" estimation purposes.

3. Analysis Approach

During the course of conducting the described indirect analysis, a chart was made using the Section III mathematical models for each helicopter type for which accident data was available. The chart for the UH-1H is presented as an example in Fig. 79. In these charts, the peak velocity was plotted as a function of radial distance at the peak velocity height (between 0.5 and 2.5 ft) and at the 10-ft height for each specific helicopter. A mid-gross weight was assumed in each case for the respective groups of accident data. For the UH-1H, the gross weight was 8000 lbs. Ambient winds of both 0 and 9 kts were also evaluated. On top of this quantitative data, a pictorial representation of several of the subject rotorcraft was drawn in order to estimate pad spacings. The assumption was made that each rotor tip was, on the average, separated by one rotor radius while on the ground. Above these pictorial representations, arrows were drawn to represent the actual or approximate radial distances that the accident reports stated were present when each accident occurred. Other information, such as type of accident and ambient wind velocity, were also noted next to the arrow. For the OH-58, UH-1H, AH-1S, CH-46, and CH-47 (Refs. 33 through 38), the wind limits for rotor startup and shutdown (from the pilot manuals) were also plotted. Wind limits of this

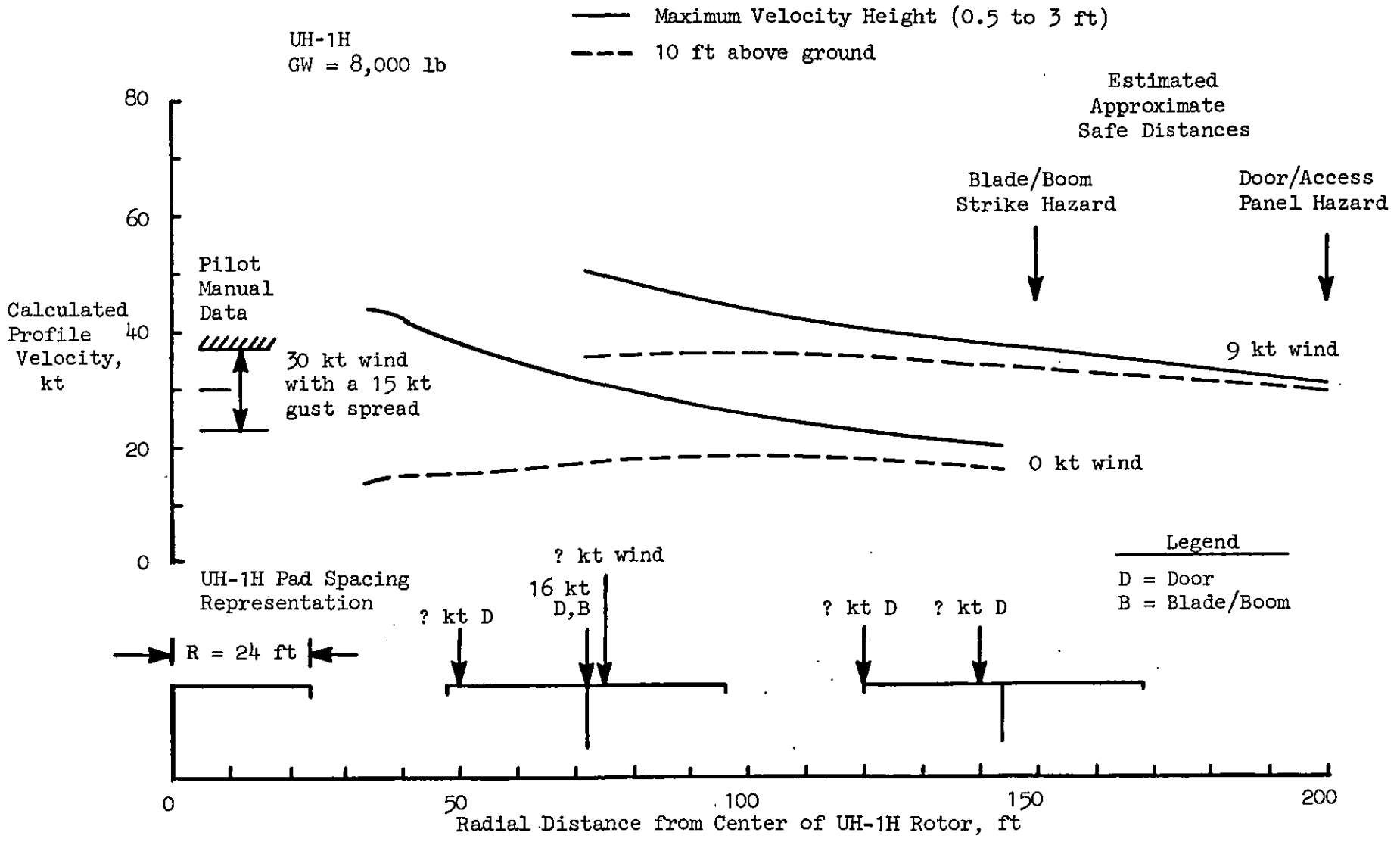

Figure 79. UH-1H Analysis Prediction Chart for Door/Access Panel and Rotor Blade/Tailboom Strike Hazards

type are provided in the pilot manual from flight test data sources in order to insure that the rotor does not flap down and strike the fuselage at very low rpm during startup or shutdown in strong gusty winds. These limiting wind values were utilized as the main basis for estimating when rotorwash peak velocity values would reach magnitudes that would become potentially hazardous in causing rotor blade/tailboom strikes.

Referring again to the example in Fig. 79, it can be seen that several interesting results can be generally deduced from the chart. For rotor blade/tailboom strikes, it can be seen that, on the next pad (a distance of approximately 72 ft) with a crosswind of 9 kt, it is possible to have a rotorwash plus ambient wind velocity such that the total velocity is above the pilot manual limit for rotor startup. At a radial distance of two pad spacings, the calculated total velocity values are below the pilot manual limits; and, interestingly enough, no blade/boom strikes are reported at this separation distance in the available accident data sources (even when considering the nonquantitative, descriptive only accident reports). From this indirect analysis, one would presume that the pilot manual limit is a good hazardous situation predictor; therefore, a separation distance of approximately 150 ft is safe for a UH-1H in the worst case analysis configuration. While separation data, as determined from this one chart, might be considered to be very speculative, the analysis approach appears to be greatly strengthened in that each of the other charts that were developed indicated similar results. The conclusion that was reached from these charts as a whole, therefore, was that, whenever the wind (ambient or ambient plus rotorwash) exceeds 30 kt ± 7.5 kt (mean plus a gust spread), a rotor blade/tailboom strike is a possibility. This limit should be further qualified, since an assumption was made that the rotor blades are not tied down and that the rotor is rotating at or below 10 to 20 percent of the operating rpm. The limited data that were available seem to indicate that, if the rotor blades were tied down or were operating at a normal rpm, operation next to a departing or landing rotorcraft was generally safe on the next takeoff/landing pad (again, this assumes a separation of one rotor radius between rotor blades).

Data plotted on the working charts to estimate separation criteria for damage to open or unlatched doors or access panels also seem to be consistent from one chart to the next. In Fig. 79, the loss of doors was reported for UH-1H helicopters out to at least 140 ft (wind unknown). Using this data and the data from the other plots, an estimated total wind plus peak velocity profile (at any height above ground) of 30 kt was assumed to be the maximum limit allowable before door or access panel damage would occur. When applying this criteria to the UH-1H data (Fig. 79), a limit distance would appear to be approximately 200 ft or three pads distances. While this separation distance may seem excessive, it must be remembered that this is a "worst case" scenario (i.e., with high winds) and not necessarily an every-day scenario. With these criteria in hand, it is now possible to evaluate the "worst offender" configurations as in previous sections.

4. Evaluation of Door, Access Panel, and Rotor Blade/Tailboom Strike Hazards

The first step that is required to analyze door/access panel and rotor blade/tailboom strike hazards is the development of charts for peak velocity estimation purposes. This is accomplished in Figs. 80 and 81 using the Section III mathematical models for ambient wind values of 0 and 9 kt, respectively, for the five "worst offender" rotorcraft configurations. Again, it should be noted that the 9-kt case, as superimposed on the hover outwash flow, is assumed to be the worst case possible, because higher wind values are assumed to break up the hover outwash flow. From these figures, the separation distances for the limiting airspeeds of 37 and 30+ kt (blade/boom and door/access panel) can be determined for each rotorcraft configuration; these are shown in Table 12. These data are also presented in Fig. 82. The previously charted data (i.e., Fig. 79) are also plotted in Fig. 82 as an aid to validation. As can be seen, the experimentally derived limits that are plotted for the OH-58, UH-1H, AH-1S, and CH-47 fall comfortably between the 0 and 9 kt ambient wind limits that were developed for the worst case configurations. This would be expected if the analysis was not excessively conservative, particularly

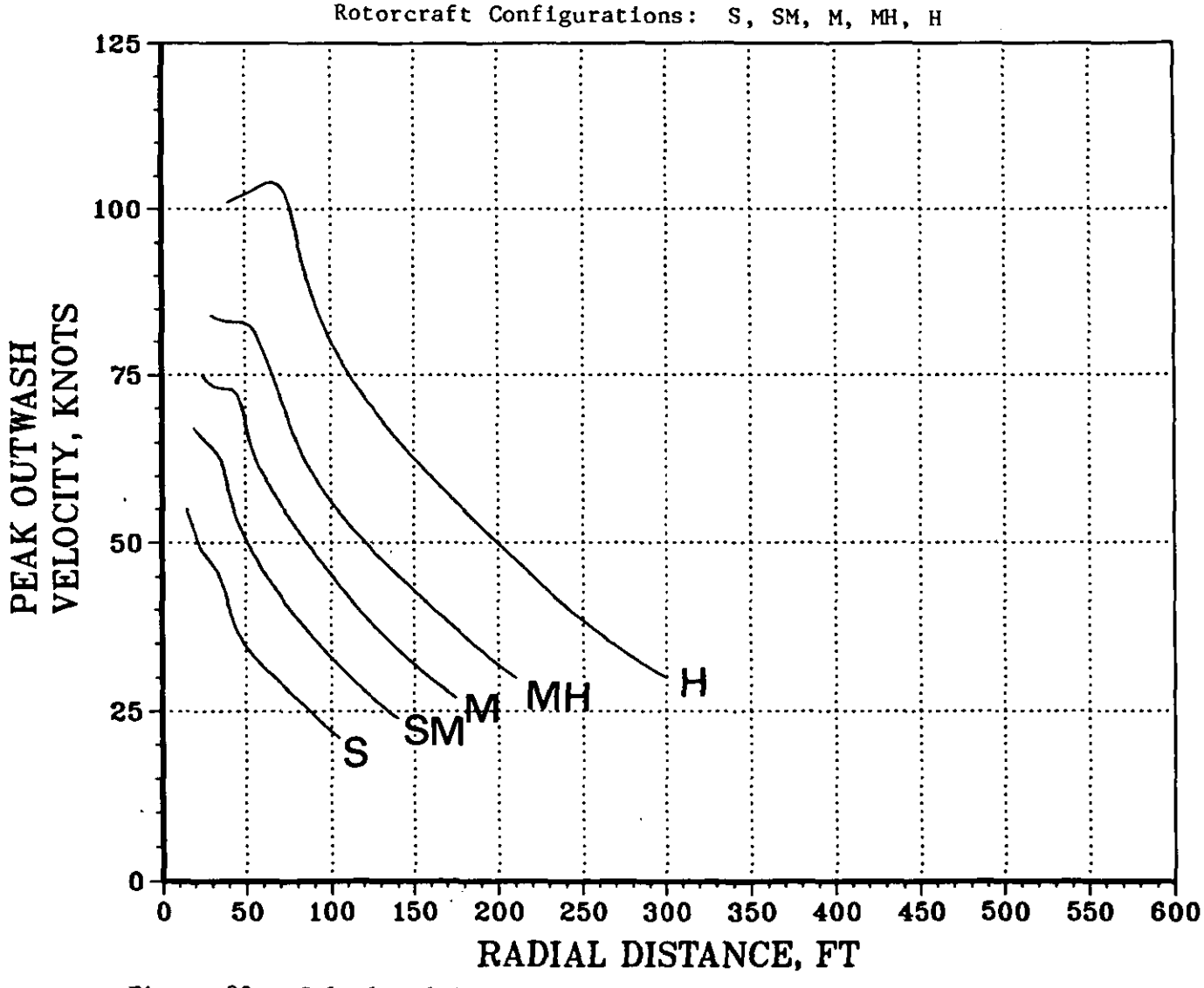

Figure 80. Calculated Peak Profile Maximum Velocities as a Function of Radial Distance (Wind = 0 kt)

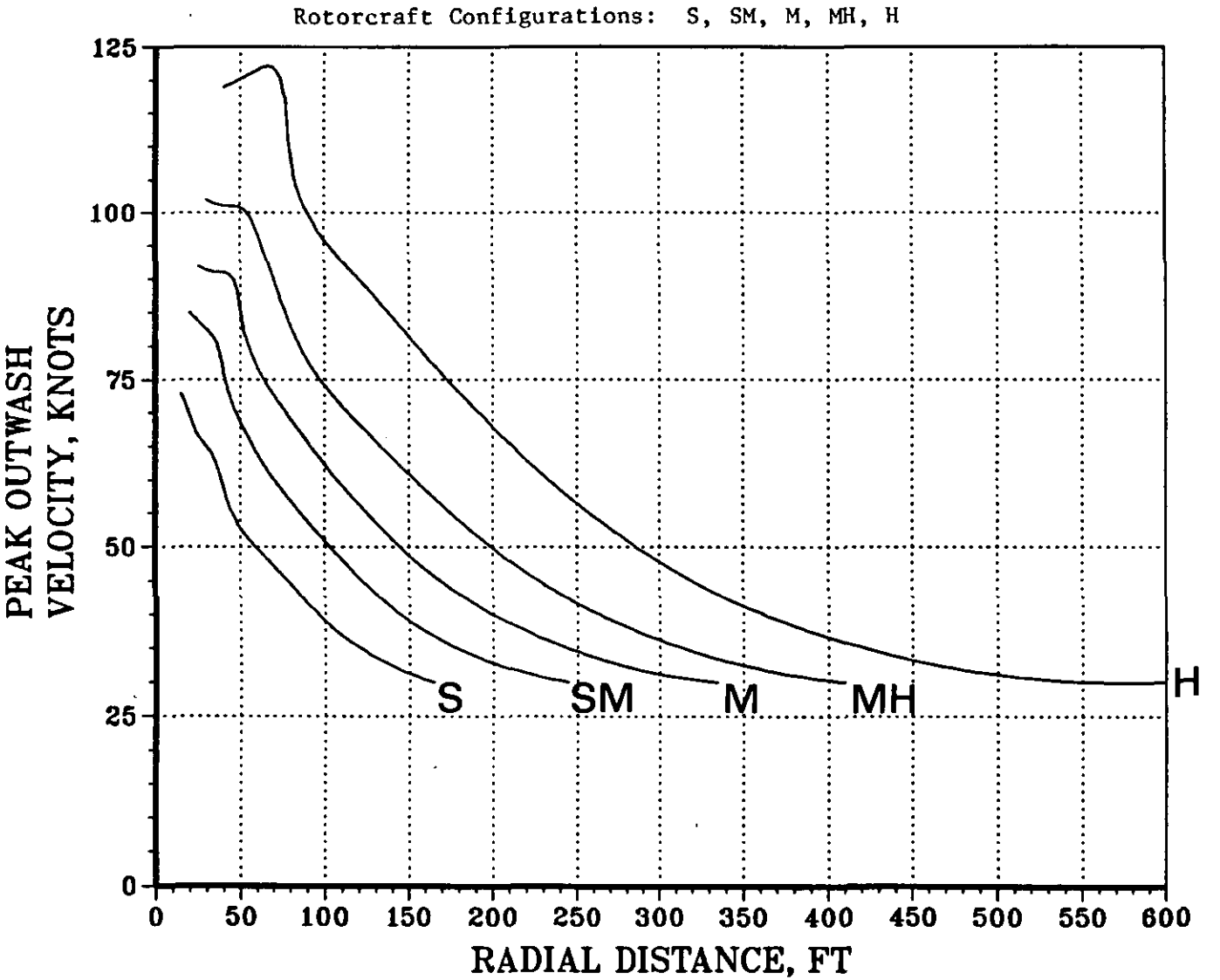

Figure 81. Calculated Peak Profile Maximum Velocities as a Function of Radial Distance (Wind = 9 kts)

TABLE 12

APPROXIMATE SEPARATION DISTANCE REQUIREMENTS NEEDED TO AVOID DOOR/ACCESS PANEL AND ROTOR BLADE/TAILBOOM STRIKE HAZARDS

Size Class	Approximate Minimum Separation Distance, ft			
	Wind = 0 kt		Wind = 9 kt	
	Door/Access Panel	Rotor Blade/ Tailboom	Door/Access Panel	Rotor Blade/ Tailboom
S	67	44	150	105
SM	110	84	220	160
M	157	125	310	220
MH	210	168	380	290
H	300	257	520	400

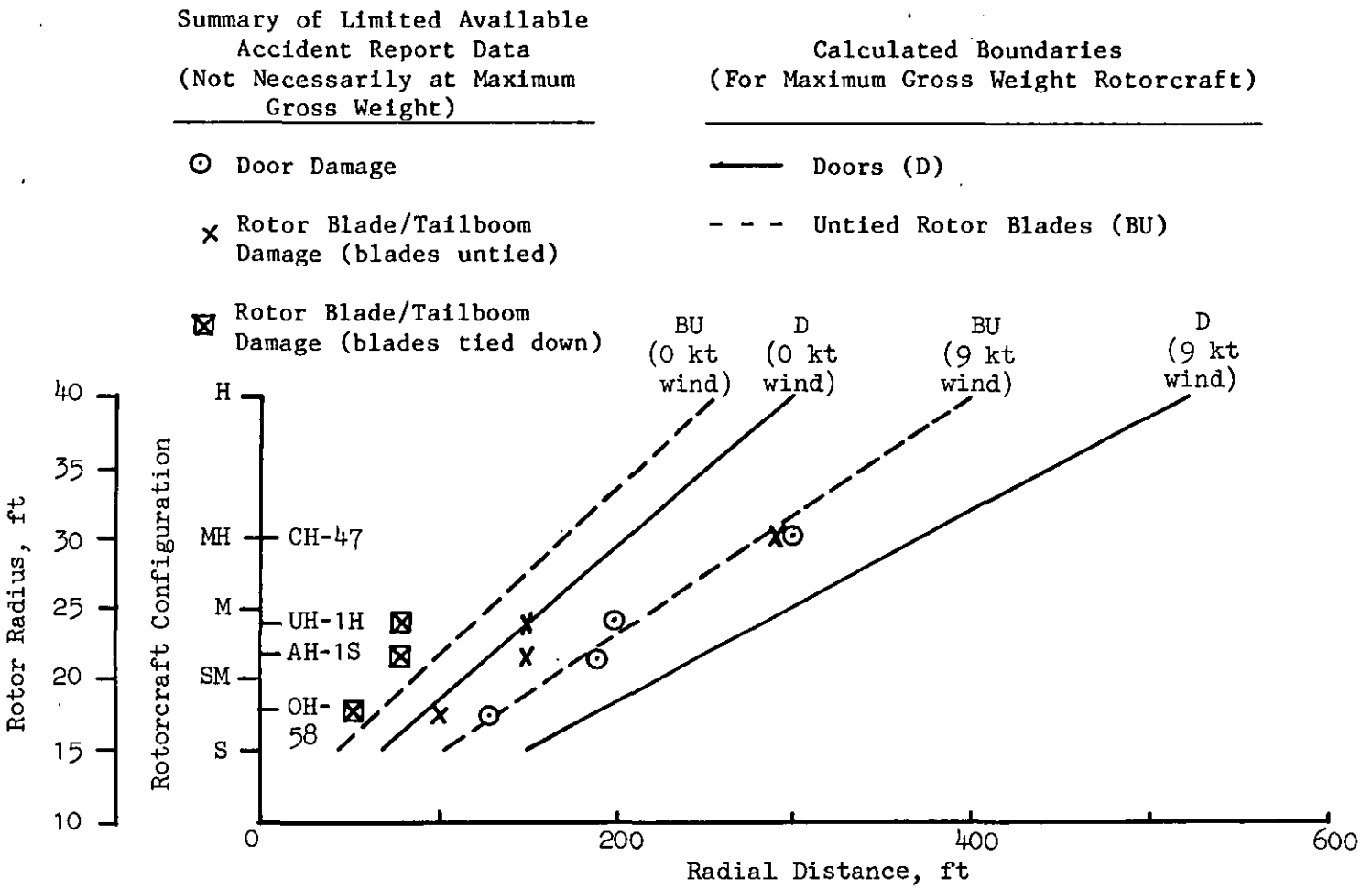

Figure 82. Separation Distance Requirements Needed to Avoid Door/Access Panel and Rotor Blade/Tailboom Strike Hazards

since the disc loadings of these four helicopters are significantly less than those of the "worst offender" configurations for the same rotor radius.

If the data presented in Table 12 (and Fig. 82) are manipulated somewhat, an interestingly new form for separation distance criteria can be introduced. This form of criteria, which will be labeled "pad separation" distance, is a measure of the number of landing pads which must separate rotorcraft in order to avoid a hazard. The centers of two landing pads are defined here as three rotor radius lengths between the centers of the rotorcraft of interest. This separation unit insures that one rotor radius exists between turning rotors. When the aforementioned data is converted to these "more nondimensionalized" units, the results are like those presented in Table 13. Separation criteria that were developed with this type of spacing concept would indicate that, on the average,

1. If the parked or low rpm rotorcraft is upwind of the departing or landing rotorcraft or the ambient wind is zero, a pad spacing of approximately two pads is probably acceptable in order to prevent door/access panel separation or rotor blade/tailboom strike hazards.

2. If the parked or low rpm rotorcraft is downwind of the departing or landing rotorcraft, the **worst case** pad spacing should be increased to three pads for elimination of rotor blade/tailboom strikes and four pads for door/access panel hazard alleviation. The four pad spacing for the door/access panel safety would also be the obvious **worst case** limit for maintenance personnel or crew/passenger loading operations.

This latter separation distance may be desirable in itself for crew/passenger operations in order to insure that, in case of crash and fire by a departing or arriving rotorcraft, the unprotected crew/passengers will be far enough away to be safe from this new hazard. This type of restriction clearly indicates the importance of the wind in the process by which controllers and pilots manage heliport operations to maximize safe operations in their limited spatial environment.

A brief analysis was also conducted in order to evaluate the ground vortex and the low-speed trailing vortex hazards as they affect separation

TABLE 13

SEPARATION DISTANCE DATA CONVERTED TO UNITS OF "PAD SEPARATION" DISTANCE

	Approximate Minimum "Pad Separation" Distance*, ft			
	Wind = 0 kt		Wind = 9 kt	
Size Class	Door/Access Panel	Rotor Blade/ Tailboom	Door/Access Panel	Rotor Blade/ Tailboom
S	1.5	1.0	3.4	2.3
SM	1.8	1.4	3.7	2.7
M	2.1	1.7	4.1	2.9
MH	2.3	1.9	4.2	3.2
H	2.5	2.1	4.3	3.3

*Where "pad separation" distance is defined as follows (in ft):

Size Class	Next Pad or 1 Pad	2 Pads	3 Pads	4 Pad
S	45	90	135	180
SM	60	120	180	240
M	75	150	225	300
MH	90	180	270	360
H	120	240	360	480

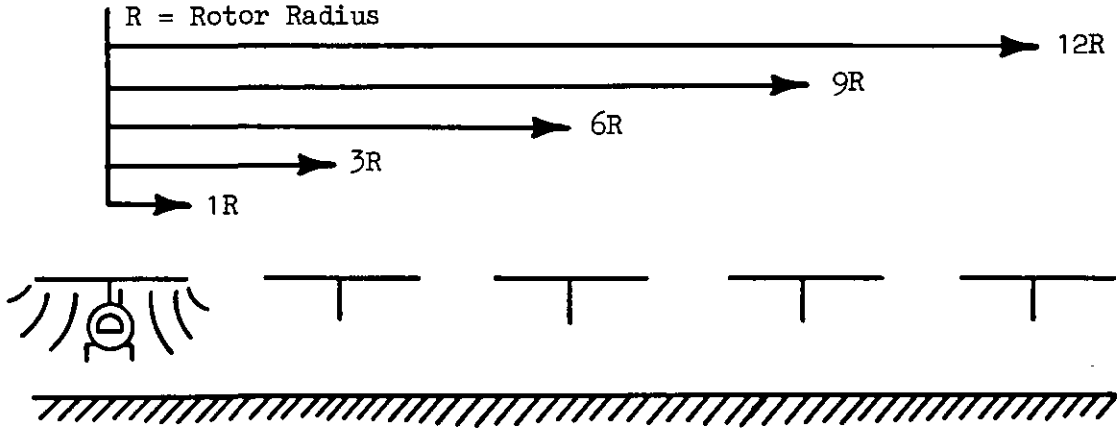

standards. Since these aerodynamic flowfields are localized and their movement with ambient winds are not clearly understood, it was not possible to develop and justify (and validate with confidence) any practical separation distance requirements in addition to those that were developed for the wall jet or interaction plane models. Therefore, the assumption is made that, until further data becomes available, separation requirements should be like those shown in Table 12.

5. Evaluation of Rotorwash Hazards to Other Hovering or Taxiing Rotorcraft

The analysis of separation standards for rotorwash hazards involving other taxiing or hovering rotorcraft was by far the least defineable type of hazard that was examined in this section. All but three of the accidents reported involved formation flights of helicopters wherein, during some part of the mission, one of the trailing helicopters got behind and below (instead of level with or above) or downwind and below (to the side of) the other helicopter(s) in the formation. In this position, the downwash and/or trailing vortices of the leading helicopter induced a sudden negative angle of attack or downdraft at the trailing helicopter's rotor. This sudden change of flight environment resulted in the trailing rotorcraft being overtorqued or making a hard landing if close to the ground, because the pilot was required to pull in an excessive amount of collective in order to maintain altitude or avoid obstacles. The number of times that this or a similar scenario went unreported because the resulting accident was narrowly avoided is unknown.

The other type of reported hazard resulted in a loss of tail rotor effectiveness following the impingement of rotorwash from another nearby helicopter. In each of the three cases where this type of hazard was reported, gusty crosswinds of 10 to 20 kt were also reported. Lateral separation distances were reported to be between "right next to" and 100 meters away as well as below the helicopter that was generating the rotorwash.

A collective review of the accidents described above leads to the conclusion that a much more detailed analysis will be required in order to study this type of hazard; however, it is questionable even then whether or not enough data exist to validate a mathematical model. As a rule of thumb, therefore, any type of formation flight probably should be restricted severely during normal operations in heliport environments. Special situations should be permitted if procedures are worked out ahead of time based on the fact that military formation flights are flown with safe separation distances all of the time. Otherwise, it is assumed, using the sparse data available, that if separation distances are maintained between hovering or taxiing rotorcraft on the same order as those required for the door/access panel and rotor blade/tailboom strike hazards, even crosswinds will probably not blow hazardous levels of rotorwash from one rotorcraft onto another. These generalized suggestions should certainly be reviewed if further data become available subsequent to completion of other ongoing FAA work directed toward an exclusive evaluation of the wake vortex hazard.

6. Summary of the Downwash/Outwash Hazard Potential of One Rotorcraft Onto Another

The previous subsections have evaluated briefly the hazard potential where one rotorcraft (hovering or taxiing) generates a rotorwash flowfield that impacts another hovering, taxiing, or parked rotorcraft (with the rotor stopped or slowly turning). The analysis showed that, given the time and resource constraints of this project, it was not possible to conduct a direct engineering analysis of the problem. Instead, an indirect approach to analysis was conducted using reported accident data. The results for this analysis appear to be consistent with what common sense would indicate might be appropriate for separation requirements. Safety factors are included inherently in the mathematical models themselves as well as in the "worst offender" rotorcraft configurations in order to provide conservative but reasonable analysis results. Significant reduction of these safety factors would require a considerable amount

of additional research that would probably not be cost effective, particularly for the ground vortex and trailing vortex cases.

E. DOWNWASH/OUTWASH HAZARDS INVOLVING FIXED-WING AIRCRAFT

The potentially hazardous effect of rotorwash on adjacent fixed-wing aircraft (while on the ground) can also be classified into categories (as was done with rotorcraft in Subsection D). These categories are defined to include the effects of hovering or taxiing rotorcraft on:

1. Other parked and shutdown fixed-wing aircraft (both tied down and not tied down).
2. Other operating fixed-wing aircraft (stationary or taxiing).

Each of these types of hazards will be discussed briefly in this section; hazards directly related to flying debris will be discussed in Subsections F and G.

1. Historical Accident Data

A review of historical accident data indicated that light fixed-wing aircraft (i.e., Cessna 150, Piper Cub) are clearly at risk when they are in close proximity to operating rotorcraft. No specific cases involving overturning accidents and "larger" fixed-wing aircraft were identified. Unfortunately, accidents of this type were not reported in large enough numbers to more fully correlate the aerodynamics and dynamics of the problem. This sparsity of accident reports was not considered to be an indication that the problem was not a potentially serious one, however, because the accident data bases were oriented primarily toward the reporting of rotorcraft accidents only. The accidents that were discovered (approximately ten in varying degrees of detail) involved UH-1 and CH-47 rotorcraft.

2. Analysis Methodology

The analysis methodology that was developed to define separation requirements for the two types of hazards previously described relies upon a combination of direct as well as indirect analysis methods. In the case of analysis for door and access panel damage, the indirect method of Subsection C was utilized, and the resulting recommended separation distances for elimination of this type of hazard are the same as those that were recommended for rotorcraft. The reason for this is that the level of detail involved in this study makes it impossible to differentiate between a rotorcraft and a fixed-wing aircraft for this particular hazard. (This assumes, of course, that there may be a reason to differentiate between the two which in itself is an unproved hypothesis).

The methodology that has been developed to analyze the fixed-wing aircraft overturning hazard uses simple aerodynamic theory. This methodology is outlined graphically in Fig. 83. The analysis approach assumes that there are two components to the aerodynamic overturning moment which contribute to the rotation of the fixed-wing aircraft about its landing gear. The analysis approach also assumes that the fixed-wing aircraft is a small, high-wing civilian model (more specifically, an Aeronca Champion 7AC, Cessna 150, Cessna 172, or Piper Cub PA18). These light-wing-loading aircraft are representative of the thousands of civilian aircraft in use in the United States today and can be shown mathematically to be more susceptible to the overturning hazard than larger all metal fixed-wing aircraft. (No specific home-built aircraft were analyzed; however, a brief survey indicated that wing loadings were, in general, no lower than the Aeronca Champion).

The two aerodynamic components of the overturning moment on a fixed-wing are those which result from lift (due to the wing) and drag (due to pressure loads on the projected side area of the fuselage). For equilibrium, these two destabilizing aerodynamic terms can be specified in conjunction with the stabilizing moment due to the fixed-wing gross weight as:

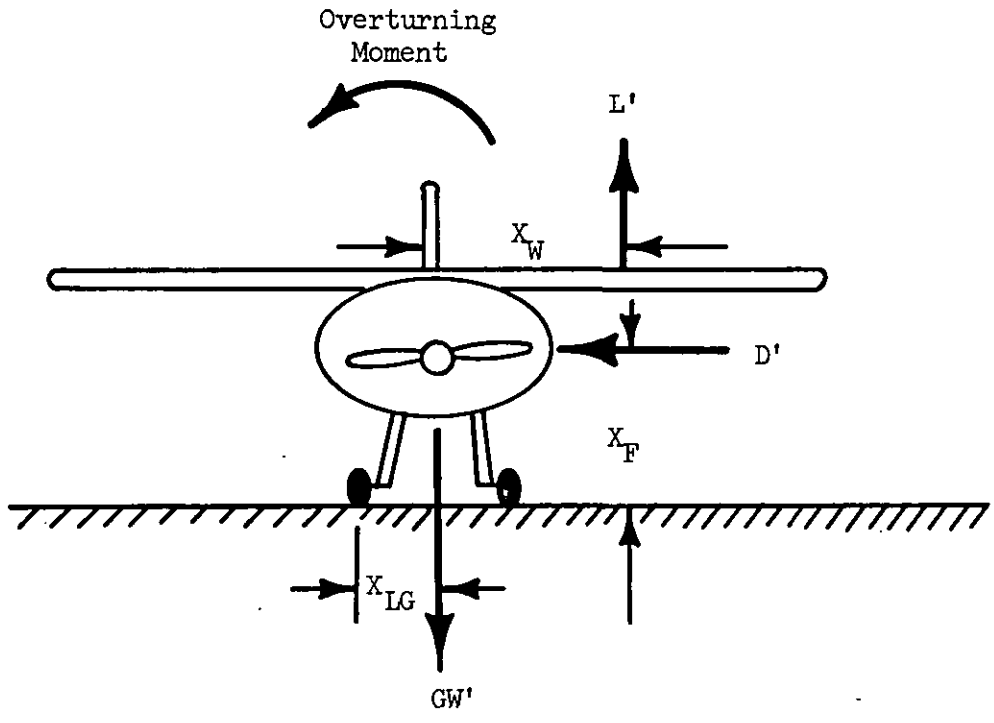

STEPS:

1. Calculate parameters to calculate the stabilizing moment $(GW')(X_{LG})$.
2. Calculate parameters to calculate the destabilizing moments $(L')(X_W)$ abd $(D')(X_F)$ in Eqs. 66 and 67.
3. Calculate minimum outwash velocity required to generate the condition where the sum of the moments is equal to zero ($\Sigma M = 0$) using Eq. 68.

Figure 83. Fixed-Wing Overturning Hazard Analysis Methodology

$$(GW')(X_{LG}) = (L')(X_W) + (D')(X_F) \quad (67)$$

Where the terms are defined as:

GW' = (0.95)(a stated empty weight for the aircraft + 100 lb)

X_{LG} = Moment arm of the landing gear (one-half the wheel stance), ft

L' = Wing generated lift, lb

X_W = Moment arm from the centerline to the point of application of L', ft

D' = Fuselage generated side force, lb

X_F = Vertical moment arm from the wheel to the point of application of D', ft

The 0.95 term in the definition of GW' provides a small safety factor to insure that the stated empty weight of the aircraft is not "high," and the 100 lb is allowed to account for any residual liquids (e.g., fuel, oil) or other flight equipment in the aircraft that are not part of the stated empty weight. X_F is also assumed for this study to be approximately equal to X_{LG} for simplicity. Developing Eq. 67 further, it can be shown that:

$$L' = (\frac{1}{2}\rho_A V^2)(\frac{S}{2})(a_{3d}\alpha_w) \quad (68)$$

and

$$D' = (\frac{1}{2}\rho_A V^2)(\frac{S}{3})(C_D) \quad (69)$$

where:

ρ_A = Atmospheric density (0.0023769 slugs/ft^3)

V = Air velocity, ft/sec

S = Wing area, ft^2

a_{3d} = Wing lift curve slope, 1/deg

C_D = Coefficient of drag

α_W = Angle of attack of the wing, deg

Assumptions made for C_D and a_{3d}, respectively, are that they equal 1.0 and 0.08 per deg. Both of these assumed values should be slightly conservative. Without a more detailed knowledge of each type of fuselage and wing involved, it is difficult to assign larger values to the parameters with confidence. The terms S/2 and S/3 in the lift and drag equations assume that only one-half of the wing provides lift for an overturning moment and that the projected side area of each fuselage is one-third that of the wing area. This assumption for the fuselage projected side area should also be slightly conservative. Again, however, without more detailed aircraft information, it is difficult to make an exact estimation. No assumptions are made with respect to additional overturning moments which might occur due to lift on the horizontal tail or the vertical tail. In addition, no reduction in the landing gear pivot arm is accounted for if the rollover occurs about one main wheel and the tail or nose wheel. The application point of L' is assumed to be one-quarter of the wing span. By substituting Eqs. 68 and 69 into Eq. 65, it can be shown that Eq. 70 will result. In this equation, VK has replaced V, and this variable equals the outwash velocity required to overturn the fixed wing in knots (1 kt = 0.592086 ft/sec).

$$VK = \sqrt{\frac{GW'}{[(0.0001356)(\alpha_W \; S \; X_W)/(X_{LG})] + (0.00113)(S)}} \quad (kt) \qquad (70)$$

If Eq. 70 is evaluated for α_W for the four fixed-wing aircraft specified in Table 14, then the curves of Figs. 84 and 85 can be obtained.

Figure 84 is the calculated overturning rotorwash velocity for Eq. 70. Figure 85 assumes that the $(D')(X_F)$ term of Eq. 70 is set to zero. As can be seen for a specified angle of attack, the critical rotorwash velocity required to produce a hazard is significantly lower when the $(D')(X_F)$ term is included. It should also be noted that the dynamics of this hazard are very unstable, once the overturning process is initiated,

TABLE 14. INPUT DATA VALUES FOR THE EVALUATED LIGHT CIVILIAN AIRCRAFT

Type	GW,* lb	S, ft^2	X_W, ft	X_{LG}, ft
Aeronca Champion 7AC	850	165	8.4	3.2
Cessna 150	1100	160	8.3	3.8
Cessna 172	1350	174	8.9	4.1
Piper Cub PA18	1030	179	8.8	3.0

* GW' = (0.95)(GW)

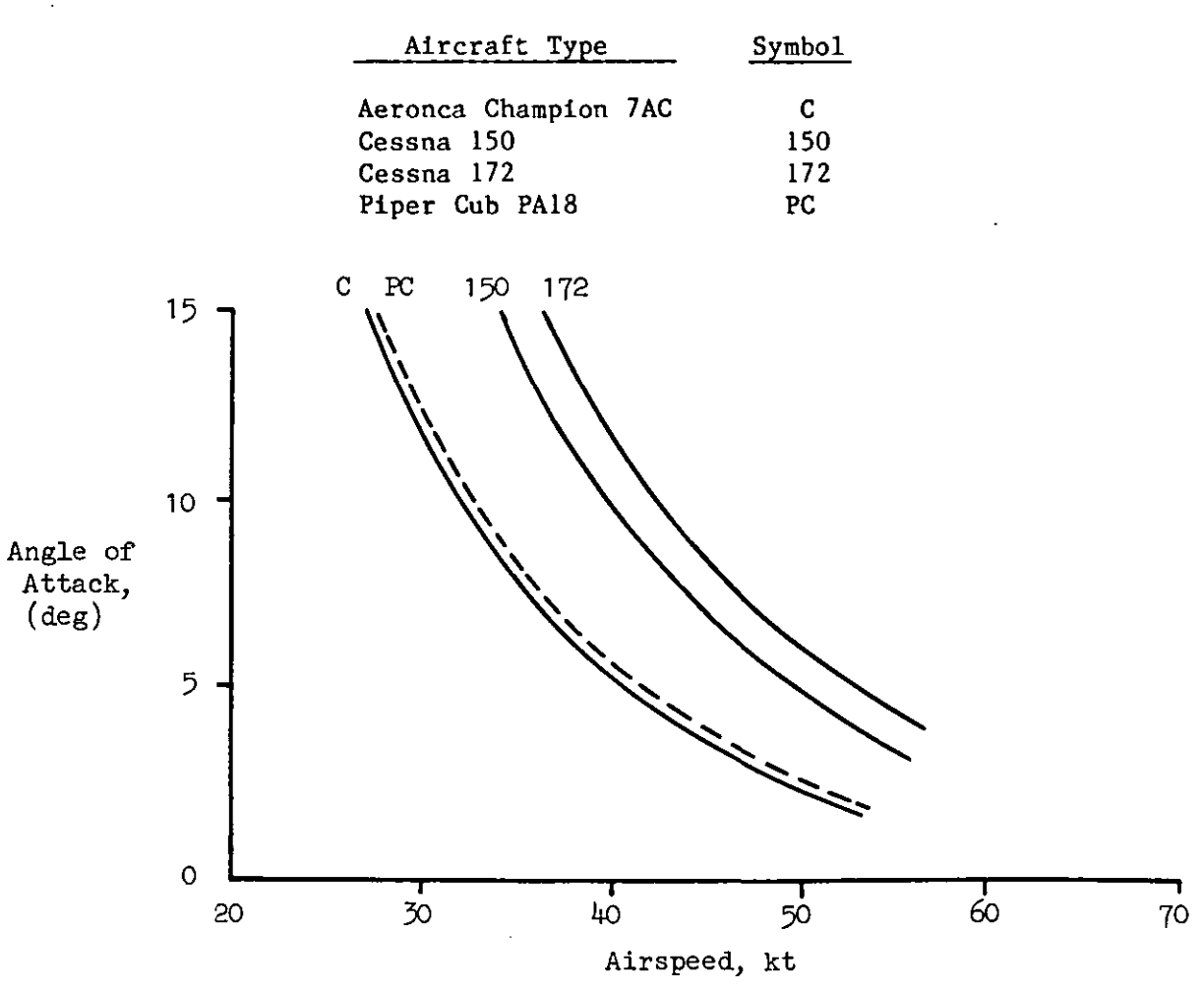

Figure 84. Minimum Airspeed/Angle-of-Attack Requirements for the Overturning of Light Fixed-Wing Aircraft

Aircraft Type	Symbol
Aeronca Champion 7AC	C
Cessna 150	150
Cessna 172	172
Piper Cub PA18	PC

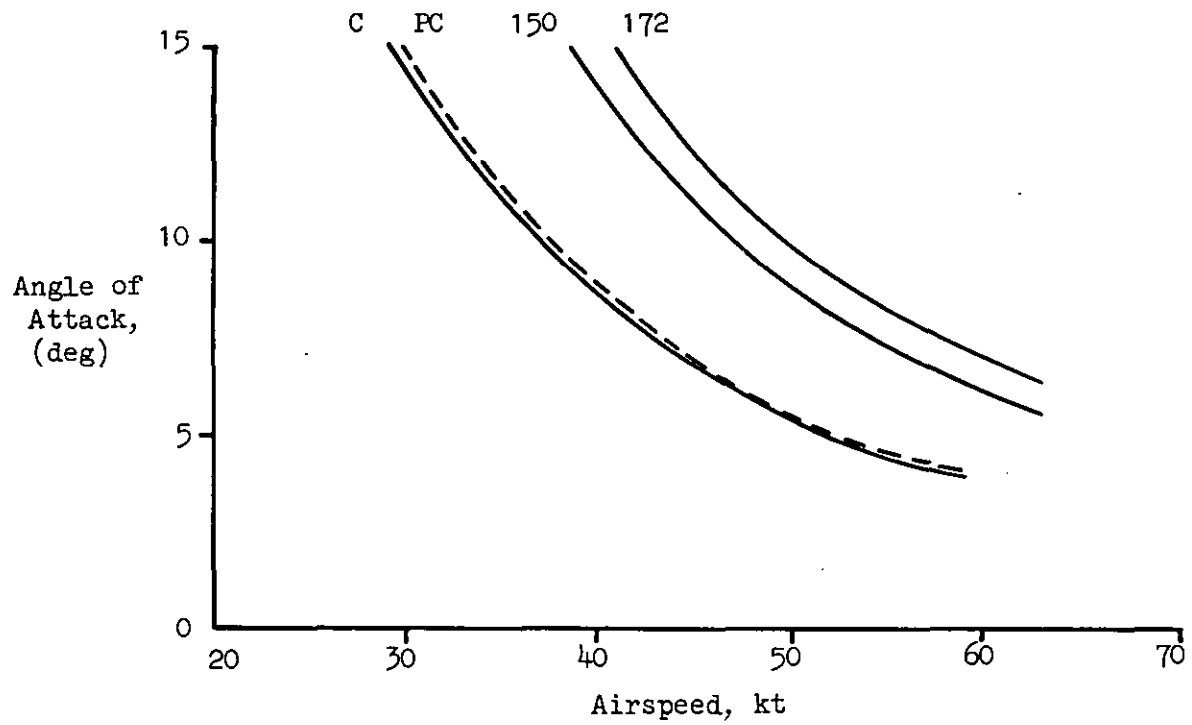

Figure 85. Minimum Airspeed/Angle-of-Attack Requirements for the Overturning of Light Fixed-Wing Aircraft with the Deletion of the $(D')(X_F)$ Term

the increase in angle of attack will rapidly accelerate the overturning process.

The next step in the logical development of the methodology presented involves at least an attempt at limited correlation of the mathematical model presented above with some actual accident data. Two of the accidents chosen for correlation involved the UH-1 (and a Cessna 150 and a Cessna 172), and two involved the CH-47 (and an unknown aircraft type). Very few details were obtainable from the "sanitized" accident reports; however, in each case, the following specifics, besides the fact that the fixed-wing aircraft were not tied down, were known:

Case	Rotorcraft	Fixed Wing	Approximate Separation Distance, ft	Approximate Wind, kts
1	UH-1H	Cessna 172	100-130	20-25 peak
2	UH-1M	Cessna 150	Nearby	Unknown
3	CH-47A	Unknown	225	12-15 peak
4	CH-47B	Unknown	Nearby, in front	10-20 peak

In the case of the UH-1, the predicted outwash velocity profile range at 100 to 130 ft can be obtained from Fig. 79. This range of calculated rotorwash velocity varies from approximately 40 to 45 kt with a 9-kt wind speed. As can be seen in Fig. 84 for angles of attack around 10 deg, an overturning moment is clearly predicted. While this analytically derived example does not compare exactly with the known information in Cases 1 or 2, the calculated range and angle-of-attack requirements nevertheless do at least seem reasonably plausible when using the accident data for comparison. It is important to note that the Aeronca Champion and the Piper Cub were clearly even more at risk. The geometric angle of attack for the wings on these two aircraft is approximately 12+ deg, since they are tail dragger configurations.

In making the same evaluation using working plots for the CH-47 in a 9-kt wind, the 40-kt outwash velocity (α_W = 10 deg) is reached at a distance of approximately 240 ft. In Cases 3 and 4, the known peak values of

wind are also reasonably in line with the value for wind input into the calculations. Therefore, if the Cessna type of aircraft was the type damaged, then the analysis method would seem to provide a reasonable approximation for the minimum required separation distance. It is also important to note in Cases 1 and 3 that the rotorcraft were known to have just refueled. While this does not quantify the gross weight, it would nevertheless indicate a medium to heavy helicopter gross weight. In the analysis case discussed here, a medium gross weight was assumed. Therefore, the probability exists that the rotorwash velocities involved were actually slightly greater than those that have been calculated. This fact should aid in assuring that the analytical method is reasonably applied if the analytical method is optimistic in its predictions.

In conclusion, the subject hazard type was reasonably predicted considering the limited correlation data that were available. The methodology would therefore appear to be sound for hazard **estimation purposes only**. It can be noted further, in several of the cases mentioned, that other "tied down" fixed-wing aircraft were equally close or closer to the subject rotorcraft, yet no other damage of any type was reported (i.e., particularly empennage/control system damage).

One other accident case was identified as having involved a fixed-wing aircraft to which control system damage did occur. A review of pilot manuals for numerous aircraft resulted in the discovery that tie-down requirements are not specified for prevention of this type of damage as a function of wind. Owners are simply told to tie down their aircraft when not in use. Considering this fact, it is assumed in the rest of this study that the methodology that is used for predicting overturning moments will also be sufficient in predicting clearance to insure that control system damage will not occur. Too little information exists to develop a reliable model that would accurately predict structural damage for this type of hazard. In all probability, it would be very surprising if a limiting rotorwash velocity value (or required separation distance) coming out of this type of analysis would be significantly less than the 30 kt as suggested for the door/access panel hazard.

3. Evaluation of "Worst Offender" Rotorcraft Configurations for the Fixed-Wing Overturning Moment Hazard

The evaluation of the five "worst offender" rotorcraft configurations was conducted using the Aeronca Champion and the Piper Cub as the affected fixed-wing aircraft. These very low-wing loading aircraft should be good representatives of the thousands of very light and home-built civilian aircraft in the United States. A rotorwash velocity of approximately 30 kt is clearly shown in Fig. 84 to be the rotorwash velocity required to overturn these aircraft when the angle of attack is greater than 12 deg. (It should be noted as before that the theory may be somewhat conservative.) Based on these results, the practical limiting rotorwash velocity chosen for these aircraft is 30 kt. (It must also be remembered that the peak rotorwash velocity that is being used in the analysis is a worst case rotorwash velocity and that the average velocity would be lower. Therefore, choosing a velocity of 25 kt would probably be unjustifiably restrictive.)

The required angle of attack of 12 deg should be easy to obtain in the typical airport scenario, since the geometric wing pitch angle of a Piper Cub on its tail dragger landing gear is approximately 12+ deg. Even in the case of the Cessna aircraft, fairly high angles of attack should still be achieveable. Two factors support this assumption. The first of these comes from the known experimental observation that outwash flowfields do travel slightly upward in direction in a very oscillatory manner as they expand. Example data for the CH-53E are shown in Fig. 86 to support this observation. The second factor requiring some upward flow of outwash airmass would be the requirement for the outwash flow to go up and over the fuselage whenever the flow impinges the fixed-wing aircraft from a non-centerline direction.

Recommended separation requirements are presented in Fig. 87 in order to insure that this hazard is avoided for the "worst offender" configurations. The distances presented are based on the outwash velocity data given in Fig. 81. Due to the fact that the "worst offender" configurations are themselves conservatively sized hypothetical rotorcraft when

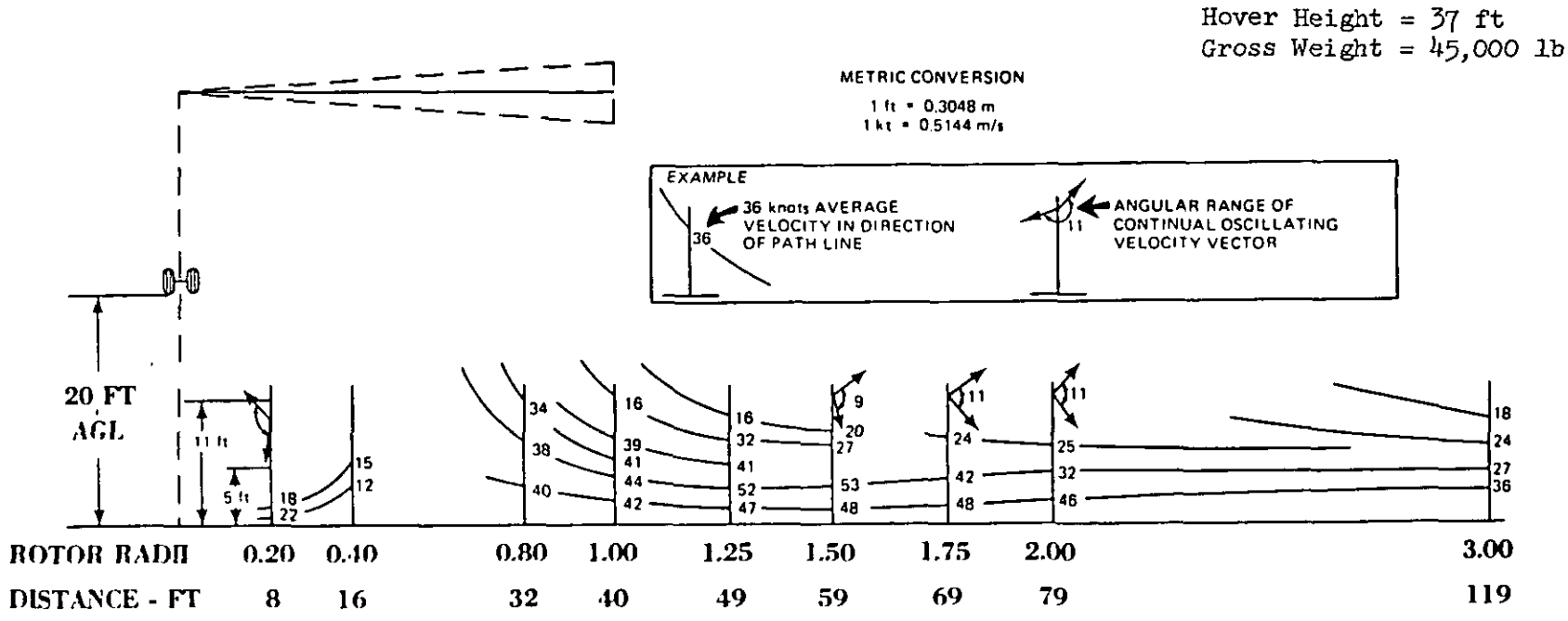

Figure 86. Streamlines of the CH-53E Downwash Wind Velocity in the Vertical Plane

(Reproduced From Ref. 11)

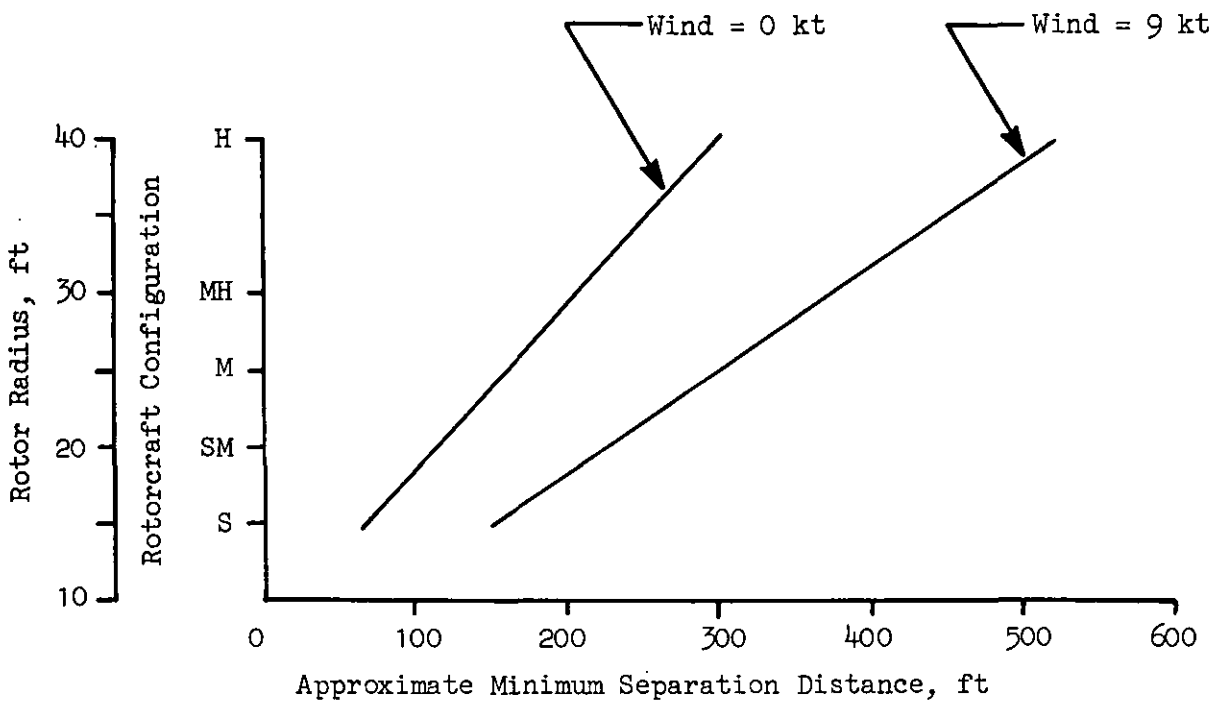

Figure 87. Separation Standard Requirements to Avoid the Overturning of Light Fixed-Wing Aircraft

compared to most operational rotorcraft today, the 9-kt wind velocity case (Fig. 81) is used as the separation requirement setting case. In addition, since winds of greater than 9 kt should result in the other types of rotorwash flowfields eventually becoming predominant (i.e., ground vortex, trailing vortices), it is hard to justify using the conservatively developed wind model of Section III to greater than 9 kt.

The scenario of a light plane being overturned with the engine running (while stopped or slowly taxiing) was also briefly examined. Rough calculations indicate that safe separation distances for this scenario would be slightly less than that for the parked and untied fixed wing. This is due to the fact that the weight of the rotorcraft is increased when passengers are on board. The intangible also exists in that the pilot can control the elevator and ailerons in order to "somewhat" prevent overturning moments (this is accomplished by the pilot in gusty winds as normal procedure). Since personnel would certainly be directly involved in this scenario if an accident were to occur, it is suggested, as a further safety factor, that the Fig. 87 separation distances still be used as the guiding criteria until further information becomes available.

Scenarios involving ground and trailing vortices were also investigated briefly for this type of hazard. Results, as shown in Table 10, would indicate that the potential exists, particularly when coupled with a crosswind, to create hazardous velocity levels. Therefore, the recommendation would certainly be appropriate that rotorcraft not be allowed to take off and land or overfly small fixed wings that are not tied down. The setting of an actual distance as a requirement is believed to be unwarranted at this time due to a lack of detailed understanding about the nature and behavior of the vortices as they descend and blow across the ground in the context of this type of hazard. Further analytical work and flight test experimentation are needed in order to validate and complete any detailed investigation. It is hoped that some of this information will be forthcoming from the planned FAA flight test experiments on trailing vortices.

4. Summary of Results

Results have been presented in this section for three specific types of hazards involving rotorcraft and fixed-wing aircraft. Separation distance requirements to prevent door/access panel damage are recommended to be the same as those derived in Subsection D for rotorcraft. Separation standards for avoidance of the hazards of fixed-wing rollover and control/empennage system damage are combined into one set of criteria. Further experimentally derived information would be highly desirable in order to aid in the validation of the methodology developed in this section so as to refine the proposed separation standards in the future.

F. DOWNWASH/OUTWASH HAZARDS INVOLVING ENTRAINED OBJECTS AND DEBRIS

One potentially hazardous environment that can be created by a rotorcraft is one in which particles, debris, or large objects are entrained in the downwash/outwash flowfield and thrown about as dangerous projectiles. Unfortunately, as stated in Ref. 8, the prediction of particle or projectile velocity as a function of time and place becomes a monumental task if the effects of most variables are to be included. Furthermore, even if time were available to develop exact solutions, experimental data does not exist with which to correlate those solutions. Therefore, one would expect that any methodology which is to be developed for the prediction of safe separation distances would have to be based on very general engineering theory (at most) and a lot of "good sense."

1. Historical Data

The effort to develop a flying object hazard avoidance methodology for quantification of safe separation distances was initiated with a review of available historical literature on the subject. Unfortunately, not a lot of work has been devoted to this topic. Reference 8 states that "full-scale experimental investigations with simulated or actual VTOL aircraft operating over sandy terrain with disc loadings as high as 50 lb/ft^2 have

produced only superficial damage to the modern airframe." Calculations are provided to further substantiate this statement. Since rotorcraft, as defined in this study in Fig. 47, operate at disc loadings of less than 20 lb/ft^2, the assumption has been made herein that sand and small pebbles will not in general be a significant hazard in causing damage to metal structures (i.e., helicopter airframes, ground equipment, hangers). It cannot be assumed, however, that these particles could not become hazards to personnel or to certain other types of material (i.e., pitting of plastic windshields or paint erosion) as well as to metal structures like rotor blades where the high velocity or damaging component of the impact is due to the rotating structure itself and not the projectile.

It has also been determined from operational data that objects or debris that have a large frontal area to weight ratio can also become entrained in the rotorwash along the ground and become a significant hazard. Examples of these types of damage-causing projectiles (as determined from U.S. Army accidents) include:

1. Sheet metal, corrugated metal, wood, or plastic panels (i.e., 3-ft square)
2. Landing zone nylon/metal markers
3. Flare/personnel parachutes
4. Dead tree branches/brush
5. Nylon, cloth, and plastic equipment bags as well as empty sandbags
6. Metal landing pad planking
7. Numerous rocks and other round objects (hitting equipment, breaking glass and windshields)
8. Maintenance stands (blown on their sides and along the ground prior to impacting other rotorcraft)
9. Rotor blade box covers, ammunition boxes, empty 55-gallon drums, tents.

Clearly, it can be seen from this brief list that the potential is almost unlimited for many types of hazardous projectile impact in the heliport environment, particularly where personnel may be involved.

2. Analysis Methodology

The discussion thus far has presented some qualitative information on hazardous types of projectiles and their impact damage potential. One very limited method for quantitative prediction of the hazard potential of various types of projectiles was discovered during the literature review in Ref. 8. This analysis method assumes a no-wind hover condition and is based on the definition of minimum energy levels for which personnel or a certain type of material can be damaged. To fully understand the assumptions, limitations, and theory associated with this **first-order estimation** methodology (as described by the authors), Ref. 8 should be consulted. The lack of correlated experimental data, a concern which the authors acknowledged in numerous paragraphs, is one of the greatest limitations to this methodology.

The methodology which is developed in Ref. 8 is basically a spreadsheet calculation method which is augmented as necessary with charts for looking up experimentally derived or analytical functions. As an aid to a practical understanding of the use of this method, an example is presented in the following paragraphs.

The first step to be taken in using the analysis technique is to define the subject rotorcraft of interest along with the operational scenario. In the example here, the S-, M-, and H-sized rotorcraft have been chosen for evaluation at rotor heights above ground equal to approximately 30 ft. This rotor height generally insures that the maximum possible peak ground velocity is reached in the outwash flow.

The second methodology requirement is that the hazardous objects be defined. This particular task, practically speaking, is almost impossible to accomplish when one considers the almost infinite variety of objects from which to choose in an airport or heliport environment. However, to aid in the development of the example in this section, some objects have

been assumed arbitrarily. These objects are listed in Table 15. Following the specification of the object type, the maximum drag area must be calculated for each object. The assumption made in the calculation procedure is that the largest surface area possible is projected in the direction of the flowfield. A calculation then must be made for the size of the object's impact area. For a circular object, this surface area is the same as the drag area. For a rectangular object, this area is not well defined. If the object impacts on a corner, there is much more potential for localized transfer of kinetic energy than there is if the impact area equals the maxiumum drag area. In this study, the impact area is arbitrarily assumed to be equal to the smallest flat side of the object. The last of the preliminary calculations made is one for "insurance purposes." Each object should be evaluated so as to calculate the minimum air velocity which is required to produce enough drag force to lift the object's weight. This can be accomplished by evaluating the following equation for objects other than sand and water (see Fig. 88 instead) where:

$$V_{min} = \sqrt{\frac{W_P}{\frac{1}{2} \rho_A A_F C_D}} \quad \text{(ft/sec)} \qquad (71)$$

The variables in this equation are:

W_P = Particle weight (lb)

ρ_A = Atmospheric density (slugs/ft^3)

A_F = Maximum drag area (ft^2)

and

C_D = Drag coefficient (often assumed to be 1.0)

Should the V_{min} value calculated in this step be less than that predicted in the rotorwash flowfield in the region of the peak dynamic pressure (q_F), then the probability of the particle becoming completely airborne is minimal. In this example, the gravel size of 0.25 ft (or 3 inches) in diameter will not become airborne for the "S"- and "M"-sized classes, because the required velocity to entrain the particle size is greater than 200 ft/sec.

TABLE 15

AN ARBITRARILY ASSUMED COLLECTION OF HAZARDOUS OBJECTS
LIKELY TO BE FOUND IN A HELIPORT ENVIRONMENT

Object Type	Approximate Mass, slugs	Approximate Size, ft	Maximum Drag Area, ft^2	Impact Area, ft^2
Sand (0.08 mm)	5.0×10^{-11}	2.6×10^{-4} (diameter)	5.4×10^{-8}	5.4×10^{-8}
Sand (3 mm)	2.65×10^{-6}	0.0099 (diameter)	7.6×10^{-5}	7.6×10^{-5}
Gravel	4.33×10^{-2}	0.25 (diameter)	4.9×10^{-5}	4.9×10^{-2}
Metal Lunch Box	0.031	0.67 × 0.58 × 0.33	0.39	0.19
Briefcase	0.25	1.5 × 1.16 × 0.5	1.74	0.58
Empty Barrel	1.24	2.0 (dia.) × 3.0 (height)	6.0	3.14

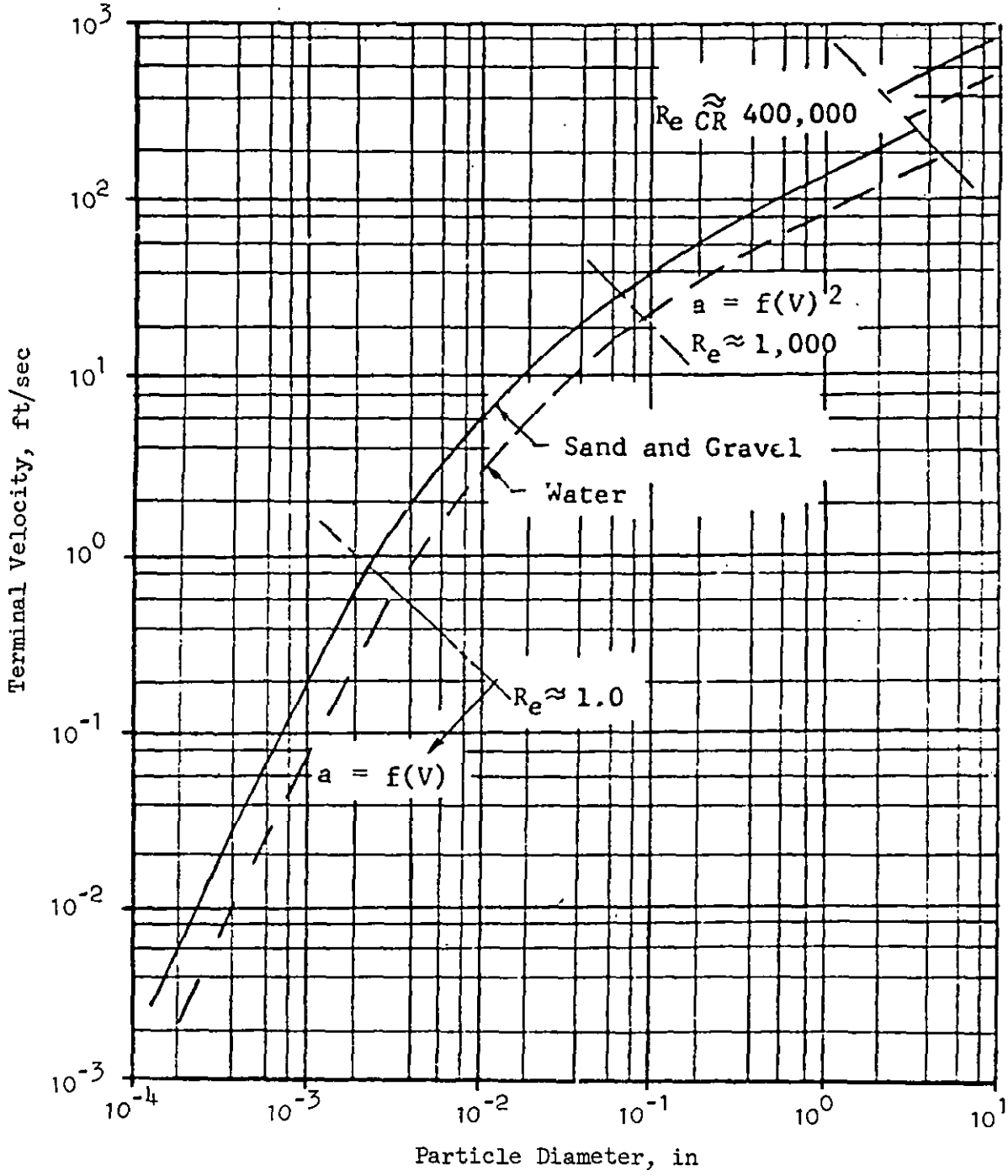

Figure 88. Variation of Terminal Velocity of Particles With Particle Diameter

(Reproduced from Ref. 8)

Upon completion of the above preliminary calculations, the analysis methodology requires the calculation of the size parameter (β), where:

$$\beta = \frac{4.24\ R\ C_D\ \rho_A\ A_F}{m_P} \tag{72}$$

and

R = Rotor radius (ft)

m_P = Mass of the particle (slugs)

For this example, ρ_A is assumed to be equal to 0.0023769 slugs/ft^3 and C_D is assumed to be equal to a value of 1.0. The calculation of β is followed by the calculation of the worst case particle velocity (V_P) which is specified in Fig. 89 (Fig. 47 from Ref. 8) as:

$$V_P = \left(\sqrt{\frac{q_F}{\rho_A}}\right)\left(1 - \frac{1}{\sqrt{\beta} + 1}\right) \text{ (ft/sec)} \tag{73}$$

The value for q_F in this equation is assumed to be (for conservatism) the maximum field dynamic pressure. For the five "worst offender" rotorcraft configurations, this value is calculated using the Section III mathematical models and is presented in Fig. 90. The calculation for V_P is then used to compute the worst case impact energies and damage potential for the specific objects of interest. The energy of the object is the object's kinetic energy which is:

$$E_P = \frac{1}{2}\rho_P V_P^2 \text{ (ft-lb)} \tag{74}$$

Another value (E_P/A_I) can also be computed for the purpose of describing the actual localized energy that is released in the impact. The respective values that are associated with the six object types for β, V_P, E_P, and E_P/A_I are tabulated in Table 16.

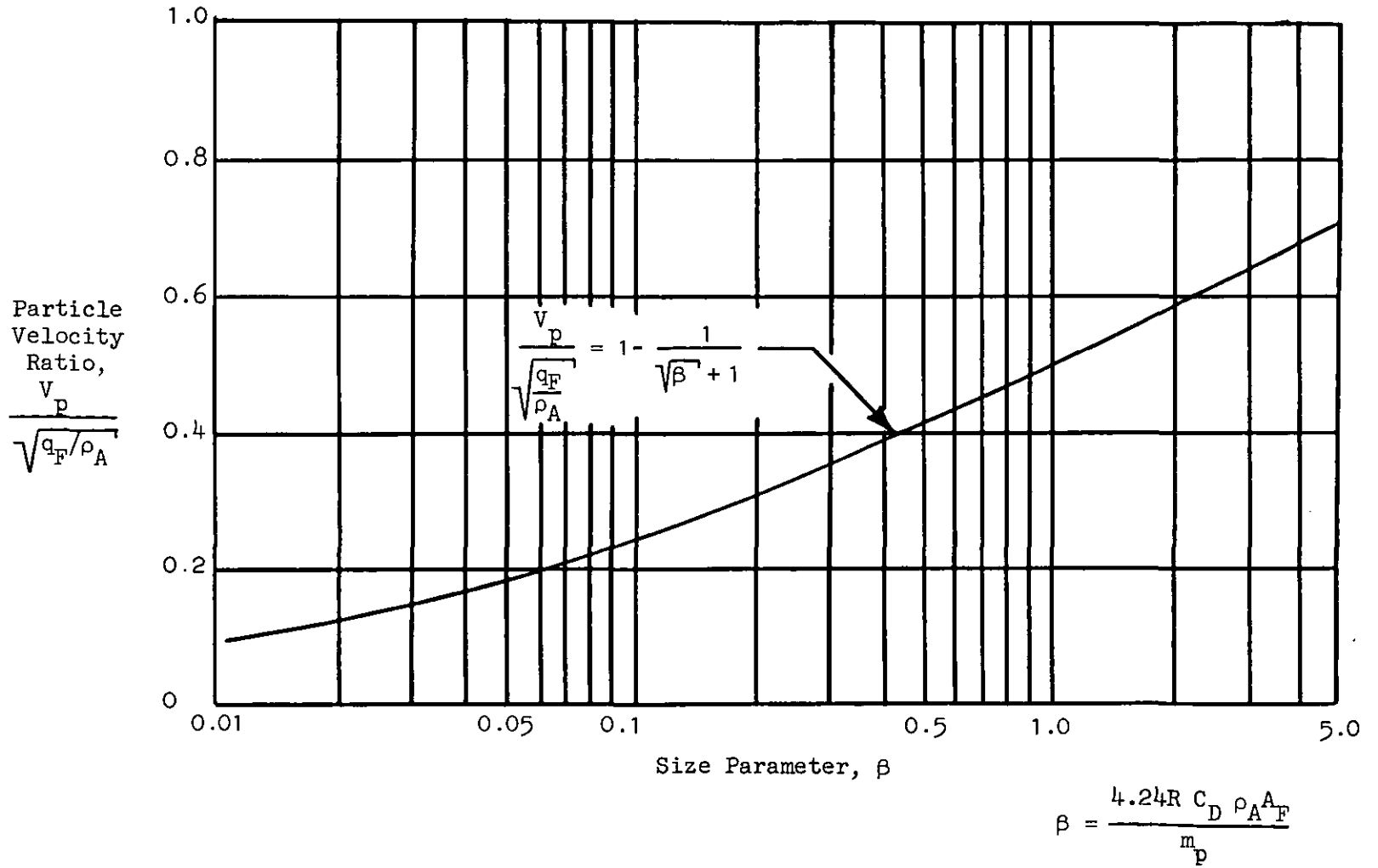

Figure 89. Entrained Particle Velocity Ratio as a Function of Size Parameter, β

Wind = 0 kt
Rotorcraft Configurations: S, SM, M, MH, H

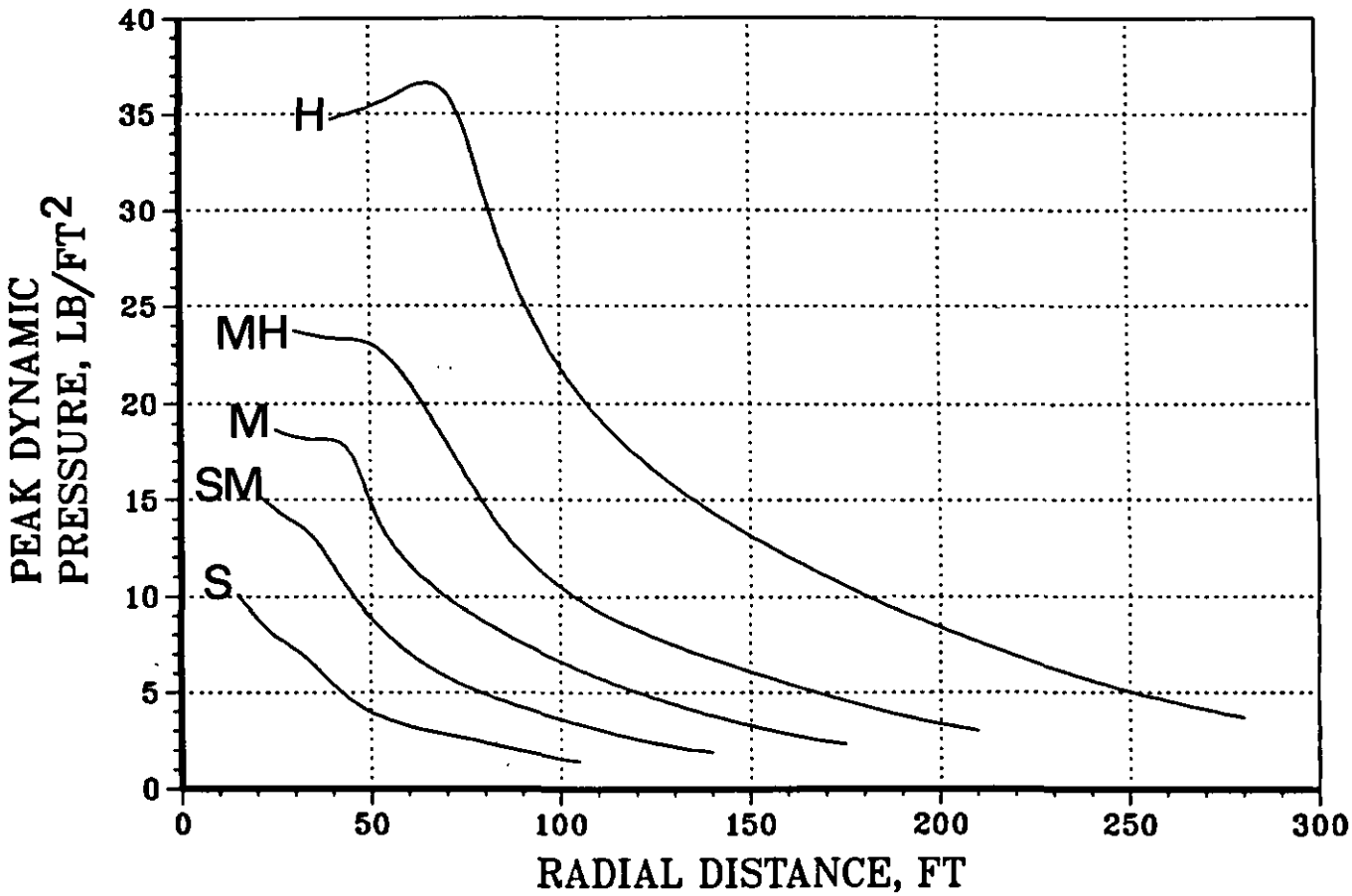

Figure 90. Peak Dynamic Pressure Loads as a Function of Radial Distance for the Five "Worst Offender" Rotorcraft Configurations (Wind = 0 kts)

3. Available Test Data

As was stated in the previous subsection, one of the weak points of the presented methodology is the almost total lack of data for correlation. In particular, very little can be said about the confidence level associated with the calculation of the impact velocity, V_p, due to numerous factors. For example, the impact velocity of the object has been observed to be altered significantly by the way in which the rotorcraft approaches the object (from above versus laterally) and by the way in which the object is placed in the flowfield. The interaction of wind with the rotorwash flowfield and a specific object is also ill defined. Therefore, one area for future research should definitely be in the development of more experimental data for correlation purposes.

The small amount of data that were discovered for aiding in the development of recommended separation requirements were all taken from U.S. Army accident reports. Several of these accident summaries are listed below for the UH-1H and AH-1 helicopters in order to provide an example of the type of data available:

1. A UH-1H was parked early in the morning on the Medivac pad. Post flight of the aircraft revealed no discrepancies. In the late morning, the crew chief reported a broken plexiglass panel in the helicopter. The UH-1H that had been parked on the adjacent spot had hovered out during the intervening time period. Due to the high volume of loose rock found around the parking pads and in the sod hover lane, it is believed that the accident was caused by rock debris thrown into the plexiglas.

2. During run-up and engine check, rotorwash blew a maintenance stand into the elevator of a nearby parked UH-1H. The locked wheels on the maintenance stand did not prevent it from being blown into the nearby helicopter.

3. After refueling at a civilian airport with a fixed-refueling point, the pilot hovered his UH-1H out for takeoff. A 55-gallon garbage drum, located approximately 55 ft away from the helicopter, was blown approximately 20 ft into a parked car. Property damage to the car exceeded $100.00.

4. A work stand was blown into a parked AH-1S during a blade tracking and alignment operation. This helicopter was damaged. In addition to the rotorwash, winds were gusting as high as 25 kt. The work stand had not been secured but it had been placed upon its side prior to the accident. Stands are recommended to be repositioned 100 ft from operating rotorcraft in the future.

If the assumption is made that the spacing between UH-1H's in Summaries 1 and 2 is approximately one rotor radius when the blades are pointed toward the other helicopter, then the safe separation distance between the impact and the center of the "offending" rotorcraft is definitely greater than 72 ft due to the geometry of the scenario. The safe distance for avoidance of the barrel impact described in Summary 3 is clearly greater than 75 ft. Lastly, the maintenance stand recommendation for safe separation in Summary 4 is approximately 100 ft (several other summaries would certainly indicate that this value for the maintenance stand should be in excess of 75 ft). While this type of data does not allow for correlation with any presented analytical method, it does aid in the application of "good judgment" later on in this study.

4. Evaluation of "Worst Offender" Configurations

The particle or object characteristics that were used in the evaluation of the "worst offender" configurations in this hazard analysis are the same ones summarized in the data presented in Table 16. The missing factor, required for the completion of the analysis at this point, is a definition for what should be considered hazardous. While not completely applicable in this particular situation, values were given in Subsection B for hazardous moments with respect to personnel. These "evenly distributed" moment limits were 120 and 60 ft-lb, respectively, for the personnel size classes of "L" and "S". Reference 24 states that the localized impact on humans of projectiles having energies in excess of 58 ft-lb is incapacitating. (This value can be reduced depending on numerous factors.) This reference also provides information on the potential for damage to the human eye as defined for small particles (see

TABLE 16

CALCULATED VALUES FOR THE PARTICAL SIZE PARAMETER, PARTICAL VELOCITY, PARTICAL ENERGY, AND PARTICLE ENERGY-TO-IMPACT AREA RATIO FOR AN ARBITRARY COLLECTION OF OBJECTS

	Object Type					
Parameter	Sand (0.08 mm)	Sand (3 mm)	Gravel	Metal Lunch Box	Briefcase	Empty Barrel
β (-ND-)						
S Class	163	4.3	0.17	1.9	1.05	0.74
M Class	272	7.2	0.28	3.2	1.75	1.22
H Class	435	11.6	0.45	5.1	2.8	1.95
V_P (ft/sec)						
S Class	60	44	18	37	32	30
M Class	84	64	30	57	50	46
H Class	119	96	50	86	78	72
E_P (ft-lb)						
S Class	9.0×10^{-8}	2.6×10^{-3}	7	21	128	558
M Class	1.8×10^{-7}	5.4×10^{-3}	20	50	312	1312
H Class	3.5×10^{-7}	1.2×10^{-2}	54	115	761	3214
E/A_I (lb/ft)						
S Class	2	34	143	110	220	177
M Class	3	71	395	263	538	418
H Class	7	150	1102	605	1312	1023

Fig. 91). Almost without question, all of the objects being discussed here will result in damage to rotorcraft or aircraft if the rotating parts--such as the rotor, engine, or propeller--are struck. The penetration potential to sheet metal of varying thicknesses can be estimated using the data presented in Fig. 92.

In further evaluating the potential hazard impact on people, it can be clearly seen that the energies present in the lunch box, briefcase, and barrel would be sufficient to injure a person, particularly if the person were struck by one of the object's corners. The UH-1H/AH-1 data presented previously confirm this for rotorcraft configurations that are slightly smaller than the "M"-sized class. The energy in the 0.25-inch diameter gravel, which results in a more localized release of energy on impact, is certainly a hazard for "H"-sized rotorcraft, based on the 58 ft-lb criteria, and it would probably at least raise a bruise on a person even for the "S" sized class of rotorcraft if it is entrained in the flowfield by some mechanism. The velocities of the two pieces of sand, which vary from approximately 44 to 138 ft/sec, can be seen in Fig. 91 to be clearly safe, since the weight of the respective sand particles in grams is less than 0.04 grams. The assumption that these particles are safe does not assume that they will not be bothersome to unprotected personnel. More discussion on this subject will be presented in Subsection G.

The potential for damage to sheet metal by flying objects is evaluated using the data in Fig. 92. If the A_I/A_F and E_p/A_I ratios, shown in Tables 15 and 16, are evaluated, it can be seen that none of the objects have the potential to actually pierce the aluminum sheets (the energies required to dent or pit the metal to various levels is not known). It should be noted, however, that if the barrel was to strike on a sharp corner, it could release enough energy to do significantly more damage than just the denting of metal.

The damage potential for any of the objects listed above, except perhaps for the smallest sand particle, is very significant if any rotating components are struck (i.e., rotor blade, propeller). Therefore, these types of impact must be avoided by insuring that these objects are not left in close proximity to rotorcraft that have their rotors turning.

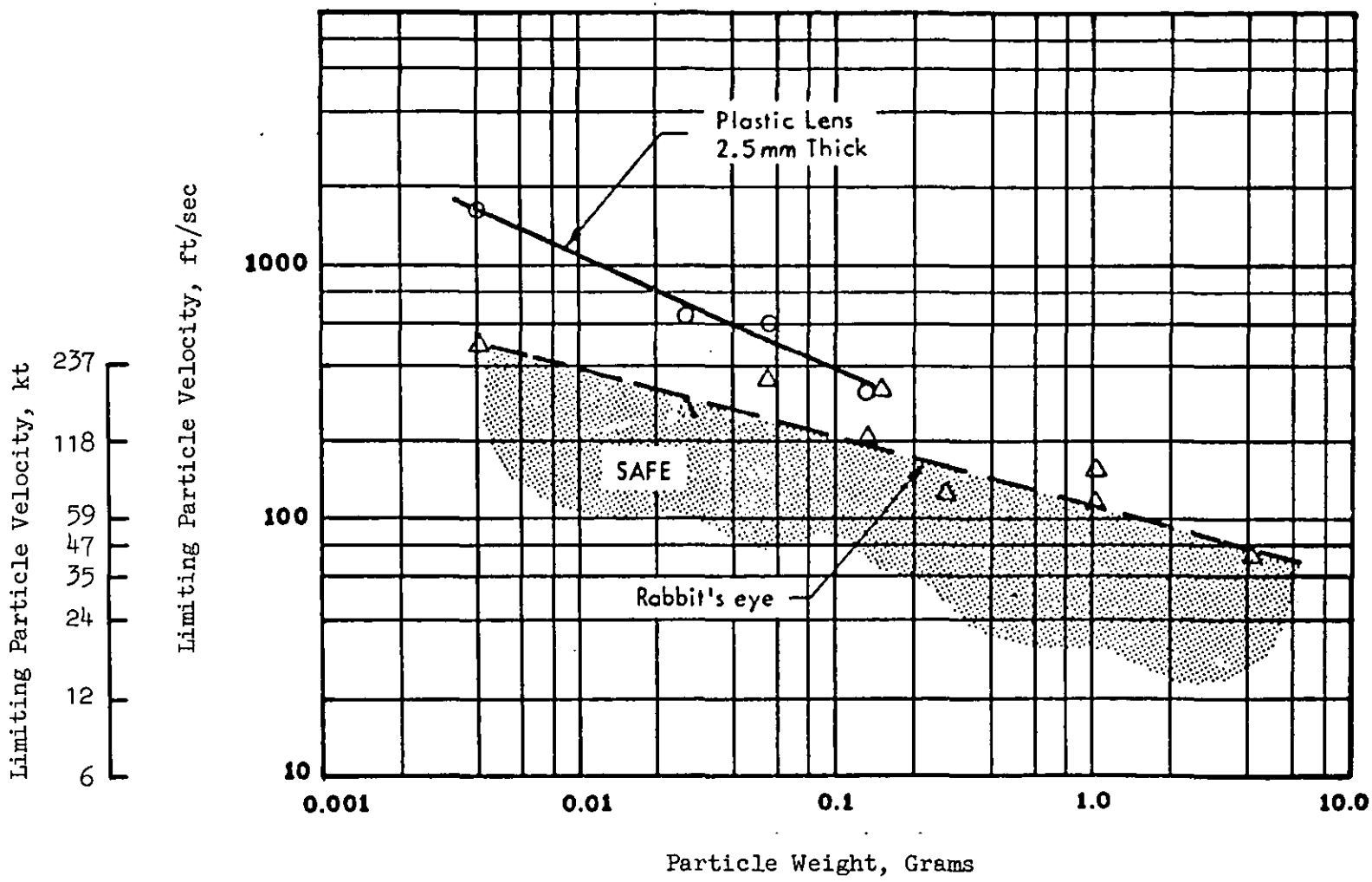

Figure 91. Maximum Particle Velocity and Weight Limits for Eye Penetration

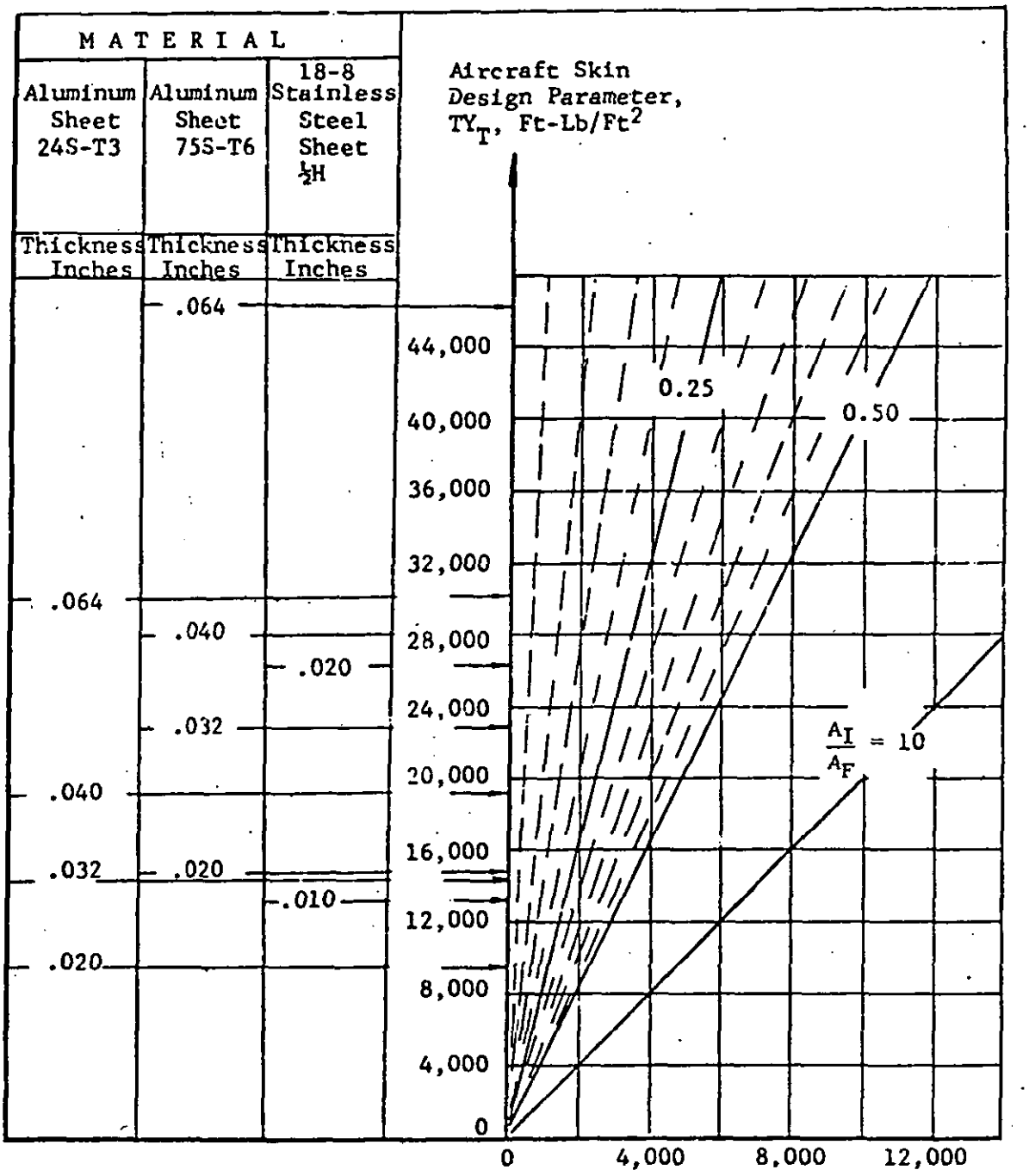

Figure 92. Minimum Particle Energy Required for Penetration Through Aircraft Skin

(Reproduced from Ref. 8)

Abrasion of rotating components is discussed in more detail in the next subsection.

The brief analysis outlined above has centered primarily on providing a rough feel for the damage potential of numerous objects. The **important missing link** in the analysis at this point is the lack of a safe separation distance being specified for association with the various objects. The methodology used in this analysis, as stated in Ref. 8, is derived using an assumption that the airstream velocity is zero at three times the effective jet diameter from the vehicle. While this assumption is not true, as evidenced by flight test data, it is nevertheless a point at which most objects (particularly the larger objects) will not be supported by the rotorwash flowfield. This choice of distance is further supported by the experimental data presented in Ref. 39 which supports the statement that large objects (i.e., rocks, dirt clods) are rarely propelled farther than 3.5 propeller diameters with twin propeller VTOL aircraft (along the interaction plane). Certainly the impact energies of all objects should be significantly less at this distance than are calculated using this methodology. The effective jet diameter for rotorcraft is approximately 0.707 times the actual rotor diameter, as calculated using momentum theory. If this calculation is made for each of the five size classes of rotorcraft in this study, then safe separation distances for each configuration might be proposed as follows:

Type Class	Rotor Radius, ft	Safe Separation Distance, ft
S	15	64
SM	20	85
M	25	106
MH	30	127
H	40	170

In the case of the UH-1H and AH-1 data that was presented earlier, where the respective rotor radius values were 24 and 22 ft, the proposed separation distance of approximately 106 ft would certainly seem to be in

line as a reasonable value for safe separation, since most of the accidents were hypothesized to be around 75 ft. This separation distance would also be in line with the recommended maintenance stand requirement for a 100-ft separation.

5. Conclusions

A methodology has been developed and utilized in this section to **roughly estimate** the damage potential for various flying objects and debris in a zero wind hover. The assumption that the wind would significantly increase the hazard potential, as predicted accurately by this methodology, cannot be made due to many unknown factors. Therefore, no analysis of this condition is presented. The methodology's greatest weakness is that very little data presently exist to correlate and verify the accuracy of the predicted results. The very limited accident data available to provide some guidelines as to the method's effectiveness do indicate that the resulting proposed separation criteria are at least reasonable. Separation standards for the ground vortex case and the trailing vortices are assumed to be insignificant when compared to the hover condition due to the low velocities that were calculated in Table 10. No method exists to compute their hazardous potential anyway. This type of hazard becomes the main hazard that influences the definition of final proposed separation standards, then it is recommended that significantly more experimental work be carried out to verify and improve where necessary the analysis methodology used in this section of this report.

G. HAZARDS INVOLVING ROTORWASH-GENERATED DUST, SNOW, AND DEBRIS CLOUDS

Throughout the operational history of rotorcraft, particulate clouds (i.e., dust, snow, water, and debris) have been a hazard to the rotorcraft that created them as well as to other nearby rotorcraft. These particulate clouds most often inflict damage by "sandblasting" rotor blades (thus shortening their useful life) and causing engine foreign object damage,

which manifests itself as a slow degradation in maximum available engine power or as a sudden engine failure. The size and density of these clouds can also obstruct pilot vision, which in turn can cause hard landings, collisions with other obstacles (e.g., other rotorcraft in a formation or trees), and crashes. Between forty and fifty of the accident summaries that were reported in the U.S. Army Safety Center accident data base were related to this type of hazard. (No record is available on the number of "near misses.")

For the purposes of this hazard analysis, the assumption has been made that terrain conditions resulting in severe degradation of visibility to the pilot are totally unacceptable for public heliport use. Because of this assumption, estimates are not made herein for parameters such as the particulate cloud density or the degree of lost visibility by the pilot when sand, loose dirt, or other particulate matter are present in heavy concentrations. [Should the reader be interested in rotorcraft operation over unimproved terrain such as this (as is the military), further study is recommended of Refs. 8, 9, 40, and 41.]

The importance of this type of hazard to this analysis effort derives from the assumption that heliport operating surfaces will, from time to time, be covered with various low-density layers of sand, snow, water, or other particulate matter. Since this particulate matter will be "blown" by rotorwash, it is desirable to know approximately where this particulate matter might be blown. The results presented in this section are therefore directed toward the **estimation** of the approximate particulate cloud boundaries for various types of common particulate matter. Detailed examinations of specific resulting hazards (e.g., engine damage) are discussed only in general terms, since cloud density and particle size are extremely important to these types of hazard estimations. General solutions for this type of analysis are, of course, also impractical, since each rotorcraft engine is different and each type of terrain can vary significantly in detailed particulate characteristics. In addition, very little data exist to correlate fully any detailed analysis results.

1. Mathematical Modeling Approach

The estimation technique that is used in this study to predict particulate cloud boundaries for various types of terrain was developed initially in Ref. 9 and is the only method of its type that was identified in the literature. A schematic representation of the assumed dust cloud geometry is presented in Fig. 93. In this estimation approach, the rotorwash is assumed to impinge the ground directly under the rotor. As the wall jet forms and flows outward, the erosion and subsequent entrainment of particulate matter generates a cloud with boundaries of R_c and H_c. These boundaries, presented in Fig. 93, are the maximum cloud radius and the cloud height, respectively. The rollup of this particulate cloud is brought about by a recirculating or tip vortex rollup mechanism which results from the interaction of the ground and the induced rotor flowfield.

Terrain erosion, as discussed in Refs. 8 and 9, is related to the maximum surface dynamic pressure in the wall jet such that an effective dynamic pressure is defined where:

$$q_{s_{eff}} = \frac{q_{s_{max}}}{\sqrt{K_T}} \tag{75}$$

The terrain erosion factor, K_T, is dependent on terrain characteristics and is further defined in Ref. 9 as:

$$K_T = \frac{\overline{D}_p \rho_p}{D_w \rho_w} \tag{76}$$

where the mean terrain particle size ($\overline{D}_p$) and density (ρ_p) are related to water droplet size and density as reported in Ref. 9. Approximate values of K_T for various types of terrain are provided in Fig. 94 (compiled from Refs. 8, 9, and 40).

Using the work of Ref. 9, it can be further shown that the particulate cloud radial boundary (R_c) can be approximated by the radial distance along the ground at which the effective surface dynamic pressure ($q_{s_{eff}}$)

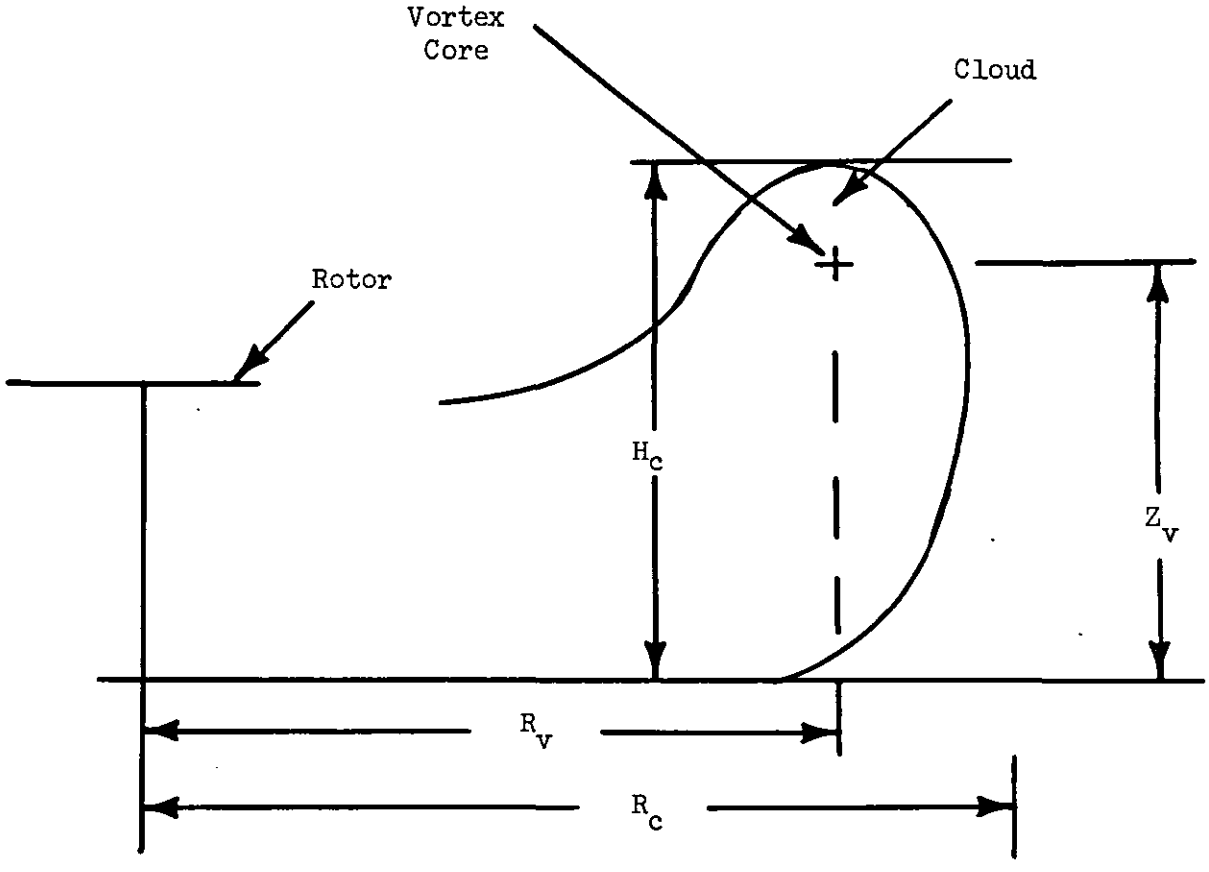

Figure 93. Schematic Representation of Dust Cloud Geometry

$$(K_T) = \frac{\text{Diameter}_P\ (\rho)_P}{\text{Diameter}_W\ (\rho)_W} = \frac{\rho_g\ g\ a}{62.4\ \text{lb/ft}^3 \times 0.10\ \text{in}}$$

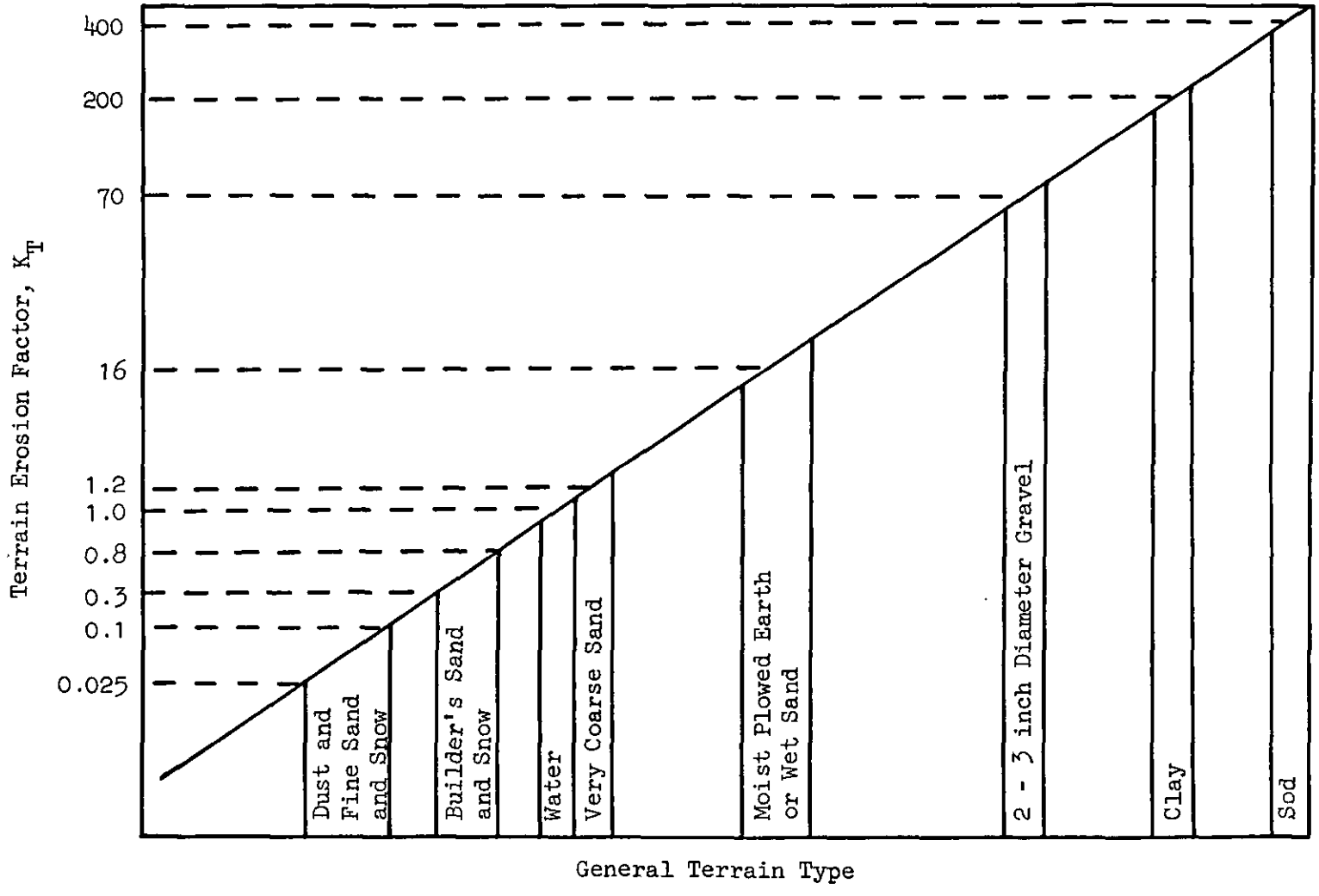

Figure 94. Approximate Values for the Terrain Erosion Factor K_T as Identified in the Literature

is approximately equal to 1.0 lb/ft^2. Using this information, Eq. 16, and Eq. 11 of Section III, which is restated here as:

$$\frac{u_m}{\overline{U}_M} = C_u \left(\frac{r}{R}\right)^{-1.143} \tag{77}$$

it can be shown that $R_c = r$ at $q_{s_{eff}} = 1.0$ lb/ft^2 such that:

$$R_c = R \left(\frac{\sqrt{K_T}}{C_3 \frac{1}{2} \rho_A \overline{U}_M^2 C_u^2}\right)^{-0.437} \tag{78}$$

where C_1 is a constant (added to improve correlation) that is equal to unity (1.0) for a single-rotor rotorcraft and 2.2 for the interaction plane of a twin-rotor rotorcraft.

The maximum height of the dust cloud, H_c, can be approximated by considering the path of the rotor blade tip vortices as they spread along the ground. A detailed analysis of the behavior of this vortex system can be made by replacing the continuous cylindrical vortex sheet with a finite number of discrete vortices. A step-by-step iteration procedure could then be applied to compute the motion of each ring vortex as it starts to expand along the ground. However, in lieu of this process which is complicated and time consuming, an attempt has been made to analyze the rollup process utilizing an analogy of the vortex sheet shed from the trailing edge of a lifting wing. The main difference between the flow mechanism of the cylindrical vortex sheet of a rotor and the vortex sheet of a lifting wing is that the former rolls up and forms a torus ring while the latter rolls up into two line vortices.

Using the analogy described above, which is discussed in more detail in Ref. 9, conventional wing vortex theory is applied to approximately predict the center of the vortex core. Using the nomenclature of Fig. 95, the coordinates for the center of this vortex core can be expressed as follows:

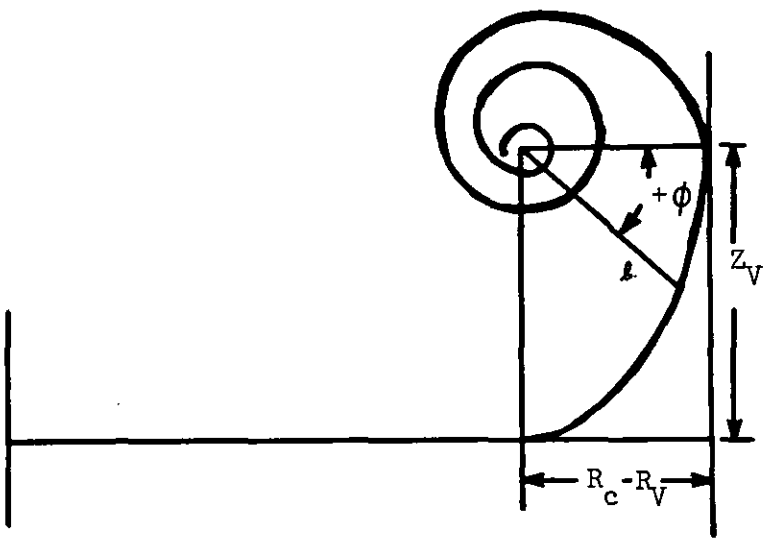

Figure 95. Logarithmic Spiral Representation of Vortex Rollup

$$R_V = 0.785\ R_c \tag{79}$$

$$Z_V = 0.329\ R_c \tag{80}$$

Once the center of the core is defined, the cloud rollup is approximated by a logarithmic spiral relationship given by:

$$\ell = e^{A(\phi + \phi_o)} \tag{81}$$

where A and ϕ_o are constants that can be determined by applying the boundary conditions of $\phi = 0$ when $\ell = R_c - R_V$ and $\phi = \pi/2$ when $\ell = Z_V$. Solutions for these constants result in the following equations:

$$A = \frac{2}{\pi} \ln \left(\frac{Z_V}{R_c - R_V}\right) \tag{82}$$

$$\phi_o = \frac{\pi}{2} \left(\frac{\ln(R_c - R_V)}{\ln(Z_V) - \ln(R_c - R_V)}\right) \tag{83}$$

(It should be noted that the equation for ϕ_o, typed as Eq. 35 in Ref. 9, was typed in error. It has been rederived here for this study.) Knowing the radial location of the dust cloud boundary (R_c) and the constants A and ϕ_o, the vertical location of the dust cloud boundary measured from the center of the vortex spiral can be computed by substituting $\phi = -\pi/2$ in Eq. 81. Thus,

$$\ell_V = e^{A(-\frac{\pi}{2} + \phi_o)} \tag{84}$$

The total dust cloud height measured from the ground is then given by the following equation for H_c.

$$H_c = \ell_V + Z_V \tag{85}$$

2. Correlation of Theory

In an effort to obtain some feel for the real-world validity of the previously described simple mathematical model, two correlation cases were evaluated. The first of these cases, described in Refs. 9 and 40, was for a sand/dust cloud generated by a tandem rotor Vertol H-21 helicopter. The second case evaluated was for the XV-15 tilt rotor while hovering over water (Ref. 42). Unfortunately, no other flight test correlation cases were identified in the literature during the available literature search time. Several scale-model tests of limited usefulness were also identified in order to aid in correlation; these results will be discussed as appropriate.

The correlation case involving the Vertol H-21 was developed in some detail in Ref. 9; however, for a full understanding of the experiment itself, it is required that Ref. 40 be reviewed also. The distribution of particle size which was used in the correlation effort was initially provided in Fig. 35 of Ref. 9, which is reproduced here as Fig. 96 (the terrain sample data is from Ft. Yuma, Arizona). The assumption was made by the authors of Ref. 9 in the correlation case that approximately the 10th to 12th percentile (by weight) size particle would be used to compute the cloud boundaries (this assumption was significantly aided by the use of photographs, movies, and particle trap results from the Ref. 40 effort). This percentile by weight particle size is approximately 0.04 mm in diameter and is representative of extremely fine sand or dust. Using this particle size and a density (ρ_p) of approximately 92 lb/ft^3 (sand), a value for K_T can be calculated where:

$$K_T = \frac{D_p \rho_p}{D_w \rho_w}$$

$$= \frac{(0.04 \text{ mm})\ (92 \text{ lb/ft}^3)}{(2.54 \text{ mm})(62.4 \text{ lb/ft}^3)}$$

$$= 0.025$$

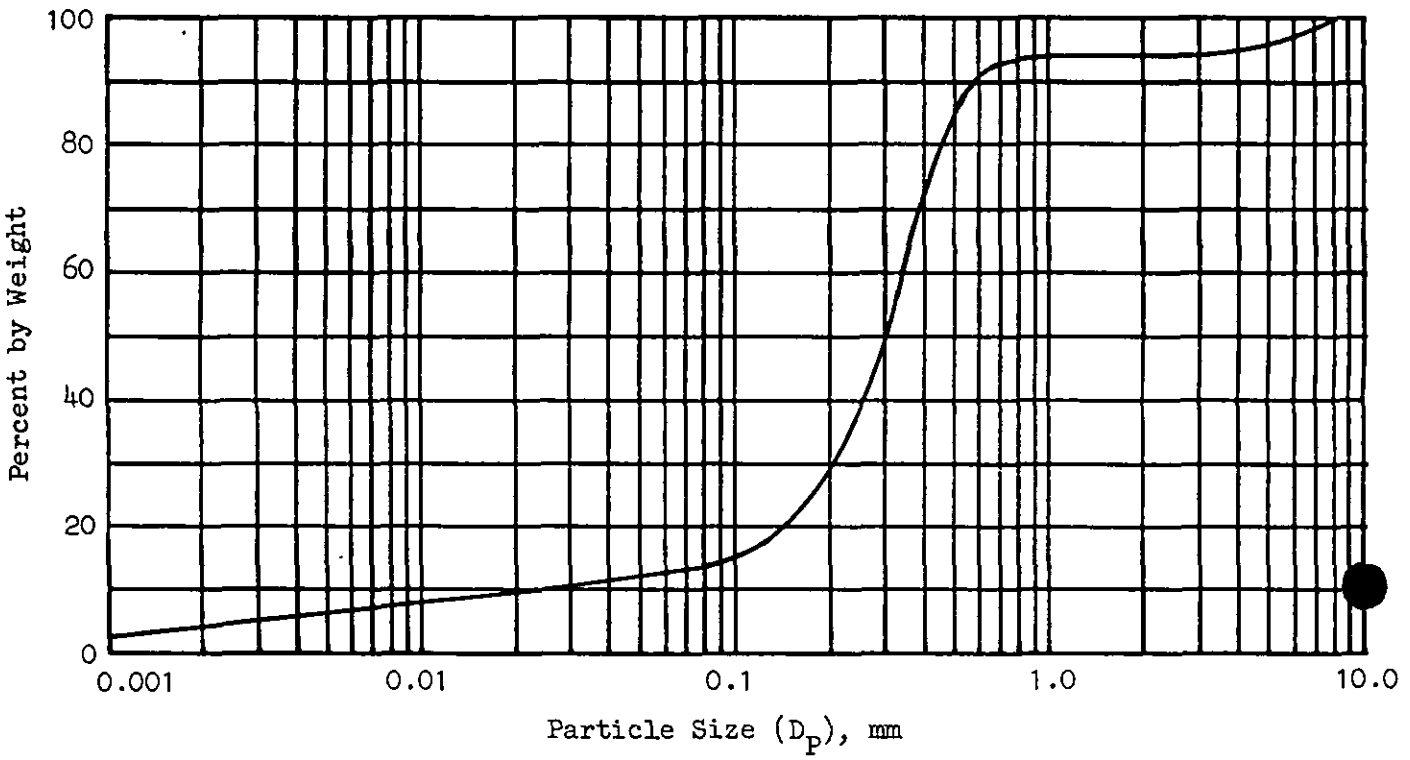

Figure 96. Ground Sample Particle Size Distribution

If this value for K_T is used, along with the input data of the H-21 (Table 17) and the theory presented earlier, then the dust cloud size can be estimated as shown in Fig. 97. Test data presented in Ref. 9 for this condition indicate the approximate boundary radius and height to be 190 ft and 95 ft, respectively. Both of these test values are quite close to what the mathematical model predicts.

Limited particle size data was also provided in Ref. 9 in order to guide in the estimation of where in the cloud larger particle size boundaries might occur. These test data are compared at 44 and 88 ft in Fig. 98 to calculated boundaries for particle sizes of approximately 0.5 mm to 2 mm. As can be seen in the graphical comparison for the non-interaction plane data (NI), the 0.5 mm boundary seems to be quite close to what was measured as the maximum particle size at approximately 5 and 10 ft (10 ft was the maximum height that particle traps were located). The 2 mm boundary would appear to be conservative, since particles of 2 mm were trapped only at heights of less than 1 ft. On the interaction plane (I), results would appear to compare similarly. One significant factor must be noted in this simple comparison, however, before any final conclusions about the quality of the correlation are reached. The first part of this factor involves a theoretical assumption made in the mathematical model that all of the particles for a certain K_T are of the same size and that they do not collide in their flight through the outwash flowfield. In addition, no loss of momentum to the flow is accounted for, since particle density is not assumed to be large enough to affect this factor. These assumptions are **rarely** correct. In the real world, particle size distribution usually varies over a wide range (i.e., Fig. 96). Also, collisions do take place, and these collisions reduce particle energy which might otherwise be utilized for further travel outward in the flowfield. If particle densities are large enough, the imparted momentum to the particles is also affected.

In conclusion, the presented test data is for only one terrain type and distribution. As a result of this fact, the data only permits "one correlation data point" to actually be plotted. Should another terrain type be evaluated, the distances at which the various particle sizes

TABLE 17

INPUT DATA FOR H-21 AND XV-15 CORRELATION CASES

Input Parameter	H-21	XV-15
Number of Rotors	2	2
Rotor Separation (ft)	42.0	32.2
Rotor Radius (ft)	22.0	12.5
Approximate Gross Weight (lb)	13000	12500
Approximate Fuselage Download (%)	1.5	13.0
Rotor Height Above Ground (ft)	17.0	62.5
Atmospheric Density Ratio	1.0	1.0
Wind (kt)	0.0	0.0

Experimental Results

- - - H-21 Flight Test Data (Ref.)

$R_c \cong 190$ ft

$H_c \cong 95$ ft

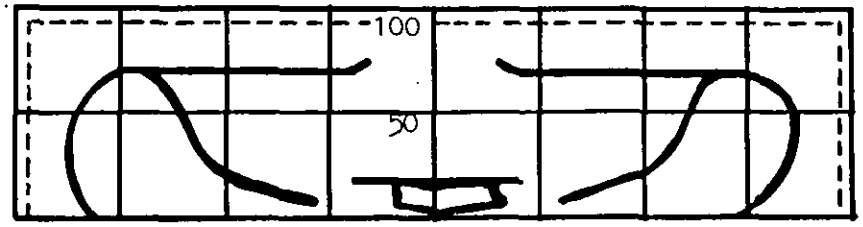

(a) Longitudinal Plane

Calculated Results*

$R_c = 150$ ft

$H_c = 70$ ft

$R_V = 117$ ft

$Z_V = 49$ ft

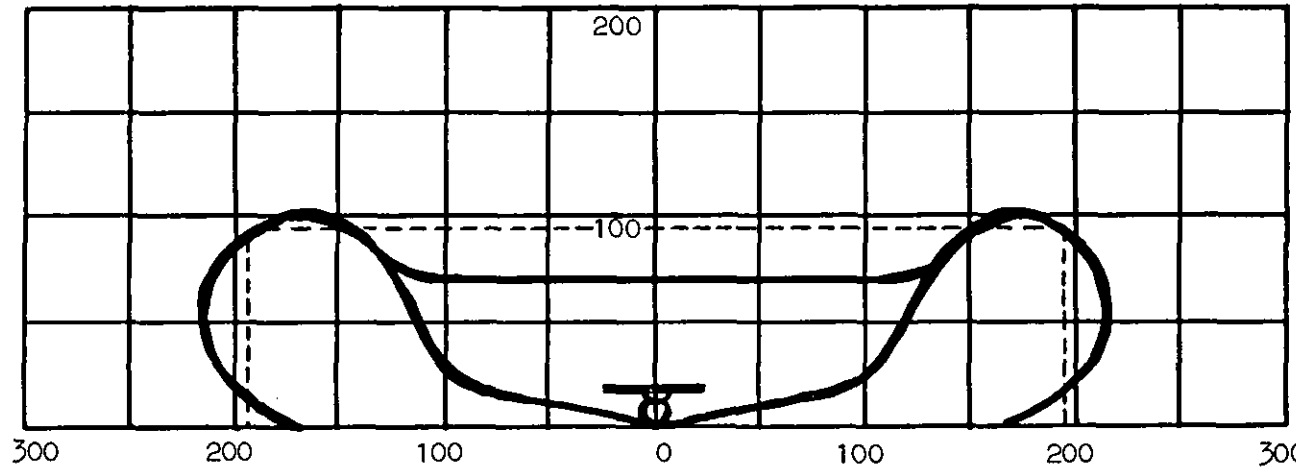

(b) Lateral Interaction Plane

Calculated Results

$R_c = 212$ ft

$H_c = 99$ ft

$R_V = 166$ ft

$Z_V = 70$ ft

*From the center of the front or rear rotor (add 22 ft to R_c and R_V before plotting)

Figure 97. Dust Cloud Size and Shape for the H-21 Helicopter

H-21 EXPERIMENTAL DATA

Particle trap radial position was either 44 or 88 ft from the center of the forward rotor (NI) or the center of both rotors (I). Maximum trap height was 10 ft. Maximum particle sizes in the traps are shown beside the data ⊙ points.

CALCULATED BOUNDARIES

——— Interaction Plane (I)

- - - Non-Interaction Plane (NI)

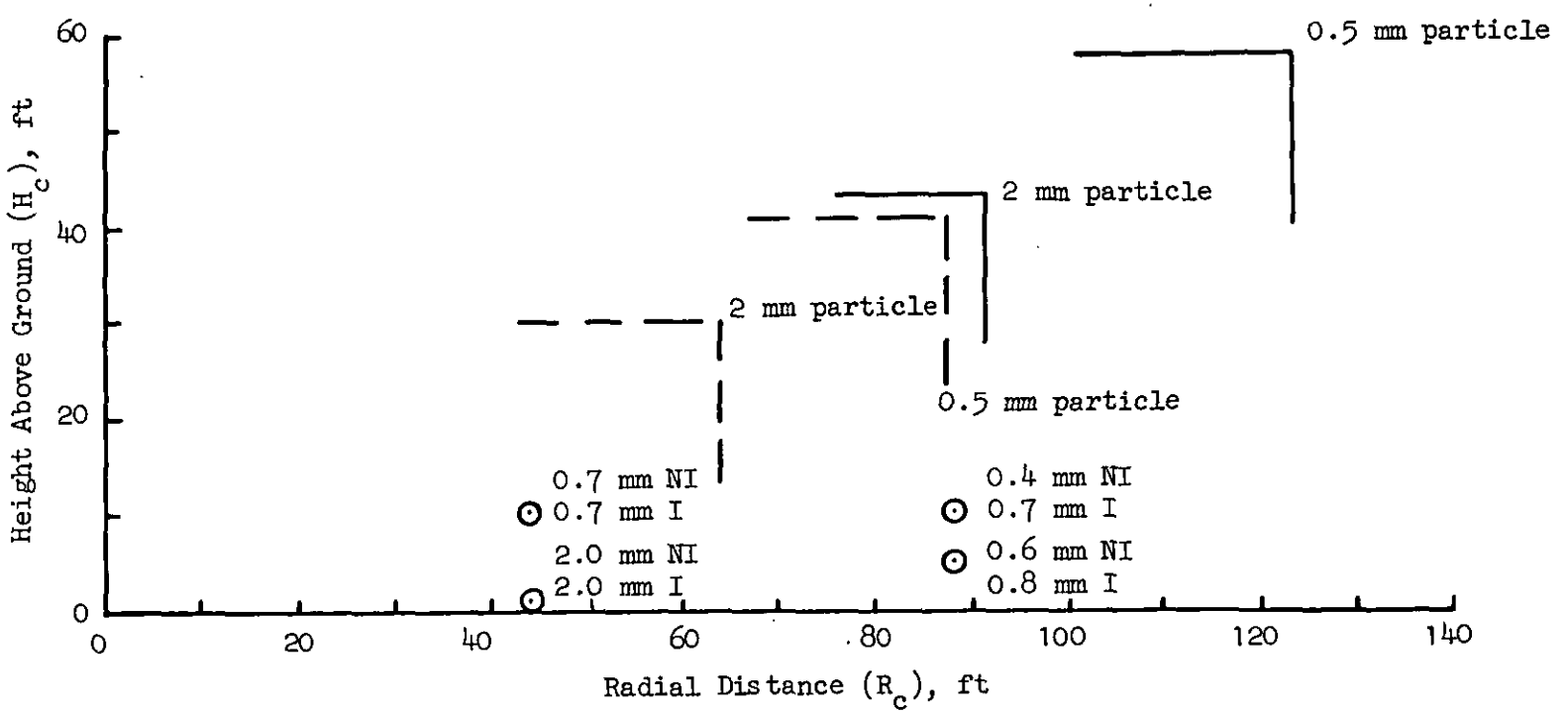

Figure 98. H-21 Particle Cloud Boundary Comparison for Particle Sizes Ranging from Approximately 0.5 mm to 2.0 mm

travel may be increased or decreased. Therefore, the correlation should only be looked upon as a very limited correlation for the presented theory. Much more data would be needed to fully validate the mathematical model.

In the second correlation case, a comparison is made with XV-15 tilt rotor data which was obtained in 1983 in an over-the-water hover test (Ref. 42). In perfectly calm air (i.e., wind less than 5 kt) at a 62.5 ft rotor height, spray was observed (from photographs) to occur to heights of approximately 3 ft. In gusty winds (12 to 20 kt), spray was observed up to approximately 20 ft. Using the input data of Table 17, and a K_T equal to 1.0, the estimated spray height is 30 ft to the side and 42 ft fore and aft. (The K_T value of 1.0 which is assumed is an estimation, because the spray droplet diameter was not recorded.) While this results in a seemingly conservative calculated discrepancy of 10 to 20 ft in predicted spray height for the gusty wind case, it is important to note that in Ref. 41, it is stated that estimates of spray height made from photographs can be very misleading, even in controlled laboratory tests. This is due to the fine, as well as transparent, nature of spray particles when photographed in lower densities in air. Therefore, it would be expected that the XV-15 spray height data for the gusty conditions might approach 30 plus ft. The simplicity of the theory presented in this section does not attempt to account directly for the effect of light-to-medium winds. Therefore, it can only be assumed that some mild choppy wave action is necessary to help lift the spray up into the rotorwash flowfield and that this theory works for these types of conditions. While this commentary might explain the gusty wind spray data, it does not explain the large discrepancy in the calm air correlation results. Another method, exclusively for spray height prediction purposes, is presented in Ref. 41. This highly empirical method (using model results) is recommended for anyone who is interested specifically in spray height calculations.

In summary, while the two correlation cases that are presented provide fairly good validation of the presented mathematical model, it would nevertheless be **extremely risky** to claim that the presented method is good for anything other than **general estimation purposes.** Use of this theory

would intuitively seem to be somewhat overpredictive of the cloud height (H_c) for many larger particle sizes. Should further correlation data be identified and similar correlation results presented, then this statement as to the method's usefulness might be modified accordingly.

3. Evaluation of "Worst Offender" Rotorcraft Configurations

An evaluation of the five "worst offender" rotorcraft configurations was made for seven values of K_T; these results are presented in Figs. 99 through 103. The presented boundaries should, in general, be considered as conservative. This would certainly be true for most rotorcraft now in civil use for the equivalent rotor radius values. However, the size of the magnitude of this conservativeness is unknown, because this method assumes no wind hovering conditions and with light, gusty winds, the effective surface dynamic pressure can significantly increase. This can be seen in the data presented in Figs. 76 and 78. In attempting to assign some practical meaning to these boundaries, several potential hazards have been assumed; these hazards include those which:

1. Might cause personnel injury.
2. Might cause engine damage.

and

3. Might cause abrasion of equipment and rotor blades.

In the first of these three cases, the exposure of an unprotected person (or animal) to the hazard for a short period of time could possibly result in severe injury. In the case of engine and abrasive related damage, a much longer duration exposure is required, along with a significant value of particulate density in the air. In each of these last two cases, a "passing" rotorcraft probably could not inflict serious damage. Only situations in which a nearby rotorcraft is required to hover or pull power for significant periods of time should be considered potentially hazardous.

Summary of Cloud Boundary Data, ft

K_T	R_c	R_V	Z_V	H_c
0.025	131	103	43	62
0.3	76	60	25	36
0.6	65	52	22	31
0.9	60	47	20	28
1.2	56	44	19	27
16.0	32	25	11	15
70.0	23	18	8	11

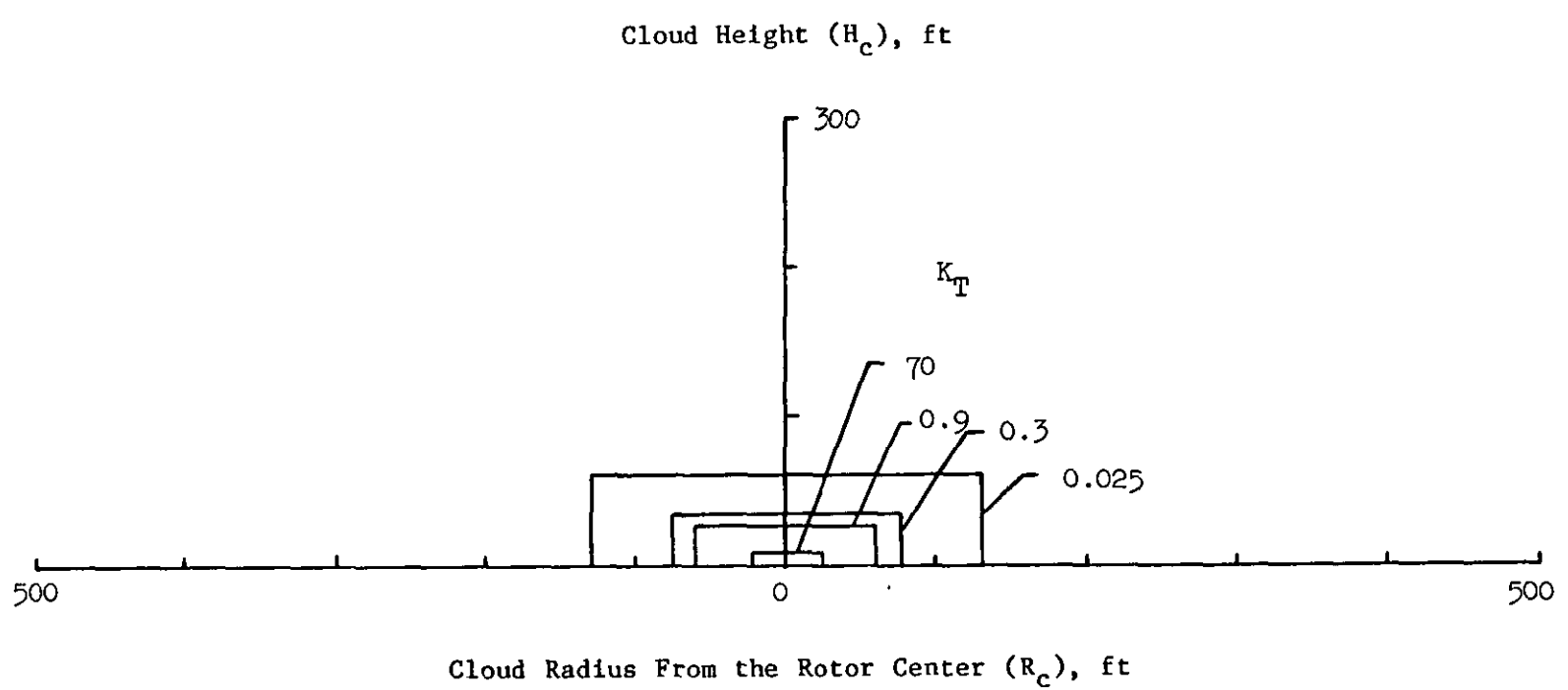

Figure 99. Cloud Boundary Summary Data for the "S" Class Rotorcraft (15 ft radius)

Summary of Cloud Boundary Data, ft

K_T	R_c	R_V	Z_V	H_c
0.025	193	152	64	91
0.3	112	88	37	53
0.6	97	76	32	45
0.9	88	69	29	42
1.2	83	65	27	39
16.0	47	37	16	22
70.0	34	27	11	16

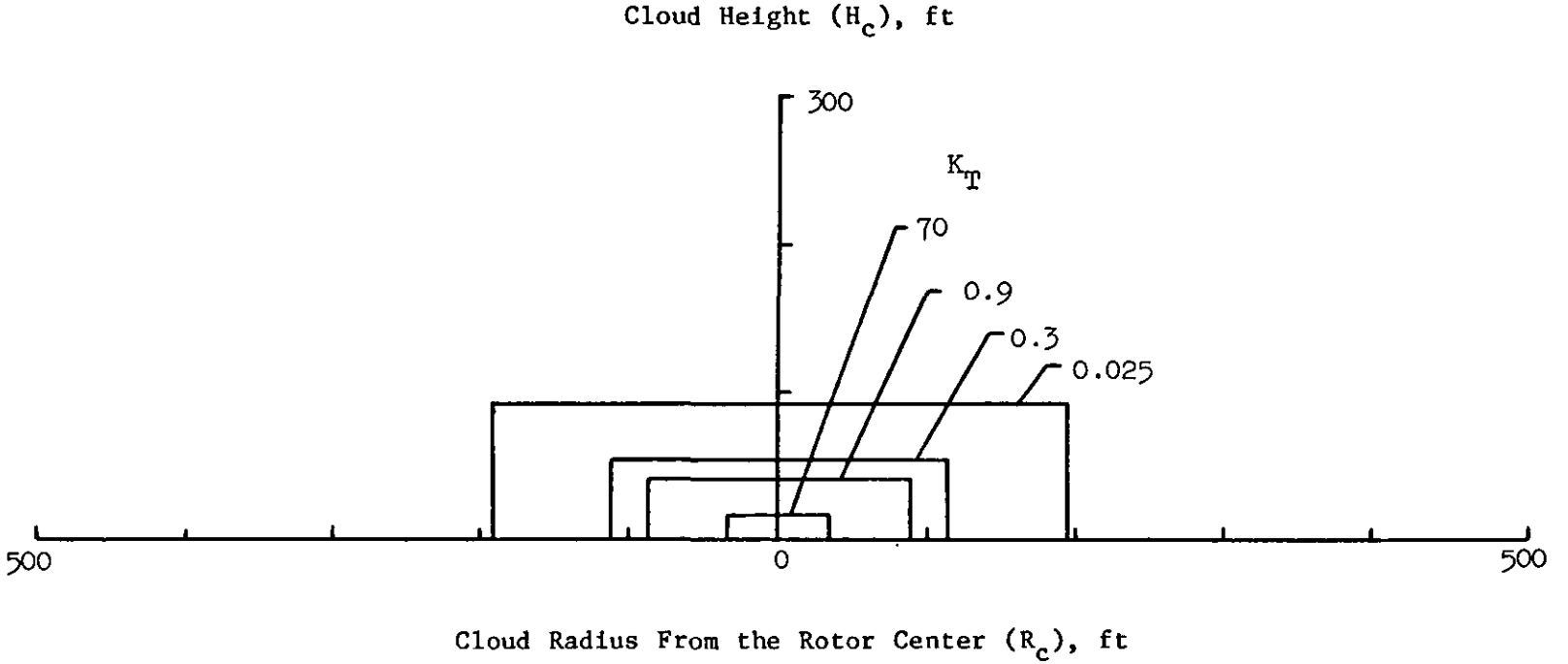

Figure 100. Cloud Boundary Summary Data for the "SM" Class Rotorcraft (20 ft radius)

Summary of Cloud Boundary Data, ft

K_T	R_c	R_V	Z_V	H_c
0.025	259	203	85	121
0.3	150	118	49	70
0.6	129	101	43	61
0.9	118	93	39	56
1.2	111	87	37	52
16.0	63	50	21	30
70.0	46	36	15	21

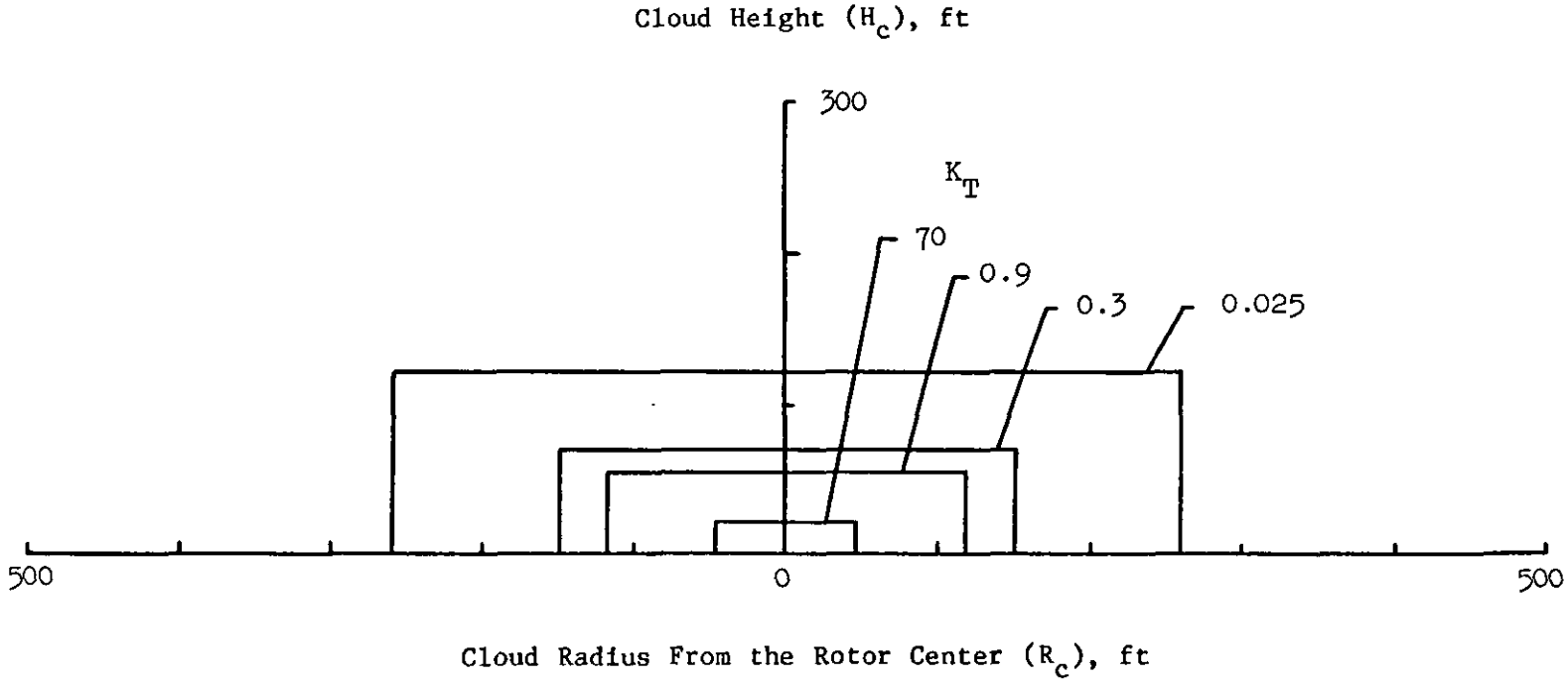

Figure 101. Cloud Boundary Summary Data for the "M" Class Rotorcraft (25 ft radius)

Summary of Cloud Boundary Data, ft

K_T	R_c	R_V	Z_V	H_c
0.025	342	269	113	161
0.3	199	156	65	93
0.6	171	134	56	80
0.9	156	123	52	73
1.2	146	115	48	69
16.0	83	66	27	39
70.0	60	47	20	28

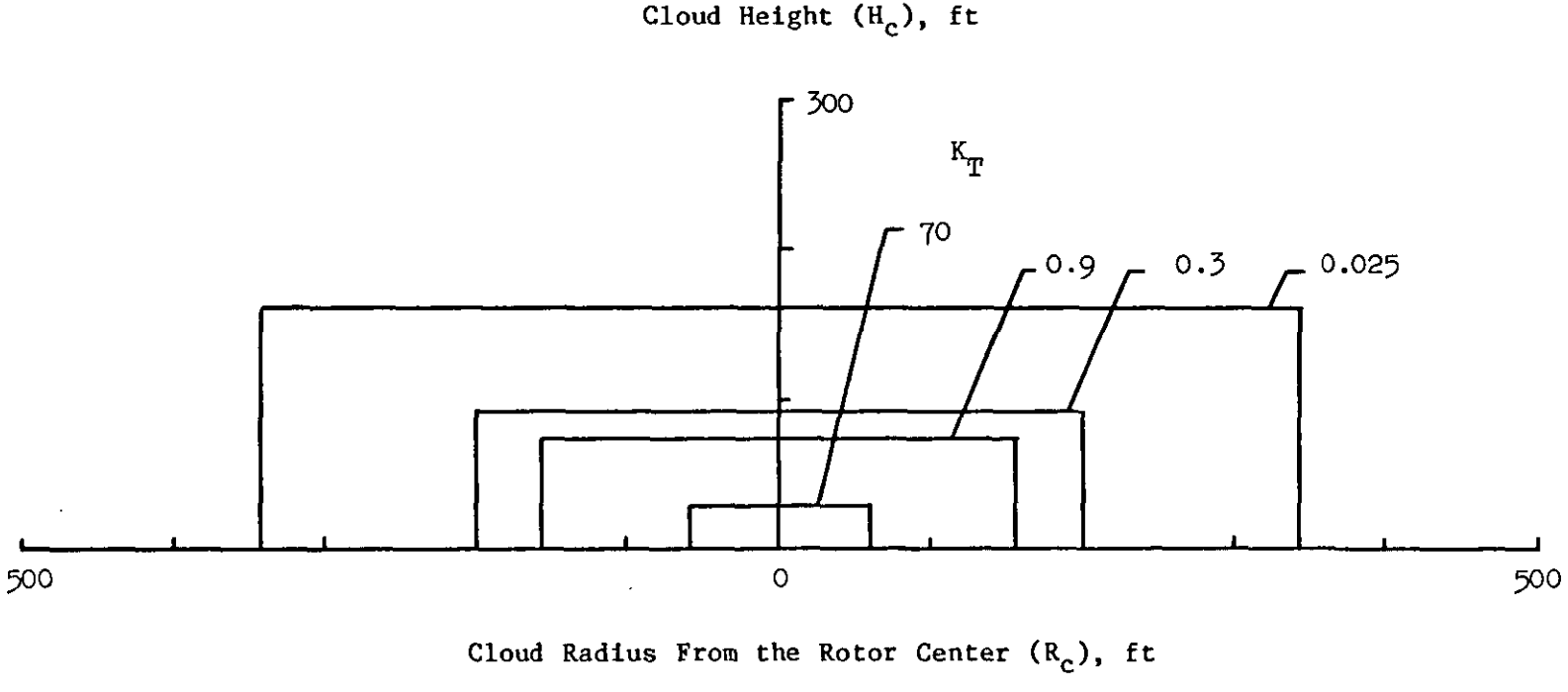

Figure 102. Cloud Boundary Summary Data for the "MH" Class Rotorcraft (30 ft radius)

Summary of Cloud Boundary Data, ft

K_T	R_c	R_V	Z_V	H_c
0.025	510	400	168	240
0.3	296	233	98	139
0.6	254	200	84	120
0.9	233	183	77	110
1.2	219	172	72	103
16.0	124	98	41	58
70.0	90	71	30	42

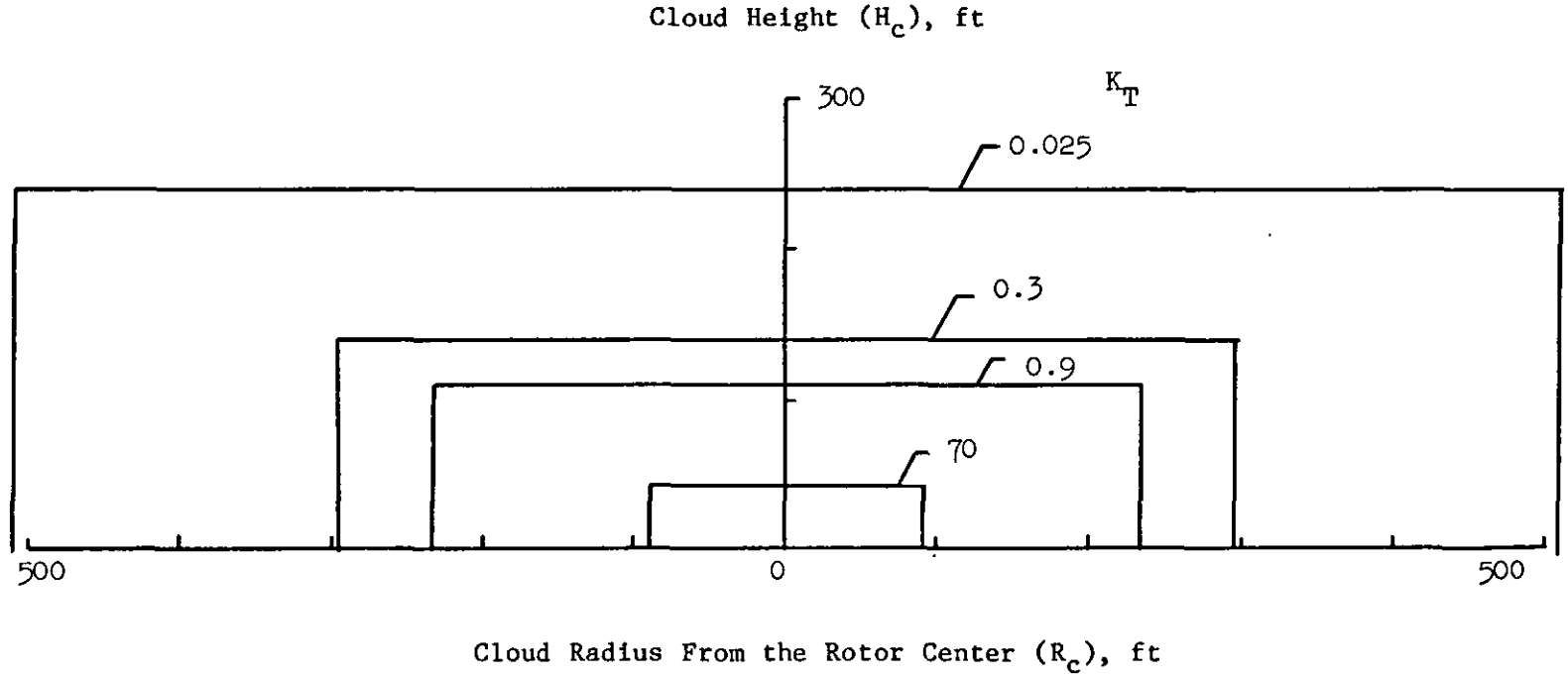

Figure 103. Cloud Boundary Summary Data for the "H" Class Rotorcraft (40 ft radius)

The personnel injury with the highest probability of occurrence, as related to debris clouds, is that of eye injury. All other parts of the human body, particularly with clothing as a protection, can withstand impacts without injury much easier than the eye. While common sense would indicate that unprotected personnel (particularly trained personnel) will close their eyes instinctively when subjected to uncomfortable levels of rotorwash, this assumption cannot be guaranteed. Therefore, for this study, the conservative assumption is made that personnel and animals will sooner or later be "surprised" by hazardous levels of rotorwash which contains dangerous sizes of particulate matter.

Reference 9 states that, as a guideline, winds of above 59 kt can clearly be expected to cause damage to the unprotected eye. (This statement must certainly be qualified in that it assumes particles of a dangerous size or weight are contained in the rotorwash.) Reference 8 provides an experimentally derived graph of particle weight versus particle velocity (steel particles) which is known to have caused corneal penetration of a rabbit's eyes. This figure was reproduced in Subsection F as Fig. 91. Unfortunately, the weight/velocity relationships to prevent abrasive damage and discomfort to the eye are not known. Builder's sand particles, as measured in Ref. 39, normally vary from approximately 0.003 to 0.05+ inches. Weights associated with these diameters are approximately 3.42×10^{-7} and 1.68×10^{-3} grams respectively. Peak rotorwash values calculated for the five analysis configurations, as shown in Fig. 104, never appear much in excess of 100 kt on a calm day. If the **conservative** assumption is made that somehow the smallest particle of sand that can be hazardous (approximately 0.2 grams) **will** be entrained at the maximum rotorcraft outwash velocity and **will** strike a human eye, then the diameter and K_T value for that size of sand particle will be approximately 0.25 inches and 3.7, respectively. The estimated worst case hazardous boundary distances associated with this value of K_T can be interpolated from the results tabulated and plotted in Figs. 99 through 103.

In reviewing these hazard boundaries with respect to the above conservative assumption, several discrepancies immediately appear. First of

Rotorcraft Configurations: S, SM, M, MH, H

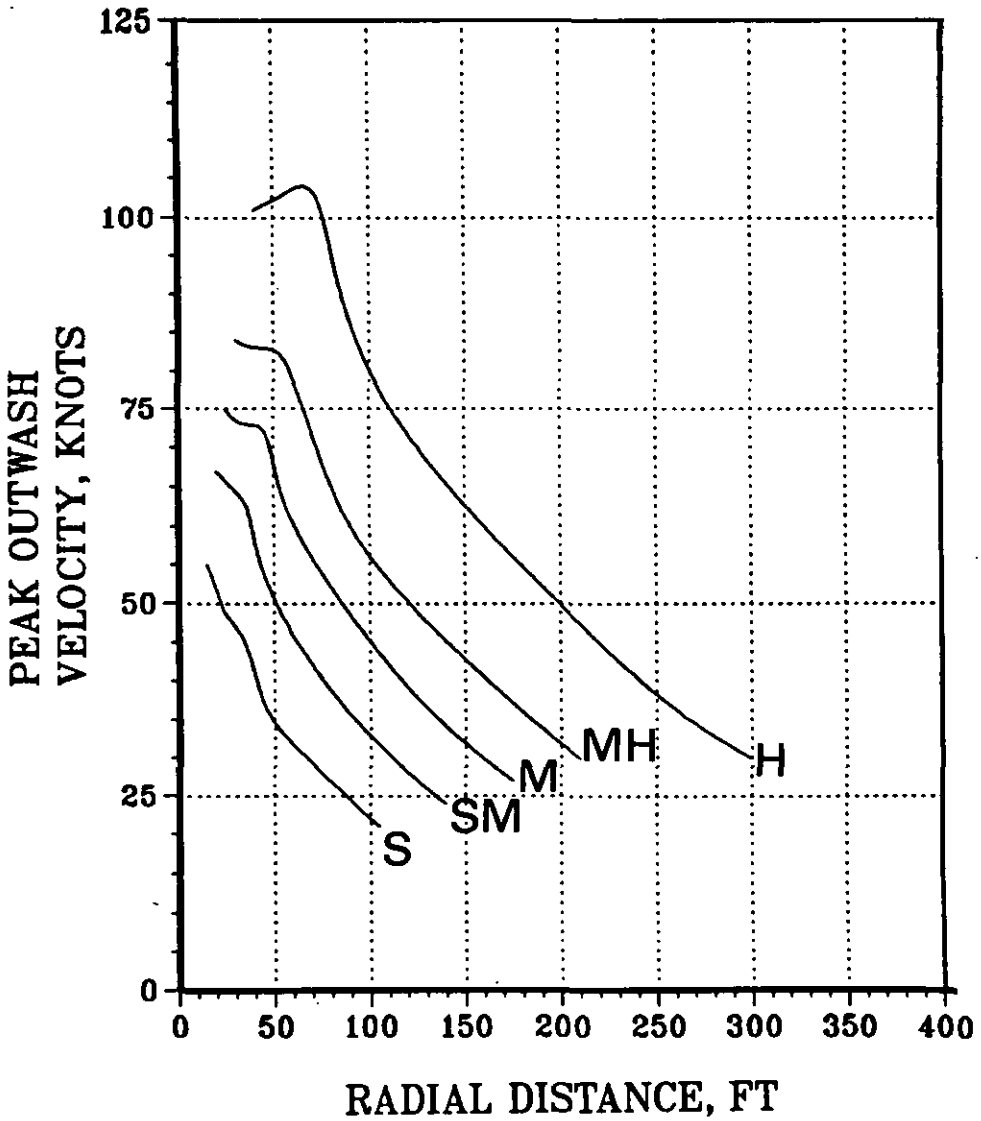

Figure 104. Calculated Peak Profile Maximum Velocities as a Function of Radial Distance (Wind = 0 kts)

all, the velocities required to damage the eye for the specified particle size are not present in the outwash flowfield to the radial boundaries specified (see Fig. 104). Therefore, it would seem impossible to have particals flying about at the boundaries which have energies of sufficient magnitude to penetrate the eye when striking it. These particles may still be very bothersome, however. (No data exist, however, to define bothersome.) If the term bothersome is assumed to be equal to a scenario in which significant abrasion of equipment can take place, then particle sizes in excess of 0.3 mm can be assumed to be hazardous. The approximate K_T value for sand particles of this size is 0.2. Another discrepancy in this analysis assumption is that no account is made for the effects of gusty wind. As can be seen in Fig. 81 (the 9-kt companion figure to Fig. 104), a gusty wind can add significantly to the particle kinetic energy at a specified radius. Thirdly, a discrepancy appears in this method in that any practical separation standard must eventually account for accidental deviations or course changes by the generating rotorcraft which may unexpectedly result in a safe separation distance becoming an unsafe distance. In summary, it is clear that a lot of uncertainty exists in assuming a value for the dangerous particle size and matching up a corresponding hazard cloud boundary. Therefore, until some of the uncertainties are further quantified by experiment, it is recommended that the suggested conservative K_T boundaries of 0.3 in in Figs. 99 through 103 remain as the personnel hazard boundaries for unprotected and untrained personnel. These boundaries are equated more with what would probably be bothersome instead of what would cause serious physiological damage. It is interesting to note that the serious injury boundary as specified by a K_T of approximately 3.7 by this method is not significantly different than that recommended in the previous section for large objects.

Boundaries for trained personnel, or personnel wearing eye protection, cannot be accurately estimated using the above technique, particularly since hazardous particles may not even be present in substantial quantities in the heliport terrain environment of interest. Also, boundaries for trained personnel may not even be relevant in that they may be required to work near the rotorcraft anyway (i.e., mechanic) even when very

hazardous rotorwash conditions exist. It is recommended that trained personnel wear eye protection at all times when in close proximity to a rotorcraft, particularly when working in close proximity to the "MH" and "H" class rotorcraft. Reference 11 provides a graphic text description of the hazardous environment associated in working near the CH-53D and CH-53E rotorcraft.

Engine and rotor blade abrasion damage can be looked at in two ways. If the engine and rotor are rotating, then particle velocity speeds become unimportant. This is because the engine component and rotor blade rotational velocities are well in excess themselves of the velocities required for particles to inflict impact damage. Only partical presence in the airstream is required for a significant hazard to occur. It must be acknowledged, though, that most modern turbine engines do have particle separators and all rotor blades have some type of an abrasion strip, because this hazard is so significant. These hardware improvements significantly reduce the hazard, and they are often installed due to the fact that rotorcraft must be able to operate in their own rotorwash environment. These particular protection features may not be assumed however for fixed wing rotating components (i.e., airplane propellors or executive jet engines). A second way to look at the problem is to assume that the endangered aircraft or rotorcraft is "parked" and that the main problem becomes one of equipment abrasion.

In briefly looking at the first of the two problem types, it is stated in Ref. 9 that significant compressor blade damage is caused by steady injestion of large size particles (greater than 0.2 mm). Continued operation in the contaminated atmosphere will produce damage which will in turn reduce engine power available levels and increase fuel consumption. Table 18 provides test data from Ref. 9 that indicates that performance loss can be most easily associated with accumulated weight of ingested sand and dust. For a 5 percent reduction in power available, the associated engine endurance times in contaminated air can be shown to vary from 7.2 to 99 minutes. While it is not the purpose of this study to estimate the mass flows which will be associated with any particular terrain environment, it is nevertheless important to note that rotorcraft

TABLE 18

RESULTS OF DUST INGESTION BY VARIOUS V/STOL ENGINES FOR A FIVE-PERCENT REDUCTION IN NORMAL RATED POWER

Engine Model	Sand Ingested (lb)	Airflow (lb/sec)	ρ_p (lb/ft^3)	Engine Endurance (minutes)
T-64(1)	29	24.5	7.7×10^{-5}	20
T-58(8)	24	12.4	34.1×10^{-5}	7.2
T-55L(5)	22.5	10.7	2.7×10^{-5}	99

should not necessarily be allowed to hover in close proximity to other rotorcraft for extended periods of time if large amounts of particulate matter is being blown about. Particle sizes of 0.2 mm for sand calculate to a K_T of approximately 0.12. Since significant densities of particles would be required to reach mass flow rates as described in Table 18, one could assume that in civilian operations, normally conducted over "particle sparse" terrains, that dust cloud hazards to engines and rotor blades should be minimal, particularly since many modern rotorcraft engines now contain integral particle separators. Much more would need to be known about specific scenarios before a signifcant hazard potential would probably need to be investigated further.

If another rotorcraft, aircraft, or piece of equipment is parked near another rotorcraft generating a particulate cloud, then the problem of abrasion can become a hazard. Very little information was identified in the literature to define what an unacceptable level of abrasion was. Reference 9 states that severe abrasion of equipment is present in winds greater than 35 kt if significant particle densities occur for particle sizes in excess of 0.3 mm. Mild abrasion of equipment occurs in winds in excess of 14 kt with significant particle densities for particle sizes in excess of 0.01 mm. K_T factor values for these sand particle sizes are below values of 0.12. While the "worst offender" results would indicate that it would be easy to generate a large dust cloud of particles of these

sizes, it again becomes important to quantify the mass flow rates which would be involved in the impact on subject pieces of equipment. For the civil heliport environment, these mass flow rates should be quite low as long as concrete and well-maintained sod are the primary terrain types in use. When considered with other potential hazards in the civilian operating environment, this particular hazard does not appear to be significant except possibly as a nuisance (i.e., deposition of a layer of dust so as to require that the inside of a vehicle be vacuumed or the outside be washed).

4. Summary of Results

In summarizing the results presented in this section, it must first be said that an assumption has been made about the analyzed civilian heliport environment. The main components of this assumption are that:

1. No heliport terrain environment will be considered acceptable by the operators or FAA if the pilot's vision is obstructed in any way due to high densities of particulate matter in the air (i.e., dust, snow, sand).

2. Concrete, asphalt, or sod are the terrain types which will be used in the approved heliport environment.

and that

3. Procedures will be in place in the heliport environment to effectively separate untrained and unprotected personnel from those which are trained and possibly intended for working in the rotorwash environment (i.e., mechanics).

As long as these components of the assumed heliport scenario are maintained, then particulate cloud related hazards should not in general be a significant worry in setting final practical separation standards. Separation guidelines for unprotected and untrained personnel are provided in this section, along with recommendations for trained personnel protection.

Should the above assumption be considered to be inaccurate for the way heliports may be designed and used, then it will become necessary to conduct a much larger and more detailed study of this hazard. This study

will need to first validate the mathematical model which is used to a greater extent than was possible here. The study will also need to define the required or acceptable terrain types (in detail) over which rotorcraft operations will be conducted. The terrain types will then need to be evaluated to determine what size particles can be eroded and at what mass flow rates the particles are blown through rotorcraft outwash flowfields.

SECTION VII

BACKGROUND INFORMATION AND A REVIEW OF THE ROTORCRAFT SEPARATION REQUIREMENT PROBLEM

A. INTRODUCTION

As stated in Section I, the Federal Aviation Administration (FAA) recently initiated a program to obtain the data necessary to improve rotorcraft separation standards. The primary topic identified requiring analytical support is the definition of safe separation distances that will be needed between rotorcraft in flight and aircraft or other vehicles on the ground. The rotorcraft pilot is currently given the responsibility for preventing damage that might result due to his rotorwash; nevertheless, the FAA has a responsibility to assure that the rotorwash hazard is reflected in the planning standards for heliport design and that air traffic controllers do not ask rotorcraft pilots to fly into areas where they can inflict damage to parked aircraft, rotorcraft, or vehicles.

The development of the recommended separation requirements presented in this report for rotorcraft operation at heliports and airports was initiated using guidelines as specified by the U. S. Department of Transportation in the issued contract statement of work (Ref. 2). This task, specified as Task 4, is reproduced below for reference.

> **Task 4.** ***Recommended Separation Requirements***
>
> This task shall result in proposed safe separation distances between classes of rotorcraft generators and classes of aircraft/vehicles on the ground. The safety factors generated in Task 3 shall be used to make the separations safe under all weather conditions. The number of classes for generation and damage should be as small as possible and preferably not exceed four for each. Thus, the separation matrix should be no larger than four by four. The study should examine the effectiveness of different classification schemes.

The following principles should be followed in defining the classes:

a. The classes should divide the existing mix of aircraft at natural breaks in size and/or characteristics.

b. The classes should be consistent with existing classes used for other purposes.

c. The classes should be consistent with the way current rotorcraft operations are carried out. For example, large military rotorcraft not normally operating at civil airports or heliports could easily be put into a separate class.

Interviews were also conducted with other members of the FAA during this contracted study, specifically people associated with the heliport planning and air traffic control groups. Guidance provided from these interviews indicated that any proposed separation requirements should also (in addition to the statement of work guidance):

1. Be as **simple** as humanly possible (certainly less than a four by four matrix, if at all possible).

2. Not rely on air traffic controllers to have to identify and classify any specific rotorcraft.

3. Be practical and easily implementable in the heliport/airport environment.

When considering the above supplied guidance as a whole, it becomes quite obvious that the development of easy to use, practical, safe, and effective recommended separation requirements is by no means a simple task.

B. GENERAL THOUGHTS ON THE EFFECTIVENESS OF VARIOUS CLASSIFICATION SCHEMES

Numerous classification schemes can be devised for specifying recommended rotorcraft separation requirements. These schemes include ones as simple as making the pilot totally responsible for safe separation distances (as is now utilized) to ones quite complex in which hazard generating rotorcraft are separated into four classes and all other

structures, vehicles, personnel, and aircraft on the ground are separated into another four classes (assumes maximum allowable matrix is four by four). Safe separation distances would then be associated with each of the sixteen boxes of the class-derived matrix. After a thorough review of these explicit approaches by the STI/CMA team, these very explicit and direct classification schemes were found to be generally unacceptable.. Reasons for the finding that the problem is not simple enough to be classified by simple matrix schemes alone include:

1. The approach does not directly take into account the operating regime of the rotorcraft.

2. The approach does not take into account the type of activity associated with the other rotorcraft, aircraft, or vehicles on the ground (i.e., maintenance in progress, personnel loading or unloading, refueling, or a lack of any type of activity at all).

3. The classification scheme does not directly take into account the way in which most rotorcraft operations are carried out.

As a result of these findings, it was decided that any practical classification schemes would also have to take into account certain procedures that would be appropriate to the situation. Several hazards not studied in Section VI were also believed to be important to indirectly consider in the developed classification scheme. An example of these would be that it would be undesirable to have nonessential (or unauthorized) personnel next to a rotorcraft on a maintenance check run as well as too close during takeoff, taxi, or landing due to the fire and explosion risks associated with a crash or ground run accident.

A search was also conducted during the evaluation of various classification schemes to identify any classification schemes that the military might be utilizing in their own definition of rotorcraft separation requirements or procedures. Discussions with the U.S. Army Safety Center and numerous pilots, however, confirmed that classification schemes of this type did not exist. Rotorcraft pilots in the services are responsible for damage caused by the rotorcraft they command.

C. APPROACHES INVESTIGATED IN AN ANALYSIS OF THE CLASSIFICATION PROBLEM

Clearly, without a good handle on classifying the various types of rotorcraft, it would be impossible to develop practical recommended separation requirements. Classification schemes involving parameters such as gross weight, rotor radius, disc loading, and even units manufactured for a specific rotorcraft type were all evaluated to some extent in an effort to develop a fair, practical, and useful classification system. For one or more reasons, however, each of these parameters was found, by itself, to be unacceptable.

The most useful classification parameter of those which were investigated was a hybrid parameter which we have defined in this report to be the Hazard Index (HI). This parameter is calculated by multiplying disc loading (DL) times the rotor radius (R) in order to obtain a parameter in units of lb/ft.

$$HI = (DL)(R) = \left(\frac{GW_{max}}{\pi R^2}\right)(R) \qquad (86)$$

While not ideal, this parameter nevertheless roughly equates the high disc loading/low-rotor radius rotorcraft with its corresponding low disc loading/large rotor radius rotorcraft which has roughly the same rotorwash generated velocity distribution at a specified finite distance away from the respective rotor hubs. Using the rotorcraft data provided in Appendix A, a chart was made of hazard index versus rotorcraft separation distance for some of the hazards identified in Section VI as well as for the five "worst offender" rotorcraft. These investigated hazards and the recommended separation distances for the five "worst offender" rotorcraft (from Section VI) are summarized in Fig. 105. In evaluating the charted data, it was discovered that almost all of the light helicopters in the United States are approximately equal to or have less hazard potential than the S class "worst offender" configuration as defined in Section V (HI = 95 lb/ft). As can be seen in Fig. 105, this size classification (or grouping) also presents a minimum of hazard potential for almost all of the specific hazard types when viewed from the perspective of the

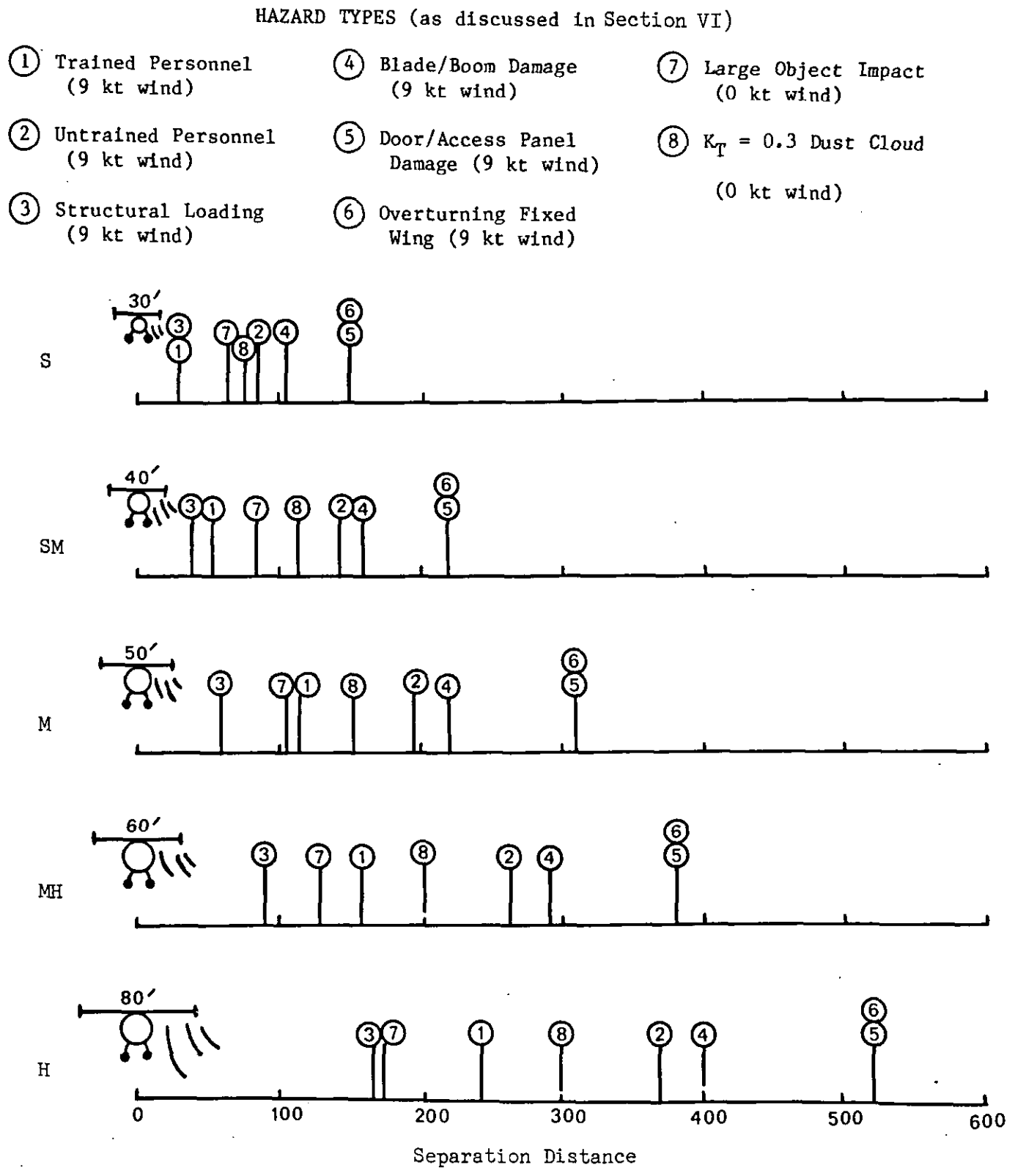

Figure 105. Summary of Individual Hazard Results

"classifying" physical unit of feet. The worst case hazard along with the worst case ambient wind level requires a safe separation distance of only one-half the length of a football field (150 ft). The required landing area therefore is nearly the minimum cleared area requirement in most cases for a rotorcraft to safely clear buildings, obstacles, and parking lots at a reasonable angle of descent. This size of open area would probably also be a desired minimum to provide space for emergency landing following an engine failure or for clearance with respect to surrounding obstacles following a surprise gust.

Since it was desirable that the chosen rotorcraft classification scheme be broken down into no more than three or four classes, it was decided that the second investigated breakpoint in the classification scheme should be the one that defined the low end of the "giant" rotorcraft class. A review of the large rotorcraft that are flying today revealed that this break point could be set justifiably at a hazard index value of approximately 260 lb/ft. This value of HI forces only the civilian rotorcraft that are a direct derivative of large, medium-to-heavy-lift military rotorcraft into a special classification group. At the present time, there are probably less than 25 to 30 registered rotorcraft of this type operating in the United States.

The last rotorcraft classification decision, considering the guidelines provided, was whether or not to break down the remaining rotorcraft, the middle size range, into two additional classification categories. After considerable review, it was decided that no clear cut criteria could be developed to fairly and equitably justify this further breakdown; therefore, all rotorcraft with HI values between 110 lb/ft and 260 lb/ft are assumed to be in one class for recommended separation requirement purposes. Further information and guidance by the FAA is needed before additional breakdown of rotorcraft in this class can be made.

As stated previously, the classification of vehicles, fixed-wing aircraft, personnel, and other rotorcraft into simple classification schemes was not deemed practical when considering the hazard analysis results. Therefore, a decision was made to provide the recommended rotorcraft separation requirements in the desired matrix format along with procedures

that should be implemented simultaneously. These recommended separation requirements and procedures are presented in detail in Section II. In the following paragraphs, some rationale will be provided for the reasoning behind the decision to provide the recommended separation requirements in the described format.

The analysis of possible classification schemes for defining separation requirements as a function of hazard type identified two operational scenarios where the recommended requirements were best presented in different forms. The first of these two scenarios involves the one in which a heliport is developed for use by only one helicopter at any one point in time (e.g., a single hospital helipad for emergency services). The second involves the scenario in which more than one rotorcraft and/or fixed-wing aircraft are involved in simultaneous operations (e.g., public use heliport or airport). The possible types of hazards involved in each of these scenarios is first of all quite different, and, more important, the operational nature of the scenarios is totally different. In the first case, an air traffic controller is not expected to be present, and the burden for preventing accidents falls solely on the pilot's ability to spot hazardous situations while also flying the rotorcraft (an extremely tough job if the weather is not ideal). In the second scenario, the pilot may or may not be in a situation in which multiple pilots and/or air traffic controllers are involved. The operations involved are also, while often extremely varied in nature, more often controlled by at least some form of safety procedures.

In an effort to attempt development of useful and practical recommendations for separation criteria for both of the aforementioned operational scenarios, a decision was made to keep each scenario independent of the other. The hazard types used in the development of criteria were chosen from the Fig. 105 hazard types as they were deemed applicable to each of the specific scenarios. This resulted, for the single rotorcraft/heliport scenario as shown in Fig. 2, in recommended separation criteria that are presented in a format which is more applicable to the design and construction of the heliport. Application of

the recommended separation requirements in this manner should aid significantly later on during actual operations by significantly reducing the pilot's mental workload in avoiding accidents when taking off and landing. Recommended separation criteria developed for the second of the two scenarios discussed above is presented in a format that is related much more to the type of rotorcraft operations being conducted. It must again be noted that the recommended separation requirements take into account the **worst case scenario** (i.e., all weather, worst case azimuth winds). The recommended separation distances presented may therefore be considered by some to be overly conservative. Reduction of the recommended separation requirements may be possible, however, if key elements of the suggested research plan in Section VIII can be conducted.

D. HAZARD TYPES USED TO DETERMINE THE QUANTITATIVE RECOMMENDED SEPARATION REQUIREMENTS

As stated previously, the types of hazards that were used in the determination of the recommended rotorcraft separation requirements, as presented in Section VI, are summarized in Fig. 105. In general, the suggested quantitative values, as presented in Section II, are slightly more conservative for the matrix approach (where only three very general size classes exist) than for the more detailed equation-related approach which is also offered.

In those scenarios where only one rotorcraft can be operated from the heliport of interest at any one particular point in time, the separation distance category parameter X (Fig. 1) is based on a merging of two hazard avoidance requirements. The first of these two requirements is related to the structural loading-related hazard type (assuming worst case winds); whereas, the second of the two requirements provides insurance that a safe and reasonable rotor blade clearance is maintained from all structures or other secure objects, particularly for the very small rotorcraft. The separation distance categories Y and Z are respectively based on rounded off analytical results which indicated safe clearance for the untrained and unprotected personnel and door/access panel related hazards (also assuming worst case winds).

The recommended separation requirements for the general heliport/ airport scenario operation, as presented in Fig. 4, are also based on a merging of the requirements for several of the hazard types, as shown in Fig. 105. For the Category I scenario, the recommended safe separation distance is based on the merged requirement to avoid both the door/access panel and the fixed-wing overturning moment hazards (assuming worst case wind conditions). The Category II and Category III scenario requirements (as explained in Fig. 4) at present are recommended to be kept the same quantitatively until further data is available. The requirements are based on a merging of the requirements for avoidance of the three hazard types labeled 3, 7, and 8, as presented in Fig. 105.

SECTION VIII

FUTURE RESEARCH OPPORTUNITIES THAT WOULD ASSIST IN REDUCTION OR IMPROVED JUSTIFICATION OF SAFETY FACTORS WHICH ARE REQUIRED IN THE DEFINITION OF ROTORCRAFT DOWNWASH-RELATED SEPARATION REQUIREMENTS

An extensive review of rotorcraft technical reports was conducted in the effort to develop analytical procedures that would predict the rotorwash hazard potential associated with low-speed rotorcraft flight. This review, which encompassed reports written over the past thirty-five years, resulted in the following important findings:

1. The U.S. military is the only organization that has shown significant long-term interest in V/STOL downwash/rotorwash-related hazards.

2. This interest resulted primarily in research directed toward the quantification of hazards related to jet engine V/STOL aircraft rather than to rotorcraft.

3. The military research assumes, in general, that the personnel who work in and around the hazard zone have knowledge (as the result of special training) of the rotorcraft downwash-related hazards and will therefore avoid most of them with specially developed procedures and protective equipment and clothing. As a result, many research topics that are of interest in civilian rotorcraft operations have not been investigated thoroughly (if investigated at all).

The purpose of this section is to outline several experiments which, if conducted in the future, would aid significantly in the development of more technically justifiable rotorcraft separation requirements.

A. PERSONNEL-RELATED HAZARDS

In the development of rotorcraft separation requirements, the most important hazards to consider are those which directly involve the safety and general welfare of people (secondarily would be the safety and welfare of animals). Unlike buildings and equipment that can be repaired or replaced if damaged, a person (or animal) who sustains serious injury or who

dies as a result of a downwash-related hazard precipitates a situation that may never be fully rectified, even in a court of law. Because of the assumption that personnel who work in potentially dangerous areas receive special hazard environment training, military research into personnel-related hazards focused primarily on quantifying the requirements for and regulating the use of protective gear. This research has, in addition, helped to quantify the parameters that are associated with the prediction of overturning moments on personnel.

Unfortunately, but understandably, military research work has not examined the civilian side of the hazard equation; therefore, little work has been conducted to quantify what is unpleasant, uncomfortable, or dangerous to the untrained and therefore unsuspecting person who is suddenly subjected to a rotorcraft downwash flowfield. No one person or group seems to know what would happen to a person standing in or passing through such a hazard environment while wearing a hat, or with a purse or briefcase in hand, or with a startled child in tow. It is therefore recommended that an experiment be conducted that would provide guidance in this important area. [Recommendation for this same kind of experiment was made in less defined terms in another recent study for the FAA (Ref. 29, p. 83).]

The proposed experiment should be conducted with protected (i.e., goggles for eye protection) but generally untrained personnel who are not familiar with the rotorwash environment in or around rotorcraft. These personnel (preferably both men and women of various body builds) should be attired and equipped in such a way as to be representative of people who would be present in a civilian heliport or airport environment (e.g., suits, hats, briefcases, sport cloths, hand-carried sport bags and equipment, various weights and types of coats and jackets, loose-fitting dresses, skirts of various lengths and fullness, bandbags, small children, diaper bags, etc.). The experiment should then require these people to approach a test rotorcraft from various directions while the rotorcraft is hovering or light on the landing gear in order to determine what could be considered as generally acceptable/unacceptable distances from the rotorcraft. The unacceptable radial distances can then be correlated to the

magnitude and shape of the peak velocity profile generated by the rotorcraft in order to provide a standard by which to evaluate acceptable distances from other rotorcraft (using mainly the developed analytical prediction techniques). This experiment should be conducted using two or three different helicopters and a statistically significant number of subjects (a definition of what constitutes statistical significance would be determined with more study; six to eight people would probably be sufficient).

The experiment outlined above should be quick and inexpensive to conduct, especially since a minimum of instrumentation, preferably that which has been used in several U.S. Navy tests and are available from the Naval Air Test Center (NATC) at Patuxent River, Maryland, would be required. Experimental design, execution of the experiment, and data reduction could be accomplished particularly easily if NATC were involved as a partner to provide the manpower for checking out the instrumentation and stripping out the experimental data for subsequent analysis.

B. AERODYNAMIC RELATED IMPROVEMENTS TO ANALYTICAL PREDICTION TECHNIQUES

As discussed earlier, most of the research uncovered during the literature search has been concerned with the prediction of the jet V/STOL rather than the rotorcraft downwash flowfield. In order to correlate further, and ultimately to better justify the analytical modeling procedures which have been developed under this contract, it would be desirable to conduct two or three special experiments. Each of these should be designed to utilize hardware that is presently available as well as to utilize previously developed data reduction techniques in order to minimize cost and manpower requirements and reduce schedule risks.

The first of the recommended experiments is designed to obtain measurements of the velocity profiles that emanate from a rotorcraft in hover and low-speed flight. This experiment would be an extension to the work already conducted by NATC, and it would use equipment and data reduction techniques that are already available. Only high disc loading rotorcraft

(i.e., the CH-53E and XV-15) have been included in tests conducted by NATC to date, not the more common rotorcraft found in civilian use (i.e., Bell 206 and Sikorsky S-76). The experimental measurement of velocity profile data for these more common types of civilian rotorcraft will aid specifically in better quantification and reduction or justification of safety factors as specified throughout this study.

The goal of the experiment should be to measure the velocity profiles (both mean and peak) for two or three of the smaller rotorcraft at several rotor heights above the ground at maximum gross weight as a function of radial distance from the rotor (i.e., see Table 19, from the CH-53E tests, as an example test plan). Some cases should also be evaluated with and without wind, because consistent data has not been found in the literature for predicting concisely this significant effect, which does not appear to be a simple vectoral velocity addition problem.

If this experiment is conducted at the Patuxent River NAS, the several rotorcraft types that are available at the Naval Test Pilot School, along with the FAA S-76, should be more than adequate for obtaining an excellent data base. The use of locally based aircraft, pilots, and proven equipment should also reduce significantly the funding requirements, especially if the project were to be co-supported in an official manner by the U.S. Navy. The previously described subjective experiment using untrained personnel would ideally be conducted concurrently with this experiment, thereby reducing overall costs still further.

A second experiment that would aid in validating the mathematical models and analytical procedures involves a full-scale (or model) rotor test. The purpose of this test would be to obtain data without contamination by secondary flows (i.e., tail rotor, engine exhausts, etc.) of the time variant or the unsteady portion of the rotorcraft outwash velocity profile (with and without ambient wind). The peak velocity component of this unsteady outwash profile is the component representing the greatest hazard potential. This component has been measured in only a small portion of previous experimental work and only then in the presence of contaminating secondary flows. The uncontaminated data from a full-scale (or model) rotor test would aid significantly in quantifying and

TABLE 19

EXAMPLE EVALUATION MATRIX FOR FLIGHT TEST/MATHEMATICAL MODEL DATA CORRELATION (TAKEN FROM THE CH-53E TEST, REF. 11)

Gross Weight, lb	Disc Loading, PSF	Rotor Height, ft	Distance From Rotor Center (DFRC), ft
56000.0	11.42	37.0	31.6,39.5,49.4,59.3,69.1,79.0,118.5,177.8
56000.0	11.42	77.0	31.6,39.5,49.4,59.3,69.1,79.0,118.5,177.8
56000.0	11.42	117.0	31.6,39.5,49.4,59.3,69.1,79.0,118.5,177.8
70000.0	14.28	37.0	31.6,39.5,49.4,59.3,69.1,79.0,118.5,177.8
70000.0	14.28	77.0	31.6,39.5,49.4,59.3,69.1,79.0,118.5,177.8
70000.0	14.28	117.0	31.6,39.5,49.4,59.3,69.1,79.0,118.5,177.8
45000.0	9.18	37.0	31.6,39.5,49.4,59.3,69.1,79.0,118.5,177.8
45000.0	9.18	77.0	31.6,39.5,49.4,59.3,69.1,79.0,118.5,177.8
45000.0	9.18	117.0	31.6,39.5,49.4,59.3,69.1,79.0,118.5,177.8

NOTE: Data taken included mean as well as peak velocity profile data as measured along the 270-deg azimuth radial (left side of helicopter from pilot's seat) which included contaminating (but worst case) secondary flows from the tail rotor and engine exhausts.

justifying empirical coefficients that are needed in any analytical modeling technique. This data could be obtained as "extra data" in many NASA- or U.S. Army-funded rotor tests using either a hover test stand or possibly one of the very large NASA wind tunnels. If data are obtained in this manner, costs that are associated with the test should result primarily from the purchase of the velocity measurement sensors (or "borrowing" of the NATC sensors) and from the manpower that would be required in data reduction and not from the execution of the full-scale (or model) rotor test.

The third experiment of interest would be an investigation and further quantification of the strength, location, and habits of rotorcraft ground vortices. This experiment would best be conducted as an extension of some very preliminary work being done by Dr. Pat Curtiss and his graduate students at Princeton University using the Princeton long track rotor evaluation facility. Very little data presently exist to quantify the position and strength of this low-speed rotorcraft hazard, yet this hazard has been associated as a probable cause with several accidents in the past.

C. HAZARDOUS OBJECT RELATED IMPROVEMENTS TO ANALYTICAL PREDICTION TECHNIQUES

It was too often stated in Sections VI-F through VI-G that insufficient information existed to fully correlate and verify the results presented. It is quite understandable that no one can affort to damage or destroy rotorcraft, fixed-wing aircraft, or vehicles in order to obtain accident data. However, it is nevertheless important that some data be obtained if safety factors are to be reduced. In order to further the goal of reducing safety factors, a broader literature review, some interviews, and one experiment are recommended to improve the situation.

The execution of a much broader literature review, using extensive use of the NTIS, Defense Department, and other technical information services is suggested in order to try to identify further available references. The literature review conducted for this study utilized search techniques

optimized to locate information in more obvious locations and was not foolproof. A greater effort should also be made to identify more accident data as might be obtainable from sources other than the U.S. Army and Navy. This data is quite useful in providing guidance for the "common sense" analysis of hazards even if the accident data is more qualitative than quantitative in nature. Interviews, if conducted with air traffic controllers from heavily utilized heliports, should aid extensively in providing good "rule of thumb" information on procedures and techniques that avoid hazardous situations of all types. **This type of involvement should also aid significantly in the acceptance of any proposed future requirements.**

The experiment that is proposed is one in which large hazardous objects (i.e., rocks, dirt clods, lunch boxes, barrels, etc.) would be evaluated in rotorwash environments in order to quantify their "destructive nature." These objects could be tethered in some cases to prevent their being blown into the "offending rotorcraft" by accident. The experiment should measure the distances, altitudes, and approach angles from which a helicopter can approach various objects before those objects will become airborne. Through the use of video tapes, it should be possible to measure how far and at what velocities the hazardous objects travel. This experiment should be quite easy and inexpensive to conduct for several different types of rotorcraft.

Experiments are not suggested at this time for the purpose of improving the techniques for prediction of dust clouds. This hazard should only be investigated if heliport criteria are needed for unimproved terrain operations.

SECTION IX

CONCLUSIONS

The analysis conducted in this study has been used to provide the U.S. Department of Transportation with a set of **recommended rotorcraft separation requirements for rotorcraft operation at airports and heliports.** These recommendations have been provided in Section II of this report in a concise format and are intended to be applicable for all weather conditions as well as being practical and consistent with the way that rotorcraft operations are presently carried out. The reasoning used in development of these recommendations has been provided in Section VII.

The mathematical models which were developed in this analysis effort to support the development of recommended rotorcraft separation requirements have been demonstrated to be quite useful in making rotorcraft separation related recommendations. Correlation of the mathematical models has been shown wherever possible in great detail, particularly with respect to the CH-53E and XV-15, in an effort to validate proposed recommendations. In many areas of the analysis, this correlation has been shown to be quite good. Clearly, however, as with all studies, more flight test data would be desirable for correlation, especially with respect to the ground vortex and trailing vortex hazards. Use of these mathematical models in future studies should be conducted with full attention given to the limitations of these mathematical models.

The hazard analysis effort using the above discussed mathematical models was conducted only after a thorough analysis of the available historical statistics on various types of accidents related to rotorcraft separation. These accident types include such things as the effects of rotorwash on personnel, structures, equipment, other rotorcraft, and light fixed-wing aircraft. The analysis conducted subsequently was primarily directed toward avoidance of these known types of accidents, and recommendations for separation distances have been provided in each

analyzed scenario for a wide range of rotorcraft configurations. A detailed listing of these accident types and the resulting analytical results were presented in Section V. Suggested further research which will result in an improvement in the recommended rotorcraft separation requirements are presented in detail in Section VIII. The recommendations for further research and the experimental data requirements are described in detail so that planning and execution of the research can be accomplished with a minimum of resources (both manpower and budget). The integration of results from these experiments into the results presented in this document will provide an improved data base for development of improved rotorcraft separation standards.

REFERENCES

1. Anon., Heliport Design Guide, Department of Transportation, Federal Aviation Administration, Advisory Circular AC 150/5390-1B, August 22, 1977.

2. Contract DTRS-57-85-R-00039, "Study of the Upset Potential of the Rotorcraft Downwash Flow Field in Order to Define Separation Standards for Rotorcraft Operations at Airports and Heliports," January 1985.

3. Glauert, M. B., "The Wall Jet," Journal of Fluid Mechanics, Vol. 1, Part 6, December 1956, pp. 625-643.

4. Hohler, D. J., An Analytical Method of Determining General Downwash Flow Field Parameters for V/STOL Aircraft, AFAPL-TR-66-90, Air Force Aero Propulsion Laboratory, Wright-Patterson AFB, Ohio, November 1966.

5. Migdal, D., W. G. Hill, Jr., R. C. Jenkins, and M. J. Siclari, VTOL In Ground Effect Flows for Closely Spaced Jets, NASA CR 152321, December 1979.

6. Ludwig, G. R., and W. G. Brady, Theoretical and Experimental Studies of Impinging Uniform and Nonuniform Jets, TRECOM Technical Report 64-42, U.S. Army Aviation Material Laboratories, Fort Eustis, Virginia, August 1964.

7. Watts, A., V/STOL Downwash Impingement Study--Velocity Estimate, Canadair Aerodynamic Memorandum MAA-284-001, January 1969, Revised April 1971.

8. George, M. M., A. A. Perlmutter, and L. Butler, Downwash Impingement Design Criteria for VTOL Aircraft, TRECOM Technical Report 64-48, U.S. Army Aviation Material Laboratories, Fort Eustis, Virginia, August 1964.

9. George, M., E. Kisielowski, and D. S. Douglas, Investigation of the Downwash Environment Generated by V/STOL Aircraft Operating in Ground Effect, USAAVLABS Technical Report 68-52, U.S. Army Aviation Material Laboratories, Fort Eustis, Virginia, July 1968.

10. Fradenburgh, E. A., "Flow Field Measurements for a Hovering Rotor Near the Ground," Fifth Annual Western Forum of the American Helicopter Society, Los Angeles, California, September 1958.

11. Harris, D. J., and R. D. Simpson, CH-53E Helicopter Downwash Evaluation. Final Report, Naval Air Test Center Technical Report No. SY-89R-78, August 1, 1978.

12. Harris, D. J., and R. D. Simpson, Technical Evaluation of the Rotor Downwash Flow Field of the XV-15 Tilt Rotor Research Aircraft, Naval Air Test Center Technical Report No. Y-14R-83, July 1983.

13. Harris, D. J., and R. D. Simpson, Downwash Evaluation Under the U.S. Army Heavy Lift Helicopter Rotor. Final Report, Naval Air Test Center Technical Report No. SY-17R-76, March 16, 1976.

14. Anon., VTOL Downwash Impingement Study, Velocity Survey, U.S. Army Transportation Research Command Technical Report No. 60-58, August 1960.

15. Michaelsen, O. E., "A Comparison of Outflows From a Helicopter, Tilt Wing, and Jet Lift Hovering Aircraft," AIAA 8th Annual Meeting and Technical Display, Washington, D.C., AIAA Paper No. 71-992, October 25, 1971.

16. Anon., A Comparison of Downwash and Outflow from a Tilt-Wing Aircraft and a Helicopter, Canadair Report RAG-084-107, February 1971.

17. Curtiss, H. C., Jr., Mao Sun, and E. J. Hanker, "Dynamic Phenomena in Ground Effect," A-83-39-76-0000, Presented at the 39th Annual National Forum of the American Helicopter Society, May 9-11, 1983.

18. Curtiss, H. C., Jr., W. Erdman, and M. Sun, "Ground Effect Aerodynamics," Presented at the International Conference on Rotorcraft Basic Research, Research Triangle Park, North Carolina, February 19-21, 1985.

19. Sun, M., "A Study of Helicopter Rotor Aerodynamics in Ground Effect," Ph.D. Thesis, Princeton University Mechanical and Aerodynamics Engineering Department, June 1983.

20. Harris, D. J., and R. D. Simpson, Tilt-Wing Vertical and Short Takeoff and Landing Downwash Evaluation. Final Report, Naval Air Test Center Technical Report No. SY-52R-76, April 9, 1976.

21. Patton, W. F., and R. D. Simpson, Investigation of SH-3/HH-3 Helicopter Downwash Environment, Naval Air Test Center Report ST-197R-71, September 24, 1971.

22. Leese, G. W., and J. T. Knight, Jr., Helicopter Downwash Data, Miscellaneous Paper S-74-17, U.S. Army Engineer Waterways Experiment Station, Vicksburg, Mississippi, June 1974.

23. O'Bryan, Thomas C., An Investigation of the Effect of Downwash from a VTOL Aircraft and a Helicopter in the Ground Environment, NASA TN D-977, October 1961.

24. Shane, W. P., Effects of Downwash Upon Man, U.S. Army Aeromedical Research Unit Report No. 68-3, November 1967.

25. Leese, G. W., Helicopter Downwash Blast Effects Study, U.S. Army Engineer Waterways Experiment Station TR-3-664, Vicksburg, Miss., October 1964.

26. Burnham, David C., and Stephen A. Teager, Preliminary Measurements of Helicopter Wake-Vortex Velocity Profiles, Unpublished DOT-TSC memorandum, March 1985.

27. Hoerner, S. F., Fluid-Dynamic Drag, Published by Author, 1958.

28. Anon., Anthropometry of U.S. Military Personnel, Military Handbook DOD-HDBK-743, October 3, 1980.

29. Schwartz, C. W., M. W. Witczak, and R. B. Leahy, Structural Design Guidelines for Heliports, DOT/FAA/PM-84/23, October 1984.

30. Jenkins, B. Z., and A. S. Marks, Rotor Downwash Velocities About the UH-1H Helicopter-Flight Test Measurements and Theoretical Calculations, Army Missile Research Development and Engineering Laboratory, Redstone Arsenal, Alabama, January 1975.

31. Leese, Grady W., UH-1H Downwash Velocity Measurements, Army Engineer Waterways Experiment Station, Vicksburg, Mississippi, August 1972.

32. Skujins, Ojars, An Experimental Investigation of Rotor Forces and Flow Field in the Vicinity of a Step Ground Plane, West Virginia University, Department of Aerospace Engineering, July 1970.

33. Anon., Operators Manual. Army OH-58C Helicopter, Headquarters, Department of the Army, Technical Manual TM 55-1520-235-10, April 7, 1978.

34. Anon., Operators Manual. Army Models. UH-1D/H and EH-1H Helicopters, Headquarters, Department of the Army, Operator's Manual TM-55-1520-210-10, May 18, 1979.

35. Anon., Operators Manual. Army AH-1S (Prod) Helicopter, Headquarters, Department of the Army, Technical Manual TM 55-1520-236-10, April 29, 1977.

36. Anon., Operators Manual. Army Model CH-47C Helicopter, Headquarters, Department of the Army, Technical Manual TM 55-1520-227-10-2, August 23, 1978.

37. Traasdahl, E. C., and S. A. Ruffa, CH-46E/LHA Engage/Disengage Dynamic Interface Test, Naval Air Test Center Report No. RW-58R-84, January 30, 1985.

38. Hurley, G. E., C. W. Pitman, and L. L. Trick, HH-46A/CV-64 Rotor Engage/Disengage Test, Naval Air Test Center Report No. RW-55R-84, October 30, 1984.

39. O'Bryan, T. C., An Experimental Study of the Effect of Downwash From a Twin Propeller VTOL Aircraft on Several Types of Ground Surfaces, NASA TN D-1239, May 1962.

40. Rogers, S. J., Evaluation of the Dust Cloud Generated by Helicopter Rotor Downwash, USAAVLABS TR-67-81, March 1968.

41. Dyke, R. W., An Investigation of the Over the Water Aspects of VTOL Airplanes at High Disc Loading, Curtis-Wright Corporation, VTOL Systems Group, Report No. 012-26, December 1963.

42. Anon., Unpublished data obtained from the XV-15 project office, NASA Ames Research Center, 1985.

TABLE A-1. ROTORCRAFT DATA SUMMARY

Rotorcraft Manufacturer/ Type	Maximum Gross Weight, lb	Main Rotor Radius, ft	Estimated Fuselage Download, PCT	Disk Loading, PSF	Number of Rotors/Blades Per Rotor	Rotor Tip Speed, fps	Rotor Height Above Ground ft	Twin Rotor Separation, ft
Agusta								
A109	5730	18.05	1.5	5.60	1/4	727	10.0	--
Aerospatiale								
SA341G	3970	17.25	1.5	4.24	1/3	683	8.9	--
AS350	4299	17.55	2.0	4.44	1/3	698	10.3	--
AS355	5291	17.55	2.0	5.47	1/3		10.7	--
SA315B	5070	18.05	1.5	4.95	1/3		10.1	--
SA319B	4960	18.05	1.5	4.84	1/3		9.8	--
SA360	6615	18.85	2.0	5.92	1/4	690	11.5	--
SA365N	8900	19.55	2.0	7.41	1/4	715	11.4	--
SA330	16315	24.75	5.0	8.48	1/4	687	14.4	--
SA332	19840	25.60	5.0	9.64	1/4	711	15.0	--
SA321	28660	31.00	5.0	9.49	1/6	688	16.3	--
Bell								
47	2850	18.50	1.0	2.65	1/2	645-716	9.5	--
206	3200	16.65	1.5	3.67	1/2	688	9.5	--
OH-58A	3200	17.65	1.5	3.26	1/2	654	9.5	--
OH-58D	4300	17.5	1.5	4.47	1/4	724	8.5	--
206L	4150	18.5	1.5	3.86	1/2	763	10.1	--
222B	8250	21.0	4.0	5.95	1/2	765	10.8	--
204	8500	22.0	2.0	5.59	1/2	746		--

TABLE A-1 (CONTINUED)

Rotorcraft Manufacturer/ Type	Maximum Gross Weight, lb	Main Rotor Radius, ft	Estimated Fuselage Download, PCT	Disk Loading, PSF	Number of Rotors/Blades Per Rotor	Rotor Tip Speed, fps	Rotor Height Above Ground ft	Twin Rotor Separation, ft
Bell (Concluded)								
UH-1M	9500	22.0	2.0	6.25	1/2	746		--
205	9500	24.0	2.0	5.25	1/2	814	11.8	--
212	11200	24.0	2.0	6.19	1/2	814	13.4	--
412	11900	23.0	2.0	7.16	1/4	780	12.8	--
214B	13800	25.0	2.0	7.03	1/2	785	14.0	--
214ST	17500	26.0	2.0	8.24	1/2	781	14.2	--
AH-1S	10000	22.0	2.0	6.58	1/2	746	12.3	--
AH-1T	14750	24.0	2.0	8.15	1/2	781		--
XV-15	13200	12.5	13.0	13.44	2/3	771	12.5	32.2
Bell/Boeing								
V-22	40000	19.0	10.0	17.63	2/3	790	20.1	46.5
Boeing/Vertol								
CH-46E	24300	25.5	7.0	5.95	2/3	705	16.6	33.3
CH-47C	46000	30.0	8.0	8.13	2/3	723	18.6	39.2
CH-47D	54000	30.0	8.0	9.55	2/3	707	18.6	39.2
Enstrom								
F28F	2600	16.0	1.5	3.23	1/3		9.1	--

TABLE A-1 (CONTINUED)

Rotorcraft Manufacturer/ Type	Maximum Gross Weight, lb	Main Rotor Radius, ft	Estimated Fuselage Download, PCT	Disk Loading, PSF	Number of Rotors/Blades Per Rotor	Rotor Tip Speed, fps	Rotor Height Above Ground ft	Twin Rotor Separation, ft
Hiller								
UH-12	2800	17.7	1.0	2.84	1/2		10.1	--
FH-1100	2750	17.7	1.5	2.79	1/2		10.2	--
Hughes								
300	2050	13.4	1.0	3.63	1/3	662	8.8	--
500D	3000	13.2	1.5	5.48	1/4	665	8.5	--
500E	3000	13.2	1.5	5.48	1/5	680	8.7	--
500F	3100	13.7	1.5	5.26	1/5		8.6	--
AH-64	14694	24.0	2.0	8.12	1/4	726	12.6	--
Kaman								
SH-2	12800	22.0	2.0	8.42	1/4	687	13.6	--
MBB								
BK105	5512	16.11	1.5	6.81	1/4	715	9.7	--
BK117	6834	18.05	2.0	6.68	1/4	725	11.0	--
Robinson								
R22	1370	12.6	1.0	2.75	1/2	699	8.8	--

TABLE A-1 (CONCLUDED)

Rotorcraft Manufacturer/ Type	Maximum Gross Weight, lb	Main Rotor Radius, ft	Estimated Fuselage Download, PCT	Disk Loading, PSF	Number of Rotors/Blades Per Rotor	Rotor Tip Speed, fps	Rotor Height Above Ground ft	Twin Rotor Separation, ft
Sikorsky								
S-62	7900	26.5	5.0	3.58	1/3			--
S-76	10300	22.0	3.0	6.77	1/4	675	10.0	--
S-76-PT6	11400	22.0	3.0	7.49	1/4	675	10.0	--
UH-60	20250	26.85	3.0	8.94	1/4	725	12.3	--
HH-60D	22000	26.85	3.0	9.71	1/4	725	12.3	--
S-61	20500	31.0	5.0	6.79	1/5		17.0	--
SH-3	20500	31.0	5.0	6.79	1/5	660	15.5	--
CH-3E	22500	31.0	5.0	7.45	1/5		16.2	--
CH-54A	42000	36.1	5.0	10.23	1/6		18.6	--
S-64E	42000	36.1	5.0	10.23	1/6		18.6	--
CH-54B	47000	36.1	5.0	11.54	1/6	700	17.6	--
CH-53D	36400	36.1	5.0	8.89	1/6	700	17.0	--
HH-53	38275	36.1	5.0	9.35	1/6		17.0	--
RH-53D	41126	36.1	5.0	10.04	1/6		17.0	--
CH-53E	70000	39.5	5.0	14.28	1/7	733	17.0	--
Westland								
Lynx	10500	21.0	2.0	7.58	1/4		9.8	--
Lynx(3)	12000	21.0	2.0	8.66	1/4		10.0	--
W-30-200	12800	21.8	2.0	8.57	1/4	745	12.5	--
W-30-300	15500	21.8	2.0	10.38	1/4			--
EH-101	31500	30.5	5.0	10.78	1/5		21.3	--

APPENDIX B

CORRELATION OF CH-53E FLIGHT TEST DATA WITH OUTPUT FROM THE ROTHAZ ANALYSIS PROGRAM

The following nine figures present correlation of CH-53E flight test data (Ref. B-1) with output from the **ROTHAZ Analysis Program** (Appendices C and D). Discussion on this correlation effort is presented in Section IV of the main report. The content of the figures is summarized in Table B-1.

TABLE B-1. EVALUATION MATRIX FOR CH-53E FLIGHT TEST/MATHEMATICAL MODEL DATA CORRELATION

Figure Number	Gross Weight, lb	Disc Loading, PSF	Rotor Height, ft	Distance From Rotor Center (DFRC), ft
B1	70000.0	14.28	37.0	31.6,39.5,49.4,59.3,69.1,79.0,118.5,177.8
B2	70000.0	14.28	77.0	31.6,39.5,49.4,59.3,69.1,79.0,118.5,177.8
B3	70000.0	14.28	117.0	31.6,39.5,49.4,59.3,69.1,79.0,118.5,177.8
B4	56000.0	11.42	37.0	31.6,39.5,49.4,59.3,69.1,79.0,118.5,177.8
B5	56000.0	11.42	77.0	31.6,39.5,49.4,59.3,69.1,79.0,118.5,177.8
B6	56000.0	11.42	117.0	31.6,39.5,49.4,59.3,69.1,79.0,118.5,177.8
B7	45000.0	9.18	37.0	31.6,39.5,49.4,59.3,69.1,79.0,118.5,177.8
B8	45000.0	9.18	77.0	31.6,39.5,49.4,59.3,69.1,79.0,118.5,177.8
B9	45000.0	9.18	117.0	31.6,39.5,49.4,59.3,69.1,79.0,118.5,177.8

NOTE: All data comparisons are for mean velocity profile data measured/computed along the 270-deg azimuth radial (left side of helicopter from pilot's seat)

REFERENCE

B-1 Harris, D. J., and R. D. Simpson, CH-53E Helicopter Fownwash Evaluation, Naval Air Test Center TR No. SY-89R-78, August 1, 1978.

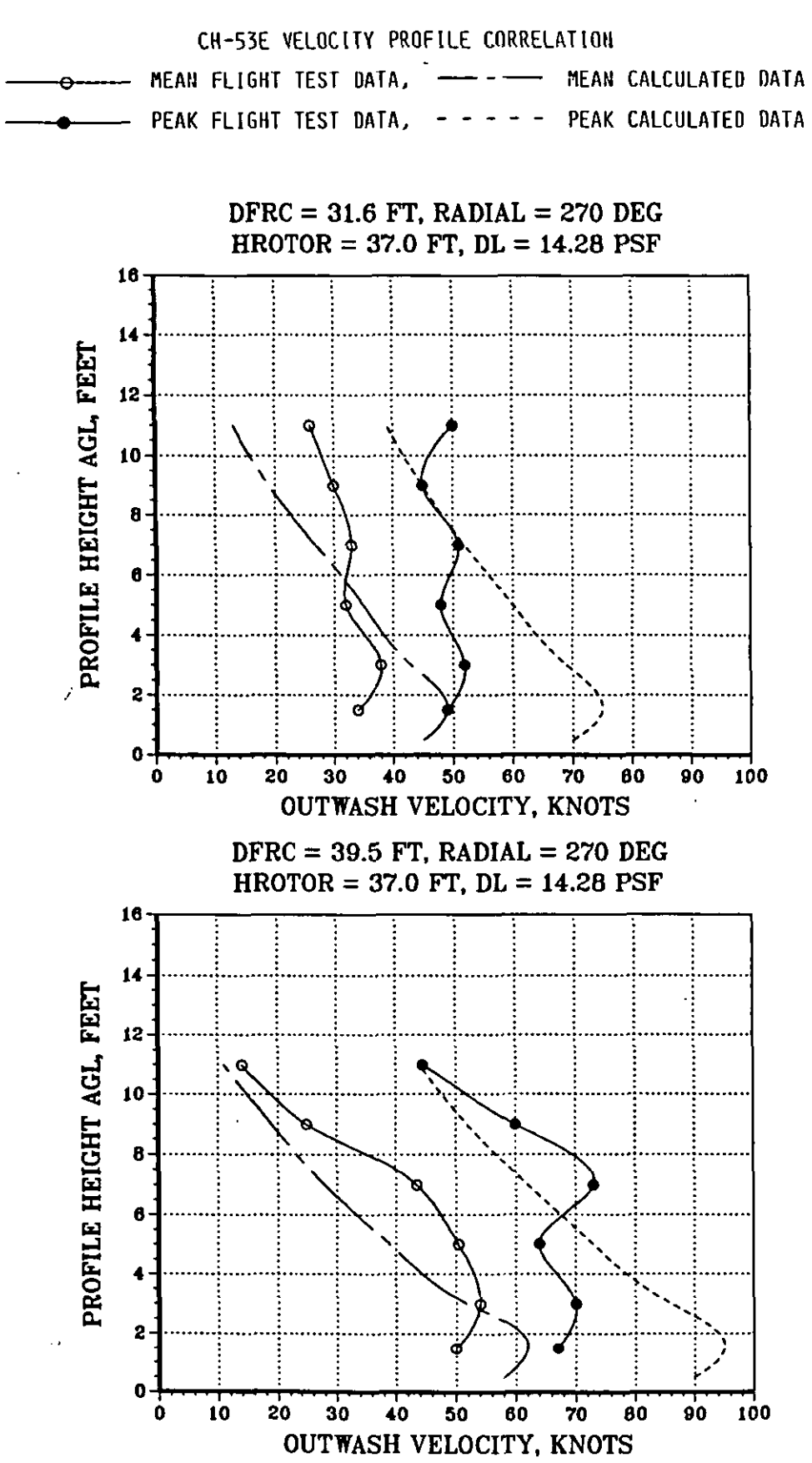

Figure B-1. CH-53E Mean and Peak Velocity Profile Correlation for Eight 270-deg Azimuth Radial Stations at a Rotor Height of 37 ft and a Gross Weight of 70000 lbs

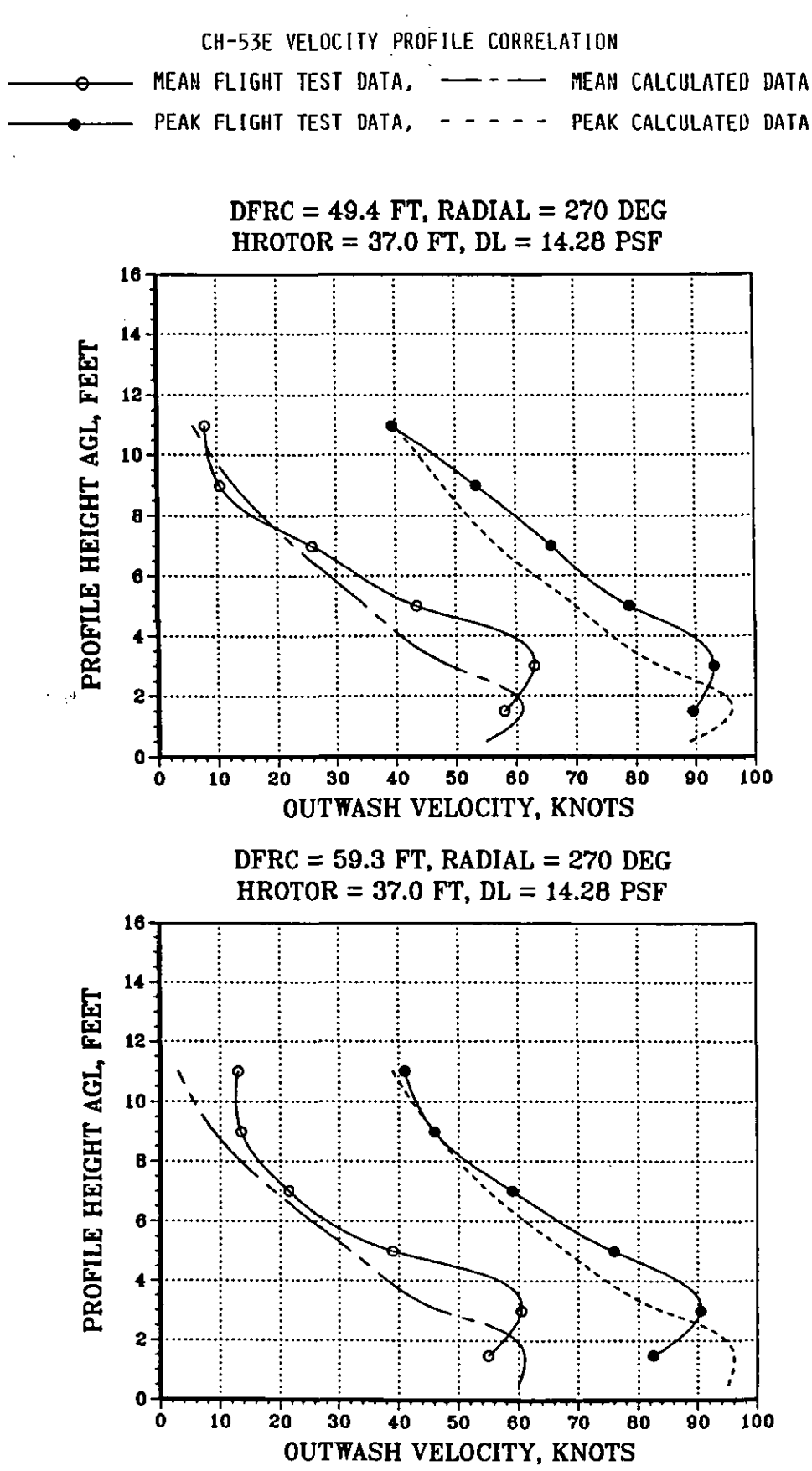

Figure B-1 (Continued)

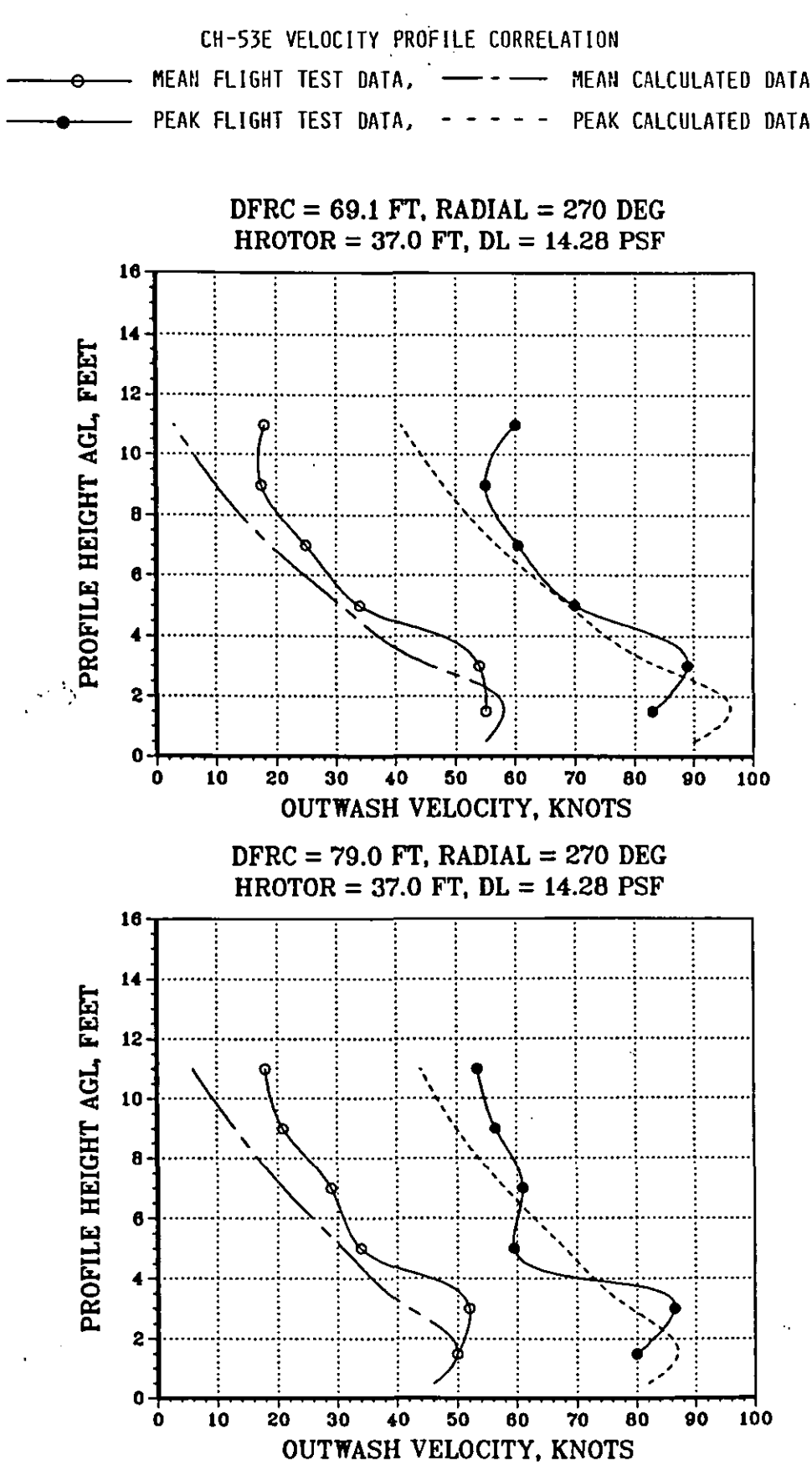

Figure B-1 (Continued)

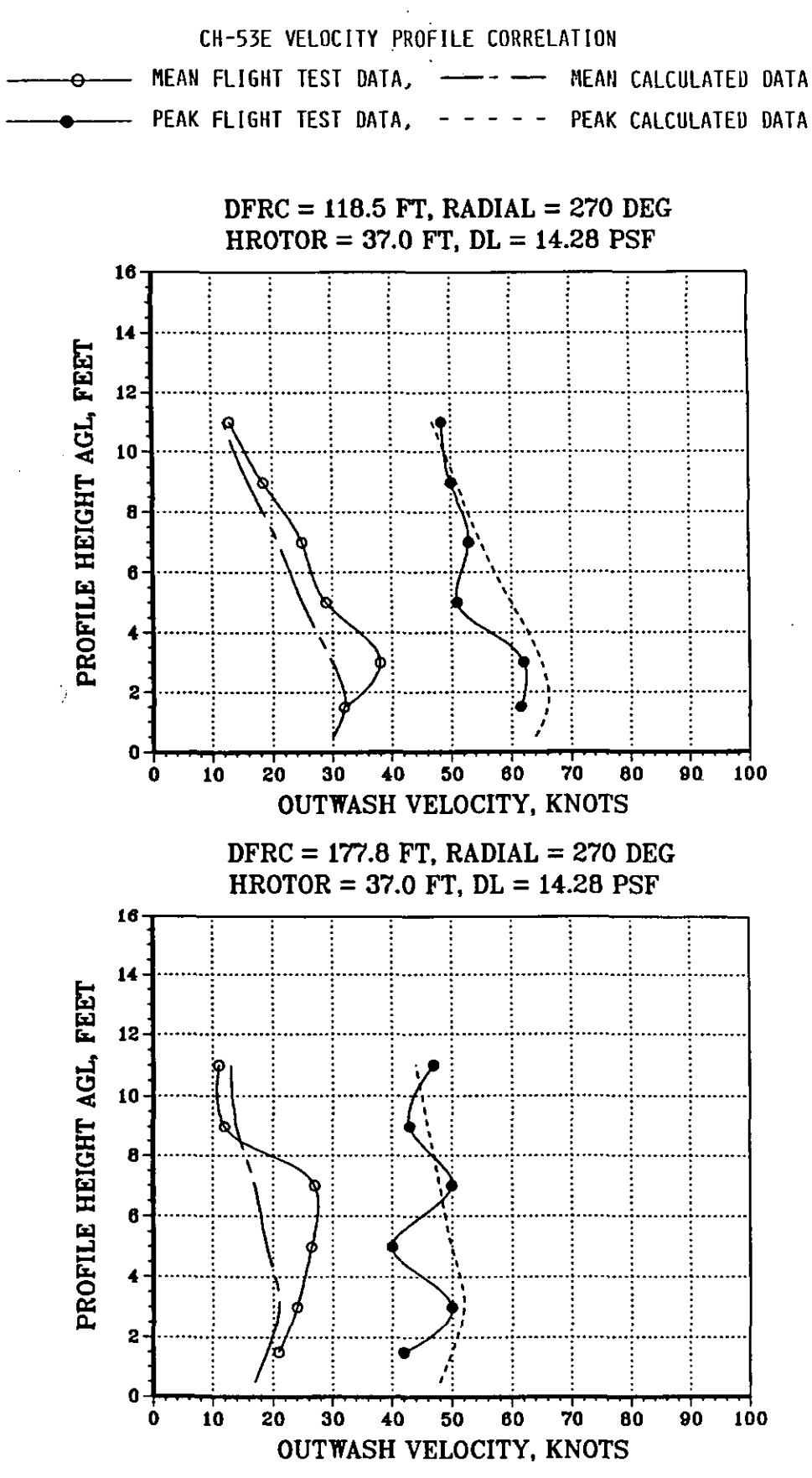

Figure B-1 (Concluded)

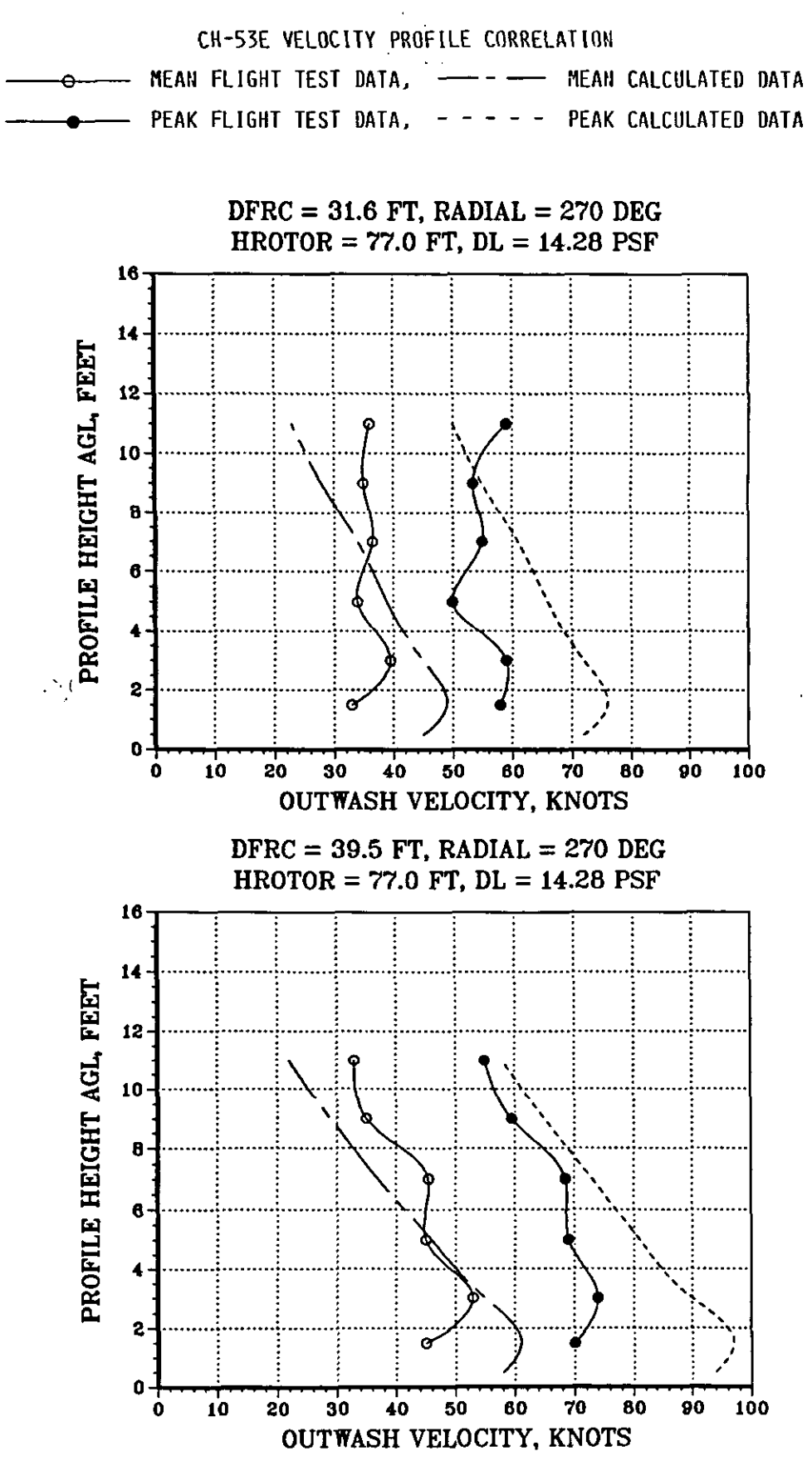

Figure B-2. CH-53E Mean and Peak Velocity Profile Correlation for Eight 270-deg Azimuth Radial Stations at a Rotor Height of 77 ft and a Gross Weight of 70000 lbs

CH-53E VELOCITY PROFILE CORRELATION

—o— MEAN FLIGHT TEST DATA, —— - —— MEAN CALCULATED DATA

—●— PEAK FLIGHT TEST DATA, - - - - - PEAK CALCULATED DATA

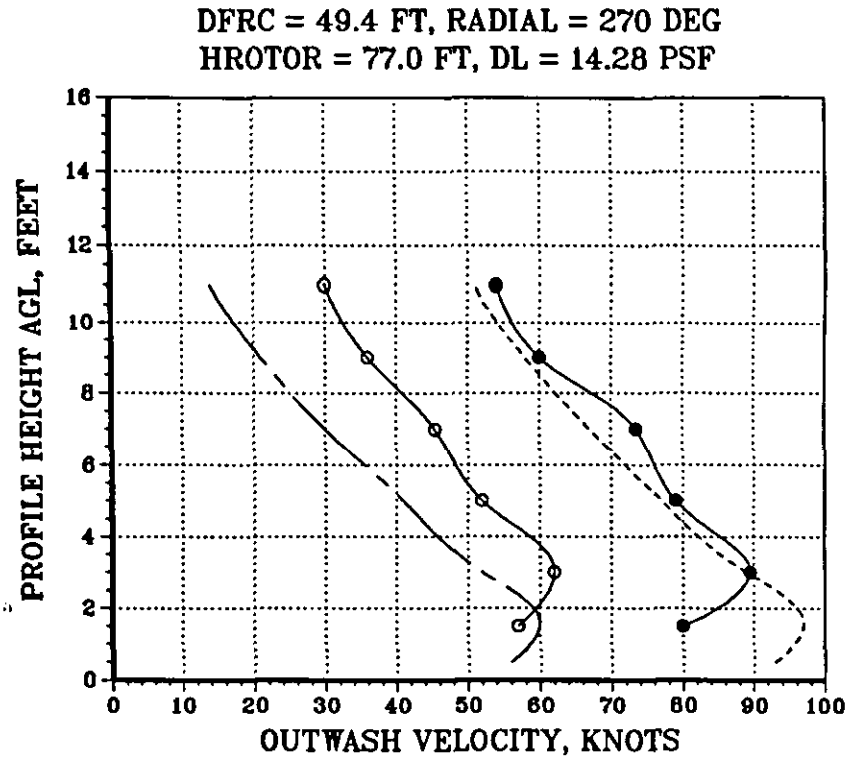

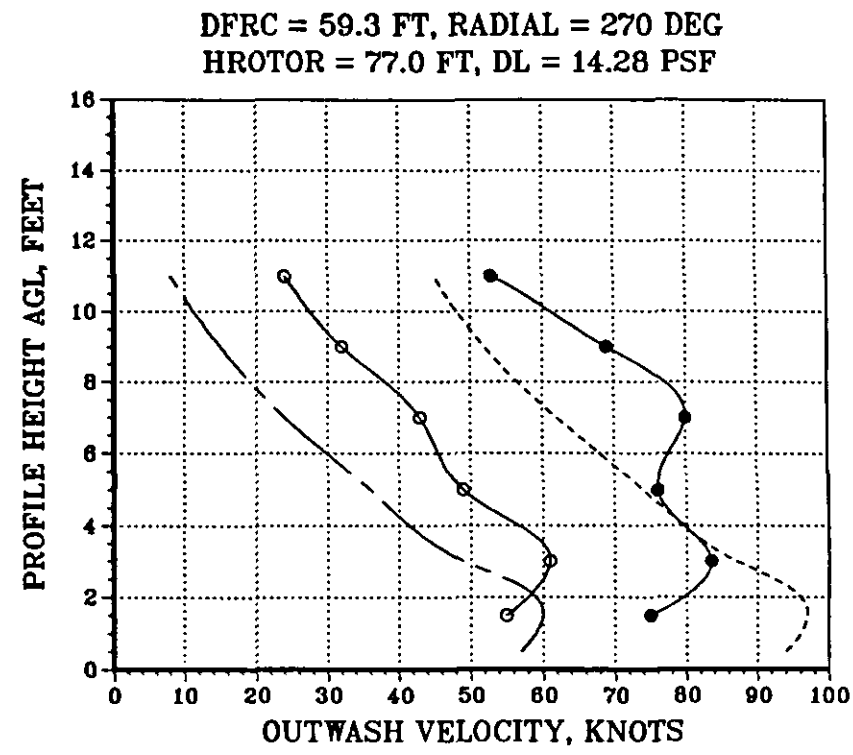

Figure B-2 (Continued)

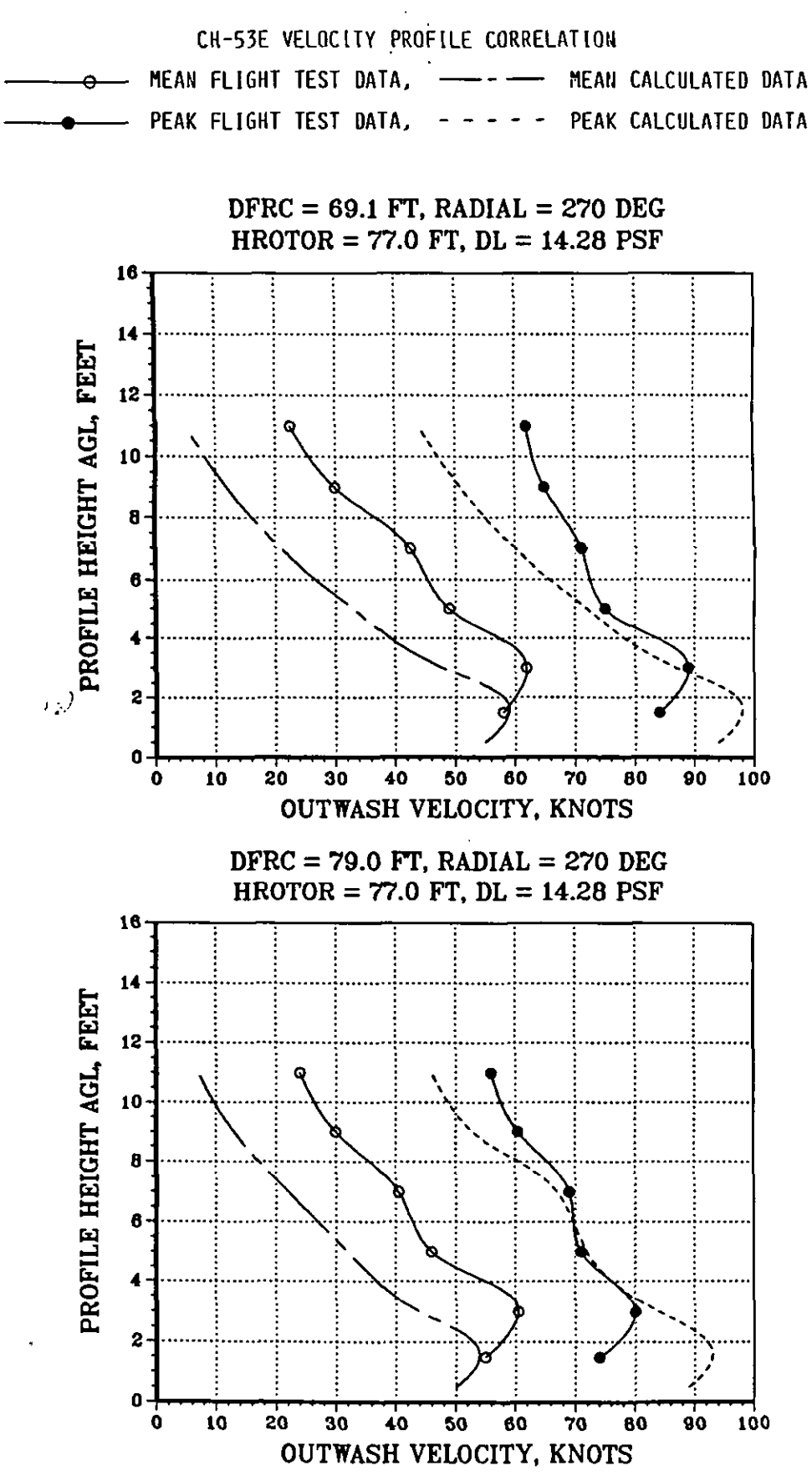

Figure B-2 (Continued)

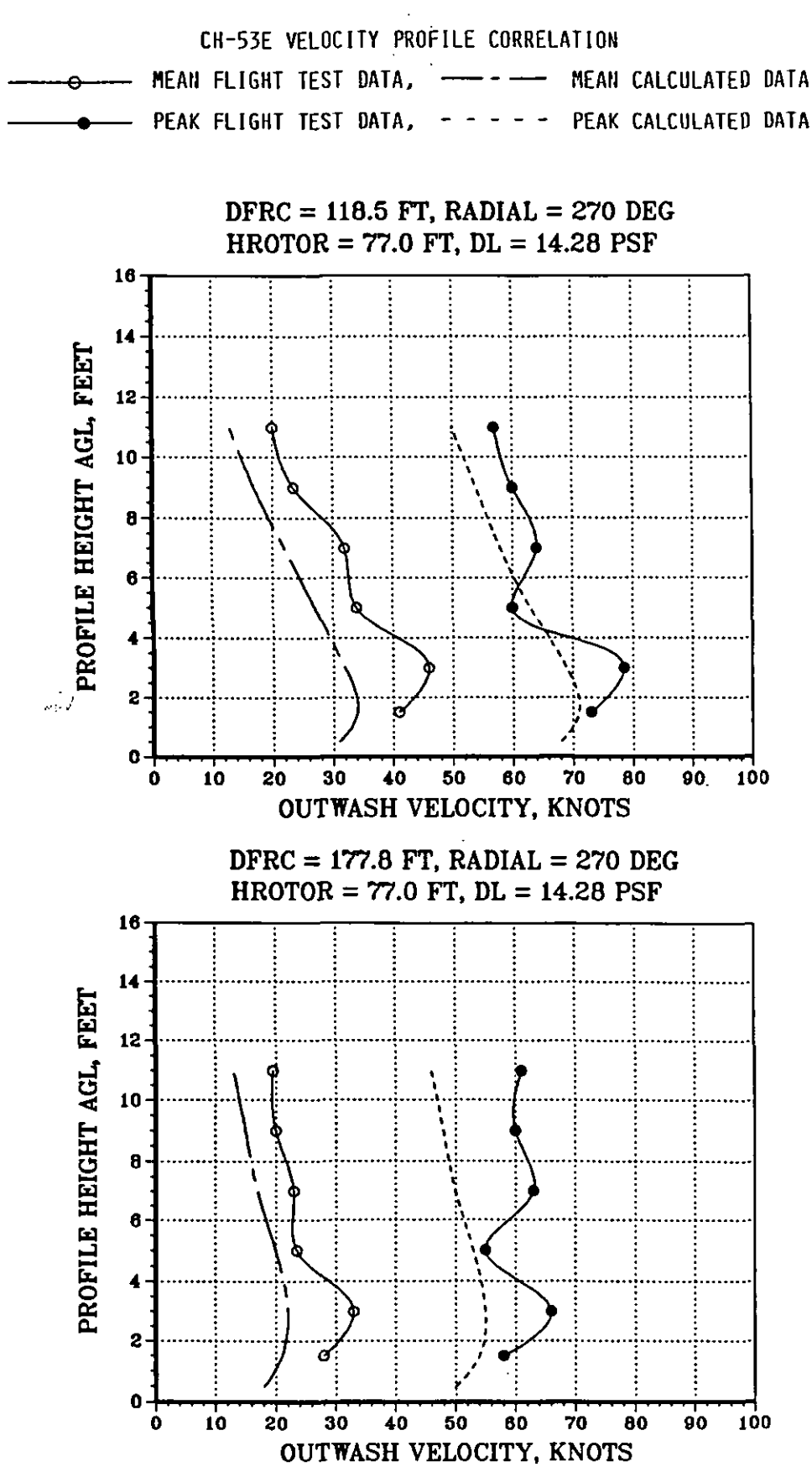

Figure B-2 (Concluded)

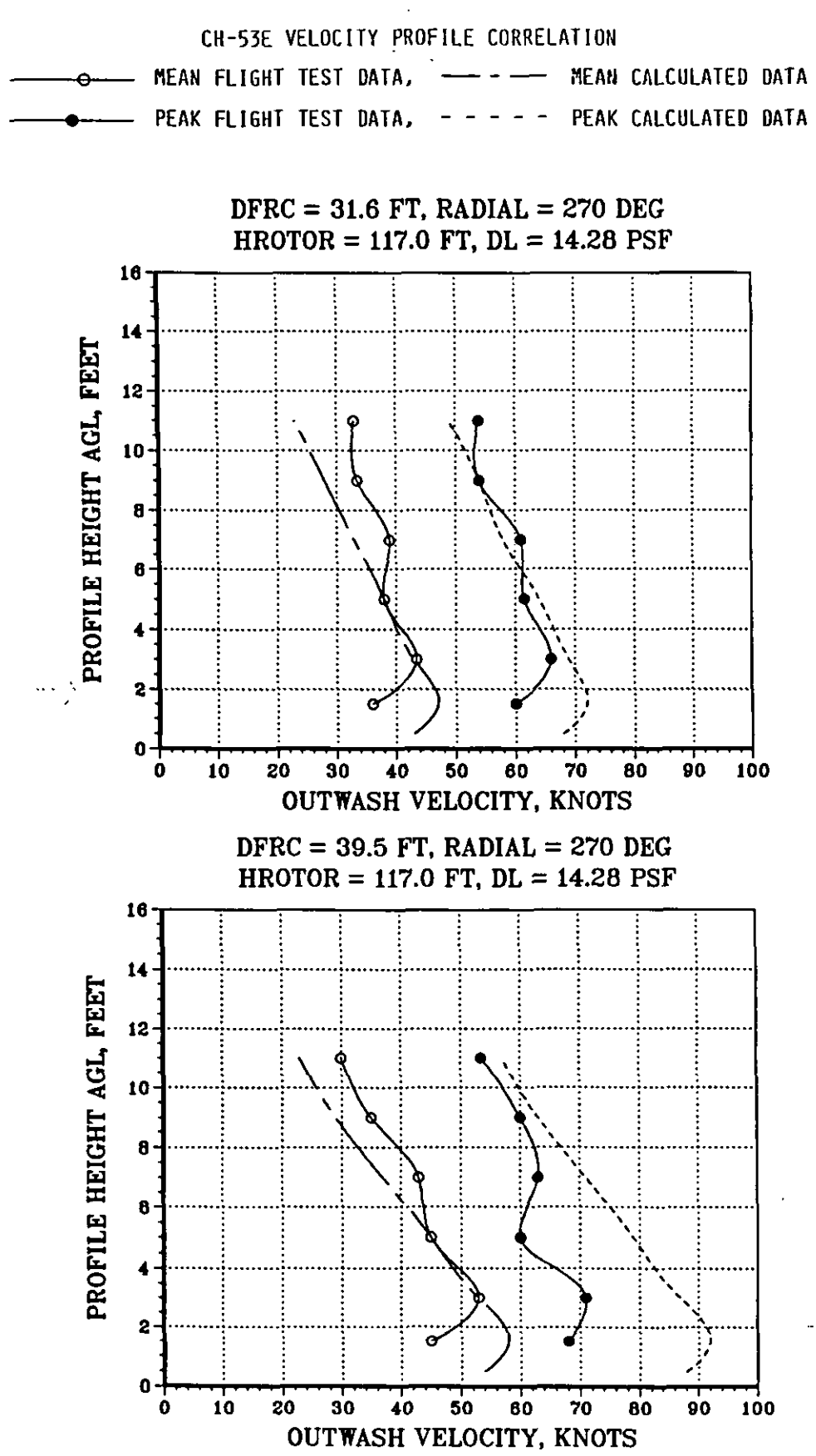

Figure B-3. CH-53E Mean and Peak Velocity Profile Correlation for Eight 270-deg Azimuth Radial Stations at a Rotor Height of 117 ft and a Gross Weight of 70000 lbs

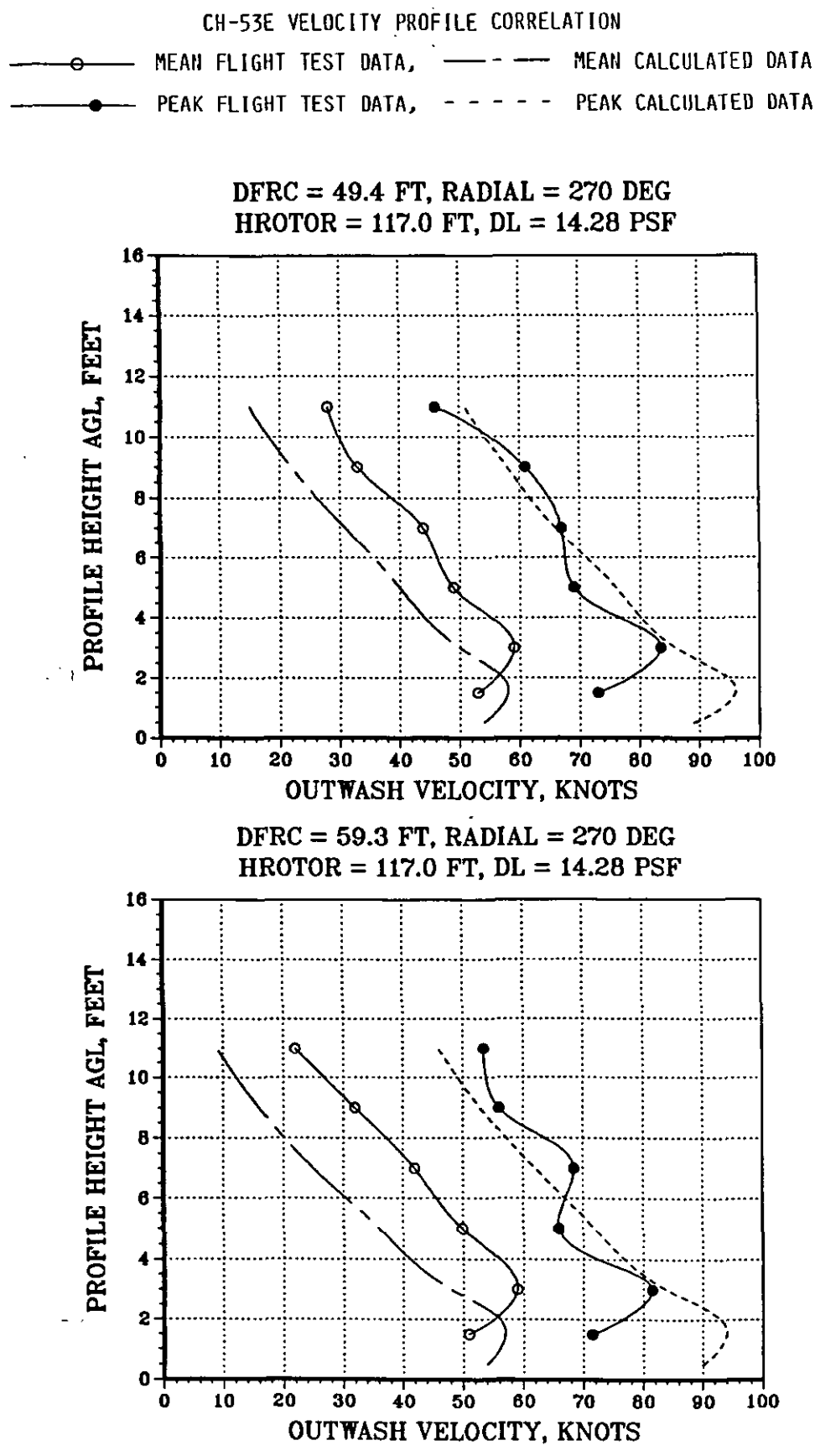

Figure B-3 (Continued)

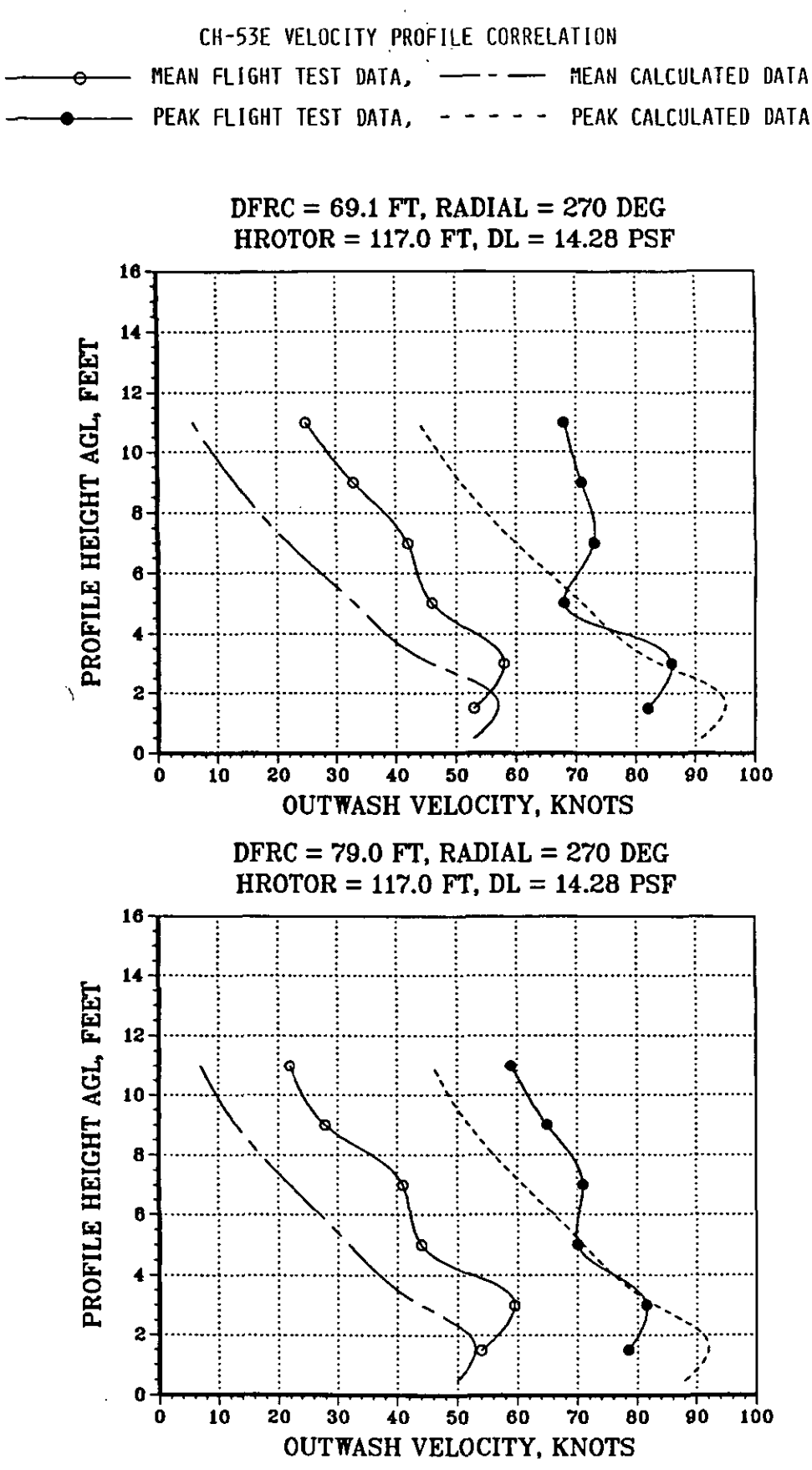

Figure B-3 (Continued)

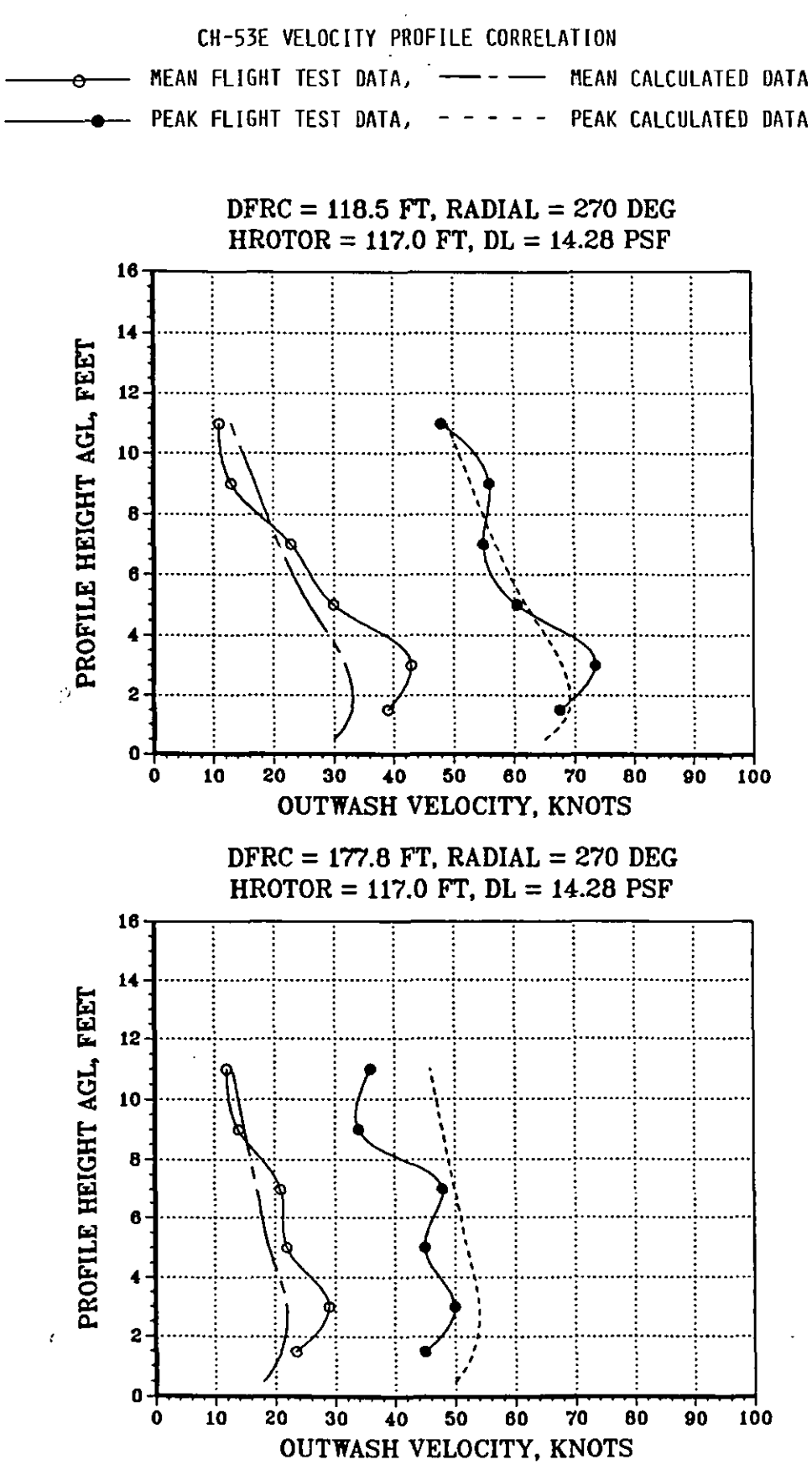

Figure B-3 (Concluded)

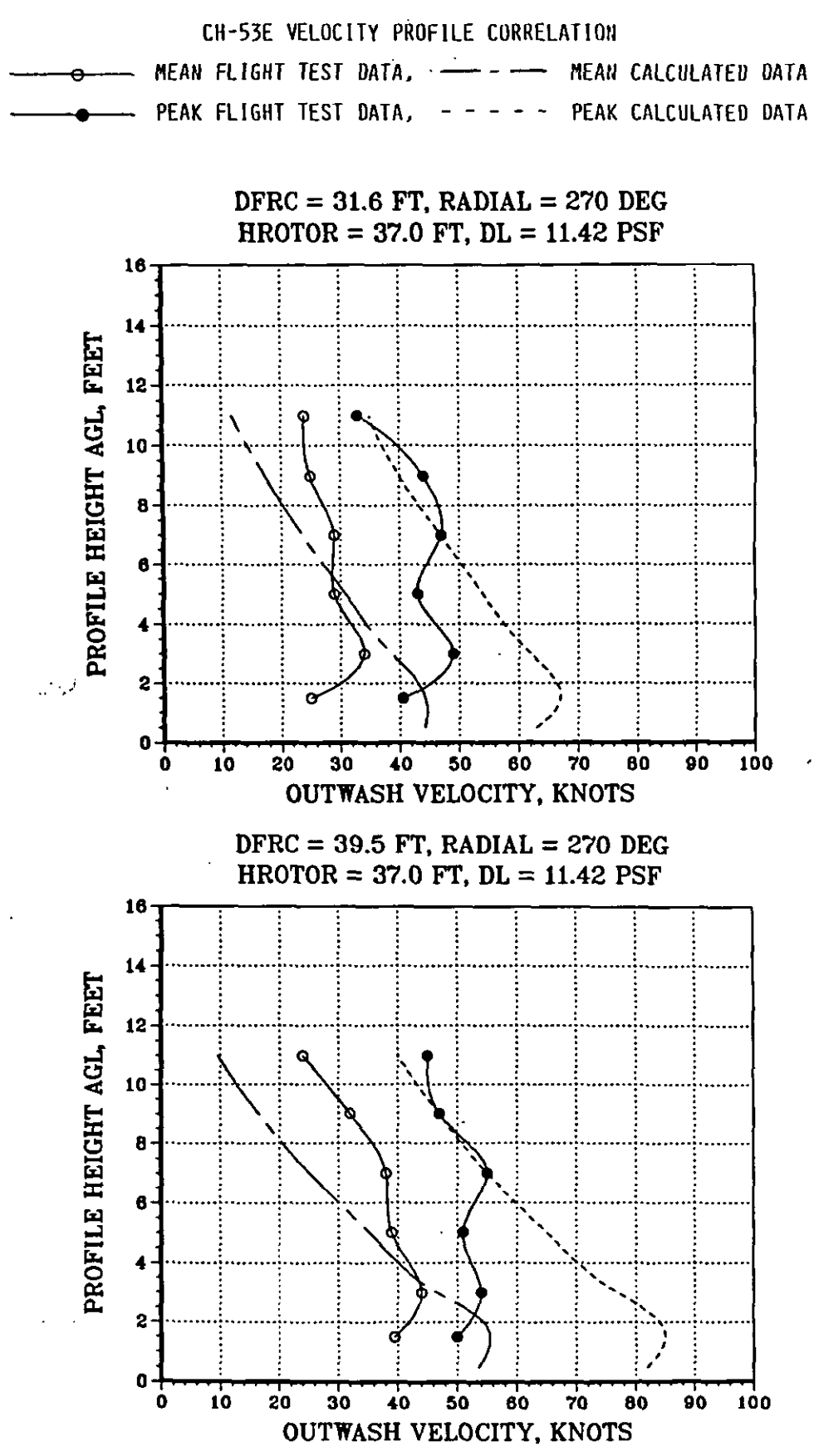

Figure B-4. CH-53E Mean and Peak Velocity Profile Correlation for Eight 270-deg Azimuth Radial Stations at a Rotor Height of 37 ft and a Gross Weight of 56000 lbs

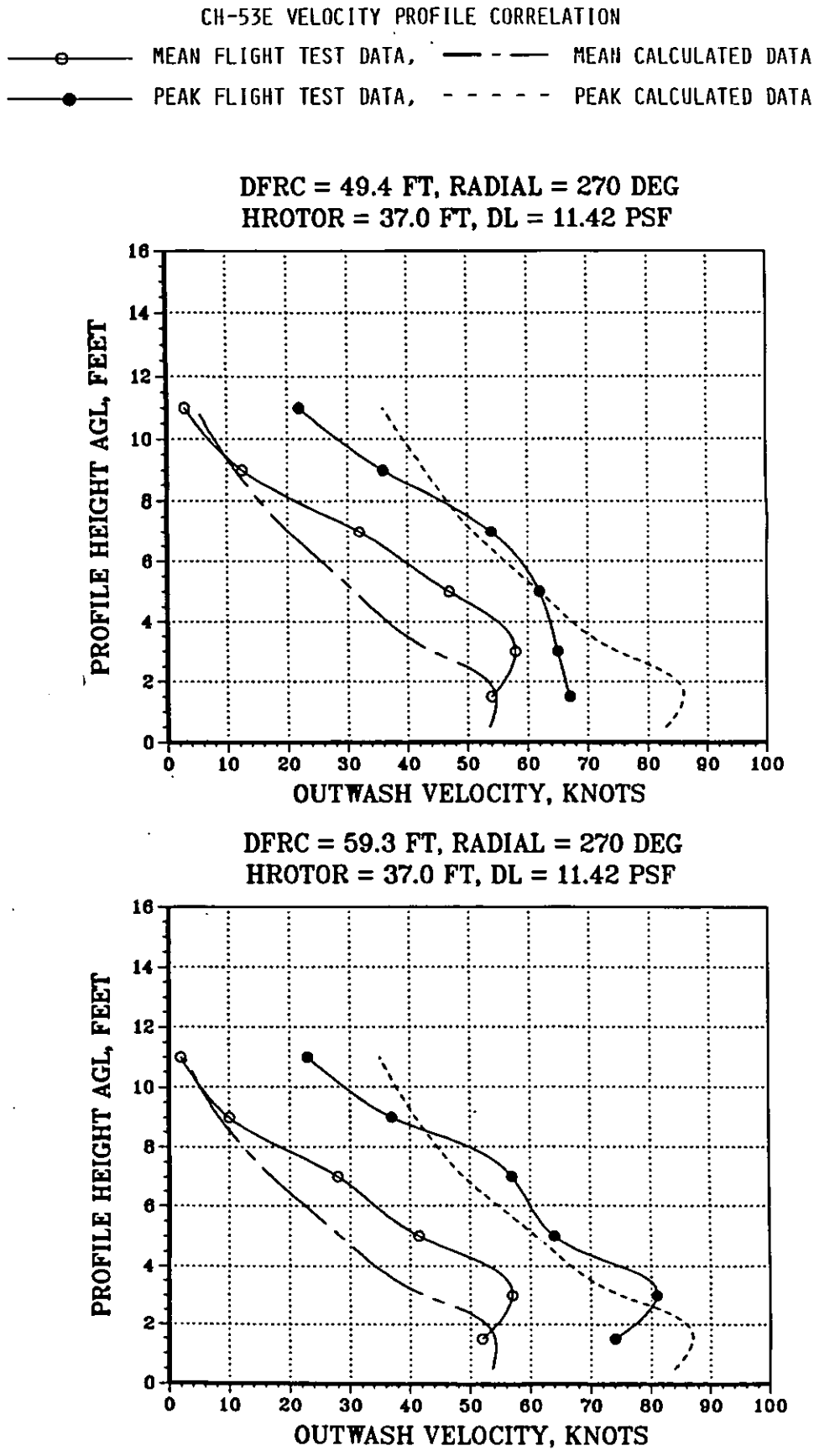

Figure B-4 (Continued)

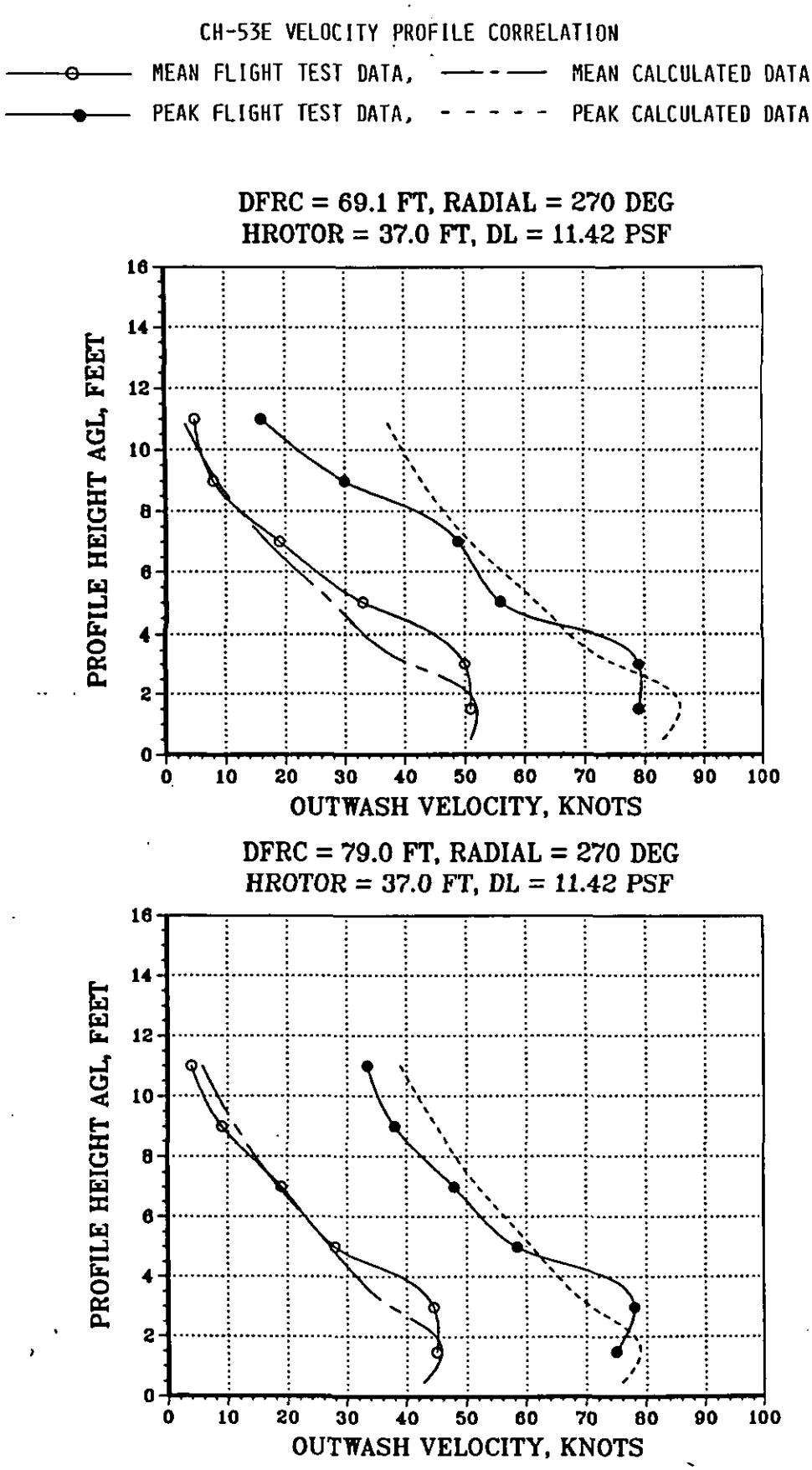

Figure B-4 (Continued)

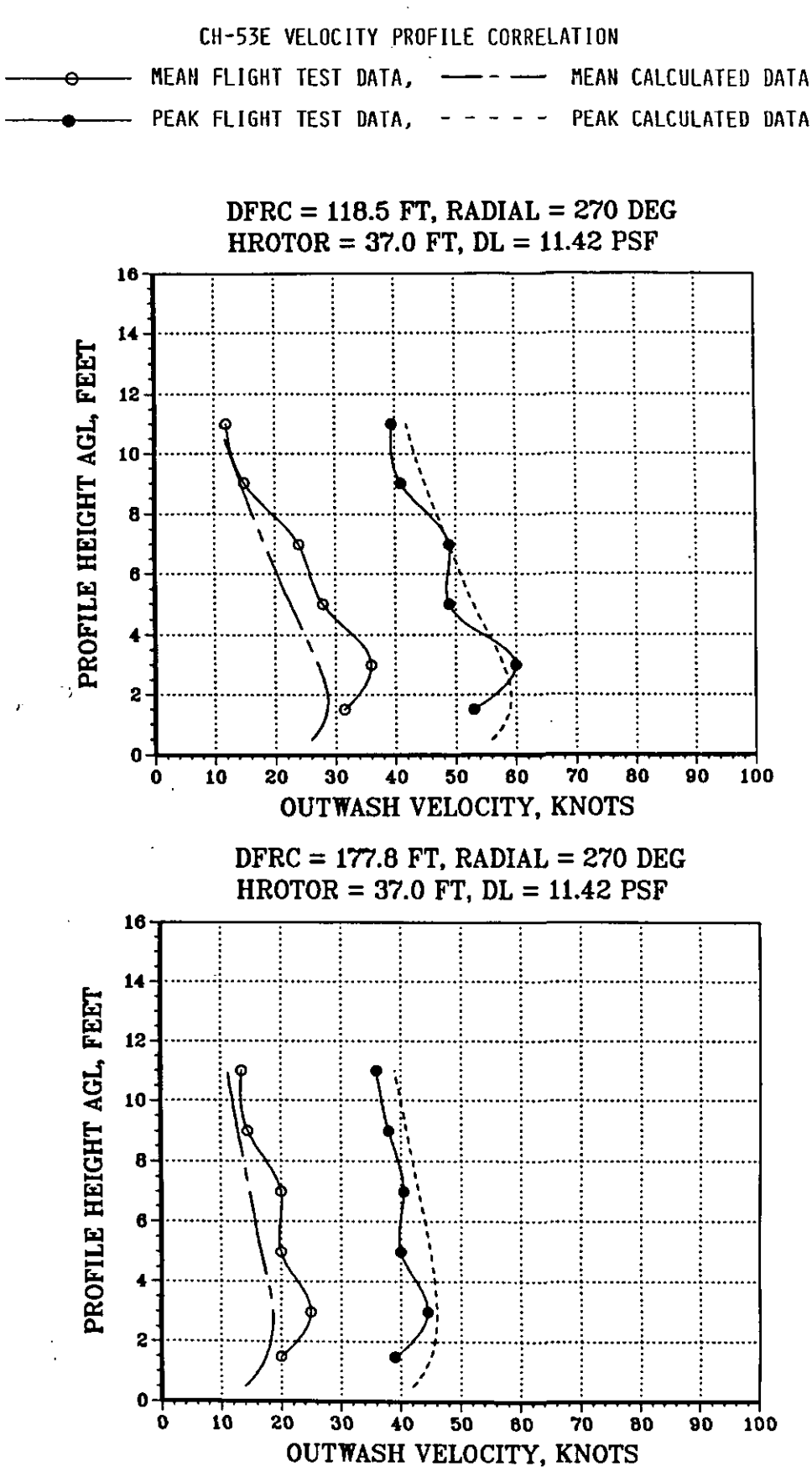

Figure B-4 (Concluded)

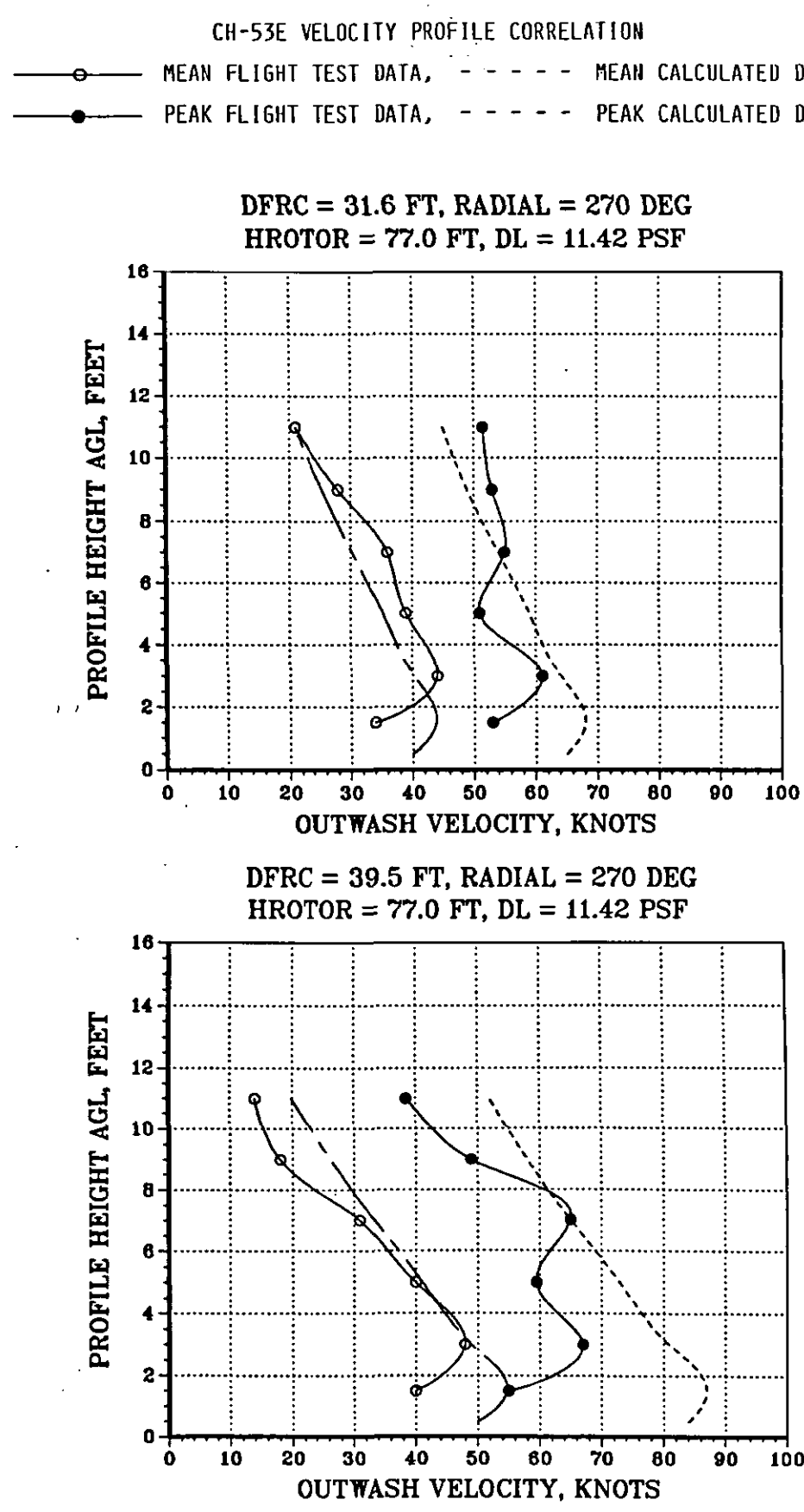

Figure B-5. CH-53E Mean and Peak Velocity Profile Correlation for Eight 270-deg Azimuth Radial Stations at a Rotor Height of 77 ft and a Gross Weight of 56000 lbs

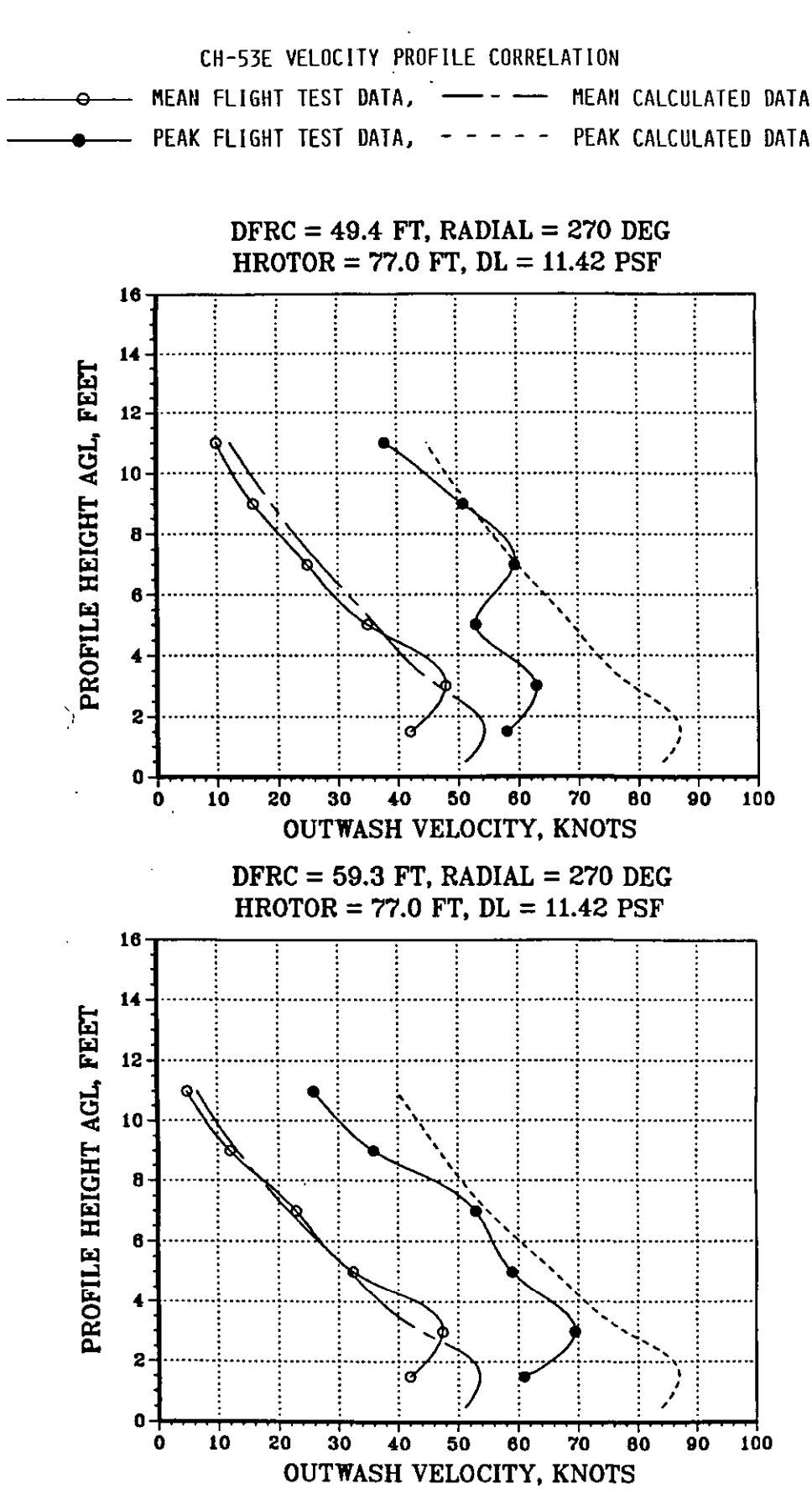

Figure B-5 (Continued)

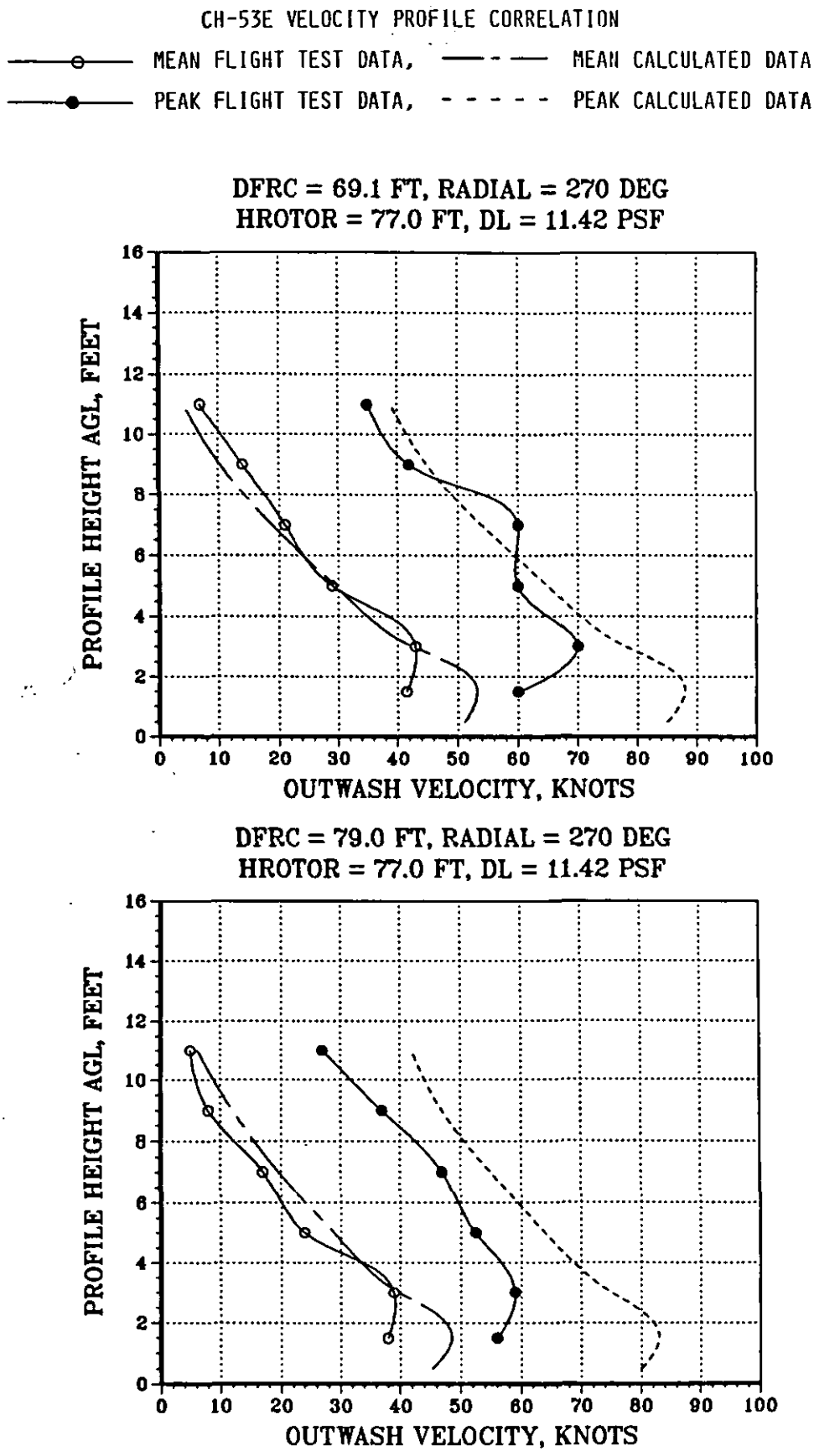

Figure B-5 (Continued)

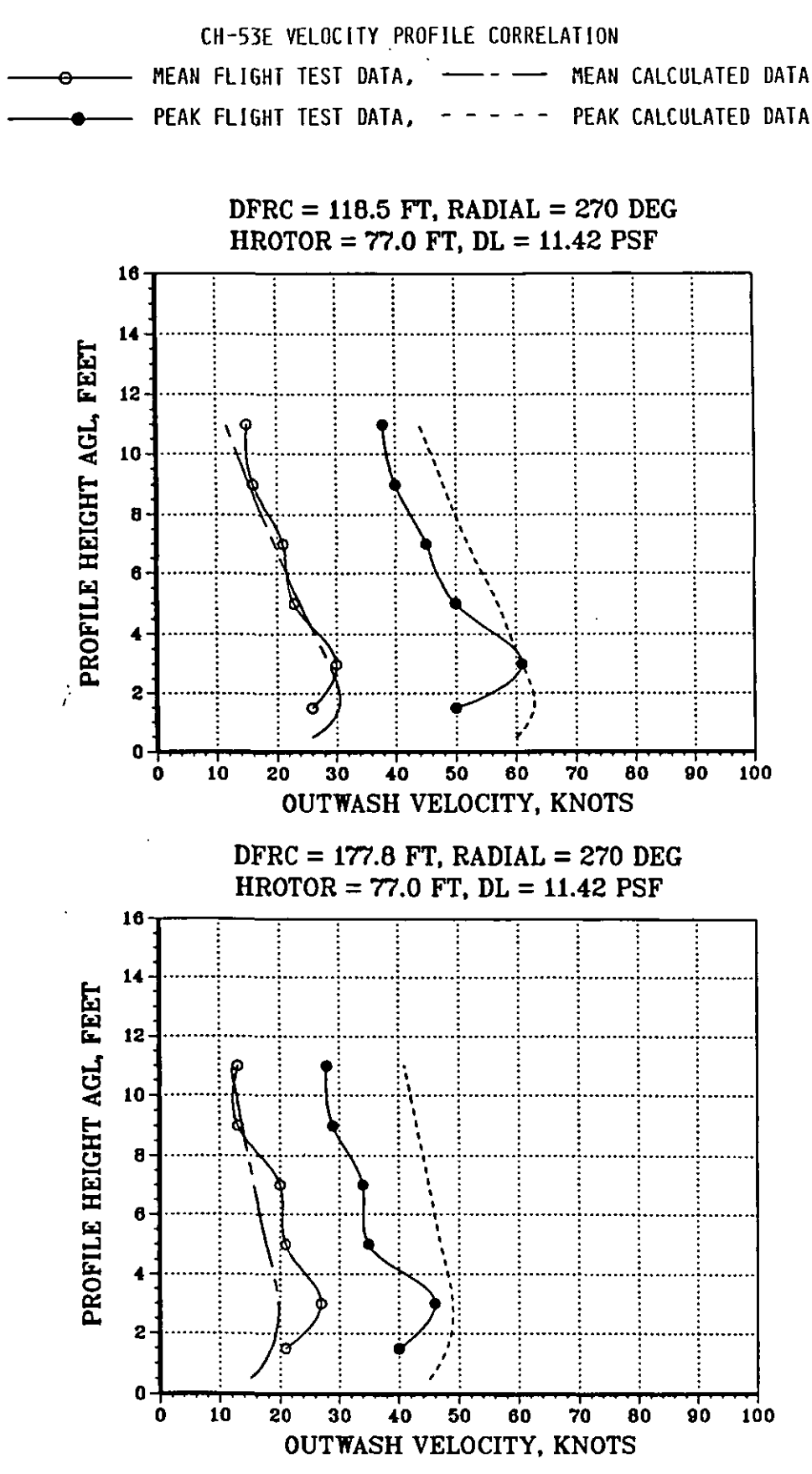

Figure B-5 (Concluded)

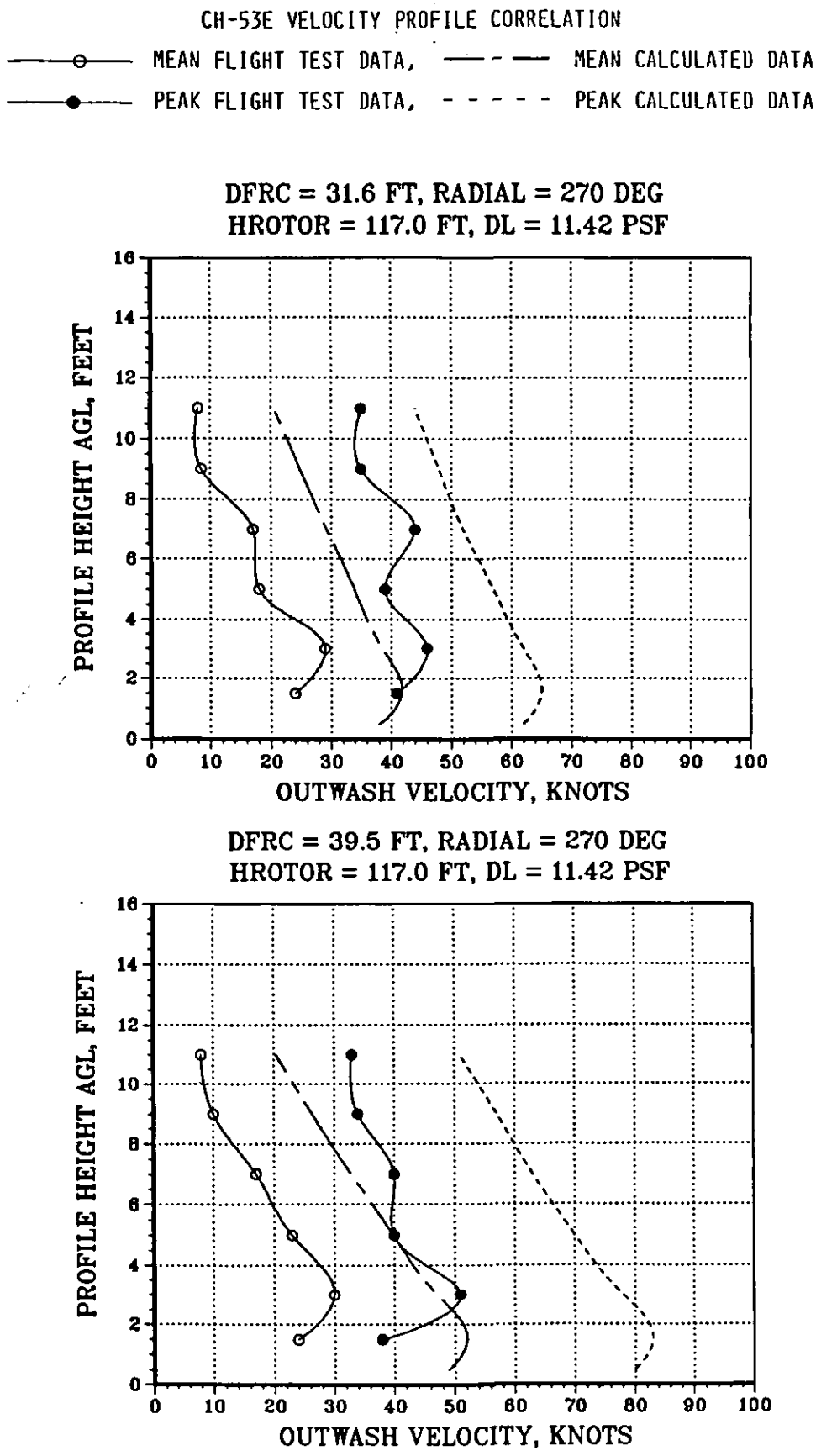

Figure B-6. CH-53E Mean and Peak Velocity Profile Correlation for Eight 270-deg Azimuth Radial Stations at a Rotor Height of 117 ft and a Gross Weight of 56000 lbs

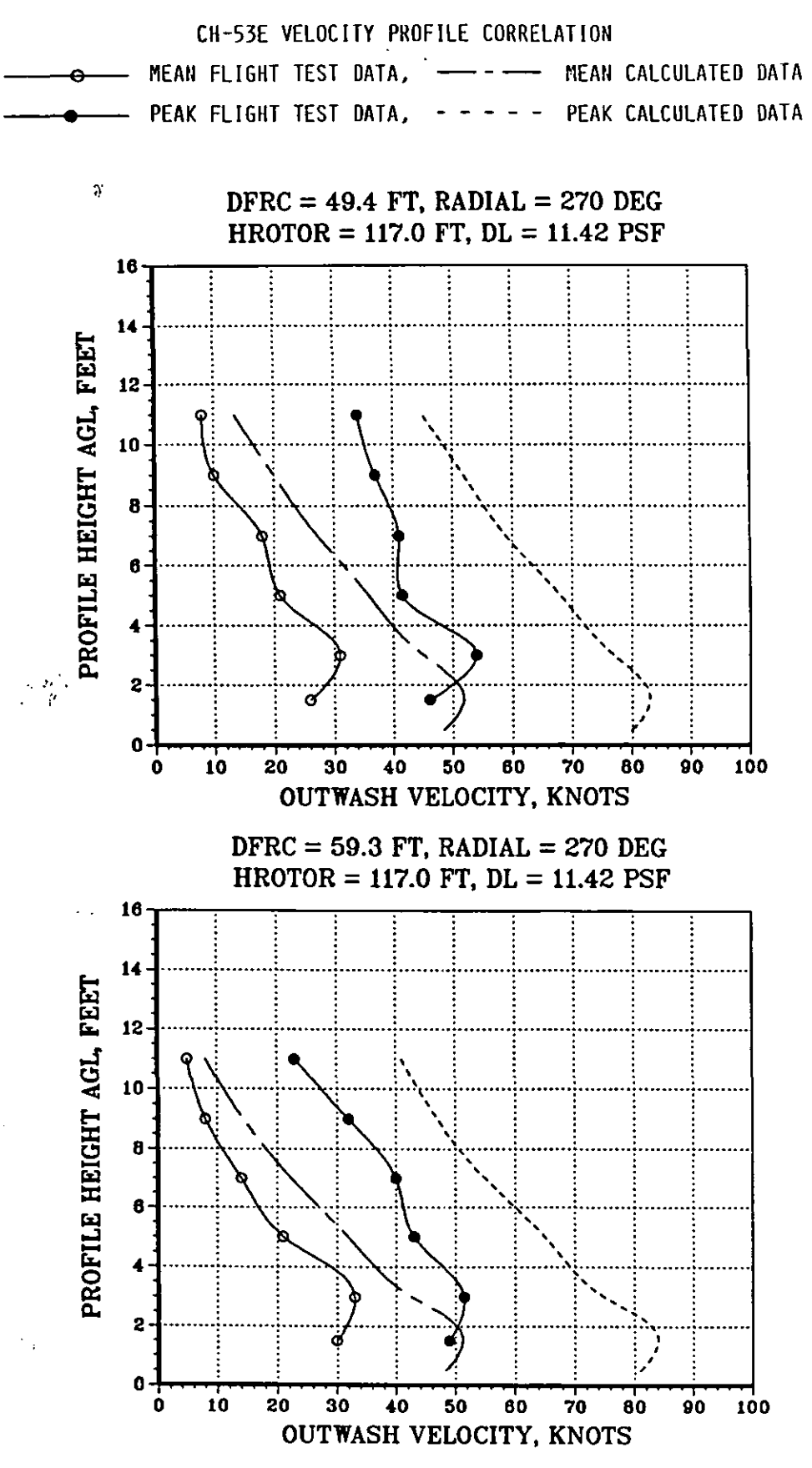

Figure B-6 (Continued)

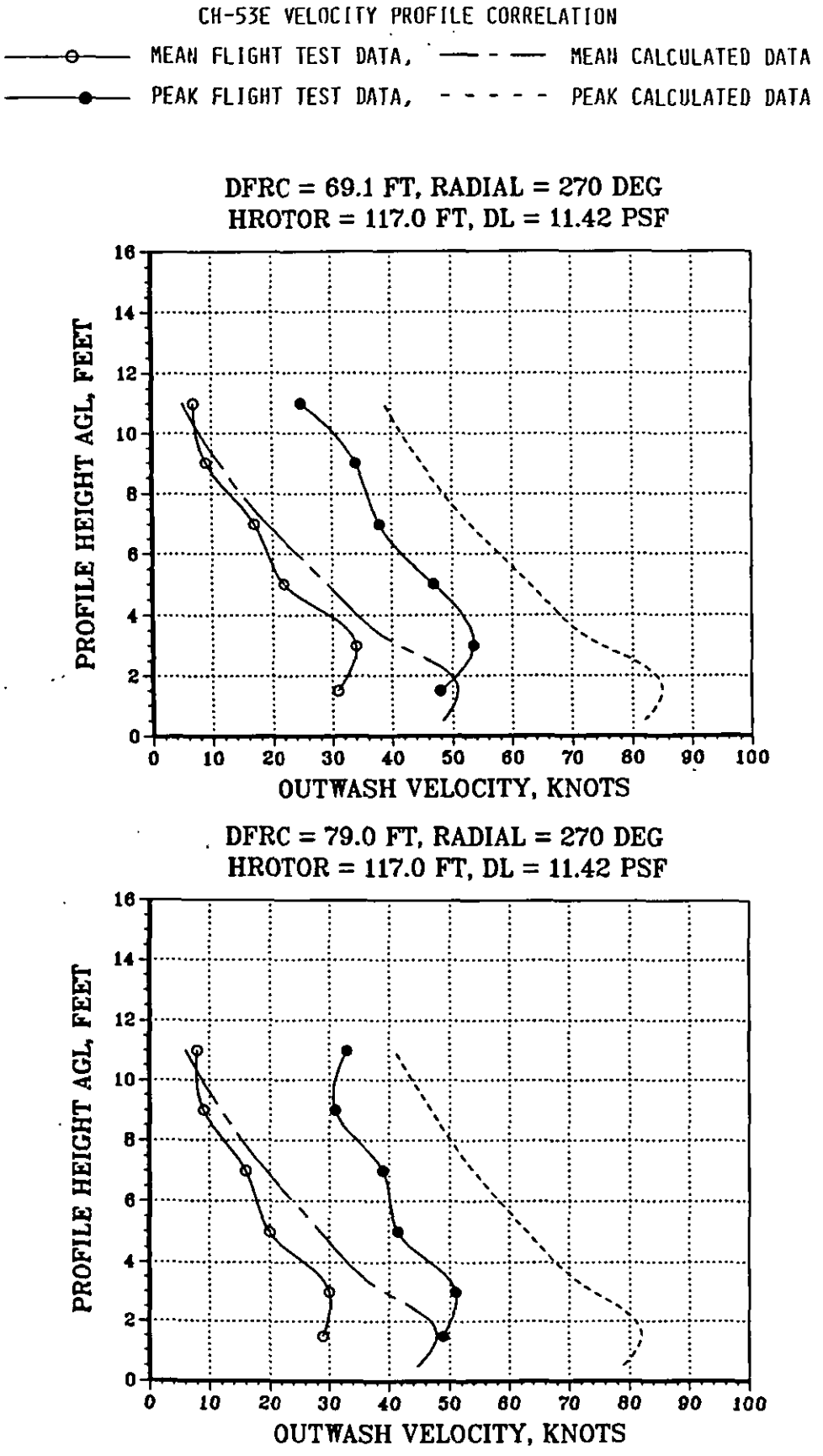

Figure B-6 (Continued)

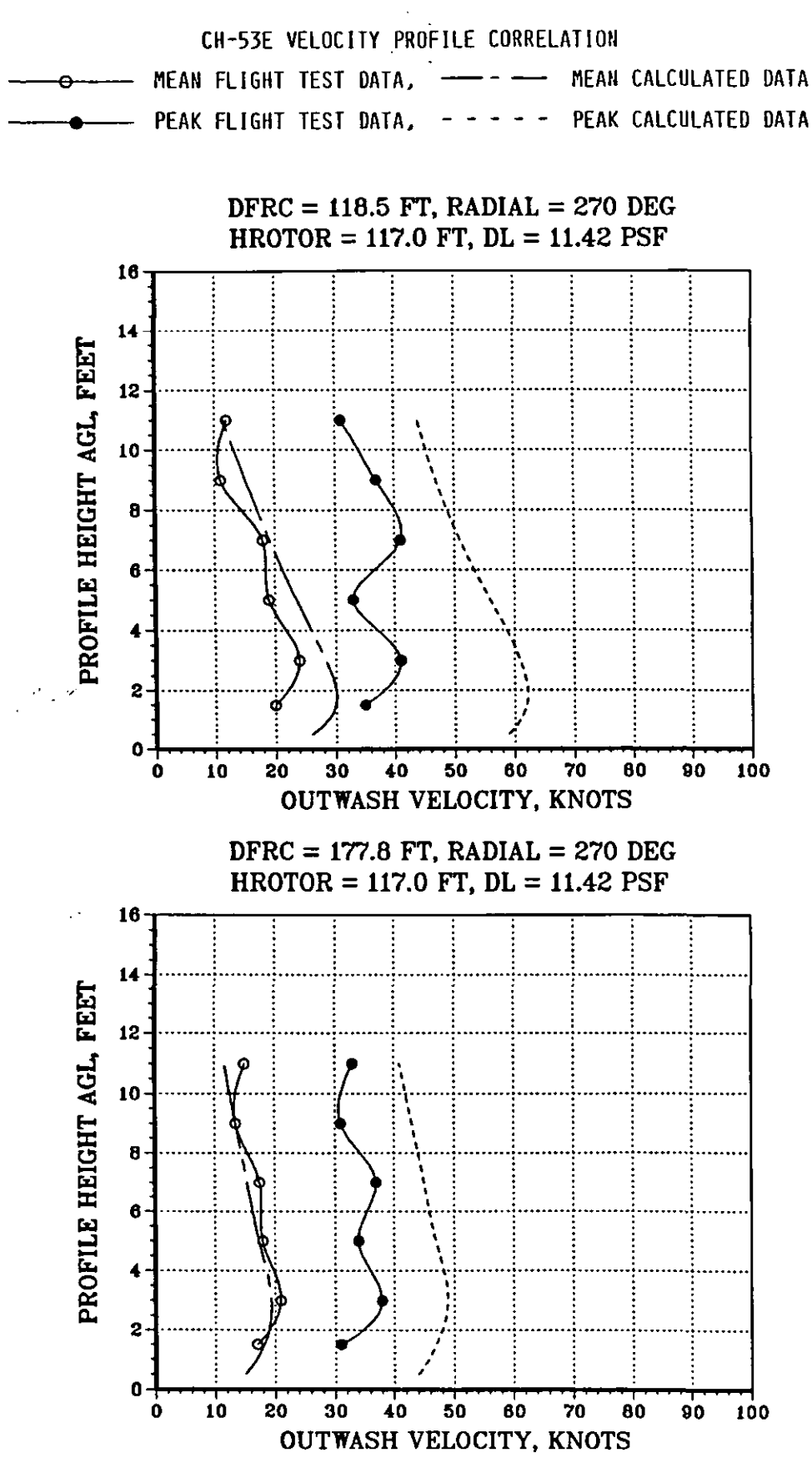

Figure B-6 (Concluded)

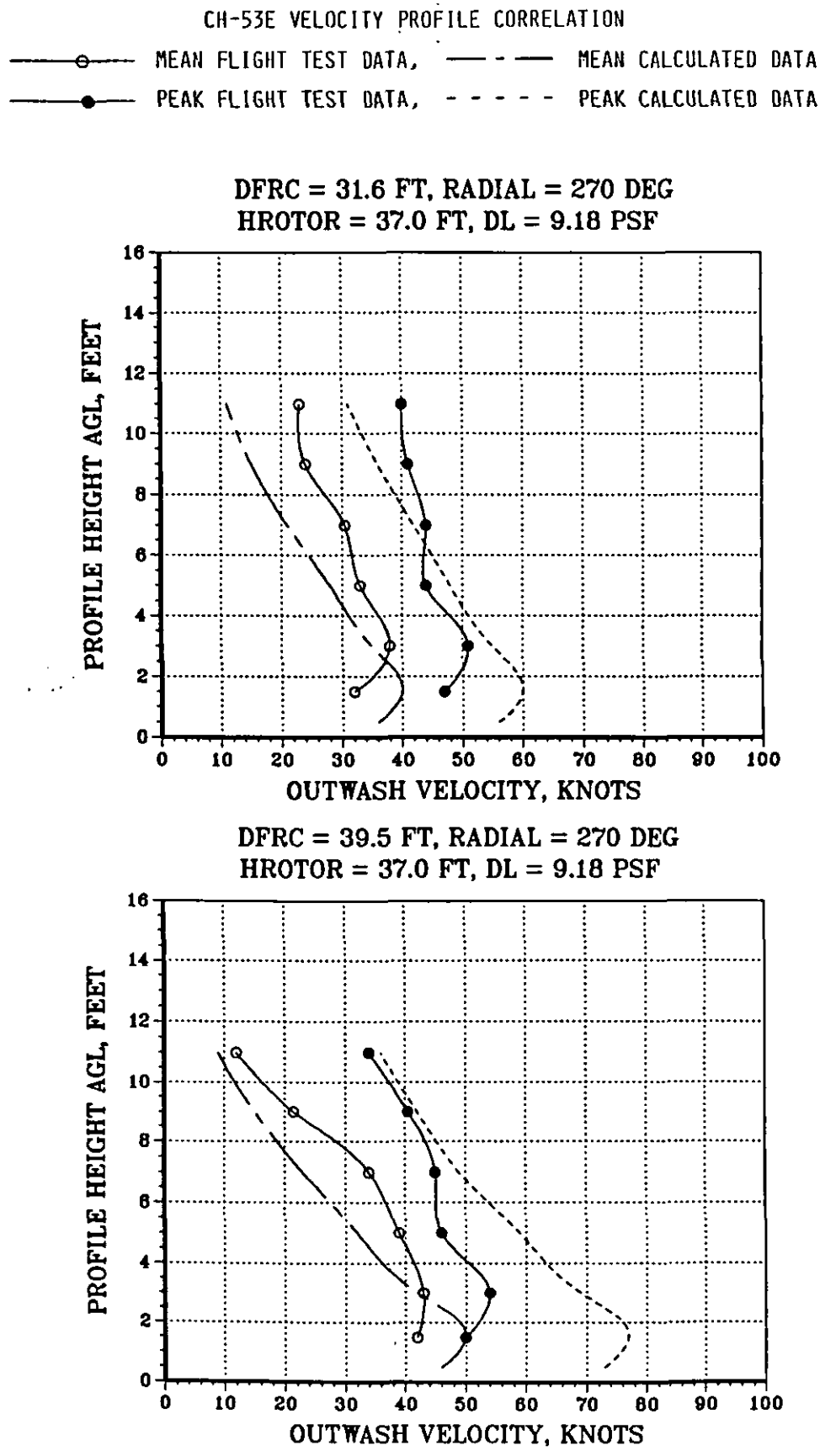

Figure B-7. CH-53E Mean and Peak Velocity Profile Correlation for Eight 270-deg Azimuth Radial Stations at a Rotor Height of 37 ft and a Gross Weight of 45000 lbs

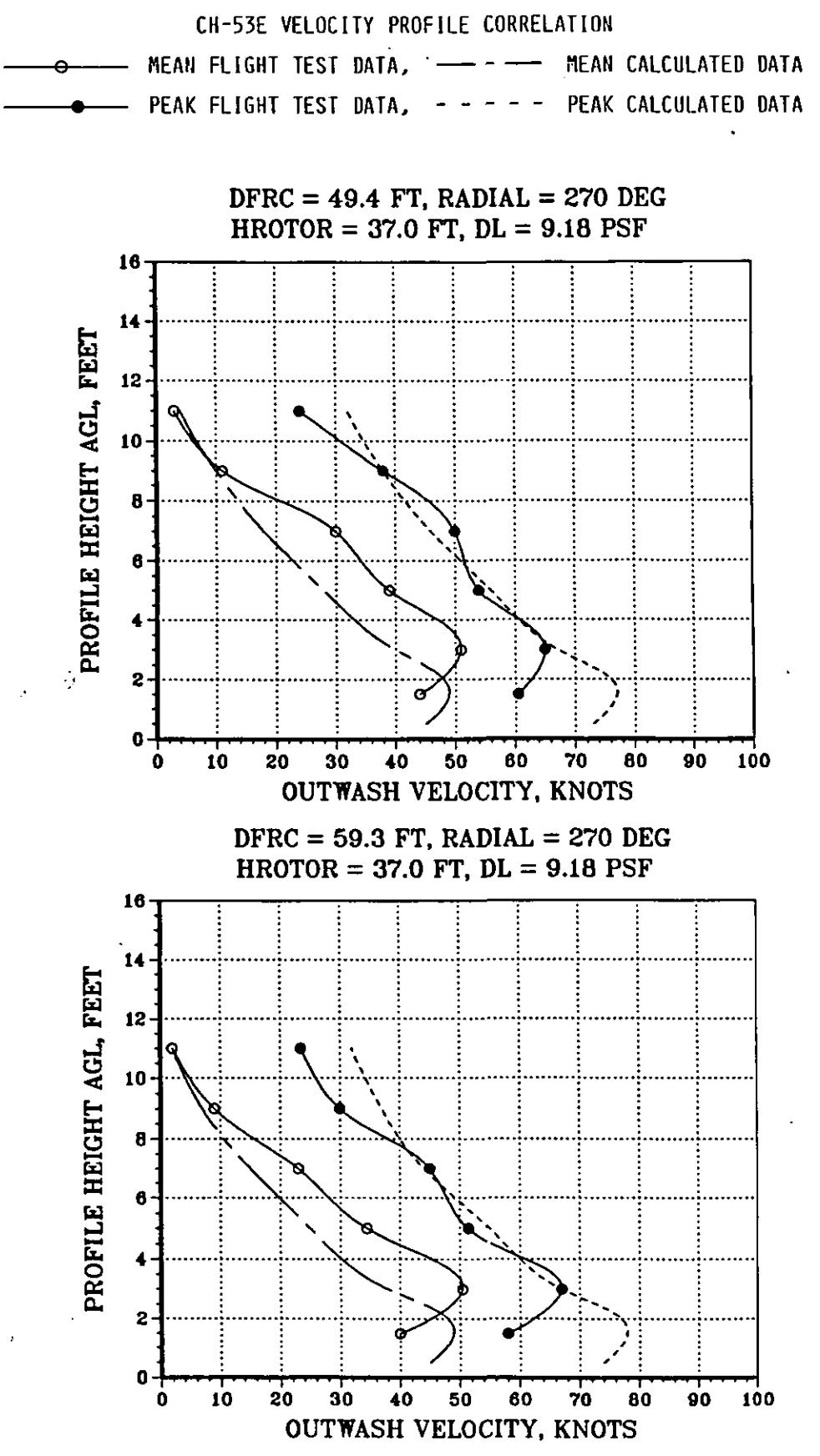

Figure B-7 (Continued)

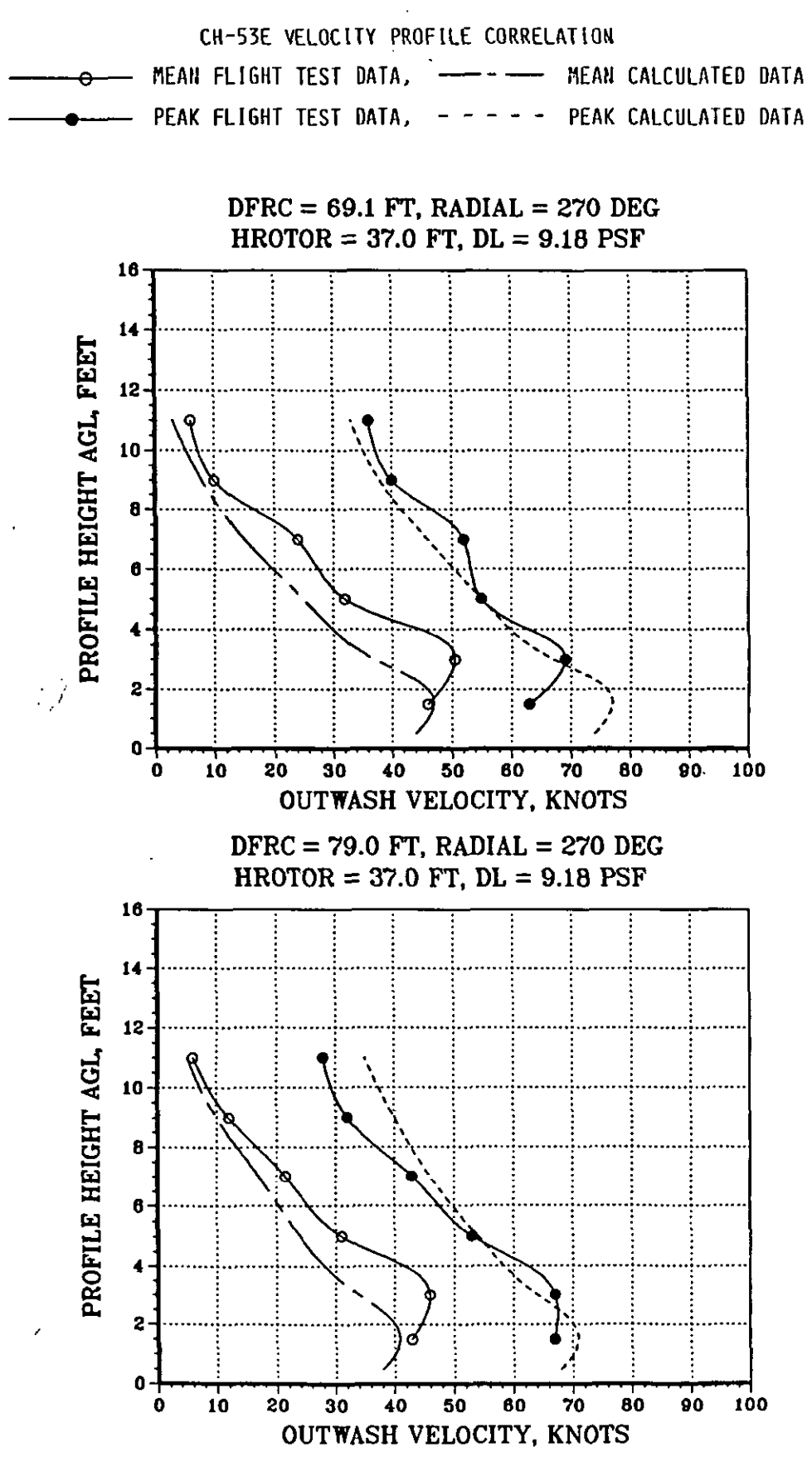

Figure B-7 (Continued)

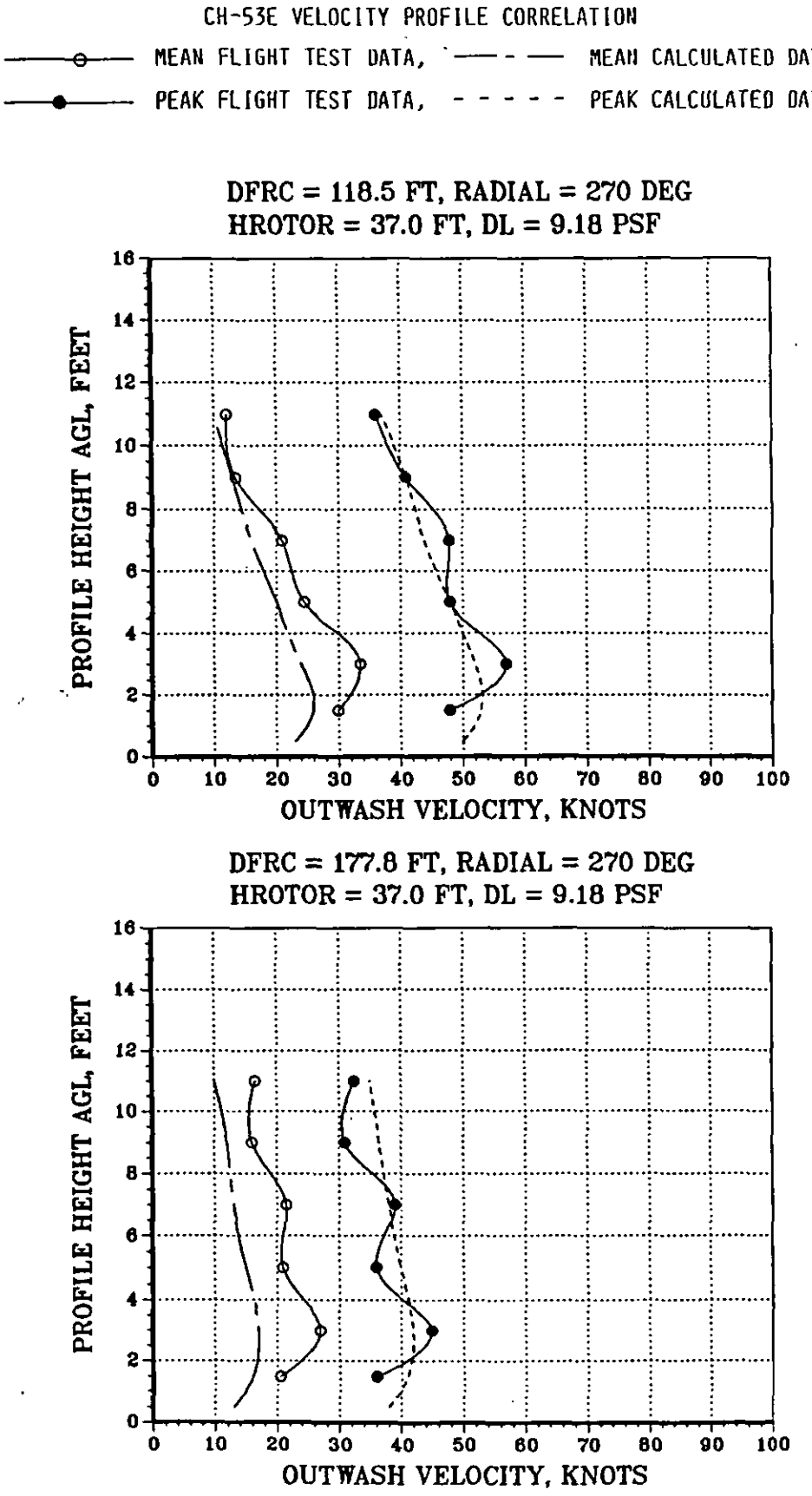

Figure B-7 (Concluded)

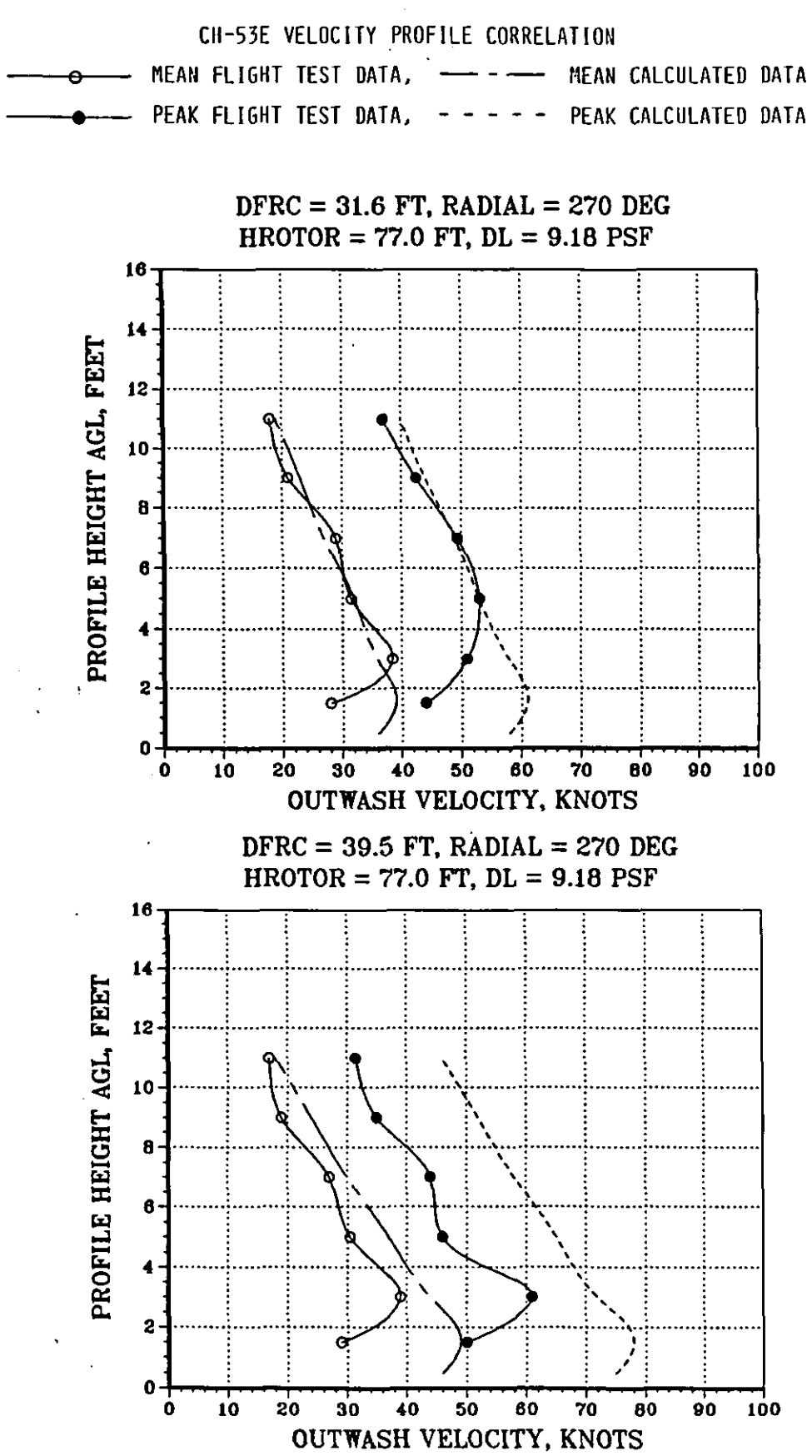

Figure B-8. CH-53E Mean and Peak Velocity Profile Correlation for Eight 270-deg Azimuth Radial Stations at a Rotor Height of 77 ft and a Gross Weight of 45000 lbs

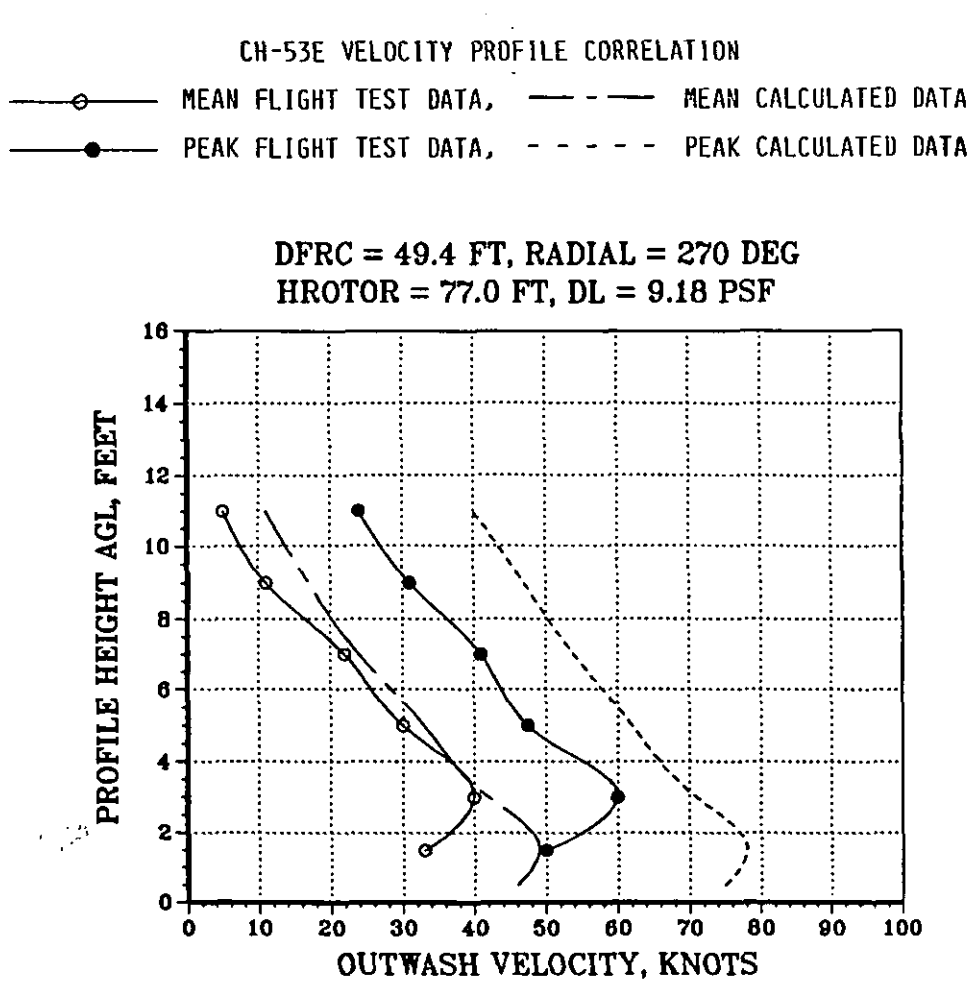

Figure B-8 (Continued)

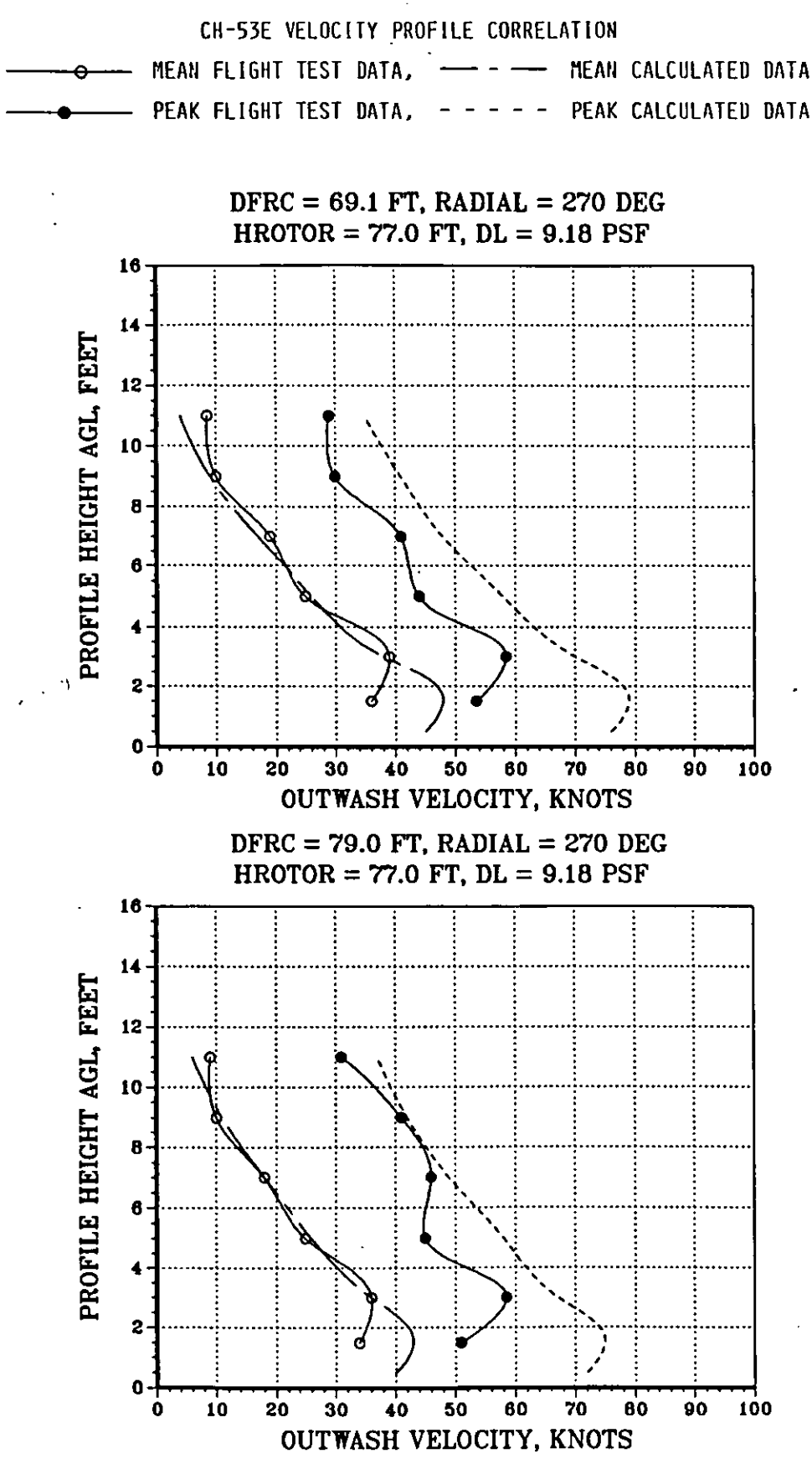

Figure B-8 (Continued)

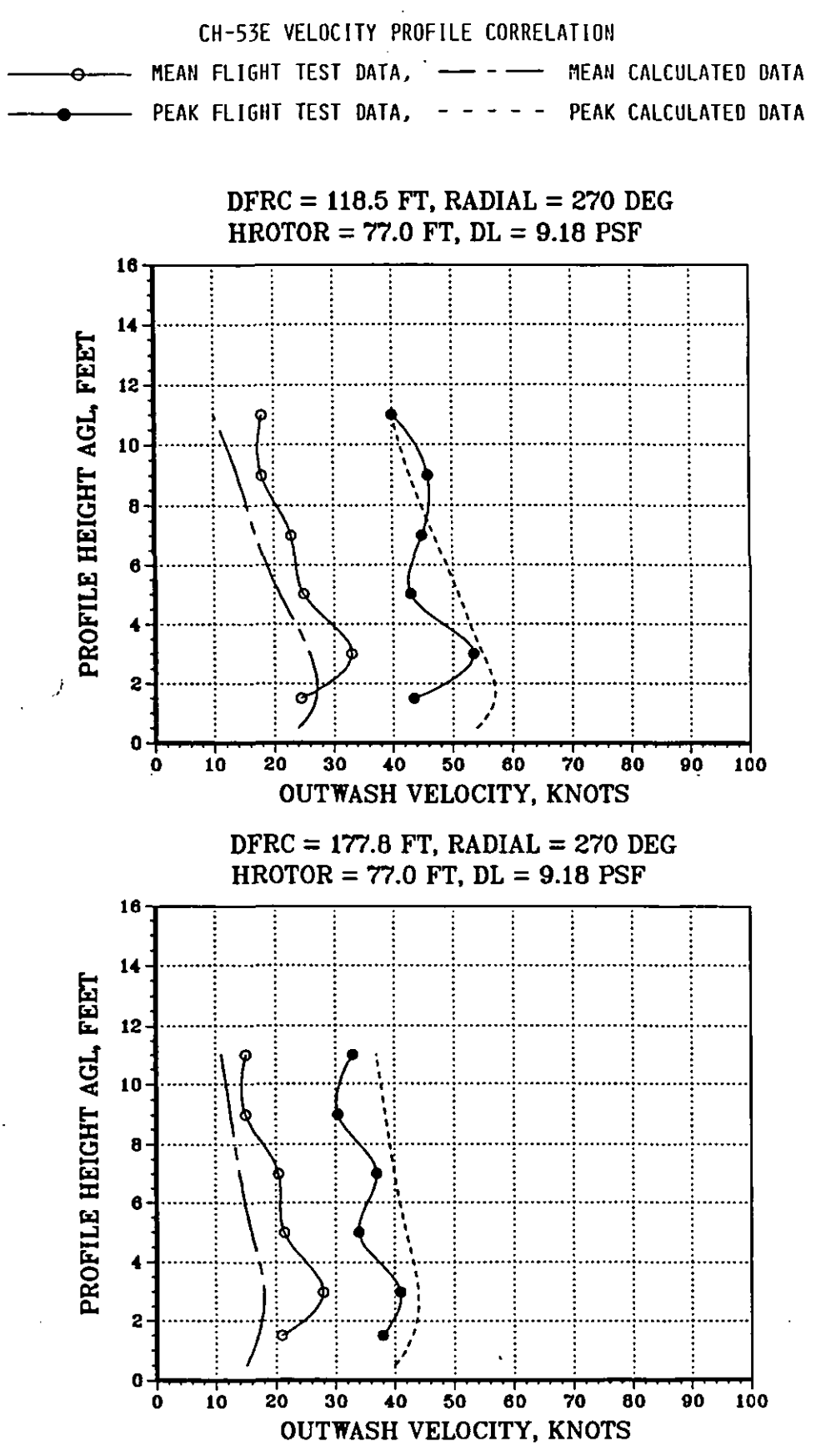

Figure B-8 (Concluded)

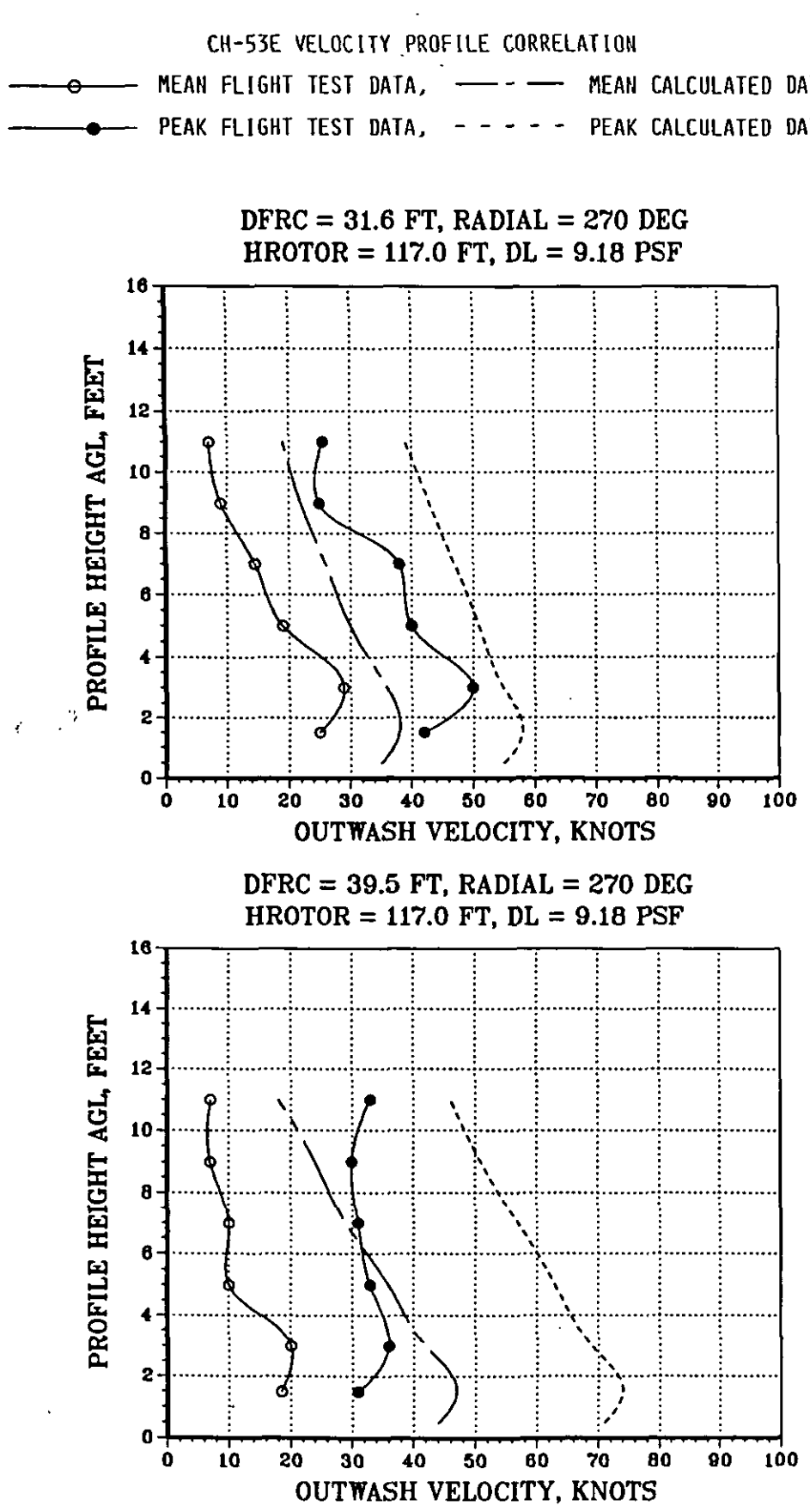

Figure B-9. CH-53E Mean and Peak Velocity Profile Correlation for Eight 270-deg Azimuth Radial Stations at a Rotor Height of 117 ft and a Gross Weight of 45000 lbs

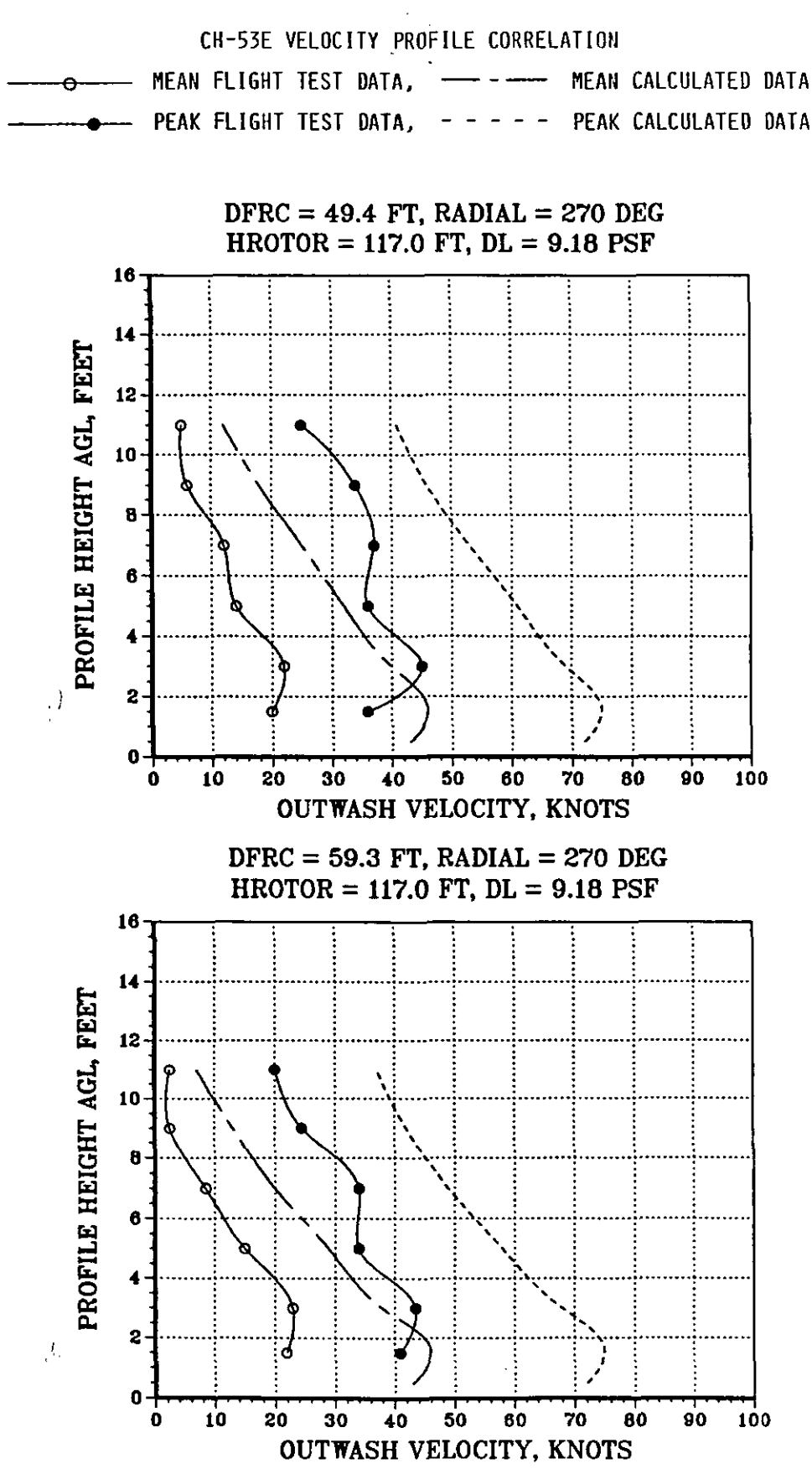

Figure B-9 (Continued)

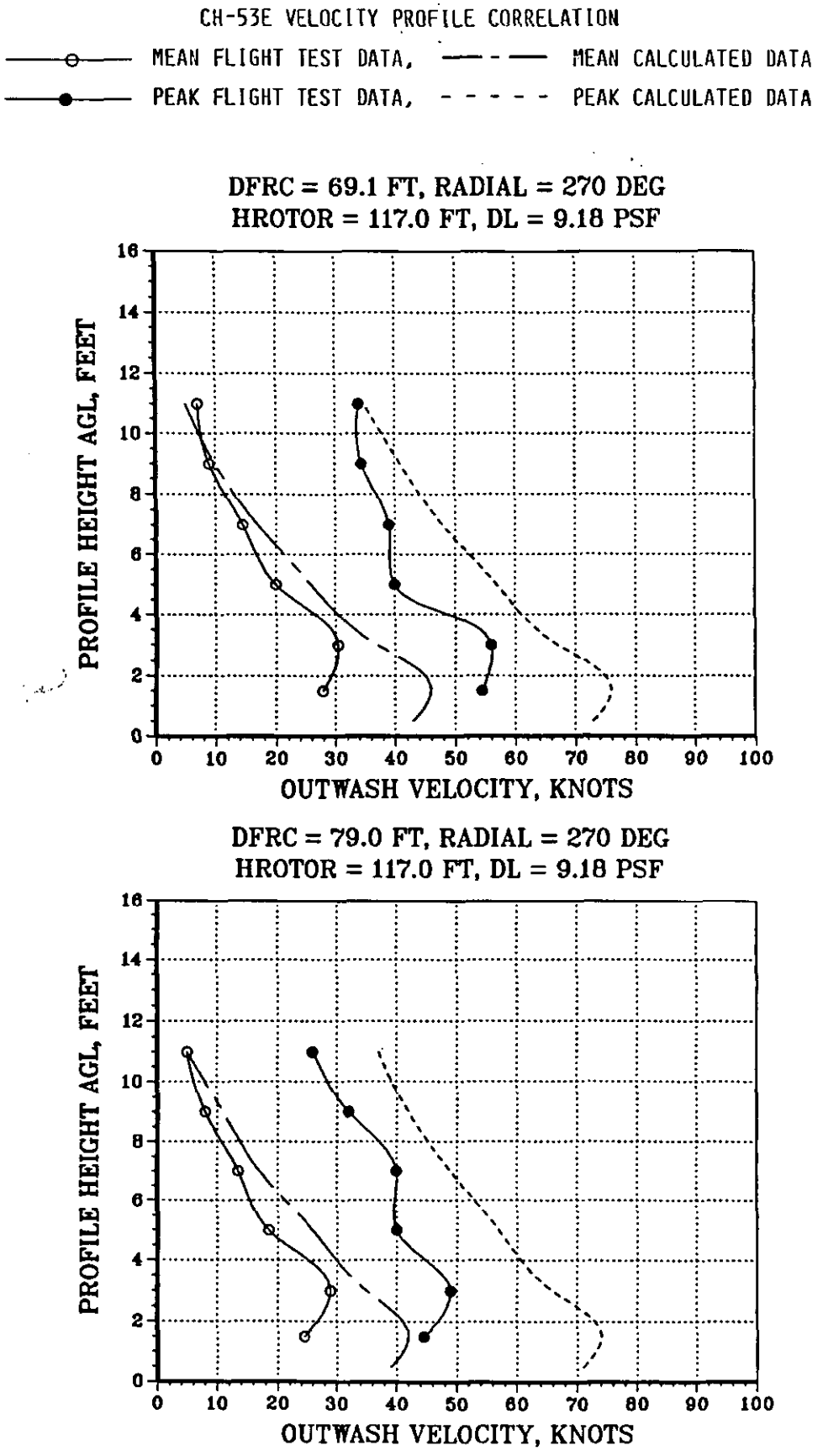

Figure B-9 (Continued)

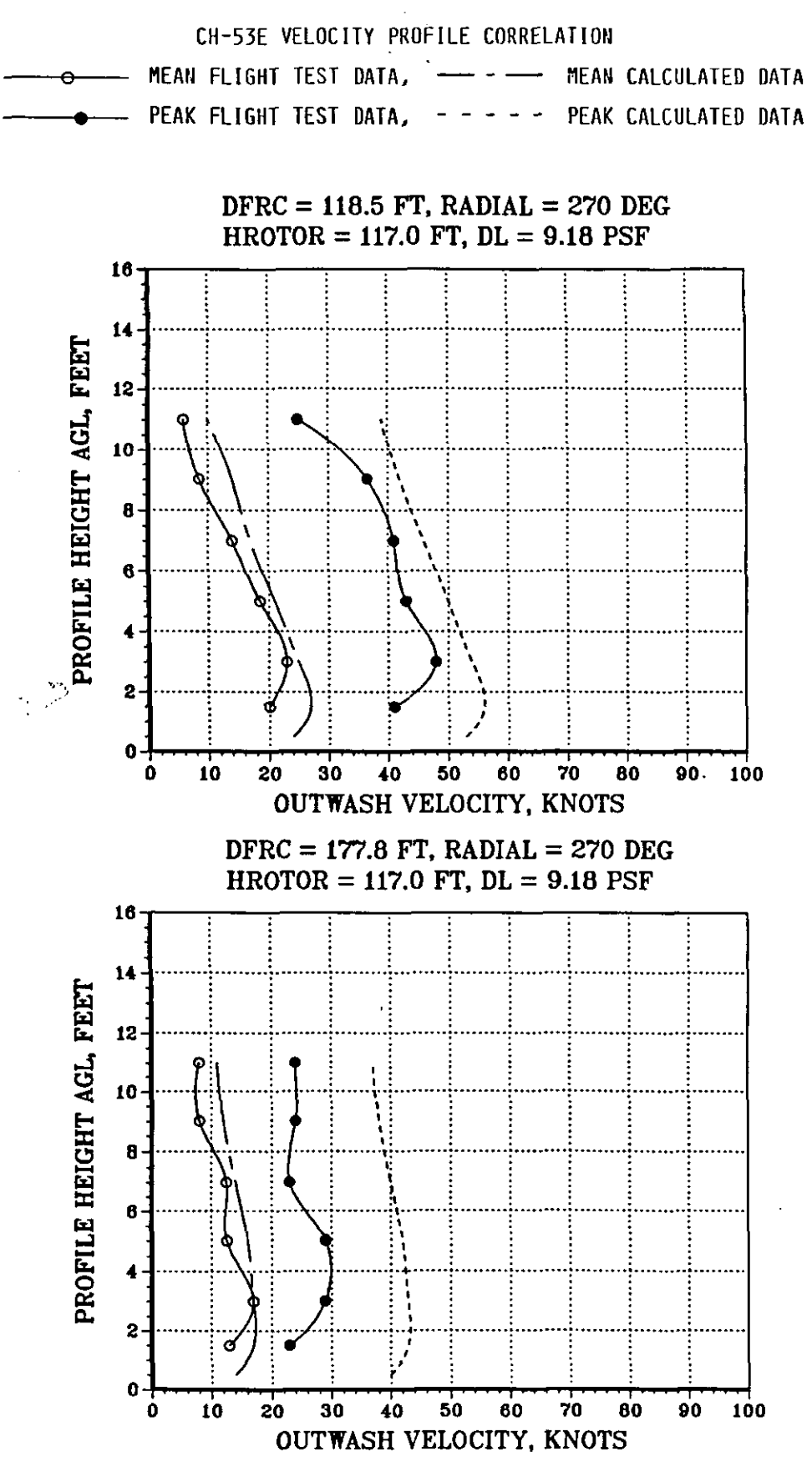

Figure B-9 (Concluded)

APPENDIX C

PROGRAM ROTHAZ LISTING

Source File: **ROTHAZ.FOR** Program Unit: **MAIN**

```
C     ************************************************************************00000010
C                                                                              00000020
C     PROGRAM ROTHAZ                                                           00000030
C                                                                              00000040
C     ROTORCRAFT DOWNWASH HAZARD ANALYSIS PROGRAM                              00000050
C                                                                              00000060
C     SYSTEMS TECHNOLOGY, INC./ COMPUTATIONAL METHODOLOGY ASSOCIATES           00000070
C     SAMUEL W. FERGUSON III/ J. DAVID KOCUREK                                 00000080
C                                                                              00000090
C     1 OCTOBER 1985                                                           00000100
C                                                                              00000110
C     PROGRAM VERSION 1.0                                                      00000120
C                                                                              00000130
C     THIS PROGRAM WAS DEVELOPED USING MICROSOFT FORTRAN VERSION 3.2           00000140
C     FOR THE MS-DOS OPERATING SYSTEM.  CONSOLE DISPLAY CONTROL                00000150
C     REQUIRES THAT THE ANSI.SYS DEVICE DRIVER BE INSTALLED WITH THE           00000160
C     THE OPERATING SYSTEM.  THE PROGRAM IS EXECUTABLE ON THE IBM PC           00000170
C     OR COMPATIBLE CLASS OF COMPUTERS.                                        00000180
C                                                                              00000190
C     ************************************************************************00000200
C                                                                              00000210
      PROGRAM MAIN                                                             00000220
C                                                                              00000230
      CHARACTER*1 KEY,KKEY,FLOW,VELHAZ                                         00000240
C                                                                              00000250
      COMMON / HELGEO / H,DL,YSEP,WSPD,RADIUS                                  00000260
      COMMON / CONSTS / PI,RHO,FPSPKN,RHOD2                                    00000270
      COMMON / UNITS  / IOU1,IOU6                                              00000280
      COMMON / PROFIL / RJ,ZBJ,ZHJ,ZMJ,UMJ,ZB,ZH,ZM,UM,CU,CY                  00000290
      COMMON / CKEY   / KEY,KKEY                                               00000300
C                                                                              00000310
C     ************************************************************************00000320
C                                                                              00000330
C     INITIALIZE MISCELLANEOUS CONSTANTS                                       00000340
C                                                                              00000350
      PI     = ACOS(-1.0)                                                      00000360
      RHOSL  = 0.0023769                                                       00000370
      FPSPKN = 1.687                                                           00000380
C                                                                              00000390
C     INITIALIZE I/O SYSTEM                                                    00000400
C                                                                              00000410
      CALL IOINIT                                                              00000420
C                                                                              00000430
   50 CONTINUE                                                                 00000440
C                                                                              00000450
      KEY = ' '                                                                00000460
      KKEY= ' '                                                                00000470
      CALL CLS                                                                 00000480
      CALL LOCATE(8,1)                                                         00000490
C                                                                              00000500
C     ****************************                                             00000510
C     OBTAIN INPUT DATA PARAMETERS                                             00000520
```

```
C     ****************************                                    00000530
C                                                                     00000540
      WRITE(*,'(''ENTER NUMBER OF ROTORS (1,2)   ===> ''\)')          00000550
      READ(*,*) ROTORS                                                00000560
      IF(ROTORS.LT.2.0) GO TO 100                                     00000570
      CALL LOCATE(10,1)                                               00000580
      WRITE(*,'(''ENTER HUB TO HUB DISTANCE BETWEEN'')')              00000590
      WRITE(*,'(''    DUAL ROTORS (FT)            ===> ''\)')       00000600
      READ(*,*) YYSEP                                                 00000610
C                                                                     00000620
  100 CONTINUE                                                        00000630
C                                                                     00000640
      CALL LOCATE(13,1)                                               00000650
      WRITE(*,'(''ENTER ROTOR RADIUS (FT)        ===> ''\)')          00000660
      READ(*,*) RADIUS                                                00000670
      CALL LOCATE(15,1)                                               00000680
      WRITE(*,'(''ENTER GROSS WEIGHT (LB)        ===> ''\)')          00000690
      READ(*,*) HELGW                                                 00000700
      CALL LOCATE(17,1)                                               00000710
      WRITE(*,'(''ENTER DOWNLOAD FACTOR (PCT)    ===> ''\)')          00000720
      READ(*,*) DWNLD                                                 00000730
C                                                                     00000740
      PAUSE ' '                                                       00000750
   51 CONTINUE                                                        00000760
      KEY = ' '                                                       00000770
      CALL CLS                                                        00000780
      CALL LOCATE(8,1)                                                00000790
C                                                                     00000800
      WRITE(*,'(''ENTER ROTOR HEIGHT AGL (FT)    ===> ''\)')          00000810
      READ(*,*) HAGL                                                  00000820
      CALL LOCATE(10,1)                                               00000830
      WRITE(*,'(''ENTER AIR DENSITY RATIO (ND)   ===> ''\)')          00000840
      READ(*,*) SIGPR                                                 00000850
   52 CONTINUE                                                        00000860
      CALL LOCATE(12,1)                                               00000870
      WRITE(*,'(''ENTER AMBIENT WIND SPEED (KT) '')')                 00000880
      WRITE(*,'('' OF <= 10 KT FOR OPT. <W>,<I>   ===> ''\)')         00000890
      READ(*,*) WSPD                                                  00000900
      IF(WSPD.LT.-10.0.OR.WSPD.GT.10.0)GOTO 52                        00000910
C                                                                     00000920
      H     = HAGL/RADIUS                                             00000930
      YSEP  = YYSEP/2.0/RADIUS                                        00000940
      EFFGW = HELGW*(1.0+(DWNLD/100.0))                               00000950
      DL    = EFFGW/ROTORS/PI/RADIUS**2                               00000960
      RHO   = SIGPR*RHOSL                                             00000970
      RHOD2 = 0.5*RHO                                                 00000980
C                                                                     00000990
      PAUSE ' '                                                       00001000
      CALL CLS                                                        00001010
      CALL LOCATE(10,1)                                               00001020
C                                                                     00001030
      WRITE(*,12)                                                     00001040
```

```
   12 FORMAT(' ',8X,'SELECT ANALYSIS PROBLEM',//,                        00001050
     1       ' ',9X,'PRESS <V> FOR VELOCITY CALCULATIONS',/,             00001060
     2       ' ',9X,'PRESS <H> FOR HAZARD CALCULATIONS   ===> '\)        00001070
      READ(*,'(A)') VELHAZ                                               00001080
C                                                                        00001090
C     SWITCHING CALLS HAZARD PROGRAM AND ALLOWS RETURN (IF DESIRED)      00001100
C     TO THE MAINLINE ROUTINE TO CHANGE ROTORCRAFT INPUT PARAMETERS      00001110
C                                                                        00001120
      IF(VELHAZ.EQ.'H') KKEY='H'                                         00001130
      IF(VELHAZ.EQ.'H') CALL HAZARD                                      00001140
C                                                                        00001150
      KKEY = 'V'                                                         00001160
      CALL CLS                                                           00001170
      CALL LOCATE(10,1)                                                  00001180
C                                                                        00001190
      IF(KEY.EQ.'R')    CALL INKEY                                       00001200
      IF(KEY.EQ.'X')    GOTO 999                                         00001210
      IF(VELHAZ.EQ.'H') GOTO 500                                         00001220
C                                                                        00001230
      CALL CLS                                                           00001240
      CALL LOCATE(10,1)                                                  00001250
C                                                                        00001260
      WRITE(*,10)                                                        00001270
   10 FORMAT (' ',8X,'SELECT TYPE OF FLOW TO BE ESTIMATED',//,           00001280
     1        ' ',9X,'PRESS <W> FOR WALL JET',/,                        00001290
     2        ' ',9X,'      <I> FOR INTERACTION PLANE',/,               00001300
     3        ' ',9X,'      <G> FOR GROUND VORTEX',/,                   00001310
     4        ' ',9X,'      <D> FOR DISK VORTEX',/,                     00001320
     5        ' ',9X,'      <X> TO EXIT                 ===> '\)        00001330
      READ(*,'(A)') FLOW                                                 00001340
C                                                                        00001350
      CALL CLS                                                           00001360
      IF(FLOW.EQ.'X') GOTO 999                                           00001370
      IF(FLOW.EQ.'G') GOTO 1000                                          00001380
      IF(FLOW.EQ.'D') GOTO 1000                                          00001390
C                                                                        00001400
C     **********************                                             00001410
C     RADIAL WALL JET FLOWS                                              00001420
C     **********************                                             00001430
C                                                                        00001440
C     ACCELERATED SLIPSTREAM MEAN VELOCITY                               00001450
C                                                                        00001460
      UN = SQRT(2.0*DL/RHO)                                              00001470
C                                                                        00001480
C     GROUND EFFECT CORRECTION                                           00001490
C                                                                        00001500
      AKG = 1.0 -0.9*EXP(-2.0*H)                                         00001510
C                                                                        00001520
C     MEAN VELOCITY AT ROTOR DISK (RATIOED TO UN)                        00001530
C                                                                        00001540
      UB = AKG/2.0                                                       00001550
C                                                                        00001560
```

```
C     FIND INITIAL RADIUS OF WALL JET                                   00001570
C                                                                       00001580
      CALL WALJET(H,UB,UN,UMB,RADIUS)                                   00001590
C                                                                       00001600
  500 CONTINUE                                                          00001610
C                                                                       00001620
      IF(KEY.EQ.'X') GOTO 999                                           00001630
      IF(KEY.EQ.'N') GOTO 50                                            00001640
      IF(KEY.EQ.'A') GOTO 51                                            00001650
C                                                                       00001660
      CALL LOCATE(10,1)                                                 00001670
C                                                                       00001680
      IF(FLOW.EQ.'I') GO TO 700                                         00001690
C                                                                       00001700
  600 CONTINUE                                                          00001710
C                                                                       00001720
C     WALL JET REGION                                                   00001730
C                                                                       00001740
      WRITE(*,'(''ENTER WALL JET RADIUS FOR V(R,Z) (FT)  ===> ''\)')    00001750
      READ(*,*) RRVZ                                                    00001760
C                                                                       00001770
      RVZ = RRVZ/RADIUS                                                 00001780
C                                                                       00001790
C     GENERATE VELOCITY PROFILE AT RVZ IN WALL JET REGION               00001800
C                                                                       00001810
      CALL WJVEL(H,UN,UMB,RVZ,RADIUS,WSPD)                              00001820
C                                                                       00001830
      GO TO 500                                                         00001840
C                                                                       00001850
  700 CONTINUE                                                          00001860
C                                                                       00001870
C     INTERACTION PLANE UPWASH DEFLECTION ZONE                          00001880
C                                                                       00001890
      WRITE(*,'(''ENTER DISTANCE ALONG INTERACTION PLANE (FT) '',       00001900
     1            ''===> ''\)')                                         00001910
      READ(*,*) XXIP                                                    00001920
C                                                                       00001930
      XIP = XXIP/RADIUS                                                 00001940
C                                                                       00001950
C     GENERATE VELOCITY PROFILE AT XIP IN INTERACTION PLANE             00001960
C                                                                       00001970
      CALL IPVEL(H,UN,RADIUS,UMB,XIP,YSEP,WSPD)                         00001980
C                                                                       00001990
      GO TO 500                                                         00002000
C                                                                       00002010
 1000 CONTINUE                                                          00002020
C                                                                       00002030
C     **********************                                            00002040
C     HORSESHOE VORTEX FLOWS                                            00002050
C     **********************                                            00002060
C                                                                       00002070
      CALL LOCATE(4,1)                                                  00002080
```

```
      WRITE(*,'(''* ************************************'')')          00002090
      WRITE(*,'('' * GROUND AND DISK VORTEX MODELS ARE *'')')          00002100
      WRITE(*,'('' * EXPLORATORY CONCEPTS - AND ARE TO *'')')          00002110
      WRITE(*,'('' * BE USED FOR RESEARCH ONLY!        *'')')          00002120
      WRITE(*,'('' * ************************************'')')          00002130
      CALL LOCATE(10,1)                                                00002140
      WRITE(*,'(''ENTER ROTOR TIP SPEED (FT/SEC)      ===> ''\)')      00002150
      READ(*,*) OMEGAR                                                 00002160
      CALL LOCATE(12,1)                                                00002170
      WRITE(*,'(''ENTER NUMBER OF BLADES              ===> ''\)')      00002180
      READ(*,*) B                                                      00002190
      CALL LOCATE(14,1)                                                00002200
      WRITE(*,'(''ENTER TRANSLATIONAL SPEED (KN)      ===> ''\)')      00002210
      READ(*,*) VF                                                     00002220
C                                                                      00002230
      VF = VF*FPSPKN                                                   00002240
      AMU = VF/OMEGAR                                                  00002250
      CT = DL/RHO/OMEGAR**2                                            00002260
C                                                                      00002270
C     ITERATE TO GET INFLOW RATIO                                      00002280
C                                                                      00002290
      ALOLD = SQRT(CT/2.0)                                             00002300
      DO 1300 ITER=1,100                                               00002310
      ALNEW  = CT/2.0/SQRT(ALOLD**2+AMU**2)                            00002320
      IF(ABS(ALNEW-ALOLD).LE.1.0E-05) GO TO 1301                       00002330
      ALOLD=ALNEW                                                      00002340
 1300 CONTINUE                                                         00002350
C                                                                      00002360
      CALL CLS                                                         00002370
      CALL LOCATE(10,1)                                                00002380
      WRITE(*,20)                                                      00002390
   20 FORMAT(' ','************************************',/              00002400
     1       ' ','ITERATIONS EXCEEDED FOR INFLOW RATIO',/              00002410
     2       ' ','************************************')               00002420
C                                                                      00002430
      STOP ' '                                                         00002440
C                                                                      00002450
 1301 CONTINUE                                                         00002460
C                                                                      00002470
      ALAMDA = ALNEW                                                   00002480
      AMUS   = AMU/SQRT(CT/2.0)                                        00002490
      GAMT   = OMEGAR*RADIUS*2.0*PI*CT/B                               00002500
      CHI    = ATAN(ALAMDA/AMU)/2.0                                    00002510
      GAMW   = PI*RADIUS*OMEGAR**2*CT/VF/2.0                           00002520
      HOD    = H/2.0                                                   00002530
C                                                                      00002540
 1100 CONTINUE                                                         00002550
C                                                                      00002560
      IF(KEY.EQ.'X') GOTO 999                                          00002570
      IF(KEY.EQ.'N') GOTO 50                                           00002580
      IF(KEY.EQ.'A') GOTO 51                                           00002590
C                                                                      00002600
```

```
      CALL CLS                                                          00002610
      CALL LOCATE(10,1)                                                 00002620
C                                                                       00002630
      IF(FLOW.EQ.'D') GO TO 1200                                        00002640
C                                                                       00002650
C     GROUND VORTEX                                                     00002660
C                                                                       00002670
      WRITE(*,1001) HOD,AMUS,AMU                                        00002680
 1001 FORMAT(' ',5X,'ROTOR HEIGHT ABOVE GROUND H/D  ',F10.5,/           00002690
     1       ' ',5X,'          ADVANCE RATIO MU-STAR ',F10.5,/         00002700
     2       ' ',5X,'          ADVANCE RATIO MU      ',F10.5)          00002710
C                                                                       00002720
C     THE VALUE INPUT HERE REQUIRES USE OF THE CHART ON PAGE 20         00002730
C     OF THE ACCOMPANYING DOCUMENTATION FOR THE GROUND VORTEX           00002740
C                                                                       00002750
      CALL LOCATE(15,1)                                                 00002760
      WRITE(*,'(''ENTER GROUND VORTEX STRENGTH RATIO '')')              00002770
      WRITE(*,'(''  (SEE CHART, PAGE 20)            ===> ''\)')         00002780
      READ(*,*) GAMG                                                    00002790
C                                                                       00002800
      GAMG = GAMG*GAMT                                                  00002810
C                                                                       00002820
      CALL GDVTX(H,RADIUS,AMU,CT,GAMG)                                  00002830
C                                                                       00002840
      GO TO 1100                                                        00002850
C                                                                       00002860
 1200 CONTINUE                                                          00002870
C                                                                       00002880
C     DISK VORTEX                                                       00002890
C                                                                       00002900
      CALL DEVTX(H,RADIUS,GAMW,CHI)                                     00002910
C                                                                       00002920
      GO TO 1100                                                        00002930
C                                                                       00002940
C     NORMAL PROGRAM EXIT                                               00002950
C                                                                       00002960
  999 CONTINUE                                                          00002970
      STOP ' '                                                          00002980
      END                                                               00002990
```

```
C     ******************************************************************00000010
C     SUBROUTINE WALJET                                                  00000020
C                                                                        00000030
C     THIS SUBROUTINE DEFINES THE START OF THE WALLJET AND ITS GROWTH    00000040
C     ******************************************************************00000050
C                                                                        00000060
      SUBROUTINE WALJET(H,UB,UN,UMB,RADIUS)                              00000070
C                                                                        00000080
      COMMON / PROFIL / RJ,ZBJ,ZHJ,ZMJ,UMJ,ZB,ZH,ZM,UM,CU,CY            00000090
      COMMON / CLOUDK / QSMAX                                            00000100
C                                                                        00000110
C     ******************************************************************00000120
C                                                                        00000130
C     INITIALIZATION OF EXPONENTS                                        00000140
C                                                                        00000150
      EXU = -1.143                                                       00000160
      EXY = 1.028                                                        00000170
      EXM = 1.0+EXU+EXY                                                  00000180
      CQ  = 0.52                                                         00000190
      CZM = 0.1944                                                       00000200
      CZB = 2.8                                                          00000210
C                                                                        00000220
C     ITERATE TO FIND INITIAL RADIUS OF WALL JET, RJ                     00000230
C                                                                        00000240
      TOL = 1.0E-05                                                      00000250
      RJ = 2.0                                                           00000260
C                                                                        00000270
      QSMAX0 = 1.0                                                       00000280
      DO 100 I=1,20                                                      00000290
C                                                                        00000300
C     EQUIVALENT JET LENGTH T/R                                          00000310
C                                                                        00000320
      TR  = H+(RJ-1.0)                                                   00000330
      TDE = 0.707*TR                                                     00000340
C                                                                        00000350
C     QSMAX CURVEFIT TO FIG. 8, USAAVLABS TECHNICAL                      00000360
C     REPORT 68-52, JULY 1968                                            00000370
C                                                                        00000380
      IF(TDE.LE.4.0) QSMAX = QSMAX0+(0.6-QSMAX0)/16.0*TDE**2             00000390
      IF(TDE.GT.4.0) QSMAX = 2.4/TDE                                     00000400
      UM  = SQRT(QSMAX)                                                  00000410
C                                                                        00000420
      RJNEW = 2.508078*(UB/UM)**(0.486)                                  00000430
C                                                                        00000440
      IF(ABS(RJNEW-RJ).LE.TOL) GO TO 200                                 00000450
      RJ = RJNEW                                                         00000460
C                                                                        00000470
  100 CONTINUE                                                           00000480
C                                                                        00000490
      WRITE(*,10)                                                        00000500
   10 FORMAT(' ','***********************************************',/     00000510
     1       ' ','ITERATIONS EXCEEDED FOR WALL JET INITIAL RADIUS',/     00000520
```

```
     2       ' ','**************************************************')      00000530
C                                                                          00000540
      STOP ' '                                                             00000550
C                                                                          00000560
  200 CONTINUE                                                             00000570
C                                                                          00000580
      RJ = RJNEW                                                           00000590
C                                                                          00000600
C     VELOCITY GROWTH FUNCTION CONSTANTS                                   00000610
C                                                                          00000620
      UMB = ((0.3586*RJ**EXM*(UM*UN)*(UB*UN)**(0.14))**(0.88))/UN          00000630
      ZHJ = 0.654/(UM/UMB)**2/RJ                                           00000640
      CU  = UM/UMB*RJ**(-EXU)                                              00000650
      CY  = ZHJ*RJ**(-EXY)                                                 00000660
C                                                                          00000670
C     MAX VELOCITY AND BOUNDARY PARAMETERS AT RJ                           00000680
C                                                                          00000690
      UMJ = CU*RJ**(EXU)*UMB                                               00000700
      ZHJ = CY*RJ**(EXY)                                                   00000710
      ZMJ = CZM*ZHJ                                                        00000720
      ZBJ = CZB*ZHJ                                                        00000730
C                                                                          00000740
      RETURN                                                               00000750
      END                                                                  00000760
```

Source File: **ROTHAZ.FOR** Program Unit: **PROPRM**

```
C     ************************************************************************00000010
C     SUBROUTINE PROPRM                                                       00000020
C                                                                             00000030
C     THIS SUBROUTINE CALCULATES THE VELOCITY PROFILE V(R,Z) PARAMETERS       00000040
C     OF THE RADIAL WALL JET FOR THE NON-INTERACTING ROTOR CASE               00000050
C     ************************************************************************00000060
C                                                                             00000070
      SUBROUTINE PROPRM(H,UN,UMB,RVZ)                                         00000080
C                                                                             00000090
      COMMON / PROFIL / RJ,ZBJ,ZHJ,ZMJ,UMJ,ZB,ZH,ZM,UM,CU,CY                 00000100
C                                                                             00000110
C     ************************************************************************00000120
C                                                                             00000130
      IF(RVZ.GE.RJ) GO TO 600                                                 00000140
C                                                                             00000150
C     RVZ .LT. RJ ==> TRANSITION REGION                                       00000160
C                                                                             00000170
      UM = UMJ*RVZ                                                            00000180
      IF(RVZ.GT.1.0) UM = UMJ                                                 00000190
      ZH = ZHJ*RVZ                                                            00000200
      IF(RVZ.GT.1.0) ZH = ZHJ                                                 00000210
      ZM = ZMJ*RVZ                                                            00000220
      IF(RVZ.GT.1.0) ZM = ZMJ                                                 00000230
C                                                                             00000240
C     BOUNDARY GROWTH IN TRANSITION REGION                                    00000250
C                                                                             00000260
      ZB0 = 1.5                                                               00000270
      IF(H.LT.1.5) ZB0 = H                                                    00000280
      ZH0 = ZB0/2.8                                                           00000290
      ZH = (ZH0-ZHJ)/RJ**2*(RJ-RVZ)**2+ZHJ                                    00000300
      ZB = 2.8*ZH                                                             00000310
C                                                                             00000320
      GO TO 700                                                               00000330
C                                                                             00000340
C     RVZ .GE. RJ ==> DEVELOPED WALL JET REGION                               00000350
C                                                                             00000360
  600 CONTINUE                                                                00000370
C                                                                             00000380
      UM = CU*RVZ**(-1.143)*UMB                                               00000390
      ZH = CY*RVZ**(1.028)                                                    00000400
      ZB = 2.8*ZH                                                             00000410
      ZM = 0.1944*ZH                                                          00000420
C                                                                             00000430
  700 CONTINUE                                                                00000440
C                                                                             00000450
      RETURN                                                                  00000460
      END                                                                     00000470
```

```
C     ************************************************************************00000010
C     SUBROUTINE WJVEL                                                        00000020
C                                                                             00000030
C     THIS SUBROUTINE GENERATES THE VELOCITY PROFILE V(R,Z)                   00000040
C     AT RVZ FOR THE NON-INTERACTING ROTOR CASE                               00000050
C     ************************************************************************00000060
C                                                                             00000070
      SUBROUTINE WJVEL(H,UN,UMB,RVZ,RADIUS,WSPD)                              00000080
C                                                                             00000090
      CHARACTER*1 KEY,KKEY                                                    00000100
C                                                                             00000110
      COMMON / CONSTS / PI,RHO,FPSPKN,RHOD2                                   00000120
      COMMON / PROFIL / RJ,ZBJ,ZHJ,ZMJ,UMJ,ZB,ZH,ZM,UM,CU,CY                  00000130
      COMMON / CKEY   / KEY,KKEY                                              00000140
      COMMON / UNITS  / IOU1,IOU6                                             00000150
C                                                                             00000160
C     ************************************************************************00000170
C                                                                             00000180
      CALL PROPRM(H,UN,UMB,RVZ)                                               00000190
C                                                                             00000200
C     DIMENSIONALIZE VELOCITY PROFILE PARAMETERS                              00000210
C                                                                             00000220
      RRVZ = RADIUS*RVZ                                                       00000230
      ZZB  = ZB*RADIUS                                                        00000240
      ZZH  = ZH*RADIUS                                                        00000250
      ZZM  = ZM*RADIUS                                                        00000260
      ZETAM = ZM/ZB                                                           00000270
C                                                                             00000280
      CALL CLS                                                                00000290
      CALL LOCATE(8,1)                                                        00000300
      IF(IOU6.NE.IOU1) WRITE(IOU6,'(''1'')')                                  00000310
      WRITE(IOU6,1000) RRVZ                                                   00000320
 1000 FORMAT(' ',5X,'SINGLE ROTOR VELOCITY PROFILE AT RADIUS (FT) ',          00000330
     1       F10.5,//)                                                        00000340
C                                                                             00000350
      WRITE(*,1001) ZZB,ZZH,ZZM                                               00000360
 1001 FORMAT(' ',9X,'PROFILE BOUNDARY HEIGHT (FT) ',F10.5,/                   00000370
     1       ' ',9X,'        HALF-VEL.HEIGHT (FT) ',F10.5,/                   00000380
     2       ' ',9X,'        MAX-VEL  HEIGHT (FT) ',F10.5)                    00000390
C                                                                             00000400
C     PROMPT FOR DISPLAY INCREMENTS AND RANGE                                 00000410
C                                                                             00000420
      CALL LOCATE(16,1)                                                       00000430
      WRITE(*,'(''ENTER VERTICAL INCREMENT DESIRED (FT) ===> ''\)')           00000440
      READ(*,*) DELZ                                                          00000450
      CALL LOCATE(18,1)                                                       00000460
      WRITE(*,'(''ENTER MAXIMUM HEIGHT FOR PROFILE (FT) ===> ''\)')           00000470
      READ(*,*) ZMAX                                                          00000480
C                                                                             00000490
      DELZ = DELZ/RADIUS                                                      00000500
      ZMAX = ZMAX/RADIUS                                                      00000510
      NPTS = IFIX(ZMAX/DELZ)+1                                                00000520
```

```
C                                                                       00000530
      PAUSE ' '                                                         00000540
      CALL CLS                                                          00000550
C                                                                       00000560
C     BOUNDARY LAYER REGION EXPONENT                                    00000570
C                                                                       00000580
C     'AN' IS ACTUALLY '= 1.0/7.0'                                      00000590
C                                                                       00000600
      AN = 0.142857142                                                  00000610
C                                                                       00000620
C     SHEAR LAYER REGION EXPONENT, TO MEET EDGE CONDITIONS              00000630
C     (FROM FIGURE 7, USAAVLABS TECHNICAL REPORT 68-52, JULY 1968)      00000640
C                                                                       00000650
      ALPW = ALOG(1.0-1.0/SQRT(2.0))/ALOG((ZH-ZM)/(ZB-ZM))              00000660
C                                                                       00000670
      VN = UN                                                           00000680
      VMN = UM                                                          00000690
C                                                                       00000700
C     CALCULATION OF THE PEAK VELOCITY CORRECTION FACTOR                00000710
C     IS MADE IN THE NEXT SECTION AT THE 3 FT POSITION                  00000720
C                                                                       00000730
      VZ3 = 3.0/RADIUS                                                  00000740
      ZETA3 = VZ3/ZB                                                    00000750
      VZM3 = 0.0                                                        00000760
      IF(ZETA3.GE.ZETAM)GOTO 51                                         00000770
C                                                                       00000780
C     THE 3 FT HEIGHT IS IN THE BOUNDARY LAYER                          00000790
C                                                                       00000800
      IF(ZETAM.GT.0.0) VZM3 = (ZETA3/ZETAM)**AN                         00000810
      GOTO 52                                                           00000820
   51 CONTINUE                                                          00000830
C                                                                       00000840
C     THE 3 FT HEIGHT IS IN THE SHEAR LAYER                             00000850
C                                                                       00000860
      IF(VZ3.LE.ZB) VZM3 = (1.0-((ZETA3-ZETAM)/(1.0-ZETAM))**ALPW)**2   00000870
   52 CONTINUE                                                          00000880
C                                                                       00000890
C     THE VELOCITY TO ADD TO THE MEAN VELOCITY TO OBTAIN THE PEAK       00000900
C     VELOCITY IS CALCULATED AS THE CONSTANT VMFD3 (FT/SEC)             00000910
C                                                                       00000920
      VZN3 = VZM3*VMN                                                   00000930
      VMF3 = VZN3*VN                                                    00000940
      VMFD3S = (RVZ*0.2444)+0.4                                         00000950
      IF(VMFD3S.GT.1.5) VMFD3S = 1.5                                    00000960
      VMFD3 = VMFD3S*VMF3                                               00000970
C                                                                       00000980
C     OUTPUT THE VELOCITY AND DYNAMIC PRESSURE PROFILE HEADER           00000990
C                                                                       00001000
      WRITE(IOU6,1005)                                                  00001010
 1005 FORMAT(' ',2X,'HEIGHT',6X,'MEAN VELOCITY',7X,'PEAK VELOCITY',5X,  00001020
     1       'MEAN Q',4X,'PEAK Q',/,                                    00001030
     2       'O',4X,'(FT)',5X,'(FPS)',6X,'(KN)',5X,'(FPS)',6X,'(KN)',5X,00001040
```

```
     3       '(PSF)',5X,'(PSF)',/)                                    00001050
C                                                                     00001060
C     CALCULATE THE VELOCITY PROFILE POINTS FOR OUTPUT                00001070
C                                                                     00001080
      LINES = 0                                                       00001090
      DO 500 I = 1,NPTS                                               00001100
C                                                                     00001110
      LINES = LINES+1                                                 00001120
      Z = DELZ*FLOAT(I-1)                                             00001130
      ZETA = Z/ZB                                                     00001140
      IF (ZETA.GE.ZETAM) GO TO 300                                    00001150
C                                                                     00001160
C     Z IS WITHIN BOUNDARY LAYER                                      00001170
C                                                                     00001180
      VZM = 0.0                                                       00001190
      IF(ZETAM.GT.0.0) VZM = (ZETA/ZETAM)**AN                         00001200
      GO TO 400                                                       00001210
C                                                                     00001220
  300 CONTINUE                                                        00001230
C                                                                     00001240
C     Z IS WITHIN SHEAR LAYER                                         00001250
C                                                                     00001260
      VZM = 0.0                                                       00001270
      IF(Z.LE.ZB) VZM=(1.0-((ZETA-ZETAM)/(1.0-ZETAM))**ALPW)**2       00001280
C                                                                     00001290
  400 CONTINUE                                                        00001300
C                                                                     00001310
      VZN = VZM*VMN                                                   00001320
C                                                                     00001330
C     DIMENSIONAL HEIGHT                                              00001340
C                                                                     00001350
      ZZ  = Z*RADIUS                                                  00001360
C                                                                     00001370
C     MEAN VELOCITIES                                                 00001380
C                                                                     00001390
      VMF = VZN*VN                                                    00001400
      VMK = VMF/FPSPKN                                                00001410
C                                                                     00001420
C     PEAK VELOCITIES                                                 00001430
C                                                                     00001440
      VPF = VMF + VMFD3                                               00001450
      IF(VMF.EQ.0.) VPF = 0.0                                         00001460
      VPK = VPF/FPSPKN                                                00001470
      IF(VPK.EQ.0.)GOTO 55                                            00001480
C                                                                     00001490
C     THE EFFECT OF WIND IS TO ADD (DOWNWIND SIDE) OR                 00001500
C     SUBTRACT (UPWIND SIDE) TWO TIMES THE AMBIENT WIND               00001510
C     VELOCITY TO THE HORIZONTAL PROFILE VELOCITY                     00001520
C                                                                     00001530
      XKW = (-0.5*H)+2.5                                              00001540
      IF(XKW.LT.1.0)XKW = 1.0                                         00001550
      WSPD2 = WSPD*XKW                                                00001560
```

```
      VMK = VMK + WSPD2                                                 00001570
      VMF = VMK*FPSPKN                                                  00001580
      VPK = VPK + WSPD2                                                 00001590
      VPF = VPK*FPSPKN                                                  00001600
   55 CONTINUE                                                          00001610
C                                                                       00001620
C     DYNAMIC PRESSURE                                                  00001630
C                                                                       00001640
      QM = RHOD2*VMF**2                                                 00001650
      QP = RHOD2*VPF**2                                                 00001660
C                                                                       00001670
      IF (IOU6.EQ.IOU1) THEN                                            00001680
        IF(LINES.LT.12) GO TO 450                                       00001690
        LINES = 1                                                       00001700
        CALL INKEY                                                      00001710
        IF(KEY.NE.'C') GO TO 999                                        00001720
        WRITE(IOU6,1005)                                                00001730
      ENDIF                                                             00001740
C                                                                       00001750
  450 CONTINUE                                                          00001760
C                                                                       00001770
C     OUTPUT THE VELOCITY AND DYNAMIC PRESSURE PROFILES                 00001780
C                                                                       00001790
      WRITE(IOU6,1002) ZZ,VMF,VMK,VPF,VPK,QM,QP                         00001800
 1002 FORMAT (' ',F8.2,6F10.3)                                          00001810
C                                                                       00001820
  500 CONTINUE                                                          00001830
      CALL INKEY                                                        00001840
C                                                                       00001850
  999 CONTINUE                                                          00001860
      RETURN                                                            00001870
      END                                                               00001880
```

```
C     ************************************************************************00000010
C     SUBROUTINE IPVEL                                                        00000020
C                                                                             00000030
C     THIS SUBROUTINE GENERATES THE VELOCITY PROFILE V(X,Z) AT                00000040
C     XVZ ALONG THE INTERACTION PLANE FOR THE TWO ROTOR CASE                  00000050
C     ************************************************************************00000060
C                                                                             00000070
      SUBROUTINE IPVEL(H,UN,RADIUS,UMB,XIP,YSEP,WSPD)                         00000080
C                                                                             00000090
      CHARACTER*1 KEY,KKEY                                                    00000100
C                                                                             00000110
      COMMON / CONSTS / PI,RHO,FPSPKN,RHOD2                                   00000120
      COMMON / PROFIL / RJ,ZBJ,ZHJ,ZMJ,UMJ,ZB,ZH,ZM,UM,CU,CY                 00000130
      COMMON / CKEY   / KEY,KKEY                                              00000140
      COMMON / UNITS  / IOU1,IOU6                                             00000150
C                                                                             00000160
C     ************************************************************************00000170
C                                                                             00000180
C     TF IS INTERACTION PLANE AMPLIFICATION FACTOR                            00000190
C                                                                             00000200
      TF = 1.55-(0.55)*EXP(-1.35*XIP)                                         00000210
C                                                                             00000220
C     OBTAIN PARAMETERS AT BASE RADIUS FOR THE 'BOUNDARY LAYER'               00000230
C                                                                             00000240
      RIPO = SQRT(XIP**2+YSEP**2)                                             00000250
C                                                                             00000260
      CALL PROPRM(H,UN,UMB,RIPO)                                              00000270
C                                                                             00000280
      ZIPB = ZB                                                               00000290
      ZIPM = ZM                                                               00000300
      ZIPH = ZH                                                               00000310
C                                                                             00000320
      RIPM = SQRT(XIP**2+(YSEP+ZIPM)**2)                                      00000330
C                                                                             00000340
      CALL PROPRM(H,UN,UMB,RIPM)                                              00000350
C                                                                             00000360
      UMM = UM                                                                00000370
C                                                                             00000380
C     PROMPT FOR DISPLAY INCREMENT AND RANGE                                  00000390
C                                                                             00000400
      CALL LOCATE(12,1)                                                       00000410
      WRITE(*,'(''ENTER VERTICAL INCREMENT DESIRED (FT)'',                    00000420
     1         ''       ===> ''\)')                                          00000430
      READ(*,*) DELZ                                                          00000440
      CALL LOCATE(14,1)                                                       00000450
      WRITE(*,'(''ENTER MAXIMUM HEIGHT FOR PROFILE (FT)'',                    00000460
     1         ''       ===> ''\)')                                          00000470
      READ(*,*) ZMAX                                                          00000480
C                                                                             00000490
      DELZ = DELZ/RADIUS                                                      00000500
      ZMAX = ZMAX/RADIUS                                                      00000510
      NPTS = IFIX(ZMAX/DELZ)+2                                                00000520
```

```
C                                                                       00000530
C     DIMENSIONALIZE VELOCITY PROFILE PARAMETERS                        00000540
C                                                                       00000550
      XXIP = RADIUS*XIP                                                 00000560
      ZZB  = ZIPB*RADIUS                                                00000570
      ZZH  = ZIPH*RADIUS                                                00000580
      ZZM  = ZIPM*RADIUS                                                00000590
C                                                                       00000600
      CALL CLS                                                          00000610
      IF(IOU6.NE.IOU1) WRITE(IOU6,'(''1'')')                            00000620
      WRITE(IOU6,1000) XXIP                                             00000630
 1000 FORMAT(' ',10X,'DUAL ROTOR VELOCITY PROFILE IN INTERACTION PLANE',00000640
     1     /,'0',12X,'           AT STATION (FT) ',F8.3,//)             00000650
C                                                                       00000660
C     OUTPUT THE VELOCITY AND DYNAMIC PRESSURE PROFILE HEADER           00000670
C                                                                       00000680
      WRITE(IOU6,1002)                                                  00000690
 1002 FORMAT(' ',2X,'HEIGHT',9X,'MEAN VELOCITY',7X,'PEAK VELOCITY',5X,  00000700
     1       'MEAN Q',4X,'PEAK Q',/,                                    00000710
     2       '0',4X,'(FT)',8X,'(FPS)',6X,'(KN)',5X,'(FPS)',6X,'(KN)',5X,00000720
     3       '(PSF)',5X,'(PSF)',/)                                      00000730
C                                                                       00000740
      LINES = 0                                                         00000750
C                                                                       00000760
C     'AN' IS ACTUALLY '= 1.0/7.0'                                      00000770
C                                                                       00000780
      AN = 0.142857142                                                  00000790
C                                                                       00000800
C     CALCULATE THE VELOCITY PROFILE POINTS FOR OUTPUT                  00000810
C                                                                       00000820
      DO 500 I = 1,NPTS                                                 00000830
C                                                                       00000840
      LINES = LINES+2                                                   00000850
      ZIP = DELZ*FLOAT(I-1)                                             00000860
C                                                                       00000870
C     GET MAX WALL JET VELOCITY AT EFFECTIVE RADIUS                     00000880
C                                                                       00000890
      RIP = SQRT(XIP**2+(YSEP+ZIP)**2)                                  00000900
C                                                                       00000910
      CALL PROPRM(H,UN,UMB,RIP)                                         00000920
C                                                                       00000930
      VN = UN                                                           00000940
      VZ = UM                                                           00000950
C                                                                       00000960
C     INTERACTION PLANE 'BOUNDARY LAYER'                                00000970
C                                                                       00000980
      IF(ZIP.LT.ZIPM) VZ = UMM*(ZIP/ZIPM)**AN                           00000990
C                                                                       00001000
C     DEVELOPED INTERACTION PLANE JET                                   00001010
C                                                                       00001020
      VH = TF*VZ*XIP/RIP                                                00001030
      VV = TF*VZ*(YSEP+ZIP)/RIP                                         00001040
```

```
C                                                                       00001050
      ZZ = ZIP*RADIUS                                                   00001060
C                                                                       00001070
C     MEAN VELOCITIES AND DYNAMIC PRESSURE                              00001080
C                                                                       00001090
      VHMF = VH*UN                                                      00001100
      VVMF = VV*UN                                                      00001110
      VHMK = VHMF/FPSPKN                                                00001120
      VVMK = VVMF/FPSPKN                                                00001130
C                                                                       00001140
C     PEAK VELOCITIES AND DYNAMIC PRESSURE                              00001150
C                                                                       00001160
      VMFD3I = (XIP*0.2444)+0.8                                         00001170
      IF(VMFD3I.GT.2.5) VMFD3I = 2.5                                    00001180
      VHPF = VMFD3I*VHMF                                                00001190
      VVPF = VMFD3I*VVMF                                                00001200
      VHPK = VHPF/FPSPKN                                                00001210
      VVPK = VVPF/FPSPKN                                                00001220
      IF(VHMF.EQ.0.)GOTO 55                                             00001230
C                                                                       00001240
C     THE EFFECT OF WIND IS TO ADD (DOWNWIND SIDE) OR                   00001250
C     SUBTRACT (UPWIND SIDE) TWO TIMES THE AMBIENT WIND                 00001260
C     VELOCITY TO THE HORIZONTAL PROFILE VELOCITY                       00001270
C                                                                       00001280
      XKW = (-0.5*H)+2.5                                                00001290
      IF(XKW.LT.1.0)XKW = 1.0                                           00001300
      WSPD2 = WSPD*XKW                                                  00001310
      VHMK = VHMK + WSPD2                                               00001320
      VHMF = VHMK*FPSPKN                                                00001330
      VHPK = VHPK + WSPD2                                               00001340
      VHPF = VHPK*FPSPKN                                                00001350
   55 CONTINUE                                                          00001360
C                                                                       00001370
C     DYNAMIC PRESSURE                                                  00001380
C                                                                       00001390
      QHM = RHOD2*VHMF**2                                               00001400
      QVM = RHOD2*VVMF**2                                               00001410
      QHP = RHOD2*VHPF**2                                               00001420
      QVP = RHOD2*VVPF**2                                               00001430
C                                                                       00001440
      IF(IOU6.EQ.IOU1) THEN                                             00001450
        IF(LINES.LT.12) GO TO 450                                       00001460
        LINES = 2                                                       00001470
        CALL INKEY                                                      00001480
        IF(KEY.NE.'C') GO TO 999                                        00001490
        WRITE(IOU6,1002)                                                00001500
      ENDIF                                                             00001510
C                                                                       00001520
  450 CONTINUE                                                          00001530
C                                                                       00001540
C     REPORT HORIZONTAL COMPONENTS OF VELOCITY PROFILE                  00001550
C                                                                       00001560
```

```
      WRITE(IOU6,1003) ZZ,VHMF,VHMK,VHPF,VHPK,QHM,QHP                00001570
 1003 FORMAT (' ',F8.2,2X,'H',6F10.3)                                00001580
C                                                                    00001590
C     REPORT VERTICAL COMPONENTS OF VELOCITY PROFILE                 00001600
C                                                                    00001610
      WRITE(IOU6,1004) VVMF,VVMK,VVPF,VVPK,QVM,QVP                   00001620
 1004 FORMAT (' ',10X,'V',6F10.3)                                    00001630
C                                                                    00001640
  500 CONTINUE                                                       00001650
      CALL INKEY                                                     00001660
C                                                                    00001670
  999 CONTINUE                                                       00001680
      RETURN                                                         00001690
      END                                                            00001700
```

```
C     ************************************************************************00000010
C     SUBROUTINE GDVTX                                                        00000020
C                                                                             00000030
C     THIS SUBROUTINE LOCATES THE GROUND VORTEX BASED ON THE                  00000040
C     EXPERIMENTS BY SUN AND CURTIS (PRINCETON UNIV.), AND THEN               00000050
C     DIRECTS THE CALCULATION OF ITS INDUCED VELOCITY FIELD                   00000060
C                                                                             00000070
C     THE OUTPUT FROM THIS SUBROUTINE SHOULD BE USED CAREFULLY                00000080
C     FOR GROSS ESTIMATION PURPOSES ONLY                                      00000090
C     ************************************************************************00000100
C                                                                             00000110
      SUBROUTINE GDVTX(H,RADIUS,AMU,CT,GAMG)                                  00000120
C                                                                             00000130
      CHARACTER*1 KEY,KKEY                                                    00000140
C                                                                             00000150
      COMMON / CONSTS / PI,RHO,FPSPKN,RHOD2                                   00000160
      COMMON / CHSVTX / XL1,YL1,ZL1,XL2,YL2,ZL2,XL3,YL3,ZL3,                  00000170
     1                  XR1,YR1,ZR1,XR2,YR2,ZR2,XR3,YR3,ZR3                   00000180
      COMMON / CKEY   / KEY,KKEY                                              00000190
      COMMON / UNITS  / IOU1,IOU6                                             00000200
C                                                                             00000210
C     ************************************************************************00000220
C                                                                             00000230
      HOD   = H/2.0                                                           00000240
      C1    = 1.0+1.2086*HOD**0.4374                                          00000250
      C2    = -0.2786*HOD**0.6757                                             00000260
      ZGV   = -10.0*AMU+0.6                                                   00000270
      XGV   = -(C1+C2*(AMU/CT))**2                                            00000280
      XXGV  = XGV*RADIUS                                                      00000290
      ZZGV  = ZGV*RADIUS                                                      00000300
C                                                                             00000310
C     ASSUME HORSESHOE SHAPE - ASSIGN LEFT AND RIGHT CORNERS                  00000320
C                                                                             00000330
      XL1 = XGV                                                               00000340
      YL1 = -1.0                                                              00000350
      ZL1 = ZGV                                                               00000360
C                                                                             00000370
      XR1 = XGV                                                               00000380
      YR1 = 1.0                                                               00000390
      ZR1 = ZGV                                                               00000400
C                                                                             00000410
C     SET UP DIRECTION POINTERS FOR TRAILER ELEMENTS                          00000420
C                                                                             00000430
      XL2 = XL1+1.0                                                           00000440
      YL2 = YL1                                                               00000450
      ZL2 = ZL1                                                               00000460
C                                                                             00000470
      XR2 = XR1+1.0                                                           00000480
      YR2 = YR1                                                               00000490
      ZR2 = ZR1                                                               00000500
C                                                                             00000510
      XL3 = XL2+1.0                                                           00000520
```

```
      YL3 = YL2                                                          00000530
      ZL3 = ZL2                                                          00000540
C                                                                        00000550
      XR3 = XR2+1.0                                                      00000560
      YR3 = YR2                                                          00000570
      ZR3 = ZR2                                                          00000580
C                                                                        00000590
      CALL LOCATE(18,1)                                                  00000600
      WRITE(*,1001) GAMG                                                 00000610
 1001 FORMAT(' ',5X,'GROUND VORTEX CIRCULATION (FT**2/SEC) ',F15.5)      00000620
      WRITE(*,1002) XXGV,ZZGV                                            00000630
 1002 FORMAT(' ',5X,' VORTEX POSITION XGV,ZGV (FT)   ',F8.3,' ,',F8.3//)00000640
      PAUSE ' '                                                          00000650
      CALL CLS                                                           00000660
C                                                                        00000670
C     GET ZMAX,DELZ FROM USER                                            00000680
C                                                                        00000690
      CALL LOCATE(10,1)                                                  00000700
      WRITE(*,'(''ENTER (XT,YT) TARGET POINTS (FT) '')')                 00000710
      WRITE(*,'(''                              XT  ===> ''\)')          00000720
      READ(*,*) XT                                                       00000730
      WRITE(*,'(''                              YT  ===> ''\)')          00000740
      READ(*,*) YT                                                       00000750
      CALL LOCATE(14,1)                                                  00000760
      WRITE(*,'(''ENTER VERTICAL INCREMENT DESIRED (FT) ===> ''\)')      00000770
      READ(*,*) DELZ                                                     00000780
      CALL LOCATE(16,1)                                                  00000790
      WRITE(*,'(''ENTER MAXIMUM HEIGHT FOR PROFILE (FT) ===> ''\)')      00000800
      READ(*,*) ZMAX                                                     00000810
C                                                                        00000820
      DELZ = DELZ/RADIUS                                                 00000830
      ZMAX = ZMAX/RADIUS                                                 00000840
C                                                                        00000850
      PAUSE ' '                                                          00000860
      CALL CLS                                                           00000870
C                                                                        00000880
C     WRITE OUTPUT HEADER                                                00000890
C                                                                        00000900
      IF(IOU6.NE.IOU1) WRITE(IOU6,'(''1'')')                             00000910
      WRITE(IOU6,1100)                                                   00000920
 1100 FORMAT(' ',2X,'HEIGHT',9X,'MEAN VELOCITY',5X,'MEAN Q',/,          00000930
     1       '0',4X,'(FT)',8X,'(FPS)',6X,'(KN)',5X,'(PSF)',/)           00000940
C                                                                        00000950
C     SET UP SWEEP OF Z AT SPECIFIED X,Y                                 00000960
C                                                                        00000970
      XT = XT/RADIUS                                                     00000980
      YT = YT/RADIUS                                                     00000990
      NPTS = IFIX(ZMAX/DELZ)+2                                           00001000
      LINES = 0                                                          00001010
C                                                                        00001020
      DO 200 I=1,NPTS                                                    00001030
      LINES = LINES + 4                                                  00001040
```

```
      ZT = (I-1)*DELZ                                                  00001050
C                                                                      00001060
      CALL HSVTX(XT,YT,ZT,VXF,VYF,VZF,GAMG,RADIUS)                     00001070
C                                                                      00001080
      ZZ = ZT*RADIUS                                                   00001090
      VTF = SQRT(VXF**2+VYF**2+VZF**2)                                 00001100
      VXK = VXF/FPSPKN                                                 00001110
      VYK = VYF/FPSPKN                                                 00001120
      VZK = VZF/FPSPKN                                                 00001130
      VTK = VTF/FPSPKN                                                 00001140
C                                                                      00001150
      QX  = RHOD2*VXF**2                                               00001160
      QY  = RHOD2*VYF**2                                               00001170
      QZ  = RHOD2*VZF**2                                               00001180
      QT  = RHOD2*VTF**2                                               00001190
C                                                                      00001200
      IF (IOU6.EQ.IOU1) THEN                                           00001210
        IF(LINES.LE.12) GO TO 100                                      00001220
        LINES = 4                                                      00001230
        CALL INKEY                                                     00001240
        IF(KEY.NE.'C') GO TO 999                                       00001250
        WRITE(IOU6,1100)                                               00001260
      ENDIF                                                            00001270
C                                                                      00001280
  100 CONTINUE                                                         00001290
C                                                                      00001300
C     REPORT X COMPONENT OF VELOCITY                                   00001310
C                                                                      00001320
      WRITE(IOU6,1101) ZZ,VXF,VXK,QX                                   00001330
 1101 FORMAT (' ',F8.2,2X,'X',3F10.3)                                  00001340
C                                                                      00001350
C     REPORT Y COMPONENT OF VELOCITY                                   00001360
C                                                                      00001370
      WRITE(IOU6,1102) VYF,VYK,QY                                      00001380
 1102 FORMAT (' ',10X,'Y',3F10.3)                                      00001390
C                                                                      00001400
C     REPORT Z COMPONENT OF VELOCITY                                   00001410
C                                                                      00001420
      WRITE(IOU6,1103) VZF,VZK,QZ                                      00001430
 1103 FORMAT (' ',10X,'Z',3F10.3)                                      00001440
C                                                                      00001450
C     REPORT TOTAL VELOCITY                                            00001460
C                                                                      00001470
      WRITE(IOU6,1104) VTF,VTK,QT                                      00001480
 1104 FORMAT (' ',10X,'T',3F10.3)                                      00001490
C                                                                      00001500
  200 CONTINUE                                                         00001510
      CALL INKEY                                                       00001520
C                                                                      00001530
  999 CONTINUE                                                         00001540
C                                                                      00001550
      RETURN                                                           00001560
```

```
C     ************************************************************************00000010
C     SUBROUTINE DEVTX                                                        00000020
C                                                                             00000030
C     THIS SUBROUTINE LOCATES THE DISK EDGE VORTEX SYSTEM, AND                00000040
C     DIRECTS THE CALCULATION OF ITS INDUCED VELOCITY FIELD                   00000050
C     ************************************************************************00000060
C                                                                             00000070
      SUBROUTINE DEVTX(H,RADIUS,GAMW,CHI)                                     00000080
C                                                                             00000090
      CHARACTER*1 KEY,KKEY                                                    00000100
C                                                                             00000110
      COMMON / CONSTS / PI,RHO,FPSPKN,RHOD2                                   00000120
      COMMON / CHSVTX / XL1,YL1,ZL1,XL2,YL2,ZL2,XL3,YL3,ZL3,                  00000130
     1                  XR1,YR1,ZR1,XR2,YR2,ZR2,XR3,YR3,ZR3                   00000140
      COMMON / CKEY   / KEY,KKEY                                              00000150
      COMMON / UNITS  / IOU1,IOU6                                             00000160
C                                                                             00000170
C     ************************************************************************00000180
C                                                                             00000190
C     ASSUME HORSESHOE SHAPE - ASSIGN LEFT AND RIGHT CORNERS                  00000200
C                                                                             00000210
      XL1 = 0.0                                                               00000220
      YL1 = -1.0                                                              00000230
      ZL1 = H                                                                 00000240
C                                                                             00000250
      XR1 = 0.0                                                               00000260
      YR1 = 1.0                                                               00000270
      ZR1 = H                                                                 00000280
C                                                                             00000290
C     SET UP DIRECTION POINTERS FOR TRAILER ELEMENTS                          00000300
C     POINT 2 IS AT GROUND IMPINGEMENT                                        00000310
C                                                                             00000320
      XL2 = XL1+H/TAN(CHI)                                                    00000330
      YL2 = YL1                                                               00000340
      ZL2 = 0.0                                                               00000350
C                                                                             00000360
      XR2 = XR1+H/TAN(CHI)                                                    00000370
      YR2 = YR1                                                               00000380
      ZR2 = 0.0                                                               00000390
C                                                                             00000400
C     POINT THREE EXTENDS TRAILER PARALLEL TO GROUND                          00000410
C                                                                             00000420
      XL3 = XL2+1.0                                                           00000430
      YL3 = YL2                                                               00000440
      ZL3 = ZL2                                                               00000450
C                                                                             00000460
      XR3 = XR2+1.0                                                           00000470
      YR3 = YR2                                                               00000480
      ZR3 = ZR2                                                               00000490
C                                                                             00000500
C     GET ZMAX,DELZ FROM USER                                                 00000510
C                                                                             00000520
```

```
      CALL LOCATE(10,1)                                                  00000530
      WRITE(*,'(''ENTER (XT,YT) TARGET POINTS (FT) '')')                 00000540
      WRITE(*,'(''                                XT  ===> ''\)')        00000550
      READ(*,*) XT                                                       00000560
      WRITE(*,'(''                                YT  ===> ''\)')        00000570
      READ(*,*) YT                                                       00000580
      CALL LOCATE(14,1)                                                  00000590
      WRITE(*,'(''ENTER VERTICAL INCREMENT DESIRED (FT) ===> ''\)')      00000600
      READ(*,*) DELZ                                                     00000610
      CALL LOCATE(16,1)                                                  00000620
      WRITE(*,'(''ENTER MAXIMUM HEIGHT FOR PROFILE (FT) ===> ''\)')      00000630
      READ(*,*) ZMAX                                                     00000640
C                                                                        00000650
      DELZ = DELZ/RADIUS                                                 00000660
      ZMAX = ZMAX/RADIUS                                                 00000670
C                                                                        00000680
C     WRITE OUTPUT HEADER                                                00000690
C                                                                        00000700
      CALL CLS                                                           00000710
      IF(IOU6.NE.IOU1) WRITE(IOU6,'(''1'')')                             00000720
      WRITE(IOU6,1000) XT,YT                                             00000730
 1000 FORMAT(' ',5X,'DISK VORTEX VELOCITY PROFILE AT POINTS X,Y (FT) ',  00000740
     1       F8.3,',',F8.3,//)                                           00000750
      WRITE(*,1001) GAMW                                                 00000760
 1001 FORMAT(' ',5X,'VORTEX CIRCULATION (FT**2/SEC) ',F12.2)             00000770
      CHID = CHI*180.0/PI                                                00000780
      WRITE(*,1005) CHID                                                 00000790
 1005 FORMAT(' ',5X,'SETTLING ANGLE (DEG)           ',F12.2//)          00000800
C                                                                        00000810
      PAUSE ' '                                                          00000820
      CALL CLS                                                           00000830
C                                                                        00000840
      WRITE(IOU6,1100)                                                   00000850
 1100 FORMAT(' ',2X,'HEIGHT',9X,'MEAN VELOCITY',5X,'MEAN Q',/,           00000860
     1       'O',4X,'(FT)',8X,'(FPS)',6X,'(KN)',5X,'(PSF)',/)            00000870
C                                                                        00000880
C     SET UP SWEEP OF Z AT SPECIFIED X,Y                                 00000890
C                                                                        00000900
      XT = XT/RADIUS                                                     00000910
      YT = YT/RADIUS                                                     00000920
      NPTS = IFIX(ZMAX/DELZ)+2                                           00000930
      LINES = 0                                                          00000940
C                                                                        00000950
      DO 200 I=1,NPTS                                                    00000960
      LINES = LINES + 4                                                  00000970
      ZT = (I-1)*DELZ                                                    00000980
C                                                                        00000990
      CALL HSVTX(XT,YT,ZT,VXF,VYF,VZF,GAMW,RADIUS)                       00001000
C                                                                        00001010
      ZZ = ZT*RADIUS                                                     00001020
      VTF = SQRT(VXF**2+VYF**2+VZF**2)                                   00001030
      VXK = VXF/FPSPKN                                                   00001040
```

```
      VYK = VYF/FPSPKN                                          00001050
      VZK = VZF/FPSPKN                                          00001060
      VTK = VTF/FPSPKN                                          00001070
C                                                               00001080
      QX  = RHOD2*VXF**2                                        00001090
      QY  = RHOD2*VYF**2                                        00001100
      QZ  = RHOD2*VZF**2                                        00001110
      QT  = RHOD2*VTF**2                                        00001120
C                                                               00001130
      IF(IOU6.EQ.IOU1) THEN                                     00001140
        IF(LINES.LE.12) GO TO 100                               00001150
        LINES = 4                                               00001160
        CALL INKEY                                              00001170
        IF(KEY.NE.'C') GO TO 999                                00001180
        WRITE(IOU6,1100)                                        00001190
      ENDIF                                                     00001200
C                                                               00001210
  100 CONTINUE                                                  00001220
C                                                               00001230
C     REPORT X COMPONENT OF VELOCITY                            00001240
C                                                               00001250
      WRITE(IOU6,1101) ZZ,VXF,VXK,QX                            00001260
 1101 FORMAT (' ',F8.2,2X,'X',3F10.3)                           00001270
C                                                               00001280
C     REPORT Y COMPONENT OF VELOCITY                            00001290
C                                                               00001300
      WRITE(IOU6,1102) VYF,VYK,QY                               00001310
 1102 FORMAT (' ',10X,'Y',3F10.3)                               00001320
C                                                               00001330
C     REPORT Z COMPONENT OF VELOCITY                            00001340
C                                                               00001350
      WRITE(IOU6,1103) VZF,VZK,QZ                               00001360
 1103 FORMAT (' ',10X,'Z',3F10.3)                               00001370
C                                                               00001380
C     REPORT TOTAL VELOCITY                                     00001390
C                                                               00001400
      WRITE(IOU6,1104) VTF,VTK,QT                               00001410
 1104 FORMAT (' ',10X,'T',3F10.3)                               00001420
C                                                               00001430
  200 CONTINUE                                                  00001440
      CALL INKEY                                                00001450
C                                                               00001460
  999 CONTINUE                                                  00001470
C                                                               00001480
      RETURN                                                    00001490
      END                                                       00001500
```

```
C     ************************************************************************00000010
C     SUBROUTINE HSVTX                                                        00000020
C                                                                             00000030
C     THIS SUBROUTINE DIRECTS THE CALCULATION OF THE INDUCED VELOCITY         00000040
C     FIELD DUE TO A HORSESHOE VORTEX SYSTEM OF UNIT STRENGTH.  POINT 1       00000050
C     (LEFT = L1, RIGHT = R1) DEFINE THE EXTENT OF THE BOUND PORTION OF       00000060
C     THE HORSESHOE.  THE TRAILERS START AT POINT 1 AND EXTEND THROUGH        00000070
C     POINT 2, AND THEN ON TO POINT 3.  THIS ALLOWS TWO ELEMENTS FOR          00000080
C     EACH TRAILER SO THAT IT CAN 'BEND' TO ACCOUNT FOR GROUND CONTACT.       00000090
C     ************************************************************************00000100
C                                                                             00000110
      SUBROUTINE HSVTX(XT,YT,ZT,VX,VY,VZ,GAMMA,RADIUS)                        00000120
C                                                                             00000130
      COMMON / CHSVTX / XL1,YL1,ZL1,XL2,YL2,ZL2,XL3,YL3,ZL3,                  00000140
     1                  XR1,YR1,ZR1,XR2,YR2,ZR2,XR3,YR3,ZR3                   00000150
      COMMON / CVLINE / IFI,XA,YA,ZA,XB,YB,ZB,XC,YC,ZC,Q1,Q2,Q3               00000160
C                                                                             00000170
C     ************************************************************************00000180
C                                                                             00000190
C     AT SPECIFIED (X,Y,Z) TARGET POINT IN VICINITY OF ROTOR, CALCULATE       00000200
C     THE VECTOR VELOCITY                                                     00000210
C                                                                             00000220
      VX = 0.0                                                                00000230
      VY = 0.0                                                                00000240
      VZ = 0.0                                                                00000250
C                                                                             00000260
      XC = XT                                                                 00000270
      YC = YT                                                                 00000280
      ZC = ZT                                                                 00000290
C                                                                             00000300
C     LEFT TRAILER CONTRIBUTION, POINT 1 TO POINT 2                           00000310
C                                                                             00000320
      IFI = 0                                                                 00000330
      XA = XL1                                                                00000340
      YA = YL1                                                                00000350
      ZA = ZL1                                                                00000360
      XB = XL2                                                                00000370
      YB = YL2                                                                00000380
      ZB = ZL2                                                                00000390
C                                                                             00000400
      CALL VLINE                                                              00000410
C                                                                             00000420
      VX = VX - Q1                                                            00000430
      VY = VY - Q2                                                            00000440
      VZ = VZ - Q3                                                            00000450
C                                                                             00000460
C     LEFT TRAILER IMAGE                                                      00000470
C                                                                             00000480
      ZA = -ZA                                                                00000490
      ZB = -ZB                                                                00000500
C                                                                             00000510
      CALL VLINE                                                              00000520
```

```
C                                                                       00000530
      VX = VX + Q1                                                      00000540
      VY = VY + Q2                                                      00000550
      VZ = VZ + Q3                                                      00000560
C                                                                       00000570
C     LEFT TRAILER CONTRIBUTION, POINT 2 TO POINT 3                     00000580
C                                                                       00000590
      IFI = 1                                                           00000600
      XA = XL2                                                          00000610
      YA = YL2                                                          00000620
      ZA = ZL2                                                          00000630
      XB = XL3                                                          00000640
      YB = YL3                                                          00000650
      ZB = ZL3                                                          00000660
C                                                                       00000670
      CALL VLINE                                                        00000680
C                                                                       00000690
      VX = VX - Q1                                                      00000700
      VY = VY - Q2                                                      00000710
      VZ = VZ - Q3                                                      00000720
C                                                                       00000730
C     LEFT TRAILER IMAGE                                                00000740
C                                                                       00000750
      ZA = -ZA                                                          00000760
      ZB = -ZB                                                          00000770
C                                                                       00000780
      CALL VLINE                                                        00000790
C                                                                       00000800
      VX = VX + Q1                                                      00000810
      VY = VY + Q2                                                      00000820
      VZ = VZ + Q3                                                      00000830
C                                                                       00000840
C     SPANWISE VORTEX CONTRIBUTION                                      00000850
C                                                                       00000860
      IFI = 0                                                           00000870
      XA = XL1                                                          00000880
      YA = YL1                                                          00000890
      ZA = ZL1                                                          00000900
      XB = XR1                                                          00000910
      YB = YR1                                                          00000920
      ZB = ZR1                                                          00000930
C                                                                       00000940
      CALL VLINE                                                        00000950
C                                                                       00000960
      VX = VX + Q1                                                      00000970
      VY = VY + Q2                                                      00000980
      VZ = VZ + Q3                                                      00000990
C                                                                       00001000
C     SPANWISE VORTEX IMAGE                                             00001010
C                                                                       00001020
      ZA = -ZA                                                          00001030
      ZB = -ZB                                                          00001040
```

```
C                                                                       00001050
      CALL VLINE                                                        00001060
C                                                                       00001070
      VX = VX - Q1                                                      00001080
      VY = VY - Q2                                                      00001090
      VZ = VZ - Q3                                                      00001100
C                                                                       00001110
C     RIGHT TRAILER CONTRIBUTION, POINT 1 TO POINT 2                    00001120
C                                                                       00001130
      IFI = 0                                                           00001140
      XA = XR1                                                          00001150
      YA = YR1                                                          00001160
      ZA = ZR1                                                          00001170
      XB = XR2                                                          00001180
      YB = YR2                                                          00001190
      ZB = ZR2                                                          00001200
C                                                                       00001210
      CALL VLINE                                                        00001220
C                                                                       00001230
      VX = VX + Q1                                                      00001240
      VY = VY + Q2                                                      00001250
      VZ = VZ + Q3                                                      00001260
C                                                                       00001270
C     RIGHT TRAILER IMAGE                                               00001280
C                                                                       00001290
      ZA = -ZA                                                          00001300
      ZB = -ZB                                                          00001310
C                                                                       00001320
      CALL VLINE                                                        00001330
C                                                                       00001340
      VX = VX - Q1                                                      00001350
      VY = VY - Q2                                                      00001360
      VZ = VZ - Q3                                                      00001370
C                                                                       00001380
C     RIGHT TRAILER CONTRIBUTION, POINT 2 TO POINT 3                    00001390
C                                                                       00001400
      IFI = 1                                                           00001410
      XA = XR2                                                          00001420
      YA = YR2                                                          00001430
      ZA = ZR2                                                          00001440
      XB = XR3                                                          00001450
      YB = YR3                                                          00001460
      ZB = ZR3                                                          00001470
C                                                                       00001480
      CALL VLINE                                                        00001490
C                                                                       00001500
      VX = VX + Q1                                                      00001510
      VY = VY + Q2                                                      00001520
      VZ = VZ + Q3                                                      00001530
C                                                                       00001540
C     RIGHT TRAILER IMAGE                                               00001550
C                                                                       00001560
```

```
      ZA = -ZA                                                  00001570
      ZB = -ZB                                                  00001580
C                                                               00001590
      CALL VLINE                                                00001600
C                                                               00001610
      VX = VX - Q1                                              00001620
      VY = VY - Q2                                              00001630
      VZ = VZ - Q3                                              00001640
C                                                               00001650
C     DIMENSIONALIZE                                            00001660
C                                                               00001670
      GDR= GAMMA/RADIUS                                         00001680
      VX = VX*GDR                                               00001690
      VY = VY*GDR                                               00001700
      VZ = VZ*GDR                                               00001710
C                                                               00001720
      RETURN                                                    00001730
      END                                                       00001740
```

```
C     ******************************************************************00000010
C     SUBROUTINE VLINE                                                  00000020
C                                                                       00000030
C     THIS SUBROUTINE APPLIES THE BIOT-SAVORT LAW TO                    00000040
C     CALCULATE THE VELOCITY INDUCED BY A LINE VORTEX                   00000050
C                                                                       00000060
C     XA,YA,ZA = STARTING POINT OF VORTEX                               00000070
C     XB,YB,ZB = ENDING POINT, OR DIRECTION POINTER                     00000080
C     XC,YC,ZC = TARGET POINT WHERE VELOCITY IS INDUCED                 00000090
C                                                                       00000100
C     IFI = 0     VORTEX IS FINITE, FROM POINT A TO POINT B             00000110
C     IFI = 1     VORTEX IS SEMI-INFINITE FROM POINT A THROUGH B        00000120
C                                                                       00000130
C     ******************************************************************00000140
C                                                                       00000150
      SUBROUTINE VLINE                                                  00000160
C                                                                       00000170
      COMMON / CONSTS / PI,RHO,FPSPKN,RHOD2                             00000180
      COMMON / CVLINE / IFI,XA,YA,ZA,XB,YB,ZB,XC,YC,ZC,Q1,Q2,Q3         00000190
C                                                                       00000200
C     ******************************************************************00000210
C                                                                       00000220
      A  = (XA-XC)**2 + (YA-YC)**2 + (ZA-ZC)**2                         00000230
      B  = 2.0*( (XA-XB)*(XC-XA) + (YA-YB)*(YC-YA) + (ZA-ZB)*(ZC-ZA) )  00000240
      C  = (XA-XB)**2 + (YA-YB)**2 + (ZA-ZB)**2                         00000250
C                                                                       00000260
      C1 = (YC-YB)*ZA + (YA-YC)*ZB + (YB-YA)*ZC                         00000270
      C2 = (ZC-ZB)*XA + (ZA-ZC)*XB + (ZB-ZA)*XC                         00000280
      C3 = (XC-XB)*YA + (XA-XC)*YB + (XB-XA)*YC                         00000290
C                                                                       00000300
      Q  = 4.0*A*C - B**2                                               00000310
C                                                                       00000320
C     CHECK FOR COLINEAR TARGET POINT                                   00000330
C                                                                       00000340
      QB = 0.0                                                          00000350
      IF(ABS(Q).LT.1.0E-06) GOTO 100                                    00000360
C                                                                       00000370
C     FINITE LENGTH VORTEX                                              00000380
C                                                                       00000390
      IF(IFI.EQ.0) QB = 1.0/Q*((2.0*C+B)/SQRT(A+B+C)-B/SQRT(A))/2.0/PI  00000400
C                                                                       00000410
C     SEMI-INFINITE VORTEX                                              00000420
C                                                                       00000430
      IF(IFI.EQ.1) QB = 1.0/Q*(2.0*SQRT(C)-B/SQRT(A))/2.0/PI            00000440
C                                                                       00000450
  100 CONTINUE                                                          00000460
C                                                                       00000470
C     VELOCITY COMPONENTS                                               00000480
C                                                                       00000490
      Q1 = C1*QB                                                        00000500
      Q2 = C2*QB                                                        00000510
      Q3 = C3*QB                                                        00000520
```

Source File: **ROTHAZ.FOR** Program Unit: **VLINE**

```
C                                                              00000530
      RETURN                                                   00000540
      END                                                      00000550
```

```
C     ************************************************************************00000010
C     SUBROUTINE INKEY                                                        00000020
C     ************************************************************************00000030
C                                                                             00000040
      SUBROUTINE INKEY                                                        00000050
C                                                                             00000060
      CHARACTER*1 KEY,KKEY                                                    00000070
C                                                                             00000080
      COMMON / CKEY   / KEY,KKEY                                              00000090
C                                                                             00000100
C     ************************************************************************00000110
C                                                                             00000120
      WRITE(*,*) ' '                                                          00000130
      IF(KKEY.EQ.'H')GOTO 20                                                  00000140
C                                                                             00000150
      WRITE(*,10)                                                             00000160
   10 FORMAT (' ',8X,'PRESS <C> TO CONTINUE',/,                               00000170
     1        ' ',8X,'       <P> FOR NEW TARGET POINT',/,                    00000180
     2        ' ',8X,'       <N> FOR NEW ROTORCRAFT',/,                      00000190
     3        ' ',8X,'       <A> FOR NEW CASE',/,                            00000200
     4        ' ',8X,'       <X> TO EXIT           ===> '\)                  00000210
      READ(*,'(A)') KEY                                                       00000220
      GOTO 30                                                                 00000230
C                                                                             00000240
   20 CONTINUE                                                                00000250
C                                                                             00000260
      WRITE(*,12)                                                             00000270
   12 FORMAT (' ',//,9X,'PRESS <C> TO CONTINUE',/,                            00000280
     1        ' ',8X,'       <P> FOR NEW TARGET POINT',/,                    00000290
     2        ' ',8X,'       <R> FOR RETURN TO MAIN PROGRAM',/,              00000300
     3        ' ',8X,'       <X> TO EXIT              ===> '\)               00000310
      READ(*,'(A)') KEY                                                       00000320
C                                                                             00000330
   30 CONTINUE                                                                00000340
      CALL CLS                                                                00000350
C                                                                             00000360
      RETURN                                                                  00000370
      END                                                                     00000380
```

```
C     ************************************************************************00000010
C     SUBROUTINE IOINIT                                                       00000020
C                                                                             00000030
C     THIS SUBROUTINE OPENS FILES FOR                                         00000040
C     I/O, AND DISPLAYS PROGRAM BANNER                                        00000050
C     ************************************************************************00000060
C                                                                             00000070
      SUBROUTINE IOINIT                                                       00000080
C                                                                             00000090
      CHARACTER*14 OPFILE                                                     00000100
C                                                                             00000110
      COMMON / UNITS / IOU1,IOU6                                              00000120
C                                                                             00000130
C     ************************************************************************00000140
C                                                                             00000150
C     ASSIGN DEFAULT VALUES TO I/O UNIT POINTERS                              00000160
C                                                                             00000170
C           CONSOLE         = IOU1                                            00000180
C           STANDARD OUTPUT = IOU6                                            00000190
C                                                                             00000200
      IOU1  = 0                                                               00000210
      IOU6  = 6                                                               00000220
C                                                                             00000230
C     CLEAR THE DISPLAY                                                       00000240
C                                                                             00000250
      CALL CLS                                                                00000260
C                                                                             00000270
C     DISPLAY PROGRAM BANNER                                                  00000280
C                                                                             00000290
      CALL LOCATE(5,1)                                                        00000300
      WRITE(*,10)                                                             00000310
   10 FORMAT(' ',10X,' PROGRAM ROTHAZ - ROTORCRAFT DOWNWASH HAZARD',          00000320
     1               ' ANALYSIS',//,                                          00000330
     2            7X,' SYSTEMS TECHNOLOGY,',                                  00000340
     3               ' INC./COMPUTATIONAL METHODOLOGY ASSOCIATES'//,          00000350
     4         /,26X,'   1 OCTOBER 1985',                                     00000360
     5         /,26X,' PROGRAM VERSION 1.0',/////)                           00000370
C                                                                             00000380
      PAUSE ' '                                                               00000390
      CALL CLS                                                                00000400
C                                                                             00000410
C     REDIRECT I/O UNITS IF REQUESTED                                         00000420
C                                                                             00000430
      CALL LOCATE(10,1)                                                       00000440
      WRITE(*,'(''TABULAR LISTINGS MAY BE WRITTEN TO A'')')                   00000450
      WRITE(*,'('' FILE OR ANY DOS OUTPUT DEVICE ...'')')                     00000460
      WRITE(*,*) ' '                                                          00000470
      WRITE(*,'('' FOR CONSOLE OUTPUT ENTER CON'')')                          00000480
      WRITE(*,'('' FOR PRINTER OUTPUT ENTER PRN, LPT1, OR LPT2'')')           00000490
      WRITE(*,*) ' '                                                          00000500
      WRITE(*,'('' ENTER OUTPUT DEVICE OR FILE   ===> ''\)')                  00000510
      READ(*,'(A)') OPFILE                                                    00000520
```

Source File: **ROTHAZ.FOR** Program Unit: **IOINIT**

```
C                                                                  00000530
      IF (OPFILE.EQ.'CON') THEN                                    00000540
         IOU6 = IOU1                                               00000550
      ELSE                                                         00000560
         OPEN (IOU6,FILE=OPFILE)                                   00000570
      ENDIF                                                        00000580
C                                                                  00000590
      RETURN                                                       00000600
      END                                                          00000610
```

```
C     ***************************************************************00000010
C     SUBROUTINE HAZARD                                               00000020
C                                                                     00000030
C     THIS SUBROUTINE IS THE MAINLINE DRIVER                          00000040
C     FOR THE CALCULATION OF SPECIFIC HAZARDS                         00000050
C     ***************************************************************00000060
C                                                                     00000070
      SUBROUTINE HAZARD                                               00000080
C                                                                     00000090
      CHARACTER*1 KEY,KKEY,FLOW,HAZTYP,HUMTYP                         00000100
C                                                                     00000110
      COMMON / CONSTS / PI,RHO,FPSPKN,RHOD2                           00000120
      COMMON / HELGEO / H,DL,YSEP,WSPD,RADIUS                         00000130
      COMMON / UNITS  / IOU1,IOU6                                     00000140
      COMMON / PROFIL / RJ,ZBJ,ZHJ,ZMJ,UMJ,ZB,ZH,ZM,UM,CU,CY         00000150
      COMMON / CKEY   / KEY,KKEY                                      00000160
C                                                                     00000170
C     ***************************************************************00000180
C                                                                     00000190
      CALL CLS                                                        00000200
      CALL LOCATE(10,1)                                               00000210
C                                                                     00000220
      WRITE(*,12)                                                     00000230
   12 FORMAT (' ',8X,'SELECT TYPE OF HAZARD',//,                      00000240
     1        ' ',9X,'PRESS <M> FOR OVERTURNING MOMENT',/,            00000250
     2        ' ',9X,'PRESS <C> FOR PARTICULATE CLOUD ',/,            00000260
     3        ' ',9X,'PRESS <X> TO EXIT                  ===> '\)     00000270
      READ(*,'(A)') HAZTYP                                            00000280
      IF(HAZTYP.EQ.'C')GOTO 14                                        00000290
C                                                                     00000300
      CALL CLS                                                        00000310
      CALL LOCATE(10,1)                                               00000320
C                                                                     00000330
      WRITE(*,10)                                                     00000340
   10 FORMAT (' ',8X,'SELECT TYPE OF FLOW TO BE ESTIMATED',//,        00000350
     1        ' ',9X,'PRESS <W> FOR WALL JET',/,                      00000360
     2        ' ',9X,'      <I> FOR INTERACTION PLANE',/,             00000370
     3        ' ',9X,'      <X> TO EXIT                  ===> '\)     00000380
      READ(*,'(A)') FLOW                                              00000390
C                                                                     00000400
   14 CONTINUE                                                        00000410
      CALL CLS                                                        00000420
      IF(FLOW.EQ.'X') GOTO 999                                        00000430
C                                                                     00000440
C     **********************                                          00000450
C     RADIAL WALL JET FLOWS                                           00000460
C     **********************                                          00000470
C                                                                     00000480
C     ACCELERATED SLIPSTREAM MEAN VELOCITY                            00000490
C                                                                     00000500
      UN = SQRT(2.0*DL/RHO)                                           00000510
C                                                                     00000520
```

```
C     GROUND EFFECT CORRECTION                                          00000530
C                                                                       00000540
      AKG = 1.0 -0.9*EXP(-2.0*H)                                        00000550
C                                                                       00000560
C     MEAN VELOCITY AT ROTOR DISK (RATIOED TO UN)                       00000570
C                                                                       00000580
      UB = AKG/2.0                                                      00000590
C                                                                       00000600
C     FIND INITIAL RADIUS OF WALL JET                                   00000610
C                                                                       00000620
      CALL WALJET(H,UB,UN,UMB,RADIUS)                                   00000630
C                                                                       00000640
  500 CONTINUE                                                          00000650
C                                                                       00000660
      IF(KEY.EQ.'X') GOTO 999                                           00000670
      IF(KEY.EQ.'R') GOTO 999                                           00000680
C                                                                       00000690
      IF(HAZTYP.EQ.'C')GOTO 15                                          00000700
C                                                                       00000710
      CALL LOCATE(10,1)                                                 00000720
      WRITE(*,16)                                                       00000730
   16 FORMAT (' ',8X,'SELECT TYPE OF HUMAN SUBJECT',//,                 00000740
     1        ' ',9X,'PRESS <L> FOR LARGE (ADULT)',/,                  00000750
     4        ' ',9X,'PRESS <S> FOR SMALL (CHILD)       ===> '\)        00000760
      READ(*,'(A)') HUMTYP                                              00000770
C                                                                       00000780
   15 CONTINUE                                                          00000790
C                                                                       00000800
      CALL CLS                                                          00000810
      CALL LOCATE(10,1)                                                 00000820
C                                                                       00000830
      IF(FLOW.EQ.'I')GOTO 700                                           00000840
      IF(HAZTYP.EQ.'C')GOTO 800                                         00000850
C                                                                       00000860
  600 CONTINUE                                                          00000870
C                                                                       00000880
C     WALL JET REGION                                                   00000890
C                                                                       00000900
      WRITE(*,'(''ENTER LOWEST OTMOMENT WJET RADIUS (FT) '',            00000910
     1            ''===> ''\)')                                         00000920
      READ(*,*) RRVZ                                                    00000930
      RVZ = RRVZ/RADIUS                                                 00000940
C                                                                       00000950
C     GENERATE VELOCITY PROFILE AT RVZ IN WALL JET REGION               00000960
C                                                                       00000970
      CALL HWJVEL(H,UN,UMB,RVZ,RADIUS,WSPD,HUMTYP)                      00000980
C                                                                       00000990
      GO TO 500                                                         00001000
C                                                                       00001010
  700 CONTINUE                                                          00001020
C                                                                       00001030
C     INTERACTION PLANE UPWASH DEFLECTION ZONE                          00001040
```

```
C                                                                       00001050
      WRITE(*,'(''ENTER LOWEST OTMOMENT IPLANE DISTANCE (FT) '',        00001060
     1            ''===> ''\)')                                         00001070
      READ(*,*) XXIP                                                    00001080
      XIP = XXIP/RADIUS                                                 00001090
C                                                                       00001100
C     GENERATE VELOCITY PROFILE AT XIP IN INTERACTION PLANE             00001110
C                                                                       00001120
      CALL HIPVEL(H,UN,RADIUS,UMB,XIP,YSEP,WSPD,HUMTYP)                 00001130
C                                                                       00001140
      GO TO 500                                                         00001150
C                                                                       00001160
  800 CONTINUE                                                          00001170
C                                                                       00001180
C     CALCULATE PARTICULATE CLOUD BOUNDARIES                            00001190
C                                                                       00001200
      CALL CLOUD(UN,UMB)                                                00001210
C                                                                       00001220
      GO TO 500                                                         00001230
C                                                                       00001240
C                                                                       00001250
C     NORMAL PROGRAM EXIT                                               00001260
C                                                                       00001270
  999 CONTINUE                                                          00001280
      RETURN                                                            00001290
      END                                                               00001300
```

```
C     ************************************************************************00000010
C     SUBROUTINE HWJVEL                                                        00000020
C                                                                              00000030
C     THIS SUBROUTINE GENERATES THE VELOCITY PROFILE AND THE FORCES            00000040
C     AND OVERTURNING MOMENTS FOR A HUMAN BEING AT A GIVEN RADIUS              00000050
C     ************************************************************************00000060
C                                                                              00000070
      SUBROUTINE HWJVEL(H,UN,UMB,RVZ,RADIUS,WSPD,HUMTYP)                       00000080
C                                                                              00000090
      CHARACTER*1 KEY,KKEY,HUMTYP                                              00000100
C                                                                              00000110
      COMMON / CONSTS / PI,RHO,FPSPKN,RHOD2                                    00000120
      COMMON / PROFIL / RJ,ZBJ,ZHJ,ZMJ,UMJ,ZB,ZH,ZM,UM,CU,CY                  00000130
      COMMON / CKEY   / KEY,KKEY                                               00000140
      COMMON / PERSON / QP(12),DSET                                            00000150
      COMMON / UNITS  / IOU1,IOU6                                              00000160
C                                                                              00000170
C     ************************************************************************00000180
C                                                                              00000190
C     PROMPT FOR INPUT TO CALCULATE THE OVERTURNING                            00000200
C     MOMENT PROFILE AT VARIOUS RADIAL POSITIONS                               00000210
C                                                                              00000220
      WRITE(*,'(''EENTER HORIZONTAL RADIAL INCREMENT (FT) ===> ''\)')          00000230
      READ(*,*) DELH                                                           00000240
      WRITE(*,'(''EENTER MAXIMUM RADIUS FOR OTMOMENT (FT) ===> ''\)')          00000250
      READ(*,*) HMAX                                                           00000260
C                                                                              00000270
      DSET = DELH                                                              00000280
      IF(DSET.EQ.0.) DELH = HMAX                                               00000290
      DELH = DELH/RADIUS                                                       00000300
      HMAX = HMAX/RADIUS                                                       00000310
      NHPTS = IFIX((HMAX-RVZ)/DELH)+1                                          00000320
C                                                                              00000330
      PAUSE ' '                                                                00000340
      CALL CLS                                                                 00000350
C                                                                              00000360
      IF(DSET.EQ.0.)GOTO 83                                                    00000370
      IF(IOU6.NE.IOU1) WRITE(IOU6,'(''1'')')                                   00000380
      WRITE(IOU6,1001)                                                         00000390
 1001 FORMAT(' ',12X,' SUMMARY OF OVERTURNING FORCES AND MOMENTS',//,          00000400
     1       ' ',19X,'RADIUS',6X,'TOTF',6X,'TOTM',/,                          00000410
     2       ' ',20X,'(FT)',7X,'(LB)',5X,'(FT-LB)',/)                         00000420
   83 CONTINUE                                                                 00000430
C                                                                              00000440
C     BEGIN LOOP INCREMENTING THE RADIAL POINTS AT WHICH                       00000450
C     THE OVERTURNING MOMENT CALCULATIONS ARE MADE                             00000460
C                                                                              00000470
      DO 565 K = 1,NHPTS                                                       00000480
C                                                                              00000490
      CALL PROPRM(H,UN,UMB,RVZ)                                                00000500
      ZETAM = ZM/ZB                                                            00000510
C                                                                              00000520
```

```
C     BOUNDARY LAYER REGION EXPONENT                                    00000530
C                                                                       00000540
C     'AN' IS ACTUALLY '= 1.0/7.0'                                      00000550
C                                                                       00000560
      AN = 0.142857142                                                  00000570
C                                                                       00000580
C     SHEAR LAYER REGION EXPONENT, TO MEET EDGE CONDITIONS              00000590
C     (FROM FIGURE 7, USAAVLABS TECHNICAL REPORT 68-52, JULY 1968)      00000600
C                                                                       00000610
      ALPW = ALOG(1.0-1.0/SQRT(2.0))/ALOG((ZH-ZM)/(ZB-ZM))              00000620
C                                                                       00000630
      VN = UN                                                           00000640
      VMN = UM                                                          00000650
C                                                                       00000660
C     CALCULATION OF THE PEAK VELOCITY CORRECTION FACTOR                00000670
C     IS MADE IN THE NEXT SECTION AT THE 3 FT POSITION                  00000680
C                                                                       00000690
      VZ3 = 3.0/RADIUS                                                  00000700
      ZETA3 = VZ3/ZB                                                    00000710
      VZM3 = 0.0                                                        00000720
      IF(ZETA3.GE.ZETAM)GOTO 51                                         00000730
C                                                                       00000740
C     THE 3 FT HEIGHT IS IN THE BOUNDARY LAYER                          00000750
C                                                                       00000760
      IF(ZETAM.GT.0.0) VZM3 = (ZETA3/ZETAM)**AN                         00000770
      GOTO 52                                                           00000780
   51 CONTINUE                                                          00000790
C                                                                       00000800
C     THE 3 FT HEIGHT IS IN THE SHEAR LAYER                             00000810
C                                                                       00000820
      IF(VZ3.LE.ZB) VZM3=(1.0-((ZETA3-ZETAM)/(1.0-ZETAM))**ALPW)**2     00000830
   52 CONTINUE                                                          00000840
C                                                                       00000850
C     THE DELTA VELOCITY TO ADD TO THE MEAN VELOCITY IS                 00000860
C     CALCULATED AS THE CONSTANT VMFD3 (FT/SEC)                         00000870
C                                                                       00000880
      VZN3 = VZM3*VMN                                                   00000890
      VMF3 = VZN3*VN                                                    00000900
      VMFD3S = (RVZ*0.2444)+0.4                                         00000910
      IF(VMFD3S.GT.1.5) VMFD3S = 1.5                                    00000920
      VMFD3 = VMFD3S*VMF3                                               00000930
C                                                                       00000940
      IF(DSET.NE.0.)GOTO 78                                             00000950
      RRVZ = RVZ*RADIUS                                                 00000960
C                                                                       00000970
      WRITE(IOU6,1000) RRVZ                                             00000980
 1000 FORMAT(' ',8X,'SINGLE ROTOR VELOCITY PROFILE AT RADIUS (FT) ',    00000990
     1       F10.5,//)                                                  00001000
      WRITE(IOU6,1005)                                                  00001010
 1005 FORMAT(' ',2X,'HEIGHT',6X,'MEAN VELOCITY',7X,'PEAK VELOCITY',5X,  00001020
     1       'MEAN Q',4X,'PEAK Q',/,                                    00001030
     2       'O',4X,'(FT)',5X,'(FPS)',6X,'(KN)',5X,'(FPS)',6X,'(KN)',5X,00001040
```

```
     3       '(PSF)',5X,'(PSF)',/)                                    00001050
    78 CONTINUE                                                       00001060
C                                                                     00001070
C     SET UP ABILITY TO CALCULATE AT 0.5 FT.                          00001080
C     INCREMENTS UP THE VELOCITY PROFILE                              00001090
C                                                                     00001100
      DELZ = 0.5/RADIUS                                               00001110
      NPTS = 12                                                       00001120
C                                                                     00001130
      DO 500 I = 1,NPTS                                               00001140
C                                                                     00001150
      Z = DELZ*(I-1)+(0.25/RADIUS)                                    00001160
      ZETA = Z/ZB                                                     00001170
      IF (ZETA.GE.ZETAM) GO TO 300                                    00001180
C                                                                     00001190
C     Z IS WITHIN BOUNDARY LAYER                                      00001200
C                                                                     00001210
      VZM = 0.0                                                       00001220
      IF(ZETAM.GT.0.0) VZM = (ZETA/ZETAM)**AN                         00001230
      GO TO 400                                                       00001240
C                                                                     00001250
  300 CONTINUE                                                        00001260
C                                                                     00001270
C     Z IS WITHIN SHEAR LAYER                                         00001280
C                                                                     00001290
      VZM = 0.0                                                       00001300
      IF(Z.LE.ZB) VZM = (1.0-((ZETA-ZETAM)/(1.0-ZETAM))**ALPW)**2     00001310
C                                                                     00001320
  400 CONTINUE                                                        00001330
C                                                                     00001340
      VZN = VZM*VMN                                                   00001350
C                                                                     00001360
C     DIMENSIONAL HEIGHT                                              00001370
C                                                                     00001380
      ZZ  = Z*RADIUS                                                  00001390
C                                                                     00001400
C     MEAN VELOCITIES                                                 00001410
C                                                                     00001420
      VMF = VZN*VN                                                    00001430
      VMK = VMF/FPSPKN                                                00001440
C                                                                     00001450
C     PEAK VELOCITIES                                                 00001460
C                                                                     00001470
      VPF = VMF + VMFD3                                               00001480
      VPK = VPF/FPSPKN                                                00001490
C                                                                     00001500
C     THE EFFECT OF WIND IS TO ADD (DOWNWIND SIDE) OR                 00001510
C     SUBTRACT (UPWIND SIDE) TWO TIMES THE AMBIENT WIND               00001520
C     VELOCITY TO THE HORIZONTAL PROFILE VELOCITY                     00001530
C                                                                     00001540
      XKW = (-0.5*H)+2.5                                              00001550
      IF(XKW.LT.1.0)XKW = 1.0                                         00001560
```

```
      WSPD2 = WSPD*XKW                                                  00001570
      VMK = VMK + WSPD2                                                 00001580
      VMF = VMK*FPSPKN                                                  00001590
      VPK = VPK + WSPD2                                                 00001600
      VPF = VPK*FPSPKN                                                  00001610
C                                                                       00001620
C     DYNAMIC PRESSURE                                                  00001630
C                                                                       00001640
      QM    = RHOD2*VMF**2                                              00001650
      QP(I) = RHOD2*VPF**2                                              00001660
C                                                                       00001670
      IF(DSET.NE.0.) GOTO 77                                            00001680
      WRITE(IOU6,1002) ZZ,VMF,VMK,VPF,VPK,QM,QP(I)                      00001690
 1002 FORMAT (' ',F8.2,6F10.3)                                          00001700
   77 CONTINUE                                                          00001710
C                                                                       00001720
  500 CONTINUE                                                          00001730
C                                                                       00001740
      IF(DSET.NE.0.) GOTO 520                                           00001750
      PAUSE ' '                                                         00001760
      CALL CLS                                                          00001770
      IF(IOU6.NE.IOU1) WRITE(IOU6,'(''1'')')                            00001780
      WRITE(IOU6,1007) RRVZ                                             00001790
 1007 FORMAT(' ',8X,'SINGLE ROTOR FORCE PROFILE AT RADIUS (FT) ',       00001800
     1       F10.5,//)                                                  00001810
      WRITE(IOU6,1008)                                                  00001820
 1008 FORMAT(' ',2X,'HEIGHT',6X,'PEAK Q',6X,'FOVER',7X,'OVERM',7X,      00001830
     1              'TOT F',7X,'TOT M',/,                               00001840
     2       ' ',3X,'(FT)',8X,'(PSF)',7X,'(LB)',6X,'(FT-LB)',7X,        00001850
     3              '(LB)',6X,'(FT-LB)',/)                              00001860
  520 CONTINUE                                                          00001870
C                                                                       00001880
C     CALL SUBROUTINE TO CALCULATE THE                                  00001890
C     FORCES AND MOMENTS ON A HUMAN BEING                               00001900
C                                                                       00001910
      CALL MOMENT(NPTS,HUMTYP,TOTF,TOTM)                                00001920
C                                                                       00001930
      IF(DSET.EQ.0.)GOTO 545                                            00001940
      HH = RVZ*RADIUS                                                   00001950
      WRITE(IOU6,1014) HH,TOTF,TOTM                                     00001960
 1014 FORMAT(' ',18X,F8.2,2F10.3)                                       00001970
  545 CONTINUE                                                          00001980
C                                                                       00001990
      RVZ = RVZ + DELH                                                  00002000
  565 CONTINUE                                                          00002010
C                                                                       00002020
      CALL INKEY                                                        00002030
C                                                                       00002040
      RETURN                                                            00002050
      END                                                               00002060
```

```
C     ************************************************************************00000010
C     SUBROUTINE HIPVEL                                                        00000020
C                                                                              00000030
C     THIS SUBROUTINE GENERATES THE VELOCITY PROFILE AND THE FORCES            00000040
C     AND OVERTURNING MOMENTS FOR A HUMAN BEING ALONG THE INTERACTION          00000050
C     PLANE FOR THE TWIN ROTOR CASE                                            00000060
C     ************************************************************************00000070
C                                                                              00000080
      SUBROUTINE HIPVEL(H,UN,RADIUS,UMB,XIP,YSEP,WSPD,HUMTYP)                  00000090
C                                                                              00000100
      CHARACTER*1 KEY,KKEY,HUMTYP                                              00000110
C                                                                              00000120
      COMMON / CONSTS / PI,RHO,FPSPKN,RHOD2                                    00000130
      COMMON / PROFIL / RJ,ZBJ,ZHJ,ZMJ,UMJ,ZB,ZH,ZM,UM,CU,CY                  00000140
      COMMON / CKEY   / KEY,KKEY                                               00000150
      COMMON / PERSON / QP(12),DSET                                            00000160
      COMMON / UNITS  / IOU1,IOU6                                              00000170
C                                                                              00000180
C     ************************************************************************00000190
C                                                                              00000200
C     PROMPT FOR INPUT TO CALCULATE THE OVERTURNING                            00000210
C     MOMENT PROFILE AT VARIOUS RADIAL POSITIONS                               00000220
C                                                                              00000230
      WRITE(*,'(''EENTER HORIZONTAL RADIAL INCREMENT (FT)'',                   00000240
     1          ''     ===> ''\)')                                             00000250
      READ(*,*) DELH                                                           00000260
      WRITE(*,'(''EENTER MAXIMUM OTMOMENT DISTANCE (FT)  '',                   00000270
     1          ''     ===> ''\)')                                             00000280
      READ(*,*) HMAX                                                           00000290
C                                                                              00000300
      DSET = DELH                                                              00000310
      IF(DSET.EQ.0.)DELH = HMAX                                                00000320
      DELH = DELH/RADIUS                                                       00000330
      HMAX = HMAX/RADIUS                                                       00000340
      NHPTS = IFIX((HMAX-XIP)/DELH)+1                                          00000350
C                                                                              00000360
      PAUSE ' '                                                                00000370
      CALL CLS                                                                 00000380
C                                                                              00000390
      IF(DSET.EQ.0.)GOTO 83                                                    00000400
      IF(IOU6.NE.IOU1) WRITE(IOU6,'(''1'')')                                   00000410
      WRITE(IOU6,1001)                                                         00000420
 1001 FORMAT(' ',12X,' SUMMARY OF OVERTURNING FORCES AND MOMENTS',//,          00000430
     1       ' ',19X,'RADIUS',6X,'TOTF',6X,'TOTM',/,                          00000440
     2       ' ',20X,'(FT)',7X,'(LB)',5X,'(FT-LB)',/)                         00000450
   83 CONTINUE                                                                 00000460
C                                                                              00000470
C     BEGIN LOOP INCREMENTING THE RADIAL POINTS AT WHICH                       00000480
C     THE OVERTURNING MOMENT CALCULATIONS ARE MADE                             00000490
C                                                                              00000500
      DO 565 K = 1,NHPTS                                                       00000510
C                                                                              00000520
```

```
C     TF IS INTERACTION PLANE AMPLIFICATION FACTOR                      00000530
C                                                                       00000540
      TF = 1.55-(0.55)*EXP(-1.35*XIP)                                   00000550
C                                                                       00000560
C     GET PARAMETERS AT BASE RADIUS FOR 'BOUNDARY LAYER'                00000570
C                                                                       00000580
      RIPO = SQRT(XIP**2+YSEP**2)                                       00000590
C                                                                       00000600
      CALL PROPRM(H,UN,UMB,RIPO)                                        00000610
C                                                                       00000620
      ZIPB = ZB                                                         00000630
      ZIPM = ZM                                                         00000640
      ZIPH = ZH                                                         00000650
C                                                                       00000660
      RIPM = SQRT(XIP**2+(YSEP+ZIPM)**2)                                00000670
C                                                                       00000680
      CALL PROPRM(H,UN,UMB,RIPM)                                        00000690
C                                                                       00000700
      UMM = UM                                                          00000710
C                                                                       00000720
C     OUTPUT HEADER                                                     00000730
C                                                                       00000740
      IF(DSET.NE.0.)GOTO 78                                             00000750
      XXIP = RADIUS*XIP                                                 00000760
C                                                                       00000770
      IF(IOU6.NE.IOU1) WRITE(IOU6,'(''1'')')                            00000780
      WRITE(IOU6,1000) XXIP                                             00000790
 1000 FORMAT(' ',18X,'IPLANE TWIN ROTOR VELOCITY PROFILE',              00000800
     1     /,'0',22X,'AT DISTANCE (FT) ',F10.5,//)                     00000810
C                                                                       00000820
      WRITE(IOU6,1002)                                                  00000830
 1002 FORMAT(' ',3X,'HEIGHT',8X,'MEAN VELOCITY',7X,'PEAK VELOCITY',5X,  00000840
     1       'MEAN Q',4X,'PEAK Q',/,                                    00000850
     2       '0',5X,'(FT)',7X,'(FPS)',6X,'(KN)',5X,'(FPS)',6X,'(KN)',5X,00000860
     3       '(PSF)',5X,'(PSF)',/)                                      00000870
   78 CONTINUE                                                          00000880
C                                                                       00000890
C     'AN' IS ACTUALLY '= 1.0/7.0'                                      00000900
C                                                                       00000910
      AN = 0.142857142                                                  00000920
C                                                                       00000930
      DELZ = 0.5/RADIUS                                                 00000940
      NPTS = 12                                                         00000950
C                                                                       00000960
      DO 500 I = 1,NPTS                                                 00000970
C                                                                       00000980
      ZIP = DELZ*(I-1)+(0.25/RADIUS)                                    00000990
C                                                                       00001000
C     GET MAX WALL JET VELOCITY AT EFFECTIVE RADIUS                     00001010
C                                                                       00001020
      RIP = SQRT(XIP**2+(YSEP+ZIP)**2)                                  00001030
C                                                                       00001040
```

```
      CALL PROPRM(H,UN,UMB,RIP)                                          00001050
C                                                                        00001060
      VN = UN                                                            00001070
      VZ = UM                                                            00001080
C                                                                        00001090
C     INTERACTION PLANE 'BOUNDARY LAYER'                                 00001100
C                                                                        00001110
      IF(ZIP.LT.ZIPM) VZ = UMM*(ZIP/ZIPM)**AN                            00001120
C                                                                        00001130
C     DEVELOPED INTERACTION PLANE JET                                    00001140
C                                                                        00001150
      VH = TF*VZ*XIP/RIP                                                 00001160
      VV = TF*VZ*(YSEP+ZIP)/RIP                                          00001170
C                                                                        00001180
      ZZ = ZIP*RADIUS                                                    00001190
C                                                                        00001200
C     MEAN HORIZONTAL VELOCITIES AND DYNAMIC PRESSURE                    00001210
C                                                                        00001220
      VHMF = VH*UN                                                       00001230
      VHMK = VHMF/FPSPKN                                                 00001240
C                                                                        00001250
C     PEAK HORIZONTAL VELOCITIES AND DYNAMIC PRESSURE                    00001260
C                                                                        00001270
      VMFD3I = (XIP*0.2444)+0.8                                          00001280
      IF(VMFD3I.GT.2.5) VMFD3I = 2.5                                     00001290
      VHPF = VMFD3I*VHMF                                                 00001300
      VHPK = VHPF/FPSPKN                                                 00001310
C                                                                        00001320
C     THE EFFECT OF WIND IS TO ADD (DOWNWIND SIDE) OR                    00001330
C     SUBTRACT (UPWIND SIDE) TWO TIMES THE AMBIENT WIND                  00001340
C     VELOCITY TO THE HORIZONTAL PROFILE VELOCITY                        00001350
C                                                                        00001360
      XKW = (-0.5*H)+2.5                                                 00001370
      IF(XKW.LT.1.0)XKW = 1.0                                            00001380
      WSPD2 = WSPD*XKW                                                   00001390
      VHMK = VHMK + WSPD2                                                00001400
      VHMF = VHMK*FPSPKN                                                 00001410
      VHPK = VHPK + WSPD2                                                00001420
      VHPF = VHPK*FPSPKN                                                 00001430
C                                                                        00001440
C     DYNAMIC PRESSURE                                                   00001450
C                                                                        00001460
      QHM   = RHOD2*VHMF**2                                              00001470
      QP(I) = RHOD2*VHPF**2                                              00001480
C                                                                        00001490
      IF(DSET.NE.0.)GOTO 77                                              00001500
C                                                                        00001510
C     REPORT HORIZONTAL COMPONENTS                                       00001520
C                                                                        00001530
      WRITE(IOU6,1003) ZZ,VHMF,VHMK,VHPF,VHPK,QHM,QP(I)                  00001540
 1003 FORMAT (' ',F8.2,2X,6F10.3)                                        00001550
   77 CONTINUE                                                           00001560
```

```
C                                                                       00001570
  500 CONTINUE                                                          00001580
C                                                                       00001590
      IF(DSET.NE.0.) GOTO 520                                           00001600
      PAUSE ' '                                                         00001610
      CALL CLS                                                          00001620
      IF(IOU6.NE.IOU1) WRITE(IOU6,'(''1'')')                            00001630
      WRITE(IOU6,1007) XXIP                                             00001640
 1007 FORMAT(' ',8X,'TWIN ROTOR FORCE PROFILE AT DISTANCE (FT) ',       00001650
     1       F10.5,//)                                                  00001660
      WRITE(IOU6,1008)                                                  00001670
 1008 FORMAT(' ',2X,'HEIGHT',6X,'PEAK Q',6X,'FOVER',7X,'OVERM',7X,      00001680
     1              'TOT F',7X,'TOT M',/,                               00001690
     2       ' ',3X,'(FT)',8X,'(PSF)',7X,'(LB)',6X,'(FT-LB)',7X,        00001700
     3              '(LB)',6X,'(FT-LB)',/)                              00001710
  520 CONTINUE                                                          00001720
C                                                                       00001730
C     CALL SUBROUTINE TO CALCULATE THE                                  00001740
C     FORCES AND MOMENTS ON A HUMAN BEING                               00001750
C                                                                       00001760
      CALL MOMENT(NPTS,HUMTYP,TOTF,TOTM)                                00001770
C                                                                       00001780
      IF(DSET.EQ.0.)GOTO 545                                            00001790
      HH = XIP*RADIUS                                                   00001800
      WRITE(IOU6,1014) HH,TOTF,TOTM                                     00001810
 1014 FORMAT(' ',18X,F8.2,2F10.3)                                       00001820
  545 CONTINUE                                                          00001830
C                                                                       00001840
      XIP = XIP + DELH                                                  00001850
  565 CONTINUE                                                          00001860
C                                                                       00001870
      CALL INKEY                                                        00001880
C                                                                       00001890
      RETURN                                                            00001900
      END                                                               00001910
```

```
C     ************************************************************************00000010
C     SUBROUTINE MOMENT                                                        00000020
C                                                                              00000030
C     THIS SUBROUTINE CALCULATE THE                                            00000040
C     FORCES AND MOMENTS ON A HUMAN BODY                                       00000050
C     ************************************************************************00000060
C                                                                              00000070
      SUBROUTINE MOMENT(NPTS,HUMTYP,TOTF,TOTM)                                 00000080
C                                                                              00000090
      CHARACTER*1 HUMTYP                                                       00000100
C                                                                              00000110
      COMMON / UNITS  / IOU1,IOU6                                              00000120
      COMMON / PERSON / QP(12),DSET                                            00000130
C                                                                              00000140
C     ************************************************************************00000150
C                                                                              00000160
C     ROUTINE TO CALCULATE FORCES AND MOMENTS                                  00000170
C     ON TWO SIZES OF HUMAN BEINGS                                             00000180
C                                                                              00000190
C     CDP IS THE COEFFICIENT OF DRAG OF THE PERSON                             00000200
C     WIDTHP IS THE WIDTH OF THE PERSON                                        00000210
C     WIDTHP IS 'L' TYPE IF 1.1 FT, WIDTHP IS 'S' TYPE IF 0.7 FT               00000220
C                                                                              00000230
C                                                                              00000240
      TOTM = 0.0                                                               00000250
      TOTF = 0.0                                                               00000260
C                                                                              00000270
      WIDTHP = 1.1                                                             00000280
      IF(HUMTYP.EQ.'S') WIDTHP = 0.7                                           00000290
      IF(HUMTYP.EQ.'S') NPTS = 8                                               00000300
      DELZZ = 0.5                                                              00000310
      CDP = 1.1                                                                00000320
C                                                                              00000330
      DO 10 J = 1,NPTS                                                         00000340
      FOVER = QP(J)*DELZZ*WIDTHP*CDP                                           00000350
      ZZ = 0.5*(J-1)+0.25                                                      00000360
      OVERM = FOVER*ZZ                                                         00000370
      TOTF = TOTF+FOVER                                                        00000380
      TOTM = TOTM+OVERM                                                        00000390
C                                                                              00000400
      IF(DSET.NE.0.)GOTO 10                                                    00000410
      WRITE(IOU6,20) ZZ,QP(J),FOVER,OVERM,TOTF,TOTM                            00000420
   20 FORMAT(' ',F8.2,5(2X,F10.3))                                             00000430
   10 CONTINUE                                                                 00000440
C                                                                              00000450
      RETURN                                                                   00000460
      END                                                                      00000470
```

```
C     ************************************************************************00000010
C     SUBROUTINE CLOUD                                                        00000020
C                                                                             00000030
C     THIS SUBROUTINE MAKES THE CALCULATIONS REQUIRED IN ESTIMATING           00000040
C     THE PARTICLE CLOUD BOUNDARIES ( NO DENSITIES ) FOR SINGLE AND           00000050
C     TWIN ROTOR CONFIGURATIONS                                               00000060
C     ************************************************************************00000070
C                                                                             00000080
      SUBROUTINE CLOUD(UN,UMB)                                                00000090
C                                                                             00000100
      CHARACTER*1 KEY,KKEY                                                    00000110
C                                                                             00000120
      COMMON / HELGEO /  H,DL,YSEP,WSPD,RADIUS                                00000130
      COMMON / CONSTS /  PI,RHO,FPSPKN,RHOD2                                  00000140
      COMMON / PROFIL /  RJ,ZBJ,ZHJ,ZMJ,UMJ,ZB,ZH,ZM,UM,CU,CY                 00000150
      COMMON / CLOUDK /  QSMAX                                                00000160
      COMMON / CKEY   /  KEY,KKEY                                             00000170
      COMMON / UNITS  /  IOU1,IOU6                                            00000180
C                                                                             00000190
C     ************************************************************************00000200
C                                                                             00000210
C     READ IN THE TERRAIN FACTOR CONSTANT                                     00000220
C                                                                             00000230
      CALL LOCATE(8,1)                                                        00000240
      WRITE(*,'(''ENTER TERRAIN ERROSION FACTOR (ND)  ===> ''\)')             00000250
      READ(*,*) XKT                                                           00000260
C                                                                             00000270
      XKT = SQRT(XKT)                                                         00000280
C                                                                             00000290
      QSMX = RHOD2*((SQRT(QSMAX)*UN)**2)                                      00000300
      ERC = -0.437                                                            00000310
      XUM = (UMB*UN)**2                                                       00000320
      XCU = CU*CU                                                             00000330
      C1 = 1.0                                                                00000340
      C2 = 2.2                                                                00000350
C                                                                             00000360
C     SINGLE ROTOR CLOUD BOUNDARY CALCULATIONS                                00000370
C                                                                             00000380
      RCR = RADIUS*((XKT/(C1*RHOD2*XUM*XCU))**ERC)                            00000390
      RVR = 0.785*RCR                                                         00000400
      ZVR = 0.329*RCR                                                         00000410
      RCVR = RCR-RVR                                                          00000420
      AR   = (2.0/PI)*ALOG(ZVR/RCVR)                                          00000430
      PHIR = (PI/2.0)*ALOG(RCVR)/ALOG(ZVR/RCVR)                               00000440
      AXLV = AR*((-PI/2.0)+PHIR)                                              00000450
      XLV = EXP(AXLV)                                                         00000460
      HCR = XLV + ZVR                                                         00000470
C                                                                             00000480
C     INITIALIZE INTERACTION PLANE BOUNDARIES                                 00000490
C                                                                             00000500
      RCI = 0.0                                                               00000510
      RVI = 0.0                                                               00000520
```

```
      ZVI = 0.0                                                          00000530
      HCI = 0.0                                                          00000540
      IF(YSEP.LE.0.1)GOTO 50                                             00000550
C                                                                        00000560
C     INTERACTION PLANE CLOUD BOUNDARY CALCULATIONS                      00000570
C                                                                        00000580
      RCI = RADIUS*((XKT/(C2*RHOD2*XUM*XCU))**ERC)                       00000590
      RVI = 0.785*RCI                                                    00000600
      ZVI = 0.329*RCI                                                    00000610
      RCVR = RCI-RVI                                                     00000620
      AR = (2.0/PI)*ALOG(ZVI/RCVR)                                       00000630
      PHIR = (PI/2.0)*ALOG(RCVR)/ALOG(ZVI/RCVR)                          00000640
      AXLV = AR*((-PI/2.0)+PHIR)                                         00000650
      XLV = EXP(AXLV)                                                    00000660
      HCI = XLV + ZVI                                                    00000670
   50 CONTINUE                                                           00000680
C                                                                        00000690
C     PRINTOUT OF BOUNDARY LIMITS                                        00000700
C                                                                        00000710
      CALL CLS                                                           00000720
      CALL LOCATE(5,1)                                                   00000730
C                                                                        00000740
      IF(IOU6.NE.IOU1) WRITE(IOU6,'(''1'')')                             00000750
      WRITE(IOU6,20)                                                     00000760
   20 FORMAT(' ',15X,' SUMMARY OF CLOUD BOUNDARIES',/,                   00000770
     1           16X,'    (ALL RESULTS IN FEET)',//,                    00000780
     2           11X,' RC ',7X,' RV ',7X,' ZV ',7X,' HC ',//)           00000790
      WRITE(IOU6,21) RCR,RVR,ZVR,HCR                                     00000800
   21 FORMAT(' ',' SR ',4F11.1)                                          00000810
      WRITE(IOU6,22) RCI,RVI,ZVI,HCI                                     00000820
   22 FORMAT(' ',' IP ',4F11.1)                                          00000830
      WRITE(IOU6,23) QSMX                                                00000840
   23 FORMAT(' ',//,' QSMAX = ',F8.2,' PSF',/)                           00000850
      WRITE(IOU6,24)                                                     00000860
   24 FORMAT(' ',///)                                                    00000870
C                                                                        00000880
      CALL INKEY                                                         00000890
C                                                                        00000900
      RETURN                                                             00000910
      END                                                                00000920
```

Source File: **ROTHAZ.FOR** Program Unit: **LOCATE**

```
C     ************************************************************************00000010
C     SUBROUTINE LOCATE                                                       00000020
C                                                                             00000030
C     POSITIONS THE CONSOLE DISPLAY CURSOR BY WRITING ANSI TERMINAL           00000040
C     CONTROL SEQUENCES TO UNIT '*'                                           00000050
C     ************************************************************************00000060
C                                                                             00000070
      SUBROUTINE LOCATE(IROW,ICOL)                                            00000080
C                                                                             00000090
      CHARACTER*8 CUP                                                         00000100
      CHARACTER*1 ECUP(8)                                                     00000110
      EQUIVALENCE (CUP,ECUP(1))                                               00000120
C                                                                             00000130
      CHARACTER*10  FMT                                                       00000140
      CHARACTER*1   EFMT(10)                                                  00000150
      EQUIVALENCE   (FMT,EFMT(1))                                             00000160
      DATA FMT      / '('' '',A? \)' /                                        00000170
C                                                                             00000180
C     ************************************************************************00000190
C                                                                             00000200
C     ANSI CONTROL SEQUENCE: CUP = ESC['ROW';'COLUMN'H                        00000210
C                                                                             00000220
      IR1 = IROW/10                                                           00000230
      IR2 = IROW-IR1*10                                                       00000240
      IC1 = ICOL/10                                                           00000250
      IC2 = ICOL-IC1*10                                                       00000260
C                                                                             00000270
      ECUP(1) = CHAR(27)                                                      00000280
      ECUP(2) = CHAR(91)                                                      00000290
      IPOS = 3                                                                00000300
C                                                                             00000310
      IF(IR1.GT.0) THEN                                                       00000320
        ECUP(IPOS) = CHAR(IR1+48)                                             00000330
      IPOS = IPOS + 1                                                         00000340
      ENDIF                                                                   00000350
C                                                                             00000360
      ECUP(IPOS) = CHAR(IR2+48)                                               00000370
      IPOS = IPOS + 1                                                         00000380
C                                                                             00000390
      ECUP(IPOS) = CHAR(59)                                                   00000400
      IPOS = IPOS + 1                                                         00000410
C                                                                             00000420
      IF(IC1.GT.0) THEN                                                       00000430
        ECUP(IPOS) = CHAR(IC1+48)                                             00000440
        IPOS = IPOS + 1                                                       00000450
      ENDIF                                                                   00000460
C                                                                             00000470
      ECUP(IPOS) = CHAR(IC2+48)                                               00000480
      IPOS = IPOS + 1                                                         00000490
C                                                                             00000500
      ECUP(IPOS) = CHAR(72)                                                   00000510
C                                                                             00000520
```

```
      EFMT(7) = CHAR(IPOS+48)                                    00000530
      WRITE (*,FMT) CUP                                          00000540
C                                                                00000550
      RETURN                                                     00000560
      END                                                        00000570
```

```
C     ************************************************************************00000010
C     SUBROUTINE CLS                                                           00000020
C                                                                              00000030
C     CLEARS THE CONSOLE DISPLAY AND HOMES THE CURSOR BY WRITING ANSI          00000040
C     TERMINAL CONTROL SEQUENCES TO UNIT '*'                                   00000050
C     ************************************************************************00000060
C                                                                              00000070
      SUBROUTINE CLS                                                           00000080
C                                                                              00000090
      CHARACTER*4  ED                                                          00000100
      CHARACTER*1  EED(4)                                                      00000110
      EQUIVALENCE  (ED,EED(1))                                                 00000120
C                                                                              00000130
      CHARACTER*10 FMT                                                         00000140
      DATA FMT     / '('' '',A4 \)' /                                          00000150
C                                                                              00000160
C     ************************************************************************00000170
C                                                                              00000180
C     ANSI CONTROL SEQUENCE: ED = ESC[2J                                       00000190
C                                                                              00000200
      EED(1) = CHAR(27)                                                        00000210
      EED(2) = CHAR(91)                                                        00000220
      EED(3) = CHAR(50)                                                        00000230
      EED(4) = CHAR(74)                                                        00000240
C                                                                              00000250
      WRITE (*,FMT) ED                                                         00000260
C                                                                              00000270
      RETURN                                                                   00000280
      END                                                                      00000290
```

APPENDIX D

PROGRAM ROTHAZ USER'S MANUAL

A narrative discussion along with example program output is provided in this appendix in order to lead the reader through a step by step usage of the **ROTHAZ Analysis Program.** An example of each one of the computer program options is covered in this fashion: numerical values or character strings contained in [ ] in the examples are input by the program user.

A. GETTING STARTED

The **ROTHAZ Analysis Program** is initiated by typing the program name:

ROTHAZ

The computer screen will then respond with the following output:

```
PROGRAM ROTHAZ - ROTORCRAFT DOWNWASH HAZARD ANALYSIS

SYSTEMS TECHNOLOGY, INC./COMPUTATIONAL METHODOLOGY ASSOCIATES

1 OCTOBER 1985
PROGRAM VERSION 1.0
```

```
Please press <return> to continue.
```

After depressing the <return> key, the user is asked in what format the program output is desired, returned to the screen or to an output device:

```
TABULAR LISTINGS MAY BE WRITTEN TO A
FILE OR ANY DOS OUTPUT DEVICE ...

FOR CONSOLE OUTPUT ENTER CON
FOR PRINTER OUTPUT ENTER PRN, LPT1, OR LPT2

ENTER OUTPUT DEVICE OR FILE    ===> [CON]
```

In this example, "CON" is typed; therefore, the output will be returned to the screen.

B. DEFINITION OF PROBLEM INPUT

Data that define the rotorcraft and the atmospheric conditions are input to the computer program following selection of the output format. In the example below, the input provided is for the Bell XV-15 Tilt Rotor. Data for other rotorcraft are provided in Appendix A.

```
ENTER NUMBER OF ROTORS (1,2)        ===>[2]

ENTER HUB TO HUB DISTANCE BETWEEN
   DUAL ROTORS (FT)                 ===>[32.2]

ENTER ROTOR RADIUS (FT)             ===>[12.5]

ENTER GROSS WEIGHT (LB)             ===>[13000.0]

ENTER DOWNLOAD FACTOR (PCT)         ===>[13.0]

Please press <return> to continue.

ENTER ROTOR HEIGHT AGL (FT)         ===>[35.0]

ENTER AIR DENSITY RATIO (ND)        ===>[1.0]

ENTER AMBIENT WIND SPEED (KT)
OF <= 10 KT FOR OPT. <W>,<I>        ===>[0.0]

Please press <return> to continue.
```

Of the inputs in the above example, the "download factor" and the "ambient wind speed" restrictions require explanation. The "download factor" is the percent of increase in thrust (where thrust is assumed initially to be equal to the gross weight) that is required to overcome the rotorcraft fuselage download which results from the rotor-induced velocity impinging upon the fuselage and/or wing. For most helicopters, this number is between approximately one and five percent. The requirement for input of an "ambient wind speed" of less than 10 kts is discussed in the main body of the report for the wall jet and interaction plane analyses. If a value greater than 10 kts is input to the program, the value is not accepted, and the user is prompted for another value.

C. ANALYSIS PROBLEM DEFINITION

There are several analysis paths that can be taken in the **ROTHAZ Analysis Program** after the input data requirements are satisfied. If the **Velocity Calculation** path is followed, the user can analyze the aerodynamics of:

1. The simple wall jet (single and twin rotor cases)

2. The interaction plane (twin rotor only)

3. The ground vortex

4. The disk edge vortex.

It is **strongly recommended** that the program user read and understand fully the limitations of the mathematical models that are associated with each of these options before executing the program. These modeling limitations are discussed in conjunction with flight test correlation cases in Sections III and IV of the main report.

If the **Hazard Calculation** option of the program is taken, the user is allowed a choice of two additional analyses for the calculation of:

1. Human overturning forces and moments (both single- and twin-rotor configurations).

2. Particle cloud boundaries (both single- and twin-rotor configurations).

The recommendation that the user read and understand fully the limitations of the mathematical models is again strongly suggested. Section V of the main report provides mathematical modeling information and flight test correlation data for both of these options.

In making the choice of which options to take, the user is prompted to input a single alphabetic character as shown below:

```
SELECT ANALYSIS PROBLEM

PRESS <V> FOR VELOCITY CALCULATIONS
PRESS <H> FOR HAZARD CALCULATIONS    ===> [V]
```

If the **Velocity Calculation** option <V> is chosen, the user is prompted further with:

```
SELECT TYPE OF FLOW TO BE ESTIMATED

PRESS <W> FOR WALL JET
      <I> FOR INTERACTION PLANE
      <G> FOR GROUND VORTEX
      <D> FOR DISK VORTEX
      <X> TO EXIT                    ===> [W]
```

If the Hazard **Calculation** option <H> is taken instead, the provided prompt is:

```
SELECT TYPE OF HAZARD

PRESS <M> FOR OVERTURNING MOMENT
PRESS <C> FOR PARTICULATE CLOUD
PRESS <X> TO EXIT                    ===> M
```

D. THE VELOCITY CALCULATION ANALYSIS

1. The Wall Jet

The **Wall Jet** option calculates the velocity profile of the single-main rotor helicopter and the noninteraction plane of the twin-rotor helicopter. The first prompt requiring input following the choice of the **Wall Jet** option <W> from the menu of the **Velocity Calculation** option <V> is for the distance from the center of the rotor at which the velocity profile calculation should be made.

```
ENTER WALL JET RADIUS FOR V(R,Z) (FT)  ===> 60.0
```

The choice of 60.0 ft that was made in the above example for the XV-15 results in the generation of information on the basic shape of the wall jet and is followed by a request for two additional inputs: the "vertical increment" and the "maximum height." These inputs are used in the presentation to the screen (or printer) of detailed information on the subject velocity profile.

```
SINGLE ROTOR VELOCITY PROFILE AT RADIUS (FT)    60.00000

     PROFILE BOUNDARY HEIGHT (FT)    12.48596
             HALF-VEL.HEIGHT (FT)     4.45927
             MAX-VEL  HEIGHT (FT)      .86688

ENTER VERTICAL INCREMENT DESIRED (FT) ===> 1.0

ENTER MAXIMUM HEIGHT FOR PROFILE (FT) ===> 12.0

Please press <return> to continue.
```

If 1 ft increments and a maximum height of 12 ft are specified, as shown above, the output of detailed information on the wall jet profile looks like the following output

HEIGHT	MEAN VELOCITY		PEAK VELOCITY		MEAN Q	PEAK Q
(FT)	(FPS)	(KN)	(FPS)	(KN)	(PSF)	(PSF)
.00	.000	.000	.000	.000	.000	.000
1.00	34.187	20.265	70.201	41.613	1.389	5.857
2.00	28.998	17.189	65.012	38.537	.999	5.023
3.00	24.009	14.232	60.023	35.580	.685	4.282
4.00	19.394	11.496	55.407	32.844	.447	3.648
5.00	15.212	9.017	51.226	30.365	.275	3.119
6.00	11.499	6.816	47.512	28.164	.157	2.683
7.00	8.277	4.907	44.291	26.254	.081	2.331
8.00	5.566	3.299	41.580	24.647	.037	2.055
9.00	3.379	2.003	39.392	23.350	.014	1.844
10.00	1.726	1.023	37.740	22.371	.004	1.693

PRESS <C> TO CONTINUE
<P> FOR NEW TARGET POINT
<N> FOR NEW ROTORCRAFT
<A> FOR NEW CASE
<X> TO EXIT ===> C

It can be seen in this output, as was indicated in the previous screen output, that the maximum velocity height (mean profile) is at approximately 1 ft, and the profile one-half velocity height is between 4 and 5 ft. Since the screen format is not designed to show more than ten points at a time, the <C> (continue) option must be invoked in order to obtain information on the last two desired heights.

HEIGHT	MEAN VELOCITY		PEAK VELOCITY		MEAN Q	PEAK Q
(FT)	(FPS)	(KN)	(FPS)	(KN)	(PSF)	(PSF)
11.00	.620	.367	36.633	21.715	.000	1.595
12.00	.067	.039	36.080	21.387	.000	1.547

PRESS <C> TO CONTINUE
<P> FOR NEW TARGET POINT
<N> FOR NEW ROTORCRAFT
<A> FOR NEW CASE
<X> TO EXIT ===>

After all of the desired information is output to the screen, the specified calculations are concluded. The user can then choose one of four other options: <P> returns the user to the first prompt for the **Wall Jet** problem; <N> allows the user to input a new rotorcraft configuration; <A> allows the user to input a new rotor height above the ground (AGL) as well as new atmospheric conditions; and <X> exits the program.

2. The Twin-Rotor Interaction Plane

The **Interaction Plane** option calculates the velocity profile along the plane perpendicular to and one-half the distance along the line connecting the rotor centers of rotation for a twin-rotor rotorcraft. Upon choosing the **Interaction Plane** option <I> from the menu of the **Velocity Calculation** option <V>, the following three prompts for the XV-15 appear:

```
ENTER DISTANCE ALONG INTERACTION PLANE (FT) ===> 50.0

ENTER VERTICAL INCREMENT DESIRED (FT)       ===> 1.0

ENTER MAXIMUM HEIGHT FOR PROFILE (FT)       ===> 10.0
```

These prompts function exactly as do the **Wall Jet** prompts. The first prompt defines the point along which the desired interaction plane velocity profile is to be calculated, and the second and third define the vertical increment and maximum height, respectively, thereof. Following the last prompt, the detailed **Interaction Plane** output format is presented.

DUAL ROTOR VELOCITY PROFILE IN INTERACTION PLANE

AT STATION (FT) 50.000

HEIGHT (FT)		MEAN VELOCITY (FPS)	MEAN VELOCITY (KN)	PEAK VELOCITY (FPS)	PEAK VELOCITY (KN)	MEAN Q (PSF)	PEAK Q (PSF)
.00	H	.000	.000	.000	.000	.000	.000
	V	.000	.000	.000	.000	.000	.000
1.00	H	58.974	34.958	104.833	62.141	4.133	13.061
	V	20.169	11.956	35.853	21.252	.483	1.528
2.00	H	58.188	34.492	103.435	61.313	4.024	12.715
	V	21.064	12.486	37.443	22.195	.527	1.666
3.00	H	57.379	34.012	101.996	60.460	3.913	12.364
	V	21.919	12.993	38.963	23.096	.571	1.804
4.00	H	56.549	33.521	100.522	59.586	3.800	12.009
	V	22.733	13.475	40.410	23.954	.614	1.941

```
PRESS <C> TO CONTINUE
      <P> FOR NEW TARGET POINT
      <N> FOR NEW ROTORCRAFT
      <A> FOR NEW CASE
      <X> TO EXIT              ===> C
```

While similar to the **Wall Jet** format, this output also provides information on the calculated vertical velocity portion of the interaction plane profile. This portion of the output is labeled with a "V" in the column to the right of the height column and appears in rows beneath each row of output for the horizontal component of velocity which are labeled with an "H."

As with the **Wall Jet**, the prompt following the output allows the user to obtain more profile information or move on to another problem.

3. The Ground Vortex

Due to the very elementary nature of its formulation, the **Ground Vortex** option, as provided in the **ROTHAZ Analysis Program**, should be used with great caution. As discussed in Section III of the main body of the report, almost no test data exist to validate this mathematical model. In addition, the mathematical model is at present formulated for use only with a single-main rotor/tail rotor helicopter configuration. With this in mind, the example that follows begins with the definition of a new rotorcraft configuration and atmospheric conditions. The input data are for the CH-53E.

```
ENTER NUMBER OF ROTORS (1,2)     ===> [1]


ENTER ROTOR RADIUS (FT)          ===> [39.5]
ENTER GROSS WEIGHT (LB)          ===> [56000.0]
ENTER DOWNLOAD FACTOR (PCT)      ===> [5.0]
Please press <return> to continue.


ENTER ROTOR HEIGHT AGL (FT)      ===> [30.0]
ENTER AIR DENSITY RATIO (ND)     ===> [1.0]
ENTER AMBIENT WIND SPEED (KT)
OF <= 10 KT FOR OPT. <W>,<I>     ===> [0.0]
Please press <return> to continue.
```

Following the data input, the **Velocity Calculation** option <V> is selected from the next menu:

```
SELECT ANALYSIS PROBLEM

PRESS <V> FOR VELOCITY CALCULATIONS
PRESS <H> FOR HAZARD CALCULATIONS    ===> [V]
```

Then the **Ground Vortex** option <G> is selected from the **Velocity Calculation** menu.

```
SELECT TYPE OF FLOW TO BE ESTIMATED

PRESS <W> FOR WALL JET
      <I> FOR INTERACTION PLANE
      <G> FOR GROUND VORTEX
      <D> FOR DISK VORTEX
      <X> TO EXIT                    ===> [G]
```

The **Ground Vortex** option requires the input of three rotorcraft parameters: the rotor tip speed, the number of rotor blades, and the rotorcraft translational velocity with respect to the surrounding air mass (i.e., an input of 15 kts can be either 15 kts ground speed on a no-wind day or 0 kts ground speed on a day with a 15-kt headwind).

```
ENTER ROTOR TIP SPEED (FT/SEC)       ===> [600.0]

ENTER NUMBER OF BLADES               ===> [7.0]

ENTER TRANSLATIONAL SPEED (KN)       ===> [16.0]
```

After these three values are entered, a listing of three calculated values is presented, followed by another prompt.

```
ROTOR HEIGHT ABOVE GROUND H/D        .37975
        ADVANCE RATIO MU-STAR        .53733
        ADVANCE RATIO MU             .04499

ENTER GROUND VORTEX STRENGTH RATIO
 (SEE CHART, PAGE 20)                ===> [4.0]
```

These values are the nondimensional rotor height above the ground and two advance ratio parameters. All three are discussed in detail in Section III of the main report. The prompt that is presented asks for input of the ground vortex strength ratio, which is obtained from Fig. D-1 (recopied from Fig. 17) using the three calculated parameters. Effective use of this figure effectively is discussed in detail in Section III, and the user is encouraged to read and understand fully this discussion so that the limits which appear on the figure (limits that define the airspeeds below and above which ground vortex formation would be extremely unlikely) are clearly understood. After the user enters the ground vortex strength ratio, the computer provides information on the calculated ground vortex circulation and position of the ground vortex core with respect to the ground axis. An example of this output for the CH-53E is:

```
GROUND VORTEX CIRCULATION (FT**2/SEC)        1192.91600
VORTEX POSITION XGV,ZGV (FT)     -69.513 ,     5.930
```

```
Please press <return> to continue.
```

The last decision that the user must make in executing the **Ground Vortex** option is the point at which the vertical velocity profile slice in the XY coordinate system is to be taken (see Fig. 18). This information is entered in response to the following prompts:

```
ENTER (XT,YT) TARGET POINTS (FT)
                              XT  ===> -80.0
                              YT  ===> 0.0

ENTER VERTICAL INCREMENT DESIRED (FT) ===> 2.0

ENTER MAXIMUM HEIGHT FOR PROFILE (FT) ===> 10.0

Please press <return> to continue.
```

The positive direction for the XY coordinate system is aft and right; therefore, in order to look at the ground vortex in front of the rotor, a negative X value is input along with a zero value for the lateral offset Y.

The screen printout resulting from input of the coordinate information is similar in format to those already presented (see the top of the next page). The velocity is output as the vectorial component in the XYZ directions as well as the resolved total magnitude. Program options following the output are identical to those discussed for the **Wall Jet.**

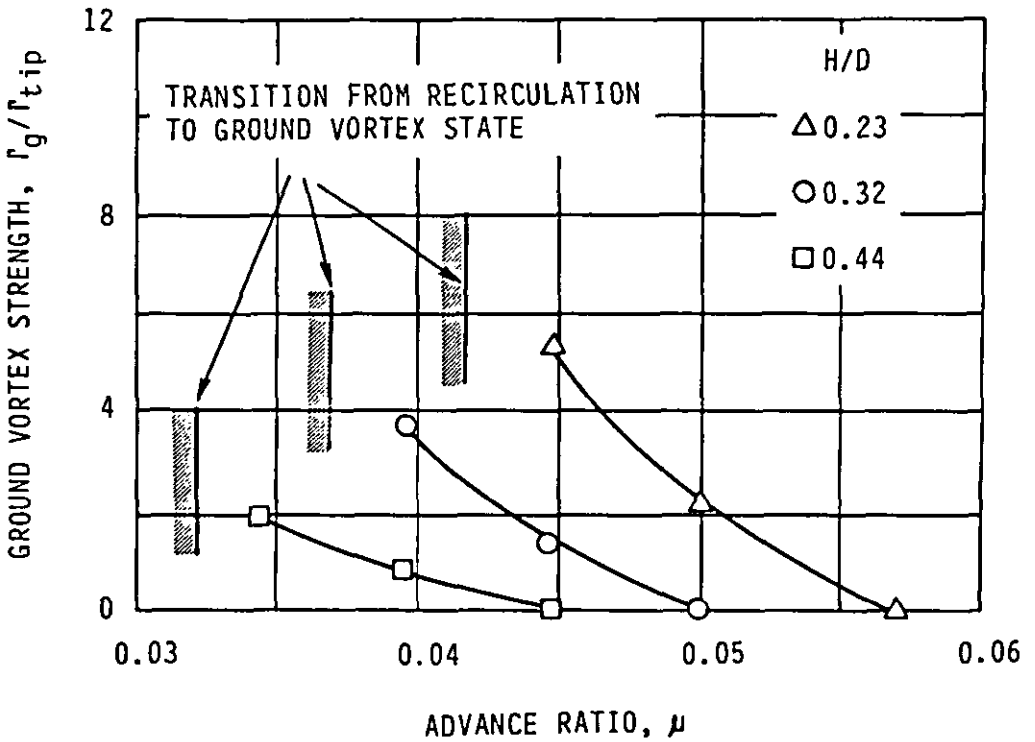

Figure D-1. Calculated Ground Vortex Circulation

HEIGHT (FT)		MEAN VELOCITY (FPS)	(KN)	MEAN Q (PSF)
.00	X	-14.839	-8.796	.262
	Y	.000	.000	.000
	Z	.000	.000	.000
	T	14.839	8.796	.262
2.00	X	-13.988	-8.291	.233
	Y	.000	.000	.000
	Z	4.257	2.523	.022
	T	14.621	8.667	.254
4.00	X	-11.601	-6.877	.160
	Y	.000	.000	.000
	Z	7.768	4.605	.072
	T	13.961	8.276	.232

PRESS <C> TO CONTINUE
<P> FOR NEW TARGET POINT
<N> FOR NEW ROTORCRAFT
<A> FOR NEW CASE
<X> TO EXIT ===> C

4. The Disk Edge Vortex

The use of the **Disk Vortex** option <D> in the **Velocity Calculation** analysis <V> path of the **ROTHAZ Analysis Program**, like the **Ground Vortex** option, should also be used with care. The text in Section III of the main body of the report provides guidance on the limitations involved in the use of this option. Vortex core size approximations can be estimated using the flight test data and correlation presented in Section IV. At present, like the **Ground Vortex** option, the mathematical model is only formulated for the single-main rotor/tail rotor helicopter configuration. With this in mind, the following example is provided, using the same input that was used for the **Ground Vortex** example (with data for the CH-53E) except that the rotor height above ground and forward airspeed are changed to 200 ft and 50 kts, respectively. The succession of input/output screens would thus present the information that begins at the top of the next page.

```
ENTER ROTOR HEIGHT AGL (FT)          ===> 200.0

ENTER AIR DENSITY RATIO (ND)         ===> 1.0

ENTER AMBIENT WIND SPEED (KT)
OF <= 10 KT FOR OPT. <W>,<I>         ===> 0.0

Please press <return> to continue.
```

```
SELECT TYPE OF FLOW TO BE ESTIMATED

PRESS <W> FOR WALL JET
      <I> FOR INTERACTION PLANE
      <G> FOR GROUND VORTEX
      <D> FOR DISK VORTEX
      <X> TO EXIT                    ===> D
```

```
ENTER ROTOR TIP SPEED (FT/SEC)       ===> 600.0

ENTER NUMBER OF BLADES               ===> 7.0

ENTER TRANSLATIONAL SPEED (KN)       ===> 50.0
```

Once the forward translational airspeed has been input, prompts request the target point in the XY coordinate plane at which the vertical velocity profile is desired. These prompts appear on the screen as follows:

```
ENTER (XT,YT) TARGET POINTS (FT)
                                     XT  ===> 150.0
                                     YT  ===> 0.0

ENTER VERTICAL INCREMENT DESIRED (FT) ===> 50.0

ENTER MAXIMUM HEIGHT FOR PROFILE (FT) ===> 150.0
```

The screen output that then follows begins the presentation of the desired results. The first frame presents the calculated vortex circulation value and the settling angle for the trailing vortex system; this is seen at the top of the next page.

DISK VORTEX VELOCITY PROFILE AT POINTS X,Y (FT) 150.000, .000

VORTEX CIRCULATION (FT**2/SEC) 3712.40
SETTLING ANGLE (DEG) 9.29

Please press <return> to continue.

After the carriage <return> is depressed, the next frame(s) of screen output provides the calculated vectorial velocity components and the total velocity at the various requested heights going up through the profile at the target XY coordinate position. At the bottom of this output, the standard menu that has been explained in the discussion of previous options is provided so that the user can continue with the presentation of more data, begin a new problem, or exit the program.

HEIGHT (FT)		MEAN VELOCITY (FPS)	(KN)	MEAN Q (PSF)
.00	X	-.996	-.590	.001
	Y	.000	.000	.000
	Z	.000	.000	.000
	T	.996	.590	.001
50.00	X	-1.113	-.660	.001
	Y	.000	.000	.000
	Z	-1.933	-1.146	.004
	T	2.230	1.322	.006
100.00	X	-1.651	-.979	.003
	Y	.000	.000	.000
	Z	-6.133	-3.636	.045
	T	6.352	3.765	.048

PRESS <C> TO CONTINUE
<P> FOR NEW TARGET POINT
<N> FOR NEW ROTORCRAFT
<A> FOR NEW CASE
<X> TO EXIT ===> C

E. THE HAZARD CALCULATION ANALYSIS

1. Personnel Overturning Moments

In the example that follows, the input data is for the XV-15 Tilt Rotor configuration:

```
ENTER NUMBER OF ROTORS (1,2)          ===> 2

ENTER HUB TO HUB DISTANCE BETWEEN
   DUAL ROTORS (FT)                   ===> 32.2

ENTER ROTOR RADIUS (FT)               ===> 12.5

ENTER GROSS WEIGHT (LB)               ===> 13000.0

ENTER DOWNLOAD FACTOR (PCT)           ===> 13.0

Please press <return> to continue.
```

```
ENTER ROTOR HEIGHT AGL (FT)           ===> 30.0

ENTER AIR DENSITY RATIO (ND)          ===> 1.0

ENTER AMBIENT WIND SPEED (KT)
OF <= 10 KT FOR OPT. <W>,<I>          ===> 0.0

Please press <return> to continue.
```

The overturning moment option of the **Hazard Calculation** path of the **ROTHAZ Analysis Program** is initiated by choosing <H> from the **Analysis Problem** menu which follows the rotorcraft input data prompting menus.

```
SELECT ANALYSIS PROBLEM

PRESS <V> FOR VELOCITY CALCULATIONS
PRESS <H> FOR HAZARD CALCULATIONS     ===> H
```

The next menu allows the user to select the **Overturning Moment** option by depressing <M>.

```
SELECT TYPE OF HAZARD

 PRESS <M> FOR OVERTURNING MOMENT
 PRESS <C> FOR PARTICULATE CLOUD
 PRESS <X> TO EXIT                    ===> [M]
```

The calculation of personnel overturning moments can be using either the single-main rotor or the twin-rotor configuration. In the following example, the choice of the single-rotor configuration is made by depressing the <W> for **Wall Jet** in response to the prompt.

```
SELECT TYPE OF FLOW TO BE ESTIMATED

PRESS <W> FOR WALL JET
      <I> FOR INTERACTION PLANE
      <X> TO EXIT                    ===> [W]
```

After the configuration is specified by choosing either the **Wall Jet** or the **Interaction Plane** option, the user must select the "type of human subject" that is of interest. The **Large** classification is for a man of approximately 6 ft in height, and the **Small** classification is for a child of approximately 3 ft. Both of these size classifications are discussed in detail in Section IV of the report. In this example, the **Large** size classification is chosen by depressing <L>:

```
SELECT TYPE OF HUMAN SUBJECT

PRESS <L> FOR LARGE (ADULT)
PRESS <S> FOR SMALL (CHILD)          ===> [L]
```

a. Wall Jet Option. The next task is to specify the radial locations at which overturning force and moment calculations are desired. For the **Wall Jet** option <W>, the user can choose between either a sequence of radial locations or a single location. The sequence of location option is specified by inputting a value for the minimum radial location of interest, followed by the inputting of values for the radial increment desired and the maximum radial location of interest. An example is provided at the top of the next page

```
ENTER LOWEST OTMOMENT WJET RADIUS (FT) ===> 30.0
ENTER HORIZONTAL RADIAL INCREMENT (FT) ===> 10.0
ENTER MAXIMUM RADIUS FOR OTMOMENT (FT) ===> 80.0
Please press <return> to continue.
```

The simple output that results from this input lists the radial station value, the total calculated body overturning force, and the total calculated body overturning moment, as shown below.

SUMMARY OF OVERTURNING FORCES AND MOMENTS

RADIUS (FT)	TOTF (LB)	TOTM (FT-LB)
30.00	31.324	51.087
40.00	34.265	74.043
50.00	34.614	84.816
60.00	31.598	82.613
70.00	25.962	70.280

```
PRESS <C> TO CONTINUE
      <P> FOR NEW TARGET POINT
      <R> FOR RETURN TO MAIN PROGRAM
      <X> TO EXIT                  ===> P
```

Again, the standard menu that provides for continuation, new data input, returning to the main program, or exiting appears at the bottom of the output data screen. Selecting the **Return to Main Program** option <R> returns the user to the mainline routine of the program where the input data prompts are provided. The **New Target Point** option <P> allows the specification of a new range of radial position values from which to calculate new force and moment data. If the <P> option is selected, the user can also choose to obtain detailed information on any one specific radial position. The way this is done is to type zero (0) in response to the **Increment** prompt as shown below:

```
ENTER LOWEST OTMOMENT WJET RADIUS (FT) ===> 40.0
ENTER HORIZONTAL RADIAL INCREMENT (FT) ===> 0.0
ENTER MAXIMUM RADIUS FOR OTMOMENT (FT) ===> 40.0
Please press <return> to continue.
```

The resulting output is provided on two consecutive screens. The first screen provides the velocity profile data that is used in the force and moment calculation procedure. The second screen provides the details of the incremental force and moment calculations as they are made vertically along the human body at 0.5 ft increments. The boxed [ ] total force and total moment values at the bottom of the TOT F and TOT M columns are equivalent to those printed in the results of the previous example; the difference is that these are calculated at a wall jet radius of 40 ft only.

SINGLE ROTOR VELOCITY PROFILE AT RADIUS (FT) 40.00000

HEIGHT	MEAN VELOCITY		PEAK VELOCITY		MEAN Q	PEAK Q
(FT)	(FPS)	(KN)	(FPS)	(KN)	(PSF)	(PSF)
.25	49.564	29.380	81.789	48.482	2.920	7.950
.75	53.605	31.775	85.830	50.877	3.415	8.755
1.25	47.280	28.026	79.505	47.128	2.657	7.512
1.75	41.132	24.382	73.356	43.483	2.011	6.395
2.25	35.299	20.924	67.523	40.026	1.481	5.419
2.75	29.840	17.688	62.064	36.790	1.058	4.578
3.25	24.787	14.693	57.012	33.795	.730	3.863
3.75	20.166	11.954	52.390	31.055	.483	3.262
4.25	15.992	9.479	48.216	28.581	.304	2.763
4.75	12.280	7.279	44.504	26.381	.179	2.354
5.25	9.041	5.359	41.265	24.461	.097	2.024
5.75	6.284	3.725	38.509	22.827	.047	1.762

Please press <return> to continue.

SINGLE ROTOR FORCE PROFILE AT RADIUS (FT) 40.00000

HEIGHT (FT)	PEAK Q (PSF)	FOVER (LB)	OVERM (FT-LB)	TOT F (LB)	TOT M (FT-LB)
.25	7.950	4.810	1.202	4.810	1.202
.75	8.755	5.297	3.973	10.107	5.175
1.25	7.512	4.545	5.681	14.651	10.856
1.75	6.395	3.869	6.771	18.521	17.627
2.25	5.419	3.278	7.376	21.799	25.003
2.75	4.578	2.770	7.616	24.568	32.620
3.25	3.863	2.337	7.595	26.905	40.215
3.75	3.262	1.973	7.401	28.879	47.616
4.25	2.763	1.672	7.104	30.550	54.720
4.75	2.354	1.424	6.764	31.975	61.484
5.25	2.024	1.224	6.428	33.199	67.912
5.75	1.762	1.066	6.131	34.265	74.043

PRESS <C> TO CONTINUE
<P> FOR NEW TARGET POINT
<R> FOR RETURN TO MAIN PROGRAM
<X> TO EXIT ===> R

b. The Interaction Plane Option. The procedure for choosing the **Interaction Plane** option <I> from the **Hazard Calculation** option <H> is exactly the same as that for the **Wall Jet** option <W>. Examples of the two output options are provided, without discussion, for the user who wishes to follow the **Interaction Plane** analysis path:

(1) Option 1—Sequence of Radial Locations

```
ENTER LOWEST OTMOMENT IPLANE DISTANCE (FT) ===> 40.0
ENTER HORIZONTAL RADIAL INCREMENT (FT)     ===> 10.0
ENTER MAXIMUM OTMOMENT DISTANCE (FT)       ===> 80.0
Please press <return> to continue.
```

SUMMARY OF OVERTURNING FORCES AND MOMENTS

RADIUS (FT)	TOTF (LB)	TOTM (FT-LB)
40.00	100.776	295.738
50.00	88.762	264.810
60.00	78.085	236.180
70.00	69.570	212.502
80.00	62.822	193.319

(2) Option 2—Single Radial Location

```
ENTER LOWEST OTMOMENT IPLANE DISTANCE (FT) ===> 50.0
ENTER HORIZONTAL RADIAL INCREMENT (FT)     ===> 0.0
ENTER MAXIMUM OTMOMENT DISTANCE (FT)       ===> 50.0
Please press <return> to continue.
```

IPLANE TWIN ROTOR VELOCITY PROFILE

AT DISTANCE (FT) 50.00000

HEIGHT	MEAN VELOCITY		PEAK VELOCITY		MEAN Q	PEAK Q
(FT)	(FPS)	(KN)	(FPS)	(KN)	(PSF)	(PSF)
.25	51.036	30.253	90.722	53.777	3.096	9.782
.75	59.531	35.288	105.822	62.728	4.212	13.309
1.25	59.210	35.098	105.251	62.390	4.166	13.165
1.75	58.814	34.863	104.547	61.972	4.111	12.990
2.25	58.412	34.625	103.833	61.549	4.055	12.813
2.75	58.004	34.383	103.108	61.119	3.999	12.635
3.25	57.591	34.138	102.374	60.684	3.942	12.455
3.75	57.173	33.891	101.631	60.244	3.885	12.275
4.25	56.751	33.640	100.880	59.799	3.828	12.095
4.75	56.324	33.387	100.122	59.349	3.770	11.913
5.25	55.893	33.132	99.356	58.895	3.713	11.732
5.75	55.459	32.874	98.584	58.438	3.655	11.550

Please press <return> to continue.

TWIN ROTOR FORCE PROFILE AT DISTANCE (FT) 50.00000

HEIGHT (FT)	PEAK Q (PSF)	FOVER (LB)	OVERM (FT-LB)	TOT F (LB)	TOT M (FT-LB)
.25	9.782	5.918	1.479	5.918	1.479
.75	13.309	8.052	6.039	13.970	7.518
1.25	13.165	7.965	9.956	21.935	17.475
1.75	12.990	7.859	13.753	29.794	31.228
2.25	12.813	7.752	17.442	37.545	48.669
2.75	12.635	7.644	21.021	45.189	69.690
3.25	12.455	7.536	24.491	52.725	94.181
3.75	12.275	7.427	27.850	60.152	122.031
4.25	12.095	7.317	31.098	67.469	153.129
4.75	11.913	7.208	34.236	74.677	187.366
5.25	11.732	7.098	37.264	81.774	224.629
5.75	11.550	6.988	40.181	88.762	264.810

PRESS <C> TO CONTINUE
<P> FOR NEW TARGET POINT
<R> FOR RETURN TO MAIN PROGRAM
<X> TO EXIT ===> R

2. Particulate Cloud Size Analysis

The particulate cloud size analysis methodology is discussed in detail in Section V of the main body of the report, along with limited flight correlation data. The method by which the terrain erosion factor is calculated and the definition of the cloud boundaries are also provided in Section V. Execution of this path of analysis begins with the depression of <C>, the **Particulate Cloud** option, from the **Hazard Calculation** <H> selection menu.

```
SELECT TYPE OF HAZARD

PRESS <M> FOR OVERTURNING MOMENT
PRESS <C> FOR PARTICULATE CLOUD
PRESS <X> TO EXIT                    ===> C
```

The next prompt asks for the terrain erosion factor, i.e., the specification of terrain type.

```
ENTER TERRAIN ERROSION FACTOR (ND)   ===> 0.1
```

The output of results is presented in a format that is designed for both single-rotor and twin-rotor vehicles. If a single-main rotor vehicle is being evaluated, the "IP" row will contain all zeros.

SUMMARY OF CLOUD BOUNDARIES
(ALL RESULTS IN FEET)

	RC	RV	ZV	HC
SR	117.0	91.8	38.5	54.9
IP	165.1	129.6	54.3	77.5

QSMAX = 12.99 PSF

In this example, using the XV-15, the single-rotor or "SR" row of information is applicable to the cloud boundary located at the calculated distance straight out from the wing tips and the interaction plane or "IP" row boundary calculations apply to the axis running out in front and aft along the XV-15 fuselage centerline. As before, standard hazard analysis continuation prompt is provided at the bottom of the screen.

```
PRESS <C> TO CONTINUE
      <P> FOR NEW TARGET POINT
      <R> FOR RETURN TO MAIN PROGRAM
      <X> TO EXIT                    ===> R
```

APPENDIX E

A COLLECTION OF REFERENCES PROVIDING INFORMATION OR FURTHER INSIGHT INTO THE ROTORWASH HAZARD ANALYSIS PROBLEM

FULL SCALE AND MODEL DOWNWASH/
OUTWASH FLOW FIELD DATA

1. Anon., VTOL Downwash Impingement Study, Velocity Survey, U.S. Army Transportation Research Command Technical Report No. 60-58, August 1960.

2. Anon., A Comparison of Downwash and Outflow From a Tilt-Wing Aircraft and a Helicopter, Canadair Report RAG-084-107, February 1971.

3. Ball, LCDR J. C., and D. A. DuFresne, Shipboard Evaluation of the XV-15 Tilt Rotor Research Aircraft, Naval Air Test Center Technical Report No. RW-54R-82, April 18, 1983.

4. Dyke, R. W., An Investigation of the Over the Water Aspects of VTOL Airplanes at High Disk Loading, Curtis-Wright Corporation, VTOL Systems Group, Report No. 012-26, December 1963.

5. Fradenburgh, E. A., "Flow Field Measurements for a Hovering Rotor Near the Ground," Fifth Annual Western Forum of the American Helicopter Society, Los Angeles, California, September 1958.

6. Harris, D. J., and R. D. Simpson, Technical Evaluation of the Rotor Downwash Flow Field of the XV-15 Tilt Rotor Research Aircraft, Naval Air Test Center Technical Report No. SY-14R-83, July 1983.

7. Harris, D. J., and R. D. Simpson, CH-53E Helicopter Downwash Evaluation. Final Report, Naval Air Test Center Technical Report No. SY-89R-78, August 1, 1978.

8. Harris, D. J., and R. D. Simpson, Tilt-Wing Vertical and Short Takeoff and Landing Downwash Evaluation. Final Report, Naval Air Test Center Technical Report No. SY-52R-76, April 9, 1976.

9. Harris, D. J., and R. D. Simpson, Downwash Evaluation Under the U.S. Army Heavy Lift Helicopter Rotor. Final Report, Naval Air Test Center Technical Report No. SY-17R-76, March 16, 1976.

10. Jenkins, B. Z., and A. S. Marks, Rotor Downwash Velocities About the UH-1H Helicopter-Flight Test Measurements and Theoretical Calculations, Army Missile Research Development and Engineering Laboratory, Redstone Arsenal, Alabama, January 1975.

11. Kuhn, Richard E., An Investigation to Determine Conditions Under Which Downwash from VTOL Aircraft will Start Surface Erosion from Various Types of Terrain, NASA TN D-56, September 1959.

12. Leese, G. W., and J. T. Knight, Jr., Helicopter Downwash Data, Miscellaneous Paper S-74-17, U.S. Army Engineer Waterways Experiment Station, Vicksburg, Mississippi, June 1974.

13. Leese, Grady W., UH-1H Downwash Velocity Measurements, Army Engineer Waterways Experiment Station, Vicksburg, Mississippi, August 1972.

14. Michaelsen, O. E., "A Comparison of Outflows From a Helicopter, Tilt Wing, and Jet Lift Hovering Aircraft," AIAA 8th Annual Meeting and Technical Display, Washington, D.C., AIAA Paper No. 71-992, October 25, 1971.

15. O'Bryan, T. C., An Experimental Study of the Effect of Downwash From a Twin Propeller VTOL Aircraft on Several Types of Ground Surfaces, NASA TN D-1239, May 1962.

16. O'Bryan, Thomas C., An Investigation of the Effect of Downwash from a VTOL Aircraft and a Helicopter in the Ground Environment, NASA TN D-977, October 1961.

17. Patton, W. G., and R. D. Simpson, Investigation of SH-3/HH-3 Helicopter Downwash Environment, Naval Air Test Center Report ST-197R-71, September 24, 1971.

18. Skujins, Ojars, An Experimental Investigation of Rotor Forces and Flow Field in the Vicinity of a Step Ground Plane, West Virginia University, Department of Aerospace Engineering, July 1970.

ANALYSIS/PREDICTION TECHNIQUES

1. Shane, W. P., Effects of Downwash Upon Man, U.S. Army Aeromedical Research Unit Report No. 68-3, November 1967.

2. George, M., E. Kisielowski, and D. S. Douglas, Investigation of the Downwash Environment Generated by V/STOL Aircraft Operating in Ground Effect, USAAVLABS Technical Report 68-52, July 1968.

3. George, M., J. Tang, S. Mills, and D. Douglas, Downwash Environment for the Boeing Model 160 V/STOL Aircraft, Dynasciences Corporation Report DCR-268, January 1968.

4. George, M. M., Downwash Impingement Design Criteria for VTOL Aircraft, TRECOM Technical Report 64-48, U.S. Army Transportation Research Command, Fort Eustis, VA, August 1964.

5. Glauert, M. B., "The Wall Jet," Journal of Fluid Mechanics, Vol. 1, Part 6, December 1956, pp. 625-643.

6. Hill, W. G., R. G. Jenkins, S. G. Kalemaris, and M. J. Siclari, Study of VTOL In-Ground-Effect Flow Field Including Temperature Effect, NASA CR-166258, April 1982.

7. Hohler, D. J., An Analytical Method of Determining General Downwash Flow Field Parameters for V/STOL Aircraft, AFAPL-TR-66-90, November 1966.

8. Leese, Grady W., and James W. Carr, Materials Evaluation for Aircraft Blast and Helicopter Downwash Protection, Army Engineer Waterways Experiment Station, Vicksburg, Mississippi, June 1975.

9. Leese, G. W., Helicopter Downwash Blast Effects Study, U.S. Army Engineer Waterways Experiment Station TR-3-664, Vicksburg, Miss., October 1964.

10. Ludwig, G. R., and W. G. Brady, Theoretical and Experimental Studies of Impinging Uniform and Nonuniform Jets, TRECOM Technical Report 64-42, U. S. Army Transportation Research Command, Fort Eustis, VA, August 1964.

11. McKinley, J. B., Evaluating Wind Flow Around Buildings on Heliport Placement, DOT/FAA/PM-84/25, October 1984.

12. Migdal, D.; W. G. Hill, Jr.; R. C. Jenkins, and M. J. Siclari, VTOL in Ground Effect Flows for Closely Spaced Jets, NASA CR 152321, December 1979.

13. Morse, A., and H. Newhouse, VTOL Downwash Impingement Study Surface Erosion Tests, U.S. Army Transportation Research Command, TREC TR 60-67, Ft. Eustis, Virginia, October 1960.

14. Rogers, S. J., Evaluation of the Dust Cloud Generated by Helicopter Rotor Downwash, USAAVLABS TR-67-81, March 1968.

15. Schwartz, C. W., M. W. Witczak, and R. B. Leahy, Structural Design Guidelines for Heliports, DOT/FAA/PM-84/23, October 1984.

16. Watts, A., V/STOL Downwash Impingement Study--Velocity Estimate, Canadair Aerodynamic Memorandum MAA-284-001, January 1969, Revised April 1971.

17. Wernicke, R. K., "Prediction of Tilt Rotor Outwash," AIAA Paper No. 81-0013, AIAA 19th Aerospace Sciences Meeting, January 12-15, 1981.

LOW SPEED INTERACTIONAL AERODYNAMICS
(I.E., GROUND VORTEX)

1. Balch, David T., "Experimental Study of Main Rotor/Tail Rotor/ Airframe Interaction in Hover," 39th Annual Forum of the American Helicopter Society, St. Louis, Missouri, May 1983.

2. Curtiss, H. C., Jr., W. F. Putman, and E. J. Hanker, Jr., Rotor Aerodynamics in Ground Effect at Low Advance Ratios, Department of Mechanical and Aerospace Engineering, Princeton University Report No. 1571-MAE, July 27, 1982.

3. Curtiss, H. C., Jr., Mao Sun, and E. J. Hanker, Jr., "Dynamic Phenomena in Ground Effect," AHS Paper No. A-83-39-76-0000, Presented at the 39th Forum of the American Helicopter Society, May 9-11, 1983.

4. Curtiss, H. C., Jr., M. Sun, W. F. Putman, and E. J. Hanker, Jr., "Rotor Aerodynamics in Ground Effect at Low Advance Ratios," Journal of the American Helicopter Society, Vol. 29, No. 1, January 1984, p. 48.

5. Curtiss, H. C., Jr., W. Erdman, and M. Sun, "Ground Effect Aerodynamics," Presented at the International Conference on Rotorcraft Basic Research, Research Triangle Park, NC, February 19-21, 1985.

6. DuWaldt, F. A., Wakes of Lifting Propellers (Rotors) in Ground Effect, Cornell Aeronautical Laboratory No. BB-1665-5-3, November 1966.

7. Hanker, E. J., Jr., and R. P. Smith, "Parameters Affecting Helicopter Interactional Aerodynamics in Ground Effect," Journal of the American Helicopter Society, Vol. 30, No. 1, January 1985.

8. Sheridan, Philip F., E. J. Hanker, and B. B. Blake, Investigation of Operational and Design Factors Resulting From Main Rotor and Tail Rotor Interactions, USAAVRADCOM-TR-82-D-40, January 1984.

9. Sheridan, Philip F., Interactional Aerodynamics of the Single Rotor Helicopter Configuration. Volume 1: Final Report, USARTL-TR-78-23A, September 1978.

10. Sun, Mao, from A Study of Helicopter Rotor Aerodynamics in Ground Effect, Ph.D. Thesis, Princeton Mechanical and Aerodynamics Engineering Department, June 1983.

11. Weisner, W., and G. Kohler, "Tail Rotor Performance in presence of Main Rotor, Ground, and Winds," Presented at the 29th Annual National Forum of the American Helicopter Society, May 1973.

WAKE VORTEX ENCOUNTERS

1. Burnham, David C., and Stephen A. Teager, Preliminary Measurements of Helicopter Wake-Vortex Velocity Profiles, DOT-TSC-FA527-PM-85-7, March 1985.

2. Johnson, Walter A., and Thomas T. Myers, A Model for Human Pilot Behavior During Wake Vortex Encounter Upsets, FAA-RD-76-8, April 1976.

3. Johnson, Walter A., and Gary L. Teper, Analysis of Vortex Wake Encounter Upsets, NASA CR-127491, August 1974.

4. Mantay, W. R., G. T. Holbrook, R. L. Campbell, and R. L. Tomaine, "Helicopter Response to an Airplane's Trailing Vortex," Journal of Aircraft, Vol. 14, No. 4, April 1977, pp. 357-363.

5. Sammonds, R. I., and G. W. Stinnett, Jr., Hazard Criteria for Wake Vortex Encounters, NASA TM X-62,473, August 1975.

OTHER REFERENCES

1. Anon., Full-Scale Tests of Grumman Design 698-411 Tilt-Nacelle V/STOL Model at the NASA-Ames Research Center, Grumman Report PDR 698-33, December 1981.

2. Donaldson, C. D., and R. S. Snedeker, "A Study of Free Jet Impingement. Part 1. Mean Properties of Free and Impinging Jets," Journal of Fluid Mechanics, Vol. 45, Part 2, 1971, pp. 281-319.

3. Heyson, H. H., Some Wake Related Operation Limitations of Rotorcraft, NASA TM-81920, December 1980.

4. Heyson, H. H., Theoretical Study of the Effect of Ground Proximity on the Induced Efficiency of Helicopter Rotors, NASA TM X-71951, May 3, 1977.

5. Hill, W. G., and R. C. Jenkins, "Effect of Nozzle Spacing on Ground Interference Forces for a Two-Jet V/STOL Aircraft," Journal of Aircraft, Vol. 17, No. 9, September 1980, pp. 684-689.

6. Hill, W. G., Jr., and R. C. Jenkins, Experimental Investigation of Multiple Jet Impingement Flows Applicable to VTOL Aircraft in Ground Effect, Grumman Research Department Memorandum RM-605, November 1975.

7. Jenkins, R. A., and W. G. Hill, Jr., Investigation of VTOL Upwash Flows Formed by Two Impinging Jets, Grumman Research Department RE-548, November 1977.

8. Kohlman, D. L., Introduction to V/STOL Airplanes, Iowa State University Press, 1981.

9. Peck, R. E., "Aerodynamics of a Round Jet in a Counterflowing Wind," Journal of Aircraft, Vol. 18, No. 1, January 1981, pp. 61-62.

10. Platzer, M. F., and R. J. Margason, "Prediction Methods for Jet V/STOL Propulsion Aerodynamics," Journal of Aircraft, Vol. 15, No. 2, February 1978, pp. 69-77.

11. Siclari, M. J.; W. G. Hill, Jr.; R. D. Jenkins; and D. Migdal, "VTOL In-Ground Effect Flows for Closely Spaced Jets," AIAA Paper No. 80-1880, AIAA Aircraft Systems Meeting, August 4-6, 1980.

12. Siclari, M. J.; W. G. Hill, Jr.; and R. C. Jenkins, "Stagnation Line and Upwash Formation of Two Impinging Jets," AIAA Journal, Vol. 19, No. 10, October 1981, pp. 1286-1293.

13. Siclari, M. J., D. Migdal, and J. L. Palcza, "Development of Theoretical Models for Jet-Induced Effects on V/STOL Aircraft," Journal of Aircraft, Vol. 13, No. 12, December 1976, pp. 936-944.

14. White, Fred, and Bruce B. Blake, "Improved Method of Predicting Helicopter Control Response and Gust Sensitivity," Presented at the 35th Annual National Forum of the American Helicopter Society, Washington, D.C., May 1979.

15. Wohllebe, F. A., and M. J. Siclari, "Fountain and Upwash Flowfields of Multijet Arrangements," Journal of Aircraft, Vol. 15, No. 8, August 1978, pp. 468-473.

Technical Report Documentation Page

1. Report No.	2. Government Accession No.	3. Recipient's Catalog No.

4. Title and Subtitle

ANALYSIS AND RECOMMENDATION OF SEPARATION REQUIREMENTS FOR ROTORCRAFT OPERATION AT AIRPORTS AND HELIPORTS

5. Report Date: September 1986

6. Performing Organization Code:

7. Author(s): Samuel W. Ferguson and J. David Kocurek

8. Performing Organization Report No.: STI TR-1224-1

9. Performing Organization Name and Address:
Systems Technology, Inc.
2672 Bayshore Parkway, Suite 505
Mountain View, California 94043

10. Work Unit No. (TRAIS):

11. Contract or Grant No.: DTRS-57-85-C-00039

12. Sponsoring Agency Name and Address:
U.S. Department of Transportation
Transport Systems Center
Kendal Square
Cambridge, Massachusetts 02142

13. Type of Report and Period Covered:
Final Report
February-December 1985

14. Sponsoring Agency Code:

15. Supplementary Notes

16. Abstract

Low-speed rotorcraft operations at airports and heliports are investigated to better understand and quantify the potential hazards associated with various types of rotorwash flowfields. Mathematical models for various types of rotor-induced flowfields are developed. These models are utilized in conjunction with hazard analysis models to evaluate the potential for rotorwash-related accidents in various operational scenarios. Correlation with available flight test and laboratory experimental data is provided wherever possible. The result from the analysis effort is a recommendation of separation requirements for rotorcraft operations at airports and heliports. Recommendations are also provided for future research that would aid in the elimination of safety factors used in the development of recommended separation criteria.

17. Key Words

Heliports
Airport Planning
Helicopter Wakes
Downwash
Ground Effect (aerodynamics)
Helicopters
Tilt-Rotor Aircraft
Rotary-Wing Aircraft
Aircraft Hazards

18. Distribution Statement

Document is available to the public through the National Technical Information Service (NTIS), Springfield, Virginia 22161

19. Security Classif. (of this report)	20. Security Classif. (of this page)	21. No. of Pages	22. Price
UNCLASSIFIED	UNCLASSIFIED		

Form DOT F 1700.7 (8-72) Reproduction of completed page authorized